

University of Memphis

University of Memphis Digital Commons

Electronic Theses and Dissertations

4-17-2012

An Analysis of Fluvial Geomorphology Parameters Affecting Meander Migration and Dynamic Equilibrium of the White River in Arkansas

Linh T. Duong

Follow this and additional works at: <https://digitalcommons.memphis.edu/etd>

Recommended Citation

Duong, Linh T., "An Analysis of Fluvial Geomorphology Parameters Affecting Meander Migration and Dynamic Equilibrium of the White River in Arkansas" (2012). *Electronic Theses and Dissertations*. 470. <https://digitalcommons.memphis.edu/etd/470>

This Thesis is brought to you for free and open access by University of Memphis Digital Commons. It has been accepted for inclusion in Electronic Theses and Dissertations by an authorized administrator of University of Memphis Digital Commons. For more information, please contact khggerty@memphis.edu.

AN ANALYSIS OF FLUVIAL GEOMORPHOLOGY PARAMETERS AFFECTING
MEANDER MIGRATION AND DYNAMIC EQUILIBRIUM OF THE WHITE RIVER
IN ARKANSAS

by

Linh Tiger Duong

A Thesis

Submitted in Partial Fulfillment of the

Requirements for the Degree of

Master of Science

Major: Civil Engineering

The University of Memphis

May, 2012

Copyright © 2012 Linh Tiger Duong
All rights reserved

This thesis is dedicated to two special individuals:

Virak Sim and Jerry Lee Anderson

ACKNOWLEDGEMENTS

Several people have been instrumental and helpful in allowing this thesis to be completed. I would like to thank my graduate advisor, Dr. Jerry Lee Anderson, and Dr. L. Yu Lin for their contributions of time and resources to this thesis. Thank you to Dr. Larry Moore for taking the time out of his busy schedule to serve on my thesis committee and for examining this thesis. I would also like to thank Dr. Ryan Csontos for providing advice and encouragement, and for sharing his expertise on geology and ArcGIS to this project. I would especially like to thank Mr. Gene McGinnis for reading and editing this thesis. Anyone who reads this thesis will surely appreciate his contribution. Other people that I would like to thank are Mr. Virak Sim and Mr. Vince T. for collecting soil field data and providing detailed descriptions of the sites, Mr. Bob Moats for allowing me to use the materials laboratory, Brother Edward Salgado for plant species biology and ecology, and Mother for giving hope and support during hard times.

ABSTRACT

Duong, Linh Tiger. M.S. Civil Engineering. The University of Memphis. May, 2012. An Analysis of Fluvial Geomorphology Parameters Affecting Meander Migration and Dynamic Equilibrium of the White River in Arkansas. Major Professor: Jerry Lee Anderson, Ph.D.

An analysis of a multitude of fluvial and morphological parameters was conducted to assess the current stability conditions of various White River reaches and to accentuate the contributions imparted by these parameters to the internal processes that governed the dynamic equilibrium within these reaches. The initial step involved the extractions and computations of pertinent fluvial and morphological parameters from the HEC-RAS Model and ArcGIS. Channel stability assessment emphasized three methodologies, namely stability assessment through parametric correlations between fluvial and morphological parameters; stability evaluation with the Rosgen Stream Classification System; and stability estimation through sediment analyses and sediment related parametric correlations. Morphological assessment implementing the Rosgen Stream Classification (RSC) system consisted of four inventory levels of classification. Sediment analyses conducted by implementing several sediment transport functions utilized the dominant bed materials attained from sieve analyses of approximately seven hundred soil samples collected from the channels of various 'reference' reaches.

TABLE OF CONTENTS

LIST OF TABLES.....	xi
LIST OF FIGURES.....	xvi
CHAPTER 1: BACKGROUND.....	1
Introduction.....	1
Objectives of the Thesis.....	3
Organization of the Thesis.....	3
Stratigraphy and Physiography.....	4
Drainage Basin/Sub-basins Landscape and Land-use.....	9
Floodplain Classification.....	14
River Biodiversity and Ecology.....	15
Human Impacts.....	19
Flow and Sediment Regimes.....	21
Tributaries, Drainage Patterns, Climate, and Miscellaneous.....	23
CHAPTER 2: LITERATURE REVIEW.....	27
Introduction.....	27
Fluvial Geomorphology.....	28
Channel Stability Assessment With Parametric Correlations.....	36
Channel Stability Assessment With The Rosgen Stream Classification System.....	45
Stability Assessment With Sediment Analyses and Parametric Correlations.....	50
CHAPTER 3: APPLICATIONS OF THE HEC-RAS MODEL AND ARCGIS.....	56
Introduction.....	56

HEC-RAS River Analysis System Modeling.....	57
HEC-RAS-Extracted Fluvial Parameters and Their Implications.....	70
Fluvial and Morphological Parameters.....	73
Entrenchment Ratio.....	73
Width to Depth Ratio.....	75
Sinuosity/Tortuosity Ratio.....	77
Longitudinal Gradient.....	81
Geometric Morphological Parameters.....	83
Meander Belt Width.....	83
Radius of Curvature.....	86
Meander Amplitude.....	88
Meander Wavelength.....	89
Empirical Correlations Between Parameters.....	90
Meander Wavelength Versus Channel Width.....	91
Meander Wavelength Versus Radius of Curvature.....	95
Meander Wavelength Versus Bend Length.....	95
Width to Depth Ratio Versus Radius of Curvature.....	97
Channel Dimensions Versus Radius of Curvature.....	99
Curvature Versus Sinuosity.....	100
Specific Energy Versus Sinuosity.....	102
Bankfull Discharge Versus Slope Versus Sinuosity.....	106
Maximum Sub-basin Width Versus Sinuosity.....	110
Correlations Involving the Transverse Water Surface Angles.....	115

ArcGIS-Extracted Morphological Parameters and Their Implications.....	122
Significance of Parametric Correlations.....	129
CHAPTER 4: FLUVIAL GEOMORPHOLOGY: THE RSC SYSTEM.....	137
Introduction.....	137
RSC Hierarchy of River Inventory and Assessment.....	138
Level I Classification: Geomorphic Characterization.....	140
Level II Classification: The Morphological Description.....	140
Batesville (RM 299.00).....	149
Newport (RM 258.94).....	152
Augusta (RM 200.30).....	155
Des Arc (RM 148.03).....	158
Devalls Bluff (RM 124.35).....	161
Clarendon (RM 100.38).....	164
St. Charles (RM 56.57).....	167
The Remaining Sections.....	170
Level III Classification: Assessment of Stream Condition and Departure.....	174
Riparian Vegetation.....	175
Streamflow Regime.....	180
Stream Size and Order.....	180
Depositional Patterns (sediment).....	183
Meander Patterns (channels).....	183
Stream Channel Stability.....	185
Streambank Erosion Potential.....	186

Level IV Classification: Field Data Verification.....	190
CHAPTER 5: SEDIMENT ANALYSES.....	226
Introduction.....	226
Sediment Transport Mechanisms.....	227
Bedforms.....	228
Sediment Transport and Supply.....	233
Correlations Between Fluvial/Morphological Parameters and Sediment Discharges.....	236
Width to Depth Ratio Versus Bed-load and Suspended-load Discharges.....	241
Channel Dimensions Versus Sediment Loads.....	244
Curvature Versus Total Sediment Concentration.....	252
Velocity Versus Total Sediment Discharge.....	254
Shear Force Versus Total Sediment Concentration.....	257
Sediment Load Rankings and Their Implications.....	260
Erosional and Depositional Activities.....	263
Specific Energy Versus Erosion and Deposition and Lateral Migrations.....	265
Channel Processes, Boundary Stability, and Morphology.....	269
Comparison of Sediment Analysis Methodologies.....	280
CHAPTER 6: RESULTS AND SOLUTIONS.....	288
Introduction.....	288
Fluvial and Morphological Contributions and Correlations.....	290
Results of Rosgen Stream Classifications.....	294
Sediment Analyses and Parametric Correlations.....	299

Drainage Patterns and Tectonic Influences.....	306
Significance of Fluvial and Morphological Parameters.....	310
Stream Restoration Solutions.....	312
Final Adjective and Numerical Ratings.....	315
CHAPTER 7: SUMMARY, CONCLUSIONS, AND RECOMMENDATIONS.....	322
Summary.....	322
Conclusions.....	324
Recommendations.....	331
REFERENCES.....	334
APPENDIX A: Procedure for Drainage Delineation (ArcGIS).....	349
APPENDIX B: Procedure for Extracting NRCS-NCGC's SSURGO Soil Data Mart...	355
APPENDIX C: Sediment Analysis Calculations.....	363
APPENDIX D: Sieve Analysis Histograms.....	371
APPENDIX E: Large Data Tables.....	438
APPENDIX F: Large Plots.....	456

LIST OF TABLES

Table 1.1. Stratigraphy of the Mississippi Alluvial Plain and the Ozark Plateaus.....	8
Table 1.2. Dimensions of Eight Drainage Sub-basins in the Vicinity of the White River.....	11
Table 1.3. A Classification of Floodplains.....	18
Table 3.1. Comparison of the HEC-RAS Model to the USACE Supermodel.....	68
Table 3.2. Fluvial Parameters Extracted from the White River HEC-RAS Model.....	72
Table 3.3. Composite Radii of Curvature for Various Reference Reaches of the White River.....	88
Table 3.4. Percentages of Occurrence of Sinuosity Values within Various Sinuosity Ranges and Sub-basins.....	112
Table 3.5. Tallies of Sinuosity Values within Various Sinuosity Ranges for the Reference Reaches.....	113
Table 3.6. Morphological Parameters Computed and Extracted from ArcGIS and HEC-RAS.....	128
Table 4.1. Geomorphic Parameters of Various Sections of the White River.....	141
Table 4.2. General Stream Type Descriptions and Delineative Criteria for Broad-level Classification (Level I).....	144
Table 4.3. Rosgen Classifications of Dominant Bed Materials.....	146
Table 4.4. Pebble Count Data for the Reference Reach at Batesville, Arkansas (RM. 299.00).....	150
Table 4.5. Field Data Form for the Reference Reach at Batesville, Arkansas (RM 299.00).....	151
Table 4.6. Pebble Count Data for the Reference Reach at Newport, Arkansas (RM 258.94).....	153
Table 4.7. Field Data Form for the Reference Reach at Newport, Arkansas (RM 258.94).....	154
Table 4.8. Pebble Count Data for the Reference Reach at Augusta, Arkansas (RM 200.30).....	156

Table 4.9. Field Data Form for the Reference Reach at Augusta, Arkansas (RM 200.30).....	157
Table 4.10. Pebble Count Data for the Reference Reach at Des Arc, Arkansas (RM 148.03).....	159
Table 4.11. Field Data Form for the Reference Reach at Des Arc, Arkansas (RM 148.03).....	160
Table 4.12. Pebble Count Data for the Reference Reach at Devalls Bluff, Arkansas (RM 124.35).....	162
Table 4.13. Pebble Count Data for the Reference Reach at Devalls Bluff, Arkansas (RM 124.35).....	163
Table 4.14. Pebble Count Data for the Reference Reach at Clarendon, Arkansas (RM 100.38).....	165
Table 4.15. Field Data Form for the Reference Reach at Clarendon, Arkansas (RM 100.38).....	166
Table 4.16. Pebble Count Data for the Reference Reach at St. Charles, Arkansas (RM 56.57).....	168
Table 4.17. Field Data Form for the Reference Reach at St. Charles, Arkansas (RM 56.57).....	169
Table 4.18. Geomorphological Characterization of the White River.....	170
Table 4.19. Riparian Vegetation Inventory/condition Survey for Section 141.....	179
Table 4.20. Categories of Stream Size as Indicated by Bankfull Surface Width and Stream Order.....	181
Table 4.21. Categories of Flow Regime for Specification in Level III Inventories.....	182
Table 4.22. Conversion of the Channel Stability Rating to a Reach Condition by Stream Type.....	187
Table 4.23a. Modified Pfankuch Channel Stability Evaluation Form.....	188
Table 4.23b. Modified Pfankuch Channel Stability Evaluation Form.....	189
Table 4.24 Conversion from Erodibility Variable Index to Numerical Bank Erosion Potential Values.....	191

Table 4.25a. Modified Pfankuch Channel Stability Evaluation for Batesville, Arkansas (RM 299.00).....	196
Table 4.25b. Modified Pfankuch Channel Stability Evaluation for Batesville, Arkansas (RM 299.00).....	197
Table 4.26a. Modified Pfankuch Channel Stability Evaluation for Newport, Arkansas (RM 258.94).....	198
Table 4.26b. Modified Pfankuch Channel Stability Evaluation for Newport, Arkansas (RM 258.94).....	199
Table 4.27a. Modified Pfankuch Channel Stability Evaluation for Augusta, Arkansas (RM 200.30).....	200
Table 4.27b. Modified Pfankuch Channel Stability Evaluation for Augusta, Arkansas (RM 200.30).....	201
Table 4.28a. Modified Pfankuch Channel Stability Evaluation for Des Arc, Arkansas (RM 148.03).....	202
Table 4.28b. Modified Pfankuch Channel Stability Evaluation for Des Arc, Arkansas (RM 148.03).....	203
Table 4.29a. Modified Pfankuch Channel Stability Evaluation for Devalls Bluff, Arkansas (RM 124.35).....	204
Table 4.29b. Modified Pfankuch Channel Stability Evaluation for Devalls Bluff, Arkansas (RM 124.35).....	205
Table 4.30a. Modified Pfankuch Channel Stability Evaluation for Clarendon, Arkansas (RM 100.38).....	206
Table 4.30b. Modified Pfankuch Channel Stability Evaluation for Clarendon, Arkansas (RM 100.38).....	207
Table 4.31a. Modified Pfankuch Channel Stability Evaluation for St. Charles, Arkansas (RM 56.57).....	208
Table 4.31b. Modified Pfankuch channel stability evaluation for St. Charles, Arkansas (RM 56.57).....	209
Table 4.32. Bank Erosion Potential for Batesville, Arkansas (RM 299.00).....	210
Table 4.33. Bank Erosion Potential for Newport, Arkansas (RM 258.94).....	211

Table 4.34. Bank Erosion Potential for Augusta, Arkansas (RM 200.30).....	212
Table 4.35. Bank Erosion Potential for Des Arc, Arkansas (RM 148.03).....	213
Table 4.36. Bank Erosion Potential for Devalls Bluff, Arkansas (RM 124.35).....	214
Table 4.37. Bank Erosion Potential for Clarendon, Arkansas (RM 100.38).....	215
Table 4.38. Bank Erosion Potential for St. Charles, Arkansas (RM 56.57).....	216
Table 4.39. Near Bank Stress Rating for Batesville, Arkansas (RM 295.27).....	217
Table 4.40. Near Bank Stress Rating for Newport, Arkansas (RM 258.94).....	218
Table 4.41. Near Bank Stress Rating for Augusta, Arkansas (RM 200.30).....	219
Table 4.42. Near Bank Stress Rating for Des Arc, Arkansas (RM 148.03).....	220
Table 4.43. Near Bank Stress Rating for Devalls Bluff, Arkansas (RM 124.35).....	221
Table 4.44. Near Bank Stress Rating for Clarendon, Arkansas (RM 100.38).....	222
Table 4.45. Near Bank Stress Rating for St. Charles, Arkansas (RM 56.57).....	223
Table 4.46. Results of Potential and Stability Assessments.....	224
Table 5.1. Numerical Quantities of Various Sediment Load Types.....	229
Table 5.2. Rankings of Bed-load, Suspended-load, and Total Sediment Discharges for Various Reaches of the White River.....	263
Table 5.3. Ranking of Erosional and Depositional Magnitudes of Various Reaches.....	265
Table 5.4. Results of Sediment Analyses.....	286
Table 6.1. Results of Fluvial and Morphological Correlations.....	294
Table 6.2. Results of RSC Classifications and Assessments.....	300
Table 6.3. Results of Sediment Analysis and Parametric Correlations.....	305
Table 6.4. Stream Restoration Solutions.....	314
Table 6.5. Criteria for the Conversions of Data into Adjective and Numerical Ratings.....	316

Table 6.6. Final Adjective Ratings.....	320
Table 6.7. Final Numerical Ratings.....	321
Table E.1. The Unified Table of Data.....	438
Table E.2. Sediment Analyses.....	448

LIST OF FIGURES

Figure 1.1. Planform of the Lower White River.....	2
Figure 1.2. Physiographic Regions of Arkansas.....	5
Figure 1.3. Textural Triangle Illustrating USDA Soil Classifications.....	7
Figure 1.4. U.S. Soil Texture Classification Map.....	7
Figure 1.5. The White River Basin.....	12
Figure 1.6. Lower White River Drainage Sub-basins and Tributaries.....	13
Figure 1.7a. Discharge Versus Slope Discriminant Diagram.....	24
Figure 1.7b. Plot of the Alluvial Sections of the White River on Discharge Versus Slope Discriminant Diagram to Predict Bed-load Materials and Meandering Range.....	24
Figure 1.8. Types of Drainage Patterns.....	25
Figure 2.1a. Fluvial Geomorphology Chart I.....	37
Figure 2.1b. Fluvial Geomorphology Chart II.....	38
Figure 2.1c. Fluvial Geomorphology Chart III.....	39
Figure 2.1d. Fluvial Geomorphology Chart IV.....	40
Figure 2.1e. Fluvial Geomorphology Chart V.....	41
Figure 3.1. Process Flow Diagram for Using HEC-GeoRAS.....	58
Figure 3.2. Loading of GeoRAS and DEM into ArcGIS, and Creating a Centerline Layer.....	60
Figure 3.3. Stream Centerline Attributing.....	62
Figure 3.4. Extraction of Station-elevation from a Digital Terrain Model.....	62
Figure 3.5. Channel Cross-section Attributing.....	64
Figure 3.6. Extraction of the GIS Data into a Formatted Data Exchange (sdf) File.....	65
Figure 3.7. The White River HEC-RAS Hydraulic Model.....	66

Figure 3.8. The White River Planform (HEC-RAS).....	69
Figure 3.9. Dimensionless Curve of Bankfull to 50-year Inundation.....	74
Figure 3.10. Width to Depth Ratios for Various Sections of the White River.....	78
Figure 3.11. Sinuosity Values for Various Sections of the White River.....	80
Figure 3.12. Schematic Diagram Identifying Terminology Used to Describe Different Components of the Meander Planform.....	84
Figure 3.13. Leopold's Empirical Formula for the Relationship Between Meander Wavelength and Channel Width.....	91
Figure 3.14. HEC-RAS Profile of the White River.....	92
Figure 3.15. Planform Illustrating ArcGIS Applications to Determine Sinuosity, Radius of Curvature, Meander Amplitude, Meander Wavelength, and Meander Belt Width.....	93
Figure 3.16. Correlation of Meander Wavelength Versus Channel Width.....	95
Figure 3.17. Correlation of Meander Wavelength Versus Mean Radius of Curvature.....	96
Figure 3.18. Correlation of Bend Length Versus Meander Wavelength.....	97
Figure 3.19. Correlation of Width to Depth Ratio Versus Radius of Curvature.....	99
Figure 3.20. Correlation of Channel Dimensions Versus Radius of Curvature.....	101
Figure 3.21. Correlation of Channel Curvature Versus Sinuosity.....	103
Figure 3.22. Correlation of Radius of Curvature Versus Sinuosity.....	103
Figure 3.23. Correlation of Specific Energy Versus Sinuosity.....	105
Figure 3.24a. Discharge Versus Slope Discriminant Diagram.....	109
Figure 3.24b. Plot of the Alluvial Sections of the White River on Discharge Versus Slope Discriminant Diagram to Predict Meandering Range.....	110
Figure 3.25. Correlation of Average Sinuosity Versus Sub-basin Width	112
Figure 3.26. Three-dimensional Surface Plot Depicting the Frequencies and Ranges of Sinuosity Values for Various Sub-basin Widths	114

Figure 3.27. Level of Significance for the Monotonic Relationship Between Average Sinuosity and Sub-basin Width.....	115
Figure 3.28. Summary Diagram for Flow Pattern and Cross-sectional Morphology at a Bend Apex.....	117
Figure 3.29. Correlation of the Transverse Water Surface Angle Versus Shear Force...	119
Figure 3.30. Correlation of the Transverse Water Surface Angle Versus Hydraulic Depth.....	120
Figure 3.31. Correlation of the Transverse Water Surface Angle Versus Janderson Curvature-shear Product.....	122
Figure 4.1. Rosgen Stream Classification's Hierarchy of River Inventory and Assessment.....	139
Figure 4.2. Broad-level Stream Classification Delineation Showing Longitudinal, Cross-Sectional, and Plan-views of Major Stream Types.....	142
Figure 4.3. Meander Width Ratio by Stream type Categories.....	142
Figure 4.4. Valley Type, Morphological Description, and Stream Type Association.....	143
Figure 4.5. Composite Wolman Pebble Count Scheme Across the Flow Transect.....	146
Figure 4.6. Illustrative Guide Showing Cross-sectional Configuration, Composition and Delineative Criteria of Major Stream Types.....	147
Figure 4.7. Classification Key for Natural Rivers.....	148
Figure 4.8. Particle Count and Calculated D_{50} for the Reference Reach at Batesville, Arkansas (RM 295.27).....	150
Figure 4.9. Particle Count and Calculated D_{50} for the Reference Reach at Newport, Arkansas (RM 258.94).....	153
Figure 4.10. Particle Count and Calculated D_{50} for the Reference Reach at Augusta, Arkansas (RM 200.30).....	156
Figure 4.11. Particle Count and Calculated D_{50} for the Reference Reach at Des Arc, Arkansas (RM 148.03).....	159
Figure 4.12. Particle Count and Calculated D_{50} for the Reference Reach at Devalls Bluff, Arkansas (RM 124.35).....	162

Figure 4.13. Particle Count and Calculated D_{50} for the Reference Reach at Clarendon, Arkansas (RM 100.38).....	165
Figure 4.14. Particle Count and Calculated D_{50} for the Reference Reach at St. Charles, Arkansas (RM 56.57).....	168
Figure 4.15. Procedure for the Tree Cramming Method of Estimating Percent Crown Exposure.....	177
Figure 4.16. Circles Drawn to Estimate Riparian Forest Density for Section 141.....	177
Figure 4.17. FAO's Landcover Classification Scheme.....	178
Figure 4.18. Illustrations of Depositional Features	184
Figure 4.19. Illustrations of Various Meander Pattern Descriptions	184
Figure 4.20. Streambank Erodibility Factors.....	191
Figure 4.21. Relationships of Particle Size Distributions for Bed-load at Bankfull Discharge, Bar Material, and Bed Material for Batesville (RM 299.00), Newport (RM 258.94), and Augusta (RM 200.30).....	194
Figure 4.22. Relationships of Particle Size Distributions for Bed-load at Bankfull Discharge, Bar Material, and Bed Material for Des Arc (RM 148.03), DeValls Bluff (RM 124.35), Clarendon (RM 100.38), and St. Charles (RM 56.57).....	195
Figure 5.1. The Schematic of Different Bedforms.....	231
Figure 5.2. Prediction of the White River's Bedforms from Transport Parameter, T , and Dimensionless Particle Diameter d^*	232
Figure 5.3. Prediction of the White River's Bedforms from Engelund's Dimensionless Shields Parameters Diagram.....	233
Figure 5.4. Sediment Rating Curve for Batesville to Newport (RM 299.00 - 258.94)....	237
Figure 5.5. Sediment Rating Curve for Newport to Augusta (RM 258.94 - 200.30).....	237
Figure 5.6. Sediment Rating Curve for Augusta to Des Arc (RM 200.30 - 148.03).....	238
Figure 5.7. Sediment Rating Curve for Des Arc to Devalls Bluff (RM 148.03 – 124.35).....	238

Figure 5.8. Sediment Rating Curve for Devalls Bluff to Clarendon (RM 124.35 – 100.38).....	239
Figure 5.9. Sediment Rating Curve for Clarendon to St. Charles (RM 100.38 – 56.57).....	239
Figure 5.10. Sediment Rating Curve for St. Charles to LMR (RM 56.57 – 0.00).....	240
Figure 5.11. Total Sediment Concentration for Batesville to LMR (RM 299.00 – 0.00).....	240
Figure 5.12. Sediment Concentration Trends for Various Sections from Batesville to LMR (RM 299.00 – 0.00).....	241
Figure 5.13. Correlation Plot of W/D Ratio Versus Bed-load Discharge.....	243
Figure 5.14. Correlation Plot of W/D Ratio Versus Suspended-load Discharge.....	244
Figure 5.15. Correlation Plot of Channel Width Versus Suspended-load Discharge.....	246
Figure 5.16. Correlation of Channel Width Versus Bed-load Discharge.....	247
Figure 5.17. Correlation of Maximum Channel Depth Versus Bed-load Discharge.....	249
Figure 5.18. Correlation of Maximum Channel Depth Versus Suspended-load Discharge.....	250
Figure 5.19. Correlation of Flow Area Versus Bed-load Discharge.....	250
Figure 5.20. Correlation of Flow Area Versus Suspended-load Discharge.....	251
Figure 5.21. Correlation of Flow area Versus Total Sediment Discharge.....	251
Figure 5.22. Correlation of Radius of Curvature Versus Total Sediment Concentration.....	254
Figure 5.23. Correlation of Velocity Versus Total Sediment Discharge (Van Rijn Results).....	258
Figure 5.24. Correlation of Velocity Versus Total Sediment discharge (Kennedy Results).....	259
Figure 5.25. Correlation of Shear Force Versus Total Sediment Concentration.....	261
Figure 5.26. Meander Area Histograms (RM 295.27 – 135.16).....	266

Figure 5.27. Meander area Histograms (RM 135.16 – 0.00).....	267
Figure 5.28. Correlations of Mean Specific Energy Versus Erosion and Deposition Activities and Lateral Migrations.....	270
Figure 6.1. Faults and Tectonic Zones of the Mississippi Alluvial Plain.....	309
Figure A.1. Open DEM Files from ArcMAP.....	349
Figure A.2. Raster to Polygon Window.....	350
Figure A.3. Aggregate Polygon Window.....	350
Figure A.4. Buffer Window.....	351
Figure A.5. Open Attributes Option.....	352
Figure A.6. Add Field Window.....	352
Figure A.7. Field Calculator.....	353
Figure A.8. VBA Script for Area Calculation.....	353
Figure A.9. Copy and Paste VBA Script to Pre-logic VBA Script Code Box.....	354
Figure A.10. Unit Selection from Calculate Geometry Window.....	354
Figure B.1. Select Survey Area: Arkansas.....	355
Figure B.2. Select Survey Area by County.....	356
Figure B.3. Select Option/Submit Request Window.....	356
Figure B.4. Download Soil Data Mart Zip File.....	357
Figure B.5. SSURGO Import Window.....	358
Figure B.6. Add Data Shapefile.....	358
Figure B.7. Add Data Mapunit.....	359
Figure B.8. Preliminary Soil Map.....	359
Figure B.9. Join Data Window.....	360
Figure B.10. Symbol Selector Window.....	361

Figure B.11. Layer Properties/Symbology Window.....	361
Figure B.12. Final Soil Map.....	362
Figure C.1. Modified Shield Diagram for Direct Determination of Critical Shear Stress.....	364

CHAPTER 1: BACKGROUND

Introduction

The White River, approximately 722 miles in length and a major tributary of the Lower Mississippi River, originates in the Boston Mountains of northwest Arkansas (35.8° N, 93.6° W) and first flows in a northerly direction toward the Arkansas-Missouri state line (River Mile 591.9). The White River then traverses easterly for about 115 miles in southwest Missouri before crossing back into Arkansas (River Mile 447.4) where it flows in a southeasterly direction to its confluence with the Black River (River Mile 264.8) near Newport. The White River then maneuvers southeast for about 265 miles before emptying into the Lower Mississippi River in the northeast corner of Desha County. The White River flows primarily through two of the five physiographic regions of Arkansas: the Ozark Plateaus and the Mississippi Alluvial Plain. From its source in the Boston Mountains to Batesville, the headwaters and mid-reaches of the White River reside within the Ozark Plateaus; an area of Karst landforms where streams incised deep valleys through sedimentary carbonate limestone and dolomite deposits (Arkansas Geological Survey, 2009). In this region, the White River is a gravel/boulder bed mountain stream with distinct sequences of pools and riffles which contribute to the rapidity of the flow. As the stream traverses southeast to Newport entering the Mississippi Alluvial Plain, an area consisting of alluvial landforms where unconsolidated sediments such as silt, sand, clay, and loess dominate, it abruptly changes to a lowland sand bed stream with extensive floodplain development and slower moving flow.

Comparisons of photographic images obtained in 2003 to quadrangle maps from 1984 indicate that excessive meandering and shifting occur in various locations along the

White River particularly along the river bends of the study area from Batesville (RM 299.00) to the confluence with the Lower Mississippi River (RM 0.00). Since natural rivers are essentially both open channel hydraulic and dynamic systems in equilibrium, various hydraulic and geomorphic parameters can affect their planform, longitudinal profile, and cross-sections. Questions central to this research revolve around the contribution of hydraulic and geomorphic parameters to the planform, longitudinal profile, cross-sections, and overall stability of the White River.

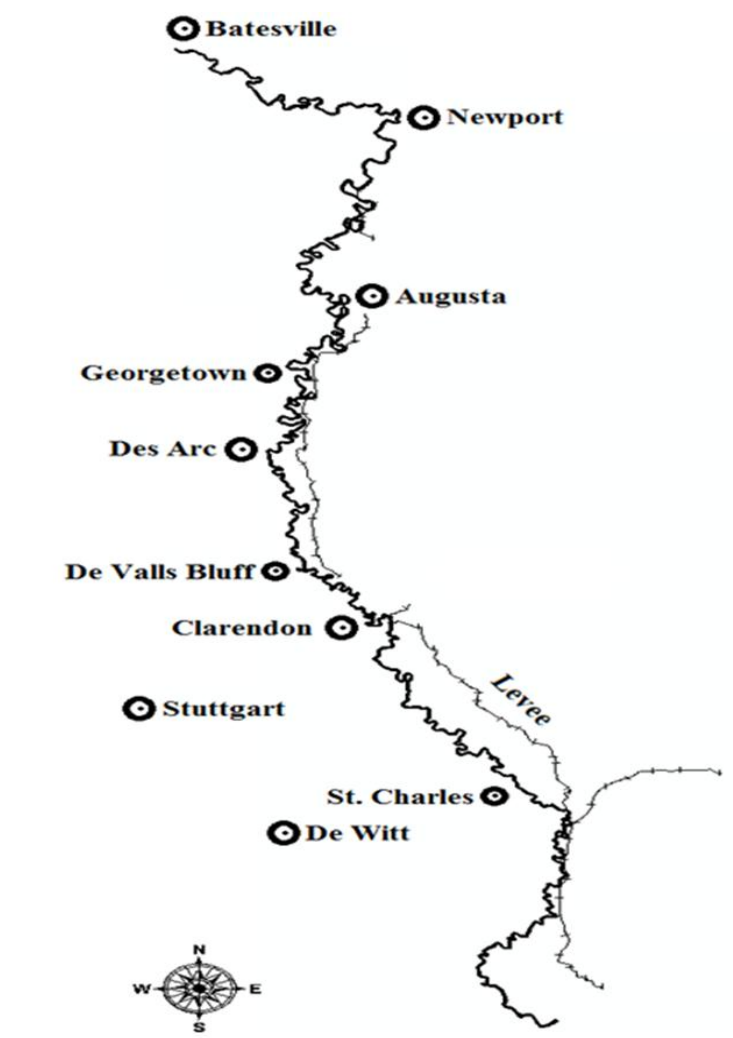


Figure 1.1. Planform of the Lower White River.

Objectives of the Thesis

The research conducted for this investigation amasses to four objectives: (1) To determine the fluvial geomorphology parameters responsible for excessive meandering/shifting along the White River, (2) to provide the geologic processes that shaped the patterns of the White River and the way its tributaries amalgamated to its main stem, (3) to determine whether the river is in dynamic equilibrium/disequilibrium in sections exhibiting excessive meandering/shifting phenomena, and (4) to provide a stream restoration solution to diminish tortuosity ratio while simultaneously helping to bring about a new dynamic equilibrium to sections in disequilibrium.

To ensure that all objectives are met, the geomorphic approach for river classification utilizing the Rosgen Stream Classification (RSC) system, classical fluvial geomorphology techniques, Pfankuch's Channel Stability Evaluation Method, and various sediment analysis methods will be implemented with the aids of ArcGIS, a HEC-RAS Model, and field data.

Organization of the Thesis

This chapter is intended to provide essential background information that serve as the basic building block for this thesis. The information presented herewith include the stratigraphy and physiography, the drainage basin/sub-basins landscape and land use, the floodplain type, the river biodiversity and ecology, the human urbanization impacts, and the intrinsic characteristics of the hydrology of the White River and its tributaries. The next chapter will introduce important fundamental hydraulics and geomorphology parameters and the correlations between the parameters that are often cited in the literature as factors contributing to the appearance and behavior of various rivers around

the world. Chapter 3 will present general procedures outlining the creation of the HEC-RAS Model as well as the procedures for determining and calculating various parameters through applications of the HEC-RAS Model and ArcGIS. Chapter 4 will present the various levels of the Rosgen Stream Classification (RSC) and its application to the White River. Chapter 5 will cover sediment analyses conducted for the reaches of the White River. Chapter 6 will present the results obtained from this study and provide a solution to help diminish lateral migrations and to stabilize section(s) in dynamic disequilibrium. Chapter 7 will summarize the conclusions of the entire thesis. The Appendices will contain field data results, sediment load computations, procedures for drainage delineation and soil data mark extraction, and large plots illustrating the entire planform and profile of the White River.

Stratigraphy and Physiography

The stratigraphy of Arkansas in a broad generalization can be described as consisting of alternating layers of sand, silt and clay underlain by poorly graded sand extending to the Tertiary suberathem. The superstratum soils vary from 5 to 25 feet in thickness while the substratum sands vary at depths ranging from 60 to 150 feet. The sands are Pleistocene at the Quaternary suberathem and Eocene at the Tertiary suberathem.

Closer inspection, with an awareness that landform tends to vary with regions, reveals that Arkansas is divided into five physiographic regions; the Ozark Plateaus, the Arkansas Valley, the Ouachita Mountains, the West Gulf Coastal Plain, and the Mississippi Alluvial Plain.

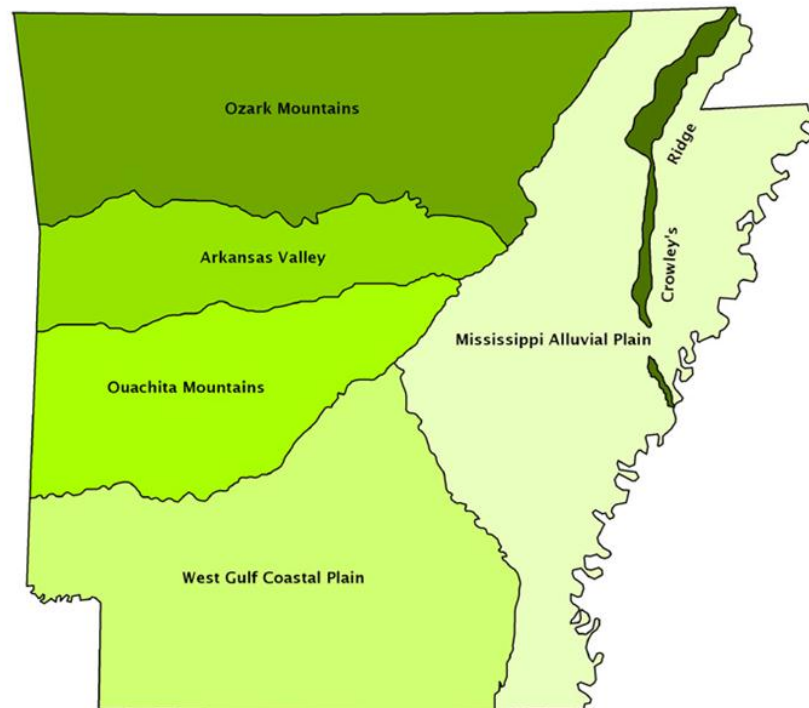


Figure 1.2. Physiographic Regions of Arkansas. From “Map of Arkansas’ six major natural geographic divisions,” by David Reed, 2011, <http://www.encyclopediaofarkansas.net/encyclopedia/media-detail.aspx?mediaID=6333>. Copyright 2011 by The Central Arkansas Library System.

The White River cuts primarily through the Ozark Plateaus at the headwaters and midreaches (from its source in the Boston Mountains to Batesville) and the Mississippi Alluvial Plain at the tailwaters and lower reaches (from Batesville to the Lower Mississippi River). The Mississippi Alluvial Plain stratigraphy consists mainly of alluvium or alluvial deposits at the Holocene epoch, followed by alternating layers of sand, silt, and clay consisting specifically of terrace deposits, dune sand, silt and sand, Aeolian loess, and sand and gravel at the Pleistocene epoch, both of which fall within the Quaternary suberathem. The subsequent Tertiary suberathem consists of sands, silts, and clays of the Jackson, Claiborne, and Wilcox Groups that make up the Eocene epoch

and the expansive clays of the Midway Group that makes up the Paleocene epoch. The Ozark Plateaus stratigraphy consists mainly of alluvial and terrace deposits at the Holocene and Pleistocene epochs of the Quaternary suberathem, sands and clays of uncertain affinities and cretaceous rocks of the Cretaceous suberathem, silty shales and sandstones at the Atokan and Morrowan epochs of the Pennsylvanian suberathem, shales and sandstones and limestones of the Mississippian, Devonian, and Silurian suberathems, and finally limestone, dolostone, and sandstone of the Ordovician suberathem. The stratigraphy of the Mississippi Alluvial Plain and Ozark Plateaus are illustrated in **Table 1.1**.

The surface soil texture in the vicinity of the White River consists primarily of loam which has a composition of approximately 40% silt, 40% sand, and 20% clay according to the USDA Soil Triangle. Loam and clay loam dominate the Ozark Plateaus while silt loam dominates the Mississippi Alluvial Plain. The soils in the Ozark Plateaus generally exhibit low infiltration and drainage rates and are less capable of absorbing high rainfall and snowmelt rates. The soils in the Mississippi Alluvial Plain exhibit high infiltration and drainage rates and are moderately capable of absorbing high rainfall and snowmelt rates. Both the Ozark Plateaus and the Mississippi Alluvial Plain exhibit moderately high soil depth to bedrock ranging from 150 to greater than 200 centimeters. For a specialized classification of the surface soils, please refer to the USDA Soil Triangle (**Figure 1.3**), the U.S. Soil Map (**Figure 1.4**), and the extracted NRCS-NCGC's SSURGO Soil Data Mart in **Appendix F**.

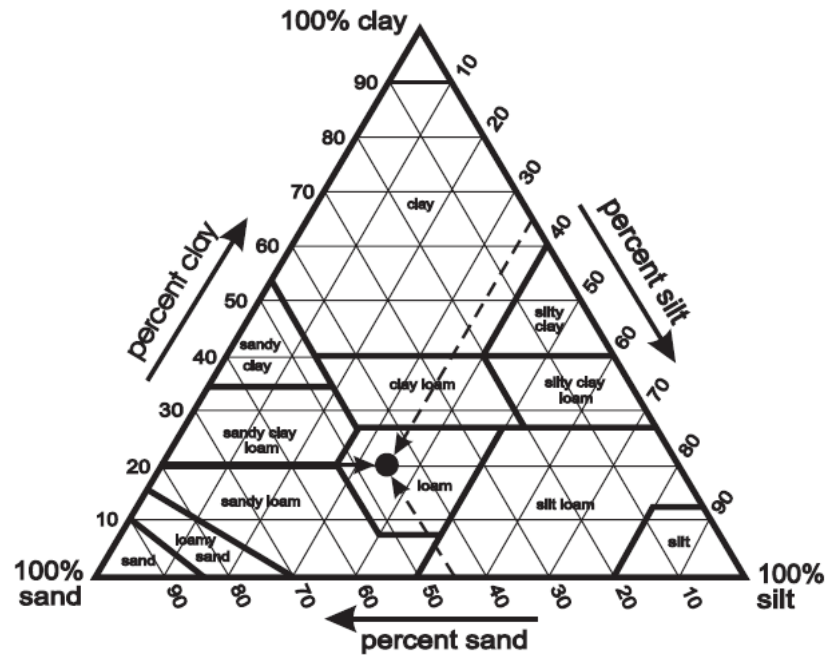


Figure 1.3. Textural Triangle Illustrating USDA Soil Classifications (USDA, Soil Survey Staff, 1951).

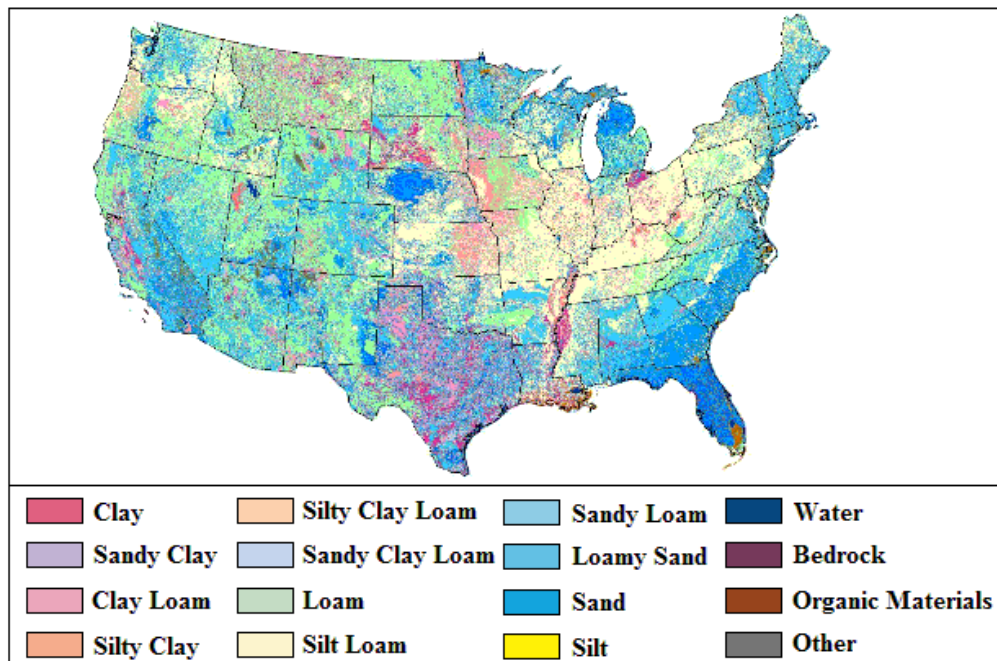


Figure 1.4. U.S. Soil Texture Classification Map. From “U.S. Soil Texture Classification Map”, by USDA/UCAR The COMET Program, http://www.meted.ucar.edu/hydro/basic/Runoff/print_version/04-soilproperties.htm. Copyright 2006 by University Corporation for Atmospheric Research.

Table 1.1. Stratigraphy of the Mississippi Alluvial Plain and the Ozark Plateaus.

MISSISSIPPI RIVER ALLUVIAL PLAIN			OZARK PLATEAUS						
ERA/ERATHM	SUBERA/SUBERATHM	EPOCH/SERIES	STRATIGRAPHIC UNIT		ERA/ERATHM	SUBERA/SUBERATHM	EPOCH/SERIES	STRATIGRAPHIC UNIT	
CENAZOIC (0-60 million yrs)	QUATERNARY	Holocene	Alluvium	PALAEZOIC (240-490 million years)	QUATERNARY	TERTIARY	Hobocene and Pleistocene	Alluvium and terrace deposits	
			Terrace deposits						
			Dune sand						
			Silt and sand						
			Loess						
	TERTIARY	Eocene	Sand and Gravel		PENNSYLVANIAN	CRETACEOUS	Atokan	Morrowan	Bloyd Shale, and Prairie Grove Member of the Hale Formation Cane Hill Member of the Hale Formation Piskin Limestone, Fayetteville Shale, and Batesville Sandstone Ruddell Shale
			Jackson Group						
			Claborne Group						
			Wilcox Group						
			Midway Group						
MESOZOIC (60-240 million years)	QUATERNARY	Holocene	Alluvium	PALAEZOIC (240-490 million years)	QUATERNARY	TERTIARY	Hobocene and Pleistocene	Alluvium and terrace deposits	
			Terrace deposits						
			Dune sand						
			Silt and sand						
			Loess						
	TERTIARY	Eocene	Sand and Gravel		PENNSYLVANIAN	CRETACEOUS	Atokan	Morrowan	Bloyd Shale, and Prairie Grove Member of the Hale Formation Cane Hill Member of the Hale Formation Piskin Limestone, Fayetteville Shale, and Batesville Sandstone Ruddell Shale
			Jackson Group						
			Claborne Group						
			Wilcox Group						
			Midway Group						
PALAEZOIC (240-490 million years)	QUATERNARY	Holocene	Alluvium	PALAEZOIC (240-490 million years)	QUATERNARY	TERTIARY	Hobocene and Pleistocene	Alluvium and terrace deposits	
			Terrace deposits						
			Dune sand						
			Silt and sand						
			Loess						
	TERTIARY	Eocene	Sand and Gravel		PENNSYLVANIAN	CRETACEOUS	Atokan	Morrowan	Bloyd Shale, and Prairie Grove Member of the Hale Formation Cane Hill Member of the Hale Formation Piskin Limestone, Fayetteville Shale, and Batesville Sandstone Ruddell Shale
			Jackson Group						
			Claborne Group						
			Wilcox Group						
			Midway Group						
MESOZOIC (60-240 million years)	QUATERNARY	Holocene	Alluvium	PALAEZOIC (240-490 million years)	QUATERNARY	TERTIARY	Hobocene and Pleistocene	Alluvium and terrace deposits	
			Terrace deposits						
			Dune sand						
			Silt and sand						
			Loess						
	TERTIARY	Eocene	Sand and Gravel		PENNSYLVANIAN	CRETACEOUS	Atokan	Morrowan	Bloyd Shale, and Prairie Grove Member of the Hale Formation Cane Hill Member of the Hale Formation Piskin Limestone, Fayetteville Shale, and Batesville Sandstone Ruddell Shale
			Jackson Group						
			Claborne Group						
			Wilcox Group						
			Midway Group						
PALAEZOIC (240-490 million years)	QUATERNARY	Holocene	Alluvium	PALAEZOIC (240-490 million years)	QUATERNARY	TERTIARY	Hobocene and Pleistocene	Alluvium and terrace deposits	
			Terrace deposits						
			Dune sand						
			Silt and sand						
			Loess						
	TERTIARY	Eocene	Sand and Gravel		PENNSYLVANIAN	CRETACEOUS	Atokan	Morrowan	Bloyd Shale, and Prairie Grove Member of the Hale Formation Cane Hill Member of the Hale Formation Piskin Limestone, Fayetteville Shale, and Batesville Sandstone Ruddell Shale
			Jackson Group						
			Claborne Group						
			Wilcox Group						
			Midway Group						
CENAZOIC (0-60 million yrs)	QUATERNARY	Holocene	Alluvium	PALAEZOIC (240-490 million years)	QUATERNARY	TERTIARY	Hobocene and Pleistocene	Alluvium and terrace deposits	
			Terrace deposits						
			Dune sand						
			Silt and sand						
			Loess						
	TERTIARY	Eocene	Sand and Gravel		PENNSYLVANIAN	CRETACEOUS	Atokan	Morrowan	Bloyd Shale, and Prairie Grove Member of the Hale Formation Cane Hill Member of the Hale Formation Piskin Limestone, Fayetteville Shale, and Batesville Sandstone Ruddell Shale
			Jackson Group						
			Claborne Group						
			Wilcox Group						
			Midway Group						
MESOZOIC (60-240 million years)	QUATERNARY	Holocene	Alluvium	PALAEZOIC (240-490 million years)	QUATERNARY	TERTIARY	Hobocene and Pleistocene	Alluvium and terrace deposits	
			Terrace deposits						
			Dune sand						
			Silt and sand						
			Loess						
	TERTIARY	Eocene	Sand and Gravel		PENNSYLVANIAN	CRETACEOUS	Atokan	Morrowan	Bloyd Shale, and Prairie Grove Member of the Hale Formation Cane Hill Member of the Hale Formation Piskin Limestone, Fayetteville Shale, and Batesville Sandstone Ruddell Shale
			Jackson Group						
			Claborne Group						
			Wilcox Group						
			Midway Group						
PALAEZOIC (240-490 million years)	QUATERNARY	Holocene	Alluvium	PALAEZOIC (240-490 million years)	QUATERNARY	TERTIARY	Hobocene and Pleistocene	Alluvium and terrace deposits	
			Terrace deposits						
			Dune sand						
			Silt and sand						
			Loess						
	TERTIARY	Eocene	Sand and Gravel		PENNSYLVANIAN	CRETACEOUS	Atokan	Morrowan	Bloyd Shale, and Prairie Grove Member of the Hale Formation Cane Hill Member of the Hale Formation Piskin Limestone, Fayetteville Shale, and Batesville Sandstone Ruddell Shale
			Jackson Group						
			Claborne Group						
			Wilcox Group						
			Midway Group						
CENAZOIC (0-60 million yrs)	QUATERNARY	Holocene	Alluvium	PALAEZOIC (240-490 million years)	QUATERNARY	TERTIARY	Hobocene and Pleistocene	Alluvium and terrace deposits	
			Terrace deposits						
			Dune sand						
			Silt and sand						
			Loess						
	TERTIARY	Eocene	Sand and Gravel		PENNSYLVANIAN	CRETACEOUS	Atokan	Morrowan	Bloyd Shale, and Prairie Grove Member of the Hale Formation Cane Hill Member of the Hale Formation Piskin Limestone, Fayetteville Shale, and Batesville Sandstone Ruddell Shale
			Jackson Group						
			Claborne Group						
			Wilcox Group						
			Midway Group						
PALAEZOIC (240-490 million years)	QUATERNARY	Holocene	Alluvium	PALAEZOIC (240-490 million years)	QUATERNARY	TERTIARY	Hobocene and Pleistocene	Alluvium and terrace deposits	
			Terrace deposits						
			Dune sand						
			Silt and sand						
			Loess						
	TERTIARY	Eocene	Sand and Gravel		PENNSYLVANIAN	CRETACEOUS	Atokan	Morrowan	Bloyd Shale, and Prairie Grove Member of the Hale Formation Cane Hill Member of the Hale Formation Piskin Limestone, Fayetteville Shale, and Batesville Sandstone Ruddell Shale
			Jackson Group						
			Claborne Group						
			Wilcox Group						
			Midway Group						
CENAZOIC (0-60 million yrs)	QUATERNARY	Holocene	Alluvium	PALAEZOIC (240-490 million years)	QUATERNARY	TERTIARY	Hobocene and Pleistocene	Alluvium and terrace deposits	
			Terrace deposits						
			Dune sand						
			Silt and sand						
			Loess						
	TERTIARY	Eocene	Sand and Gravel		PENNSYLVANIAN	CRETACEOUS	Atokan	Morrowan	Bloyd Shale, and Prairie Grove Member of the Hale Formation Cane Hill Member of the Hale Formation Piskin Limestone, Fayetteville Shale, and Batesville Sandstone Ruddell Shale
			Jackson Group						
			Claborne Group						
			Wilcox Group						
			Midway Group						
PALAEZOIC (240-490 million years)	QUATERNARY	Holocene	Alluvium	PALAEZOIC (240-490 million years)	QUATERNARY	TERTIARY	Hobocene and Pleistocene	Alluvium and terrace deposits	
			Terrace deposits						
			Dune sand						
			Silt and sand						
			Loess						
	TERTIARY	Eocene	Sand and Gravel		PENNSYLVANIAN	CRETACEOUS	Atokan	Morrowan	Bloyd Shale, and Prairie Grove Member of the Hale Formation Cane Hill Member of the Hale Formation Piskin Limestone, Fayetteville Shale, and Batesville Sandstone Ruddell Shale
			Jackson Group						
			Claborne Group						
			Wilcox Group						
			Midway Group						
CENAZOIC (0-60 million yrs)	QUATERNARY	Holocene	Alluvium	PALAEZOIC (240-490 million years)	QUATERNARY	TERTIARY	Hobocene and Pleistocene	Alluvium and terrace deposits	
			Terrace deposits						
			Dune sand						
			Silt and sand						
			Loess						
	TERTIARY	Eocene	Sand and Gravel		PENNSYLVANIAN	CRETACEOUS	Atokan	Morrowan	Bloyd Shale, and Prairie Grove Member of the Hale Formation Cane Hill Member of the Hale Formation Piskin Limestone, Fayetteville Shale, and Batesville Sandstone Ruddell Shale
			Jackson Group						
			Claborne Group						
			Wilcox Group						
			Midway Group						
PALAEZOIC (240-490 million years)	QUATERNARY	Holocene	Alluvium	PALAEZOIC (240-490 million years)	QUATERNARY	TERTIARY	Hobocene and Pleistocene	Alluvium and terrace deposits	
			Terrace deposits						
			Dune sand						
			Silt and sand						
			Loess						
	TERTIARY	Eocene	Sand and Gravel		PENNSYLVANIAN	CRETACEOUS	Atokan	Morrowan	Bloyd Shale, and Prairie Grove Member of the Hale Formation Cane Hill Member of the Hale Formation Piskin Limestone, Fayetteville Shale, and Batesville Sandstone Ruddell Shale
			Jackson Group						
			Claborne Group						
			Wilcox Group						
			Midway Group						
CENAZOIC (0-60 million yrs)	QUATERNARY	Holocene	Alluvium	PALAEZOIC (240-490 million years)	QUATERNARY	TERTIARY	Hobocene and Pleistocene	Alluvium and terrace deposits	
			Terrace deposits						
			Dune sand						
			Silt and sand						
			Loess						
	TERTIARY	Eocene	Sand and Gravel		PENNSYLVANIAN	CRETACEOUS	Atokan	Morrowan	Bloyd Shale, and Prairie Grove Member of the Hale Formation Cane Hill Member of the Hale Formation Piskin Limestone, Fayetteville Shale, and Batesville Sandstone Ruddell Shale
			Jackson Group						
			Claborne Group						
			Wilcox Group						
			Midway Group						
PALAEZOIC (240-490 million years)	QUATERNARY	Holocene	Alluvium	PALAEZOIC (240-490 million years)	QUATERNARY	TERTIARY	Hobocene and Pleistocene	Alluvium and terrace deposits	
			Terrace deposits						
			Dune sand						
			Silt and sand						
			Loess						
	TERTIARY	Eocene	Sand and Gravel		PENNSYLVANIAN	CRETACEOUS	Atokan	Morrowan	Bloyd Shale, and Prairie Grove Member of the Hale Formation Cane Hill Member of the Hale Formation Piskin Limestone, Fayetteville Shale, and Batesville Sandstone Ruddell Shale
			Jackson Group						
			Claborne Group						
			Wilcox Group						
			Midway Group						
CENAZOIC (0-60 million yrs)	QUATERNARY	Holocene	Alluvium	PALAEZOIC (240-490 million years)	QUATERNARY	TERTIARY	Hobocene and Pleistocene	Alluvium and terrace deposits	
			Terrace deposits						
			Dune sand						
			Silt and sand						
			Loess						
	TERTIARY	Eocene	Sand and Gravel		PENNSYLVANIAN	CRETACEOUS	Atokan	Morrowan	Bloyd Shale, and Prairie Grove Member of the Hale Formation Cane Hill Member of the Hale Formation Piskin Limestone, Fayetteville Shale, and Batesville Sandstone Ruddell Shale
			Jackson Group						
			Claborne Group						
			Wilcox Group						
			Midway Group						
PALAEZOIC (240-490 million years)	QUATERNARY	Holocene	Alluvium	PALAEZOIC (240-490 million years)	QUATERNARY	TERTIARY	Hobocene and Pleistocene	Alluvium and terrace deposits	
			Terrace deposits						
			Dune sand						
			Silt and sand						
			Loess						
	TERTIARY	Eocene	Sand and Gravel		PENNSYLVANIAN	CRETACEOUS	Atokan	Morrowan	Bloyd Shale, and Prairie Grove Member of the Hale Formation Cane Hill Member of the Hale Formation Piskin Limestone, Fayetteville Shale, and Batesville Sandstone Ruddell Shale
			Jackson Group						
			Claborne Group						
			Wilcox Group						
			Midway Group						
CENAZOIC (0-60 million yrs)	QUATERNARY	Holocene	Alluvium	PALAEZOIC (240-490 million years)	QUATERNARY	TERTIARY	Hobocene and Pleistocene	Alluvium and terrace deposits	
			Terrace deposits						
			Dune sand						
			Silt and sand						
			Loess						
	TERTIARY	Eocene	Sand and Gravel		PENNSYLVANIAN	CRETACEOUS	Atokan	Morrowan	Bloyd Shale, and Prairie Grove Member of the Hale Formation Cane Hill Member of the Hale Formation Piskin Limestone, Fayetteville Shale, and Batesville Sandstone Ruddell Shale
			Jackson Group						
			Claborne Group						
			Wilcox Group						
			Midway Group						
PALAEZOIC (240-490 million years)	QUATERNARY	Holocene	Alluvium	PALAEZOIC (240-490 million years)	QUATERNARY	TERTIARY	Hobocene and Pleistocene	Alluvium and terrace deposits	
			Terrace deposits						
			Dune sand						
			Silt and sand						
			Loess						
	TERTIARY	Eocene	Sand and Gravel		PENNSYLVANIAN	CRETACEOUS	Atokan	Morrowan	Bloyd Shale, and Prairie Grove Member of the Hale Formation Cane Hill Member of the Hale Formation Piskin Limestone, Fayetteville Shale, and Batesville Sandstone Ruddell Shale
			Jackson Group						
			Claborne Group						
			Wilcox Group						
			Midway Group						
CENAZOIC (0-60 million yrs)	QUATERNARY	Holocene	Alluvium	PALAEZOIC (240-490 million years)	QUATERNARY	TERTIARY	Hobocene and Pleistocene	Alluvium and terrace deposits	
			Terrace deposits						
			Dune sand						
			Silt and sand						
			Loess						
	TERTIARY	Eocene	Sand and Gravel		PENNSYLVANIAN	CRETACEOUS	Atokan	Morrowan	Bloyd Shale, and Prairie Grove Member of the Hale Formation Cane Hill Member of the Hale Formation Piskin Limestone, Fayetteville Shale, and Batesville Sandstone Ruddell Shale
			Jackson Group						
			Claborne Group						
			Wilcox Group						
			Midway Group						
PALAEZOIC (240-490 million years)	QUATERNARY	Holocene	Alluvium	PALAEZOIC (240-490 million years)	QUATERNARY	TERTIARY	Hobocene and Pleistocene	Alluvium and terrace deposits	
			Terrace deposits						
			Dune sand						
			Silt and sand						
			Loess						
	TERTIARY	Eocene	Sand and Gravel		PENNSYLVANIAN	CRETACEOUS	Atokan	Morrowan	Bloyd Shale, and Prairie Grove Member of the Hale Formation Cane Hill Member of the Hale Formation Piskin Limestone, Fayetteville Shale, and Batesville Sandstone Ruddell Shale
			Jackson Group						
			Claborne Group						
			Wilcox Group						
			Midway Group						
CENAZOIC (0-60 million yrs)	QUATERNARY	Holocene	Alluvium	PALAEZOIC (240-490 million years)	QUATERNARY	TERTIARY	Hobocene and Pleistocene	Alluvium and terrace deposits	
			Terrace deposits						
			Dune sand						
			Silt and sand						
			Loess						
	TERTIARY	Eocene	Sand and Gravel		PENNSYLVANIAN	CRETACEOUS	Atokan	Morrowan	Bloyd Shale, and Prairie Grove Member of the Hale Formation Cane Hill Member of the Hale Formation Piskin Limestone, Fayetteville Shale, and Batesville Sandstone Ruddell Shale
			Jackson Group						
			Claborne Group						
			Wilcox Group						
			Midway Group						
PALAEZOIC (240-490 million years)	QUATERNARY	Holocene	Alluvium	PALAEZOIC (240-490 million years)	QUATERNARY	TERTIARY	Hobocene and Pleistocene	Alluvium and terrace deposits	
			Terrace deposits						
			Dune sand						
			Silt and sand						
			Loess						
	TERTIARY	Eocene	Sand and Gravel		PENNSYLVANIAN	CRETACEOUS	Atokan	Morrowan	Bloyd Shale, and Prairie Grove Member of the Hale Formation Cane Hill Member of the Hale Formation Piskin Limestone, Fayetteville Shale, and Batesville Sandstone Ruddell Shale
			Jackson Group						
			Claborne Group						
			Wilcox Group						
			Midway Group						
CENAZOIC (0-60 million yrs)	QUATERNARY	Holocene	Alluvium	PALAEZOIC (240-490 million years)	QUATERNARY	TERTIARY	Hobocene and Pleistocene	Alluvium and terrace deposits	
			Terrace deposits						
			Dune sand						
			Silt and sand						
			Loess						
	TERTIARY	Eocene	Sand and Gravel		PENNSYLVANIAN	CRETACEOUS	Atokan	Morrowan	Bloyd Shale, and Prairie Grove Member of the Hale Formation Cane Hill Member of the Hale Formation Piskin Limestone, Fayetteville Shale, and Batesville Sandstone Ruddell Shale
			Jackson Group						
			Claborne Group						
			Wilcox Group						
			Midway Group						
PALAEZOIC (240-490 million years)	QUATERNARY	Holocene	Alluvium	PALAEZOIC (240-490 million years)	QUATERNARY	TERTIARY	Hobocene and Pleistocene	Alluvium and terrace deposits	
			Terrace deposits						
			Dune sand						
			Silt and sand						
			Loess						
	TERTIARY	Eocene	Sand and Gravel		PENNSYLVANIAN	CRETACEOUS	Atokan	Morrowan	Bloyd Shale, and Prairie Grove Member of the Hale Formation Cane Hill Member of the Hale Formation Piskin Limestone, Fayetteville Shale, and Batesville Sandstone Ruddell Shale
			Jackson Group						
			Claborne Group						
			Wilcox Group						
			Midway Group						
CENAZOIC (0-60 million yrs)	QUATERNARY	Holocene	Alluvium	PALAEZOIC (240-490 million years)	QUATERNARY	TERTIARY	Hobocene and Pleistocene	Alluvium and terrace deposits	
			Terrace deposits						
			Dune sand						
			Silt and sand						
			Loess						
	TERTIARY	Eocene	Sand and Gravel		PENNSYLVANIAN	CRETACEOUS	Atokan	Morrowan	Bloyd Shale, and Prairie Grove Member of the Hale Formation Cane Hill Member of the Hale Formation Piskin Limestone, Fayetteville Shale, and Batesville Sandstone Ruddell Shale
			Jackson Group						
			Claborne Group						
			Wilcox Group						
			Midway Group						
PALAEZOIC (240-490 million years)	QUATERNARY	Holocene	Alluvium	PALAEZOIC (240-490 million years)	QUATERNARY	TERTIARY	Hobocene and Pleistocene	Alluvium and terrace deposits	
			Terrace deposits						
			Dune sand						
			Silt and sand						
			Loess						
	TERTIARY	Eocene	Sand and Gravel		PENNSYLVANIAN	CRETACEOUS	Atokan	Morrowan	Bloyd Shale, and Prairie Grove Member of the Hale Formation Cane Hill Member of the Hale Formation Piskin Limestone, Fayetteville Shale, and Batesville Sandstone Ruddell Shale
			Jackson Group						
			Claborne Group						
			Wilcox Group						
			Midway Group						
CENAZOIC (0-60 million yrs)	QUATERNARY	Holocene	Alluvium	PALAEZOIC (240-490 million years)	QUATERNARY	TERTIARY	Hobocene and Pleistocene	Alluvium and terrace deposits	
			Terrace deposits						
			Dune sand						
			Silt and sand						
			Loess						
	TERTIARY	Eocene	Sand and Gravel		PENNSYLVANIAN	CRETACEOUS	Atokan	Morrowan	Bloyd Shale, and Prairie Grove Member of the Hale Formation Cane Hill Member of the Hale Formation Piskin Limestone, Fayetteville Shale, and Batesville Sandstone Ruddell Shale
			Jackson Group						
			Claborne Group						
			Wilcox Group						
			Midway Group						
PALAEZOIC (240-490 million years)	QUATERNARY	Holocene	Alluvium	PALAEZOIC (240-490 million years)	QUATERNARY	TERTIARY	Hobocene and Pleistocene	Alluvium and terrace deposits	
			Terrace deposits						
			Dune sand						
			Silt and sand						
			Loess						
	TERTIARY	Eocene	Sand and Gravel		PENNSYLVANIAN	CRETACEOUS	Atokan	Morrowan	Bloyd Shale, and Prairie Grove Member of the Hale Formation Cane Hill Member of the Hale Formation Piskin Limestone, Fayetteville Shale, and Batesville Sandstone Ruddell Shale
			Jackson Group						
			Claborne Group						
			Wilcox Group						
			Midway Group						
CENAZOIC (0-60 million yrs)	QUATERNARY	Holocene	Alluvium	PALAEZOIC (240-490 million years)	QUATERNARY	TERTIARY	Hobocene and Pleistocene	Alluvium and terrace deposits	
			Terrace deposits						
			Dune sand						
			Silt and sand						
			Loess						
	TERTIARY	Eocene	Sand and Gravel		PENNSYLVANIAN	CRETACEOUS	Atokan	Morrowan	Bloyd Shale, and Prairie Grove Member of the Hale Formation Cane Hill Member of the Hale Formation Piskin Limestone, Fayetteville Shale, and Batesville Sandstone Ruddell Shale
			Jackson Group						
			Claborne Group						
			Wilcox Group						
			Midway Group						
PALAEZOIC (240-490 million years)	QUATERNARY	Holocene	Alluvium	PALAEZOIC (240-490 million years)	QUATERNARY	TERTIARY	Hobocene and Pleistocene	Alluvium and terrace deposits	
			Terrace deposits						
			Dune sand						
			Silt and sand						
			Loess						
	TERTIARY	Eocene	Sand and Gravel		PENNSYLVANIAN	CRETACEOUS	Atokan	Morrowan	Bloyd Shale, and Prairie Grove Member of the Hale Formation Cane Hill Member of the Hale Formation Piskin Limestone, Fayetteville Shale, and Batesville Sandstone Ruddell Shale
			Jackson Group						
			Claborne Group						
			Wilcox Group						
			Midway Group						
CENAZOIC (0-60 million yrs)	QUATERNARY	Holocene	Alluvium	PALAEZOIC (240-490 million years)	QUATERNARY	TERTIARY	Hobocene and Pleistocene	Alluvium and terrace deposits	
			Terrace deposits						
			Dune sand						
			Silt and sand						
			Loess						
	TERTIARY	Eocene	Sand and Gravel		PENNSYLVANIAN	CRETACEOUS	Atokan	Morrowan	Bloyd Shale, and Prairie Grove Member of the Hale Formation Cane Hill Member of the Hale Formation Piskin Limestone, Fayetteville Shale, and Batesville Sandstone Ruddell Shale
			Jackson Group						
			Claborne Group						
			Wilcox Group						
			Midway Group						
PALAEZOIC (240-490 million years)	QUATERNARY	Holocene	Alluvium	PALAEZOIC (240-490 million years)	QUATERNARY	TERTIARY	Hobocene and Pleistocene	Alluvium and terrace deposits	
			Terrace deposits						
			Dune sand						
			Silt and sand						
			Loess						
	TERTIARY	Eocene	Sand and Gravel		PENNSYLVANIAN	CRETACEOUS	Atokan	Morrowan	Bloyd Shale, and Prairie Grove Member

Drainage Basin/Sub-basins Landscape and Land-use

The White River drainage basin covers an area of approximately 27870 square miles, of which 11684 square miles occupy northern Arkansas. The Arkansas State Water Plan separates the White River Basin into the Upper White River Basin, the area that covers the Ozark Plateaus physiographic region, and the Lower White River Basin, the area that covers the Mississippi Alluvial Plain physiographic region. The Upper White River Basin in the northern part of the Ozark Plateaus physiographic region makes up the Central Mixed U.S. Hardwood Forest terrestrial ecoregion, which has for the most part remained forested as its soils are too thin for row-crop agriculture production. The southern portion of the upper basin which makes up the Ozark Mountain Forest terrestrial ecoregion has for the most part been cleared of its diverse riparian vegetation and planted with fescue, a nonnative pasture grass of importance for agricultural land and livestock (A. Brown, K. Brown, Jackson, & Pierson, 2005). The Lower White River Basin in the Mississippi Alluvial Plain physiographic province contains the Mississippi Lowland Forests terrestrial ecoregion, which has also been cleared of its natural forests for agricultural crop production (Ricketts et al., 1999).

Landuse in the Mississippi Alluvial Plain area is dominated by row-crop production of cotton, soybeans, and rice while silviculture and cattle production is characteristic of the upper basin in the Ozark Plateaus area. Landuse in the upper and middle region consists of 28% agriculture (excluding silviculture), 70% forest, and 1% urban. Landuse in the lower region consists distinctively as 83% agriculture (excluding silviculture), 8% forest, and 1% urban (Brown et al., 2005).

Agriculture diversions constitute approximately 90% of out-of-stream water use

in the Lower White River Basin, of which 14% of water withdrawn comes from surface water and 86% from groundwater sources. The amounts diverted from Jackson, White, Woodruff, Prairie, Monroe, and Arkansas counties are 981 million, 690 million, 171 million, 1.6 billion, 298 million, and 4 billion gallons, respectively (Arkansas Soil and Water Conservation Commission [ASWCC], 2000).

The White River Basin is made up of nine sub-basins, of which the Cache River sub-basin and the Black River sub-basin are notable. The long and narrow Cache River sub-basin covers about 2300 square miles of flat alluvial deposits of silt, clay, and sand. The natural vegetation of the basin consists of cypress-tupelo gum swamps and lowland forests abundant in oaks, hickories, ashes, and willows. The Black River sub-basin covers an area of 8520 square miles in Arkansas and Missouri, nearly 30% of the total White River Basin, and consists of natural vegetation characteristics of both the Ozark Plateaus and Mississippi Alluvial Plain provinces.

There are eight sub-basins of importance in the proximity of the White River. Each sub-basin has been numbered sequentially for ease of reference as indicated by **Figure 1.6**. The area Digital Elevation Models (DEMs) for the drainage areas are obtained from the U.S. Environmental Protection Agency website and are extracted and delineated via ArcGIS. The maximum length and width are also measured for each sub-basin. The slopes for the sub-basins are determined through a simple procedure that includes creating a point shapefile, placing points along the longest length of each sub-basin, extracting raster elevation values to the point shapefile through the *Spatial Analyst's Extraction* tool, calculating the distance between each elevation point, plotting elevation versus distance, and finally estimating the numerical value of the slope through

linear regression. The values of length, width, area, and slope for each sub-basin are tabulated in **Table 1.2**.

The area through which the White River crossed sub-basin I consists mostly of tiny creeks and waterways. The Lower Mississippi River extends directly along the right boundary of this sub-basin. A very tortuous Big Creek also extends from near the vertex of sub-basin I and continues into sub-basin II. Upstream, the Bayou Deview traverses across sub-basins I and II and heads, from the northeast direction along the lower boundary of sub-basin III (the Cache River sub-basin), into the White River. The Cache River, running along the center of sub-basin III, merges with the Bayou Deview in the proximity of the northeast boundary of sub-basin I. As the White River crossed sub-basin IV, an area consisting of many oxbow lakes not far from the limit of the meander belt width, it encounters one of its major tributaries in the Little Red River, which runs northwest well into sub-basin V. As the White River heads north, it goes back into sub-basin III for a span of about 24,000 feet and continues into sub-basin VI, where it eventually meets the Black River near the intersection of the borders of sub-basins VI,

Table 1.2. Dimensions of Eight Drainage Sub-basins in the Vicinity of the White River.

<u>Sub-basin</u>	<u>Area</u> (sq miles)	<u>Max Length</u> (ft)	<u>Max Width</u> (ft)	<u>Valley Slope</u>
1	1684.85	373491	147057	0.0002
2	1143	305279	183197	0.0002
3	2298.35	773106	125756	0.0002
4	1357.95	325347	215210	0.0005
5	2115.76	471000	171261	0.0023
6	981.02	444179	130143	0.0002
7	1785.12	428387	202400	0.0013
8	1086.52	324637	125142	0.0025

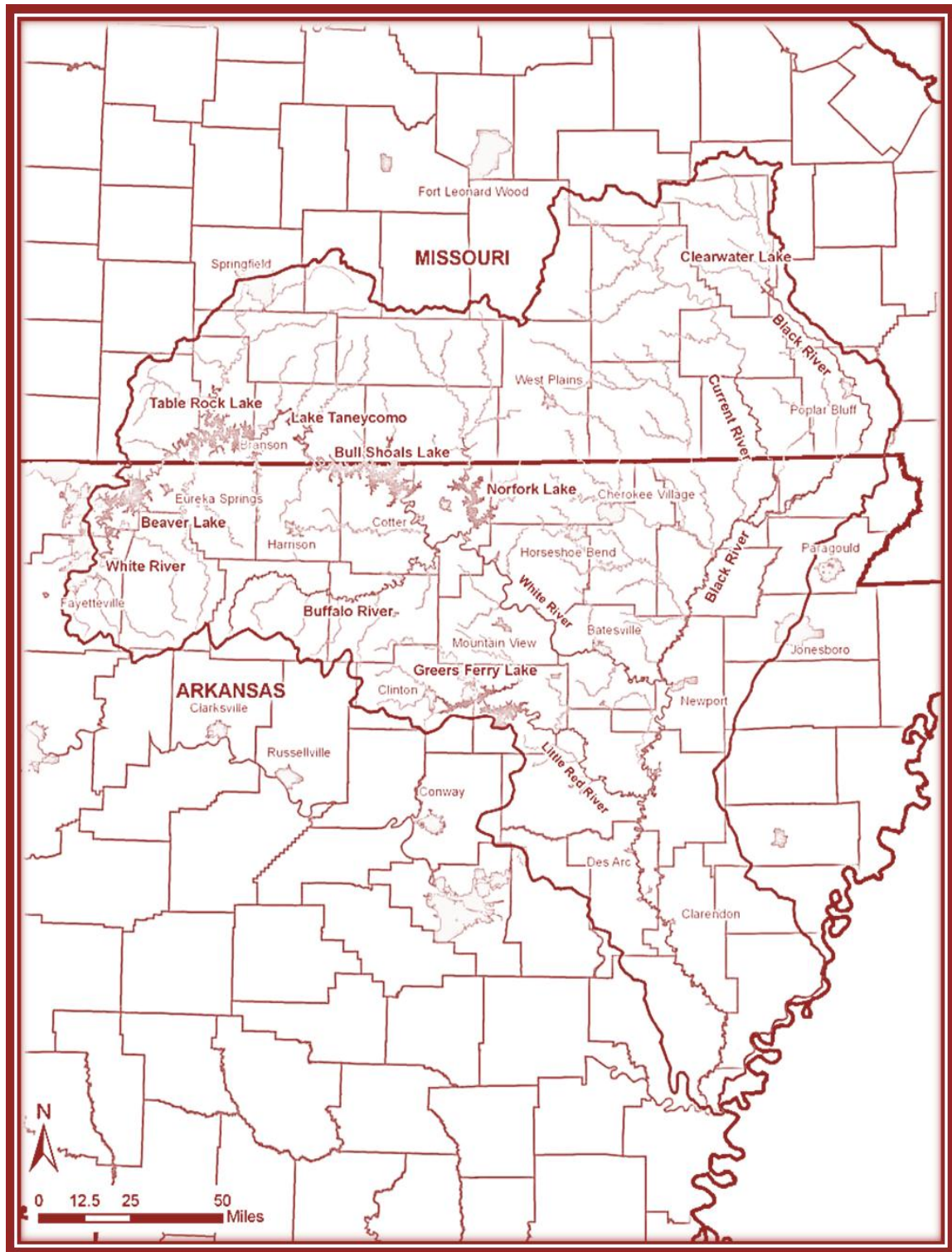


Figure 1.5. The White River Basin (U.S. Army Corps of Engineers, 2009).

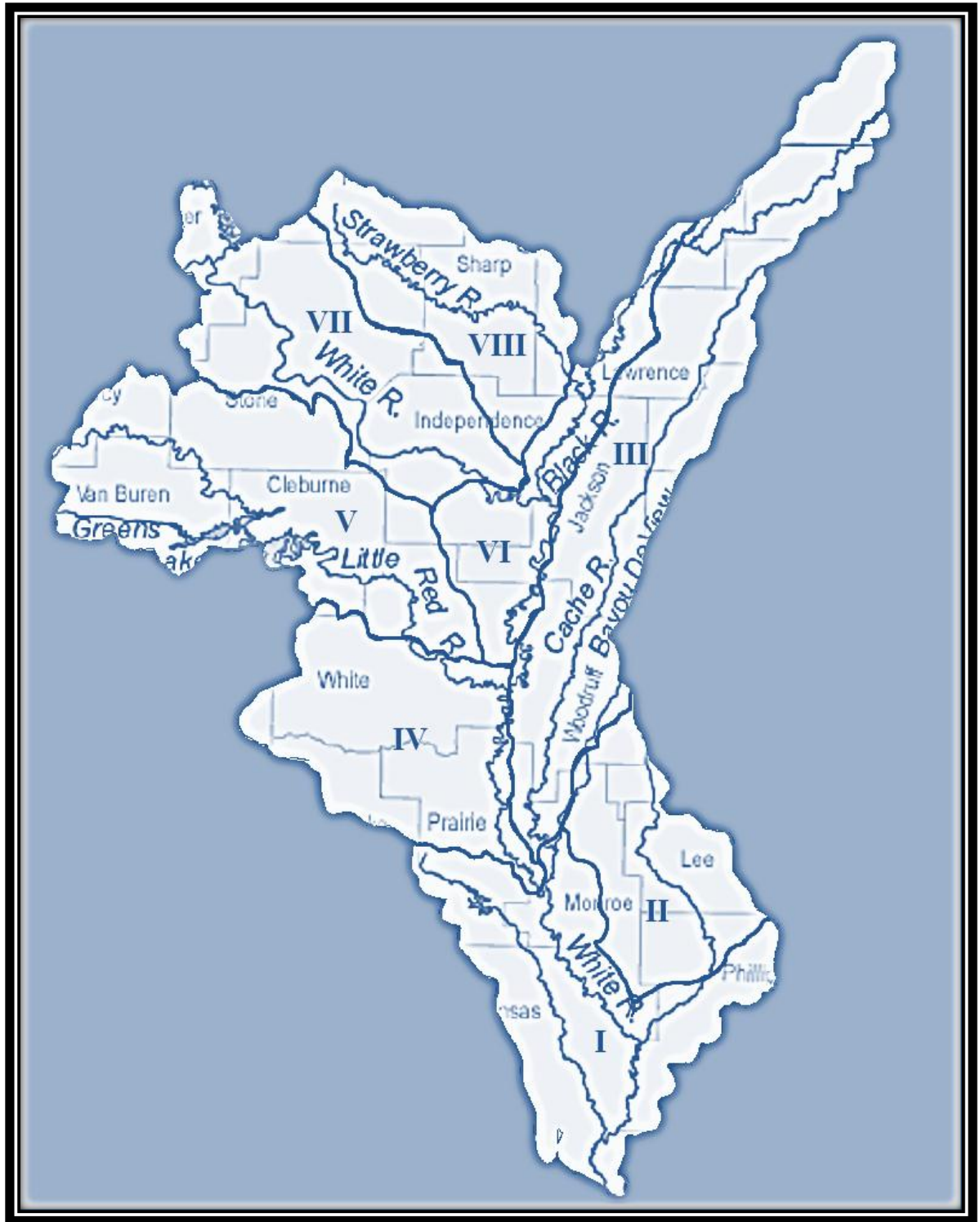


Figure 1.6. Lower White River Drainage Sub-basins and Tributaries.

VII, and VIII. The river then heads northwest into sub-basin VII. It should also be noted that the elevations and slopes in sub-basins I, II, III, and VI are low compared to other sub-basins because these sub-basins are in the vicinity of the Mississippi Alluvial Plain.

Floodplain Classification

Hydrologists and engineers often defined a floodplain as “the surface next to the channel that is inundated once during a given return period” (U. S. Army Corps of Engineers Hydrologic Engineering Center, 1976, as cited in Nanson & Croke, 1992, p. 460). This terminology, however, is broad and ambiguous since it does not take in account the geomorphic history and fluvial processes that shaped the floodplain. To provide an accurate classification of floodplain, a more specialize floodplain definition “the largely horizontally-bedded alluvial landform adjacent to a channel, separated from the channel by banks, and built of sediment transported by the present flow-regime” (Nanson & Croke, 1992, p. 460) is adopted.

Although the genesis of floodplains often involved multifarious interactions between fluvial processes, their evolution and character can be adequately described by unit stream power, the stream’s ability to entrain and transport sediment, and sediment characteristic (Nanson & Croke, 1992). These two geomorphic parameters formed the basis for an energy-based genetic classification system proposed by Nanson and Croke. The classification of the White River floodplain relies exclusively on this system in part due to the availability of stream power from the HEC-RAS Model as well as the soil distribution from the Soil Data Mart. However, it should be noted that specific sedimentary data within the White River’s channel are not readily available and that the soil distribution extracted from the Soil Data Mart is merely a representation of the

depositions that have occurred in the past or are expected to occur during high-magnitude, low-frequency inundations. The deduction that the Soil Data Mart could possibly epitomize the sedimentary characteristics within the White River's channel relies on the knowledge that its floodplain lies within an alluvial plain, specifically the Mississippi Alluvial Plain, which is often created over time through sediment erosions and depositions as indicated by the floodplain definition defined previously.

Utilizing the classification system proposed by Nanson and Croke, the White River floodplain is classified as a low-energy cohesive floodplain of order C1, which is a flat laterally stable floodplain abundant in silts and clays from overbank accretions. An overall conclusion that the White River is stable should not be made from the previous statement considering that in reality fluvial systems rarely fall neatly into a category, and that all classification systems are “[anthro]-contrivances or simplifications of reality” (Nanson & Croke, 1992, p. 465).

River Biodiversity and Ecology

“The White River Basin occurs in two freshwater ecoregions, the Ozark [Plateaus] and the Mississippi [Alluvial Plain]” (Abell et al., 2000, as cited in Brown et al., 2005). Information regarding the biological communities and ecological relationships are much more voluminous and are better apprehended for the Ozark Plateaus regions than for the Mississippi Alluvial Plain although the levels and patterns of production of biota are at best partially known or understood. However, the energetic interactions of the faunas, especially among invertebrates and fishes, have been more thoroughly studied.

Little is known about the algae and cyanobacteria of the White River although studies of streams from the same ecoregion have implied that a diverse array of

periphytic diatoms may occur in the winter to early spring. Planktons, a rarity in the the White River, are only found in pools in the third and fifth order reaches. Plankton and periphyton in the lower reaches of the White River are expected to be scarce due to frequent fluctuation of the water levels and turbid (as with suspended sediment) water conditions.

The floras of the native riparian forests in the Upper White River Basin regions consist primarily of stands of hardwoods dominated by various species of oaks and hickories. Flowering dogwoods, eastern red cedars, red maples, sassafras, mulberries, sugarberries, and shortleaf pines also exist in the regions along with major riparian plants such as willows, witchhazels, American sycamores, river birches, buttonbushes, cottonwoods, green ashes, box elders, sweetgums, hackberries, and many others.

Adjacent floodplain forests of the Lower White River Basin are dominated by bald cypress and water tupelo and are also abundant in oaks, hickories, and ashes. A diverse array of clambering and herbaceous plants such as cucumber vines, wild grapes, poison ivies, greenbriers, trumpet creepers, and cat's claws also colonize the riverbanks and stream margins along with hardwoods such as willows, cottonwoods, river birches, red maples, witchhazels, sycamores, and buttonbushes. The faunas of the White River's ecoregions consist of various species of invertebrates and vertebrates. Invertebrates common to the White River's ecoregions include crayfish, bivalves, mussels, mayflies, caddisflies, chironomid midges, beetles, dragonflies, damselflies, and oligochaete worms. The diversity and abundance of crayfish and bivalves is one distinctive characteristic of the White River invertebrate assemblage. Vertebrates common to the White River's ecoregions include various species of fish, amphibians and reptiles, and mammals. The

most abundant fish found in the White River are mimic shiner, emerald shiner, channel catfish, blue catfish, western sand darter, bluegill, spotted bass, bullhead minnow, white crappie, and Mississippi silvery minnow. Amphibians and reptiles such as western cottonmouths, water snakes, softshell turtles, alligator snapping turtles, stinkpot turtles, map turtles, false map turtles, bullfrogs, greenfrogs, pickerel frogs, and southern leopard frogs are common. Mammals detected along the entire length of the White River includes raccoons, minks, river otters, muskrats, and beavers.

The complexity in the ecological interactions and bioenergetics pathways in the ecoregions of the White River are attributable to the diversity and abundance of flora and fauna species, and to the physical and chemical environments. The high P/R ratios ($P/R > 1$), of the gross production to total community respiration, of the White River suggest that its ecosystem is classified as autotrophic, meaning that its “energy is [furnished] through instream photosynthesis” (Allan & Castillo, 2007, p. 308), and its ecosystem supported primarily by autochthonous production. Little else is known about the ecology of the White River except that it is a highly productive system, judging from the diversity and abundance of “plant, invertebrate, and vertebrate animal species assemblages” that it sustains (Brown et al., 2005, p. 249). The dynamic, movement, distribution, and interactions of the biota are influenced by the size, flow regime, depth, substrate composition, and disturbances (Brown & Brussock, 1991; Doisy, Rabeni, & Galat, 1997; Peterson & Rabeni, 2001). Disturbances such as gravel mining seem to have altered the ecological functioning of gravel-bed streams in the Ozark Plateaus physiographic region (A. Brown, Lyttle, & K. Brown, 1998; Rabeni, 2000; Zweifel, Hayward, & Rabeni, 1999).

Table 1.3. A Classification of Floodplains (Nanson & Croke, 1992).

Order/Suborder	Floodplain Type	Specific Stream Power, ω [W/m ²]	Sediment	Erosional and depositional processes	Landforms	Channel planform	Environment	References
Class A: High-Energy Non Cohesive Floodplains ($\omega > 300$ W/m²). Disequilibrium floodplains which erode in response to extreme events, typically located in steep headwater areas where channel migration is prevented by valley confinement.								
A1	Confined coarse-textured floodplains	> 1000	Poorly sorted boulders and gravels; buried soils	Catastrophic floodplain erosion and overbank vertical accretion; abandoned-channel accretion; minor lateral accretion	Boulder levees; sand and gravel splays; back channels abandoned channels and scour holes	Single-thread straight/irregular	Steep upland headwater valleys	Stewart and Lamarche (1967)*; Baker (1977)*
A2	Confined vertical accretion floodplains	300-1000	Basal gravels and abundant sand with silty overburden	Catastrophic floodplain erosion and overbank vertical accretion	Large levees and deep back channels and scour holes	Single-thread straight/irregular	Upland headwater valleys	Nanson (1986)*; Croke (1991)*
A3	Unconfined vertical accretion sandy floodplains	300-600	Sandy-strata inter-bedded muds	Catastrophic channel widening; overbank vertical accretion; island deposition and abandoned-channel accretion. Minor lateral accretion	Flat floodplain surface	Single-thread wandering	Semi-arid open valleys	Schumm and Lichty (1963)*; Burkham (1972)*
A4	Cut and fill floodplains	app. 300	Sand, silts and organics	Catastrophic gullying; overbank vertical accretion; abandoned-channel accretion	Flat floodplain surface; channel fills; swampy meadows	Straight/irregular	Upland dells and semi-arid alluvial-filled valleys	Graf (1983a, 1983b); Young (1986)*; Prosser (1988)*
Class B: Medium-Energy Non-Cohesive Floodplains ($\omega = 10-300$ W/m²). Equilibrium floodplains formed by regular flow-events in relatively unconfined valleys.								
B1	Braided-river floodplains	50-300	Gravels, sand and occasional silt	Braided-channel accretion and incision; overbank vertical accretion; minor lateral and abandoned-channel accretion	Undulating floodplain of abandoned channels and bars; backswamps	Braided	Abundant sediment load in tectonically and/or glacially active areas	Doeglas (1962); Fahnstock (1963)*; William and Rust (1969)*; Ferguson (1981)*; Carson (1984); Brierley and Hickin (1991)
B2	Wandering gravel-bed river floodplains	30-200(?)	Gravels, sands, silts and organics	As for braided and meandering rivers	Abandoned channels; sloughs; braidbars; islands; back channels	Braided, meandering and anastomosing	Abundant sediment load; alternating sedimentation zones in tectonically and/or glacially active areas	Church (1983); Desloges and Church (1987); Brierley and Hicin (1991)
B3	Meandering river, lateral migration floodplains	10-60	Gravels, sands and silts	Cut-bank erosion; lateral point bar accretion; overbank vertical and abandoned-channel accretion. Counterpoint accretion; minor oblique accretion	Flat to undulating floodplain surface; oxbows; backswamps	Meandering	Usually middle to lower valley reaches	Sundborg (1956); Wolman and Leopold (1957); Jackson (1976); Nanson (1980); Ferguson (1981)*; Hickin and Nanson (1984)*
B3a	Lateral migration, non-scrolled floodplains	ditto	ditto	ditto	ditto	ditto	ditto	ditto
B3b	Lateral migration, scrolled-floodplains	ditto	sands and minor gravels	As for B3 with scroll-bar formation	Distinctly scrolled floodplains	ditto	ditto	Jackson (1976); Nanson (1980)
B3c	Lateral migration/back swamp flood-plains	ditto	Sands, silts and organics	As for B3b	Central scrolled floodplain with flanking backswamps	ditto	ditto	Fisk (1947); Speight (1965); Blake and Ollier (1971); Woodroffe et al. (1989)
B3d	Lateral migration, counterpoint floodplains	ditto	Sands with abundant silts and organics	As B3 with pronounced counterpoint accretion	Concave benches with scrolled floodplains	Confined meandering	ditto	Hickin (1979); Lewin (1983); Nanson and Page (1983)
Class C Low-Energy Cohesive Floodplains ($\omega \leq 10$ W/m²). Floodplains formed by regular flow-events along laterally stable single-thread or anastomosing low-gradient channels.								
C1	Laterally stable, single-channel floodplains	< 10	Abundant silts and clays with organics	Overbank vertical accretion	Flat floodplains with low levees; backswamps	Single-thread straight/meandering	Abundant fine sediment load middle-lower reaches	Beckinsale and Richardson (1964); Nanson and Young (1981)*; Brown (1983); Croke (1991)*
C2	Anastomosing-river floodplains	ditto	Gravel and sands with abundant silts and clays	Overbank vertical accretion; island deposition	Flat floodplains with extensive levees, islands and floodplains crevasse-channels and splays	Anastomosing	Very low gradient with wide floodplains	Smith and Smith (1980); Rust (1981); Smith (1983); Nanson et al. (1986); Smith. pers com. (1990)*
C2a	Anastomosing-river, organic rich floodplains	ditto	As for C2 with abundant organics and lacustrine deposits	As for C2 with peat formation, and lacustrine sedimentation	As for C2 with lakes and peat swamps	ditto	As for C2 in humid environments	Smith and Smith (1980); Smith (1983)
C2b	Anastomosing-river, inorganic floodplains	ditto	As for C2 but with little or no organics	As for C2	As for C2	Anastomosing channels and coexisting floodplain-surface braid channels	As for C2 in semi-arid environments	Nanson et al. (1986); Rust and Nanson (1986)

*Specific stream-power estimated from data in these papers.

Human Impacts

The Upper White River on the fourth and fifth order reaches are characterized by numerous impoundments created for the purposes of flood control and generation of hydroelectric power for the region. The upper White River Projects include Beaver, Table Rock, Taneycomo, and Bull Shoals Lakes on its main stem and Norfolk, Clearwater, and Greers Ferry Lakes on its tributaries the North Fork, the Little Black, and the Little Red, respectively. These projects, managing approximately 48% of the White River's total drainage area, have metamorphosed its ecological characteristics from a continuous system to a discontinuous system, thus resetting the river continuum and making the tailwater reaches similar to the headwater reaches in some aspects (Ward & Stanford, 1983). In addition, it has been documented that the hypolimnetic water released from the reservoirs have altered the temperature cycles both daily and annually, and may have contributed to a substantial decrease in endemic invertebrates and vertebrates such as mollusks and pallid sturgeons. The low dissolved oxygen concentrations in reservoir-released hypolimnetic water have also been documented to be responsible for fish kills and as a result chronic impacts on fish species, which may contribute to the decline in their harvests in the last 80 years, are suspected (Brown et al., 2005).

In contrast to the Upper White River, the flat terrain of the Lower White River below Newport prohibits the construction of reservoirs. The 250-mile-long Lower White River extending from Newport to the Lower Mississippi River, however, is "dredged and snagged to maintain [an 8-foot] deep" (Brown et al., 2005, p. 251) channel (90% of the time) that facilitates barge traffic. Currently, the USACE is planning to deepen this channel to 9 feet to expand navigational capacity and to facilitate passage of

larger barges. Dredging at the inflection points of meanders where the thalwegs vacillate is employed to maintain the mandated depth. Negative impacts of dredging include the introduction of sediments to the channel, resuspension of contaminants embedded and absorbed by the sediments particles, and the induction of plumes of turbidity downstream. Implementing the proposal to increase vertical depth of the White River by one foot would lower its water levels and leads to ecological alteration or diminishment in flood pulse rhythm; an ecological process that yields lateral energy inputs for the rivers that inundate their floodplains. During inundation, nutrients from the river are dissipated to its floodplain where communities of secondary and primary producers expend to produce organic materials that the aquatic hordes and terrestrial consumers used, resulting in high productions. “Internal cycles of organic material and correlated nutrient among terrestrial and aquatic phases result in the accumulation [of nutrients] in the floodplain [which] makes the system [function at] at a [higher] tropic level” (Junk, 1999, as cited in Kawakami, 2004, p. 283). During the annual flood pulse, the lateral exchanges between the White River and its floodplain as well as the terrestrial and aquatic phases make substantial contributions to the production (and diversity) of the river-floodplain biota (Allen & Castillo, 2007). Diminishment in the flood pulse rhythm of the White River would reduce and devastate floodplain habitats available for aquatic species (Buchanan, 1997; Chordas & Harp, 1991; Gordon, Chordas, Harp, & Brown, 1995; Wright, 2000).

Levees adjacent to the White River from Augusta to the confluence with the Lower Mississippi River may also contribute to alterations in the natural ecological functioning of the White River floodplain as they are the primary features responsible for

abnegating the river access to the floodplain (flood pulse concept), which reduced relative percentages of a variety of habitats available to endemic and nonnative species resulting in diminishment of biota diverseness. Artificial cut-offs, forcing the river to take a shorter path downstream by directing flows across depositional bars or necks of meanders, and revetments have also been implemented to decrease channel meanderings. Revetments of gabions, rocks, logs, tires, fences, and automobile bodies used extensively to stabilize the banks and artificial cutoffs used to straighten, shorten, and deepen channels for navigational purposes as well as subsiding floodwater “have altered the relative percentages of different types of habitat” (Baker, Killgore, & Kasul, 1991, as cited in Brown et al., 2005, p. 235). Constructions of dikes, floodways, and other tributary basin modifications for analogous purposes have also resulted in similar impacts (Baker et al., 1991).

Other activities involving agriculture landuse and agriculture diversion also disrupt the “natural interaction between the river and its riparian zone” and may influence the morphology, function, water quality, and stability of the White River (Thorp & Delong, 1994, as cited in Brown et al., p. 245).

Flow and Sediment Regimes

The White River in the Ozark Plateaus is classified as a crooked, narrow cold-water channel that is structurally controlled. The rapid flow in this reach generates sufficient energy to erode through the bedrock in numerous places. The streambed is composed of gravel, rocks, and boulders while the banks are composed of comparatively stable materials. The White River’s reach from Batesville to Newport, the transition zone from the Ozark Plateaus to the Mississippi Alluvial Plain or the transition zone from cold

to warm water, is classified as a low-gradient, wide and meandering channel with relatively flat bank slopes. The dominant bed material consists of gravel and sand while the banks are composed of unconsolidated, heterogeneous alluvial materials such as sand, silt, and clay. One distinguishable characteristic of this reach is the transparency of the water which signifies that it transports or entrains only a small quantity of sediment. At Newport, near the confluence with the Black River, the White River abruptly changes into a lowland, twisting channel with sluggish flow and turbid water. Stream banks are composed of unconsolidated alluvium while the streambed is prevalently sand. The average longitudinal gradient of the White River is approximately 0.4 feet per mile in the lower valley. The upstream one third of the White River possesses channel widths ranging from 200 to 600 feet with bank heights ranging from 20 to 25 feet while the downstream two thirds possess channel widths ranging from 400 to 800 feet with bank heights ranging from 25 to 30 feet (U.S. Army Corps of Engineers, 2009).

According to Brown et al. (2005), the bed of the channel of the White River portion above Newport is dominated by gravel. At and below Newport, the White River is a sand bed river with an extensively developed floodplain. Due to a lack of channel sedimentary data, verification of their assertion is accomplished by the classical discharge-slope relation introduced by Leopold and Wolman (1957). Although the discharge-slope empirical equation was initially used as a discriminant between braided and meandering river types, extensive analyses by Carson (1984a) and Ferguson (1987) of the Leopold and Wolman's threshold have shown that it is too high for sand bed rivers and too low for gravel bed rivers, or that it overestimates sand bed rivers and underestimates gravel bed rivers. This information, coupled with the fact that slope and

discharge are a product of stream power, indicates that a sand bed river has a tendency to exist where stream power is low, which is a prerequisite for the White River.

The White River sediment load type can best be described as mixed, a combination of both bed-load and suspended-load. The bed-load consists of sand and gravel that is transported, at velocities slower than the river flow, along the bed by sliding, rolling, and saltation. The low flow regime, measured as strength of flow by the Froude Number, suggests an intermittent mechanism of grain motion. This is an implication that a large amount of sediment, mainly sand, is stored in the bed and is migrating slowly downstream over time. The suspended-load consists of silt and clay that is held in suspension by the flow through electrostatic attraction between unfulfilled valence of the grain's surface and the water molecules. The relatively small grain size of silt and clay and the available velocities of the White River via the HEC-RAS Model suggest a continuous mechanism of grain motion.

Tributaries, Drainage Patterns, Climate, and Miscellaneous

The major tributaries of the White River that span proximal to the eight sub-basins include the Big Creek, the Bayou Deview, the Cache River, the Little Red River, and the Black River. The streams or tributaries that developed along the upper portion of the White River exhibit a trellis pattern while the streams along the lower portion of the White River exhibit a dendritic pattern. The dendritic drainage pattern, which resembles the branches of a tree, has a tendency to develop in regions “underlain by flat-lying or uniformly eroded sedimentary rock” (AGS, 2009, p. 23). The trellis pattern has a tendency to occur in regions “where rocks have been folded and bent into long folds and eroded into resistant ridges and valleys” (AGS, 2009, p. 23). Explanations of specific

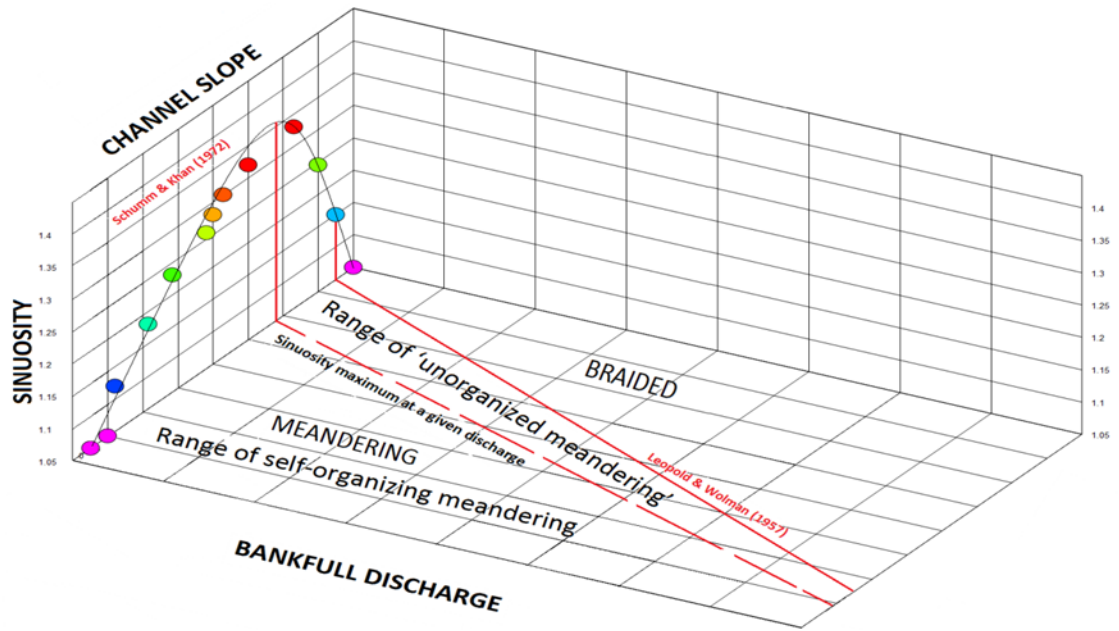


Figure 1.7a. Discharge Versus Slope Discriminant Diagram (after Leopold & Wolman, 1957; Schumm & Khan, 1972).

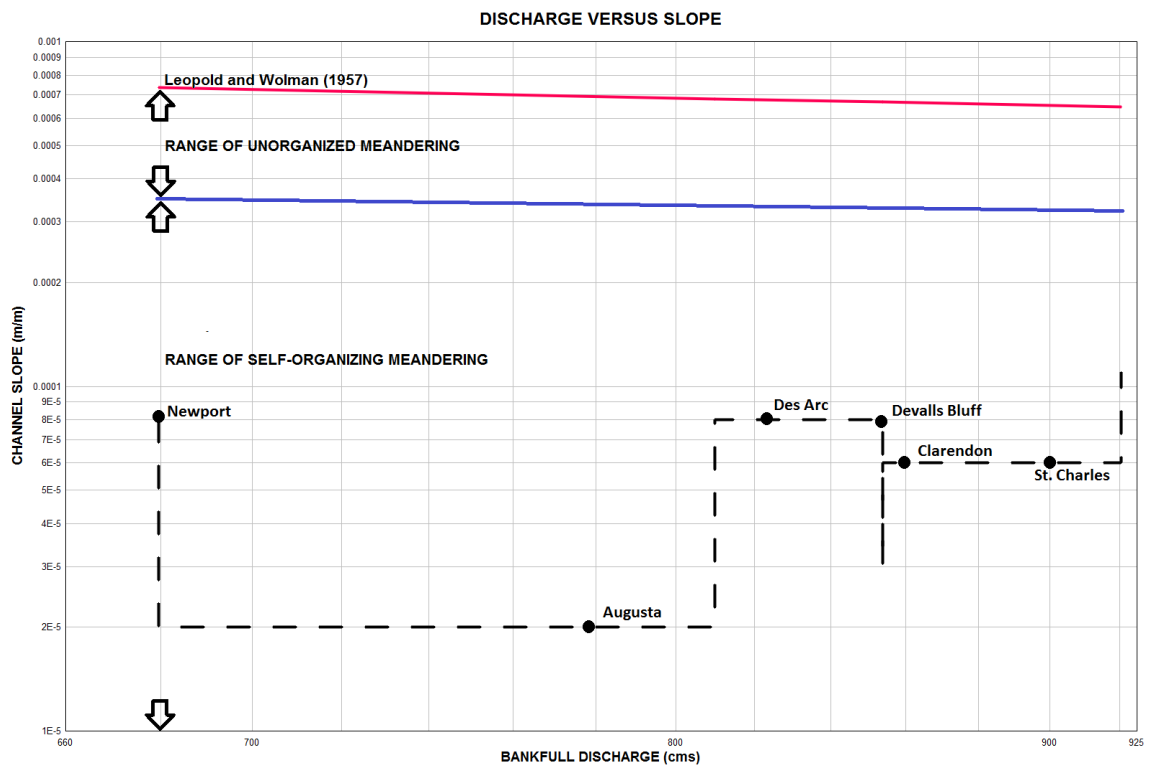


Figure 1.7b. Plot of the Alluvial Sections of the White River on Discharge Versus Slope Discriminant Diagram to Predict Bed-load Materials and Meandering Range.

processes that formulate these drainage patterns will be covered in detail in a subsequent chapter or section.

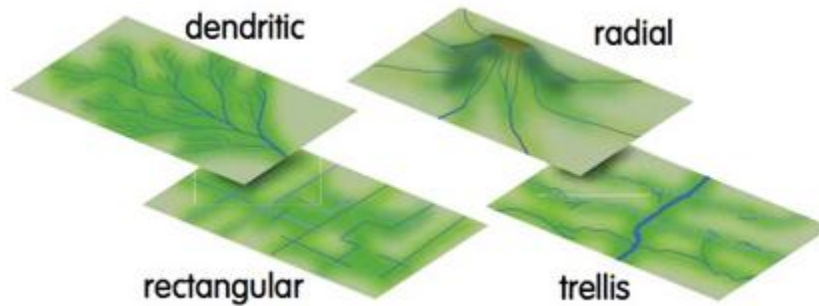


Figure 1.8. Types of Drainage Patterns. From “earthscience_f20”, by Sparknotes,2004, http://sparkcharts.sparknotes.com/gensci/geology_earthsci/section13.php. Copyright 2004 by Sparknotes.

With the exception of the Little Red River and the Black River, the tributaries along the White River all reside within the lowlands. In fact, most of the White River below Newport resides within the lowlands. Precipitation, mainly in the form of rainfall, is approximately 130 centimeters per year for the lowlands and 110 centimeters per year for the highlands. Mean annual temperature is estimated to be close to 16.4 degrees Celsius, with a range of 1 through 16 degrees, for the lowlands and 14 degrees Celsius for the highlands, with a range of 4 through 27 degrees. Mean monthly temperatures are highest for July, approximately 27 degrees Celsius, and lowest for January, around 2 degrees Celsius. Monthly precipitations for the region indicate a peak of 12.6 centimeters in May and a base of 7.4 centimeters in January.

The White River has a mean annual discharge of about 980 cubic meters per second with an annual runoff close to 43 centimeters. Mean monthly runoff tends to

exhibit a seasonal pattern with a peak in March of 5.6 centimeters and a base in September of 1.5 centimeters. In the upper and midreaches of the White River and most of the tributaries in the proximity of the Ozark Plateaus, where there are man-made reservoirs, the water temperatures are cooler than normal in the summer and warmer than normal in the winter due mainly to the mixture with dam-released hypolimnetic water. The average water temperature of the White River is approximate 19 degrees Celsius.

Tributaries such as Big Creek, Bayou Deview, and Cache River that reside within the Mississippi Alluvial Plains have maintained lower slopes and consequently lower stream power than the tributaries proximal to the Ozark Plateaus such as the Black River and the Little Red River. Since the White River and all of its tributaries are substantially wide, Reynolds numbers computed generally fall within the range of turbulent flows.

CHAPTER 2: LITERATURE REVIEW

Introduction

In attempting to determine an appropriate course of action to take in order to evaluate the stability condition of the White River fluvial system and to decipher the contributions of the internal processes that occurred within the channels of its meander bends as they pertain to dynamic stability, an extensive review of existing literature on fluvial geomorphology was conducted. During the literature search, it became apparent that within the area of fluvial geomorphology there existed a multitude of theories and approaches to explicate changes in river meanders and many differing ideas on the definitions of what constituted dynamic stability in rivers, “with sometimes a lack of communication between the proponents of [various] theories and approaches” (Hooke, 2007a, p. 237). This issue prompted questions “as to whether these frameworks and types of explanations [were] mutually exclusive, or whether they [were] compatible, or whether different explanations [applied] in different times and places [and for different situations]” (Hooke, 2007a, p. 237). In addition, many explanations, principles, and theoretical concepts that emerged from the field of fluvial geomorphology, a topic of importance that has yet to reach its pinnacle of expansion into applicable science and seemingly distinguished by scatterings of information and ideas that appeared mutually exclusive or possessed little to no perceivable connections, were considered to some extent impractical from an engineering perspective as few available and detailed guidelines/procedures were formulated to better assess channel planform metamorphoses and to pinpoint specific stimulus (or stimuli) spurring anomalous phenomena in channel form. Conversely, the assemblages of literature materials that were deemed useful and

applicable essentially provided the foundation for the development of a concrete method to assess the stability condition of the White River fluvial system. Since the quantities of literature utilized in the process of identifying and developing effective channel stability evaluation methods are quite voluminous to discuss in detail in this chapter and for this thesis, focus was placed upon three alternatives of channel stability evaluation approaches, namely stability assessment through parametric correlations with the assistance of aerial photographs, quadrangle maps, and a hydraulic model; stability evaluation through the Rosgen Stream Classification System with the assistance of aerial photographs, quadrangle maps, a hydraulic model, and field data/observations; and stability estimation through sediment analyses and sediment-related parametric correlations of data attained from the field and via ArcGIS images and the HEC-RAS Model. In view of this fact, the results of the literature search are presented in the following sections to highlight the background information that led to the three primary channel stability approaches implemented for the White River system and its alluvial reaches. Brief discussions on additional findings in regard to the general correlations between significant constituents, as outlined by the bulks of research papers arising from various proponents in the field of fluvial geomorphology, will also be covered subsequently.

Fluvial Geomorphology

It is evident that, since a multitude of factors was deemed critical to the developments of fluvial systems and since emphasis was placed upon different contributing determinants by different investigators, there existed an extensive network of categories and subcategories (detailing various aspects of or) within the field of fluvial

geomorphology. Examinations of the bulk of research papers and journal articles contributed by various proponents of fluvial geomorphology conveyed a plethora of ideas, concepts, theories, and perspectives that for the most part lacked unity or provided no perceivable connections. This section, however, focused on the similarities prevalent in the literature and highlighted significant and consistent correlations among contributing constituents as adduced by the assemblages of papers collected for this research.

One common similarity that emerged from the early stage of literature review involved the promulgations of the principle of energy expenditure from various sources. According to Harnischmacher (2007), this theory insinuated that a fluvial system with a stream power below a certain critical threshold dissipated excess energy by developing bends and meanders while a fluvial system secernated by a stream power exceeding a certain critical threshold dissipated excess energy by flowing turbulently. The particular mechanism of energy dissipation via water flowing in bends and meanders, as suggested by Kolla, Posamentier, and Wood (2007), is apparently colligated with the formation of corkscrew-like flow patterns known as helicoidal circulations. These helicoidal circulations, that formed synchronously with the emergences of transient and intermittent bedforms (riffles and pools) and non-linear flow proclivities, are responsible for directing rapid flowing water to the concave bank initiating erosion and sluggish water to the convex bank triggering deposition; thus prompting sinuosity enhancements and channel width variations (Harnischmacher, 2007; Hooke, 2008; Kolla et al., 2007). Lagasse, Zevenbergen, Spitz, and Thorne (2004b) in their inspections of roughly 1503 meander bends on 89 U.S. rivers for the purpose of developing “a practical methodology to predict

the rate and extent of channel migration in proximity to transportation facilities” (p. ix) mentioned many references that point to the influences of channel curvature (R_c/W) on helicoidal flow formations and their aftereffects on channel planforms. In *NCHRP Web-Only Document 67 (Project 24-16): Methodology for Predicting Channel Migration*, these investigators suggested that channel curvature values within the interval of 2 to 3 correspond to rapid migrations, channel curvatures greater than 3 correspond to bend growths, and channel curvatures less than 2 correspond to double headings (Lagasse et al., 2004b). The implication that helicoidal circulation was most critical in promoting erosion/deposition was also inferred within this source by the confirmation that maximum bend migrations occur as R_c/W approaches 3, a condition that marks the instance where the river does the least work in turning or when helical flow is at maximum strength (Chang, 1984a, as cited in Lagasse et al., 2004b, p. 14). In addition, the correlation between channel curvature and channel width variation, is also denoted by Luchi, Hooke, Zolezzi, and Bertoldi (2010) in their investigation of the River Bollin. As for the transient and intermittent bedforms encompassing riffles and pools, which formed at the inflection regions and bend apices of meandering bends, respectively, their emergence as cited by Hooke (2007a) was essentially equivalent to energy dissipation in the vertical direction. Research conducted by Hooke (2007a) on meandering rivers also indicated that the spacing and abundance of riffle structures were highly correlated to channel curvature while Hudson’s (2002) investigation on the Lower Mississippi River and Harnischmacher’s (2007) investigation of rivers of varying sizes in Western Germany produced results that greatly asseverated the contributions of curvature and stream power, a product of slope and discharge, on pool depths and spacings,

respectively. In simple and specific terms, Hooke's (2007a) results denoted that the spacings of riffles were smaller and their numbers greater when channel curvature or R_c/W values were low, and vice versa; Hudson's (2002) results confirmed that curvature and pool depth were inversely related, curvature and pool spacing proportional; and Harnischmacher's (2007) results affirmed that pool depth was monotonically proportional to stream power at and below the critical stream power values of approximately 100 W/m^2 and inversely proportional to stream power values greater than 100 W/m^2 .

An alternate and unique common theme arising from these research papers and journal articles revolves around the great emphasis placed upon the role of the longitudinal gradient, the bankfull or dominant discharge, and sediment characteristics in controlling the form, dynamic, and stability condition of fluvial channels. Petts and Foster's (1985) and Van den Berg's (1995) suggestions that bankfull discharges govern channel size, shape, and conveyance of sediment in proximity to the channel bottom, Schumm and Khan's (1972) assertion that the longitudinal gradients control sediment conveyance and flow strength (to some extent), and Hooke's (2008) inference that sediment movements within a channel reflect ongoing adjustments in response to flow and slope variations distinctly corroborated the interdependent relationship existing between these parameters. It is obvious then that the pairing of the longitudinal gradient and discharge as early as the 1950s by Lane (to predict channel planform) possibly prompted the derivation of the highly significant and actively implemented parameter 'stream power', which, according to Lewin and Brewer (2001) and Van den Berg (1995), represents the product of the longitudinal gradient and discharge or simply the ability of

river to do work (i.e., entrain and transport sediment). Since stream power governs sediment texture and load, controls sinuosity to some extent, and serves as a predictor of channel dynamic and susceptibility to form change, this versatile capability in application is the justification as to why stream power is often included in fluvial geomorphology research papers as a complement to discharge, gradient, and sediment characteristics. Specific relationships pertaining to stream power and other parameters included (1) the positively monotonic correlations between stream power and sediment particle grain size as suggested by Nanson and Croke (1992) and Richards (1982), (2) the positively monotonic correlation between stream power and sinuosity below the critical power threshold of 100 W/m^2 , (3) the negatively monotonic correlation between stream power and sinuosity above the critical power threshold of 100 W/m^2 , (4) the monotonically increasing sequence of pool depth and step steepness versus stream power at or below the 100 W/m^2 value, (5) the monotonically decreasing sequence of pool depth and step steepness versus stream power above 100 W/m^2 (Harnischmacher, 2007), and (6) the monotonically proportional relationship between stream power and slope as suggested by many proponents of fluvial geomorphology (Laczay, 1977, due to channelization; Lewin & Brewer, 2001, as concluded from the definition of unit stream power; Nanson & Croke, 1992; Schumm & Khan, 1972, as drawn from results of flume experiments). Given that stream power is equivalently a composite counterpart to discharge, slope, and sediment, its utilization for the classification of floodplains and the determination of planform patterns were visible in the works of Ferguson (1981, 1987), Keller and Brookes (1984), Nanson and Croke (1992), Schumm and Lichty (1963), and Van den Berg (1995). Actual stream power values differentiating straight channels from actively

meandering channels, meandering channels from braided channels, and braided channels from high energy straight channels are shown in **Figure 2.1d**. Actual stream power values discriminating cohesive floodplains from non-cohesive floodplains and other types of floodplains were included in Nanson and Croke (1992) as well as the literary references cited within this source (see **Table 1.3**).

In the case pertaining to sedimentation, sediment characteristics within a fluvial system are characterized by erosion and deposition phenomena, which were previously stated to be driven by thalweg-oscillations-induced helicoidal circulations and flow non-uniformities, and are often linked to width variations to describe the dynamic and condition of a fluvial system (or lack thereof). Many investigators, Hooke being the most recent and persistent advocate, have continuously associated width variations with channel disequilibrium based on the fact that high annual differences between erosion and deposition occurrences have often been observed (over time) to produce outcomes involving channel expansions and constrictions. Hooke (2007a, 2007b, 2008), Kolla et al. (2007), and Van den Berg (1995) together revealed that high differences in erosion and deposition designated low sediment bypassing and high sensitivity to discharge variations, thus stimulating width and lateral developments. It was therefore well established that a channel in a disequilibrium condition (or a laterally active channel) was easily distinguishable from a channel possessing dynamic equilibrium (or a stable channel) in that it exhibited a highly sinuous planform, width constriction at or near bend apices (when deposition is identified as the dominant phenomenon), and width expansion at or proximal to bend apices (when erosion is identified as the dominant activity) (Brice, 1982; Hooke, 2007b; Kolla et al., 2007). Through deduction, constant width as an

indicator of channel condition must represent the equilibrium state when erosion and deposition activities were identical in occurrences and magnitudes. These findings permit a quick and viable predictor of channel dynamic and stability in the inspection for width alterations.

As for the long term evolution of river planform, the theory of equilibrium and adjustment known as Mackin's concept of "graded stream" is often adduced in many of the research papers and journal articles assembled for this research. Central to this concept is the idea of autogenic adjustments in channel form, i.e., width, depth, slope, and particularly planform, to develop an equilibrium configuration that promotes maximum efficiency for the transport of water and sediment load delivered to the channel (Mackin, 1948). This means that on a long time scale on the order of several hundred years, if true equilibrium state is not attained, continuous adjustments, therefore, may cause the river to undergo a series of planform metamorphoses that should greatly alter its patterns. When it comes to specific planform alterations, whether catalyzed by helicoidal circulations, transient bedforms, the propensities for flowing fluid to depart from a straight path, or the simultaneous interactions between these activities, the literature review indicates a general planform metamorphosis progression that begins with a straight channel undergoing meandering and migration, then growth, and finally cut-off(s) (Hooke, 2007b). The planform metamorphosis cycle, also equivalent to the long-term evolution of sinuosity or bend morphology, suggests that the initial departure from a straight course as a mean to dissipate excess flow energy accelerates point bar development or the lateral and vertical accretions of sediment particles, thus encouraging a meandering pattern (Cserkesz-Nagy, Toch, Vajk, & Sztano, 2010; Miall, 1977;

Schumm & Khan, 1972). As point bar development heightens through erosion and deposition of the channel boundaries and bedforms adjust themselves (to provide a roughness consistent with the depth and flow velocity), the river bends undergo migration, translation, and further development. Intensive point bar development, if it persists, then lengthens the river and decreases its gradient resulting in bend growth or a compounded form distinguished by very high sinuosity. Additional planform development finally increases the sinuosity to a maximum critical state of 3.14 at which a clustering of meander cutoffs take place (Stolum, 1996; 1998). These phenomena bring about a significant increase in the longitudinal gradient and a pronounced decrease in sinuosity followed by a period in which sinuosity oscillates (and bed form changes) to maintain equilibrium, and the cycle is repeated when excess energy accumulates (Cserkesz et al., 2010; Stolum, 1996; 1998; Timar, 2003).

During the planform metamorphosis progression, transient and intermittent changes in bedforms (to attain a roughness consistent with the depth and velocity necessary to convey sediment discharge) may range from ripples and less-developed dunes to highly developed dunes, anti-dunes, and flats (Garcia, 2008). Pool and riffle structures also formed in conjunction with these bed features at the inflection regions and apices of meandering bends, respectively.

The classifications of rivers based on planform or sinuosity also parallel the theory of equilibrium and adjustment. Straight (and braided) rivers are characterized with sinuosity values ranging from 1.0 to 1.3, meandering rivers are classified as having sinuosity greater than 1.3, and compounded rivers near chute cut-off are distinguished by sinuosity values ranging from 2 to 3 (Bledsoe & Watson, 2001; Miall, 1977; Van den

Berg, 1995). Other attributes, such as longitudinal gradient range, width to depth ratio range, stream power strength, sediment characteristics, and general channel cross-sectional form, of these common types of rivers are shown in **Figure 2.1b**. Correlations including the inversely related relationship between sinuosity and longitudinal gradient and the monotonically proportional relationship between width to depth ratio and boundary shear stress are also shown in **Figure 2.1b**. Additional findings stemming from various research papers and journal articles are included in **Figures 2.1a** through **2.1e**. The assemblage of literature information represents the foundation for the development of the three channel stability evaluation methodologies that will be covered in the following sections.

Channel Stability Assessment With Parametric Correlations

The inception of the utilization of empirical correlations to describe channel form and patterns began with the period of quantification of the 1950s and 1960s. The formulation of equations and relationships between meander parameters at this stage, when the underlying conceptual framework was marked “by that of equilibrium and [the] assumption of stabilization of natural forms after development” (Hooke, 2007a, p. 237), was intended to justify the conjecture that channel form and patterns of typical, stable fluvial systems developed “naturally [...] to provide for the dissipation of kinetic energy of moving water, and the transportation of sediment” (Rosgen & Silvey, 1996, p. 2-7). Notable empirical correlations encompassing that of discharge and slope by Lane (1957) and Leopold and Wolman (1957), width and wavelength by Leopold and Wolman (1960), and discharge and wavelength by Carlston (1965) and Dury (1965) were implemented as thresholds discriminating meandering patterns from braided patterns, as

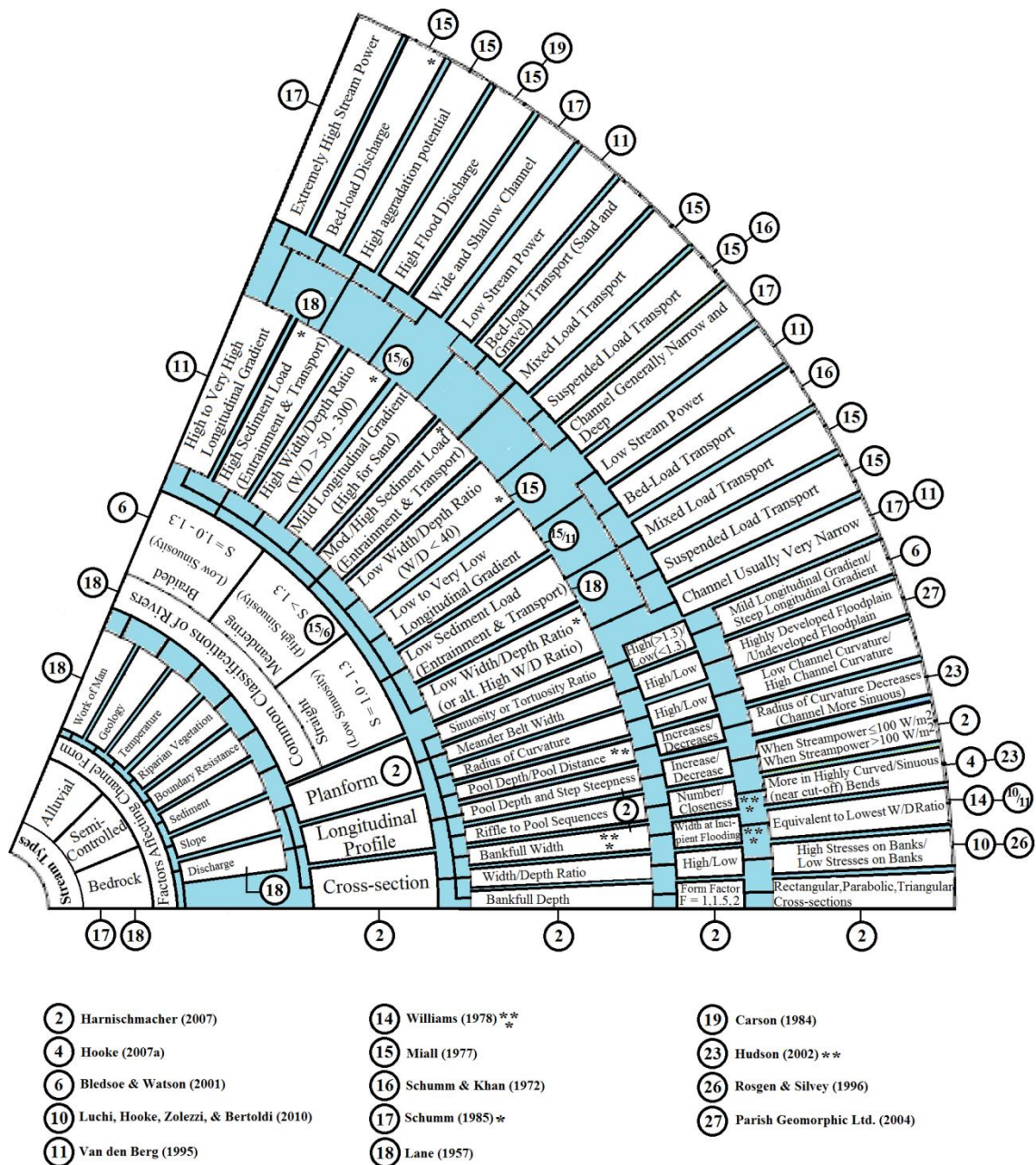


Figure 2.1b. Fluvial Geomorphology Chart II.

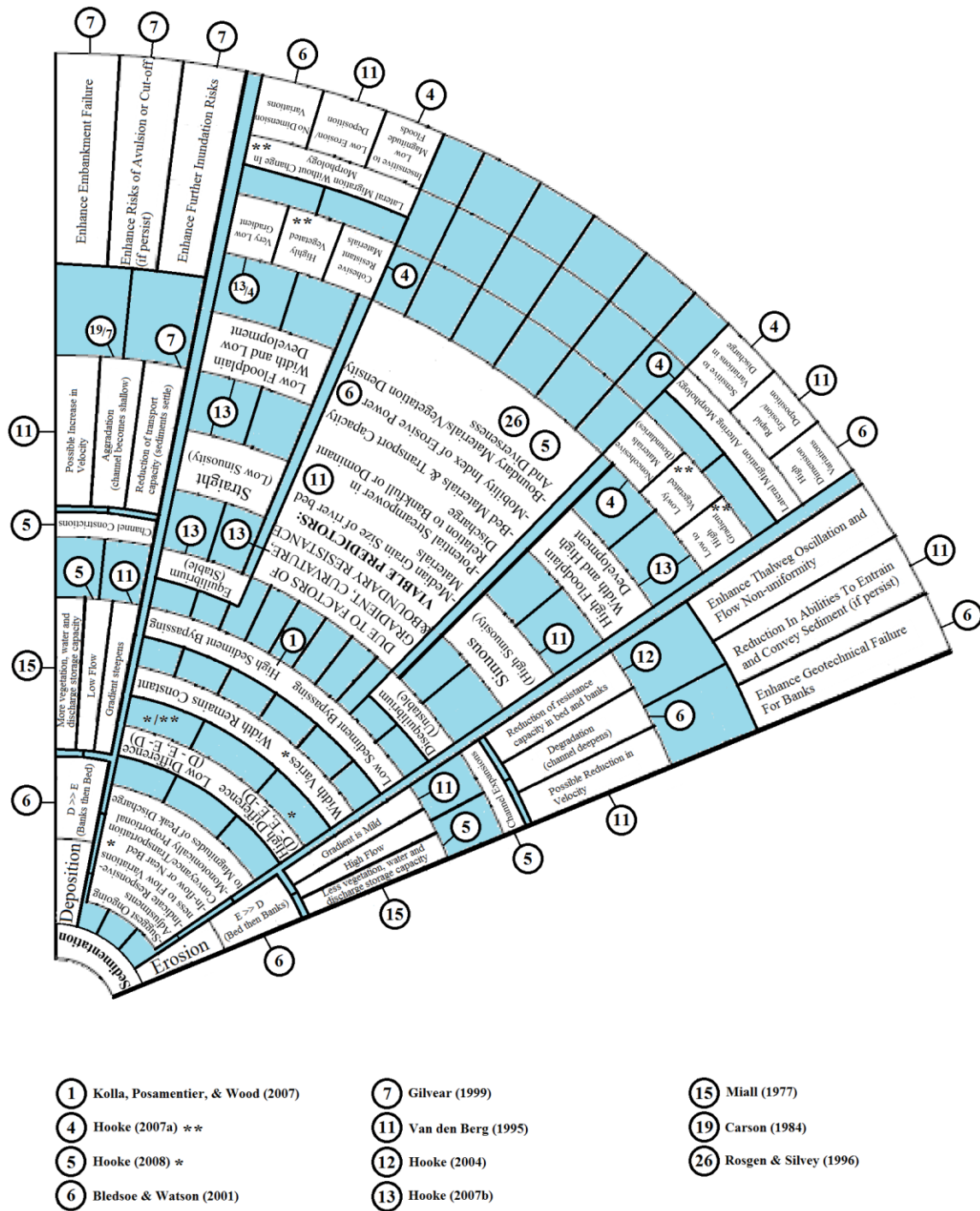


Figure 2.1c. Fluvial Geomorphology Chart III.



meander geometry to describe the configuration of a meandering bend, and as predictors of meander response to discharge variations, respectively. As the quantification period of the 1950s and 1960s concluded, a new phase of empirical work associated with the 1970s and 1980s began. The formulation of numerous empirical correlations between geomorphic, hydrologic, and geologic parameters during this period, when the underlying conceptual framework expanded to include non-linear and non-equilibrium developments (of channel forms and meanders) on historical timescales, not only conveyed ideas of instability and dynamic imbalances in fluvial systems and provided quick assessments for departure from stability for these systems, but also slightly altered the definitions and applications of erstwhile empirical equations to include instability conditions. Empirical functions involving discharge and slope, such as those belonging to Ackers (1964), Ackers and Charlton (1971), Lane (1957), Leopold and Wolman (1957), and Schumm and Khan (1972), still defined the thresholds discriminating straight rivers from meandering rivers and meandering rivers from braided rivers; however, the term straight had become synonymous with stability while meandering and braided had become interchangeable with departure from stability and instability, respectively. Proofs, within the works of Ackers and Charlton (1970a, 1970b), Schumm (1981), and Schumm and Khan (1972), that once a threshold was crossed rapid changes in the shape of the channel pattern followed before a new equilibrium status was attained suggested that the focus (of the use of empirical correlations) had shifted from mere channel form and pattern classifications to simple stability analyses. A multitude of empirical relationships involving the meander wavelength and width and the meander wavelength and discharge that were derived during the quantification period (1950s – 1960s) and during the new era

of empirical work (1970s – 1980s), most notably the equations of Carlston (1965), Dury (1965), Leopold and Wolman (1960), and Richards (1982), also became increasingly popular in stability analyses of meander bends. Proponents of these hydraulic geometry relationships (primarily relationships involving wavelength and width) including Leopold, Richards, Soar, and Thorn proposed that they may be implemented to “indicate stream instability if meander wavelength for a given stream did not plot closely to the predicted [correlations]” (U.S. Department of Agriculture - Natural Resources Conservation Service [USDA-NRCS], 2007, p. 12-5). The consistency of the results attained from various studies of rivers and flumes by various investigators later prompted adoption of a stable meander wavelength range (11.26W to 12.47W) suitable for engineering design (*see USDA-NRCS National Engineering Handbook Part 654, 2007*).

The periods of quantification and expansion in empirical work also spawned a multitude of relationships involving discharge, radius of curvature, channel dimensions (e.g., width, depth, and cross-sectional flow area), sinuosity, W/D ratio, and the dominant bed material. Empirical correlations involving radius of curvature versus other parameters, such as radius of curvature versus discharge by Chang and Toebes (1970, 1980), radius of curvature versus channel dimensions by Williams (1986) (using data of earlier researchers), radius of curvature versus meander length by Leopold, Wolman, and Miller (1964), just to name a few, however, became more prevalent in the literature because they were considered to provide an accurate depiction of meander geometry as well as an appropriate interpretation of channel boundary resistance to flow. For these reasons, the radius of curvature relationships were also “often used to evaluate channel resistance to erosion and bend or migration rates” (Rosgen & Silvey, 1996, p. 2-7), or in

more generalized terms to evaluate the stability condition of a channel or a bend. The proponents of these parametric relationships involving the radius of curvature and other parameters also suggested that they may be employed to indicate the instability condition if the radius of curvature for a given stream deviated from the regression lines of the predicted correlations, or when the regression lines of these parametric relationships for a given stream did not match the trends shown by the predicted correlations.

Other parametric correlations or functions, for example channel slope to Froude number versus width to depth ratio (Parker & Anderson, 1975) or sinuosity ratio versus the ratio of bend apex width to inflection point width (USDA-NRCS, 2007), “may be applied in river engineering projects [and river investigations], provided that the channel dimension width, depth, and channel slope are known in advance” (Van den Berg, 1995, p. 261).

In the case pertaining to the White River (RM 299.00 – RM 0.00), the first part of stability assessment was conducted through parametric correlations of significant hydraulic and geomorphic parameters (much in the same manner as those shown in research papers and journal articles of various aforementioned proponents). The HEC-RAS Model initially provided many static and dynamic hydraulic parameters while other geomorphic parameters were determined with the simultaneous use of aerial photographs, quadrangle maps, and the hydraulic model. Guidance for determining various geomorphic parameters was provided by Leopold (1994), Parish Geomorphic Ltd. (2004), Rosgen (1994), Rosgen and Silvey (1996), etc. Parameters lacking clear guidelines were determined via simultaneous employment of the HEC-RAS Model and ArcGIS (quadrangle maps and aerial photographs) based on the definitions and results

provided by various proponents in their investigations of other fluvial systems.

Assessment of the stability conditions of various segments of the White River through parametric correlations basically involved meticulous inspections of data point(s) that deviated from the created regression lines. During stability assessment, the regression lines (or empirical functions) of parameters arising from this investigation were also compared with the regression lines (or empirical functions) belonging to various proponents of the similarly predicted correlations for anomalous properties or behaviors.

Channel Stability Assessment With The Rosgen Stream Classification System

To comprehend the need for an organized classification of rivers like the Rosgen Stream Classification system, one must look into the literature for previous scientific works that inspired the formulation of such a system. Inspection of the history of river works revealed that the earliest case of the effort to classify streams was presented in Davis (1899), where rivers were separated into classes of young, mature, and old streams. By the early to mid-1900s, the emergence of additional river classification systems, most notably those developed by Melton (1936) and Matthes (1956), based upon qualitative and descriptive delineations became customary. Rivers types were then essentially separated into three classes of straight, meandering, and braided streams by Leopold and Wolman (1957), and were quantitatively discriminated with slope-discharge relationships introduced by Lane (1957). The formulation of these river classification systems also gave way to classification systems (of the 1960s) based on descriptive and interpretative characteristics such as those encompassing Schumm (1963) where delineation was contingent upon stability conditions (i.e., whether the channel is stable, aggrading, or degrading) and mode of sediment transport (i.e, suspended-load, bed-load, and mixed

load), Thornbury (1969) where delineation was based on valley types, and Culbertson, Young, and Brice (1967) where delineation was supported by the utilization and inclusion of elements consisting of planimetric patterns, riparian vegetation, sinuosity, meander scrolls, bank heights, floodplain types, and depositional features (i.e., different types of bars). However, departure from the typical delineative criteria of these earlier stream classification systems, once inconsistencies were identified with the mandated qualitative geomorphic interpretations, was also common, and prompted the development of stream classification systems based primarily on quantitative delineation. An example of such a system was the classification of sand-bed streams by Khan (1971) where delineation was based on planimetric patterns, longitudinal gradients, and sinuosity ratios.

In the 1970s, the popularity of a descriptive classification scheme utilizing both aerial photography delineation and classic delineation techniques yielded a detailed inventory of channel and valley features that accounted for a wide range of stream morphologies. The implementation of this scheme was reflected in the works of Galay, Kellerhals, and Bray (1973), Kellerhals et al. (1972, 1976), and Mollard (1973) on a collection of Canadian rivers, and the independent work of Brice (1974) on over 350 rivers in the continental United States. These works provided the inspiration and data for the development of the highly comprehensive, hierarchically organized Rosgen Stream Classification system.

In view of the fact that the RSC system was developed from morphological measurements of a large collection of rivers throughout the continental United States, Canada, and New Zealand over the course of nearly thirty years (1969 through 1994),

that the hierarchical inventory approach of RSC had been successfully utilized to evaluate rivers in Colorado and other regions of the United States, and that the techniques involved in this classification method were continually tested over many years for improvements, its use in the classification and evaluation of the White River (RM 299.00 – 0.00) was considered appropriate. Details regarding the implementation of RSC for the White River system are elaborated in the following paragraph. Slight modifications made at particular phases are also discussed subsequently.

Evaluating the stability condition of the White River by utilizing the Rosgen Stream Classification (RSC) system mandated following a hierarchical inventory approach based on common characteristics inherent to channel morphology and the assumptions that stream morphology relies upon landscape arrangement (Rosgen & Silvey, 1996). This RSC hierarchical inventory, which consisted of four levels of classifications, included Geomorphic Characterization (Level I), the Morphological Description (Level II), Assessment of Stream Condition and Departure (Level III), and Field Data Verification (Level IV). The broad-level classification (Level I) of the White River was contingent on knowing its vertical and horizontal containment (i.e., mean width to depth and entrenchment ratios), general pattern (i.e., mean sinuosity ratio), longitudinal gradient, and channel shape, and the landform features associated with its adjacent floodplain; all of which were visible and easily computed, by following the guidelines provided in the works of Dr. David Rosgen and other investigators, from aerial photographs, and the HEC-RAS Model. The delineation process during this stage of classification basically provided a general classification of landform, and identified the corresponding major stream type (A through G) and valley type (I through X) that

matched this fluvial system and the valley through which it flowed. Unlike the classification associated with geomorphic characterization (Level I) that depended on river features observable on aerial photographs and quadrangle maps, the morphological description of the White River at Level II depended on actual measurements taken from specific channel reaches known as ‘reference’ reaches and fluvial features within the vicinity of these reaches. Measurements of sinuosity, width/depth ratio, entrenchment ratio, longitudinal gradient, and meander belt width for these reaches were determined primarily with the assistance of high resolution aerial photographs and the HEC-RAS Model while measurements of riparian vegetation characteristics (such as density, vigor, diversity), bank characteristics (i.e., materials and slope), and dominant bed material for these reaches were determined from the actual sites. The dominant bed material D_{50} , or the median grain size bed material, for each ‘reference’ site was attained from a particle size distribution curve developed from sieve analyses of 100 soil samples collected using a modified Wolman Pebble Count method. Step by step procedures were provided in Wolman (1954), but the count scheme across the flow transect was greatly modified due to the high depth of the ‘reference’ reach. With the aforementioned features measured, the primary delineative criteria and classification key of natural rivers provided by Rosgen and Silvey (1996) were applied to classify the ‘reference’ reaches, which were then extrapolated to areas having similar landforms and fluvial features via the simultaneous utilization of aerial photographs, quadrangle maps, digital elevation models, and the hydraulic model to classify the remaining reaches. In view of the established fact that in reality reaches with similar morphologies were not imperative to possess similar conditions or ‘states’ and that the baseline or natural conditions may not be in agreement

with the current conditions, Level III classifications of various White River ‘reference’ reaches, which permitted a quantitative assessment of departure from an accepted range of morphological values validated for these reaches, focused on field elements controlling their conditions and their departures from the natural conditions. Guidelines and forms used for categorizing and assessing riparian vegetation, streamflow regime, stream size and stream order, depositional patterns, stream channel stability, and streambank erosion potentials were provided in *Applied River Morphology* by Rosgen and Silvey (1996). Several modifications made to the guidelines and forms of some of these elements include, for riparian vegetation, the additions of landcover types based on *Food and Agriculture Organization of the United Nations: Forest Resources Assessment* (1996), functioning condition categories based on *U.S. Department of the Interior, Bureau of Land Management: Riparian Area Management* (1998), and an alternate procedure for density estimation of riparian forest based on the tree “cramming” method provided in Hays, Summers, and Seitz (1981) and Paine and Kiser (2003); and for stream channel stability using the Pfankuch’s (1975) method, the replacement of bank slope gradient with the Bank Height Ratio (BHR) of Rosgen (2001) for predicting boundary stability, and the additions of the Mobility Index and Hjulström Diagram from Bledsoe and Watson (2001) and Hjulström (1939), respectively, to evaluate the erosive power and sediment transport capability or ultimately streambed aggradation/degradation potentials. Using the conversion table provided in Rosgen and Silvey (1996), the total numerical ratings applied to the ‘reference’ reaches through Pfankuch Channel Stability Evaluation were then converted to reach conditions or adjective ratings by stream types, and extrapolated to other areas (in the same manner as Level II classification) to classify the

remaining reaches. Level IV of RSC involved analyzing the results of laboratory sieve analyses of core samples obtained from the mid-sections of depositional point bar features and the apexes of the banks at various locations, which represented bed-load sizes being transported and/or deposited at bankfull discharge.

Stability Assessment With Sediment Analyses and Parametric Correlations

Regardless of the existence of a general unanimity indicating the influence power of the sediment regime on the shapes, patterns, gradients, and stability conditions of alluvial streams, its initial applications had been somewhat limited to the differentiations of channel patterns. In the early experimental works of Schumm (1968) and Schumm and Khan (1972) on laboratory flume models, it was demonstrated that, when discharge remained relatively constant and sediment load augmentations accompanied longitudinal gradient enhancements, the rate at which sediment moved through the channel greatly coincided with changes in thalweg or channel pattern. It was therefore concluded by these proponents upon additional investigations on the patterns of the Mississippi River, the Murrumbidgee River, and an assortment of rivers of the Great Plains that changes in the mode of sediment conveyance (i.e., from bed-load to suspended-load) were necessary prior to the transition from one stream pattern to the next (i.e., straight to meandering). Alternate inferences emerging from the experimental study of channel patterns by Schumm and Khan (1972), most notably the corollary that depicted enhancements in thalweg sinuosity in reaction to augmentations in the longitudinal gradient and sediment load and the corollary that illustrated the substantial changes in channel patterns as a reverberation of insignificant changes in sediment loads, insinuated that the amount and texture of sediment load may also play key role in the determination of channel and

floodplain geomorphology, the development of meander bends, and the stability condition of channel bed and banks. These connotations were verified by the subsequent works of Carson (1984b, 1984c) which denoted the equivalency between sediment size and texture and stream power (or the ability of river to perform work), Ackers and Charlton (1975) which demonstrated the initiation of meanders in a formerly straight channel and the actuation of sinuosity enhancements in a meandering channel in response to an initial augmentation in sediment load, Neill (1984) which averred the colligation of elevated levels of bed-load to enhancements in bank erosion rate, and Hickin and Nanson (1984) which alluded to the controlling power of sediment properties (i.e., size and texture) on “the sedimentary composition of the floodplain, which in turn [influenced] the resistance of stream bank to erosion” (Nanson & Croke, 1992, p. 465). The impact of sediment conveyance on bend development was also reinforced by Chang (1984b) via “a theoretical explanation [illustrating] the sensitivity of meandering to sediment supply” (Lagasse et al., 2004b, p. 27), which specifically involved the action of allowing the bed-load/discharge ratio to fluctuate or enhanced meandering/sinuosity augmentation to occur in response to discharge variation, and Yen and Ho (1990) via the provision of concrete evidence detailing the influence of sediment movement on bend evolution, especially through its impression on bedforms.

Since it was shown and suggested by various investigators that the sediment regime of open channel flow in a river may be held accountable for the bed and bank instability, it was not unexpected to see explanations regarding the magnitude and rate of migration be isolated to just the sediment regime. As interests in the ability to forecast adjustments in planform became more prominent in the late seventies to eighties, one

could conclude that in the effort to develop empirical relations for the estimations of bankline migrations based on sediment-related attributes, the focus of the use of sediment had shifted from mere pattern differentiations to simple stability assessments. This was seen in the early work of Schumm (1977) where it was shown that “an increase in the ratio of the bed material load to the total sediment load with a corresponding increase in channel gradient [led] to a decrease in [channel] stability” (Rosgen, 1994, p. 171) causing channel patterns to shift. Based on this work, Selby (1985) derived a relationship illustrating the changes in the form of alluvial channels with specific types and textures (particle sizes) of sediments. The mutually exclusive works of Dr. Dave Rosgen on a multitude of alluvial streams also produced relationships involving the types of sediments to channel stability ratings developed by Pfankuch (1975). The long established conjecture that “the rate of bank migration at a given location [was] a function of erosional and resisting forces [actuated by sediment movements]” (USDA-NRCS, 2007, p. 12-25) was corroborated within the work of Lewin (1978), in which “historical records of bend movement over a period of 100 years [...] illustrated the influence of sediment transport pattern on bend migration rate, with the spatial distribution of rapid shifting being associated [primarily] with changes in the local sediment transport pathways” (Lagasse et al., 2004b, p. 27). Critical influences of the sediment supply and bed material size on bank erosion and meander migration, or the stability condition of a channel within its floodplain, was confirmed by the long-term investigations conducted by Brook and Luft (1987) on the Oconee River in Georgia as well as the statistical analyses conducted by Nanson and Hickin (1986) on eighteen meandering rivers in western Canada. The results of the latter work not only indicated the dependency of bank erosion and meander

migration on sediment transport capacity of flows, but also distinctively demonstrated “that [approximately] 70 percent of the variability in migration rates could be explained by variability in bed sediment size” (Lagasse et al., 2004b, p. 27).

It was not surprising then that bed sediment size, especially the median grain size river bed material D_{50} , was often indicated as a highly critical parameter (for use in sediment analysis) to describe and predict river pattern stability. Emphasis placed upon the dominant bed material initially originated from the works of Henderson (1966), Carson (1984a), and Ferguson (1984, 1987), where it was originally shown that this parameter was critical in defining the threshold criterion separating one channel pattern from the next. The significance of the dominant bed sediment size D_{50} in predicting river pattern stability was also often promulgated in scientific works involving sediment transport functions. Its use in a variety of sediment transport functions to predict the magnitudes or concentrations of sediment loads (in preparation for stability analysis) had demonstrated high degrees of reliability.

As for existing correlations between sediment loads being conveyed within a channel and other static and dynamic fluvial/geomorphic parameters, only a few were mentioned in the literature. However, it was often suggested by many proponents that once these sediment-related empirical relationships became more available, they could be implemented in the same manner as those involving purely hydraulic and geomorphic parameters to assess boundary stability, dynamic stability, and aggradation/degradation potential of a channel.

The third and final part of the stability assessment for the White River (RM 299.00 – RM 0.00) fluvial system was contingent on the integration of sediment analyses

results with a multitude of hydraulic and geomorphic parameters. The HEC-RAS Model initially provided many static and dynamic hydraulic parameters while other geomorphic parameters were determined with the simultaneous use of aerial photographs, quadrangle maps, and a hydraulic model. Guidance for determining various geomorphic parameters was provided by Leopold (1994), Parish Geomorphic Ltd. (2004), Rosgen (1994), Rosgen and Silvey (1996), etc. Parameters lacking clear guidelines were determined via simultaneous employment of the HEC-RAS Model and ArcGIS (quadrangle maps and aerial photographs) based on the definitions and results provided by various proponents in their investigations of other fluvial systems. Sediment analyses were conducted by implementing several well-established sediment transport functions (i.e., Van Rijn, Yang, Kennedy, and Karim-Kennedy) by consulting and following guidelines provided in the works of Karim (1988, 1995, 1999), Karim and Kennedy (1990), Kennedy (1961, 1963), Van Rijn (1982, 1984a, 1984b, 1984c), and Yang (1972, 1973, 1996). Prior to the initiation of sediment analyses and sediment computations, the median grain size bed materials D_{50s} were determined from particle size distribution curves of soil samples collected from the sites. Step by step guidelines for collecting soil samples were provided in Wolman (1954), but the count scheme across the flow transect was greatly modified due to the high depths of the reaches. Justifications and additional guidelines of the use of D_{50} in sediment analyses were provided by Bathurst, Graf, and Cao (1987) and Sturm (2001), respectively. During sediment analyses, bedform features were predicted for various reaches of the White River using procedures and diagrams provided by Engelund (1967), Engelund and Hansen (1967), and Van Rijn (1984c). Nomenclatures and descriptions of bedform features were supplied by Garcia (2008). After sediment

analyses, the approach utilized for the creations of sediment rating curves (to predict flow related changes in sediment supply and transport) was furnished by Rosgen and Silvey (1996). Sediment-related correlations were determined through regression of the sediment-analyses resulting data and the fluvial and geomorphological data. Sediment results and sediment-related parametric correlations were then utilized to gain insights into the transport mechanisms, the trends of sediment transport and supply, the erosional and depositional patterns, the boundary stability conditions, the channel dimensions and sediment mobility relationships, the interactions between channel boundaries and flow regimes, and the aggradation and degradation potentials of various reaches of the White River.

CHAPTER 3: APPLICATIONS OF THE HEC-RAS MODEL AND ARCGIS

Introduction

The assemblages of the quantitative values of fluvial and morphological parameters and the correlations between parameters are acquired by implementing procedures through the applications of the HEC-RAS Model and ArcGIS. Specific geometric relationships, or specific stream channel patterns, are quantitatively defined through measurements of parameters such as meander wavelength, radius of curvature, meander amplitude, meander belt width, and sinuosity via ArcGIS. Specific stream channel dimensions encompassing width, depth, cross-sectional area, and slope, and other dynamic hydraulic parameters such as discharge, velocity, and stream power are determined from simulation output of the HEC-RAS Model based on SUPER run W95X02's discharge frequency data. Additional morphological parameters, such as width to depth, entrenchment, radius of curvature to width, and meander belt width ratios are acquired by synthesizing HEC-RAS and ArcGIS output data into one unified table. The amalgamation of simulated HEC-RAS and measured ArcGIS output data assist in the determination of empirical relationships of channel dimensions with stream patterns, channel dimensions with morphological parameters, and other combinations of correlations between fluvial and morphological parameters. The objectives of this chapter are to briefly outline the procedures involved in the creation of the HEC-RAS Model, the procedures for determining and calculating various fluvial and morphological parameters through applications of the HEC-RAS Model and ArcGIS, and the significance of the parameters on the meandering/shifting, dynamic equilibrium, and overall stability of the White River.

HEC-RAS River Analysis System Modeling

The creation of the hydraulic model for the White River required extensive implementations of HEC-GeoRAS, an ArcGIS extension that provides users with “a set of procedures, tools, and utilities for processing geospatial data in ArcGIS using a graphical user interface (GUI)” (U.S. Army Corps of Engineers Hydrologic Engineering Center [USACE HEC], 2005, p. 3-1), and HEC-RAS simultaneously. HEC-GeoRAS is a medium for exchanging data between ArcGIS and HEC-RAS as “the interface allows for the preparation of geometric [or GIS] data for import into HEC-RAS” and the generation and processing of output simulation data exported from HEC-RAS (USACE HEC, 2005, p. 3-1). A specifically formatted data exchange file (sdf) is responsible for the transference of data between ArcGIS and HEC-RAS. The general procedures involved (1) importing an existing 30-meter by 30-meter digital terrain model (DTM) in a triangulated irregular network (TIN) or GRID format of the White River floodplain, (2) creating point, line, and polygon RAS layers, such as *Stream Centerline*, *Flowpath*, *Main Channel Banks*, and *Cross Section Cut Lines*, that are pertinent to the development of geometric data for the HEC-RAS Model, (3) completing and importing geometric data, entering discharge data (obtained from USACE-Little Rock District’s Super Model W95X02), and performing hydraulic computations in HEC-RAS, and finally (4) exporting results obtained from HEC-RAS hydraulic computations back to ArcGIS for spatial analysis. Step by step procedures followed in the creation of the White River HEC-RAS Model is outlined by the process flow diagram shown in **Figure 3.1**, and explicate in details subsequently. It should be noted that *Floodplain Mappings* or *Floodplain Delineations* for specific recurrence intervals of inundation are circumvented

due to difficulty experienced in the current version of ArcGIS.

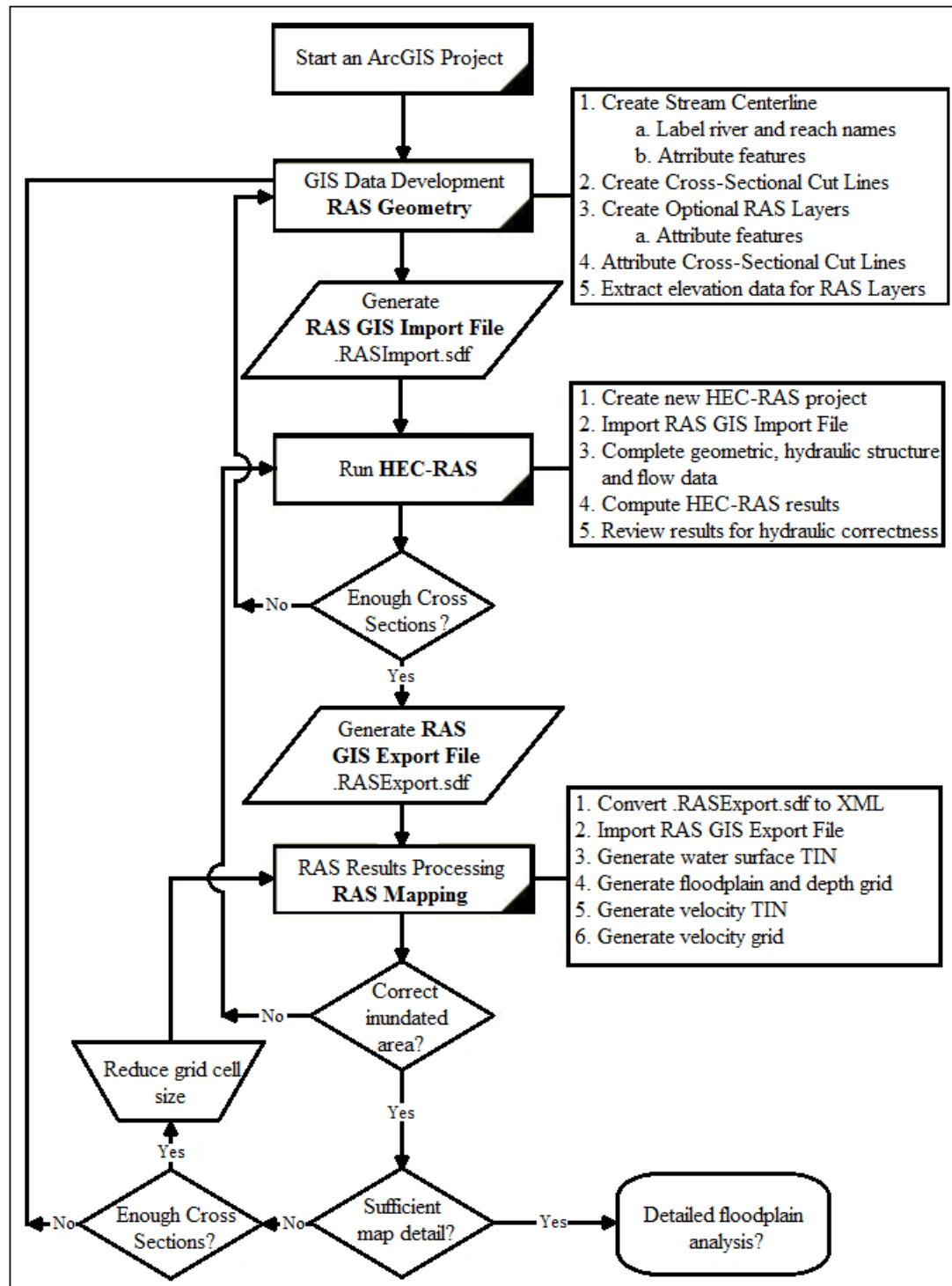


Figure 3.1. Process Flow Diagram for Using HEC-GeoRAS (USACE HEC, 2005).

Prior to importing the digital terrain model of the White River system, HEC-GeoRAS is loaded into ArcGIS by selecting the option *Customize* under the *Tools* menu, and checking the *Spatial Analyst* and *3D Analyst* extensions. Once the extensions load, menu and toolbars are added into the ArcGIS interface to aid in the development of geometric data. The vector Digital Elevation Model (DEM) of the White River floodplain is then loaded into the ArcGIS interface by pressing the *Add Layer* button. Since all cross-sectional data will be extracted from the DEM, it is imperative that it is high resolution, as well as containing a continuous surface that includes the river bottom and the floodplain for hydraulic modeling. For this reason the 30 meter by 30 meter DEM, attained from the U.S. Geological Survey, is chosen as it is sufficient to produce accurate and detailed cross-sections of the White River channel. The subsequent steps involved creating RAS layers for geometric data development and extraction beginning with a *Stream Centerline* layer which is made by selecting *Create RAS layers* under the *RAS Geometry* item of the HEC-GeoRAS toolbar. When the layer appeared on the ArcGIS interface, the user must manually draw the centerline by using the available *Sketch tool*. It should be noted that it is mandatory that river reaches be drawn from upstream to downstream in the direction of flow, and each reach be assigned a name via the *Reach and River ID* tool. By selecting the appropriate items under the *Create RAS Layers* menu and following the same methodology for the creation of the *Stream Centerline* layer, *Main Channel Banks* and the *Flowpath* layers are created. Separate lines are used to designate the left and right banks as well as the left and right overbanks. The stream centerline is equivalent to the flow path in the main channel, therefore, is copied to the *Flowpath* layer. The left and right overbanks are drawn such that they

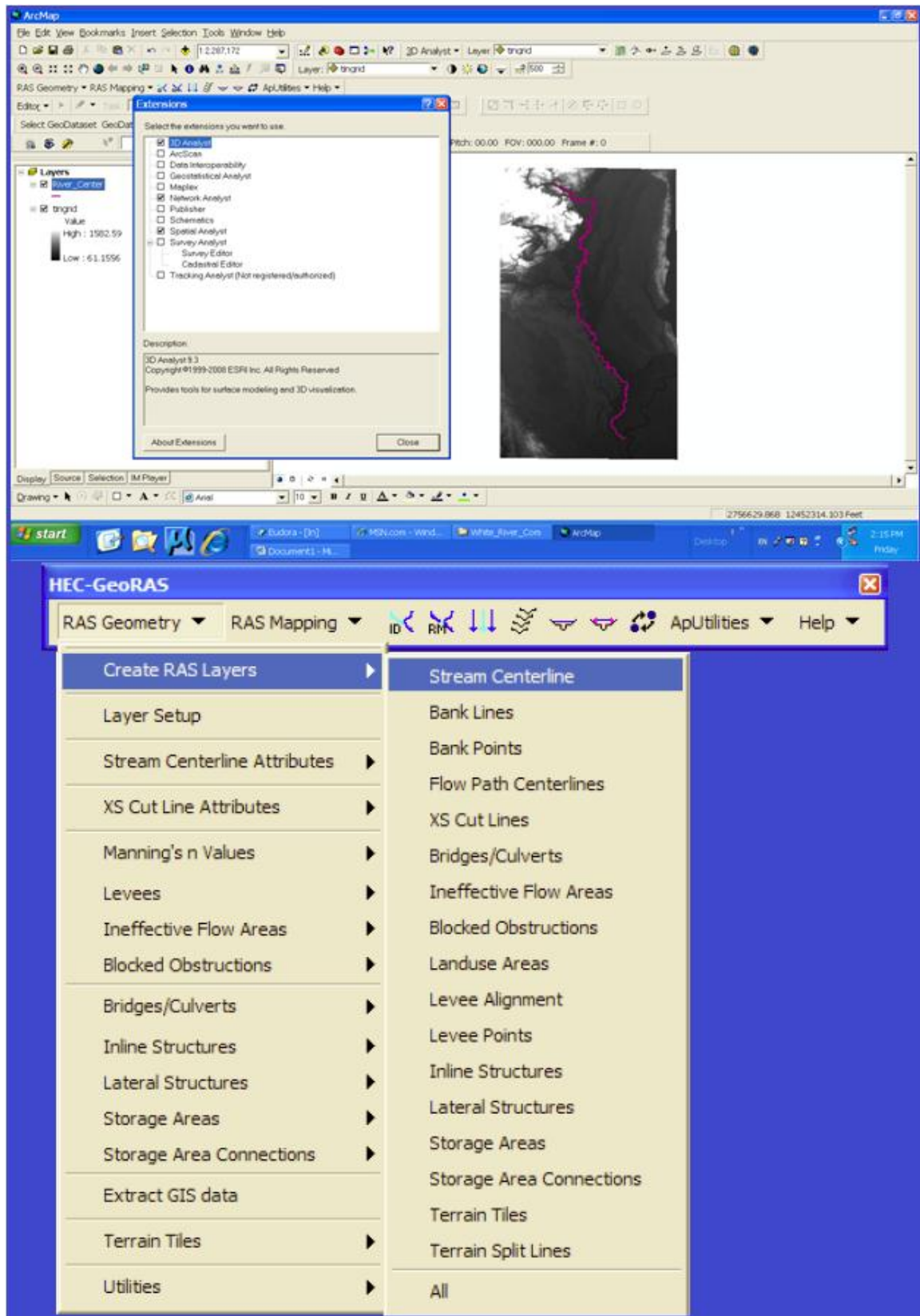


Figure 3.2. Loading of GeoRAS and DEM into ArcGIS, and Creating a Centerline Layer.

superimposed the extent of the water level at two-year recurring inundation. Next, the *Cross-Sectional Cut Lines* layer is created and the cut lines are drawn at locations where cross-sectional data are extracted from the terrain model. The criteria for placing the cross-sectional cut lines include (1) Each cross-sectional cut line should be drawn from the left overbank to the right overbank when facing downstream, (2) Each cross-sectional cut line should be drawn perpendicular to the flow path lines, (3) Each cross-sectional cut line must cross the main channel only once, and (4) Each cross-sectional cut line must in no way intersect or cross another cross-sectional cut line (USACE HEC, 2005). Manual manipulations of the RAS layers should follow the included guidelines as they are crucial to the geometric data extraction process and have a specific function during the extraction process. Specifically cross-sectional bank stations are assigned based on the intersections of the *Main Channel Banks* theme and the *Cross-Sectional Cut Lines* theme, downstream reach lengths are calculated between the cross-sectional cut lines for the left overbank, the main channel, and the right overbank of the *Flowpath* theme, and the stage-elevations are extracted along the cross-sectional cut lines from the digital terrain model of the floodplain.

When the manual manipulations are completed for each of the RAS layers, the geometric data extraction process begins. The initial step involves the attributing of the *Stream Centerline* layer which is located under *Stream Centerline Attributes* of the *RAS Geometry* menu. Essentially there are three processes that take place during centerline attributing. The processes include (1) *Topology*, which “establishes the connectivity and orientation (upstream and downstream ends) of the river network, (2) *Lengths/Stations*, which “computes the river reach lengths”, and (3) *Elevations*, which extracts the

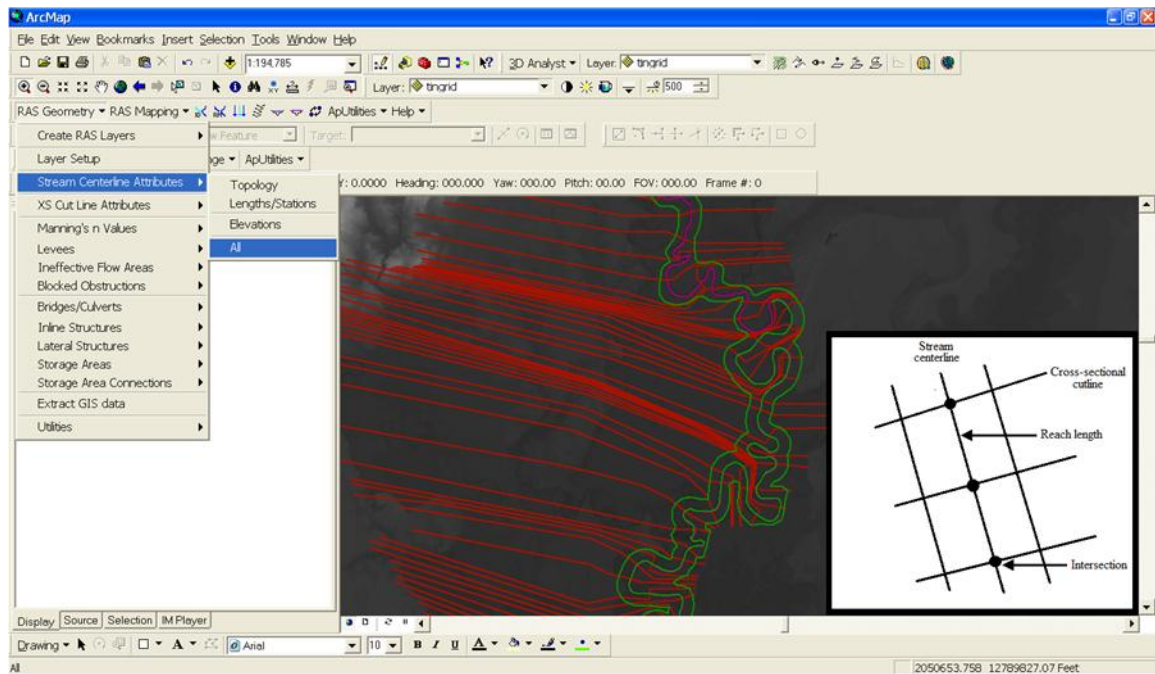


Figure 3.3. Stream Centerline Attributing.

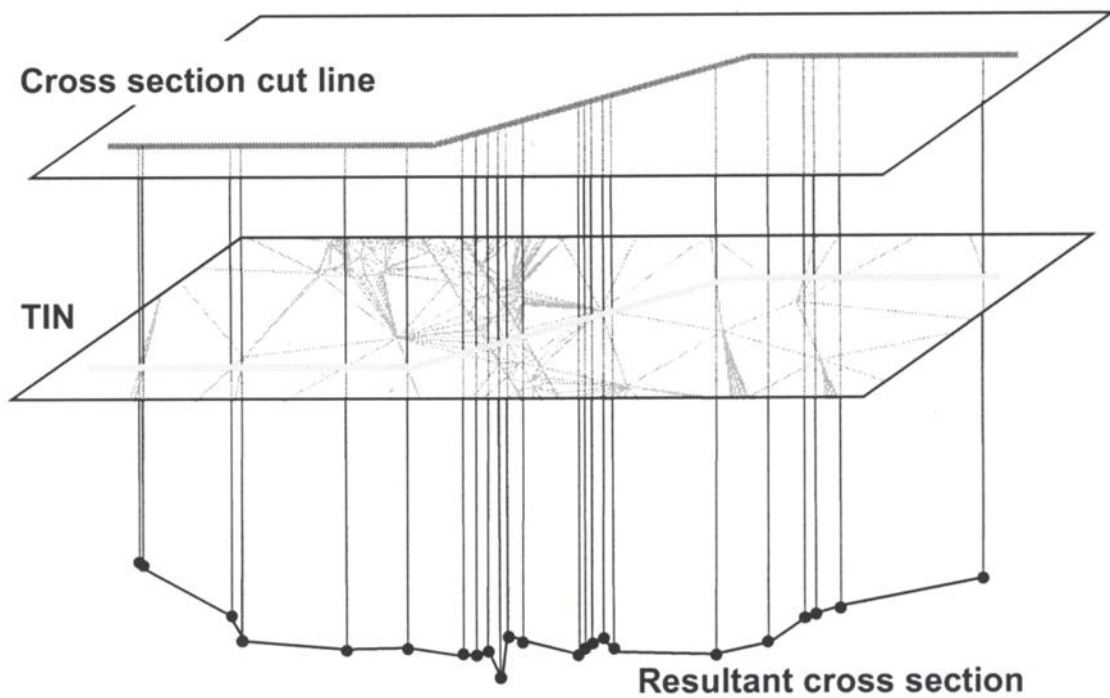


Figure 3.4. Extraction of Station-elevation from a Digital Terrain Model (USACE HEC, 2005).

elevations and creates a three dimensional shapefile from the *Stream Centerline* layer (U.S. Army Corps of Engineers Hydrologic Engineering Center [USACE HEC], 2000, p. 31). By selecting all three processes, the stations are computed for each of the cross-sectional cut lines at the intersection with the centerline, the reach lengths are computed between the cross-sectional cut lines, and the elevations are calculated for each individual section of the centerline; all of which are arranged in specific order from the upstream end to the downstream end. Identical processes are implemented for the left and right banks. In a similar manner, cross section attributes are added to the *Cross-Sectional Cut Lines* layer by first selecting *XS Cutlines Attributes* option under the *RAS Geometry* menu. The processes that take place in cross-sectional attributing include (1) *River/Reach Names*, which adds stream and reach ID to each cross-section “based on the intersection of the cut line with the stream centerline”, (2) *Stationing*, which “adds the cross-sectional stationing based on the intersection of the cross-sectional cut lines and the stream centerline (2D)”, (3) *Bank Stations*, which adds “bank station positions for each cross section from the intersection of the cross-sectional cut lines and bank station lines”, (4) *Downstream Reach Lengths*, which “adds downstream reach lengths to each cross section cut lines based on the intersection of the flow path centerlines and the cut lines”, and (5) *Elevations*, which extracts the stage-elevation data from the digital terrain model at the edge of each triangle along a cut line, and creates a three dimensional shapefile from the *Cross Sectional Cut Lines* layer (USACE HEC, 2000, pp. 32-34). The final step involves The extraction of the GIS data into a formatted data exchange file, which is executed by selecting the *Extract GIS Data* item under the *RAS Geometry* profile. When this function is selected, the heading and reach information within the Stream Centerline theme, and

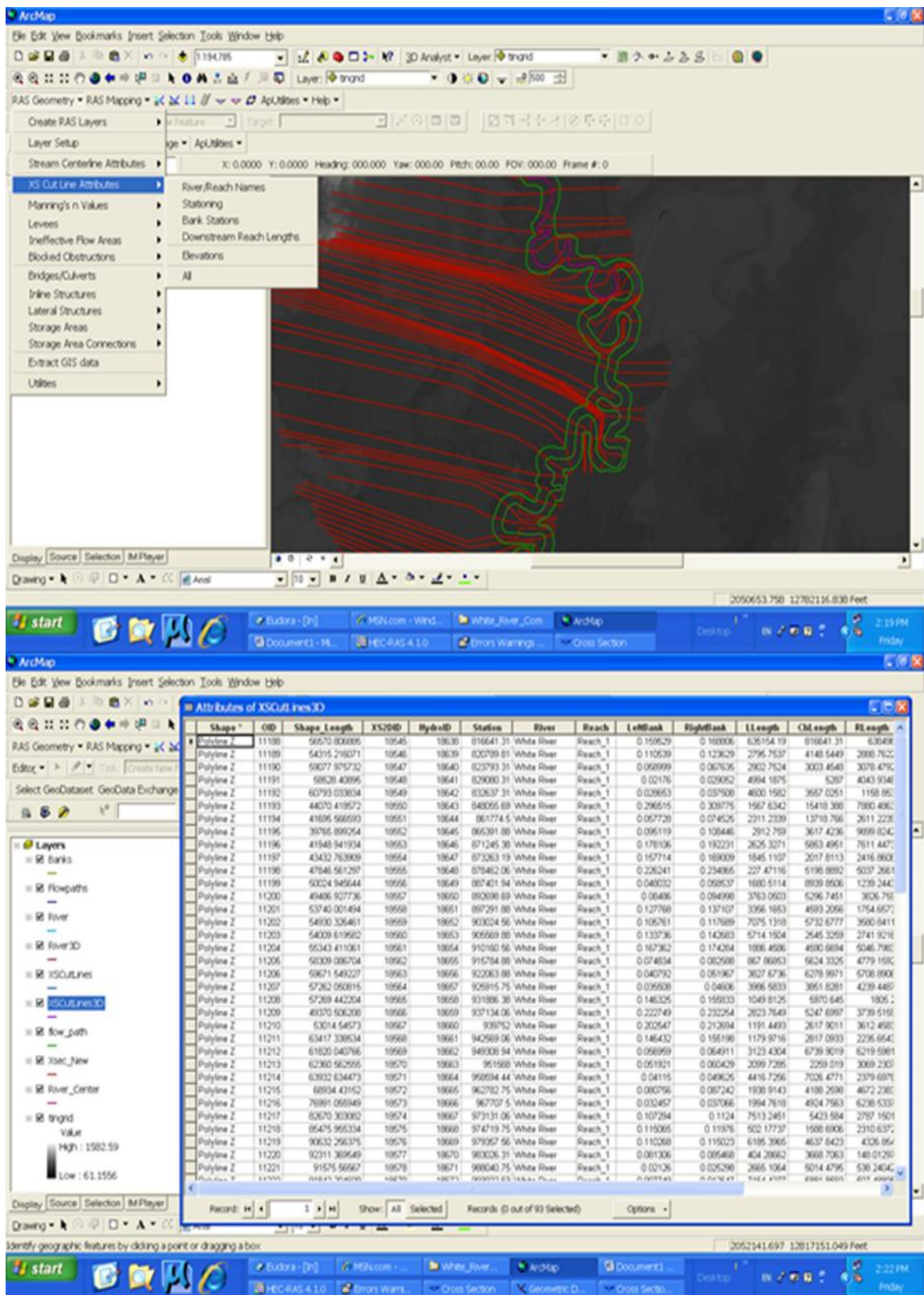


Figure 3.5. Channel Cross-section Attributing.

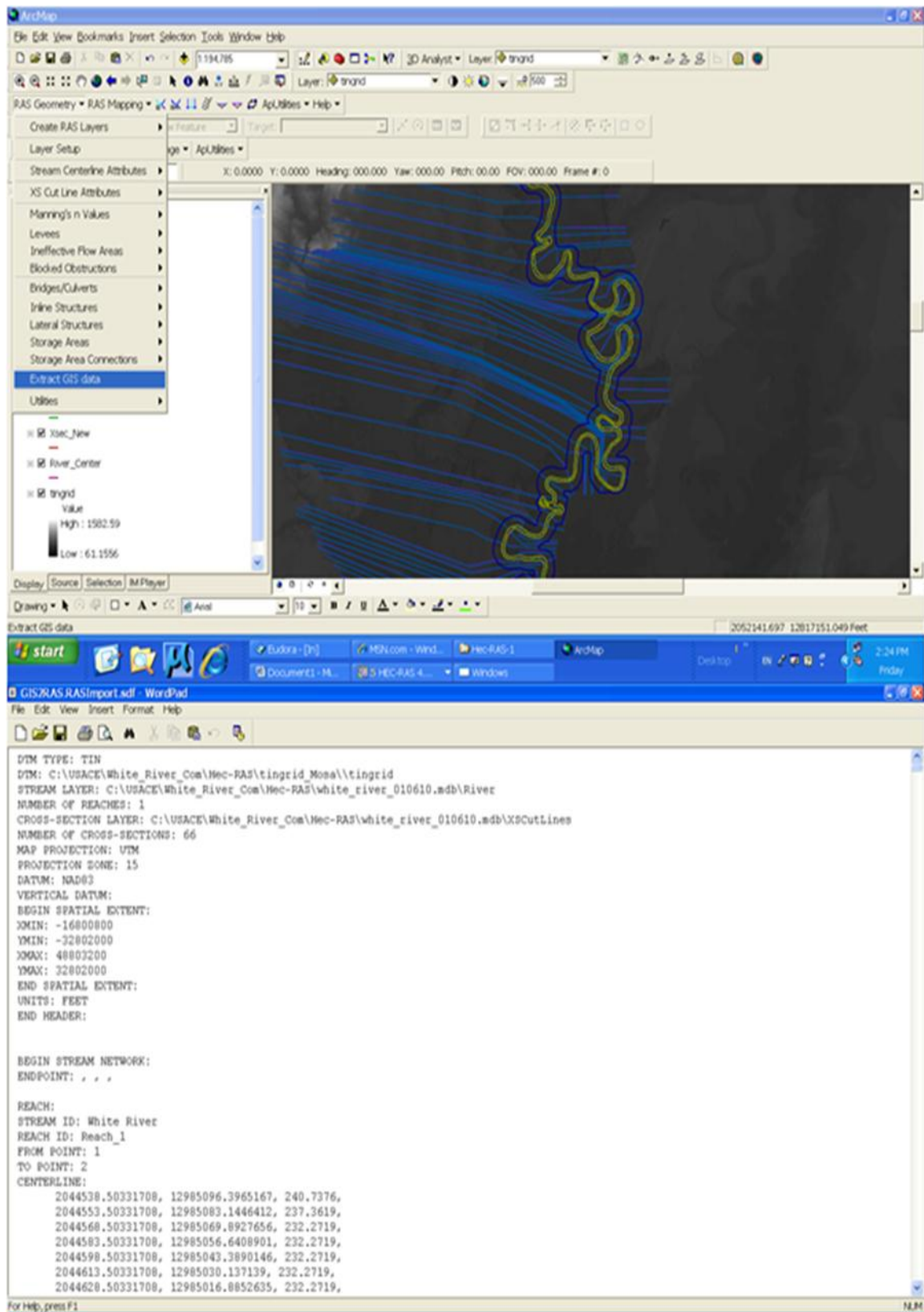


Figure 3.6. Extraction of the GIS Data into a Formatted Data Exchange (sdf) File.

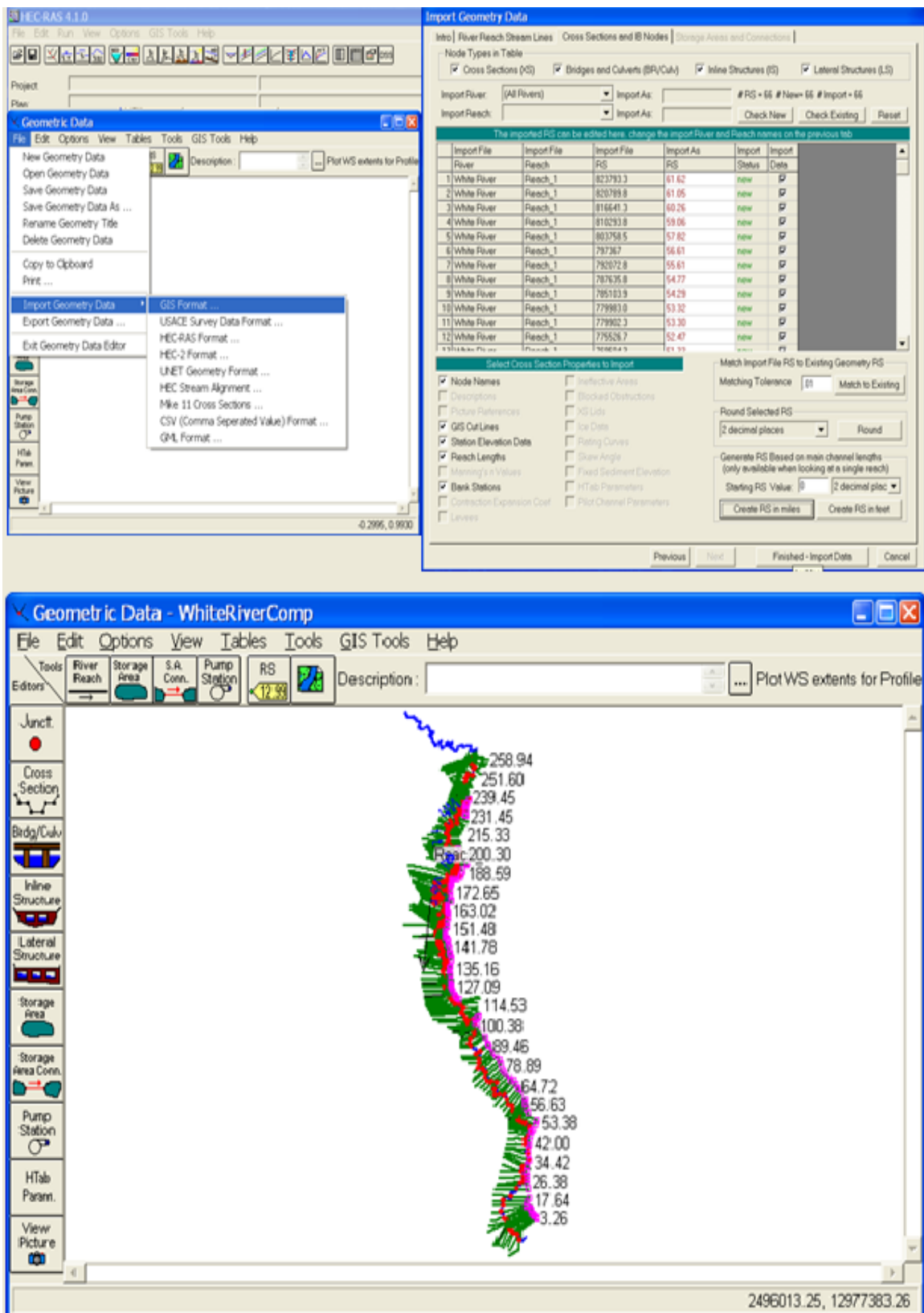


Figure 3.7. The White River HEC-RAS Hydraulic Model.

the cross-sectional information contained in the *Cross-Sectional Cut Lines* theme are then written into a GIS import file that comes in two formats: a sdf format and a XML format. Once the sdf file is created, it is imported into HEC-RAS from the *Geometric Schematic* by selecting the *GIS Data* option from the *Import Geometry Data* submenu, which is located under the *File* menu. In the *Import Options* dialog window after the appropriate units system to import data into is selected, in this case in miles, clicking the *Finished-Import Data* button results in a HEC-RAS Model with pertinent attributes. Input of flow data for various recurrence intervals are obtained from the USACE Supermodel W95x02's discharge-frequency curve for simulation purposes. Several simulations of the White River Model are required to ensure that (1) the conveyance R is between 0.7 and 1.4, (2) the stages are similar to HEC-SSP output for various gages, and (3) the flow data are within reasonable ranges of the USACE Supermodel simulation output. In the case where the conveyance criterion is not met, additional cross-sectional cut lines, hence additional cross-sections, are added and the process is reiterated. Since the surface elevation is dependent on Manning coefficients, they are predicted and adjusted based on land use until they produce water surface elevations that matched the gage (HEC-SSP) water surface elevations. The White River HEC-RAS Model required roughly two hundred cross-sections and an average Manning coefficient of approximately 0.03 to satisfy all criteria. Comparisons of stage and flow are shown in **Table 3.1**.

Table 3.1. Comparison of the HEC-RAS Model to the USACE Supermodel.

	HEC-RAS MODEL					SUPER MODEL			
	River Stations					River Stations			
	Newport	Augusta	Georgetown	Clarendon		Newport	Augusta	Georgetown	Clarendon
Discharge (cfs)									
100	250000	259000	227000	243000		337000	259000	227000	243000
50	220000	220000	195000	213000		274000	220000	195000	213000
25	201000	186000	166000	184000		221000	186000	166000	184000
10	162000	144000	132000	147000		162000	144000	132000	147000
5	123000	120000	108000	120000		123000	116000	108000	120000
2	77800	79100	75400	78500		77800	79100	75400	78500
1	24000	28600	30150	32500		29300	33500	33900	32500
Stage (1000 feet)									
100	229000	208890	201500	175760		228690	208350	201180	174810
50	227700	207580	199540	174440		227790	207550	199580	174110
25	226730	206370	197630	173220		226790	206750	198080	173310
10	224760	204770	195180	171570		224990	205450	195980	172310
5	222500	203700	193850	170230		223390	204450	194280	171410
2	218840	201320	190290	167660		219990	202750	191680	169810
1	206630	194810	182270	161660		210290	199150	186780	166410
Depth (feet)									
100	35.79	38.61	31.23	35.44		34.60	38.50	31.10	34.90
50	34.59	37.86	30.16	34.54		33.70	37.70	29.50	34.20
25	33.24	37.03	28.98	33.57		32.70	36.90	28.00	33.40
10	31.11	35.74	27.14	32.14		30.90	35.60	25.90	32.40
5	29.06	34.53	25.40	30.84		29.30	34.60	24.20	31.50
2	24.96	32.18	22.01	28.46		25.90	32.90	21.60	29.90
1	11.65	24.99	11.56	22.13		16.20	29.30	16.70	26.50

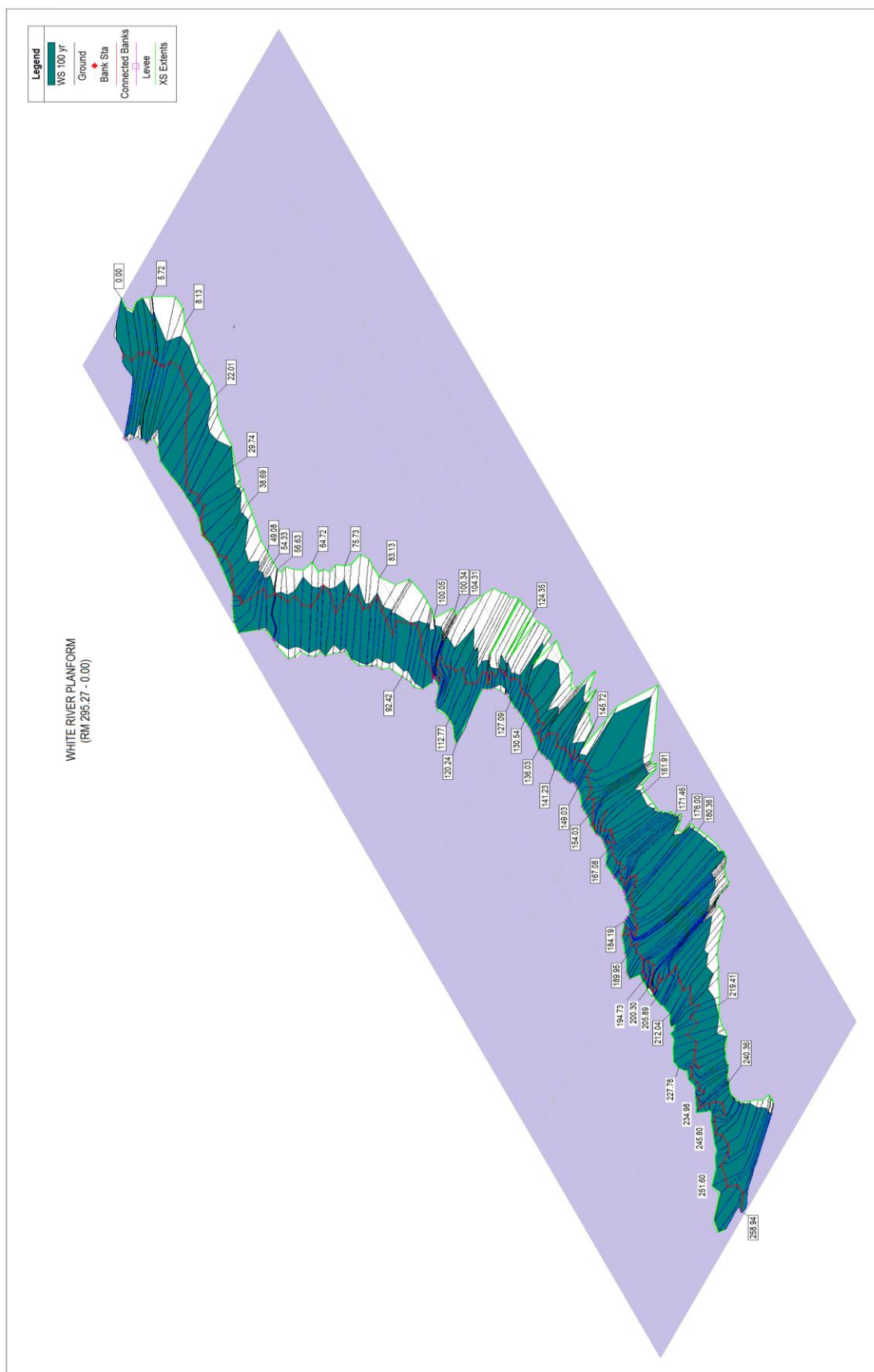


Figure 3.8. The White River Planform (HEC-RAS).

HEC-RAS-Extracted Fluvial Parameters and Their Implications

Post-simulation extractions of significant fluvial parameters from the White River HEC-RAS Model result in a table summarizing the mean quantities of these parameters for specific reference reaches. Similar to various correlation plots depicting the relationships between parameters, mean values of static and dynamic parameters encompassing the longitudinal gradient, width, depth, cross-sectional area, discharge, velocity, stream power, shear force, and Manning's roughness coefficient may permit percipience into the current conditions of the studied sections as well as possible anomalies associated with channel dimensions, boundary resistance, and flow strength and regime. Inspection of the tabulated data reveals that the reach extending from Batesville to Newport, which possesses a longitudinal gradient in excess of the remaining alluvial reaches, is marked by low channel dimensions, specifically insufficient channel depth and mean hydraulic depth, and a low cumulative flow discharge quantity exhibiting considerable velocity and stream power. The shear force exerted on the channel boundaries, especially the banks, is slightly higher than the downstream alluvial sections while the resistance to flow, represented by Manning's roughness coefficient, of approximately 0.026 is considerably lower; a minimum value in comparison to other alluvial reaches of the White River. A Manning's roughness coefficient numerical quantity of 0.026 is also characteristic of predominantly gravelly earth streams possessing top widths at flood-stage exceeding 100 feet where the banks offer less effective resistance, and a regular section devoid of boulders and brush (Chow, 1959). On the contrary, the reach extending from Devalls Bluff to Clarendon, distinguished by an extremely flat longitudinal gradient, consists of very high channel dimensions,

specifically channel depth and cross-sectional flow area, and an apparent deficiency in boundary shear force. The Manning n-value of approximately 0.03, however, denotes a weedy stream with irregular cross-sections. Similarly, the reference reach extending from Clarendon to St. Charles also exhibits high magnitudes in channel dimensions, an optimum top width and mean hydraulic depth, in addition to a maximum numerical quantity in boundary resistance associated with a major river residing in a floodplain of pasture and farmland. Since the top width at flood stage exceeds 100 feet, a Manning's roughness coefficient of 0.035 would imply that the channel of this major stream may be differentiated by irregular and rough sections. Other distinctive features emanating from the table include high magnitudes of stream power and flow velocity for Newport to Augusta, substantial amount of shear forces exerted on the boundaries of the channels extending from Augusta to Devalls Bluff, and an exceptional degree of boundary roughness for St. Charles to LMR. In addition, the average Manning's roughness coefficients of the remaining alluvial sections including Newport to Augusta, Augusta to Des Arc, and Des Arc to Devalls Bluff, all appear to fall within the category of weedy major streams with irregular and rough sections. It should be noted that the findings hitherto do not take into account the effects induced on channel roughness and other fluvial parameters by anthro-related activities; most notably dredging, realignment, and construction in proximity to the channel, but rather predicated upon the assumption that the White River is a natural fluvial system.

Table 3.2. Fluvial Parameters Extracted from the White River HEC-RAS Model.

Section	Station, RM	Gradient, S	Top Width, W	Max Depth, D_{max}	Mean Depth, H_d	Flow Area, A	Flow, Q	Velocity, V	Stream Power, Ω	Shear Force, τ	Manning n-value
			(feet)	(feet)	(feet)	(ft ²)	(cfs)	(ft/s)	lb/ft s	lb/ft ²	
Batesville – Newport (1-17)	295.27 through 256.89	0.000112	507.79	18.02	12.51	6390	18598	3.20	0.36	0.09	0.026
Newport – Augusta (18 – 38)	256.89 through 197.27	0.000050	520.96	27.74	20.06	10283	21991	2.17	0.10	0.05	0.029
Augusta - Des Arc (39 – 62)	197.27 through 147.19	0.000078	552.62	27.08	18.42	10054	26765	2.73	0.25	0.09	0.032
Des Arc – Devalls Bluff (63 – 74)	147.19 through 124.33	0.000080	555.55	31.68	18.86	10160	29155	2.93	0.26	0.09	0.030
Devalls Bluff – Clarendon (75 – 88)	124.33 through 100.34	0.000045	522.37	33.34	23.48	12443	25236	2.19	0.12	0.05	0.030
Clarendon – St. Charles (89 – 109)	100.34 through 55.30	0.000060	569.64	29.80	30.38	11659	26655	2.29	0.16	0.07	0.035
St. Charles – LMR (110 – 141)	55.30 through 0.00	0.000093	557.73	31.05	20.39	11844	28909	2.53	0.23	0.08	0.035

Fluvial and Morphological Parameters

The following sections cover fluvial and morphological parameters pertinent to the White River fluvial system. Brief discourses accentuating the procedures implemented to determine these constituents via applications of the HEC-RAS Model and ArcGIS are also included.

Entrenchment ratio. Some rivers incised deeply into the floodplains while others passed gradually through the adjacent floodplains. The relationship of the river to its valley and floodplains is often described with the term “entrenchment” or “entrenchment ratio”, which has been quantitatively defined as the vertical containment of a river or equivalently the extent of the river incision to its valley floor (Kellerhalls, Neill, & Bray, 1972). The entrenchment ratio, derived empirically from measurements of the flood prone areas and the bankfull cross-sections and in part by the dimensionless rating curves of the ratio of mean depth to bankfull depth versus the ratio of the mean discharge to bankfull discharge (Dunne & Leopold, 1978), is tantamount to the ratio of flood-prone width to bankfull width. Based on studies conducted by Dr. Dave Rosgen involving a variety of stream types, the flood-prone width is representative of the width at the 50-year recurrence interval flood discharge which occurs at an average of twice the maximum bankfull depth (Rosgen, 1994). In the case pertaining to the White River, the flood-prone width corresponding to twice the maximum bankfull depth is associated with the 100-year recurrence interval inundation, thus Rosgen’s empirical equation for entrenchment cannot fully be implemented. Modification of Rosgen’s empirical equation follows a procedure in which the ratio of 50-year depth to bankfull depth (d_{50}/d_{bkf}) is plotted against the corresponding discharge ratio (Q_{50}/Q_{bkf}) in a dimensionless rating curve

(Figure 3.9). The ordinate intercept of 1.5 on the dimensionless rating curve signifies that the flood-prone width of the White River occurs at 1.5 times the maximum bankfull depth, therefore the quotient of the width at 1.5 times the maximum bankfull depth to the bankfull width is adopted to calculate entrenchment ratios for various reach segments. The entrenchment ratios computed for the reaches from Batesville to the confluence with the Lower Mississippi River indicate that (1) the White River is only slightly entrenched in its valley, (2) flows exceeding bankfull discharge increase in width much faster than in depth, and (3) flows exceeding bankfull discharge extend onto the floodplain thus greatly dissipating shear stresses.

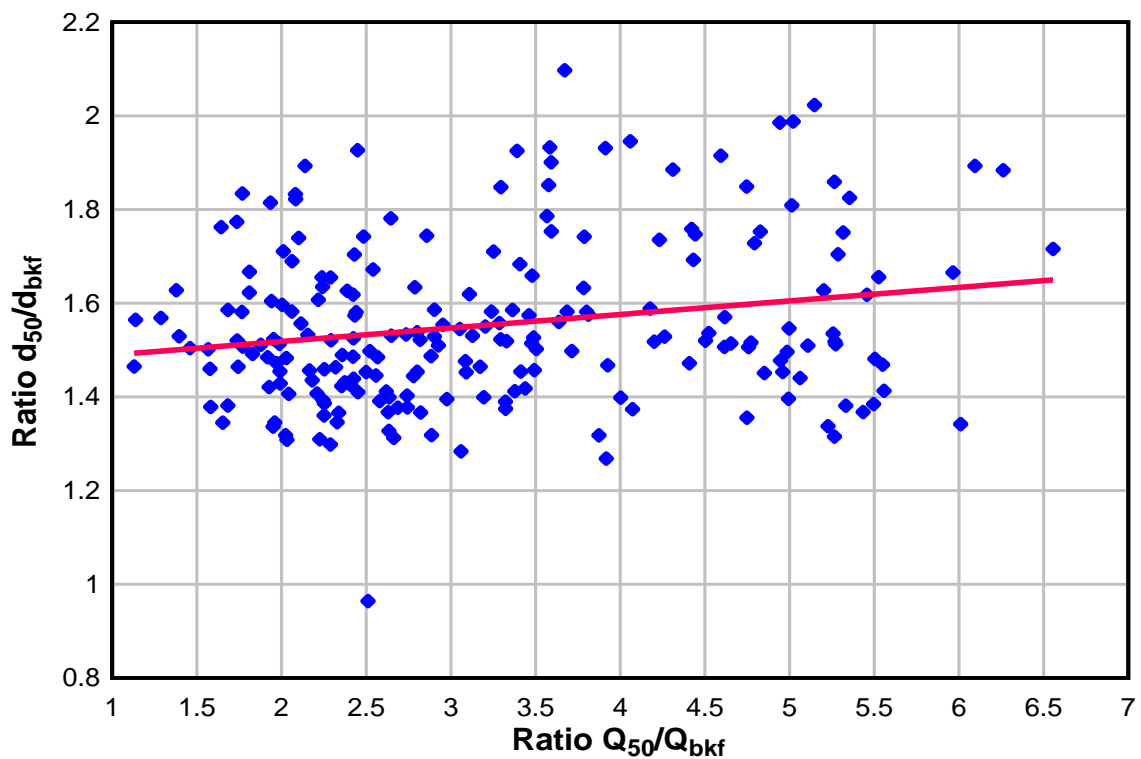


Figure 3.9. Dimensionless Curve of Bankfull to 50-year Inundation.

Width to depth ratio. Lateral migrations are common phenomena that occur in fluvial sinuous channels. A channel exhibiting lateral migrations without significant changes in width and depth are deemed dynamically stable. Uniformity of width and invariability of depth as indicators of stability also represent equilibrium of erosion and deposition activities (Hooke, 2007a). Since the major mechanisms by which fluvial systems dissipate excess energy often involve increases in width and alterations in depth, a combination of width and depth into the width/depth (W/D) ratio provides “the key to understanding the distribution of available energy within a channel, and the ability of various discharges occurring within the channel to move sediment” (Rosgen & Silvey, 1996, pp. 5-21 – 5-22). Measurements of the width/depth ratio also provide a visual assessment of channel cross-section shape. Channels with high W/D ratios (i.e. relatively wide and shallow channels) are sensitive to variations in discharge as the distributions of energy are such that stresses are directed toward the near bank regions. A substantial increase in the W/D ratio (i.e. channel becomes wider and shallower) may trigger a progressive sequence of activities that includes an increase in bank stress, an acceleration in bank erosion, an increase in sediment supply within the channel, a reduction in sediment transport capability (as the channel becomes an over widened channel), and finally an enhancement in deposition which may result in channel aggradation if the cycle persists. The W/D ratios, computed by utilizing data from the HEC-RAS Model and aerial photographs via ArcGIS, are also implemented to classify the stream type (Level I) and provide morphological descriptions (Level II) of the reaches of the White River (refer to chapter 4). The W/D ratios for various reaches of the White River are extremely high, averaging a value of approximately 29.5. The numerical quantity suggests that the

White River channel capacity is inadequate, in that its cross-sectional shape is too wide and shallow, suggesting that overbank flows are frequent. Comparison of aerial photos to quadrangle maps also indicates that multiple reaches of the White River, particularly the reaches below Augusta, have undergone channel widening or that its W/D ratios have increased in the last twenty plus years. Alterations in W/D ratios appear to suggest ongoing channel adjustments and reflect annual differences between erosion and deposition occurrences and magnitudes (Hooke, 2008). Plots of changes in the W/D ratios for various sections of the White River from the 1980s to the 2000s, computed based on the assumption that depth remains constant, indicates a dominant characteristic of width, hence W/D ratio, augmentation and a recessive characteristic of width diminishment. High degrees of W/D ratio augmentation imply high magnitudes of erosional activities of the banks and degradation of the bed while high degrees of W/D ratio diminishment indicate a prevalence in depositional activities as well as aggradation of the bed. Reaches exhibiting low occurrence, high numerical values of W/D ratio enhancement and distinct patterns of W/D ratio enhancement and reduction include Batesville to Augusta, Des Arc to Devalls Bluff, and St. Charles to LMR. Reaches exhibiting higher frequency of lower magnitudes W/D ratio enhancement include Augusta to Des Arc, Devalls Bluff to Clarendon, and Clarendon to St. Charles.

In single-thread meandering channels, with a W/D ratio of approximately 40 or less, channel incisions and meander widenings are characteristics of erosive behavior while point bar formations are characteristic of depositional behavior (Miall, 1977). Similar to other single-thread meandering channels, the physical manifestations of erosional and depositional activities within the channel of the White River occurred more

frequently in close proximity but not limited to the river bends rather than the inflection regions between the bends. Point bar formations, ranging from 100 feet to 200+ feet in width, and W/D ratio enhancements proximal to the river bends denote a larger susceptibility or variability for increasing values of discharge, denote that insignificant changes in water level may cause consequential changes in channel width or W/D ratio, and connote that the preponderance of excess energy dissipation may have been actuated by augmentation of velocity as the thalweg advances closer to the banks. The correlation between the asymmetrical channel cross-sections and high W/D ratios in the bend sections of the White River concurs with the latter part of the previous statement. In addition, the widths at the bend sections have often been found to exceed the widths at the inflection sections by a magnitude of two during bankfull condition, the elevations at which the W/D ratios become minima (Luchi et al., 2010). Generally, the width/depth (W/D) ratio is a robust indicator of trends in channel stability because W/D sensitivity to variations in discharge suggests a short-term evolution that may control meander development, contribute to compounded forms, and influence the curvature of the White River channel.

Sinuosity/Tortuosity ratio. Sinuosity, a geomorphologic parameter that generally describes the deviation of the planform of a river from a straight path, is the ratio of the length of the stream channel to the linear length of the valley. The sinuosity of a channel is also equivalent to the ratio of valley slope to channel slope. A variety of factors that controls sinuosity evolution includes valley or floodplain gradient, sediment load and calibre, cohesiveness of the banks and beds, initial morphologies of the floodplain (e.g. W/D ratio), and stream power (Kolla et al., 2007). Sinuosity is also often

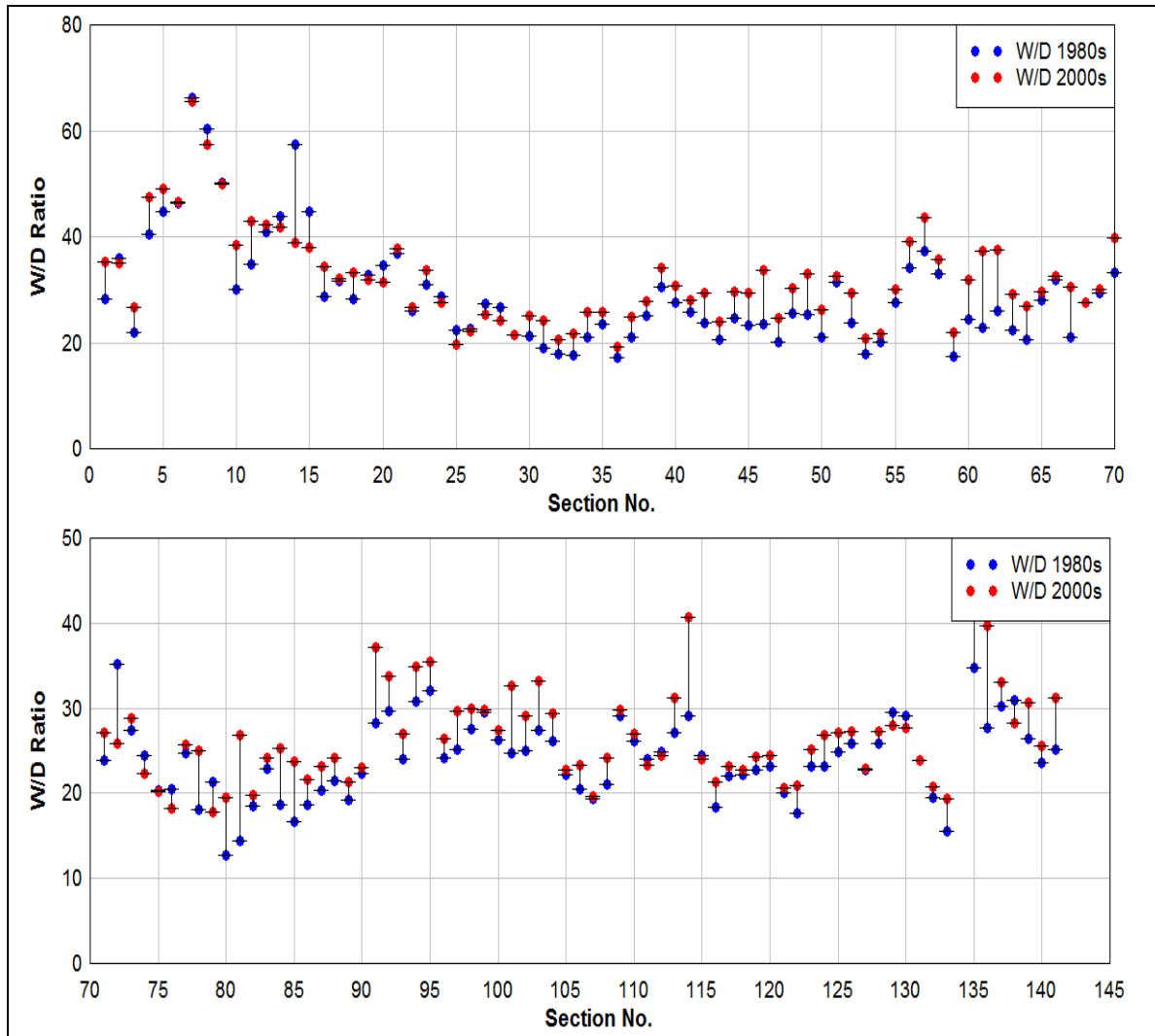


Figure 3.10. Width to Depth Ratios for Various Sections of the White River.

colligated with the principle of energy expenditure that justifies that in the attempt to build equilibrium profiles to maintain a dynamic equilibrium, or adjust its slope to that of its valley slope, (1) a fluvial system with stream power less than a certain threshold has to continually adjust to alterations in discharge and sediment load by meandering and (2) a fluvial system with stream power exceeding a certain threshold has to flow more turbulently to dissipate excess energy. Since stream power is a product of slope and discharge, the former alternative of the previous conjecture corresponds to a system with

a relatively flat longitudinal gradient while the latter alternative of the previous conjecture corresponds to a system with a steep longitudinal gradient. The flat gradient and the tortuous planform of the White River and its floodplain, respectively, suggests that the mechanism by which the White River developed a meander pattern involves convergent and divergent patterns of flow that result in the formation of pools and riffles. Water flowing through pools and riffles create helicoidal circulation and asymmetry in flow strength responsible for directing rapid flowing water to the concave bank causing erosion and sluggish water to the convex bank causing deposition, thus increasing the channel sinuosity.

Single-thread alluvial reaches that have maintained a sinuosity of approximately 1.3 without intensive point bar development or changes in width are deemed dynamically stable (Bledsoe & Watson, 2001). The long-term evolutions of sinuosity and bend morphology assert that major changes in sediment load and discharge are catalysts responsible for the initial progressive increase of sinuosity which triggers point bar development. Intensive point bar developments increase the sinuosity to an optimal critical state ($S = \pi$) at which a clustering of meander cutoffs take place (Stolum, 1996; 1998). Meander cutoffs result in a pronounced decrease in sinuosity followed by a period in which sinuosity oscillates to maintain equilibrium, and the cycle is repeated. In the case pertaining to the White River, the sinuosity ratios (S) are computed with the assistance of aerial photographs and quadrangle maps available in ArcGIS. The procedure implemented to determine sinuosity for the White River initially involved dividing the White River into various sections in such a way that each cutline intersects the channel perpendicularly (see **Figure 3.15**). The spacing criteria between cutlines follow a trial and error observational method that includes measuring the straight and

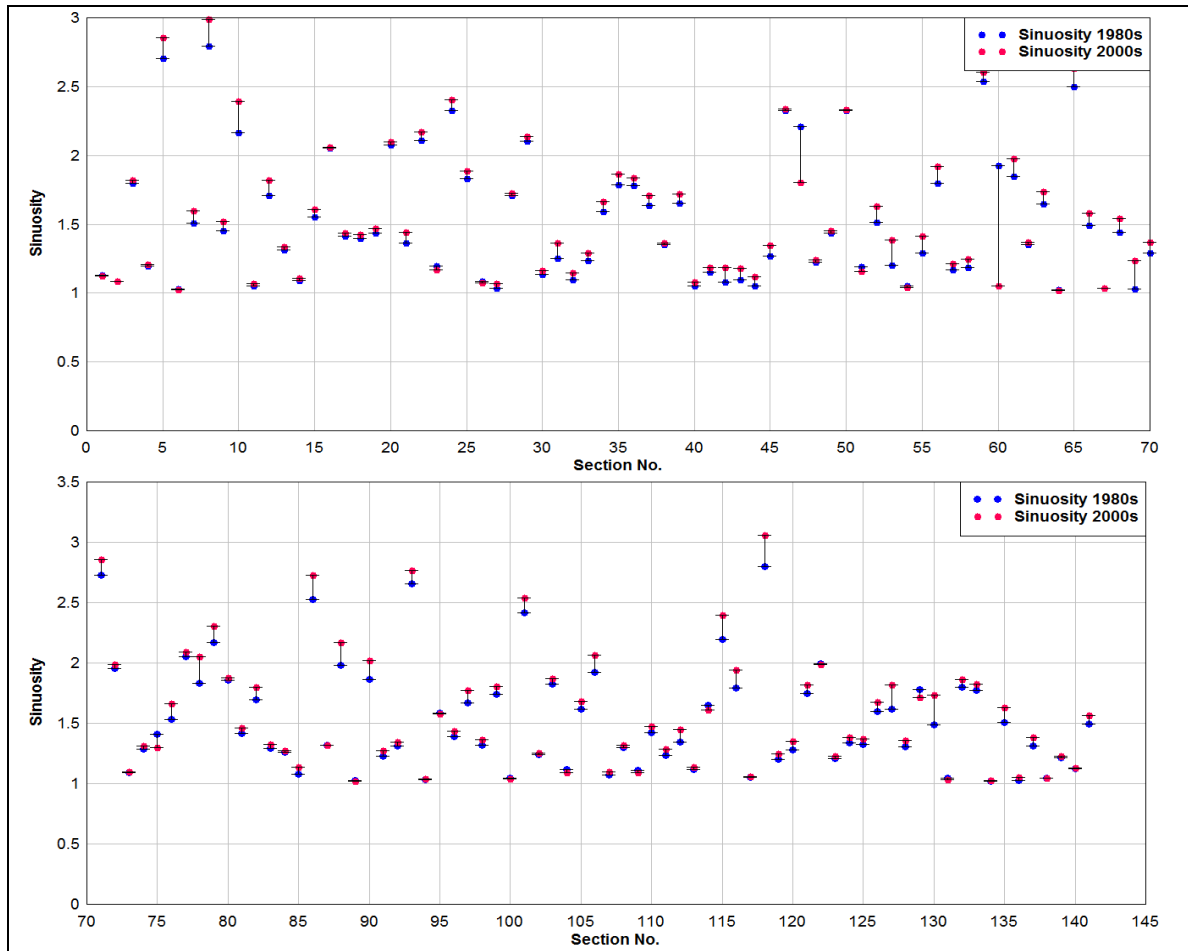


Figure 3.11. Sinuosity Values for Various Sections of the White River.

curve distances of a section, computing a numerical value for sinuosity, and checking the validity of the sinuosity value with the criteria that (1) if the sinuosity value is equivalent to unity based on the White River planform, the spacing interval between the cutlines is an underestimation and (2) if the sinuosity value equals or exceeds 3.14, the spacing interval between the cutlines is an overestimation. The sinuosity ratios for various reaches of the White River are high averaging an overall value of approximately 1.53. This numerical quantity coupled with numerous accounts of point bar developments and lateral migrations visible through aerial photos suggest that the White River is an actively

dynamic or meandering channel. Inspections of aerial photos and quadrangle maps also indicate a dominant characteristic of sinuosity enhancement and a less prevalent characteristic of sinuosity diminishment for various reaches of the White River. Plots of sinuosity ratios for various sections of the White River from the 1980s to 2000s show high degrees of sinuosity augmentations from Batesville to Newport, Des Arc to Devalls Bluff, and Devalls Bluff to Clarendon, and sinuosity diminishments at several sections from Augusta to Des Arc and Clarendon to St. Charles. Sections exhibiting the highest average value of sinuosity are proximal to the region extending from Devalls Bluff to Clarendon. Sections that decreased in sinuosity are sections proximal to oxbow lakes or previous cut-offs, specifically sections 23, 47, 60, and 75 (see the White River Planform in **Appendix F**). Alterations in sinuosity ratios appear to suggest ongoing channel adjustments as stream power and longitudinal gradient are significantly low for the White River.

Longitudinal gradient. Channel slope is “a major determinant of river channel morphology, and of the related sediment, hydraulic, and biological functions” (Rosgen & Silvey, 1996, p. 5-27). According to Lane (1957), the principal factors controlling stream channel form are slope, discharge, bed-bank material, and sinuosity. Of the principal factors controlling stream channel form, slope or the longitudinal gradient is the most significant as all other factors are contingent upon it. Since a fluvial system is continually adjusting its slope to that of its valley slope, the characteristics of all factors inherent to a fluvial system can be linked to slope. Relevant energy parameters, such as the magnitudes of flow volume and velocity of a discharge (i.e. stream power), is significant when the longitudinal gradient is steep and insignificant when the longitudinal gradient is

flat, i.e., stream power generally decreases with decreasing slope and increases with increasing slope. The effect of slope on sediment is such that steepening of the slope will likely result in an increase in the river's erosional power or sediment load, and vice versa (Cserkesz-Nagy et al., 2010). In addition, a sufficient array of slope data may provide valuable insights on the frequency and specific characteristics of bed features, such as riffles and pools, of a fluvial system. In regards to the principle of energy expenditure for a fluvial system with low stream power in which the primary mechanism of energy dissipation involves flowing in bends and meanders, an accompanying reduction of channel gradient is immanent (Harnischmacher, 2007). Consequently, a single-thread meandering fluvial system tends to possess a high sinuosity and a corresponding flat longitudinal gradient. The gradient also appears to affect bend development in that it decreases when meanders grow and steepens when meanders cut off. The White River reach extending from Batesville to the Lower Mississippi River is characterized by an average longitudinal gradient of approximately 0.00006, and it possesses an array of values that fall within the flat gradient category. The longitudinal gradient of the White River is obtained from the HEC-RAS Model by a procedure that includes setting a steady flow boundary condition to a normal depth criteria of 0.000018, performing a steady flow simulation, and measuring the one-year frequency inundation water surface slope from the HEC-RAS profile plot. The numerical value of 0.000018 is selected for the simulation as it warrants that the water surface slope (S) would be nearly parallel to the channel slope (S_o).

Geometric Morphological Parameters

The integration between the physical attributes of the setting in which a channel is situated and the water and sediment regimes that are conveyed through it are crucial to the development of the natural meandering pattern that the system exhibits. Adjustments in the planform of a fluvial system are colligated to the process in which the fluvial system continually attempts to develop a configuration that promotes optimum efficiency of water and sediment conveyance while simultaneously minimizing the energy expenditure mandatory for transport of water and sediment downstream. Analyses conducted by Leopold and Wolman (1960) of numerous river planform configurations, appearing as being simple and/or compounded, indicate that all rivers in general shared patterns that can be quantified by geometric variables. The planimetric view of river patterns, classified as either straight, meandering, braided, or anastomosis, are often described by the specific relationships of various geometric variables that include radius of curvature, meander wavelength, meander amplitude, and meander belt width. The strong correlation between the mentioned variables, often expressed as a function of bankfull width, enables the derivation of empirical formulae widely accepted as ‘meander geometry relations’ (after Leopold et al., 1964). The schematic diagram identifying components of a meander pattern are shown in **Figure 3.12**. Each individual component is briefly defined and discussed subsequently.

Meander belt width. The meander belt, or meander belt width, is defined as “the space [on either side of the belt axis] that a meandering watercourse occupies [or can be expected to occupy] on its floodplain, and in which all of the natural channel processes occur” (Parish Geomorphic Ltd., 2004, p. 3). The area interior to the imaginary meander

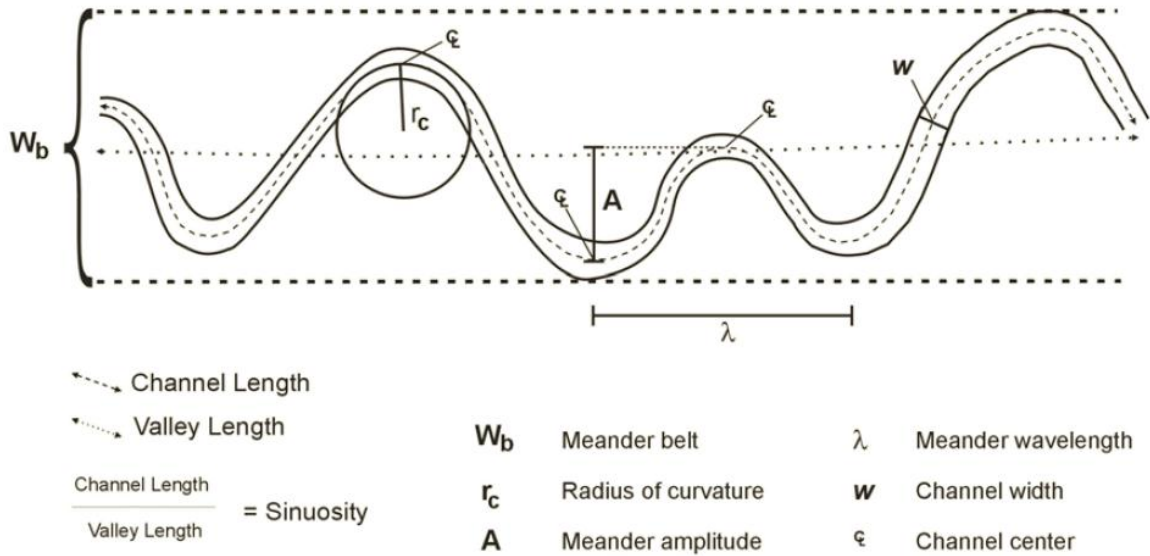


Figure 3.12. Schematic Diagram Identifying Terminology Used to Describe Different Components of the Meander Planform (Parish Geomorph Ltd., 2004).

belt width boundary lines represents the spatial interval that a watercourse can occupy while the area exterior to the meander belt width boundary lines represents the spatial region beyond which a watercourse can occupy. The conceptual line known as the meander belt axis, termed “the down-valley orientation of the meander pattern” (p. 21) by Parrish Geomorph Ltd. (2004), typically divides the meander belt into two equivalent regions. The preparatory steps undertaken prior to actual delineation of the White River’s meander belt width include (1) determining the meander belt axis based on general meander patterns observable through aerial photographs, and (2) addressing the limitations and assumptions of the delineative procedure. Since observations of the quadrangle maps and aerial photographs in ArcGIS clearly showed variabilities in radii, shapes, and frequencies of all meanders in a sequence of meanders along the White River, or that the meander patterns along the White River are irregular, the conceptual line that follows “the trends of the meandering pattern” is appropriately the meander belt

axis (Carson & Lapointe, 1983, as cited in Parish Geomorphic Ltd., 2004, Appendix B p. 5) (see **Figure 3.15**). The meander belt axis of the alluvial reaches of the White River is adjusted to follow the compound or irregular meander trends of two time periods (1980s and 2000s). The assumptions and limitations made are as follow: (1) the meander migration or evolution processes are ongoing, (2) the belt width of the channel varies since floodplain properties (e.g., gradient, vegetation, sediment) vary spatially, (3) “meander belt encompasses the area in which all future meandering and migration tendencies of the watercourse are anticipated to occur”, (4) meander belt ignores lateral and vertical confinements (e.g., levee and valley wall), (5) meander belt delineation procedure does not take into account alterations in hydrologic regime, and (6) meander belt delineation procedure involves a degree of subjectivity (Parish Geomorphic Ltd., 2004, pp. 41-42). The procedure implemented to delineate the White River’s meander belt involved placing lines, on both sides of the meander belt axis, tangential to the outside bends of the laterally extreme meander bends in a sequence of meanders. Since the assumption that the spatial occupation of the floodplain by the channel is unlimited, the meander belt boundary lines are placed in such a way that they follow the general unconfined valley trend while simultaneously being parallel to the meander belt axis. The meander belt widths are then measured normal to the tangential boundary lines and are tabulated for various reaches of the White River. The meander belt widths for various reaches of the White River averaged an overall value of approximately 17,000 feet with the reaches proximal to Newport and Clarendon averaging high values in the range of 20,000 to 23,000 feet. Variations in the meander belt widths within the White River drainage network, attributable to the characteristics of the local influences that include

longitudinal gradient, discharge, floodplain vegetation, bank height, and boundary materials, and irregularities in the meander patterns suggest dissimilarities in the degree of meander migration and heterogeneity in lenses and strata of resistant materials, respectively. In addition, “the width of the meander belt [also] represents the sum[mation] of the driving and resisting forces operative in the [White River] channel and in [its] floodplain” (Parish Geomorphic Ltd. , 2004, Appendix B p. 7). The aforementioned statement in conjunction with the irregular or compound configuration, which is discovered to occur when varying discharges influenced channel form, implies that the meander belt initiation and development within the White River basin are the resultant of the interaction between discharges (the driving factor) and the properties the floodplain (the limiting factor). Although the measurement of the meandering belt width does not provide specific information on the rate of meander adjustment and migration, it does provide an outline of the general meander pattern or sequence, an insight into the potential future evolution of a meandering planform in the across-valley and downstream directions, and a meandering boundary limit for planning purposes.

Radius of curvature. The radius of curvature of a sequence of meander bends describes not only the general planform of a fluvial system, but also the characteristics of its bedforms and flows. The influence of channel curvature on bedforms and flows is responsible for the spacing and frequency of riffle and pool features and the non-uniformity in flows or velocities within the channel, respectively. The frequency and spacing of riffles and pools are correlated to the radius of curvature such that a high magnitude of the radius of curvature usually corresponds to a high spacing interval of riffle and pool sequences and a low quantity of riffle and pool features. In other words,

“the riffle [and pool] numbers are [smallest] and the spacing [interval] is widest in the lowest curvature bend” and vice versa (Hooke, 2007a, p. 252). The divergent and convergent patterns of flow that formed riffles and pools, which are responsible for helicoidal circulation that directs rapid flowing water to the concave bank and sluggish water to the convex bank, implied a general conjecture that water moves faster in bends with smaller radii of curvature and the contrary is anticipated. The factual information that verifies the previous conjecture is the presence of point bars at the bend apex sections of a channel, which denote erosional and depositional activities actuated by a higher flow velocity toward the concave bank of the meander bend. Wider widths at the apex sections of a channel also suggest a high correlation between radius of curvature and width variation (i.e., wider width is correlated to low radii of curvature). In the case pertaining to the White River, the radii of curvature for various meander bends are acquired through ArcGIS by a procedure that includes placing a circular buffer zone to superimpose the curve of the exterior channel boundary, locating and placing a focal point within the circular buffer zone, and measuring the radius of curvature from the focal point to the border of the buffer zone. Since the White River exhibits irregular or compounded meander patterns, possibly a resultant of localized erosion at various sections that has metamorphosed low curvature loops into compounded forms over time, the array of the radii of curvature measured also exhibits a significant degree of variability. The variation in radius of curvature reflects the “adjustments that occur within the channel that change the radius of curvature towards an equilibrium relation with the flow” (Parish Geomorphic Ltd., 2004, Appendix B p. 4). The reach from St. Charles to the Lower Mississippi River appears to have maintained very low ranges of radii of

curvature while the reach from Clarendon to St. Charles indicates a very high degree of disparity. For comparison purposes with other morphological parameters and considering that the tortuous planform in most cases showed clusters of the radii of curvature per section, a composite quantitative value of radius of curvature is applied to each individual sinuosity section as indicated by the unified table (see **Table E.1**).

Table 3.3. Composite Radii of Curvature for Various Reference Reaches of the White River.

Sections	Mean R_C (ft)	Minimum R_C (ft)	Maximum R_C (ft)	Standard Deviation
Batesville - Newport	2671.34	1310.36	4837.48	1076.58
Newport - Augusta	2242.83	1150.57	3886.28	735.53
Augusta - Des Arc	1923.02	845.41	3554.61	597.07
Des Arc - Devalls Bluff	2319.68	1509.01	5013.58	1046.11
Devalls Bluff - Clarendon	1795.99	1187.56	3471.25	608.42
Clarendon - St. Charles	2524.85	1296.46	9814.67	1795.25
St. Charles - LMR	1826.33	841.54	3709.69	731.03

Meander amplitude. Migration tendencies to move laterally across a floodplain and/or in a downstream direction and to occur at discrete locations at any one time in response to the interaction or adjustment between the controlling factors such as flow and sediment regimes, boundary materials, longitudinal gradient, and vegetation are exclusively accountable for the configurations of individual meanders and meander sequences which can be quantified by the meander belt width (Burke 1984; Mathes, 1941). Like the meander belt width, the meander amplitude is also a term that “quantif[ies] the lateral extent of a river’s occupation on the floodplain” (Parish Geomorphic Ltd., 2004, p. 7). The distinction that separates the meander amplitude from

the meander belt width is that the meander amplitude is the lateral distance measured perpendicular to two “tangential lines drawn to the center of two successive meander bends” (Leopold et al., 1964, as cited in Parish Geomorphic Ltd., 2004, p. 7). Because the meander amplitude is measured to the center of the channel as opposed to the exterior bends of the laterally extreme meander bends, it is always smaller than the meander belt width even in instances where one and only one bend innately defined the meander belt (Parish Geomorphic Ltd., 2004). Unlike the meander belt width, which can be measured directly from one boundary line to another regardless of configuration, the meander amplitudes for meander bends with irregular forms are difficult to measure due to a lack of available guidelines. In the case pertaining to the White River’s irregular meander bends or sections, the meander amplitudes are measured perpendicularly from the line that makes up the straight distance of a sinuosity section to the channel centerline of the laterally extreme meander bends. For comparison purposes with other morphological parameters and considering that a section may exhibit several amplitude values, one composite amplitude quantity represents each individual sinuosity section. The variation in amplitude values indicates that the presence of "resistant materials in the [White River] floodplain may interfere with the [direction and] rate of meander [movement (e.g. meander shift, elongation, and rotation)], [thus] contributing to the [perceivable] irregular planform” (Parish Geomorphic Ltd., 2004, Appendix B p. 3).

Meander wavelength. Meander wavelength is another component that describes the meander planform of a fluvial system. Meander wavelength is often defined as the linear distance between two consecutive inflection points in the channel. Alternately, meander wavelength also represents “twice the linear distance between two consecutive

points of similar condition (i.e., pools or crossings) in the channel” (Watson, Biedenharn, & Scott, 1999, p. 32). The latter definition of wavelength is often referred to as the axial meander wavelength to distinguish it from the former definition. Since width and meander wavelength are dependent upon the discharge and sediment load conveyance of a channel, meander wavelength versus width relationship is often regarded to be the most significant geometric relationship for channel form. Various hydraulic geometry relationships or empirical formulae indicate that stable meander wavelengths generally fall in the range of 11 to 12.5 times the width (Hey, 1976; Leopold & Wolman, 1960; Richard, 1992; Thorne, Hey, & Newson, 1997; USDA-NRCS, 2007). According to Leopold (1994), the relationship between meander wavelength and width could be implemented to predict channel instability if meander wavelength(s) of a given stream deviate from the linear empirical relationship. The wavelengths for various sections of the White River, as measured from aerial photographs via ArcGIS, illustrate high degrees of disparity or non-uniformity which confirm the heterogeneity of boundary materials implied previously. High degrees of disparity between measured meander wavelength quantities also corroborate the fact that the waveforms in bed topography and planform, which are associated with the mechanics of the flow that shaped the channel forms and features, are the resultant of an irregular mechanism of erosion and deposition.

Empirical Correlations Between Parameters

Various fluvial and morphological parameters presented by the unified table (**Table E.1**), a product resulted from the synthesization of the HEC-RAS Model and ArcGIS data, are plotted to determine the specific formulae associated with discernible correlations among parameters. Since a considerable quantity of available data may

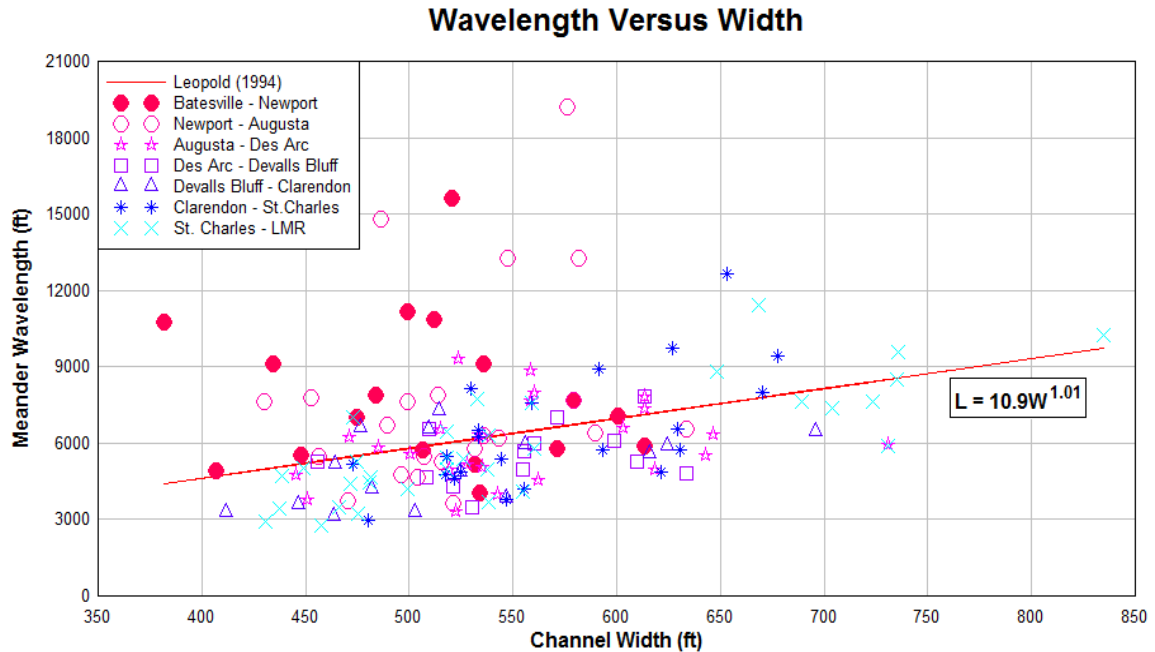


Figure 3.13. Leopold's Empirical Formula for the Relationship Between Meander Wavelength and Channel Width.

permit multitudinous relationships between parameters, only apposite correlations that exhibit an acceptable degree of agreement or an adequate correlation coefficient are included, presented, and briefly discussed subsequently.

Meander wavelength versus channel width. Wavelength versus width relationship, as mentioned previously, is often regarded to be the most significant geometric relationship for channel form because it could be implemented to predict channel instability. Leopold suggests that dispersion of meander wavelength(s) in a wavelength versus width relationship signifies channel instability while others elaborate that a stable meander wavelength falls within the range of 11 to 12.5 times the width (Leopold & Wolman, 1960; Hey, 1976; Richards, 1982; Thorn, 1997; USDA-NRCS, 2007). In the case pertaining to the White River, the empirical relationship of wavelength

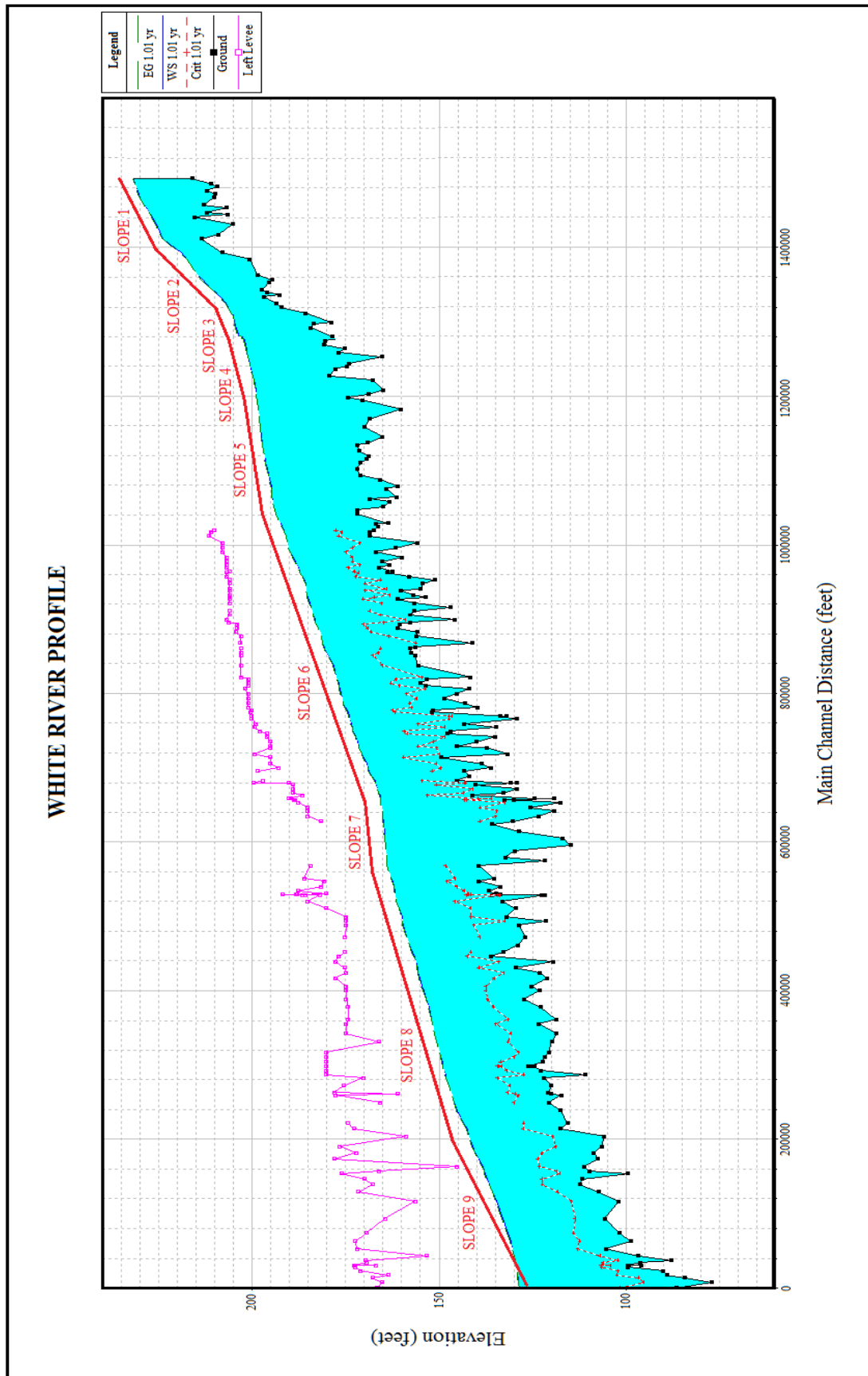


Figure 3.14. HEC-RAS Profile of the White River.

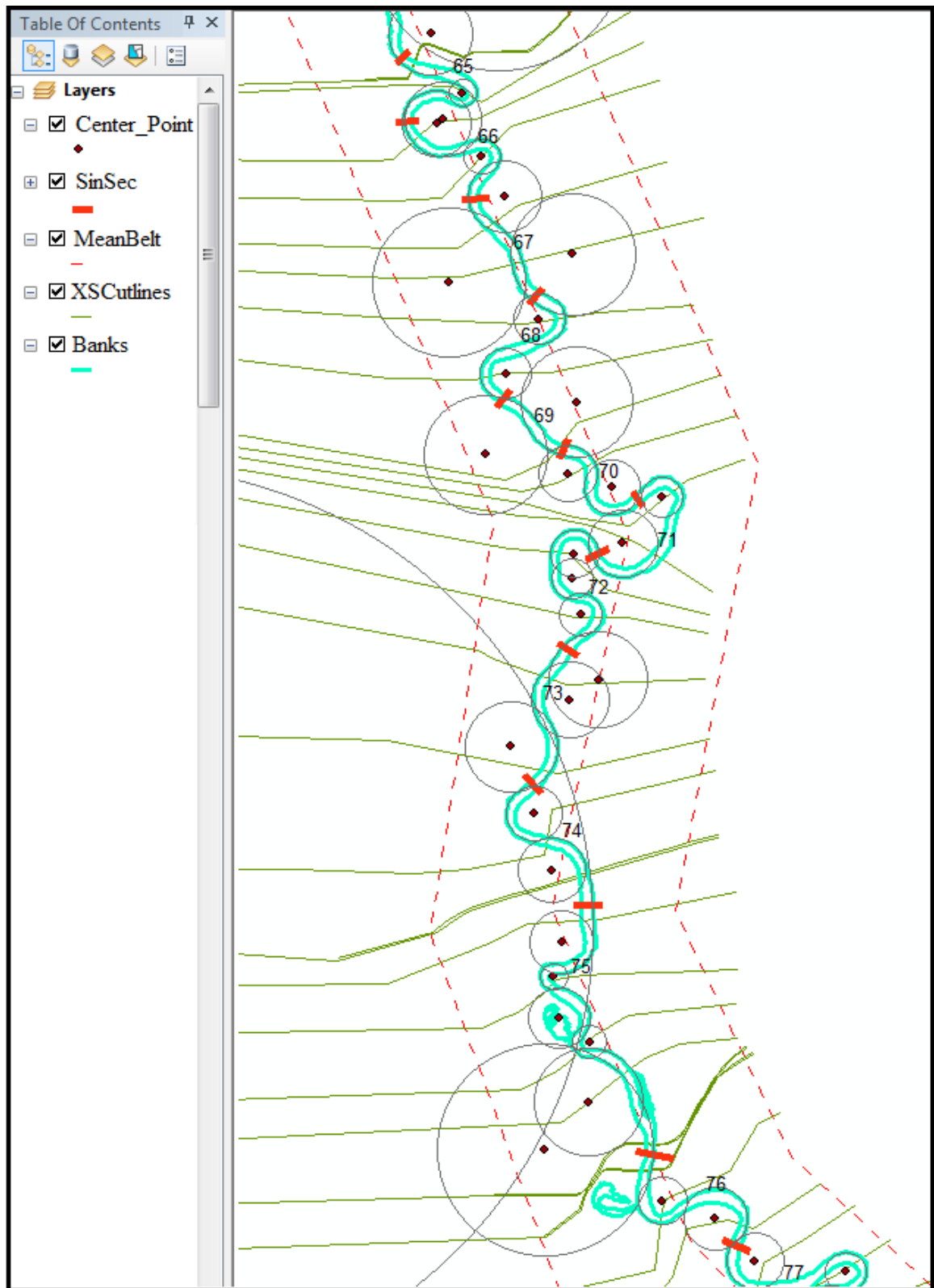


Figure 3.15. Planform Illustrating ArcGIS Applications to Determine Sinuosity, Radius of Curvature, Meander Amplitude, Meander Wavelength, and Meander Belt Width.

and width indicates a degree of instability in channel form as the array of wavelengths, approximately 16 times the width, exceeds the stability thresholds. Reaches exhibiting very high disparities in wavelengths include Batesville to Newport, Newport to Augusta, and Clarendon to St. Charles. In comparison to other reaches, the reaches from Batesville to Newport and Newport to Augusta exhibit the highest degrees of disparity as predicted. It is suspected that for Batesville to Newport, which represents the transition zone from the Ozark Plateaus to the Mississippi Alluvial Plain, variations in wavelengths may be attributed to the crooked and rapid flow that generated sufficient energy to erode through the bedrock (i.e. the channel is structurally controlled). In addition, variations of valley slopes, and ultimately sinuosity ratios and wavelengths, may be attributed to the southeast-trending White River Fault Zones that formed the spatial boundaries that the Batesville to Newport segment occupies. For the reach from Newport to Augusta, it is possible that intense weathering occurring along the intersection of the Rift Margin Fault and the northwest trending faults, which are coincident with the White River Fault Zone, may contribute to higher wavelength variations. Dispersion in meander wavelengths for Clarendon to St. Charles, which does not exhibit any data points on the linear regression line, is contributed by highly erodible beds and banks and high dune wavelengths and amplitudes, and may be influenced by the Rift Margin Fault and the Big Creek fault zone. Overall, heterogeneity in lenses and strata of resistant materials and variations in rates and patterns of sediment yield are primarily responsible for the dispersion of wavelength quantities on the reaches of the White River.

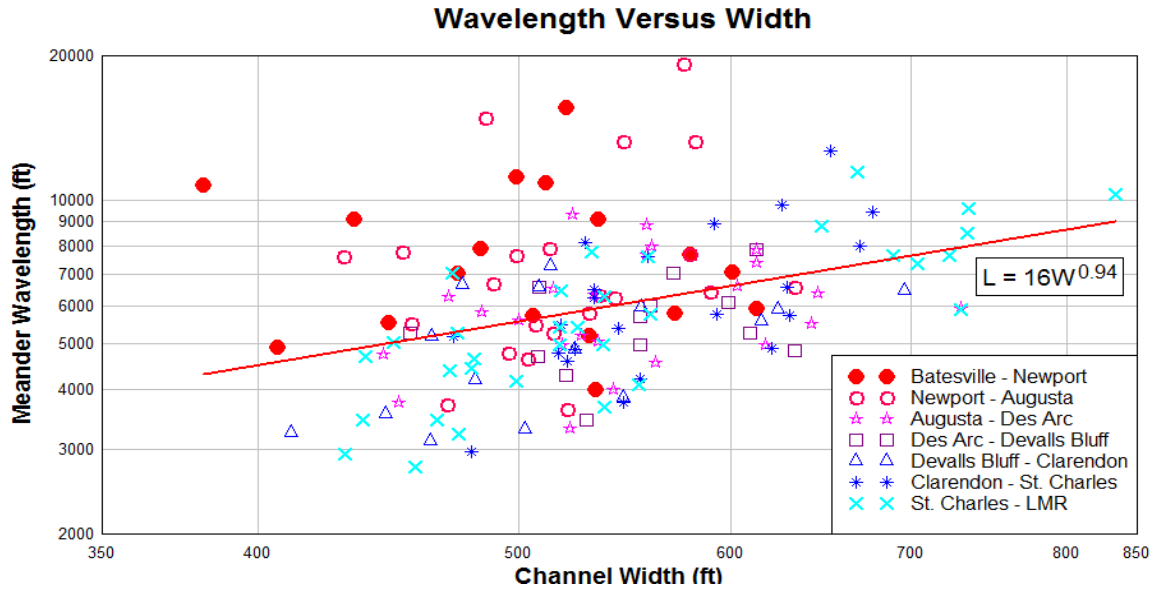


Figure 3.16. Correlation of Meander Wavelength Versus Channel Width.

Meander wavelength versus radius of curvature. Meander wavelength versus radius of curvature shows a positive monotonic correlation. The array of meander wavelengths is approximately 146 times the square root of the radius of curvature. **Figure 3.17** suggests that higher wavelengths correspond to a more linear channel planform while lower wavelengths correspond to a meandering planform. Irregular patterns of erosional and depositional activities actuated by non-uniformity in flow through heterogeneous resistant material are responsible for the reduction and augmentation of both wavelength and radius of curvature, thus resulting in the correlation shown by the subsequent figure.

Meander wavelength versus bend length. Bend length and wavelength also exhibit a positive correlation. The strength of the relationship between bend length and wavelengths is greater, or the correlation coefficient is higher, as the plot displays sufficient degree of perceptibility in trend and less scattering of data points. The

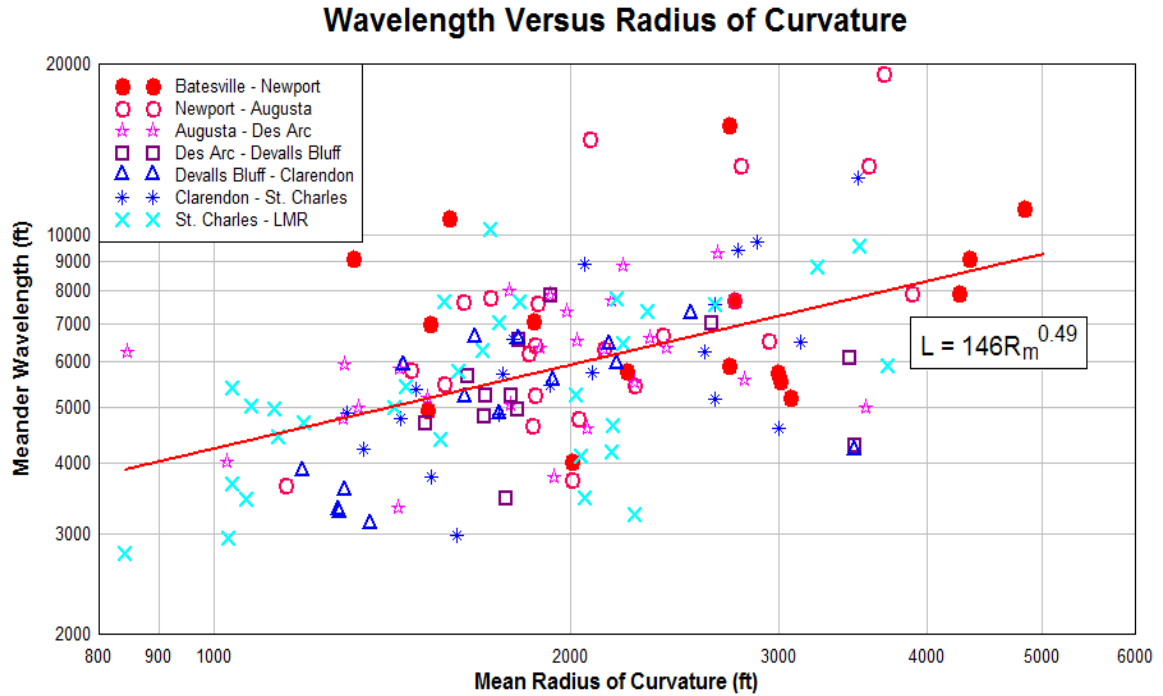


Figure 3.17. Correlation of Meander Wavelength Versus Mean Radius of Curvature.

correlation of bend length versus wavelength that indicates that bend length augmentation corresponds to wavelength augmentation and vice versa, however, contradicts the correlation between wavelength and radius of curvature which implies that higher wavelengths would accommodate a more linear planform. Perhaps the method implemented to determine the wavelengths are inaccurate as the overall White River planform is very irregularly tortuous. However, the correlation may just be the resultant of implementing sinuosity sections of varying scales.

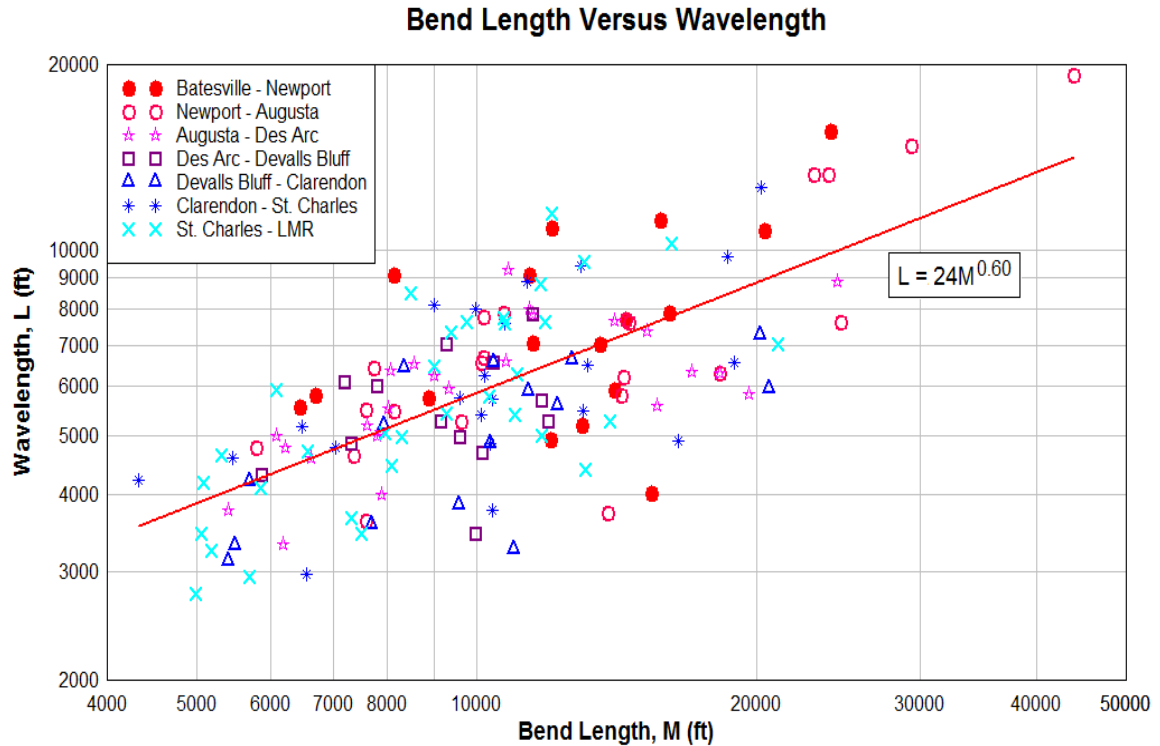


Figure 3.18. Correlation of Bend Length Versus Meander Wavelength.

Width to depth ratio versus radius of curvature. As shown by **Figure 3.19**, the width to depth ratio is also positively correlated to the radius of curvature. The correlation indicates that as the W/D ratio increases, an increase in radius of curvature (i.e., the channel is becoming straighter) is immanent. The segments from Batesville to Newport and St. Charles to LMR appear to exhibit high magnitudes of W/D ratio and deviation from the correlation line. The greatest deviation of W/D ratios from the regression line, however, clearly corresponds to high magnitudes of radii of curvature. Conversely, for the segment from Devalls Bluff to Clarendon, a majority of data points that possessed low magnitudes of radii of curvature also possessed low magnitudes of W/D ratios that deviate greatly from the regression line. In contrast to W/D ratios for the segments from Batesville to Newport and St. Charles to LMR, which exhibit the highest

degrees of deviation above the regression lines, the majority of the W/D ratios for the segment from Devalls Bluff to Clarendon that deviate from the regression line deviate below the regression line. The apparent trend is that the segment from Devalls Bluff to Clarendon with an array of low magnitude curvatures and W/D ratios constitute a tortuous planform (i.e., high sinuosity). The opposite applies to segments from Batesville to Newport and St. Charles to LMR. It is speculated that the correlation between W/D ratio and radius of curvature in conjunction with an accepted conjecture that high W/D ratios represent susceptibility to frequent overbank flows as well as sensitivity to variations in discharge (due to greater exertion of stresses toward the near bank regions) is analogous to the theory associated with braided channels, which are often unstable despite possessing sinuosity values of lower magnitudes. In this context, significant departure of W/D ratios above the steady augmentation of the array of radii of curvature represented by the regression line would likely signify instability of the banks and attenuation of the capability to transport sediment while significant departure of W/D ratio below the regression line would likely represent less susceptibility to discharge variations and less uniformity in flow; the latter of which appears to corroborate Schumm's (1969) conclusion that small width to depth ratios correspond to large sinuosity values. Significant departure of W/D ratios below the regression line, as is the case for the reach extending from Devalls Bluff to Clarendon, may also imply a high percentage of silt-clay contents within the channel; a speculation based on Schumm's study of 39 alluvial rivers which indicated that a larger percentage of silt-clay contents in the sediment that forms the channel bed and banks always accompany a smaller width to depth ratio.

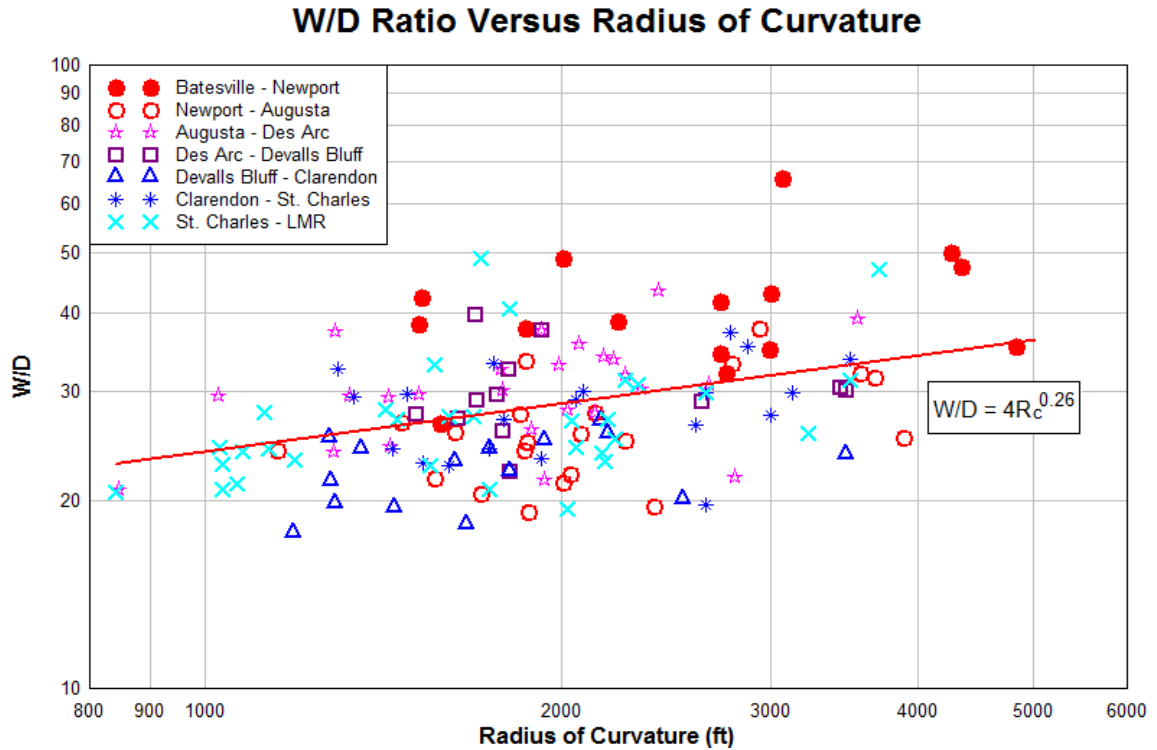


Figure 3.19. Correlation of Width to Depth Ratio Versus Radius of Curvature.

Channel dimensions versus radius of curvature. The correlation of channel dimensions to meander-bend radius of curvature distinctively shows high values of cross-sectional area, width, and mean depth for the segments from Devalls Bluff to Clarendon and St. Charles to LMR, and, conversely, for the segment from Batesville to Newport. Mean depth and cross-sectional area are negatively correlated to radius of curvature while channel width is positively correlated to radius of curvature. The correlations of channel cross-sectional area to meander-bend radius of curvature and depth to meander-bend radius of curvature for the White River appear to contravene the principle that depth and area amplify with curvature augmentation, as shown by Williams (1986) using separate data taken from 79 sites. The relationship between radius of curvature and channel width is highly perceptible as data points are less dispersed while the relationships between

radius of curvature and depth and radius of curvature and cross-sectional area are imperceptible due to high degrees of data scattering. This is especially noticeable for the segments from Batesville to Newport, Devalls Bluff to Clarendon, and St. Charles to LMR. It is speculated that high degrees of deviation from the regression line may represent discrepancies between channel dimensions and radii of curvature, and that reaches that exhibit such discrepancies are likely more sinuous. Therefore, unusually low depths and cross-sectional areas for the reach extending from Batesville to Newport and extremely high depths and cross-sectional areas for the reach extending from Devalls Bluff to Clarendon may imply the possibility of dynamic disequilibrium for the channel of these sections. Similarly, for the reaches extending from St. Charles to LMR, high channel dimensions of area, width, and depth with respect to radii of curvature may constitute dynamic disequilibrium.

Curvature versus sinuosity. Substantial evidence from detailed studies of river bends by Hooke (1987), Biedenharn, Combs, Hill, Pinkard, and Pinkston (1989), and Hickin and Nanson (1975, 1984) have shown that the rates of channel migration are controlled by channel curvature as represented by R_c/W . Previous findings have demonstrated that the optimal rate of channel migration, or maximum erosion rate, tends to occur when the ratio of radius of curvature to channel width value is between 2 and 3. Beyond this range on either side, attenuations in the rate of migration are observable. Since “the loss of energy [is] associated with flow through a bend, a maximum bend sharpness exists beyond which further significant lateral erosion is unlikely to occur” (Lagasse, Spitz, Zevenbergen, & Zachmann, 2004a, p. 11). When the channel curvature (R_c/W) falls below a value of 2, diminishments in the rate of lateral migration are

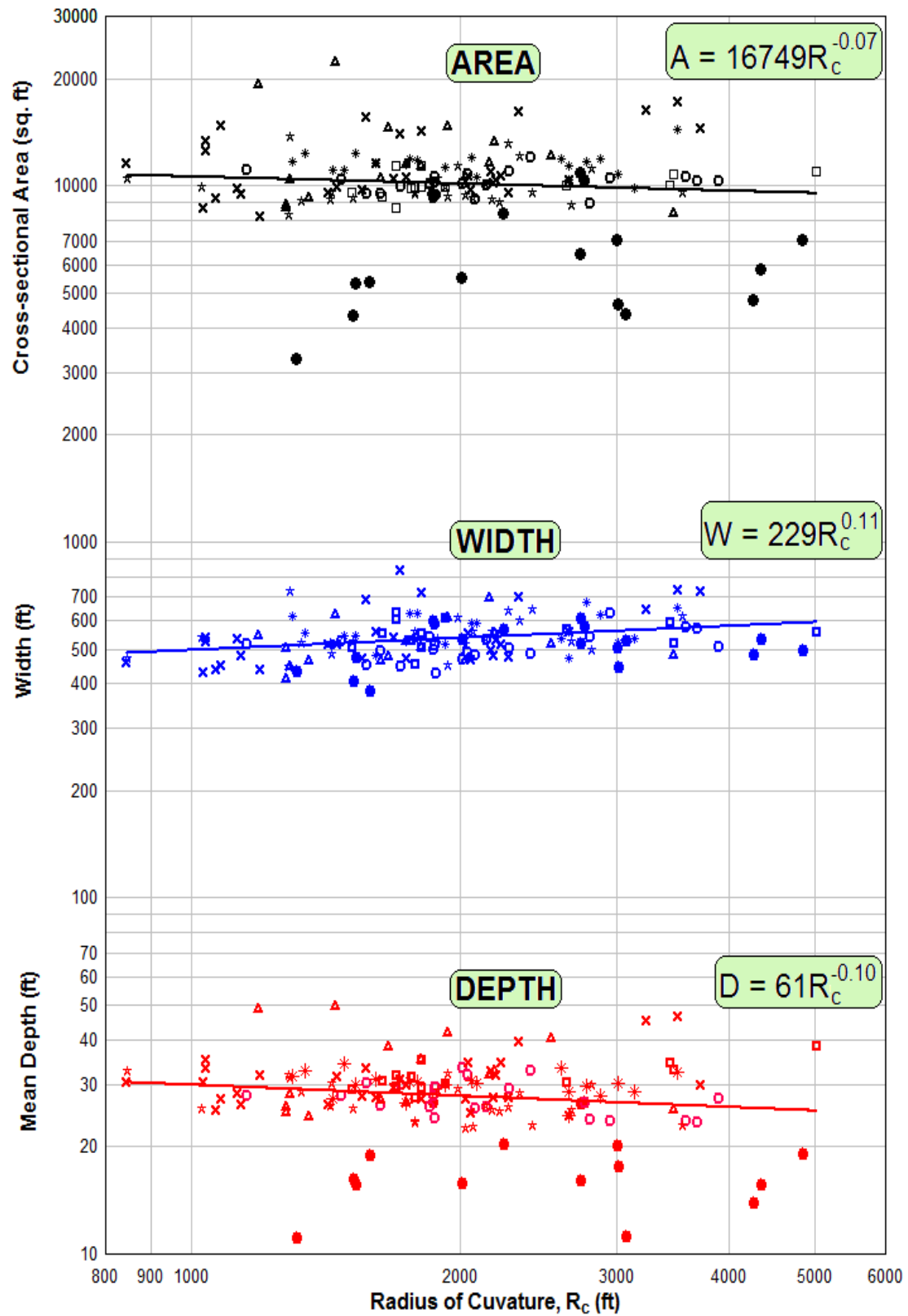


Figure 3.20. Correlation of Channel Dimensions Versus Radius of Curvature.

attributable to energy loss in the bend, augmentation in resistance, and diminishment in outer-bank radial force which may constitute deposition along the outer bank of the meander bend. In the case pertaining to the White River where the rate of lateral migration is unavailable, the correlation between sinuosity and channel curvature indicates a similar overall pattern. The envelope curve demonstrates that optimal magnitudes of sinuosity tend to fall within a channel curvature value of between 2.75 and 3.75. The finding suggests that the rate of lateral migration is coincident to sinuosity. An additional plot of sinuosity versus radius of curvature also displays an analogous pattern which denotes that when the radius of curvature is approximately 1250 to 2000 feet, high sinuosity quantities and high lateral migration rates are anticipated. Furthermore, when the lines of demarcation are applied to sinuosity values of 1.5, 2.0, 2.5, and 3, the reaches that exhibit highest frequencies of sinuosity quantities above 1.5 are Batesville to Newport, Devalls Bluff to Clarendon, and St. Charles to LMR. The discovery affirms the conjecture that high degrees of deviation of channel dimensions (i.e., cross-sectional areas, widths, and mean depths) from the channel dimensions versus radius of curvature regression lines correspond to high sinuosity values.

Specific energy versus sinuosity. In contrast to previous correlations among various parameters that have resulted in simple monotonic power functions, the relationship between sinuosity and specific energy, or the total energy of the flow with reference to the channel bed as the datum, is distinguished by a third-order polynomial function illustrating an oscillating pattern. The cubic function, which shows mean specific energy as a function of average sinuosity for the alluvial reference reaches, distinctively illustrates fluctuations in sinuosity values as specific energy increases. The

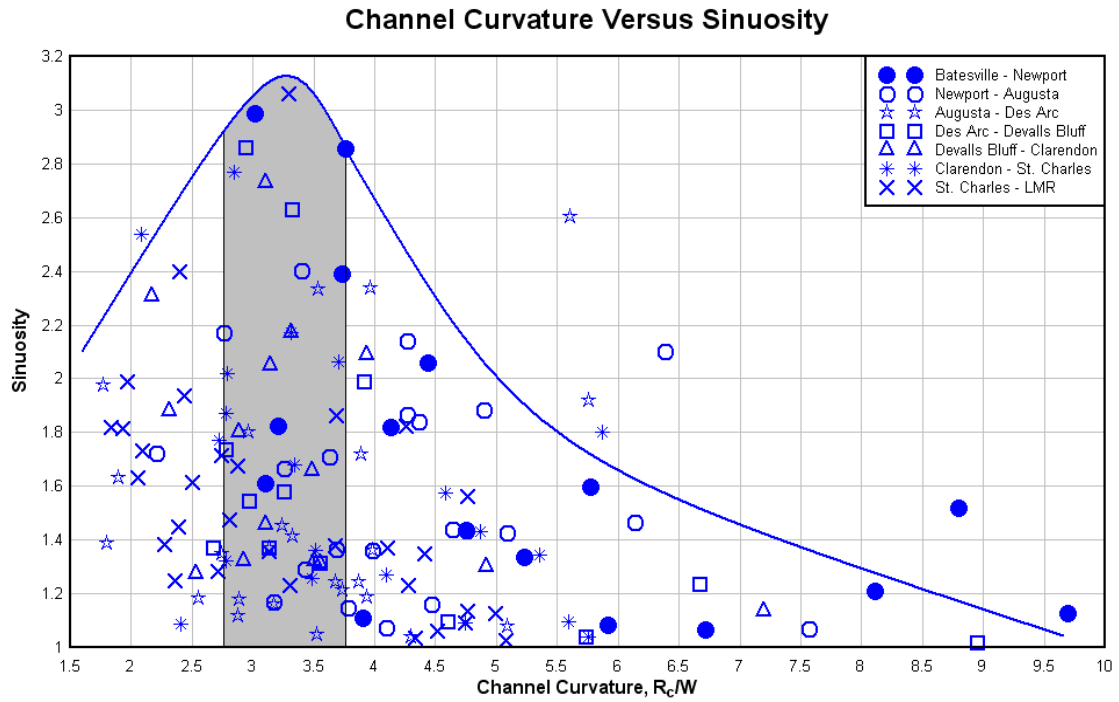


Figure 3.21. Correlation of Channel Curvature Versus Sinuosity.

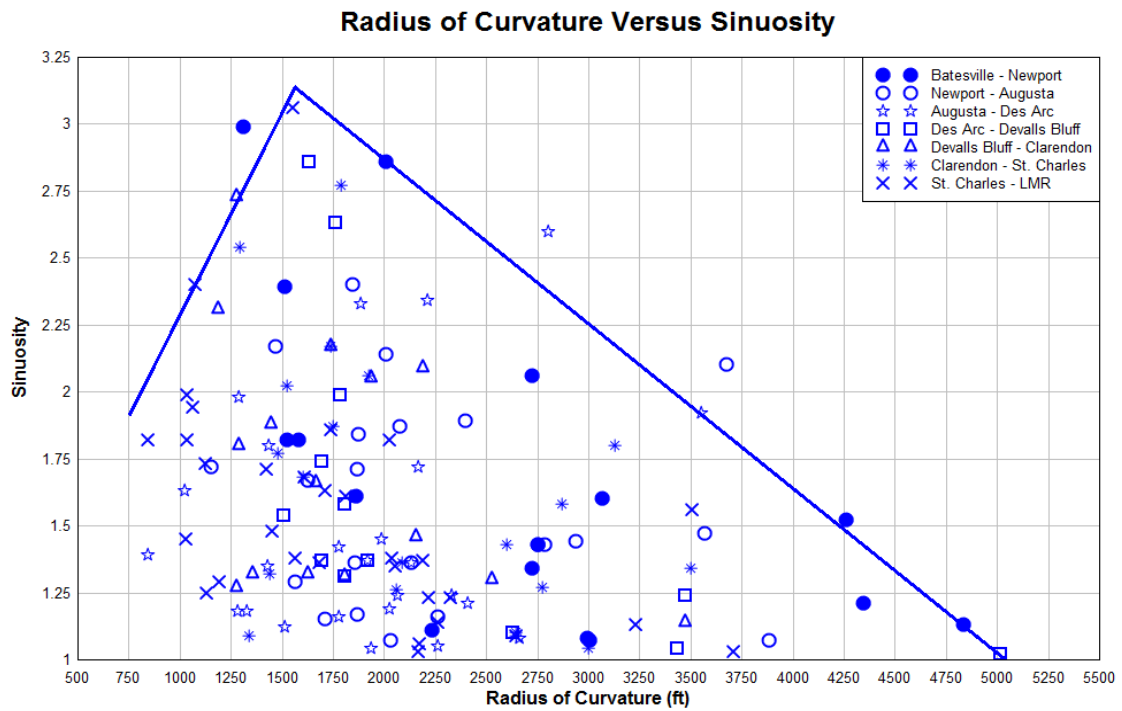


Figure 3.22. Correlation of Radius of Curvature Versus Sinuosity.

presence of both diminishments and augmentations in sinuosity values with respect to general amplifications in specific energy, however, does not impede the conception of the conjecture that, for the case involving the White River system and its alluvial sections, high specific energy is tantamount to high susceptibility to alteration in discharge. This speculation is derived from both the steep acclivities shown in the correlation plots for the reaches extending from Des Arc to Devalls Bluff and Devalls Bluff to Clarendon, which possess sinuosity and specific energy values that occupy the upper high ranges, and the high channel depths shown in the HEC-RAS river profile for these reaches. Since the channel depth within the aforementioned reaches greatly exceeds the remaining alluvial sections and since the channel depth represents the potential energy term during computation of specific energy, a product of the sum of a potential energy term and a kinetic energy term, high magnitude of channel depth must therefore account for much of the energy of the flow within the channel of the reaches extending from Des Arc to Devalls Bluff and Devalls Bluff to Clarendon and constitutes a high potential for flooding as the channel bed elevation is lower or the channel more incised in the valley. In terms of flow energy expenditure without taking into account the contribution of stream power and the influence exerted by the longitudinal gradient on discharge, it is reasonable to anticipate that the distributions of potential and kinetic energy within the terminology of specific energy are crucial to excess energy dissipation mechanisms (within various localities of this fluvial system) in the sense that reaches exhibiting preponderance in kinetic energy over potential energy, or reaches with low channel depth, possess higher propensity for excess energy dissipation while reaches displaying preponderance of potential energy over kinetic energy, or reaches secernated by high channel depth, yield

lower propensity for excess energy dissipation. The implication of this inference is that reaches characterized by dominances of potential energy or reaches distinguished by high-order magnitudes in depth are not only prone to inundation episodes, which appear to connote an outcome encompassing sinuosity augmentations as erosion and deposition transpire when the water level rises and falls, but also likely feature a dearth of an effective and exuberant mode of energy dissipation, which likewise signify the imminence of an alternate mode of energy dissipation via thalweg and bedform oscillations resulting in the promotion of sinuosity enhancements. This explains why high specific energy, hence high channel depth or potential energy, generally conform to a high sinuosity for the White River fluvial system and related reference reaches. Additionally, the rationalization involving energy distribution and energy expenditure also appears to denote connectivities between high specific energy and high lateral migration and high specific energy and high erosional and depositional activities.

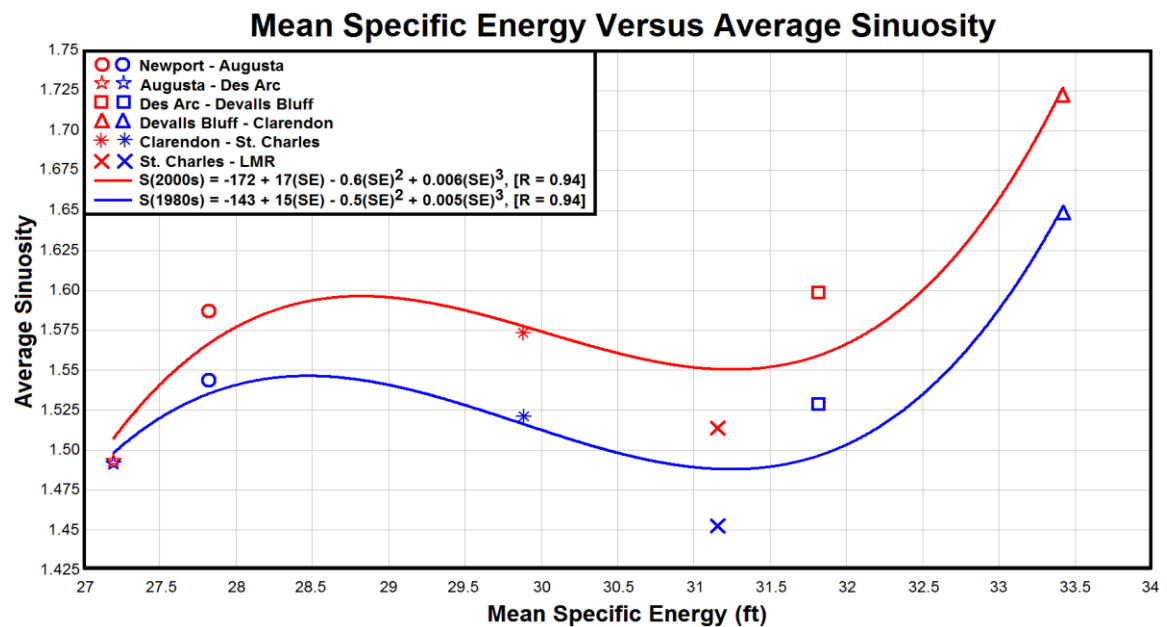


Figure 3.23. Correlation of Specific Energy Versus Sinuosity.

Bankfull discharge versus slope versus sinuosity. Conventional theory suggests that the apperception of “the interpretation of morphology and morphological changes in fluvial geomorphology” is tightly entwined with the theory of equilibrium and adjustment otherwise known as Mackin’s concept of “graded stream” (Hooke, 2007a, p. 237; Mackin, 1948). Central to this concept is the idea of autogenic adjustments in channel form to develop an equilibrium configuration that promotes optimal mobility of water and sediment load delivered to the channel. Autogenic adjustments in channel form, whether gradual or spasmodic or both, are set forth by the initial responses in the fluvial system to changes in intrinsic and extrinsic controlling factors. Responses of the fluvial system to allogenic causes of change in the basic external factors, which may be promoted by climate change, land-use change, and other human induced changes, and to progressive and fulminant changes in the intrinsic controlling factors, which may be initiated by an imbalance in the inflow and outflow sediment discharges, occurred at what are referred to as the extrinsic and intrinsic thresholds, respectively (Schumm, 1985). On a short time scale, the evolution of the channel form of a fluvial system, explained as an adjustment to changed intrinsic factors when longitudinal gradient and water discharge are considered independent variables, will transpire during the instance when the intrinsic threshold is reached (Schumm, 1985; Sturm, 2001). Conversely, on a much longer time scale, the evolution of channel form is colligated to the extrinsic threshold under circumstances where water and sediment discharges become the independent variables. Since remarkable variability in sinuosity has been found to be dependent on the longitudinal gradient and water and sediment discharges, the range of pattern adjustments or the adjustments in the channel planform from straight to meandering to braided are

characteristics of both the effects of intrinsic and extrinsic threshold conditions. For this reason, a parametric correlation expressing sinuosity as a function of the channel slope and bankfull discharge for the White River can reveal pertinent information on the long and short term evolution of its channel form as well as the effects induced by the long-term and short-term bed adjustments, or channel aggradations and degradations, on its planform at a given discharge. The creation of a three-dimensional chart showing sinuosity as a function of both channel slope and bankfull discharge follows a procedure that includes (1) plotting changes in sinuosity to different values of longitudinal gradient as the vertical axis, (2) plotting the bankfull discharge versus the longitudinal gradient as the horizontal axis, and (3) deriving a new discriminant line or threshold to predict the meandering range within the alluvial sections of the White River. The correlation that makes up the vertical axis is based on flume model experiments conducted by Schumm and Khan (1972) to illustrate the dependency of thalweg sinuosity on varying angles of the longitudinal gradient. The results indicate that for a given discharge with constant sediment load, the sinuosity of a meandering river increases with an accompanying augmentation in the longitudinal gradient until it arrives at a critical dip; beyond this critical gradient angle, the thalweg sinuosity progressively declines and the channel straightens and eventually attains a braided pattern. The horizontal axis represents the classic slope versus discharge diagram of Leopold and Wolman (1957), which separates the natural range of meandering from braided patterns. Synthesizing the two diagrams and assuming that the correlation of Schumm and Khan (1972) is valid for differing values of discharge permit the projection of an optimum sinuosity value onto the slope versus discharge correlation plot, thus defining a new discriminant line separating the

range of self-organizing meandering from the range of unorganized meandering. Plotting the discharge and slope values extracted from the HEC-RAS Model for the alluvial sections of the White River with the composite diagram showed that the White River fluvial system resides within the range of self-organizing meandering or well below the range of unorganized meandering. The implication is that since the alluvial sections of the White River fall well below the range of unorganized meandering, any progressive or spasmodic augmentation and diminishment in longitudinal gradient and discharge will result in an enhancement of sinuosity. The occupation of the White River well within the range of self-organizing meandering also suggests that “the formation and maintenance of patterns [are prevalently] attributable to the internal dynamics of the system [and secondarily to external controls or inputs]” (Hooke, 2007a, p. 239). In simple terms, the White River fluvial system has not reached the critical limit, or the critical longitudinal gradient angle where sinuosity peaks, that forces the channel to undergo radical morphological adjustments to maintain proper functioning. This means that, on an engineering time scale, adjustments or readjustments in channel form or planform are impacted more so by imbalances in the inflow and outflow sediment discharges, and possibly by flood incidences that may induce temporary but fundamental changes in form, than external influences such as climate change, land-use change, and other changes elicited by human activities. Since the reaches of the White River also exhibit quantities of longitudinal gradient well below its valley slope, the bedforms have to adjust themselves through sediment storage (plus or minus), also known as temporary aggradation or degradation, to produce an appropriate depth-velocity combination to indemnify for a lack in channel gradient to carry equilibrium sediment discharge.

Obviously as the configuration of the White River becomes more sinuous, or more linear, whether by natural or man-made contributions, changes in other parameters have to take place, e.g., alterations in width or W/D ratio or the emergences of point bar features. In conclusion, one theme evident from the composite correlation between bankfull discharge, channel slope, and sinuosity is that meander development of the White River's channel form follows a short term evolution. Comparisons of the planform geometries of the study section of the White River at different time periods, i.e., the 1980s and 2000s, with the correlation between channel slope, bankfull discharge, and sinuosity also reveal implications that the sinuosity ratios of various reaches of the White River may be correlated with fault positions as well as subsidence and uplift anomalies.

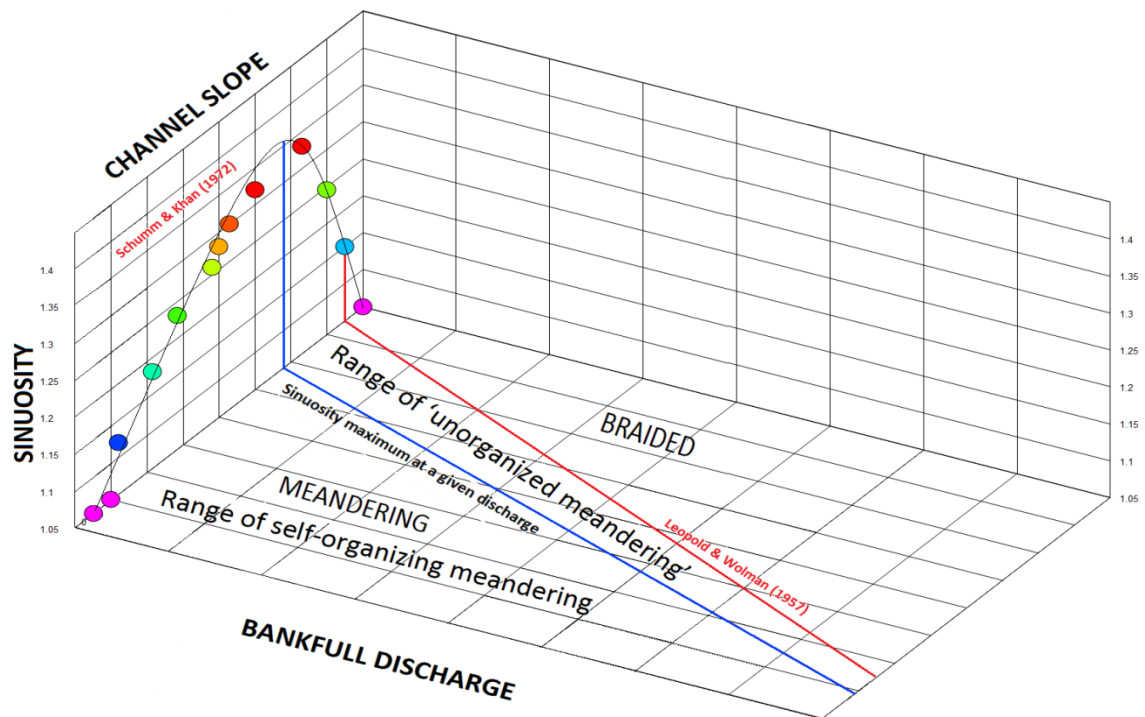


Figure 3.24a. Discharge Versus Slope Discriminant Diagram (after Leopold & Wolman, 1957; Schumm & Khan, 1972).

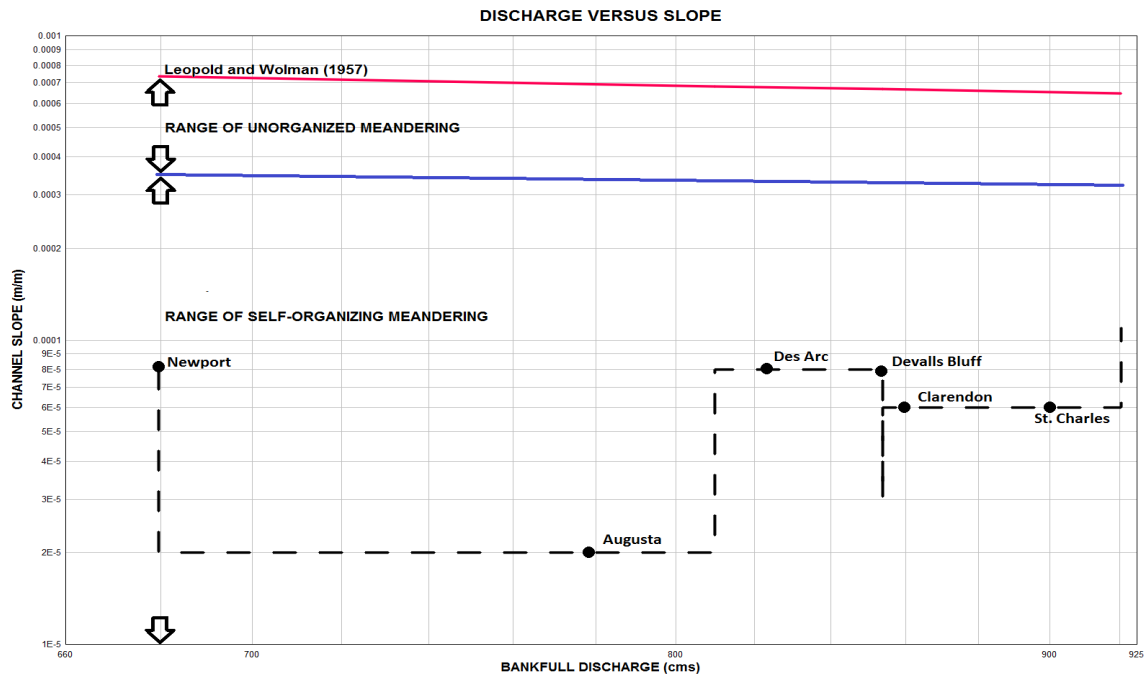


Figure 3.24b. Plot of the Alluvial Sections of the White River on Discharge Versus Slope Discriminant Diagram to Predict Meandering Range.

Maximum sub-basin width versus sinuosity. Of the pertinent dimensions extracted and measured from the drainage area DEMs via ArcGIS, the maximum widths of the sub-basins through which the White River traverses appear to display the most discernible connection to the sinuosity quantities measured from its bends. The three-dimensional surface plot depicting the frequency of sinuosity values for various sinuosity ranges indicates that within the sub-basins possessing a higher order of magnitude of width, the probability of occurrence for sinuosity quantities exceeding 2.5 is greater. The step-like surface plot also illustrates wider treads corresponding to an enhancement in sinuosity values for sub-basin widths equivalent to and exceeding 180,000 feet, albeit an apparent attenuation in gradation intensity or frequency of occurrence for high sinuosity intervals. The implication is that similar to the meander belt width, which represent the

products of the interaction between discharges, the driving factor, and the properties of the floodplain, the limiting factor, sub-basins exhibiting high optimal magnitudes in width are characteristics of dynamic areas more probable to experience flooding events and more susceptible to high and low recurring inundation activities accountable for further expansion of the floodplain. Since a drainage area is often considered as the source of water and sediment that advances through the fluvial system and reshapes the channel configuration, its optimum width is indicative of the lateral extents or boundaries by which the channel may oscillate in extreme conditions; thus explicating the higher occurrence of large sinuosity quantities within the White River's sub-basins that possessed substantial width dimensions. Closer inspection of the tabulated data extracted from the HEC-RAS Model and ArcGIS's aerial photos shows that within sub-basins IV, VII, and I, which are distinguished by maximum widths in excess of 140,000 feet and high degrees of dispersion in sinuosity values across various arrays of sinuosity range, the frequency of bends exhibiting sinuosity quantities in the order of 2 or above is higher than the narrower sub-basins VI and III where the majority of sinuosity values clustered the lower ranges of 2 and below. Similarly, when the average sinuosity of the bends occupying particular sub-basins of interest are plotted against the maximum sub-basin widths for comparison purposes, high sinuosity values are ostensibly coincident to high width values and vice versa. The conjecture that sub-basin widths represent the lateral boundary limits or the levels of lateral confinement, or lack thereof, that affect the extent by which the channel planform may vacillate is further affirmed by the polynomial regression line fitted through the data; a trend line, discerned by a correlation coefficient of approximately 0.80, that indubitably shows a significant complementary relationship

between sinuosity augmentation and width enhancement, and conversely sinuosity diminishment with width attenuation.

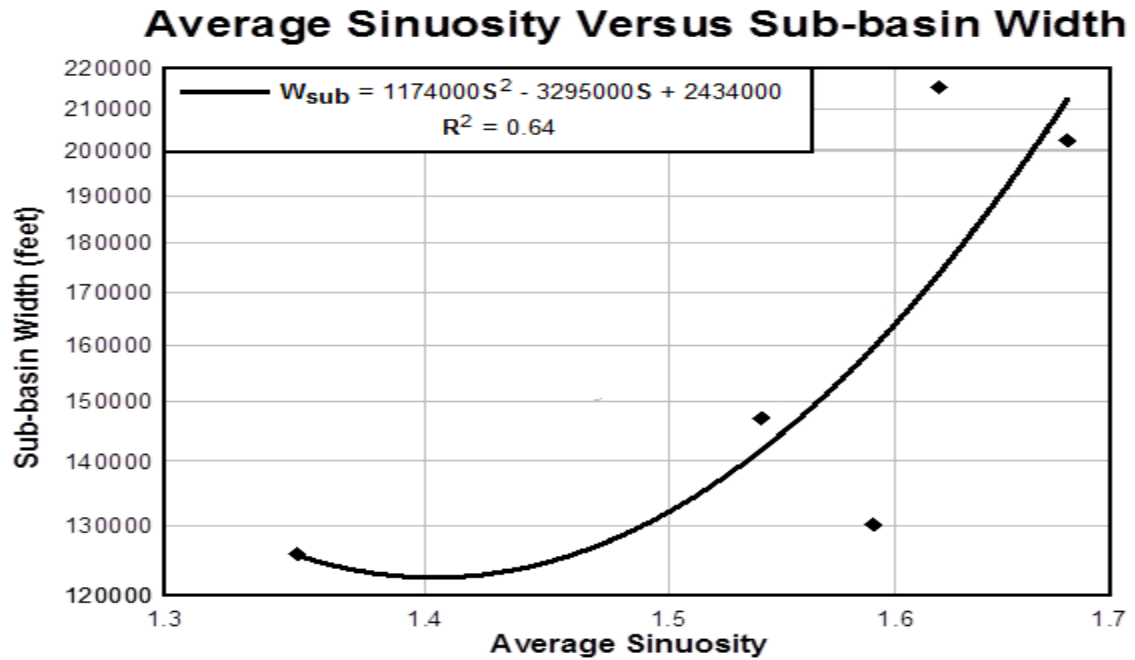


Figure 3.25. Correlation of Average Sinuosity Versus Sub-basin Width.

Table 3.4. Percentages of Occurrence of Sinuosity Values within Various Sinuosity Ranges and Sub-basins.

Sinuosity Range	Sub-basin IV	Sub-basin VII	Sub-basin I	Sub-basin VI	Sub-basin III
	47 - 89	1 - 13	90 - 141	14 - 39	40 - 46
1 through 1.25	28.00%	39.00%	29.00%	23.00%	72.00%
1.25 through 1.50	25.00%	8.00%	27.00%	27.00%	14.00%
1.50 through 1.75	12.00%	15.00%	15.00%	19.00%	0.00%
1.75 through 2.00	14.00%	15.00%	17.00%	12.00%	0.00%
2.00 through 2.25	7.00%	0.00%	4.00%	15.00%	0.00%
2.25 through 2.50	5.00%	8.00%	2.00%	4.00%	14.00%
2.50 through 2.75	7.00%	0.00%	2.00%	0.00%	0.00%
2.75 through 3.00	2.00%	15.00%	2.00%	0.00%	0.00%
3.00 +	0.00%	0.00%	2.00%	0.00%	0.00%
Average sinuosity	1.62	1.68	1.54	1.59	1.35

When the lines of demarcation are applied to sinuosity values of 1.5, 2.0, 2.5, and 3.0, and tabulated with the seven reference sections, the reaches that exhibit highest sums of sinuosity quantities above 2.0 are Batesville to Newport, Devalls Bluff to Clarendon, and Clarendon to St. Charles, which apparently resides within sub-basins VII, IV, and I, respectively. Additionally, it should be noted that the mean sinuosity ratios of the sections occupying primarily within sub-basins IV, VII, and I, which in descending order possessed optimum width values of 215,210 feet, 202,400 feet, and 147,057 feet, respectively, are also perfectly compatible to sub-basin widths in term of rank or order. Specifically, the positive monotonic relationship between sub-basin widths of IV, VII, and I, and thalweg sinuosity values possessed both a Pearson's product-moment and a Spearman's rank-order correlation coefficients of approximately 1.00, which denote a significance level within 1% and further reinforced the connection between these constituents to the alluvial sections of the White River.

Table 3.5. Tallies of Sinuosity Values within Various Sinuosity Ranges for the Reference Reaches.

Sections	Sinuosity Range					Sum 2.0 +
	3.0 +	2.5 +	2.0 +	1.5 +	1.5 -	
Batesville - Newport (1 - 17)	0	2	2	5	8	4
Newport - Augusta (18 - 38)	0	0	4	6	11	4
Augusta - Des Arc (39 - 62)	0	1	2	5	16	3
Des Arc - Devalls Bluff (63 - 74)	0	2	0	4	6	2
Devalls Bluff - Clarendon (75 - 88)	0	1	4	4	5	5
Clarendon - St. Charles (89 - 109)	0	2	2	5	12	4
St. Charles - LMR (110 - 141)	1	0	1	12	18	2

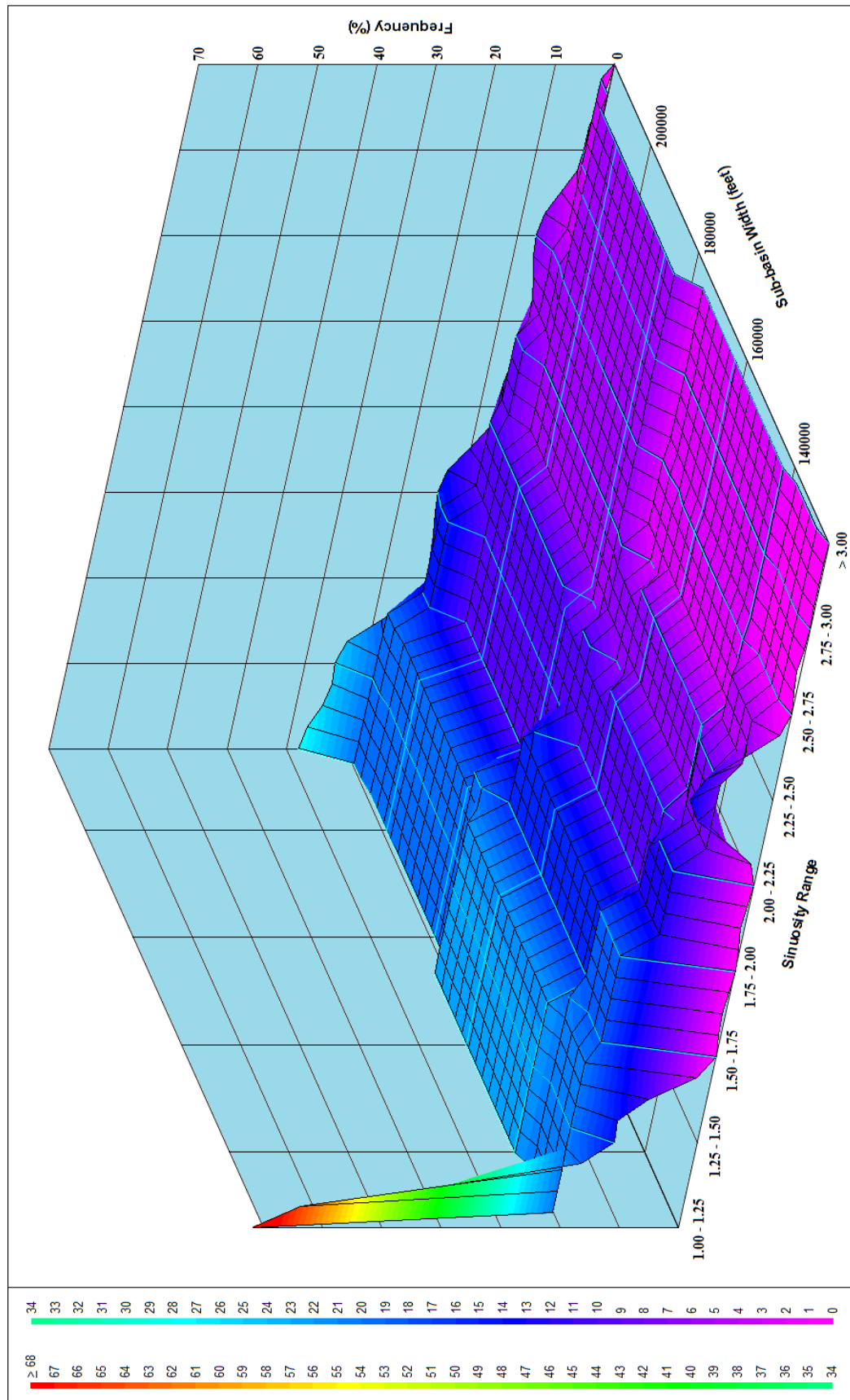


Figure 3.26. Three-dimensional Surface Plot Depicting the Frequencies and Ranges of Sinuosity Values for Various Sub-basin Widths.

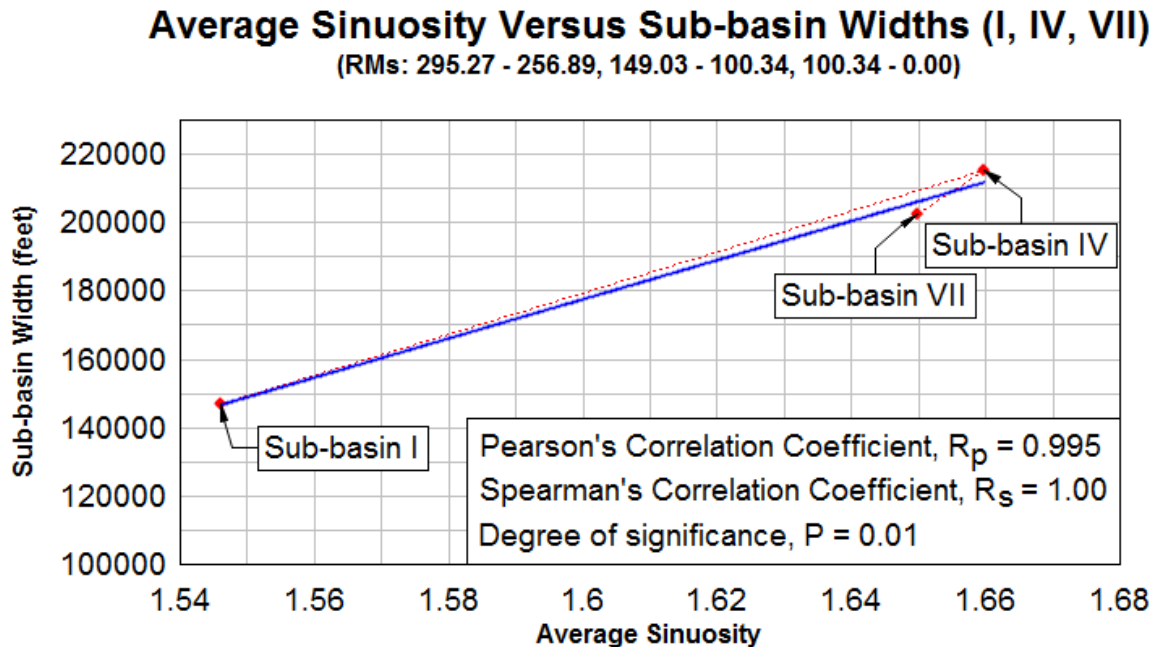


Figure 3.27. Level of Significance for the Monotonic Relationship Between Average Sinuosity and Sub-basin Width.

The correlations involving the transverse water surface angles. In spite of a dearth of empirical equation(s) underpinning the fundamental causes and mechanisms of meandering, the notion that “the propensity for flowing fluids to meander [...] is inherent to shear flows” is a consensus suggested in the literature by many proponents content with the elucidation that meandering is a natural attribute of alluvial rivers and, therefore, cannot be ascribed “solely to local non-uniformity in sediment transport or bank erosion, although both [are requisites for the development of meanders in alluvial channels]” (Lagasse et al., 2004b, p. 12). Ambiguity associated with the precise cause of meandering, however, does not impede investigators from establishing a rationalization that the complex nature of flow at bends induced by curvature effects are driven by a dominant helicoidal, or corkscrew-like, circulation generated by primary and secondary currents. The interaction between the currents consisting of “the main skew-induced

secondary cell directing rapid, near surface water to the outwards at a bend and carrying sluggish, near-bed water inwards” and “the small, counter-rotating cell [directing water to the outer bank]” helps generate non-uniform, “elevated velocities and high local boundary shear stresses on the lower bank and bend adjacent to the outer banks [causing undercutting of the bank and scouring of the bed near] the toe to promote erosion, instability, and rapid banks retreat [which in turn] enables active meanders to shift and migrate” (Lagasse et al., 2004b, pp. 12-13). The asymmetry in velocity and boundary shear stress distributions associated with helical flows induced by curvature effects also leads to the formation of pools and riffles, which further strengthen the overall effects of curvature and, consequently, set in motion additional modifications in velocity and shear stress distributions as the bend evolves. Therefore, closer inspection of the patterns of flow at bends and related constituents may permit percipience into the magnitudes of changes in bend geometry and migration rate. In the case pertaining to the White River, where the HEC-RAS Model is inadequate in providing animation illustrating specific patterns of flow, the transverse water surface angle is implemented to reinforce the degree of symmetry, or lack thereof, in velocity distributions at the bend and to impart the level of intensity of shear force exerted on the bank by converging fluid shear flows. Since channel shifting and migration are discontinuous processes that depend on the occurrence of morphogenetically significant hydrologic events such as recurring inundation episodes; are contributed primarily by local non-uniformity in velocity distributions and vacillating flow patterns; and are especially imminent and observable more so proximal to or in bend apices, all of which points to the propensity of fluid to meander and the curvature effects phenomenon, their derivation must, therefore, stem

from the tendency of flowing fluid to emulate the principle of centrifugal force, which in this case may be explained by the superelevated water surface angle formed with respect to or adjacent to the horizontal plane. The transverse water surface angles for various bends are acquired through ArcGIS, via the digital elevation models and aerial photographs, and the HEC-RAS Model by a procedure that includes (1) measuring the elevation at the focal point within the circular buffer zone antecedently implemented for the calculation of the radius of curvature, (2) measuring the elevation at the border of the circular buffer zone, which superimposed the curve of the exterior channel boundary representative of the location and instance that the bank is completely occupied by water, and finally (3) employing the inverse sine trigonometric function to determine the angle between the horizontal plane and the incline or hypotenuse equivalent to the radius of curvature. In comparison with the velocity distributions of the cross-sections within the White River HEC-RAS Model, an acclivity or positive transverse water surface angle typically indicates exertions of high velocities and high boundary shear stresses toward the outer or concave bank, a declivity or negative transverse water surface angle indicates exertions of high velocities and boundary shear stresses toward the inner or convex bank,

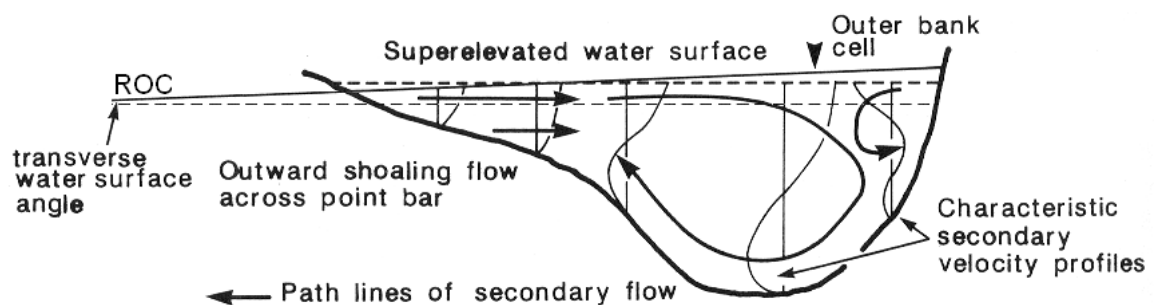


Figure 3.28. Summary Diagram for Flow Pattern and Cross-sectional Morphology at a Bend Apex (adapted from Markham & Thorne, 1992).

and a horizontal exhibiting a transverse water surface angle of approximately zero implies a perfectly symmetrical flow cross-section with high flow velocities in the center of the channel as well as equivalent boundary shear stresses on both banks. In colligation to the principle of centrifugal force where channel curvature implies elevated velocities and high local boundary shear stresses away from the center of curvature, a significant numerical quantity of the transverse water surface angle denotes not only higher force of water exerted on the external boundary of the channel but also a higher degree of bend sharpness. Inspection of subsequent figures reveals that the transverse water surface angles, computed for various bends extending from Batesville to the Lower Mississippi River, are correlated to shear forces and hydraulic depths. The monotonically increasing sequence of the correlation between the transverse water surface angles and shear stresses, secernated by a Pearson correlation coefficient of approximately 0.76, indicates that increases in the transverse water surface angles correspond to enhancements of boundary shear stresses in the near bank region adjacent to the outer banks. If the fitted trendline represents an established norm for shear stresses given a particular magnitude of the transverse surface angle, then it could be justified that, for most cases, the bends within the reaches from Devalls Bluff to Clarendon, Clarendon to St. Charles, and St. Charles to LMR are characterized by near-bank shear stresses exceeding the mean or anticipated shear stresses. Bends within these reference reaches that exhibit substantial deviation above the correlation line, therefore, must possess a high perceptibility to bank erosion, a high inclination for lateral migration, and a high degree of bend sharpness. As for the comparison between the hydraulic depth and the transverse water surface angle, distinguished by a Pearson's correlation coefficient of approximately 0.5, the

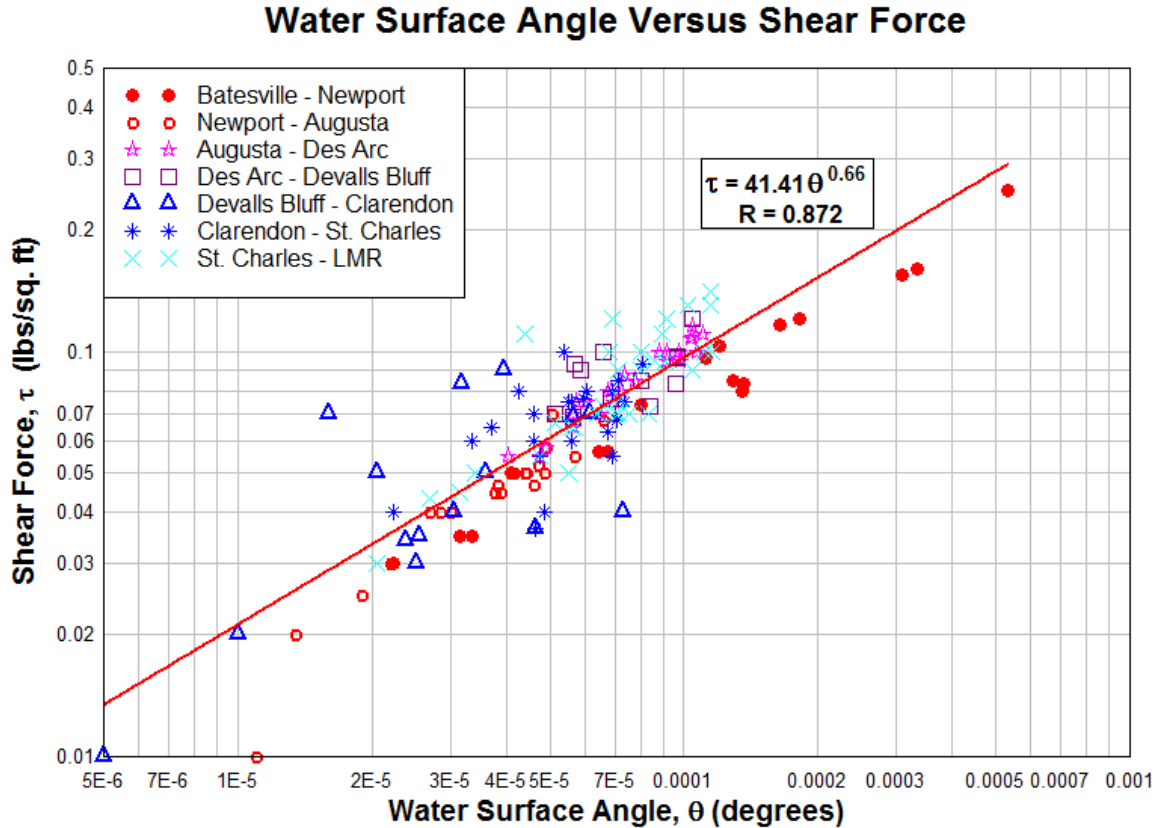


Figure 3.29. Correlation of the Transverse Water Surface Angle Versus Shear Force.

monotonically decreasing sequence indicates that augmentations in the transverse water surface angles correspond to diminishment in hydraulic depths. The implication is that when boundary shear stresses are immense and the longitudinal gradient is excessively mild to promote efficient mobility of sediment through the system, the channel bed will likely aggrade or sediment will likely accumulate to the bed, thus inducing a reduction in hydraulic depth. In addition, if the correlation line signifies the average hydraulic depths for specific values of the transverse water surface angles, then it could be concluded that the reaches from Devalls Bluff to Clarendon, Clarendon to St. Charles, and St. Charles to LMR, which are characterized by hydraulic depths in excess of the regression line, are

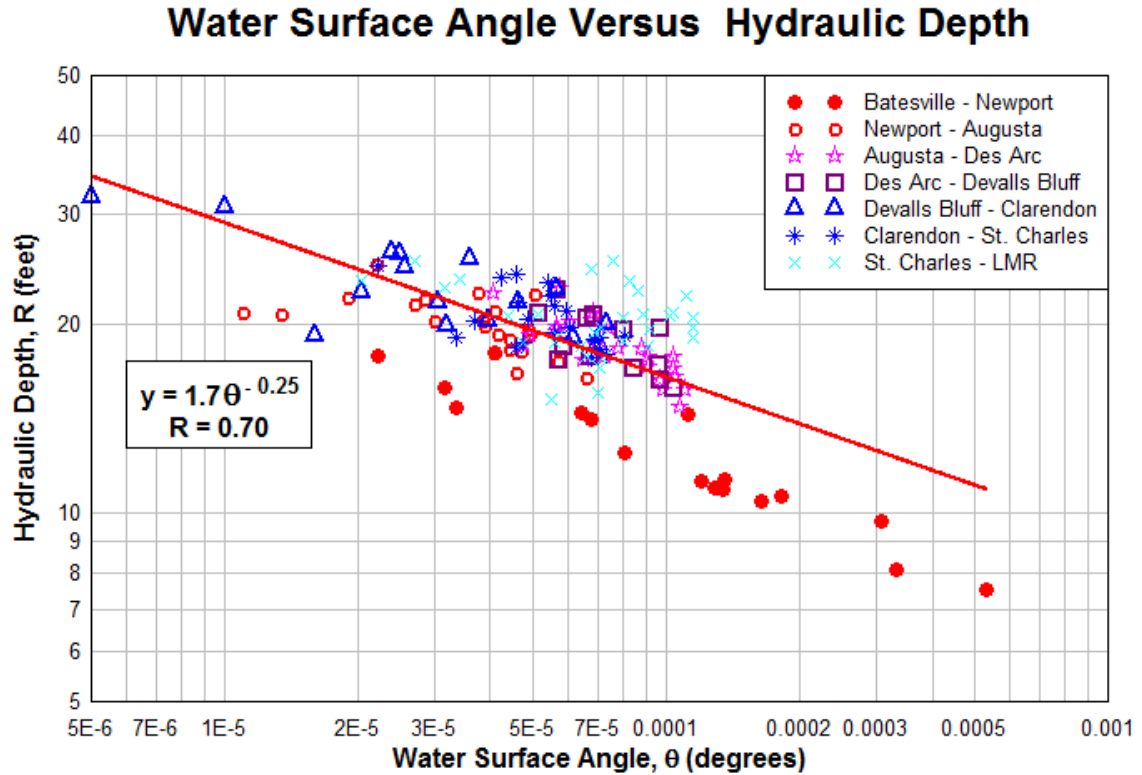


Figure 3.30. Correlation of the Transverse Water Surface Angle Versus Hydraulic Depth.

highly susceptible to boundary erosion due to immense shear stresses exerted by the flow. Specifically, the channel of the reference reaches from Devalls Bluff to Clarendon and Clarendon to St. Charles, due to high boundary stresses and a mild longitudinal gradient, is highly vulnerable to undergo bed aggradation while the channel of St. Charles to LMR, marked by high boundary stresses and a moderately steep longitudinal gradient, is likely susceptible to bed degradation. Since channel curvature (R_c/W) and shear stress are viable predictors of lateral migration and erosion potential more so than velocity on account of the consideration of the fluid flow scheme and water force exerted on the boundary of the channel, respectively, the product of shear stress and channel curvature, termed Janderson curvature-shear product, is compared to the

transverse water surface angle. The results depicted by **Figure 3.30** appear to denote that augmentations in the transverse water surface angle from straight conditions are inversely correlated to the Janderson curvature-shear stress product. In contrast to the monotonically increasing sequence of the correlation between shear stresses and the transverse water surface angles, the perceivable transformation to a monotonically decreasing sequence for the relationship between curvature-shear stress products and the transverse water surface angles, with the inclusion of channel curvatures (R_c/W_s) to shear stresses to form the curvature-shear stress products, suggests that channel curvatures induce a greater impact to alterations in the transverse water surface angles than shear stresses; therefore channel curvature may be a more viable and reliable predictor of lateral migration and erosion potential. This discovery confirms the validity of the conjectures of Hooke (1987a), Biedenharn et al. (1989), and Hickin and Nanson (1975, 1984) that the rates of channel migration are controlled by channel curvature. In colligation to previous findings by said investigators and other researchers, which suggests that the optimal rate of channel migration tends to occur at channel curvature values between 2 and 3, the patterns shown in **Figure 3.21** and **Figure 3.30** connote that curvature effects and helical flow may “strengthen[.] as bend amplitude grows and radius shortens” (Lagasse et al., 2004b, p. 15). Assuming that the arrays of data representing the correlations between sinuosity and channel curvature and transverse water surface angle and Janderson curvature-shear stress product are legitimate indicators of planform metamorphosis, considerable rates of lateral migration, substantial erosion potential, and large values of sinuosity are anticipated for the bends that constitute the reaches from Devalls Bluff to Clarendon, Clarendon to St. Charles, and St. Charles to LMR. It should

be noted, however, that these speculations are based primarily on parametric correlations emanating from the measurements, quantifications, and computations of variables within ArcGIS and the HEC-RAS Model of the White River rather than on-site observations, monitoring, and data collection and extraction. Such actions are covered in detail in chapters 4 and 5 to verify the stability conditions of the alluvial reaches of the White River.

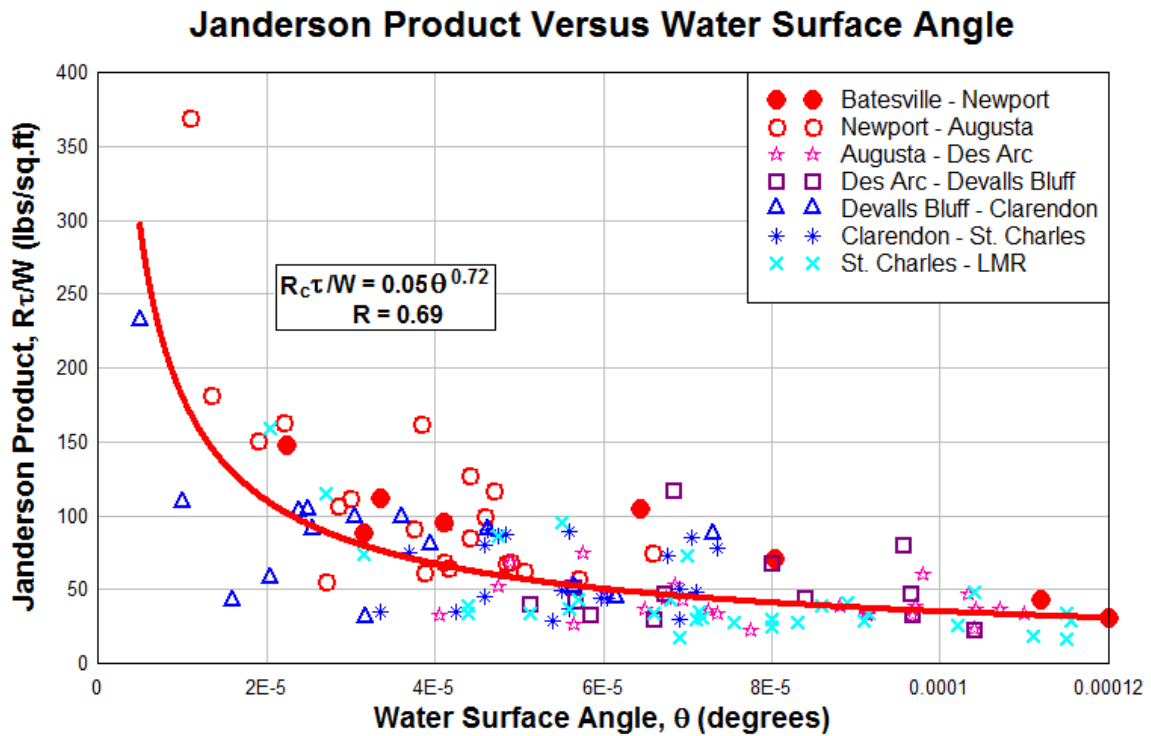


Figure 3.31. Correlation of the Transverse Water Surface Angle Versus Janderson Curvature-shear Product.

ArcGIS-Extracted Morphological Parameters and Their Implications

Synonymous with the formulation of a table displaying static and dynamic fluvial parameters for specific reaches of the White River, the amalgamation of extracted,

measured, and calculated post-simulation HEC-RAS data and aerial-photography-derived ArcGIS data assisted in the composition of a similar table outlining various critical morphological parameters inherent to these reaches. The inclusion of a multitude of channel planform metamorphoses, such as the extent of lateral migrations and frequencies of cut-offs, constrictions and expansions perceivable from the superimposition of aerial photographs to quadrangle maps, to the assemblages of morphological parameters encompassing sinuosity, radius of curvature, meander wavelength, meander amplitude, flood-prone width, meander width ratio, width to depth ratio, entrenchment ratio, radius of curvature to width ratio, and the transverse water surface angle in a single table provides insights into the degree of influence contributed by these constituents on the meandering/shifting propensity, dynamic equilibrium, and overall stability of the reaches composing the White River. Inspection of the tabulated data reveals that for the segment extending from Batesville to Newport, where a majority of morphological parameters including radius of curvature, wavelength, flood-prone width, meander width ratio, width to depth ratio, entrenchment ratio, channel curvature, and the transverse water surface angle are considerably higher than the downstream alluvial reaches, accounts of channel and channel planform changes are relatively infrequent. Substantially high quantities of mean radius of curvature and meander wavelength indicate that the bends residing in the vicinity of Batesville to Newport are more linear and the channel planform less compounded while high values of meander width ratio and width to depth ratio are indicative of a greater spatial boundary for channel meandering, an acute sensitivity to variations in discharge, and an efficient mode of excess energy dissipations. Flood-prone widths and entrenchment ratios in excess of

downstream alluvial reaches reestablish the connotation that the channel extending from Batesville to Newport is distinguished by a lack of vertical containment or incision to its valley floor, and insinuates that flows exceeding the bankfull discharge frequently overtop streambanks and extend onto the adjacent floodplain. An extremely high composite magnitude of the transverse water surface angle, influenced and controlled by a concoction of a considerable longitudinal gradient, the natural propensity for flowing fluid to meander, and subsurface materials, not only suggests that higher forces of water exerted on the external boundaries of the channel and greater degrees of bend sharpness at various localities, but also reinforce the notion that the primary mode of excess energy dissipation within this reach is through means of a crooked and turbulent shear flow; an attribute often associated with fluvial systems residing within the Ozark Plateaus region above Newport. One perplexing phenomenon emanating from the resulting table for Batesville to Newport involves an apparent synchronism between a substantial magnitude of sinuosity and a high quantity of channel curvature, or radius of curvature to width ratio. It is speculated that despite both parameters designating contrasting implications on pattern developments, one explanation that would suffice both circumstances revolve around the idea that channel pattern developments driven by symmetrical vacillating flow patterns may permit both high sinuosity values as well as a relatively non-compounded sinusoidal planform marked by significant magnitudes of radii of curvature or channel curvature with diminutive variations. This conjecture corroborates the conception that sinuosity ratio is only highly coincident to channel curvature, hence lateral migration, within the channel curvature and radius of curvature intervals of 2.75 to 3.75 and 1250 to 2000 feet, respectively, both of which signify the critical zones of optimum rate of bend

migration. Consequently and regardless of the display of high sinuosity values for this 'reference' reach, radius of curvature and channel curvature in excess of the critical intervals for optimum lateral migration rate appear to account for the low occurrences of channel cut-offs, constrictions, and expansions associated with its bends. The finding herewith elicits evidence that curvature may be a more viable indicator of meander geometry and planform metamorphoses than morphological parameters such as meander wavelength, meander amplitude, and tortuosity ratio. Other distinctive and prominent attributes manifested from the resulting morphological parameters table include maximum quantity of amplitude for the bends composing the reach from Newport to Augusta; minimum magnitudes and changes in sinuosity ratios and extremely high observable occurrences of channel constriction and expansion for the bends of Augusta to Des Arc; characteristically low magnitudes of flood-prone width, meander width ratio, and entrenchment ratio for Des Arc to Devalls Bluff; significantly low quantities of radius of curvature, meander wavelength, width to depth ratio, and transverse water surface angle accompanied by immense extent of lateral shift, optimum frequency of cut-offs and maximum magnitude and enhancement of sinuosity for Devalls Bluff to Clarendon; modest degrees of lateral shift or migration for Clarendon to St. Charles; and low and high occurrences of cut-off and narrowing/widening, respectively, as well as low values of sinuosity, meander amplitude, and channel curvature for the reach extending from St. Charles to the confluence with the Lower Mississippi River.

Albeit a dearth of a definitive inference underpinning the weight of influence imparted specifically by individual morphological parameters on the meandering/shifting propensity, dynamic equilibrium, and overall stability of the reaches that personify the

alluvial portion of the White River, a common theme evident from the meticulous inspection of the resulting table resonates with the connectivity of radius of curvature and channel curvature to sinuosity and occurrences of channel cut-off, narrowing and widening. Significant enhancements in sinuosity and high frequencies of either channel cut-off or channel narrowing and widening, as the data insists, are highly colligated with radius of curvature and channel curvature values within the critical ranges of 1250 to 2000 feet and 2.75 to 3.75, respectively, for reaches extending from Augusta to Des Arc, Devalls Bluff to Clarendon, and St. Charles to the Lower Mississippi River. For the reach extending from Devalls Bluff to Clarendon, which is secernated by radius of curvature and channel curvature values falling well within the critical intervals of significance, the most convincing confirmation that the channel curvature exerted the highest degree of influence on planform metamorphoses or deformations pivots around the immense numerical quantities of sinuosity and sinuosity enhancement, the substantially high frequencies of channel cut-off, narrowing and widening, and the excessive magnitude of lateral migration detected for this segment. The implication that channel curvature may be the most influential and significant morphological parameter representing channel geometry, planform development, and channel stability has also often been promulgated in the literature by many investigators content with the elucidation that river metamorphoses are actuated by the natural propensity of flowing fluid to meander and are accelerated by the complex nature of flow at bends induced primarily by curvature effects. In spite of the fact that every fluvial system differs or that no fluvial system is completely identical to another, the results manifested from studies and experiments conducted by Bagnold (1960), Chang (1984a), Harvey (1989), Hooke (1987), Hickin

(1974), Hickin and Nanson (1983, 1984, 1986), and Leeder and Bridges (1975), and on various fluvial systems around the world revealed that migration rates are highest when the radius of curvature to channel width ratio is in the range of 2 to 3; a range not far off from the critical interval of 2.75 to 3.75 established for the White River fluvial system. Explanations provided for this discovery involve the development of inner and outer bank flow separations as amplitude increases and radius of curvature decreases when the bend tightens. As bends develop and tighten, the “spatially organized pattern of [helical circulation is stalled], resulting in intense [flow] turbulence, [initiations in bank erosions, rapid increases in lateral and downstream migrations, and massive increases in energy losses]” (Bagnold, 1960, as cited in Lagasse et al., 2004b, p. 14). A channel curvature of 2 to 3, therefore, “corresponds to a minimum in the energy losses generated by the bend” (Lagasse et al., 2004b, p. 14) and characterizes migration, a channel curvature of exactly 3 corresponds to the instance when “the river does least work in turning” (Chang, 1984a, as cited in Lagasse et al., 2004b, p. 14) and characterizes maximum rate of bend migration while channel curvatures of greater than 3 and less than 2 correspond to “the lack of flow convergence and energy loss” (Lagasse et al., 2004b, p. 36) and characterize bend growth and double heading, respectively.

Table 3.6. Morphological Parameters Computed and Extracted from ArcGIS and HEC-RAS.

Section	Station, RM	Sinuosity (1984)	Sinuosity (2003)	Radius of curvature, R_c	Wave- length, L	Amplitude, A	Flood Prone Width (50-yr)	Meander Width Ratio	Width/ Depth Ratio	Entrench- ment Ratio	Channel Curvature, R_c/W	Water Surface Angle, θ	Lateral Shift	Freq. of cut- off	Freq of narrowing/ widening
				(feet)	(feet)	(feet)	(feet)					(degrees)	(feet)		
Batesville to Newport (1 – 17)	295.27 through 256.89	1.59	1.65	2671.34	7847.94	3194.89	34071.52	36.55	42.43	66.15	5.27	0.000146	285.0	1	7
Newport to Augusta (18 – 38)	256.89 through 197.27	1.54	1.59	2242.83	7736.30	3270.34	30707.03	34.37	26.43	60.00	4.26	0.000038	206.53	7	9
Augusta to Des Arc (39 – 62)	197.27 through 147.19	1.49	1.49	1923.02	6044.09	2513.68	25569.48	31.81	30.48	47.75	3.47	0.000079	274.02	11	19
Des Arc to Devalls Bluff (63 – 74)	147.19 through 124.33	1.53	1.60	2319.68	5538.96	2254.52	14232.12	28.42	29.83	25.44	3.79	0.000074	347.90	3	11
Devalls Bluff to Clarendon (75 – 88)	124.33 through 100.34	1.65	1.72	1795.99	5045.09	2688.04	25630.55	32.33	22.50	49.48	3.47	0.000032	369.41	13	13
Clarendon to St. Charles (89 – 109)	100.34 through 55.30	1.52	1.57	2524.85	6422.86	2546.51	24336.40	32.11	28.36	43.24	3.86	0.000056	182.36	2	9
St. Charles to LMR (110 – 141)	55.30 through 0.00	1.45	1.51	1826.33	5910.97	2020.22	22461.10	28.98	27.82	42.35	3.26	0.000072	268.34	1	17

Significance of Parametric Correlations

Germinating from the amalgamation of simulated HEC-RAS data and extracted ArcGIS data, the multifarious empirical correlations existing between fluvial and morphological parameters presented in this chapter permitted not only percipience into the intrinsic attributes of the White River fluvial system, but also ascertained the degree of influence contributed by each parameter to the meandering/shifting propensity, dynamic equilibrium, and overall stability of its alluvial reaches. Results indicate that individual static and dynamic fluvial parameters as well as morphological parameters distinctively provide differing facets that, as a whole, constitute characteristics inherent to the White River system and animate the processes inherent to its channel. Entrenchment ratio, quantitatively defined as the vertical containment of a river or equivalently the extent of the river incision to its valley floor, indicates that the White River, in the most satisfactory conditions, is only slightly entrenched in its valley, and insinuates that flows exceeding bankfull discharge increase in width much faster than in depth and frequently extend onto the adjacent floodplain to dissipate kinetic energy. Width to depth ratio, averaging a numerical quantity of approximately 29.5, also suggests a high frequency of overbank flows and, from a slightly different angle, denotes channel sensitivity to variations in discharge in addition to providing a rough visual assessment of channel cross-sectional shapes; all of which suggests a short-term evolution of meander development that influences bend curvature and contributes to the compounded forms of the White River. Mild longitudinal gradient and low stream power in colligation to enhancements in sinuosity ratios observable for various bends over a span of approximately 20 years show that, with the exception of the reach extending from

Batesville to Newport, the primary mechanism of energy dissipation involves fluid flowing in bends and meanders. Energy dissipation by means of bends and meanders, generally accompanied by a reduction in the longitudinal gradient, also appears to control the frequency and spacing of bed features such as riffles and pools. Delineation of the meander belt width for the White River floodplain to estimate a meandering boundary limit reveals that, with the presence of distinctive variations in the meander belt width and observable irregular meander patterns, the evolution of the meandering planform in the cross-valley and downstream directions is contributed by heterogeneity in lenses and strata of resistant materials. Similarly, the variation in amplitude values also connotes that the presence of “resistant materials in the [White River] floodplain may interfere with the [direction and] rate of meander [movement (e.g., meander shift, elongation, and rotation)], [thus] contributing to [its] irregular planform” (Parish Geomorphologic Ltd., 2004, Appendix B p. 3). High degrees of dispersion in measured wavelength quantities of various White River bends, distinguished by a regression line showing that wavelengths are approximately 16 times the width or that the wavelengths exceed the stability range of 11 to 12.5 times the width, corroborate the notion that waveforms in bed topography and planform are the resultant of an irregular mechanism of erosion and deposition. Despite strong implications that heterogeneity in lenses and strata of resistant materials and variations in rates and patterns of sediment yield are primarily accountable for the scatterings of wavelength quantities, dispersions in meander wavelengths associated with the reaches from Batesville to Newport, Newport to Augusta, and Clarendon to St. Charles are also controlled specifically by the crooked and rapid flow possessing sufficient energy to erode into bedrock, by intense weathering that occurs along the

intersections of faults proximal to the river course, and by highly erodible bed and banks and considerable magnitudes of dune wavelengths and amplitudes, respectively. Through the creation of a three-dimensional surface plot depicting the frequency of sinuosity values for various sinuosity ranges, which has shown that higher occurrence of large sinuosity quantities exists within the sub-basins that possessed substantial width dimensions, it is concluded with certainty that the maximum widths of the sub-basins through which the White River traversed are highly connected to the sinuosity quantities measured from its bends. With the implication that high sinuosity values are ostensibly coincident to high sub-basin widths and vice versa, it is adduced that, congruous with the meander belt width which represents the products of the interaction between discharges and the properties of the floodplain, sub-basins exhibiting high optimal magnitudes in width are characteristics of dynamic areas prone to flooding events and more susceptible to high and low recurring inundation activities accountable for further expansion of the floodplain; thus explicating the higher occurrence of large sinuosity values within the reaches extending from Batesville to Newport, Devalls Bluff to Clarendon and Clarendon to St. Charles, which apparently reside within the sub-basins VII, IV, and I, respectively, that possessed substantial width dimensions in excess of 140,000 feet. A common theme evident from the meticulous inspection of the resulting data resonates with the radius of curvature and channel curvature being connected to many parameters and attributes (i.e., sinuosity, flow patterns, bedforms, channel dimensions, lateral migration, and occurrences of channel cut-off, narrowing and widening) that define the White River fluvial system. In regard to bedforms and flow patterns, radii of curvature are directly responsible for the asymmetry in flow or velocity, the formation of helical flow patterns,

and the creation and spacing of riffle and pool sequences within the White River channel; all of which are catalysts evoking further modifications that affect channel forms and dynamic stability. The function of curvature in generating changes in velocity and shear stress distributions as the bends evolve also affects channel shape and stability to an extent that is visible from the correlation plot of width to depth ratio versus radius of curvature which indicates that (1) the reach extending from Devalls Bluff to Clarendon, with width to depth ratios well below the regression line of the width to depth ratio versus radius of curvature relationship (i.e., the channel is narrow and deep in comparison to the remaining reaches), signifies less susceptibility to discharge variations and less uniformity in flow, large sinuosity, and a high percentage of silt-clay contents within the channel and (2) the reaches extending from Batesville to Newport and St. Charles to LMR, distinguished by width to depth ratios well above the regression line of the width to depth ratio versus radius of curvature relationship (i.e., relatively wide and shallow channels), insinuate instability of the banks and attenuation of the capability to transport sediment. Additional findings perceived from correlating channel dimensions encompassing width, depth, and cross-sectional flow area to radius of curvature include the inference that high degrees of deviation from the resulting regression line may represent discrepancies between channel dimensions and radius of curvature, and reaches that exhibit such discrepancies are likely more sinuous and less stable. Specifically, the unusually low depths and cross-sectional flow areas are indicators of a possible imbalance in the dynamic processes within the segment from Batesville to Newport, the extremely high depths and flow cross-sectional areas are signifiers of possible dynamic disequilibrium for the reach from Devalls Bluff to Clarendon, and the high channel

dimensions of area, width, and depth with respect to radius of curvature are evidence of possible offsets in equilibrium within the reach extending from St. Charles to LMR. Metamorphoses in channel forms initiated by the natural propensity for flowing fluid to meander and accelerated by the asymmetry in velocity and boundary shear stress distributions induced by curvature effects are also emphasized by the correlations involving the transverse water surface angles. Revelations emanating from the correlation plots of the transverse water surface angles versus shear stresses and the transverse water surface angles versus hydraulic depths include immense shear stresses exerted by converging fluid shear flows on the boundaries of the reaches that constitute Devalls Bluff to Clarendon, Clarendon to St. Charles, and St. Charles to LMR and excessively high hydraulic depths, hence high perceptibility to boundary erosions due to immense shear stresses exerted by the flow, for the reaches extending from Devalls Bluff to Clarendon, Clarendon to St. Charles, and St. Charles to LMR. When the longitudinal gradients are taken into account, the aforementioned correlations between the transverse water surface angles and shear stresses and the transverse water surface angles and hydraulic depths also revealed that the channels of the reference reaches from Devalls Bluff to Clarendon and Clarendon to St. Charles are highly vulnerable to undergo bed aggradations while the channel of the reach extending from St. Charles to LMR is susceptible to bed degradation. The most profound indicator of channel stability or lack thereof, however, clearly pivots around the correlations of radius of curvature versus sinuosity and channel curvature versus sinuosity which not only confirmed the conception that large sinuosity ratios are highly coincident to radii of curvature and channel curvatures within the critical intervals of 2.75 to 3.75 and 1250 to 2000 feet,

respectively, but also validated the often promulgated-in-the-literature consensus that the optimal rate of channel migration tends to channel curvature quantities between 2 and 3. Substantial augmentations in sinuosity and high magnitudes and occurrences of either channel cut-off or channel narrowing and widening, as the data insists, are also highly attributable to radius of curvature and channel curvature quantities within the critical ranges of 1250 to 2000 feet and 2.75 to 3.75, correspondingly, for the reaches extending from Augusta to Des Arc, Devalls Bluff to Clarendon, and St. Charles to LMR. A similar, yet simplistic and convincing, confirmation that curvature may impose greater impacts on planform metamorphoses or deformations than other fluvial and morphological parameters appertains to combinations of the immense numerical quantities of sinuosity and sinuosity enhancement, the high frequencies of channel cut-off, narrowing, and widening, and the excessive magnitudes of lateral migration detected for the segments from Augusta to Des Arc, Devalls Bluff to Clarendon, and St. Charles to LMR. The phenomena encompassing lateral migrations, sinuosity augmentations, and channel dimension modifications may also be explicated for these reaches in terms of discharge and its interdependent relationship with channel curvature. Explanations specifically involve the development of inner and outer bank flow separations as bends develop and tighten, which stall the spatially organized vacillating pattern of helical flow, resulting in intense flow turbulence that operates as a catalyst for the initiations of rapid bank erosions, accelerations of lateral and downstream migrations, and ultimately escalations in energy losses (Bagnold, 1960; Lagasse et al., 2004b). Therefore, a channel curvature range of 2 or below corresponds to energy loss and attenuation in erosion rate and characterizes double heading, a channel curvature interval of 2 to 3 corresponds to “a

minimum in the energy losses generated by the bend” and characterizes rapid migration, and a channel curvature range of 3 and above corresponds to the absence of flow convergence and amplification in erosion rate and characterizes bend growth (Lagasse et al., 2004b).

The assemblages of parametric correlations between fluvial and morphological parameters as a whole evinced concrete evidence to support the classifications of the reach extending from Devalls Bluff to Clarendon, which is characterized by dimensional disparities in association to an array of quantified radii of curvature, substantial magnitudes of depths or boundary stresses, large sinuosity ratios in accompaniment to high optimal sub-basin widths, high potential for bed aggradation, channel curvature occupation within the critical range of rapid channel migration, considerable and perceivable extent of lateral shift or migration, and high occurrences of channel cut-off and widening or narrowing; the reach extending from Clarendon to St. Charles, which is distinguished by significant dispersions in meander wavelengths, a wide or developed sub-basin with numerous accounts of large sinuosity values across various arrays of higher order numerical ranges, substantial magnitudes of depths or boundary stresses, and high potential for channel bed aggradation; and the reach extending from St. Charles to the confluence with the Lower Mississippi River, which is secernated by high channel dimensions in colligation to measured radii of curvature, substantial magnitudes of depths and boundary stresses, high probability for bed degradation, bountiful channel curvature values within the critical range of accelerated channel migration, and high frequencies of channel widening and narrowing, as unstable or destitute of dynamic stability.

It should be noted that the conclusions made regarding the meandering/shifting propensity, dynamic equilibrium, and overall stability of these alluvial reaches are derived primarily from parametric correlations emerging from the measurements, quantifications, and computations of variables via ArcGIS and HEC-RAS rather than field observations, monitoring, and data extraction. Field activities will be covered in detail in chapter 4 and 5 to validate the flow and sediment regimes and stability conditions of the studied reaches of the White River. Verifications of channel degradation/aggradation potentials in the form of detailed sediment analyses will also be included in chapter 5. In summary, the key findings herewith elicit concrete evidence that channel curvature represents a viable prognosticator of meander geometry and planform metamorphoses more so than other fluvial and morphological parameters although the arrays of data representing multifarious correlations between these constituents together may also provide a fairly legitimate interpretation of planform metamorphosis, lateral migration, flow divergence and convergence, boundary shear stress and velocity distributions, and overall channel condition.

CHAPTER 4: THE ROSGEN STREAM CLASSIFICATION SYSTEM

Introduction

The Rosgen Stream Classification (RSC) system is a method for classifying streams and rivers by utilizing a hierarchical inventory approach based on common characteristics inherent to channel morphology. RSC is also a derivative of physical processes established upon assumptions that stream morphology is reliant upon landscape arrangement (Rosgen & Silvey, 1996). Significant constituents of channel morphology include various parameters that constitute stream channel dimensions, patterns, and profiles.

Stream channel dimensions consist of width, depth, and bankfull cross-sectional area. “Stream width is a function of streamflow occurrence and magnitude, size and type of transported sediment, and the bed and bank materials of the channel” and can be altered by channelization, and a change in streamflow regime, sediment regime, and riparian vegetation (Rosgen & Silvey, 1996, pp. 2-4 – 2-5). Stream depth, which varies from section to section, is a function of streamflow regime, sediment regime, basin relief, and the nature of the bed and bank materials. Bankfull cross-sectional area, a function of both stream channel width and depth, is often “correlated with streamflow and drainage area as an expression of channel size” (Rosgen & Silvey, 1996, p. 2-5). The geomorphic parameters often associated with stream channel dimensions include width/depth ratio, entrenchment ratio, and riffle/pool sequence.

Stream channel patterns are utilized to depict the planform of a stream. Stream patterns of river, classified as either straight, meandering, braided, or anastomosis, are developed naturally to dissipate the kinetic energy of water movement and sediment

conveyance within a flow regime. The dynamic equilibrium and stability of a stream are maintained by the river through an autogenic balancing of sediment loads and stream energy. The geomorphic parameters often associated with stream channel patterns include radius of curvature, meander wavelength, meander amplitude, and sinuosity.

Stream channel profile deals primarily with the stream gradients which were discovered by Lane (1957) to be directly proportional to sediment size and load and inversely proportional to stream discharge. Streams with steep gradients are generally found to be straight, dissipating kinetic energy along the longitudinal profile through steps and pools while streams with gentle gradients are generally found to be sinuous/tortuous, dissipating kinetic energy by shifting and meandering (erosion and deposition). Parameters associated with the profile are energy gradient, channel slope, and valley slope.

RSC Hierarchy of River Inventory and Assessment

The objective of this chapter is to utilize the Rosgen Stream Classification System to characterize the geomorphology of the White River. The assessment of the White River fluvial morphology will follow a hierarchy comprised of four inventory levels. The first level will describe the White River's geomorphological characterization. The second level will provide a morphological description of the White River's characteristics. The third level will assess the White River's "state" or condition and its stability. The fourth level will serve as verification of the predictions made in Level III. The hierarchy of river morphology is also illustrated by **Figure 4.1**.

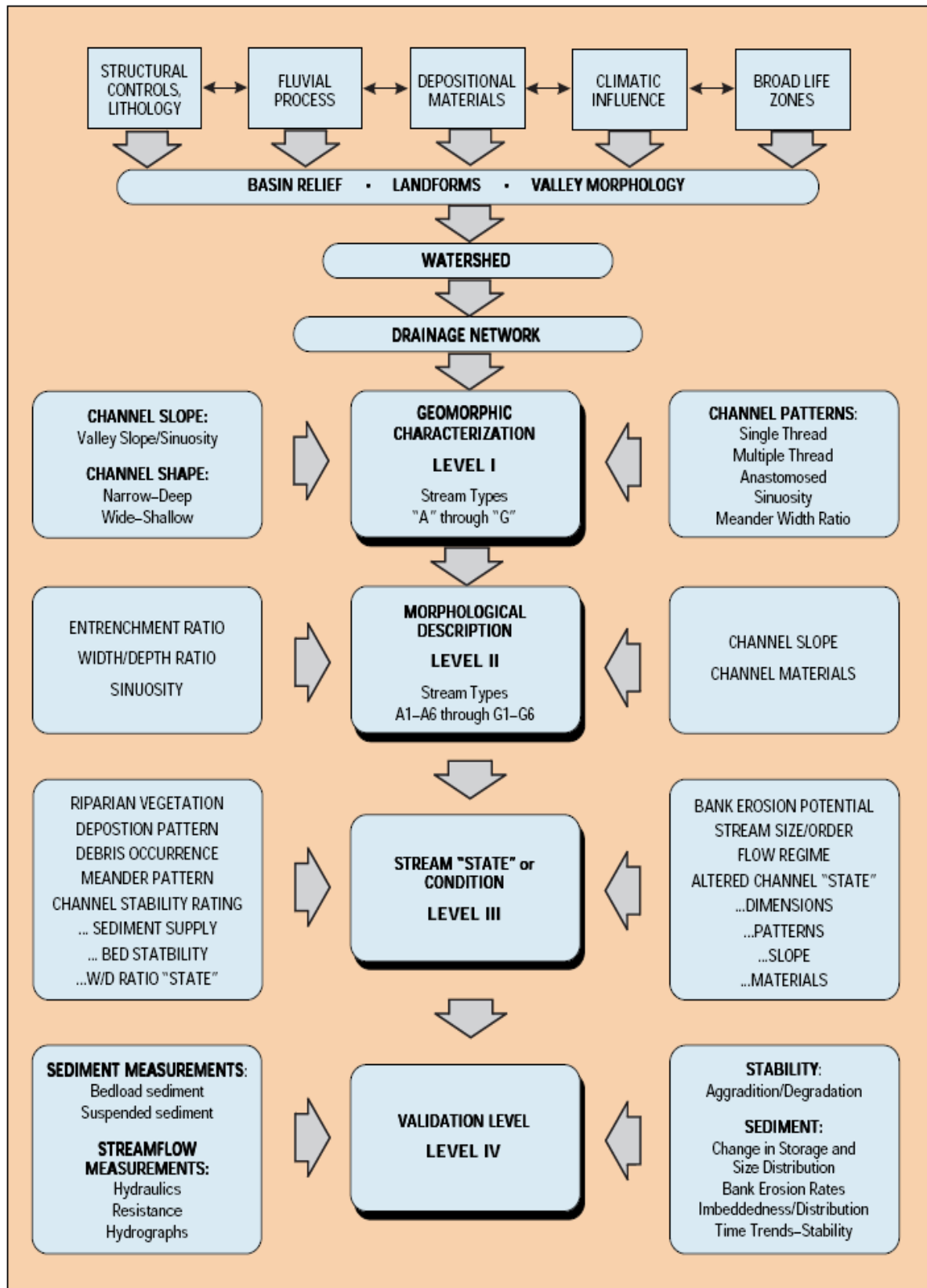


Figure 4.1. Rosgen Stream Classification's Hierarchy of River Inventory and Assessment (Rosgen & Silvey, 1996).

Level I Classification: Geomorphic Characterization

This section provides an initial morphological delineation of stream type(s) and valley morphology related to the White River. The broad classification is dependent on the stream's overall vertical containment, patterns, slope, and shapes obtained and computed via the HEC-RAS Model and Aerial Photographs in ArcGIS.

Based on the criteria of **Table 4.2**, **Figure 4.2**, and **Figure 4.3**, the White River is classified as a type "C" stream developed within a type "X" valley. The White River at the delineation level exhibits morphological features such as a sinuous planform, low relief profile, "point bars" features, and an extensively developed floodplain often associated with a "C" stream. The quantitative values of the geomorphic parameters such as the longitudinal channel slope, width-depth ratio, entrenchment ratio, sinuosity, and meander width ratio presented in **Table 4.1** also indicate that the White River fits the description of a type "C" river. The wide valley through which the White River incised has a very gentle gradient and an extensive floodplain constructed with alluvium; a criterion of the valley type "X". Landforms associated with this valley type are coastal plains, alluvial flats, and wetlands which are often encountered in the Mississippi Alluvial Plain physiographic region.

Level II Classification: The Morphological Description

In contrast to the classification associated with Level I's geomorphic characterization, the classification of the morphological description of the White River's characteristics is reach-specific. Morphological variables possess the tendency for change in relatively short distances along the river channel and are attributable to changes in geology and tributary influence, thus stream type classification cannot be averaged or

generalized over the entire length of the river (Rosgen & Silvey, 1996). A method to account for a variety of stream types encountered along the White River is dependent upon data obtained from selected ‘reference’ reaches, which are then extrapolated to areas having similar landforms and fluvial features through the use of aerial photos, topographic maps, and a hydraulic model. Aerial photos and topographic maps are used to determine the channel sinuosity, radius of curvature, and meander belt width, the HEC-RAS Model is used to determine the channel slope, the channel cross-section, the width to depth and entrenchment ratios, and field measurements on ‘reference’ reaches are used to determine the dominant bed material and riparian vegetation. Knowledge pertaining to the size of the dominant bed material “helps determine the extent of sediment transport in [the White River]” (Arnwine, James, & Sparks, 2003, p. 59) while riparian vegetation has a significant influence on the stability and condition of the White River, all of which will be presented in detail in the third level of RSC.

The dominant bed material D_{50} or the median grain size river bed material is determined from a particle size distribution curve developed from data obtained by a

Table 4.1. Geomorphic Parameters of Various Sections of the White River.

Sections	Gradient	Entrenchment. Ratio	W/D Ratio	Sinuosity	Meander Belt Ratio
Batesville - Newport	0.000112	66.15	42.43	1.65	36.54
Newport - Augusta	0.000050	60.00	26.43	1.59	34.37
Augusta - Des Arc	0.000078	47.75	30.48	1.49	31.81
Des Arc - Devalls Bluff	0.000080	25.44	29.83	1.60	28.42
Devalls Bluff - Clarendon	0.000045	49.48	22.50	1.72	32.33
Clarendon - St. Charles	0.000060	43.24	28.36	1.57	32.11
St. Charles - LMR	0.000093	42.35	27.82	1.51	28.98

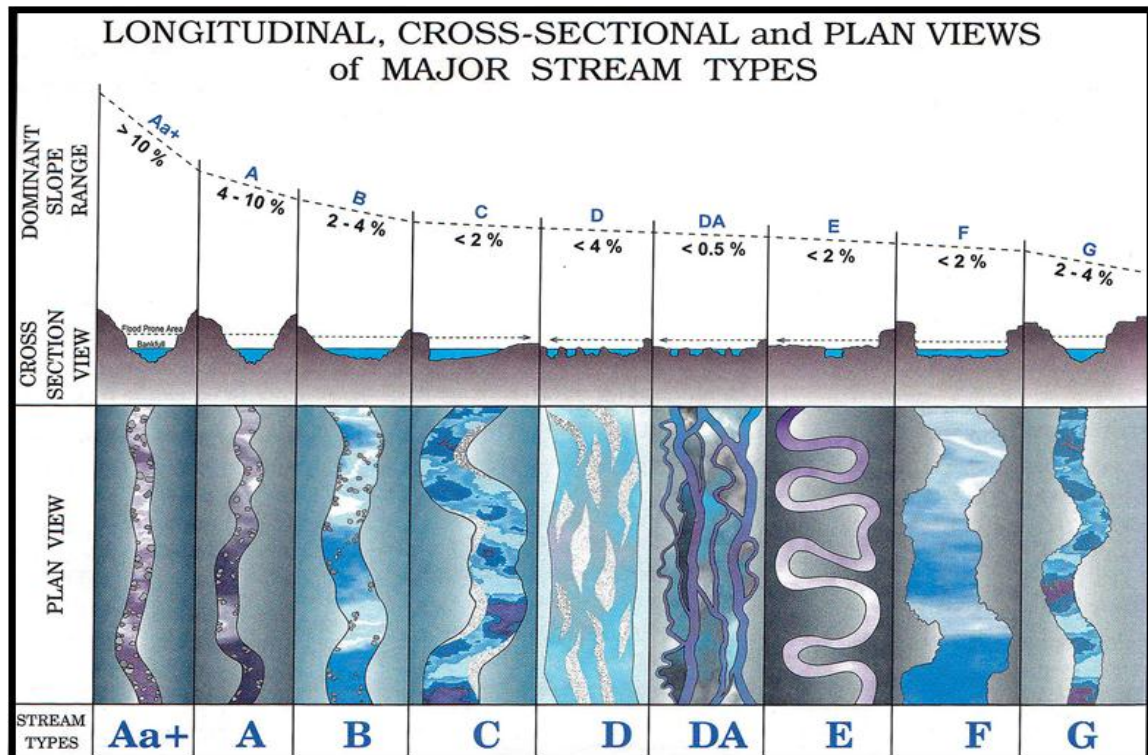


Figure 4.2. Broad-level Stream Classification Delineation Showing Longitudinal, Cross-sectional, and Plan-views of Major Stream Types (Rosgen & Silvey, 1996).

STREAM TYPE	A	D	B & G	F	C	E
PLAN VIEW						
CROSS-SECTION VIEW						
AVERAGE VALUES	1.5	1.1	3.7	5.3	11.4	24.2
RANGE	1-3	1-2	2-8	2-10	4-20	20-40

Figure 4.3. Meander Width Ratio by Stream Type Categories (Rosgen, 1994).


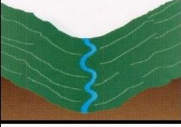




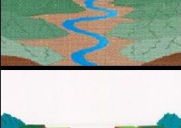




	Valley type	Description	Stream type association
I		Steep V-shaped confined, highly dissected fluvial slopes greater than 2 percent	A and Aa+
II		Moderate relief gentle sloping side slopes with a parabolic valley bottom form often in colluvial valleys	B
III		Primarily depositional, usually steep, greater than 2 percent valley slope with debris-colluvium or alluvial fan landform	A, B, G, and D
IV		Gentle gradient canyons, gorges and confined alluvial valleys such as the Grand Canyon. Valley floors are typically less than 2 percent	F
V		U-shaped glacial-fluvial troughs with slopes generally less than 4 percent. Landforms typically include lateral or terminal moraines, alluvial terraces and flood plains. Trough is typically the result of glacial scouring process	C, D, G
VI		Fault control valleys, structurally controlled and dominated by colluvial slope building processes. Moderately steep with slopes less than 4 percent. G stream types observed under fault disequilibrium	Mostly B with C and F; some G
VII		Steep highly dissected fluvial slopes typically in either colluvium, alluvium or in residual soil. Active lateral and vertical accretion (Badlands of SD)	A and G
VIII		Mature wide gentle valley slopes with well developed flood plain features adjacent to river terraces. Alluvial terraces and flood plains are predominate landforms. Depending on local streambed and riparian conditions D, F, and G stream types can be found. Gentle slopes with the alluvial valley fills	C and E D, F, and G
IX		Glacial outwash and/or eolian sand dunes. Moderate to gentle slopes. High sediment supply either single- or multiple-threaded channels	C and D
X		Very broad and very gentle slopes with extensive flood plain development. Often associated with lacustrine and gentle alluvial slopes. G and F streams are common when local base grades have been changed	E or C and DA, G, and F
XI		Large river deltas and tidal flats constructed of fine alluvial materials originating from riverine and estuarine depositional processes. Extremely gentle slopes with base grade controlled by sea or lake levels. Most often distributary channels, wave, or tide dominated	DA C and E

Figure 4.4. Valley Type, Morphological Description, and Stream Type Association (as modified from Rosgen & Silvey, 1996).

Table 4.2. General Stream Type Descriptions and Delineative Criteria for Broad-level Classification (Level I) (Rosgen & Silvey, 1996).

Stream type	General description	Entrench ratio	Width-to-depth ratio	Sinuosity	Slope	Landform/soils/features
Aa+	Very steep, deeply entrenched, debris transport streams	<1.4	<12	1.0 – 1.2	>.10	Very high relief. Erosional, bedrock, boulder, or depositional features; debris flow potential. Deeply entrenched streams. Vertical steps with deep scour pools; waterfalls
A	Steep, entrenched, cascading, step-pool streams. High energy/debris transport with depositional soils. Very stable if bedrock or boulder-dominated channel	<1.4	<12	1.0 – 1.2	.04–.10	High relief. Erosional bedrock forms. Entrenched and confined streams with cascading reaches. Frequently spaced, deep pools in associated step-pool bed morphology
B	Moderately entrenched, moderate gradient dominated channel, with infrequently spaced pools. Very stable plan and profile. Stable banks	1.4 – 2.2	>12	>1.2	.02–.039	Moderate relief, colluvial riffle deposition, and/or residual soils. Moderate entrenchment and width-to-depth ratio. Narrow, moderately sloping valleys. Rapids predominate with occasional pools
C	Low gradient, meandering point-bar, riffle-pool, alluvial channels with broad, well-defined flood plains	>2.2	>12	>1.4	<.02	Broad valleys w/terraces, in association with flood plains, alluvial soils. Slightly entrenched with well-defined meandering channel. Riffle-pool bed morphology
D	Braided channel with longitudinal and transverse bars. Very wide channel with eroding banks	N/a	>40	N/A	<.04	Broad valleys with alluvial and colluvial fans. Glacial debris and depositional features. Active lateral adjustment with abundance of sediment supply
DA	Anastomosing (multiple channels) narrow and deep with expansive well-vegetated flood plain and associated wetlands. Very gentle relief with highly variable sinuosity's, stable streambanks	>4.0	<40	Variable	<.005	Broad, low-gradient valleys with fine alluvium and/or lacustrine soils. Anastomosed (multiple channel) geologic control creating fine deposition with well-vegetated bars that are laterally stable with broad wetland flood plains. Stream type common in estuaries
E	Low gradient, meandering riffle-pool stream with low width-to-depth ratio and little deposition. Very efficient and stable. High meander width ratio	>2.2	<12	>1.5	<.02	Broad valley/meadows. Alluvial materials with flood plain and/or lacustrine soil. Highly sinuous with stable well-vegetated banks. Riffle-pool morphology with very low width-to-depth ratio
F	Entrenched meandering riffle-pool channel on low gradients with high width-to-depth ratio	<1.4	>12	>1.4	<.04	Entrenched in highly weathered material. Gentle gradients usually less than .02 ft/ft, but may range up to .04 ft/ft with a high width-to-depth ratio. Meandering, laterally unstable with high bank erosion rates. Riffle-pool morphology.
G	Entrenched gully step-pool and low width-to-depth ratio on moderate gradients	<1.4	<12	>1.2	.02–.039	Gully, step-pool morphology with moderate slopes and low width-to-depth ratio. Narrow valleys, or deeply incised in alluvial or colluvial materials (fans or deltas). Unstable with grade control problems and high bank erosion rates

modified Wolman Pebble Count method. The method involves randomly selecting and measuring 100 particles at a particular site. The common schemes include collecting and measuring 100 particles within the thalweg at systematic distance intervals, collecting and measuring 100 particles on a 45 degree zig-zag pattern across the flow transect, and collecting and measuring a total of 100 particles from parallel systematically-spaced intervals across the flow transects. In the case pertaining to the White River, a composite of the two latter schemes was employed mainly in part due to the great depth of the transect near the thalweg, which limited manual pebble count as it exceeded the data collector's height. The composite method consisted of a team of two members starting at one common point at the wetted edge where an initial sample was taken by the team leader. The team leader then ventured into the channel at a 45 degree angle while the other member of the team walked along the wetted edge. The team leader took two samples at evenly spaced intervals between the starting point along the wetted edge and a distance of 10 feet along the wetted edge. The team leader then returned to the river edge at a 45 degree angle and took two more samples, at evenly spaced intervals, to meet the other member at an additional distance of 10 feet along the wetted edge. The process was repeated until 100 samples were obtained. The composite pebble count scheme is illustrated in **Figure 4.5**. Grouping of the median grain size river bed material (D_{50}) into one of six categories of Rosgen classifications for dominant bed material is also shown in **Table 4.3**.

Samples dominated by fine sediments such as sands, silts, and clays are oven dried and analyzed in the laboratory through sieve analyses. The U.S. standard sieve numbers used and the sizes of openings are given in **Appendix D**. Particle sizes smaller

Table 4.3. Rosgen Classifications of Dominant Bed Materials.

Particle Size (mm)	Description	Rosgen Classification
> 4096	Bedrock	1
256 - 4096	Boulder	2
64 - 256	Cobble	3
2 - 64	Gravel	4
0.062 - 2	Sand (5 categories from very fine to very coarse)	5
< 0.062	Silt/Clay	6

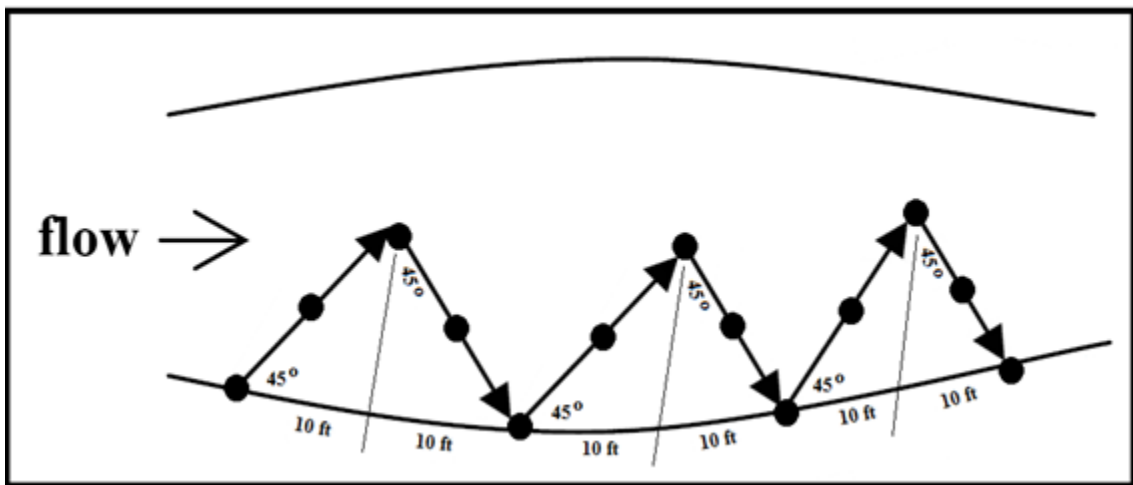


Figure 4.5. Composite Wolman Pebble Count Scheme Across the Flow Transect.

than 0.075 mm in diameter, i.e., silts and clays, are not separated by hydrometer analysis and are classified as a one soil class. Sieve analysis results are also presented as bar histograms in **Appendix D**. Samples dominated by gravels or retained on U.S. standard sieve number 4 are measured individually for the intermediate axis or the width. Particle size distribution curves are constructed by tabulating the results obtained from laboratory analyses.

Multiple ‘reference’ reaches are selected along the White River in cities or

towns located close to the river. The ‘reference’ reaches are Batesville (RM 299.00), Newport (RM 258.94), Augusta (RM 200.30), Des Arc (RM 148.03), Devalls Bluff (RM 124.35), Clarendon (RM 100.38), and St. Charles (RM 56.57). Fluvial and morphological descriptions for each ‘reference’ reach are tabulated and discussed in greater detail in the following sections.

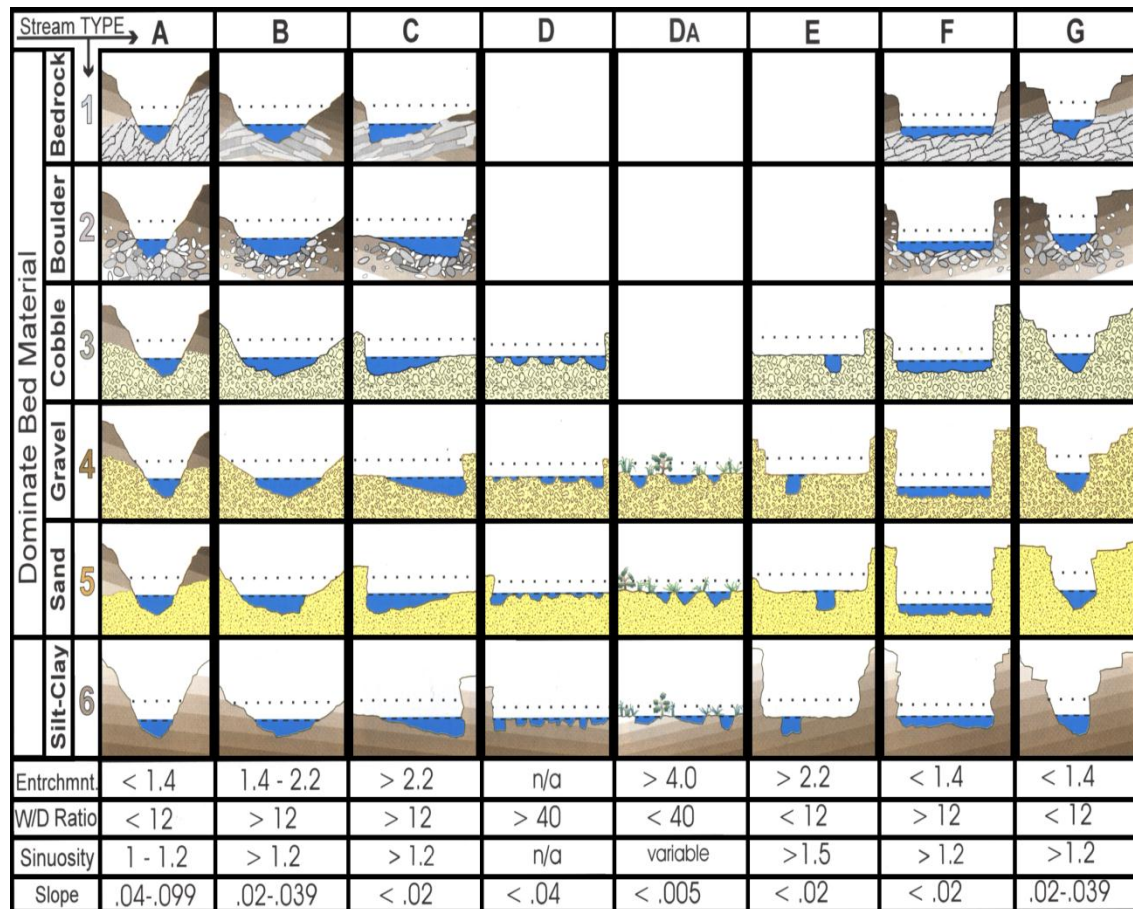


Figure 4.6. Illustrative Guide Showing Cross-sectional Configuration, Composition and Delineative Criteria of Major Stream Types (Rosgen & Silvey, 1996).

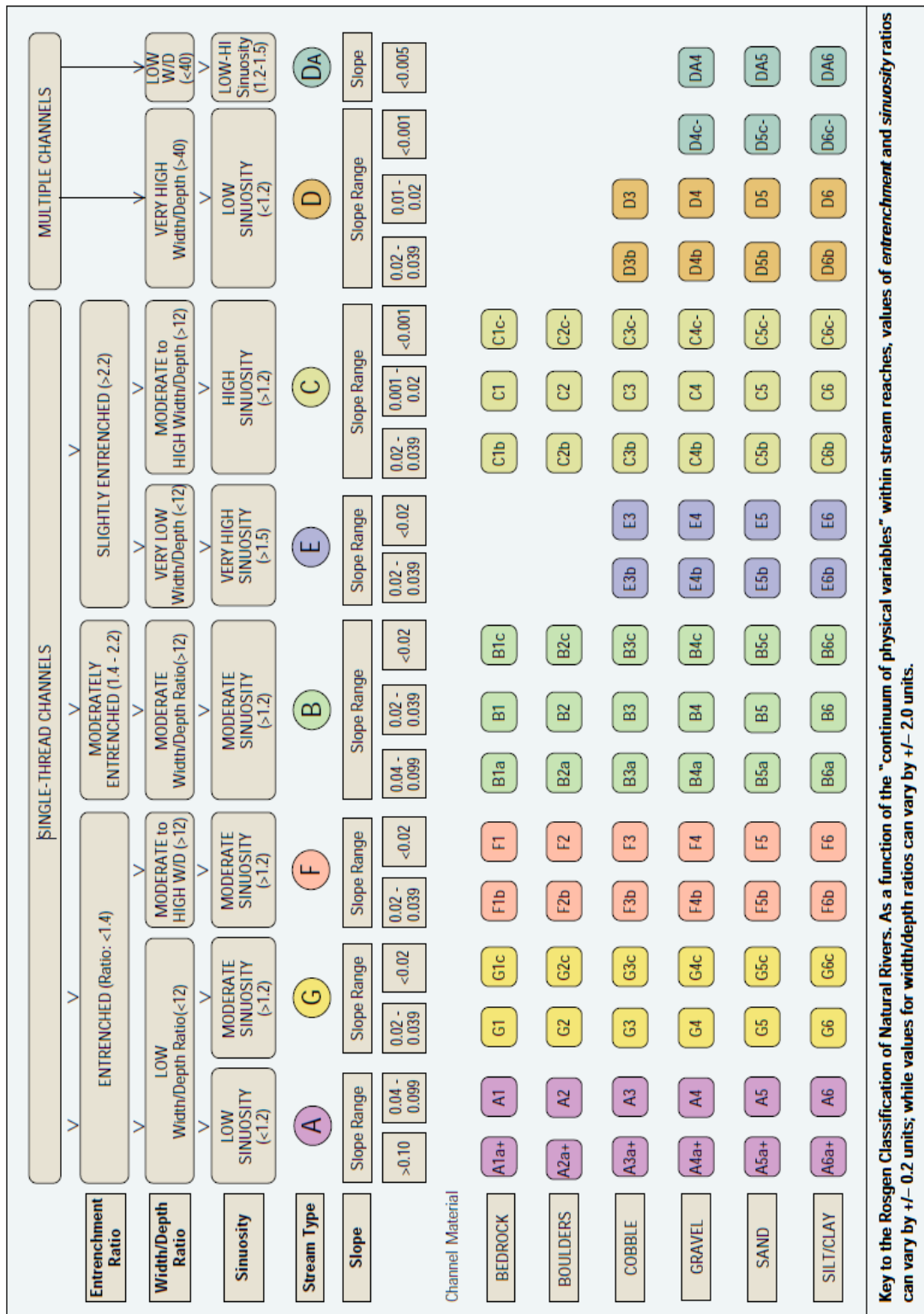


Figure 4.7. Classification Key for Natural Rivers (Rosgen & Silvey, 1996).

Batesville (RM 299.00). Based on the particle size distribution curve developed from data obtained by the Wolman Pebble Count method and the morphological and fluvial features obtained from the HEC-RAS Model and aerial photographs, the White River's 'reference' reach at Batesville (RM 299.00) is classified as a type "C4c-" stream within a type "X" valley. The reach had a width of about 500 feet, a bank height ranging from 15 feet to 20 feet, a gentle gradient of less than 2%, displayed a width/depth ratio of approximately 35, an entrenchment ratio of 9.9, a meander width ratio of about 29, and an average sinuosity of 1.65. The dominant bed material D_{50} consisted of very coarse gravels while the banks were composed of unconsolidated, heterogeneous, non-cohesive materials. Riffle and pool sequences, which contributed to the rapidity of the flow, were very distinct and were spaced approximately 7.40 times the channel width in length. The reach was characterized by point bars and other depositional features such as islands and mid-bars; an indicator of susceptibility to lateral and vertical shifts generally evoked by alterations in flow and sediment regimes. Field observations in the vicinity revealed non-uniform flow and very low water temperatures possibly due to the presence of riffle and pool sequences and the mixture of stream water and dam-released hypolimnetic water, respectively, and suggested an ecological environment stressing a healthy terrestrial habitat for insects and diversified riparian habitats of hard hardwoods encompassing oaks, hickories, sycamores, maples, walnuts, and mulberries; soft hardwoods such as sugar berries and sassafras; clambering plants/vines such as wild grapes and greenbriers, and monocots such as goldenrod and grass. Pebble count data, the particle distribution curve, and the field form detailing fluvial and morphological and parameters are shown in **Table 4.4, Table 4.5 and Figure 4.8.**

Table 4.4. Pebble Count Data for the Reference Reach at Batesville, Arkansas (RM. 299.00).

PEBBLE COUNT							
Site: Batesville, AR (RM 299.00)				Date: 09/15/2010			
Party: Linh & Vince				Reach: Upper White River			
INCHES	PARTICLE	MILLIMETER		Particle Count	TOT #	ITEM %	% CUM
	Silt/Clay	< .062	S/C	I	1	1	1
.04 - .08	Very Fine	.062 - .125	S	III	3	3	4
	Fine	.125 - .25	A	HHH HHH III	13	13	17
	Medium	.25 - .50	N	III	4	4	21
	Coarse	.50 - 1.0	D	I	1	1	22
	Very Coarse	1.0 - 2.0	S		0	0	22
.08 - .16	Very Fine	2.0 - 4.0	G	I	1	1	23
.16 - .31	Fine	4.0 - 8.0	R	II	2	2	25
.31 - .63	Medium	8.0 - 16.0	V	III	4	4	29
.63 - 1.26	Coarse	16.0 - 32.0	L	HHH HHH HHH HHH HHH I	31	31	60
1.26 - 2.5	Very Coarse	32.0 - 64.0	S	HHH HHH HHH HHH HHH HHH II	37	37	97
2.5 - 5.0	Small	64.0 - 128.0	C O	III	3	3	100
5.0 - 10.0	Large	128.0 - 256.0	B L		0	0	100
10.0 - 20.0	Small	256.0 - 512.0	B		0	0	100
20.0 - 40.0	Medium	512.0 - 1024.0	L		0	0	100
40.0 - 160	Lrg-Very Lrg	1024.0 - 4096.0	D R		0	0	100
	BEDROCK		BDRK				
TOTALS					100	100	100

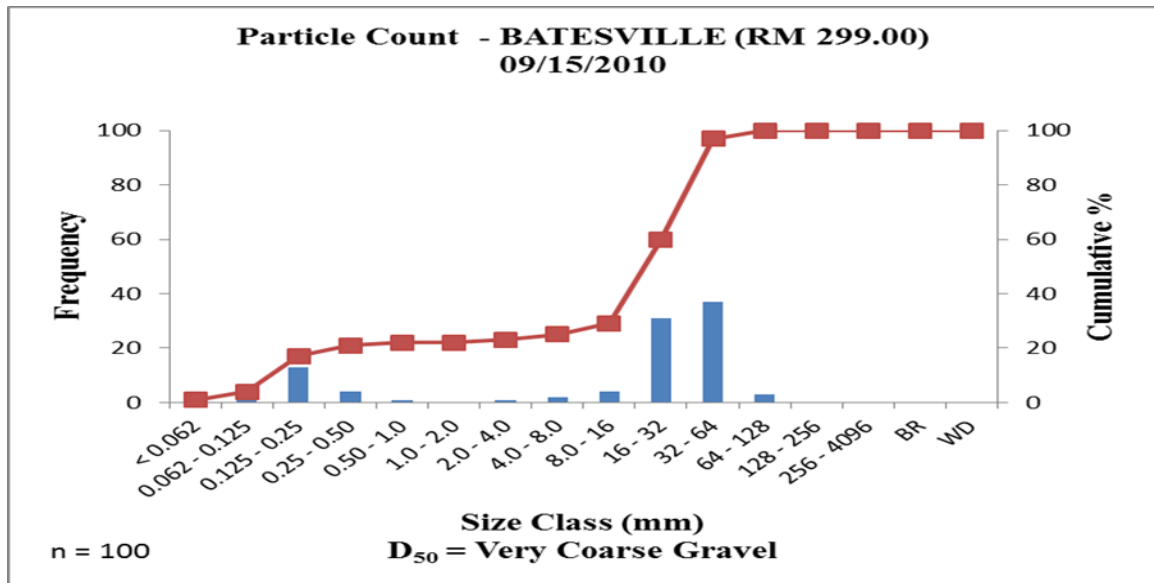




Figure 4.8. Particle Count and Calculated D_{50} for the Reference Reach at Batesville.

Table 4.5. Field Data Form for the Reference Reach at Batesville, AR (RM 299.00)

REFERENCE REACH FIELD FORM STREAM CHANNEL CLASSIFICATION LEVEL II		STREAM TYPE: C4c-	
STREAM NAME: White River		DRAINAGE AREA: 1785.12 Sq. mi.	
BASIN NAME: White River Basin		DATE: 09/15/2010	
OBSERVERS: Linh & Vince		Twp. Sec. 299.00 Qtr.	
LOCATION: Batesville, Arkansas		Rge.	
Bankfull WIDTH 499.00 Ft. (W_{bkt})	Bankfull MAX DEPTH 19.23 Ft. (d_{max})	Channel SLOPE 0.0001	Ft/Ft < 0.01 %
Bankfull Mean DEPTH 15.71 Ft. (d_{bkt})	Flood Prone Area WIDTH 4.9k Ft. (W_{fp})	Valley SLOPE 0.0013	Ft/Ft 0.13 %
WIDTH/DEPTH Ratio 35.00	ENTRENCHMENT Ratio 9.90	SINUOSITY 1.65	
Channel Materials: Medium to very coarse gravels with fine sands			
			
<ul style="list-style-type: none"> - Wide channel with flat longitudinal gradient and flat wide banks with noncohesive materials, gravels, cobbles, and boulders in some areas. - Distinct sequences of riffles and pools. - Rapid flow 		<ul style="list-style-type: none"> - Healthy insect terrestrial habitat. - Diverse riparian habitat consists of oaks (<i>Quercus palustris</i> and <i>Quercus nigra</i>), <i>Carya</i> spp., <i>Juglans</i>, <i>Populus deltoides</i>, <i>Plantanus occidentalis</i>, <i>Acer rubrum</i>, <i>sassafras albidum</i>, <i>poaceae</i>, and thick clusters of <i>Celtis laevigata</i>, <i>Morus alba</i>, wild <i>vitis</i>, <i>Smilax rotundifolia</i> L., and <i>solidago</i> sp. 	

Newport (RM 258.94). Particle size distribution results, morphological and fluvial features local to the White River's 'reference' reach at Newport (RM 258.94) suggest that it is a "C5c-" stream within a type "X" valley. The reach had a width of about 580 feet, a bank height ranging from 20 feet to 25 feet, a gentle gradient of less than 1%, a width/depth ratio of about 32, an entrenchment ratio of 106, a meander width ratio of about 37, and a sinuosity of about 1.43. The dominant bed material D_{50} consisted of fine sands while the banks consisted of mostly fine sand, silt, and clay. Riffle and pool sequences averaged approximately about 6.65 times the channel width in length. The reach was characterized by point bars, an indicator of susceptibility to lateral and vertical shifts generally evoked by alterations in flow and sediment regimes, although not as prevalent as the upstream reaches. It is suspected that sediment supply ranges from high to very high especially at the confluence with the Black River. Field observations in the vicinity revealed rapid non-uniform flow influenced by the Black River, low water temperature and an ecological environment emphasizing a healthy terrestrial habitat for caterpillars, butterflies, and other insects. Zonation was very apparent for the mixed hardwood riparian forest with smaller trees near the river bank and larger trees away from the bank. The riparian forest was diverse in hardwoods such as oaks, hickories, sycamores, and maples. Smaller hardwoods such as silver maples, Shagbark and bitternut hickories, and various species of sycamores occupied the river banks along with thick clusters of mulberries, wild grape vines, and herbaceous monocots and dicots. Fallen trees and exposed roots were common at steep banks near man-made structures or bridges. For specific data pertaining to Pebble Count, particle distribution curve, and reference reach observations, refer to **Table 4.6**, **Table 4.7**, and **Figure 4.9**.

Table 4.6. Pebble Count Data for the Reference Reach at Newport, Arkansas (RM 258.94).

PEBBLE COUNT							
Site: Newport, AR (RM 258.94)				Date: 08/27/2010			
Party: Linh & Virak				Reach: White River			
INCHES	PARTICLE	MILLIMETER		Particle Count	TOT #	ITEM %	% CUM
	Silt/Clay	< .062	S/C	HHH HHH HHH I	16	16	16
.04 - .08	Very Fine	.062 - .125	S	HHH HHH	10	10	26
	Fine	.125 - .25	A	HHH HHH HHH HHH HHH HHH HHH HHH	39	39	65
	Medium	.25 - .50	N	HHH HHH HHH HHH I	21	21	86
	Coarse	.50 - 1.0	D	HHH HHH	10	10	96
	Very Coarse	1.0 - 2.0	S	II	2	2	98
.08 - .16	Very Fine	2.0 - 4.0	G	II	2	2	100
.16 - .31	Fine	4.0 - 8.0	R		0	0	100
.31 - .63	Medium	8.0 - 16.0	V		0	0	100
.63 - 1.26	Coarse	16.0 - 32.0	L		0	0	100
1.26 - 2.5	Very Coarse	32.0 - 64.0	S		0	0	100
2.5 - 5.0	Small	64.0 - 128.0	C O		0	0	100
5.0 - 10.0	Large	128.0 - 256.0	B L		0	0	100
10.0 - 20.0	Small	256.0 - 512.0	B		0	0	100
20.0 - 40.0	Medium	512.0 - 1024.0	L D		0	0	100
40.0 - 160	Lrg-Very Lrg	1024.0 - 4096.0	R		0	0	100
	BEDROCK		BDRK				
TOTALS					100	100	100

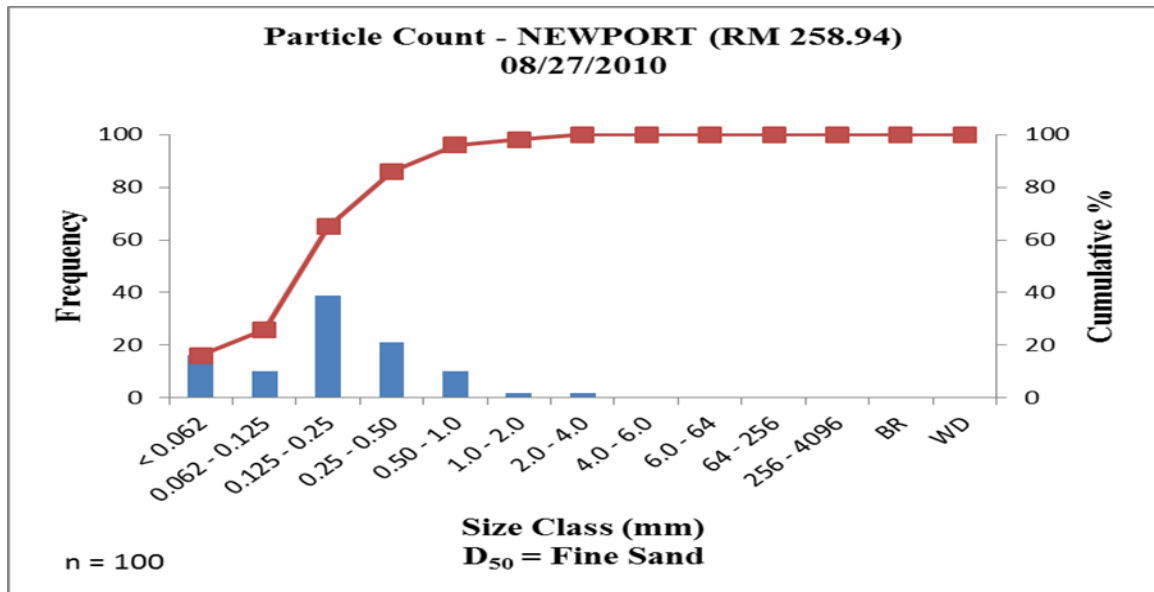

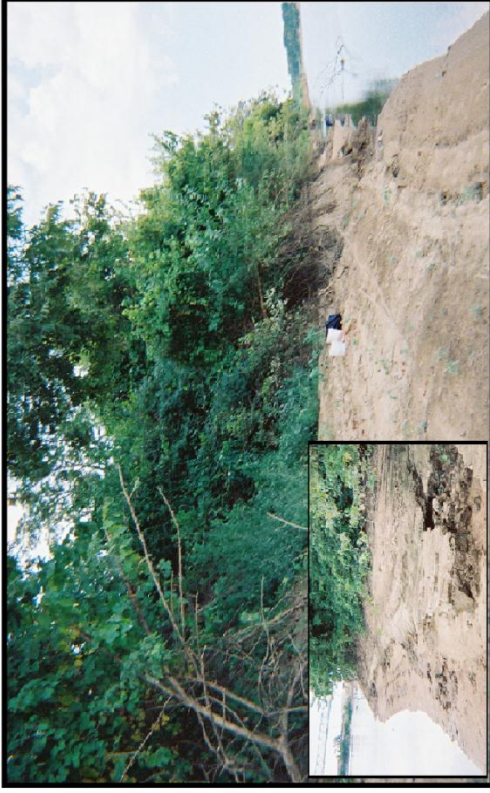


Figure 4.9. Particle Count and Calculated D₅₀ for the Reference Reach at Newport.

Table 4.7. Field Data Form for the Reference Reach at Newport, AR (RM 258.94).

<div style="border: 1px solid black; padding: 5px; margin-bottom: 10px;"> REFERENCE REACH FIELD FORM STREAM CHANNEL CLASSIFICATION LEVEL II </div> <div style="border: 1px solid black; padding: 5px;"> <p>STREAM NAME: <u>White River</u> DRAINAGE AREA: <u>981.02 Sq. mi.</u> BASIN NAME: <u>White River Basin</u></p> <p>OBSERVERS: <u>Linh & Virak</u> DATE: <u>08/27/2010</u></p> <p>LOCATION: <u>Newport, Arkansas</u> Twp. _____ Rge. _____ Sec. <u>258.94</u> Qtr. _____</p> <p>Bankfull WIDTH <u>579.16</u> Ft. (W_{bkt}) Bankfull MAX DEPTH <u>28.26</u> Ft. (d_{max}) Channel SLOPE <u>0.00008</u> Ft/Ft <u>0.008</u> %</p> <p>Bankfull Mean DEPTH <u>26.80</u> Ft. (d_{bkt}) Flood Prone Area WIDTH <u>61k</u> Ft. (W_{fp}) Valley SLOPE <u>0.0002</u> Ft/Ft <u>0.02</u> %</p> <p>WIDTH/DEPTH Ratio <u>32.00</u> ENTRENCHMENT Ratio <u>105.50</u> SINUOSITY <u>1.43</u></p> <p>Channel Materials: <u>Silts, Clays, and Sands (Abundant in fine sands)</u> D50 <u>Sands (fine)</u></p> </div>	<div style="border: 1px solid black; padding: 5px; margin-bottom: 10px;"> STREAM TYPE: <u>C5c-</u> </div> <div style="display: flex; justify-content: space-around;">   </div> <div style="border: 1px solid black; padding: 5px; margin-top: 10px;"> <p>- Wide channel with flat longitudinal gradient and relative flat banks with distinct point bars of noncohesive materials.</p> <p>- Healthy terrestrial habitat with presence of caterpillars, butterflies, and other insects.</p> <p>- Apparent zonation with smaller trees near river banks and larger trees farther from the plain.</p> <p>- Fallen trees and root exposure proximal to steeper banks and bridges.</p> </div>
<p>- Riparian forest abundant in hickories (<i>Carya ovata</i> and <i>Carya cordiformis</i>) and oaks (<i>Quercus velutina</i>, <i>Quercus alba</i>, <i>Quercus rubra</i>, <i>Quercus laurifolia</i>, and <i>Quercus phellos</i>).</p> <p>- Small <i>Acer saccharinum</i>, <i>Carya ovata</i>, and <i>Platanus occidentalis</i> at tops of river banks with thick clusters of <i>Morus alba</i>, wild vitis, and herbaceous monocotyledonae and dicotyledons.</p>	

Augusta (RM 200.30). Particle size distribution results, morphological and fluvial features of the White River's reference reach at Augusta (RM 200.30) suggest that it is a "C5c-" stream within a type "X" valley. The reach had a width of about 536 feet, a bank height ranging from 25 feet to 30 feet, a gentle gradient of less than 1%, a width/depth ratio of approximately 28, an entrenchment ratio of 66, a meander width ratio of about 31, and a sinuosity of about 1.36. The dominant bed material D_{50} consisted of very fine sands while the banks consisted of mostly cohesive soils as well as lesser quantities of non-cohesive materials. Riffle and pool sequences averaged approximately 5.88 times the channel width in length. The reach was characterized by point bars, an indicator of susceptibility to lateral and vertical shifts generally evoked by alterations in flow and sediment regimes. Field observations indicated slightly steep banks and non-uniform slower flow (in comparison to upstream reaches) due in part to a decrease in the longitudinal slope. Several miles downstream, Oxbow lakes were present as the river maneuvered into swamp lands of the alluvial floodplain. The area also exhibited tortuously compounded bends on the verge of neck cut-off. The riparian forest was abundant in hickories and various species of oaks with thick walls of clambering plants or vines such as poison ivies, wild grapes, and cat's claws thriving vigorously along the face of the river banks proximal to the water edge. Mississippi Hackberries and clusters of herbaceous monocots such as greenbriers and grasses also lined the banks. Fallen trees and exposed roots occupied areas along the banks exhibiting slightly steeper slope and distinct breaks in slope. Data and results pertaining to the morphological and fluvial parameters of the 'reference' reach are shown in **Table 4.8**, **Table 4.9**, and **Figure 4.10**.

Table 4.8. Pebble Count Data for the Reference Reach at Augusta, Arkansas (RM 200.30).

PEBBLE COUNT							
Site: Augusta, AR (RM 200.30)				Date: 09/04/2010			
Party: Linh & Virak				Reach: White River			
INCHES	PARTICLE	MILLIMETER		Particle Count	TOT #	ITEM %	% CUM
	Silt/Clay	< .062	S/C	HHH HHH HHH III	18	18	18
.04 - .08	Very Fine	.062 - .125	S	HHH HHH HHH HHH HHH HHH HHH I	41	41	59
	Fine	.125 - .25	A	HHH HHH HHH HHH III	23	23	82
	Medium	.25 - .50	N	HHH III	8	8	90
	Coarse	.50 - 1.0	D	HHH III	8	8	98
	Very Coarse	1.0 - 2.0	S		0	0	98
.08 - .16	Very Fine	2.0 - 4.0	G	II	2	2	100
.16 - .31	Fine	4.0 - 8.0	R		0	0	100
.31 - .63	Medium	8.0 - 16.0	V		0	0	100
.63 - 1.26	Coarse	16.0 - 32.0	L		0	0	100
1.26 - 2.5	Very Coarse	32.0 - 64.0	S		0	0	100
2.5 - 5.0	Small	64.0 - 128.0	C		0	0	100
5.0 - 10.0	Large	128.0 - 256.0	B		0	0	100
10.0 - 20.0	Small	256.0 - 512.0	L		0	0	100
20.0 - 40.0	Medium	512.0 - 1024.0	D		0	0	100
40.0 - 160	Lrg-Very Lrg	1024.0 - 4096.0	R		0	0	100
	BEDROCK		BDRK				
TOTALS					100	100	100

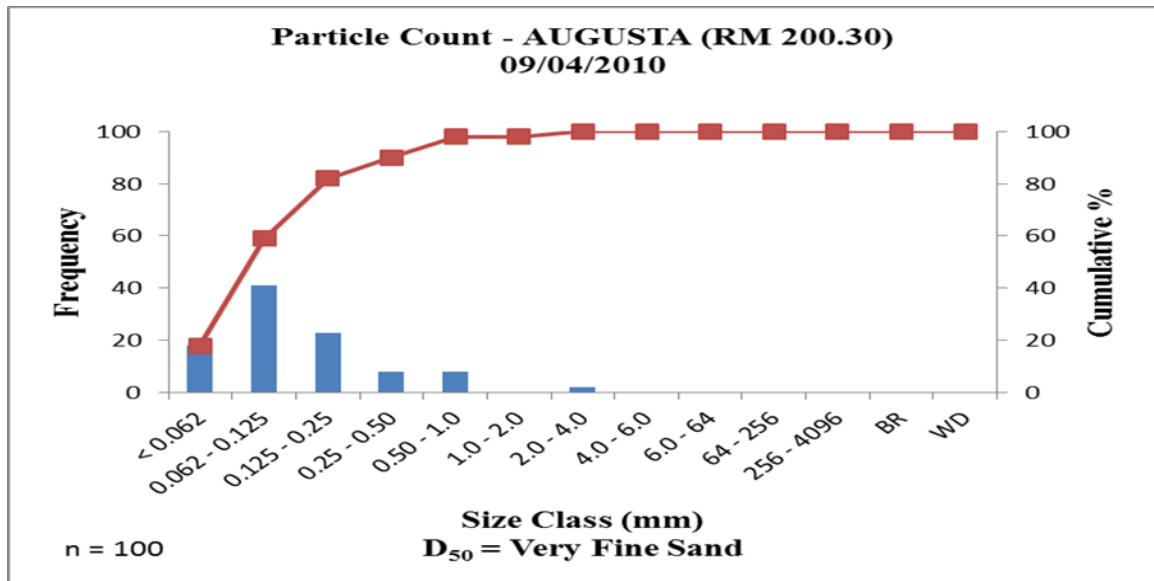




Figure 4.10. Particle Count and Calculated D_{50} for the Reference Reach at Augusta.

Table 4.9. Field Data Form for the Reference Reach at Augusta, AR (RM 200.30)

<div style="border: 1px solid black; padding: 5px; margin-bottom: 5px;"> REFERENCE REACH FIELD FORM STREAM CHANNEL CLASSIFICATION LEVEL II </div> <div style="border: 1px solid black; padding: 5px;"> <p>STREAM NAME: White River DRAINAGE AREA: 981.02 Sq. mi. BASIN NAME: White River Basin</p> <p>OBSERVERS: Linh & Virak DATE: 09/04/2010</p> <p>LOCATION: Augusta, Arkansas Twp. Rge. Sec. 200.30 Qtr.</p> <p>Bankfull WIDTH 535.71 Ft. (W_{bkt}) Bankfull MAX DEPTH 31.34 Ft. (d_{max}) Channel SLOPE 0.00002 Ft/Ft 0.002 %</p> <p>Bankfull Mean DEPTH 26.15 Ft. (d_{bkt}) Flood Prone Area WIDTH 35k Ft. (W_{fp}) Valley SLOPE 0.0002 Ft/Ft 0.02 %</p> <p>WIDTH/DEPTH Ratio 27.70 ENTRENCHMENT Ratio 65.60 SINUOSITY 1.36</p> <p>Channel Materials: Very fine to medium sands with silts and clays D50 Sands (very fine)</p> </div>	<div style="border: 1px solid black; padding: 5px; margin-bottom: 5px;"> STREAM TYPE: C5c- </div> <div style="border: 1px solid black; padding: 5px;">  <p>- Wide channel with very flat longitudinal gradient and slightly steep banks. - Fallen trees and root exposure along river banks in areas with distinct breaks in slope. - Riparian forest abundant in <i>Carya</i> spp. and various species of oaks (<i>Quercus rubra</i>, <i>Quercus bicolor</i>, <i>Quercus pagoda</i>, <i>Quercus falcata</i>, and <i>Quercus phellos</i>) with thick walls of</p> </div> <div style="border: 1px solid black; padding: 5px;">  <p>clambering plants in close proximity to river banks. - <i>Celtis laevigata</i>, clambering plants/vines (<i>toxicodendron radicans</i> and wild <i>vitis</i>), and herbaceous monocotyledonae (<i>smilax rotundifolia</i> L., <i>distichlis spicata</i>, <i>macfadyena unguis-cati</i> and <i>poaceae</i>) along river banks.</p> </div>
--	---

Des Arc (RM 148.03). From the Wolman Pebble Count data and various fluvial and morphological parameters obtained via aerial photographs and the HEC-RAS Model, the White River at Des Arc (RM 148.03) was classified as a “C5c-” stream residing within a type “X” valley. The reach had a width of about 614 feet, a bank height approximately 20 feet, a gentle channel slope less than 2%, a width/depth ratio of 38, an entrenchment ratio of 55, a meander belt ratio of 28, and a sinuosity around 1.37. The dominant bed materials D_{50s} were very fine sands with a fair amount of cohesive materials including silts and clays. The banks were relatively flat and were composed primarily of finer grained cohesive materials. However, locations half-way between the bankfull stage and the normal stage exhibited large amounts of a very fine sand. Riffle and pool sequences were spaced approximately 6.40 times the channel width in length. The reach was characterized by very wide point bars ranging from 100 feet to 200 feet in width, indicating susceptibility to accelerated bank erosion and deposition evoked by alterations in flow and sediment regimes. Site observation in the area revealed sluggish flow and suggested an anthro-altered environment with small fairly dense riparian forests consisting of hickories, sycamores, and oaks. Downstream anthro-altered areas cleared of diverse vegetation, were abundant in other grasses and fescue, a nonnative pasture grass of importance for agricultural land and livestock. Zonation was indistinct, and river banks lacked diversity in clambering plants/vines and herbaceous monocots and dicots. Oxbow lakes, formerly channels of the White River, were abundant several miles downstream of Des Arc (RM 148.03) as the river maneuvered toward Devalls Bluff. Specific tallies of pebble count and estimations of the numerical values of fluvial and morphological parameters can be found in **Table 4.10**, **Table 4.11**, and **Figure 4.11**.

Table 4.10. Pebble Count Data for the Reference Reach at Des Arc, Arkansas (RM 148.03).

PEBBLE COUNT								
Site: Des Arc, AR (RM 148.03)				Date: 09/01/2010				
Party: Linh & Virak				Reach: White River				
INCHES	PARTICLE	MILLIMETER		Particle Count	TOT #	ITEM %	% CUM	
	Silt/Clay	< .062	S/C	HH HH HH HH HH HH HH IIII	39	39	39	
.04 - .08	Very Fine	.062 - .125	S	HH HH HH HH HH HH HH HH I	41	41	80	
	Fine	.125 - .25	A	HH HH HH HH	20	20	100	
	Medium	.25 - .50	N		0	0	100	
	Coarse	.50 - 1.0	D		0	0	100	
	Very Coarse	1.0 - 2.0	S		0	0	100	
.08 - .16	Very Fine	2.0 - 4.0	G		0	0	100	
.16 - .31	Fine	4.0 - 8.0	R		0	0	100	
.31 - .63	Medium	8.0 - 16.0	V		0	0	100	
.63 - 1.26	Coarse	16.0 - 32.0	L		0	0	100	
1.26 - 2.5	Very Coarse	32.0 - 64.0	S		0	0	100	
2.5 - 5.0	Small	64.0 - 128.0	C		0	0	100	
5.0 - 10.0	Large	128.0 - 256.0	O		0	0	100	
10.0 - 20.0	Small	256.0 - 512.0	B		0	0	100	
20.0 - 40.0	Medium	512.0 - 1024.0	L		0	0	100	
40.0 - 160	Lrg-Very Lrg	1024.0 - 4096.0	D		0	0	100	
	BEDROCK		BDRK					
TOTALS					100	100	100	

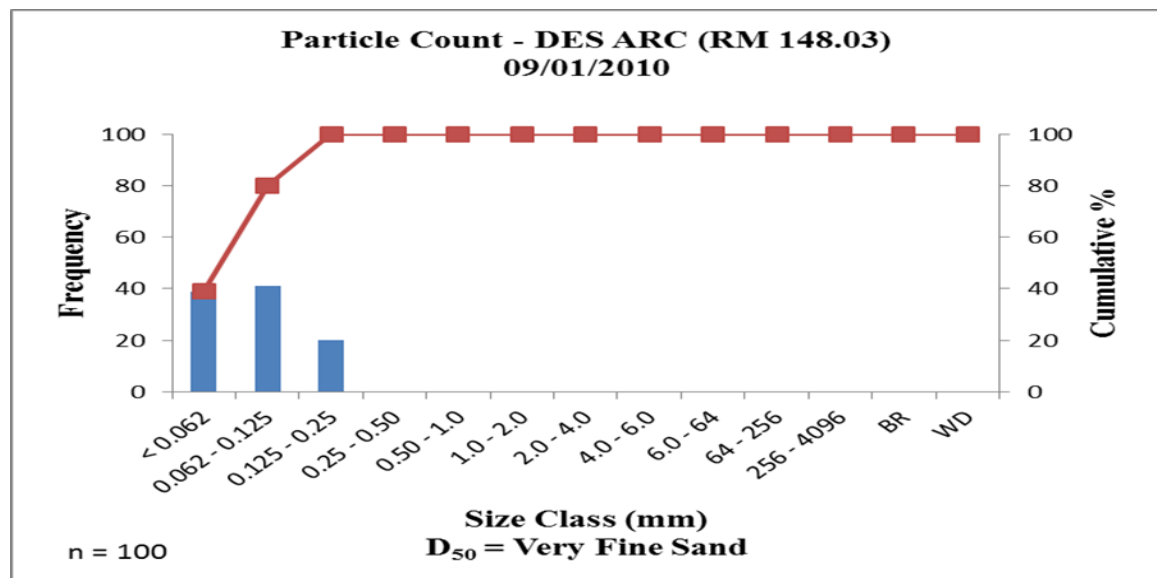




Figure 4.11. Particle Count and Calculated D₅₀ for the Reference Reach at Des Arc.

Table 4.11. Field Data Form for the Reference Reach at Des Arc, AR (RM 148.03).

REFERENCE REACH FIELD FORM STREAM CHANNEL CLASSIFICATION LEVEL II		STREAM TYPE: C5c-	
STREAM NAME: <u>White River</u>	DRAINAGE AREA: <u>1357.95</u> Sq. mi.	BASIN NAME: <u>White River Basin</u>	
OBSERVERS: <u>Linh & Virak</u>	DATE: <u>09/01/2010</u>		
LOCATION: <u>Des Arc, Arkansas</u>	Twp. _____ Rge. <u>148.03</u>	Sec. _____ Qtr. _____	
Bankfull WIDTH <u>613.52</u>	Ft. (W_{bkt}) Bankfull MAX DEPTH <u>35.24</u> Ft. (d_{max})	Channel SLOPE <u>0.00008</u>	Ft/Ft <u>0.008</u> %
Bankfull Mean DEPTH <u>30.25</u>	Ft. (d_{bkt}) Flood Prone Area WIDTH <u>34k</u> Ft. (W_{fp})	Valley SLOPE <u>0.0005</u>	Ft/Ft <u>0.05</u> %
WIDTH/DEPTH Ratio <u>37.50</u>	ENTRENCHMENT Ratio <u>55.10</u>	SINUOSITY <u>1.37</u>	
Channel Materials: <u>Silts, clays, and very fine to fine sands</u>			
			
<ul style="list-style-type: none"> - Wide channel with flat longitudinal gradient and flat banks with cohesive materials. - Mid-banks exhibit high amounts of very fine noncohesive soils. - Moderately dense riparian forest abundant in various species of <i>Carya</i> spp., <i>Quercus</i>, and <i>Platanus occidentalis</i>. 		<ul style="list-style-type: none"> - Anthro-altered areas abundant in poaceae, but scarce in herbaceous monocotyledonae and dicotyledons. - Zonation is indistinct. No diversity in plant species near river banks. 	

Devalls Bluff (RM 124.35). Using the classification key for natural rivers with morphological and fluvial parameters obtained through field data, aerial photographs, and the HEC-RAS Model, the section of the White River at Devalls Bluff (RM 124.35) was classified as a “C5c-” stream existing within a type “X” valley. The reach has a width of about 509 feet, a bank height ranging from 25 feet to 30 feet, a gentle gradient of less than 1%, a width/depth ratio of approximately 22, an entrenchment ratio of 15, a meander width ratio of about 28, and a sinuosity of about 1.31. The dominant bed material D_{50} consisted of fine sands while the banks were composed of mostly cohesive soils as well as lesser quantities of non-cohesive materials and fine gravels. Riffle and pool sequences averaged approximately about 6.45 times the channel width in length. The reach was characterized by point bars especially in compounded bends, an indicator of susceptibility to lateral and vertical shifts generally evoked by alterations in flow and sediment regimes. Field observations indicated flat banks and non-uniform sluggish flow due in part to a significant decrease in the longitudinal slope. The reach was located in an area of swamp land abundant in Oxbow lakes. The area also exhibited tortuously compounded bends on the verge of neck cut-off as well as wandering and compounded mini-channels. The riparian forest was abundant in hickories, oaks, maples, and sycamores. Defoliated or sick yellow and red sycamores were very apparent in some of the riparian forests. Zonation was very indistinct, and the river banks lacked diversity in herbaceous monocots and dicots. Data and results pertaining to the numerical values of the morphological and fluvial parameters of the ‘reference’ reach are shown in **Table 4.12**, **Table 4.13**, and **Figure 4.12**.

Table 4.12. Pebble Count Data for the Reference Reach at Devalls Bluff, Arkansas (RM 124.35).

PEBBLE COUNT							
Site: Devalls Bluff, AR (RM 124.35)				Date: 09/03/2010			
Party: Linh & Virak				Reach: White River			
INCHES	PARTICLE	MILLIMETER		Particle Count	TOT #	ITEM %	% CUM
	Silt/Clay	< .062	S/C	HHH HHH HHH HHH HHH	25	25	25
.04 - .08	Very Fine	.062 - .125	S	HHH HHH HHH HHH HHH HHH	30	30	55
	Fine	.125 - .25	A	HHH HHH HHH HHH HHH HHH II	32	32	87
	Medium	.25 - .50	N	HHH	5	5	92
	Coarse	.50 - 1.0	D	IIII	4	4	96
	Very Coarse	1.0 - 2.0	S		0	0	96
.08 - .16	Very Fine	2.0 - 4.0	G	II	2	2	98
.16 - .31	Fine	4.0 - 8.0	R	I	1	1	99
.31 - .63	Medium	8.0 - 16.0	V	I	1	1	100
.63 - 1.26	Coarse	16.0 - 32.0	L		0	0	100
1.26 - 2.5	Very Coarse	32.0 - 64.0	S		0	0	100
2.5 - 5.0	Small	64.0 - 128.0	C O		0	0	100
5.0 - 10.0	Large	128.0 - 256.0	B L		0	0	100
10.0 - 20.0	Small	256.0 - 512.0	B		0	0	100
20.0 - 40.0	Medium	512.0 - 1024.0	L D		0	0	100
40.0 - 160	Lrg-Very Lrg	1024.0 - 4096.0	R		0	0	100
	BEDROCK		BDRK				
TOTALS					100	100	100

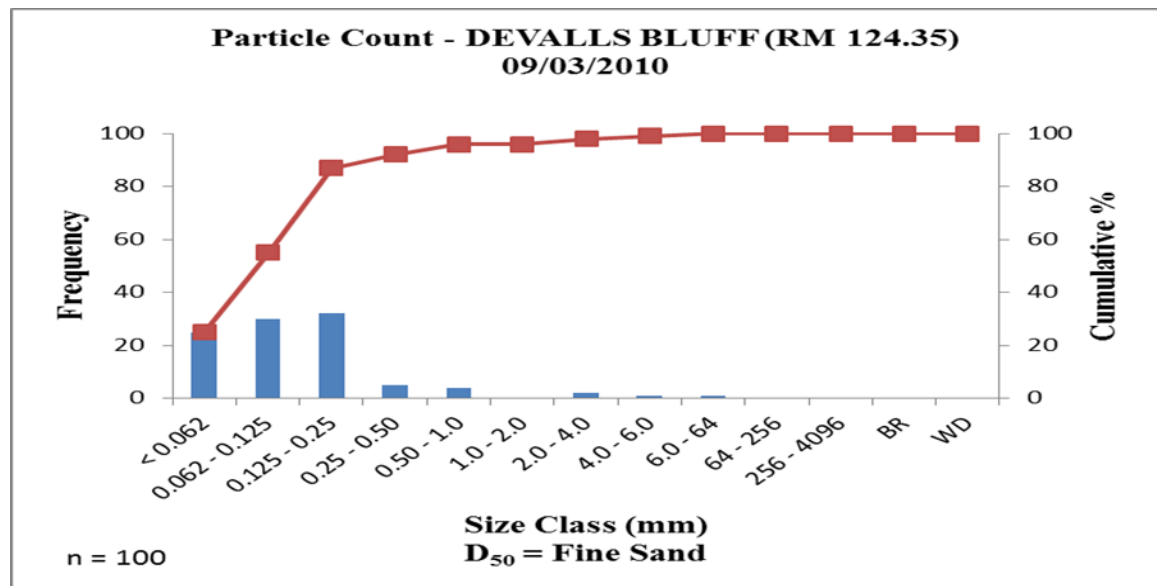




Figure 4.12. Particle Count and Calculated D_{50} for the Reference Reach at Devalls Bluff.

Table 4.13. Field Data Form for the Reference Reach at Devalls Bluff, AR (RM 124.35).

<div style="border: 1px solid black; padding: 5px; margin-bottom: 10px;"> REFERENCE REACH FIELD FORM STREAM CHANNEL CLASSIFICATION LEVEL II </div> <div style="border: 1px solid black; padding: 5px;"> <p>STREAM NAME: <u>White River</u> DRAINAGE AREA: <u>1357.95 Sq. mi.</u> BASIN NAME: <u>White River Basin</u></p> <p>OBSERVERS: <u>Linh & Virak</u> DATE: <u>09/03/2010</u></p> <p>LOCATION: <u>DeValls Bluff, Arkansas</u> Twp. <u> </u> Rge. <u> </u> Sec. <u>124.35</u> Qtr. <u> </u></p> <p>Bankfull WIDTH <u>509.27</u> Ft. (W_{bkt}) Bankfull MAX DEPTH <u>35.67</u> Ft. (d_{max}) Channel SLOPE <u>0.00003</u> Ft/Ft <u>0.003</u> %</p> <p>Bankfull Mean DEPTH <u>35.12</u> Ft. (d_{bkt}) Flood Prone Area WIDTH <u>8k</u> Ft. (W_{fp}) Valley SLOPE <u>0.0005</u> Ft/Ft <u>0.05</u> %</p> <p>WIDTH/DEPTH Ratio <u>22.35</u> ENTRENCHMENT Ratio <u>15.50</u> SINUOSITY <u>1.31</u></p> <p>Channel Materials: <u>Silts, clays, very fine to medium sands with fine gravels</u> D50 <u>Sands (fine)</u></p> </div>	<div style="border: 1px solid black; padding: 5px; margin-bottom: 10px;"> STREAM TYPE: <u>C5c-</u> </div> <div style="display: flex; justify-content: space-around;">   </div> <div style="border: 1px solid black; padding: 5px; margin-top: 10px;"> <p>- Wide channel with extremely flat longitudinal gradient and flat banks with cohesive-dominant materials and fine gravels.</p> <p>- Salix negras within wetted water edge and robinia pseudoacacia at the top of banks.</p> <p>- Riparian forest abundant in hickories (Carya ovata and Carya cordiformis), oaks, (Quercus</p> </div> <div style="border: 1px solid black; padding: 5px; margin-top: 10px;"> <p>Quercus michauxii, Quercus bicolor, Quercus oalustris, Quercus nigra, Quercus velutina, Quercus rubra, Quercus alba, etc.), and sycamores (Plantanus occidentalis), and maples (Accer saccharinum and Acer rubrum).</p> <p>- Apparent presence of defoliated or possibly sick yellow and red sycamores.</p> </div>
---	---

Clarendon (RM 100.38). The White River's reference reach at Clarendon (RM 100.38) was classified as a "C5c-/C6c-" stream existing within a type "X" valley. The reach had a width of about 525 feet, a bank height ranging from 25 feet to 30 feet, a gentle gradient of less than 1%, a width/depth ratio of approximately 24, an entrenchment ratio of 30, a meander width ratio of about 34, and a sinuosity of about 2.17. The reach did not feature a dominant bed material D_{50} , and the banks were composed of mixed cohesive and non-cohesive materials such as clays, silts, sands and gravels. Riffle and pool sequences, although indistinct in comparison to other sections of the White River, averaged approximately about 4.6 times the channel width in length. The reach was characterized by wide point bars in tortuous and sharp bends, which indicated the susceptibility to lateral shifts generally evoked by alterations in flow and sediment regimes. Field observations in the area revealed relatively flat banks and extremely slow murky water. The reach was located within the heart of the swamp land where Oxbow lakes and wandering compounded mini-channels and water loops were abundant. It is suspected that sediment load is high to very high with much of the sediment supply originating from the Cache River as well as upstream reaches. Extremely sluggish flow and low stream power indicated a bed-load type with the main mode of sediment transportation occurring along the bed by sliding, rolling, and saltation. Zonation of plant species was indistinct, and the riparian forest was abundant in hardwoods such as oaks, maples, and sycamores. Hard hardwoods and soft hardwoods such as elms and ashes, respectively, were also present and were less abundant. The classification of the reach at Clarendon based on RSC key in **Figure 4.7** was dependent upon morphological and fluvial data presented in **Table 4.14**, **Table 4.15**, and **Figure 4.13**.

Table 4.14. Pebble Count Data for the Reference Reach at Clarendon, Arkansas (RM 100.38).

PEBBLE COUNT							
Site: Clarendon, AR (RM 100.38)				Date: 09/10/2010			
Party: Linh & Virak				Reach: White River			
INCHES	PARTICLE	MILLIMETER		Particle Count	TOT #	ITEM %	% CUM
	Silt/Clay	< .062	S/C	HHH HHH HHH HHH HHH HHH HHH	35	35	35
.04 - .08	Very Fine	.062 - .125	S	HHH HHH HHH HHH HHH HHH HHH I	36	36	71
	Fine	.125 - .25	A	III	4	4	75
	Medium	.25 - .50	N	II	2	2	77
	Coarse	.50 - 1.0	D	III	3	3	80
	Very Coarse	1.0 - 2.0	S		0	0	80
.08 - .16	Very Fine	2.0 - 4.0	G	I	1	1	81
.16 - .31	Fine	4.0 - 8.0	R	I	1	1	82
.31 - .63	Medium	8.0 - 16.0	V	HHH HHH III	13	13	95
.63 - 1.26	Coarse	16.0 - 32.0	L	III	3	3	98
1.26 - 2.5	Very Coarse	32.0 - 64.0	S	II	2	2	100
2.5 - 5.0	Small	64.0 - 128.0	C O		0	0	100
5.0 - 10.0	Large	128.0 - 256.0	B L		0	0	100
10.0 - 20.0	Small	256.0 - 512.0	B		0	0	100
20.0 - 40.0	Medium	512.0 - 1024.0	L D		0	0	100
40.0 - 160	Lrg-Very Lrg	1024.0 - 4096.0	R		0	0	100
	BEDROCK		BDRK				
TOTALS					100	100	100

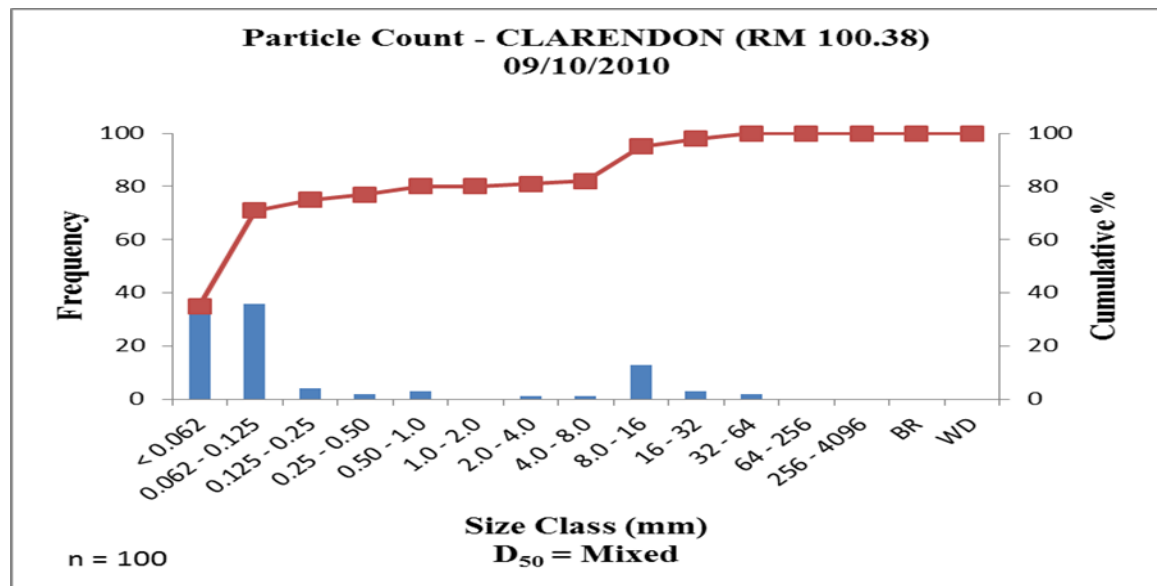




Figure 4.13. Particle Count and Calculated D_{50} for the Reference Reach at Clarendon.

Table 4.15. Field Data Form for the Reference Reach at Clarendon, AR (RM 100.38).

<div style="border: 1px solid black; padding: 5px; margin-bottom: 10px;"> REFERENCE REACH FIELD FORM STREAM CHANNEL CLASSIFICATION LEVEL II </div> <div style="border: 1px solid black; padding: 5px;"> <p>STREAM NAME: <u>White River</u> DRAINAGE AREA: <u>1357.95</u> Sq. mi. BASIN NAME: <u>White River Basin</u></p> <p>OBSERVERS: <u>Linh & Virak</u> DATE: <u>09/10/2010</u></p> <p>LOCATION: <u>Clarendon, Arkansas</u> Twp. <u> </u> Rge. <u> </u> Sec. <u>100.38</u> Qtr. <u> </u></p> <p>Bankfull WIDTH <u>524.71</u> Ft. (W_{bkt}) Bankfull MAX DEPTH <u>27.15</u> Ft. (d_{max}) Channel SLOPE <u>0.00006</u> Ft/Ft <u>0.006</u> %</p> <p>Bankfull Mean DEPTH <u>26.59</u> Ft. (d_{bkt}) Flood Prone Area WIDTH <u>16k</u> Ft. (W_{fp}) Valley SLOPE <u>0.0005</u> Ft/Ft <u>0.05</u> %</p> <p>WIDTH/DEPTH Ratio <u>24.18</u> ENTRENCHMENT Ratio <u>30.16</u> SINUOSITY <u>2.17</u></p> <p>Channel Materials: <u>Silts, clays, and sands</u> D50 <u>Mixed</u></p> </div>	<div style="border: 1px solid black; padding: 5px; margin-bottom: 10px;"> STREAM TYPE: C5c-/C6c- </div> <div style="display: flex; justify-content: space-around;">   </div> <div style="border: 1px solid black; padding: 5px; margin-top: 10px;"> <p>- Wide channel with extremely flat longitudinal gradient and relatively flat banks of mixed materials.</p> <p>- Observations indicate very slow moving flow or extremely low stream power.</p> <p>- Indistinct zonation of plant species along river banks.</p> </div> <div style="border: 1px solid black; padding: 5px; margin-top: 10px;"> <p>- Riparian forest abundant with mixture of various species of oaks (Quercus palustris, Quercus shumardii, Quercus phellos, Quercus bicolor, Quercus rubra, etc.), sycamores (Platanus occidentalis) and maples (Acer saccharum, Acer rubrum, Acer saccharum, Acer nigrum, etc.)</p> <p>- Also present are Fraxinus nigra and Ulmus Americana although not very abundant.</p> </div>
---	---

St. Charles (RM 56.57). The White River at St. Charles (RM 56.57) was classified as a “C5c-” stream residing within a type “X” valley. The reach had a width of about 559 feet, a bank height of approximately 25 to 30 feet, a gentle channel slope less than 1%, a width/depth ratio of about 30, an entrenchment ratio of 38, a meander belt ratio of 30, and a sinuosity around 1.09. The dominant bed material D_{50} consisted of fine sands while the banks were composed of a mixture of cohesive and non-cohesive materials. Riffle and pool sequences averaged approximately 6.78 times the channel width in length. The reach was characterized by wide point bars in the range of 180 feet to 200+ feet and other depositional features which served as indicators of susceptibility to lateral shifts evoked by alterations in flow and sediment regimes. Field observations indicated slightly steep banks and non-uniform sluggish flow. The reach was located within the swamp land where Oxbow lakes and wandering compounded mini-channels and water loops were abundant. A majority of the bends were compounded having small radii of curvature while others were sharper having larger radii of curvature. Bends in the area were not free to meander due to the constraint of a nearby levee. The riparian forest was abundant in hickories and various species of sycamores, oaks, tulips, and maples. Clusters of clambering plants/vines and herbaceous monocots such as poison ivies, wild grapes, greenbriers, and trumpet creepers were bountiful at bank tops and were found extending to the water edge along the face of the river banks. Fallen and tilted trees and exposed roots occupied areas along the banks that exhibited slightly steeper slopes. Pebble count data, particle distribution curve, and the reference reach field form detailing morphological and fluvial parameters are shown with **Table 4.16**, **Table 4.17**, and **Figure 4.14**.

Table 4.16. Pebble Count Data for the Reference Reach at St. Charles, Arkansas (RM 56.57).

PEBBLE COUNT							
Site: St. Charles, AR (RM 56.57)				Date: 09/12/2010			
Party: Linh & Vince				Reach: Lower White River			
INCHES	PARTICLE	MILLIMETER		Particle Count	TOT #	ITEM %	% CUM
	Silt/Clay	< .062	S/C	HHH HHH HHH II	17	17	17
.04 - .08	Very Fine	.062 - .125	S	HHH HHH HHH HHH HHH HHH	30	30	47
	Fine	.125 - .25	A	HHH HHH HHH HHH HHH HHH II	32	32	79
	Medium	.25 - .50	N	I	1	1	80
	Coarse	.50 - 1.0	D		0	0	80
	Very Coarse	1.0 - 2.0	S		0	0	80
.08 - .16	Very Fine	2.0 - 4.0	G		0	0	80
.16 - .31	Fine	4.0 - 8.0	R		0	0	80
.31 - .63	Medium	8.0 - 16.0	V		0	0	80
.63 - 1.26	Coarse	16.0 - 32.0	L	III	4	4	84
1.26 - 2.5	Very Coarse	32.0 - 64.0	S	HHH III	8	8	92
2.5 - 5.0	Small	64.0 - 128.0	C O	III	3	3	95
5.0 - 10.0	Large	128.0 - 256.0	B L	HHH	5	5	100
10.0 - 20.0	Small	256.0 - 512.0	B		0	0	100
20.0 - 40.0	Medium	512.0 - 1024.0	L D		0	0	100
40.0 - 160	Lrg-Very Lrg	1024.0 - 4096.0	R		0	0	100
	BEDROCK		BDRK				
TOTALS					100	100	100

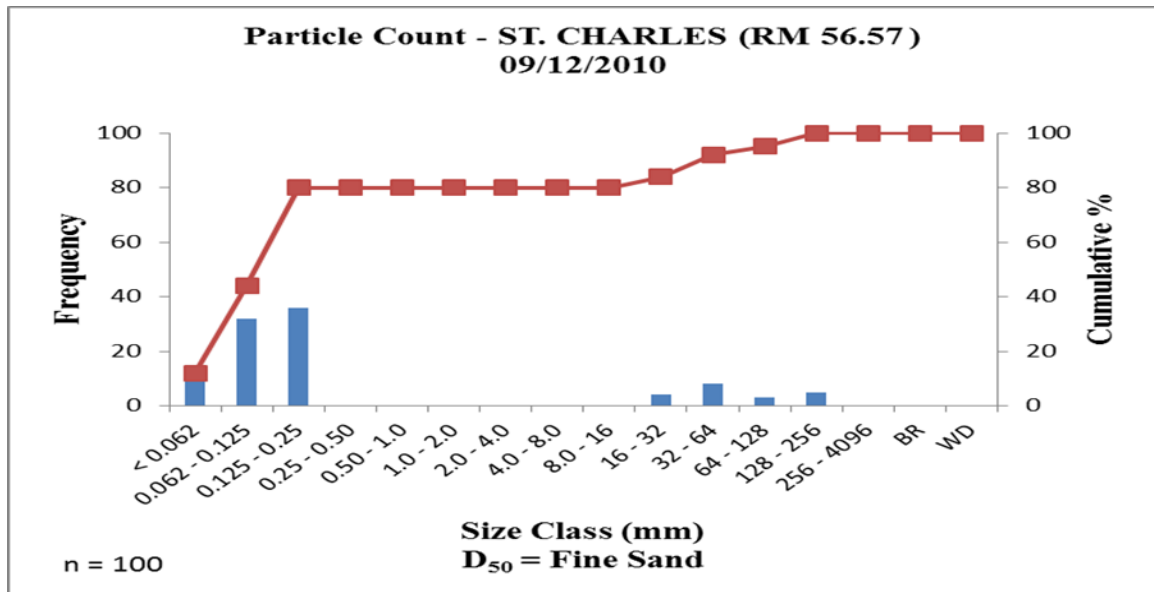




Figure 4.14. Particle Count and Calculated D₅₀ for the Reference Reach at St. Charles.

Table 4.17. Field Data Form for the Reference Reach at St. Charles, AR (RM 56.57).

<div style="border: 1px solid black; padding: 5px; margin-bottom: 10px;"> REFERENCE REACH FIELD FORM STREAM CHANNEL CLASSIFICATION LEVEL II </div> <div style="border: 1px solid black; padding: 5px;"> <p>STREAM NAME: White River DRAINAGE AREA: 1684.85 Sq. mi. BASIN NAME: White River Basin</p> <p>OBSERVERS: Linh & Vince DATE: 09/12/2010</p> <p>LOCATION: St. Charles, Arkansas Twp. Rge. Sec. 56.57 Qtr.</p> <p>Bankfull WIDTH 558.75 Ft. (W_{bkt}) Bankfull MAX DEPTH 24.45 Ft. (d_{max}) Channel SLOPE 0.00006 Ft/Ft 0.006 %</p> <p>Bankfull Mean DEPTH 22.66 Ft. (d_{bkt}) Flood Prone Area WIDTH 21.5k Ft. (W_{fp}) Valley SLOPE 0.0002 Ft/Ft 0.02 %</p> <p>WIDTH/DEPTH Ratio 29.84 ENTRENCHMENT Ratio 38.60 SINUOSITY 1.09</p> <p>Channel Materials: Silts, clays, and sands with coarse to very coarse gravels D50 Sands (fine)</p> </div>	<div style="border: 1px solid black; padding: 5px; margin-bottom: 10px;"> STREAM TYPE: C5c- </div> <div style="display: flex; justify-content: space-around;">   </div> <div style="border: 1px solid black; padding: 5px; margin-top: 10px;"> <p>- Wide channel with flat longitudinal gradient and slightly steep banks with point bars of noncohesive materials.</p> <p>- Mid-bank and water edge exhibit very fine sand with silty clay.</p> <p>- Root exposure and fallen trees proximal to areas with steeper bank.</p> <p>- Riparian forest abundant in hickories (<i>Carya</i> spp.), oaks (<i>Quercus palustris</i>, <i>Quercus shumardii</i>, <i>Quercus phellos</i>, <i>Quercus bicolor</i>, <i>Quercus rubra</i>, etc.), sycamores (<i>Platanus occidentalis</i>) and maples (<i>Acer saccharinum</i>, <i>Acer rubrum</i>, <i>Acer saccharum</i>, <i>Acer nigrum</i>, etc.)</p> <p>- <i>Liriodendron tulipifera</i>, clambering plants/vines (<i>Toxicodendron radicans</i>, <i>Campsis radicans</i>, and wild vitis), herbaceous monocotyledonae (<i>Smilax rotundifolia</i> L.) and dicotyledons at tops of banks extending to water edge.</p> </div>
--	---

The remaining sections. Geomorphological characterizations of the remaining 134 sections of the White River based on 7 ‘reference’ reaches are shown in **Table 4.19**.

Stream type and valley type are based on the Rosgen Classification System.

Table 4.18. Geomorphological Characterization of the White River.

Section	River Mile	W.S. Elev. (ft)	D ₅₀	Stream Type	Valley Type
1	295.27 - 293.21	231.32	Gravel	C4c-	V
2	293.21 - 291.27	230.63	Gravel	C4c-	V
3	290.54 - 287.90	229.01	Gravel	C4c-	V
4	286.54 - 285.34	227.13	Gravel	C4c-	V
5	285.34 - 283.60	226.24	Gravel	C4c-	X
6	281.04 - 280.00	224.05	Gravel	C4c-	X
7	280.00 - 276.57	221.43	Gravel	C4c-	X
8	276.57	219.12	Gravel	C4c-	X
9	276.57 - 274.71	218.37	Gravel	C4c-	X
10	270.75	215.02	Gravel	C4c-	X
11	270.75 - 268.78	213.99	Gravel	C4c-	X
12	268.78 - 266.28	212.01	Gravel	C4c-	X
13	266.28 - 262.47	210.35	Gravel	C4c-	X
14	262.47 - 260.98	209.34	Gravel	C4c-	X
15	260.98 - 258.72	208.99	Gravel	C4c-	X
16	258.72 - 257.25	208.69	Gravel	C4c-	X
17	258.94 - 256.89	206.04	Sand (F)	C5c-	X
18	256.89 - 253.08	205.13	Sand (F)	C5c-	X
19	253.08 - 248.95	204.00	Sand (F)	C5c-	X
20	247.80 - 240.36	202.56	Sand (F)	C5c-	X
21	240.36 - 238.48	201.46	Sand (F)	C5c-	X
22	238.48 - 234.98	200.83	Sand (F)	C5c-	X
23	234.98 - 234.22	200.38	Sand (F)	C5c-	X
24	232.55 - 231.45	199.47	Sand (F)	C5c-	X
25	231.45 - 228.89	199.23	Sand (F)	C5c-	X
26	228.89 - 227.78	198.98	Sand (F)	C5c-	X
27	227.78 - 226.14	198.72	Sand (F)	C5c-	X
28	226.14	198.59	Sand (F)	C5c-	X
29	223.9 - 221.53	198.12	Sand (F)	C5c-	X
30	221.53	197.95	Sand (F)	C5c-	X

Table 4.18(Continued...). Geomorphological characterization of the White River.

Section	River Mile	W.S. Elev. (ft)	D ₅₀	Stream Type	Valley Type
31	219.41	197.83	Sand (F)	C5c-	X
32	219.41 - 216.97	197.72	Sand (F)	C5c-	X
33	216.97 - 215.33	197.43	Sand (F)	C5c-	X
34	215.33 - 213.33	197.10	Sand (F)	C5c-	X
35	213.33 - 207.17	196.34	Sand (F)	C5c-	X
36	207.17 - 203.71	195.12	Sand (F)	C5c-	X
37	201.56 - 201.01	194.54	Sand (F)	C5c-	X
38	201.01 - 197.27	194.15	Sand (VF)	C5c-	X
39	197.27 - 195.01	193.06	Sand (VF)	C5c-	X
40	195.01 - 192.68	191.91	Sand (VF)	C5c-	X
41	192.68 - 191.64	191.06	Sand (VF)	C5c-	X
42	191.64 - 189.95	190.64	Sand (VF)	C5c-	X
43	189.95 - 188.59	190.33	Sand (VF)	C5c-	X
44	188.59 - 187.55	190.01	Sand (VF)	C5c-	X
45	187.55 - 186.26	189.46	Sand (VF)	C5c-	X
46	186.26 - 181.29	187.72	Sand (VF)	C5c-	X
47	181.29 - 177.81	185.83	Sand (VF)	C5c-	X
48	177.81 - 176.00	185.27	Sand (VF)	C5c-	X
49	175.50 - 172.65	184.40	Sand (VF)	C5c-	X
50	172.65 - 169.52	183.41	Sand (VF)	C5c-	X
51	169.52 - 167.08	182.36	Sand (VF)	C5c-	X
52	167.08 - 166.08	181.52	Sand (VF)	C5c-	X
53	166.08 - 164.39	181.22	Sand (VF)	C5c-	X
54	164.39 - 163.40	180.91	Sand (VF)	C5c-	X
55	163.40 - 161.91	180.46	Sand (VF)	C5c-	X
56	161.91 - 161.23	179.91	Sand (VF)	C5c-	X
57	161.23 - 158.63	179.00	Sand (VF)	C5c-	X
58	158.63	178.27	Sand (VF)	C5c-	X
59	155.71 - 155.04	177.43	Sand (VF)	C5c-	X
60	155.04 - 152.68	176.87	Sand (VF)	C5c-	X
61	152.68 - 149.03	176.07	Sand (VF)	C5c-	X
62	149.03 - 147.19	175.04	Sand (VF)	C5c-	X
63	147.19 - 145.72	174.26	Sand (VF)	C5c-	X
64	145.72 - 143.75	173.79	Sand (VF)	C5c-	X
65	143.75 - 141.78	173.15	Sand (VF)	C5c-	X
66	141.78 - 140.39	172.59	Sand (VF)	C5c-	X
67	140.39 - 139.21	172.04	Sand (VF)	C5c-	X
68	139.21 - 138.01	171.57	Sand (VF)	C5c-	X

Table 4.18(Continued...). Geomorphological characterization of the White River.

Section	River Mile	W.S. Elev. (ft)	D ₅₀	Stream Type	Valley Type
69	138.01 - 136.03	171.05	Sand (VF)	C5c-	X
70	136.03 - 135.16	170.31	Sand (VF)	C5c-	X
71	133.65 - 132.61	169.26	Sand (VF)	C5c-	X
72	132.61 - 130.54	168.66	Sand (VF)	C5c-	X
73	130.54 - 128.70	167.24	Sand (VF)	C5c-	X
74	128.70 - 124.33	166.02	Sand (F)	C5c-	X
75	124.33 - 122.36	165.39	Sand (F)	C5c-	X
76	122.36 - 118.19	165.02	Sand (F)	C5c-	X
77	118.19 - 116.4	164.71	Sand (F)	C5c-	X
78	116.4 - 114.53	164.47	Sand (F)	C5c-	X
79	114.53 - 112.77	164.35	Sand (F)	C5c-	X
80	111.34	164.32	Sand (F)	C5c-	X
81	109.77 - 108.75	164.07	Sand (F)	C5c-	X
82	108.75 - 107.67	163.91	Sand (F)	C5c-	X
83	107.67	163.74	Sand (F)	C5c-	X
84	107.67 - 103.51	162.99	Sand (F)	C5c-	X
85	104.31 - 103.51	162.61	Sand (F)	C5c-	X
86	103.51 - 102.25	162.23	Sand (F)	C5c-	X
87	102.25 - 101.14	161.93	Sand (F)	C5c-	X
88	101.14 - 100.34	161.80	Mixed	C5c-/C6c-	X
89	100.34 - 98.48	161.66	Mixed	C5c-/C6c-	X
90	98.48 - 96.72	161.03	Mixed	C5c-/C6c-	X
91	96.72 - 94.57	160.32	Mixed	C5c-/C6c-	X
92	94.57 - 92.42	159.71	Mixed	C5c-/C6c-	X
93	89.46 - 87.41	158.20	Mixed	C5c-/C6c-	X
94	87.41 - 84.62	157.11	Mixed	C5c-/C6c-	X
95	84.62 - 81.65	156.16	Mixed	C5c-/C6c-	X
96	80.31 - 78.89	155.33	Mixed	C5c-/C6c-	X
97	78.89	155.17	Mixed	C5c-/C6c-	X
98	76.87 - 75.73	154.32	Mixed	C5c-/C6c-	X
99	75.73 - 73.62	153.74	Mixed	C5c-/C6c-	X
100	75.73 - 68.51	153.02	Mixed	C5c-/C6c-	X
101	71.59 - 68.51	152.31	Mixed	C5c-/C6c-	X
102	68.51 - 67.21	151.82	Mixed	C5c-/C6c-	X
103	67.21 - 64.72	151.42	Mixed	C5c-/C6c-	X
104	64.72	151.15	Mixed	C5c-/C6c-	X
105	64.72 - 60.12	150.45	Mixed	C5c-/C6c-	X
106	62.7 - 60.12	150.11	Mixed	C5c-/C6c-	X

Table 4.18(Continued...). Geomorphological characterization of the White River.

Section	River Mile	W.S. Elev. (ft)	D ₅₀	Stream Type	Valley Type
107	60.12 - 58.79	149.61	Mixed	C5c-/C6c-	X
108	58.79 - 57.61	149.27	Mixed	C5c-/C6c-	X
109	57.61 - 55.30	148.89	Sand (F)	C5c-	X
110	55.30 - 54.33	148.47	Sand (F)	C5c-	X
111	54.33 - 53.38	148.12	Sand (F)	C5c-	X
112	54.33 - 51.45	147.86	Sand (F)	C5c-	X
113	51.45	147.35	Sand (F)	C5c-	X
114	49.77 - 49.08	146.55	Sand (F)	C5c-	X
115	49.08 - 47.19	146.20	Sand (F)	C5c-	X
116	47.19	145.94	Sand (F)	C5c-	X
117	45.31	145.09	Sand (F)	C5c-	X
118	45.31 - 42.00	144.22	Sand (F)	C5c-	X
119	42.00 - 40.52	142.93	Sand (F)	C5c-	X
120	40.52	142.50	Sand (F)	C5c-	X
121	40.52 - 38.69	142.21	Sand (F)	C5c-	X
122	38.69	141.91	Sand (F)	C5c-	X
123	36	141.01	Sand (F)	C5c-	X
124	36	141.01	Sand (F)	C5c-	X
125	34.42 - 32.81	139.80	Sand (F)	C5c-	X
126	30.88 - 29.74	138.02	Sand (F)	C5c-	X
127	29.74 - 29.13	137.75	Sand (F)	C5c-	X
128	29.13 - 26.38	137.05	Sand (F)	C5c-	X
129	26.38 - 24.47	136.01	Sand (F)	C5c-	X
130	24.47	135.56	Sand (F)	C5c-	X
131	22.01	134.55	Sand (F)	C5c-	X
132	22.01 - 17.64	133.74	Sand (F)	C5c-	X
133	17.64	132.92	Sand (F)	C5c-	X
134	14.01	131.62	Sand (F)	C5c-	X
135	14.01 - 11.80	131.23	Sand (F)	C5c-	X
136	11.8	130.83	Sand (F)	C5c-	X
137	9.97 - 6.92	129.83	Sand (F)	C5c-	X
138	6.92 - 5.32	129.25	Sand (F)	C5c-	X
139	4.31 - 3.26	128.90	Sand (F)	C5c-	X
140	3.26 - 1.36	128.70	Sand (F)	C5c-	X
141	1.36 - 0.00	128.51	Sand (F)	C5c-	X

Level III Classification: Assessment of Stream Condition and Departure

While the reach-specific morphological description presented as Level II Classification may provide significant physical attributes of various stream sections, it does not provide a “base datum of normality” depicting hydrologic, biological, ecological, and human factors influential to the conditions or “state” of the sections as they pertain to stability, potential, and function. Stream stability in the morphological sense is defined as “the ability of the stream to maintain, over time, its dimension, pattern, and profile in such a manner that is it neither aggrading nor degrading and is able to transport [sediments] without adverse consequence the flows and detritus of its watershed” (Rosgen & Silvey, 1996, pp. 6-1 – 6-2). Stream potential is referred to as the best channel condition when physical and biological functions operate at maximum efficiency which may be “quantitatively described in terms of channel size and shape, low erodibility factors, low lateral migration rates, and comparatively low rates of sediment supply” (Rosgen & Silvey, 1996, pp. 6-4 – 6-5). The current classification level deals primarily with the idea that in reality streams with similar morphologies are not imperative to have similar conditions or “states” and that the baseline or “natural” conditions are not often in agreement with the existing conditions. Thus the stream classification at Level III also permits a quantitative assessment of stream departure from an accepted range of morphological values validated for different stream types. Level III field parameters having an impact on the condition of a stream having a given morphology are riparian vegetation, streamflow regime, stream size and stream order, depositional patterns, meander patterns, channel stability rating, and streambank erosion potential; all of which will be presented in subsequent passages as applicable to the

various reaches or sections of the White River.

Riparian vegetation. The native riparian forests encountered along various sections of the White River reside within riparian wetland areas that have been, for the most part, altered by human activities. The functioning condition of the wetland areas, whether classified as lentic or lotic, is a result of the interactions between geology, soil, water and vegetation of which the latter two are particularly significant for the situation pertaining to the stability of the White River. However, identification of existing riparian vegetation via aerial photographs and field observations is most economical as it requires fewer trials and less time. Existing riparian vegetation often defines existing stream morphology, function, water quality, and stability. The influence of riparian vegetation on the morphology, function, water quality, and stability of the White River, possessing an equivalent magnitude to other Rosgen 'C' streams, is very high, therefore alterations in composition, vigor, and density of riparian vegetation promote corresponding changes that encompass rooting depth and density, water temperature and quality, physical resistance to bank erosion processes, terrestrial habitat, and contribution of detritus to various sections of the river. An inspection of the native riparian forests through which the White River traverses reveal stands of hardwoods dominated by various species of oaks (i.e., red, white, and black oaks, pin oaks, cherrybark oaks, nuttall oaks, willow oaks, shumard oaks, bur oaks, and overcup oaks) and hickories (i.e., shagbark hickories and bitternut hickories). Flowering dogwoods, eastern red cedars, red maples, sassafras, mulberries, sugarberries, and shortleaf pines also exist in these regions. Riparian forests in the lowland regions also support water oaks, swamp chestnut oaks, swamp white oaks, laurel oaks, black gums, sycamores, cottonwoods, black willows, water willows, cypress,

water tupelo, water hickories, red maples, silver maples, Mississippi hackberries, green ashes, river birches, water birches, water locusts, black locusts and yellow poplars in addition to the previously mentioned hardwoods. Clambering plants/vines and herbaceous monocots such as poison ivies, wild grapes, greenbriers, cucumbers, trumpet creepers, cat's claws, golden rods, and various species of grass also thrived on the bank apexes of the White River. Hardwoods of the riparian forests are classified as flood adaptable having the means of transferring oxygen to roots by producing ethylene, an unsaturated hydrocarbon, that creates pore spaces through which air is pumped downward to the roots during flood events when the water tables become significantly high. Hardwoods near the banks generally exhibit root systems that do not grow deep since resources are readily available while hardwoods farther from the banks generally exhibit deep and extensive root systems as nutrients and water are not readily available. Although hardwoods do not contribute to soil stability or bank erosion resistance on the same magnitude as smaller shrubs and bushes, the "natural recruitment of large woody debris [is] needed for fisheries habitat and stream-bed stability" (Rosgen & Silvey, 1996, p. 6-15). Riparian vegetation inventory or condition survey to identify composition, vigor, density, and potential, or overall current patterns in riparian communities are applied to 141 sections of the White River to determine reaches that may be vulnerable to disturbances. The terminologies, procedures, and scorecards utilized to describe and document the riparian condition are based on a combination of USDI BLM's Riparian Area Management (1998) and FAO'S Forest Resources Assessment (1996). Density classifications of woodland areas are based on the FAO's FAR criteria shown in **Figure 4.17** and Peurifoy and Oberlender (2002), and are executed by aerial photograph

observations implementing the tree “cramming” method (Hays et al., 1981). Circles with radii of 131 feet are drawn along sections of the White River to cover 1.24 acres or 0.5 hectares for estimating percent crown closure. A sample riparian vegetation evaluation for a reach, i.e., reach 141, is shown below in **Table 4.20**.

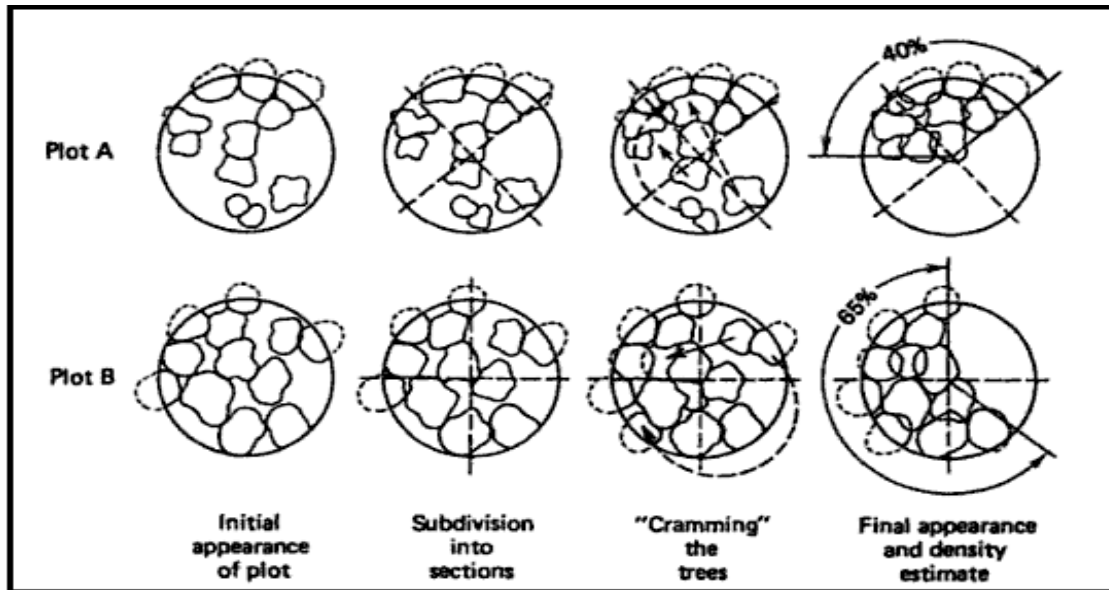
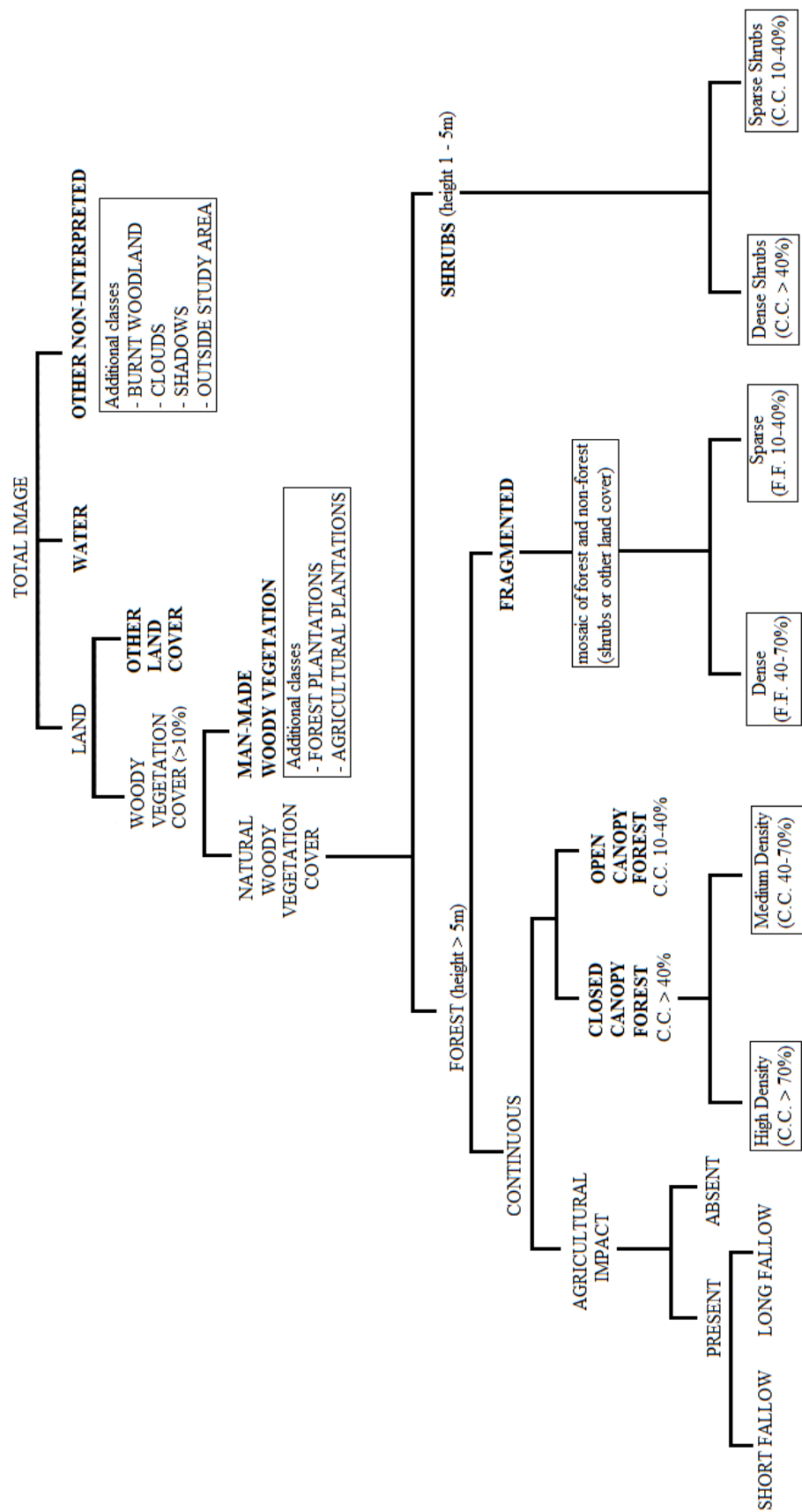


Figure 4.15 Procedure for the Tree Cramming Method of Estimating Percent Crown Exposure (Paine & Kiser, 2003).



Figure 4.16 Circles Drawn to Estimate Riparian Forest Density for Section 141.



* Note: Bold characters belong to the main classification level.
C.C. = Canopy cover and F.F. = Forest Fraction.

Figure 4.17. FAO's Landcover Classification Scheme.

Table 4.19. Riparian Vegetation Inventory/condition Survey for Section 141.

RIPARIAN VEGETATION River Section 141		
<u>Existing Vegetation:</u>		
Type: Fragmented Forest		
Composition: 8b,3b,4b,6c,12c		
Vigor/Density: Moderate (M)		
Potential: F (Functioning at risk)		
Summary Categories (Identify individually and/or in combination)		
Bare		RV 1
Forbs only	Low Density	2a
	Moderate Density	2b
Grass with forbs and or brush	Low Density	3a
	Moderate Density	3b
	High Density	3c
Perennial and/or rhizomatous grasses	Low Density	4a
	Moderate Density	4b
	High Density	4c
Low Brush	Low Density	5a
	Moderate Density	5b
	High Density	5c
High Brush	Low Density	6a
	Moderate Density	6b
	High Density	6c
Deciduous and/or perennial overstory	Low Density	7a
	Moderate Density	7b
	High Density	7c
Overstory with brush/grass understory	Low Density	8a
	Moderate Density	8b
	High Density	8c
Wetland vegetation community		12a
	Bog	12b
	Fen	12c
	Marsh	RV 12d
Condition	Proper Functioning Condition (P)	
	Functional-At Risk (F)	
	Nonfunctional (N)	
	Unknown (U)	

Streamflow regime. Streamflow regime, an important factor influencing the aquatic habitat, the riparian vegetation, and the morphology of a river channel, is classified into general categories that include (E) ephemeral, (I) intermittent, (P) perennial, and (S) subterranean for specification in Level III inventories pertaining to the White River. Specific additional categories for streamflow patterns include (1) streamflow dominated by snowmelt runoff, (2) streamflow dominated by stormflow runoff, (3) streamflow dominated by spring-fed condition, (4) streamflow dominated by glacial melt, (5) streamflow dominated by ice flows, (6) streamflow dominated by tidal influence, (7) streamflow dominated by regulated flow, and (8) streamflow altered by development. Streamflow regime classification for a reach is designated by an alphanumeric descriptor indicating its general classification and specific flow pattern(s). For example, a (E;2,4) streamflow classification would indicate a hydrologic regime described as ephemeral flow with a flow pattern dominated by stormflow and glacial melt. Distinctions between the flow regime general categories and specific streamflow pattern notations are depicted in **Table 4.22** with definitions obtained from the indicated sources.

Stream Size and Order. Stream size and order are observable stream dimensions utilized to further describe the state of the various sections of the White River. Bankfull channel width is selected to be the primary ingredient representing stream size in part due to many “hydrologic and geomorphic interpretations that can be derived from width measurements” (Rosgen & Silvey, 1996, p. 6-17). Bankfull channel width is classified into thirteen categories ranging from less than 1 foot, designated as S-1, to greater than 1000 feet, designated as S-13. The primary function of stream order at the Level III

classification is as a biological stratification providing “indices of the diversity in the food web” (Rosgen & Silvey, 1996, p. 6-18). Stream order determination is based on Strahler’s stream order numbering system. Categories of stream size are shown in **Table 4.21.**

Table 4.20. Categories of Stream Size as Indicated by Bankfull Surface Width and Stream Order (Rosgen & Silvey, 1996).

STREAM SIZE	
S-1	Bankfull width less than 1 foot
S-2	Bankfull width 1-5 feet
S-3	Bankfull width 5-15 feet
S-4	Bankfull width 15-30 feet
S-5	Bankfull width 30-50 feet
S-6	Bankfull width 50-75 feet
S-7	Bankfull width 75-100 feet
S-8	Bankfull width 100-150 feet
S-9	Bankfull width 150-250 feet
S-10	Bankfull width 250-350 feet
S-11	Bankfull width 350-500 feet
S-12	Bankfull width 500-1000 feet
S-13	Bankfull width greater than 1000 feet
STREAM ORDER	
Add categories in parenthesis for specific stream order of reach. For example a third order stream with a bankfull width of 20 feet would be indexed as: S-4(3).	

Table 4.21. Categories of Flow Regime for Specification in Level III Inventories (Rosgen & Silvey, 1996; Meinzer, 1923).

FLOW REGIME	
<u>General Category</u>	
E.	A stream that flows only in direct response to precipitation, and whose channel is at all times above the water table. Often used in conjunction with intermittent (Meinzer, 1923).
S.	A stream that flows parallel to and near the surface for various seasons - a subsurface flow which follows the stream bed (Rosgen & Silvey, 1996).
I.	A stream that flows only at certain times of the year when it receives water from springs or from some surface source such as melting snow in mountainous areas. Often this term is associated with flows that reappear along various locations of a reach, then run subterranean (Meinzer, 1923).
P.	A stream that flows continuously. Perennial streams are generally associated with a water table in the localities through which they flow (Meinzer, 1923).
<u>Specific Category</u>	
1.	Seasonal variation in streamflow dominated primarily by snowmelt runoff.
2.	Seasonal variation in streamflow dominated primarily by stormflow runoff.
3.	Uniform stage and associated streamflow due to spring fed condition, backwater etc.
4.	Stream flow regulated by glacial melt.
5.	Ice flows, ice torrents from ice dam breaches.
6.	Alternating flow/backwater due to tidal influence.
7.	Regulated stream flow due to diversions, dam release, dewatering, etc.
8.	Altered due to development, such as urban streams, cut-over watersheds, vegetation conversions (forested to grassland) that changes flow response to precipitation events.

Depositional patterns (sediment). Depositional patterns or features are the physical manifestations of the interaction between sediments and flow regime within a channel. Unique depositional features are the results of sediment supply, sediment storage, and sediment conveyance patterns reflecting channel adjustments initiated by inundations, direct channel disturbances, and alterations in riparian vegetation and flow regime. In terms of energy, depositional patterns are the resultant of the work performed or organized to dissipate excessive kinetic energy through means of channel aggradation/degradation and oscillation. Therefore, meticulous inspection of observable depositional features through aerial photographs can help interpret stream condition and verify interpretations of vertical and lateral channel stability. Depositional feature classifications for various sections of the White River are based on the forms presented initially by Mollard (1973) and Galay et al., (1973) and modified by Rosgen (1985) (**Figure 4.18**).

Meander Patterns (channels). Meander patterns are the oscillations or lateral adjustments initiated by inundations, direct channel disturbances, and alterations in riparian vegetation and flow regime to dissipate excess kinetic energy within a stream channel. The analyses of meander patterns observable through aerial photographs can provide the “potential onset of disequilibrium and evolutionary adjustments” as well as meander geometry relationships for a stream channel, which allows for interpretation to assess the effects of the manner in which the channel adjusted its channel gradient to its valley gradient, banks erosion estimates, and changes in pattern and dimensions on channel stability (Rosgen & Silvey, 1996, p. 6-25). Meander pattern classifications for various sections of the White River are based on the descriptions provided initially by Mollard (1973) and Galay et al. (1973) and modified by Rosgen (1985) (**Figure 4.19**).

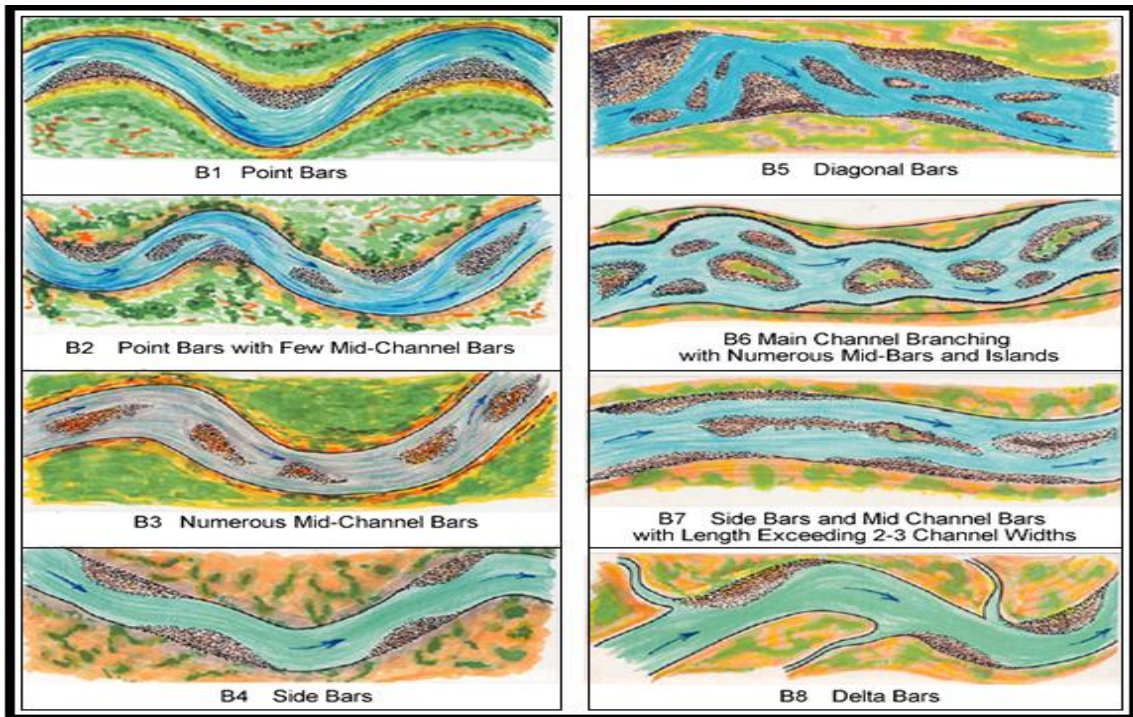


Figure 4.18. Illustrations of Depositional Features as modified from Galay et al. (1973).

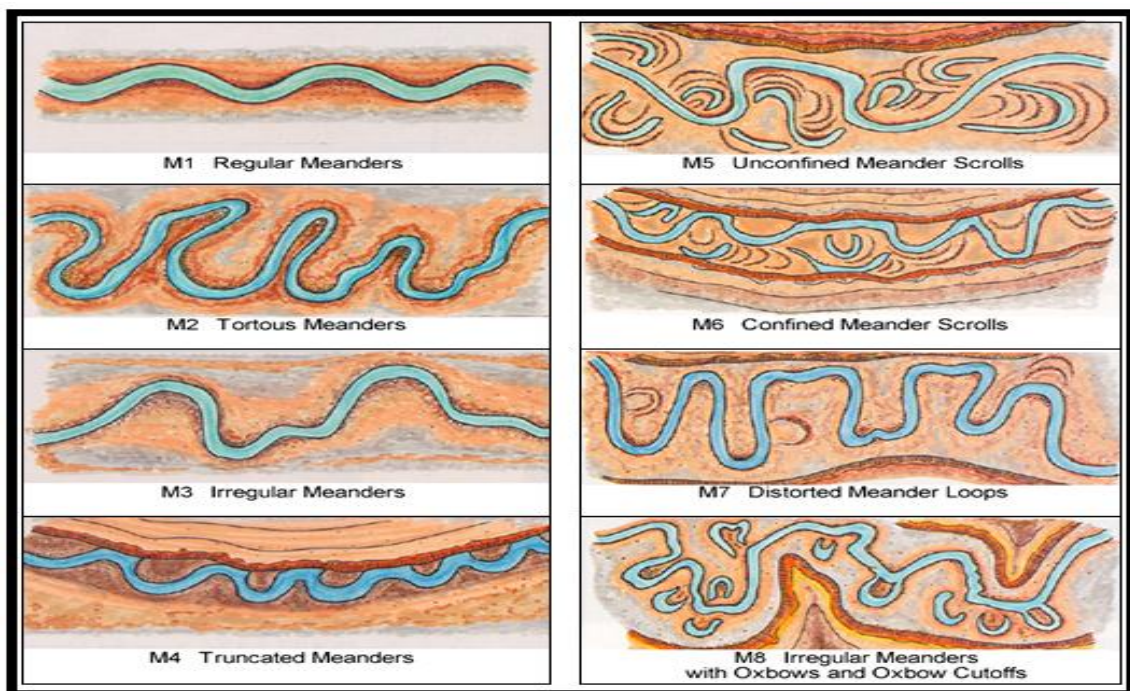


Figure 4.19. Illustrations of Various Meander Pattern Descriptions as modified from Galay et al.(1973).

Stream channel stability. Stream channel stability is the most significant indicator of natural stream function and condition considering that it conveys the lateral and vertical stability or bank and bed stability, respectively, by encompassing visible features resulting from the interaction of components such as vegetation, landform/soils, and hydrology. The modified Pfankuch evaluation method is utilized to quantitatively describe the degree of stability inherent to a specific Rosgen stream system, in this case the type “C” White River fluvial system, by applying numerical ratings to measurable and observable vegetative, geomorphic/geotechnical, and hydrologic categories such as landform slope, mass wasting, debris potential, vegetative protection, depositional patterns, and particle size distribution. A specific numerical value is applied to each of the mentioned categories for various levels denoted as Excellent, Good, Fair, and Poor. The cumulative value obtained from the Pfankuch channel stability rating is then converted to different stability criteria, for various levels specified, for a certain Rosgen stream type to assess its condition. Cumulative values greater than the mean values of stream types indicate “[increased system sensitivity and potential for increased erosion/ sediment supply if there are commensurate increases of streamflow magnitude and duration, or] potential departure from typical stability conditions [...], and suggest onset or existence of channel instability” while cumulative values smaller than the average values indicate a “system sensitivity to potential change associated with channel disturbance” (Rosgen & Silvey, 1996, p. 6-28). Data categories such as sediment supply, streambed stability, and width/depth ratio condition are also included for recording field observations and interpretations. In contrast to sediment supply which can be estimated by observing depositional patterns and water transparency and width/depth ratio which

can be determined from aerial photographs and the HEC-RAS Model, stream bed stability is difficult to determine as it requires extensive documentations of locations where aggradation/degradation has raised/lowered bed elevations. For this reason, stream bed stability is replaced with a Mobility Index and Hjulström's plot of velocity and particle size to evaluate the erosive power and sediment transport capability of the studied channel which ultimately serve as an unrefined predictor of whether the streambed is aggrading or degrading. The Mobility Index is computed as $S(Q/D_{50}v)^{0.5}$ where S is the slope, Q is the discharge, D_{50} is the diameter of the dominant bed material, and v is the kinematic viscosity of water at 20 degrees Celsius. The stability rating criteria table for Rosgen's stream types and the modified Pfankuch channel stability evaluation forms are shown in **Table 4.23** and **Tables 4.24a-b**, respectively.

Channel stability evaluations for the Level II 'reference' reaches are shown at the end of chapter 4. Similar channel stability evaluations are also applied for each of the remaining sections and are summarized at the finale of Level IV classification. It should be noted that the numerical values obtained are simply an index to channel stability and not the actual stability. The actual channel stability will be validated by sediment data collection and sediment analysis methods covered in Level IV.

Streambank erosion potential. Streambank erosion is a natural river adjustment process often responsible for lateral migrations of a river channel. Lateral migrations are accelerated by alterations in the reciprocally connected variables, such as riparian vegetation, rooting depth and density, velocity and velocity gradient, stream power, near bank shear stress, and discharge. The distributions of vegetation, velocity gradient, stream power, streamflow, and shear stress play important roles in the bank erodibility

hazard rating procedures developed by Dr. Dave Rosgen (1994), and their conversions into numerical indices of bank erosion potential provide a guideline to assess the stability conditions of the banks of the White River. The specific streambank erodibility factors implemented are (1) the ratio of streambank height to bankfull depth, (2) the ratio of root depth to bankfull depth, (3) the degree of rooting density, (4) the streambank angle or

Table 4.22. Conversion of the Channel Stability Rating to a Reach Condition by Stream Type (Rosgen & Silvey, 1996).

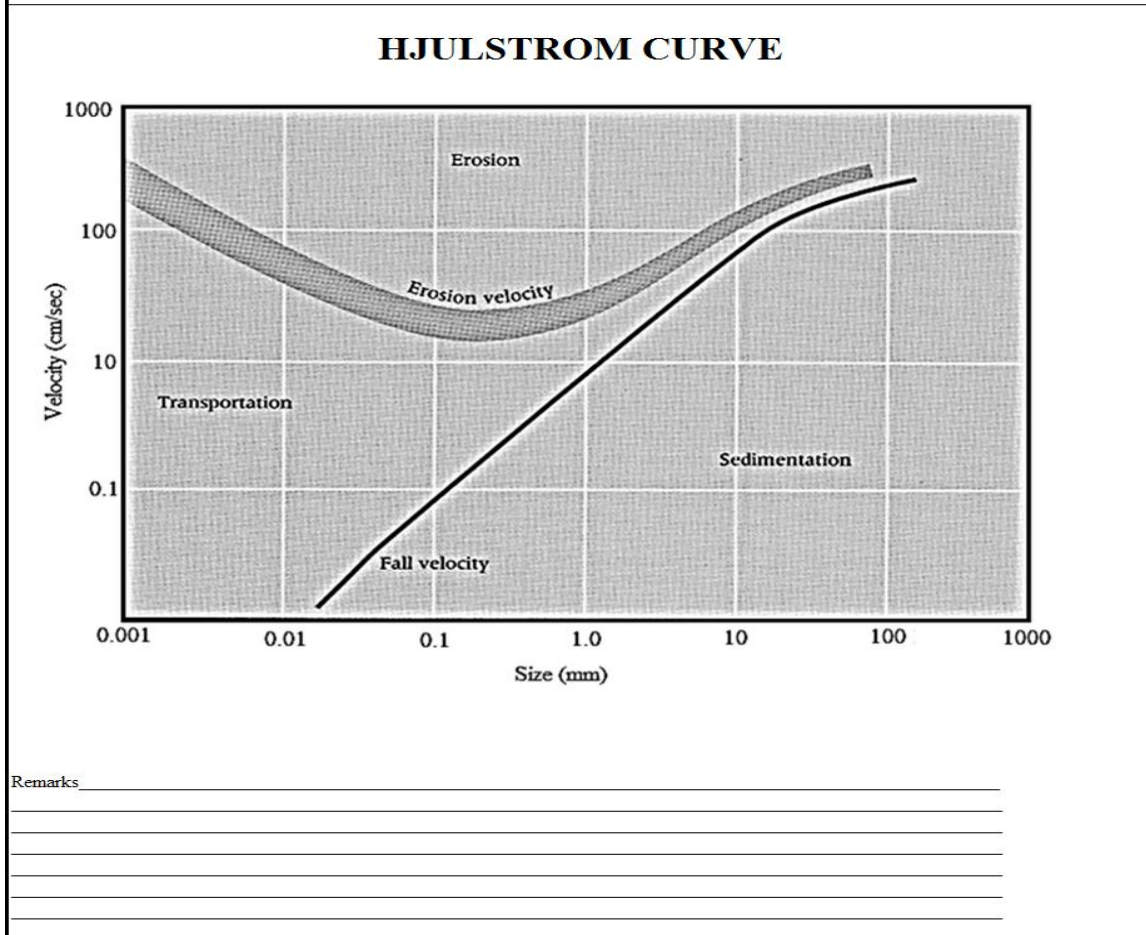
Conversion of Stability Rating To Reach Condition By Stream Type*							
Stream Type	A1	A2	A3	A4	A5	A6	B1
GOOD	38-43	38-43	54-90	60-95	60-95	50-80	38-45
FAIR	44-47	44-47	91-129	96-132	96-142	81-110	46-58
POOR	48+	48+	130+	133+	143+	111+	59+
Stream Type	B2	B3	B4	B5	B6	C1	C2
GOOD	38-45	40-60	40-64	48-68	40-60	38-50	38-50
FAIR	46-58	61-78	65-84	69-88	61-78	51-61	51-61
POOR	59+	79+	85+	89+	79+	62+	62+
Stream Type	C3	C4	C5	C6	D3	D4	D5
GOOD	60-85	70-90	70-90	60-85	85-107	85-107	85-107
FAIR	86-105	91-110	91-110	86-105	108-132	108-132	108-132
POOR	106+	111+	111+	106+	133+	133+	133+
Stream Type	D6	DA3	DA4	DA5	DA6	E3	E4
GOOD	67-98	40-63	40-63	40-63	40-63	40-63	50-75
FAIR	99-125	64-86	64-86	64-86	64-86	64-86	76-96
POOR	126+	87+	87+	87+	87+	87+	97+
Stream Type	E5	E6	F1	F2	F3	F4	F5
GOOD	50-75	40-63	60-85	60-85	85-110	85-110	90-115
FAIR	76-96	64-86	86-105	86-105	111-125	111-125	116-130
POOR	97+	87+	106+	106+	126+	126+	131+
Stream Type	F6	G1	G2	G3	G4	G5	G6
GOOD	80-95	40-60	40-60	85-107	85-107	90-112	85-107
FAIR	96-110	61-78	61-78	108-120	108-120	113-125	108-120
POOR	111+	79+	79+	121+	121+	126+	121+
<i>*Generalized relations...need additional Level IV data to expand data base for validation.</i>							

Table 4.23a. Modified Pfankuch Channel Stability Evaluation Form (Pfankuch, 1975).

PFANKUCH'S CHANNEL STABILITY EVALUATION			
Reach Location _____		Date _____	Observers _____
Stream Type _____			
	Category	EXCELLENT	Score
UPPER BANKS	1 Landform Slope	Bank Height Ratio approximately 1.0	2
	2 Mass Wasting	No evidence of past or future mass wasting.	3
	3 Debris Jam Potential	Essential absent from immediate channel area.	2
	4 Vegetative Bank Protection	90%+ plant density. Vigor and variety suggest a deep dense soil binding root mass.	3
LOWER BANKS	5 Channel Capacity	Ample for present plus some increases. Peak flows contained. W/D ratio < 7.	1
	6 Bank Rock Content	65%+ with large angular boulders. 12" + common.	2
	7 Obstructions to Flow	Rocks and logs firmly imbedded. Flow pattern without cutting or deposition.	2
	8 Cutting	Little or none. Infreq. Raw banks less than 6".	4
BOTTOM	9 Deposition	Little or no enlargement of channel or point bars.	4
	10 Rock Angularity	Sharp edges and corners. Plane surfaces rough.	1
	11 Water Brightness	Surface dull, dark or stained. Generally not bright.	1
	12 Consolidation of Particles	Assorted sizes tightly packed or overlapping.	2
	13 Bottom Size Distribution	No size change evident. Stable material 80-100%	4
	14 Scouring and Deposition	<5% of bottom affected by scour or deposition.	6
	15 Aquatic Vegetation	Abundant Growth moss-like, dark green perennial. In swift water too.	1
SUM			
	Category	GOOD	Score
UPPER BANKS	1 Landform Slope	Bank Height Ratio approximately 1.1	4
	2 Mass Wasting	Infrequent. Mostly healed over. Low future potential.	6
	3 Debris Jam Potential	Present, but mostly small twigs and limbs.	4
	4 Vegetative Bank Protection	70-90% density. Fewer species or less vigor suggest less dense or deep root mass.	6
LOWER BANKS	5 Channel Capacity	Adequate, Bank overflows rare. W/D ratio 8-15	2
	6 Bank Rock Content	40-65%. Mostly small boulders to cobbles 6-12"	4
	7 Obstructions to Flow	Some present causing erosive cross currents and minor pool filling. Obstr. newer and less firm.	4
	8 Cutting	Some, intermittently at outcures and constrictions. Raw banks may be up to 12"	6
BOTTOM	9 Deposition	Some new bar increase, mostly from coarse gravel.	8
	10 Rock Angularity	Rounded corners and edges, surfaces smooth, flat.	2
	11 Water Brightness	Mostly dull, but may have < 35% bright surfaces.	2
	12 Consolidation of Particles	Moderately packed with some overlapping.	4
	13 Bottom Size Distribution	Distribution shift light. Stable material 50-80%	8
	14 Scouring and Deposition	5-30% affected. Scour at constrictions and where grades steepen. Some deposition in pools.	12
	15 Aquatic Vegetation	Common. Algae forms in low velocity and pool areas. Moss here too.	2
SUM			
	Category	FAIR	Score
UPPER BANKS	1 Landform Slope	Bank Height Ratio approximately 1.45	6
	2 Mass Wasting	Frequent or large, causing sediment nearly year long.	9
	3 Debris Jam Potential	Moderate to heavy amounts, mostly larger sizes.	6
	4 Vegetative Bank Protection	<50-70% density. Lower vigor and fewer species from a shallow, discontinuous root mass.	9
LOWER BANKS	5 Channel Capacity	Barely contains present peaks. Occasional overbank floods. W/D ratio 15 to 25.	3
	6 Bank Rock Content	20-40% with most in the 3-6" diameter class.	6
	7 Obstructions to Flow	Moderately frequent, unstable obstructions move with high flows causing bank cutting and pool filling.	6
	8 Cutting	Significant. Cuts 12-24" high. Root mat overhangs and sloughing evident.	12
BOTTOM	9 Deposition	Moderate deposition of new gravel and coarse sand on old and some new bars.	12
	10 Rock Angularity	Corners and edges well rounded in two dimensions.	3
	11 Water Brightness	Mixture dull and bright, i.e. 35-65% mixture range.	3
	12 Consolidation of Particles	Mostly loose assortment with no apparent overlap.	6
	13 Bottom Size Distribution	Moderate change in sizes. Stable materials 20-50%.	12
	14 Scouring and Deposition	30-50% affected. Deposits and scour at obstructions, constrictions, and bends. Some filling of pools.	18
	15 Aquatic Vegetation	Present but spotty, mostly in backwater. Seasonal algae growth makes rocks slick.	3
SUM			
	Category	POOR	Score
UPPER BANKS	1 Landform Slope	Bank Height Ratio approximately 1.63	8
	2 Mass Wasting	Frequent or large causing sediment supply nearly year long or imminent danger of same.	12
	3 Debris Jam Potential	Moderate to heavy amounts, predominantly larger sizes.	8
	4 Vegetative Bank Protection	<50% density, fewer species and less vigor indicate poor, discontinuous and shallow root mass.	12
LOWER BANKS	5 Channel Capacity	Inadequate. Overbank flows common. W/D ratio > 25.	4
	6 Bank Rock Content	<20% rock fragments of gravel sizes, 1-3" or less.	8
	7 Obstructions to Flow	Sediment traps full, channel migration occurring.	8
	8 Cutting	Almost continuous cuts, some over 24" high. Failure of overhangs frequent.	16
BOTTOM	9 Deposition	Extensive deposits of predominantly fine particles. Accelerated bar development.	16
	10 Rock Angularity	Well rounded in all dimensions, surfaces smooth.	4
	11 Water Brightness	Predominantly bright, 65%+ exposed or scoured surface.	4
	12 Consolidation of Particles	No packing evident. Loose assortment easily moved.	8
	13 Bottom Size Distribution	Marked distribution change. Stable materials 0-20%.	16
	14 Scouring and Deposition	More than 50% of the bottom in a state of flux or change nearly year long.	24
	15 Aquatic Vegetation	Perennial types scarce or absent. Yellow-green, short term bloom may be present.	4
SUM			
TOTAL			

Table 4.23b. Modified Pfankuch Channel Stability Evaluation Form (Pfankuch, 1975).

Stream Width	X avg. depth	X mean velocity	Reach Gradient
Stream Order	Sinuosity	Width/bkf	Depth/bkf
W/D Ratio	Discharge	Drainage Area	Belt Width
Stream Length	Entrenchment Ratio	Meander Length	Mobility Index
Sediment Supply	Width/Depth Ratio Condition		
Extreme	Normal		Stream Type
Very High	High		
High	Very High		Pfankuch Rating
Moderate	TOTAL SCORE E__ + G__ + F__ + P__ =		
Low			Reach Condition
Remarks			



slope, (5) and bank surface protection provided by vegetation and debris. Bank Erosion Hazard Indices shown in **Table 4.25** are determined from the mentioned factors with the total BEHI rating indicating bank erosion potential. In addition, it should be noted that numerical adjustments relating to the bank materials and stratification are also made to determine the grand total BEHI rating. Numerical adjustments relating to the bank materials are made based on the defined criteria: (1) Bedrock – bank erosion potential very low, (2) Boulders – bank erosion potential low, (3) Cobble – subtract 10 points. If sand/gravel matrix is over 50%, then do not adjust, (4) Gravel – Add 5-10 points depending on percentage of bank material that is composed of sand, (5) Sand – Add 10 points, and (6) Silt/Clay – No adjustment. Numerical adjustment for stratification involves adding 5-10 points depending on position of unstable layers in relation to bankfull stage. Near bank stresses are also estimated for the various sections of the White River by using field method 6 from Rosgen (2004), and are converted to adjective rating based on the criteria shown in **Table 4.40**. Method 6 estimates the near bank stress (NBS) from the ratio of near-bank area to bankfull area. Near bank shear stresses for various segments of the White River are also available from the HEC-RAS Model for sections at which field data could not easily be obtained. BEHI's and NBS's representing the stability conditions of the streambanks of various White River reaches are shown at the end of the RSC Level IV classification.

Level IV Classification: Field Data Verification

Stream inventory Level IV analyses are conducted to confirm the assessments of stream condition, potential, and stability as predicted in the previous section. The confirmation of the stream condition, potential, and stability of each section of the White

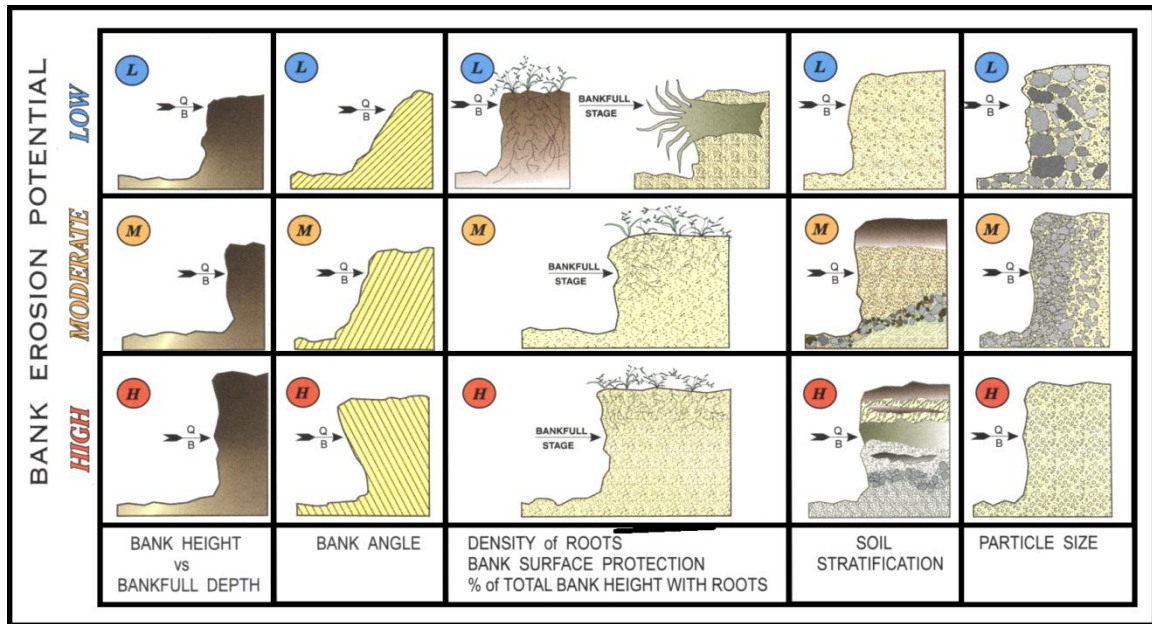


Figure 4.20. Streambank Erodibility Factors (Rosgen & Silvey, 1996).

Table 4.24 Conversion from Erodibility Variable Index to Numerical Bank Erosion Potential Values (as modified from Rosgen & Silvey, 1996).

		BANK EROSION POTENTIAL					
ERODIBILITY VARIABLE		V. Low	Low	Mod.	High	V. High	Extr.
	Bank Ht./	Value	1-1.1	1.1-1.2	1.2-1.5	1.6-2	2.1-2.8
	Bkf Ht.	Index	1-1.9	2-3.9	4-5.9	6-7.9	8-9
	Rt. Depth/	Value	1-.9	.89-.5	.49-.3	.29-1.15	.14-.05
	Bank Ht.	Index	1-1.9	2.3-3.9	4-5.9	6-7.9	8-9
	Rt. Density	Value	80-100	55-79	30-54	15-29	5-14
	(%)	Index	1-1.9	2-3.9	4-5.9	6-7.9	8-9
	Bk. Angle	Value	0-20	21-60	61-80	81-90	91-119
	(deg)	Index	1-1.9	2-3.9	4-5.9	6-7.9	8-9
	Surface	Value	80-100	55-79	30-54	15-29	10-15
	Prot.(%)	Index	1-1.9	2-3.9	4-5.9	6-7.9	8-9
	Total Score		5-9.9	10-19.9	20-29.9	30-39.9	40-45
	BEHI Rating		V. Low	Low	Mod.	High	V. High
							Extr.

River is accomplished through reach-specific observation and analyses of sediment condition, and stream flow and stability via the HEC-RAS Model, ArcGIS, and field data collected from reference “reaches”.

Since it is established that sediment plays an important role in influencing the channel stability and morphology of a river channel, sediment analyses emphasizing field measurements of suspended and bed-load sediment are mandatory for validation purposes. In practice, however, sediment data are often predicted by utilizing various prediction methodologies available in the literature rather than measured directly from the site. In the case pertaining to the White River, the primary sediment data consisted of core samples obtained from the mid-sections of depositional point bar features as well as the apexes of the banks. The core samples from depositional bars, obtained from an open bottom bucket to not exceed twice the depth of the maximum particle size diameter encountered, are sieved and weighted in order to determine the particle size distribution representative of bed-load sizes available that are being transported and/or deposited at the bankfull stage or the normal high flows. Suspended-load is presently ignored based on the premise that since it is “associated with a supply limitation in relation to its transport” rather than an energy limitation, a prerequisite of the White River, it is less critical to stability assessment since the fine sediment is less sensitive to an energy requirement for transport (Rosgen & Silvey, 1996, p. 7-3). Bed-load size distribution at or near the bankfull discharge for various reference “reaches” are shown in **Figure 4.23** and **Figure 4.24**. Sediment data obtained from the field will also be analyzed in chapter 5 to express the numerical quantities of bed-load and suspended-load inherent to specific reference reaches.

Stream stability, as defined as the “ability of the stream, over time, to transport the flows and sediment of its watershed in such a manner that the dimension, pattern and profile of the river is maintained without either aggrading nor degrading” (Rosgen & Silvey, 1996, p. 7-11). Verification of the current stability conditions of various reaches of the White River are determined via aerial photograph and quadrangle map comparisons to identify the emergence of depositional bar features, alterations in planform or sinuosity, and contrasts in landforms and vegetation; via the HEC-RAS Model to identify hydraulic geometry relations between parameters, i.e., discharge and velocity, discharge and width, discharge and depth, discharge and cross-sectional area, shear stress and velocity, etc., (refer to chapter 3); and via field observation for bed/bank materials and sediment data. These actions are adjoining and inclusive to the assessments initiated in Level III classification. The results are tabulated in the figures and tables shown below.

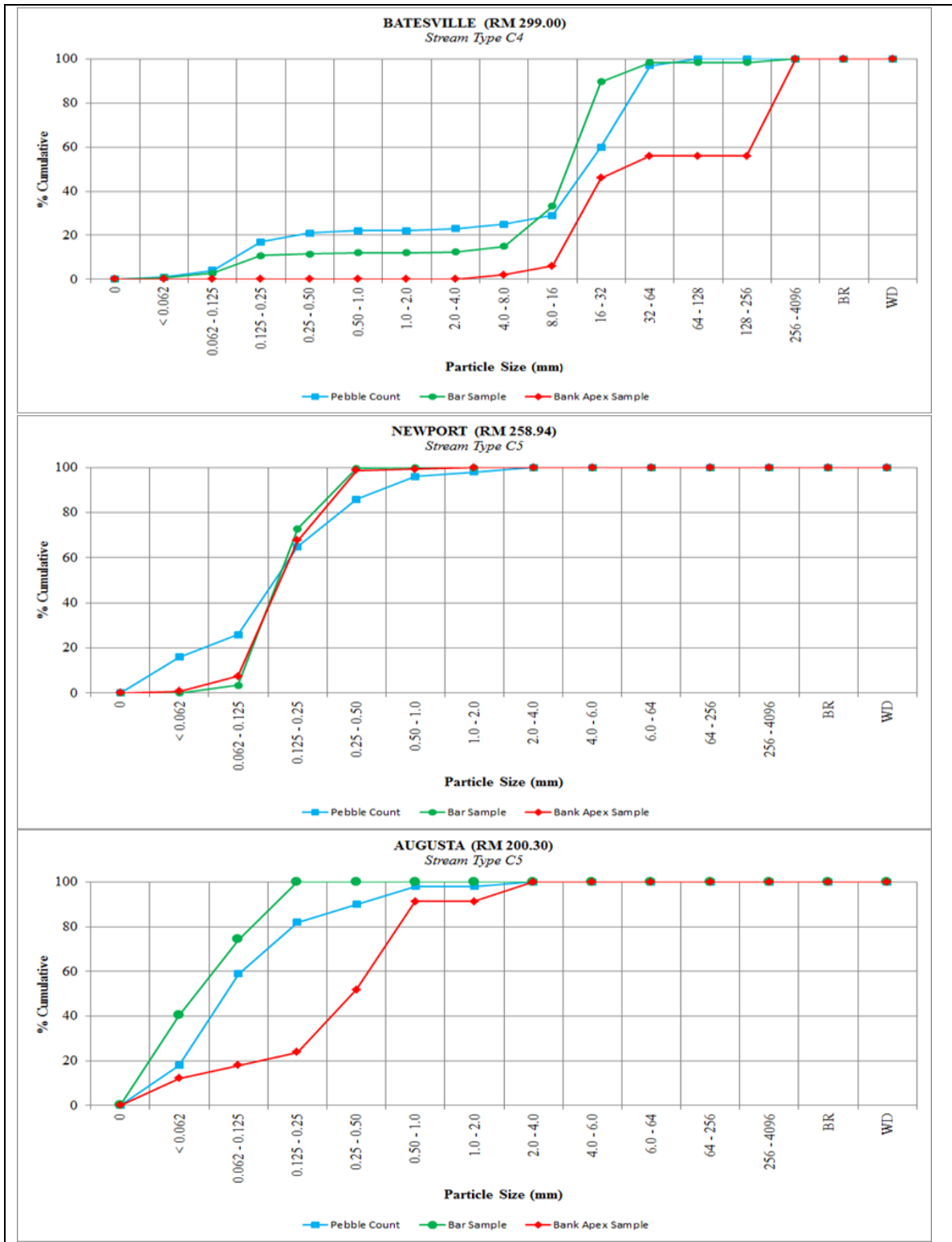


Figure 4.21. Relationships of Particle Size Distributions for Bed-load at Bankfull Discharge, Bar Material, and Bed Material for Batesville (RM 299.00), Newport (RM 258.94), and Augusta (RM 200.30).

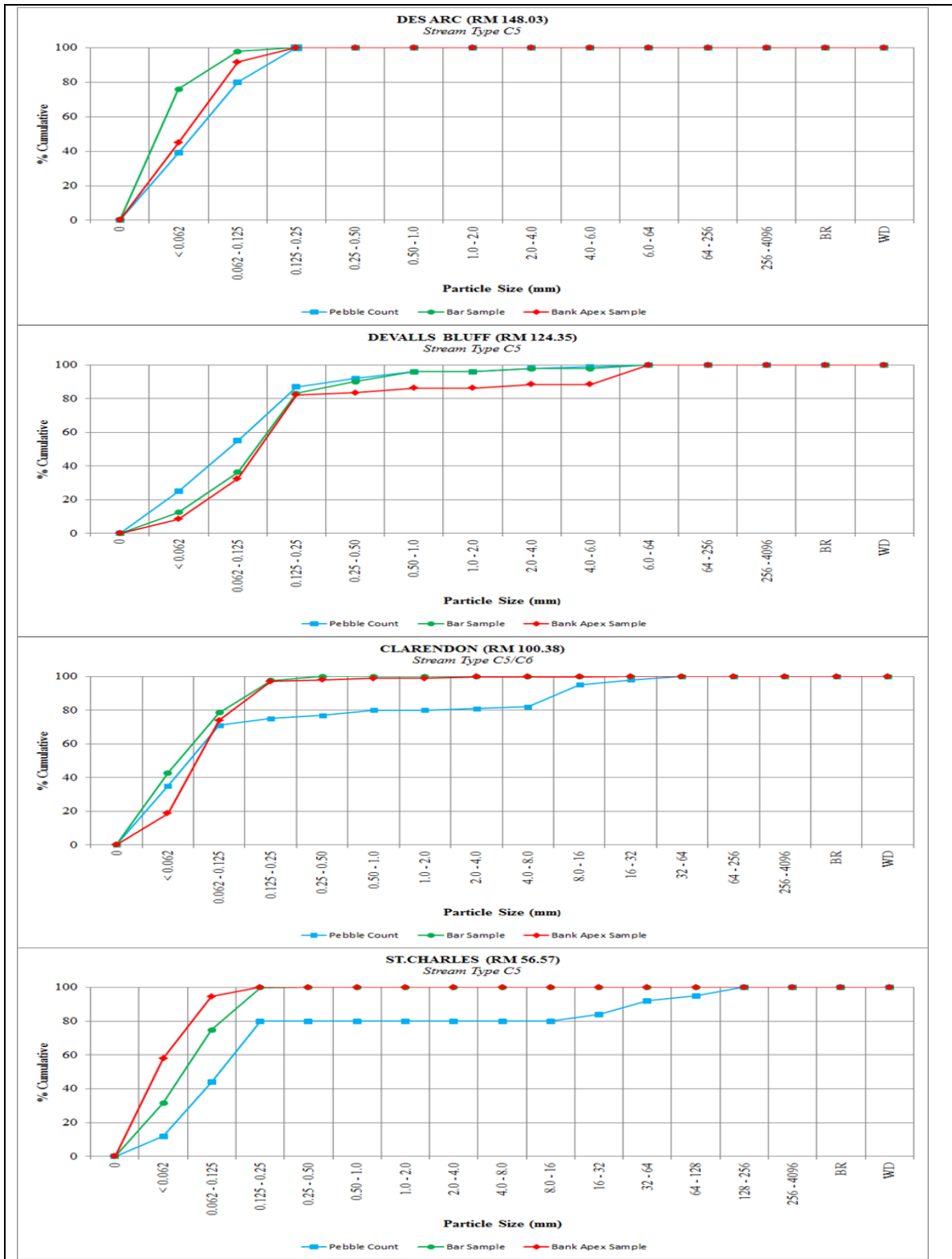


Figure 4.22. Relationships of Particle Size Distributions for Bed-load at Bankfull Discharge, Bar Material, and Bed Material for Des Arc (RM 148.03), DeValls Bluff (RM 124.35), Clarendon (RM 100.38), and St. Charles (RM 56.57).

Table 4.25a. Modified Pfankuch Channel Stability Evaluation for Batesville (RM 299.00).

PFANKUCH'S CHANNEL STABILITY EVALUATION			
Reach Location	BATESVILLE (RM 299.00)	Date	9/15/2010
Stream Type	C4C-	Observers	Linh & Vince
Category	EXCELLENT		Score
UPPER BANKS	1 Landform Slope	Bank Height Ratio approximately 1.0	2
	2 Mass Wasting	No evidence of past or future mass wasting.	3
	3 Debris Jam Potential	Essential absent from immediate channel area.	2
	4 Vegetative Bank Protection	90%+ plant density. Vigor and variety suggest a deep dense soil binding root mass.	3
LOWER BANKS	5 Channel Capacity	Ample for present plus some increases. Peak flows contained. W/D ratio < 7.	1
	6 Bank Rock Content	65%+ with large angular boulders. 12" + common.	2
	7 Obstructions to Flow	Rocks and logs firmly imbedded. Flow pattern without cutting or deposition.	2
	8 Cutting	Little or none. Infreq. Raw banks less than 6".	4
BOTTOM	9 Deposition	Little or no enlargement of channel or point bars.	4
	10 Rock Angularity	Sharp edges and corners. Plane surfaces rough.	1
	11 Water Brightness	Surface dull, dark or stained. Generally not bright.	1
	12 Consolidation of Particles	Assorted sizes tightly packed or overlapping.	2
	13 Bottom Size Distribution	No size change evident. Stable material 80-100%	4
	14 Scouring and Deposition	<5% of bottom affected by scour or deposition.	6
	15 Aquatic Vegetation	Abundant Growth moss-like, dark green perennial. In swift water too.	1
SUM			12
Category	GOOD		Score
UPPER BANKS	1 Landform Slope	Bank Height Ratio approximately 1.1	4
	2 Mass Wasting	Infrequent. Mostly healed over. Low future potential.	6
	3 Debris Jam Potential	Present, but mostly small twigs and limbs.	4
	4 Vegetative Bank Protection	70-90% density. Fewer species or less vigor suggest less dense or deep root mass.	6
LOWER BANKS	5 Channel Capacity	Adequate, Bank overflows rare. W/D ratio 8-15	2
	6 Bank Rock Content	40-65%. Mostly small boulders to cobbles 6-12"	4
	7 Obstructions to Flow	Some present causing erosive cross currents and minor pool filling. Obstr. newer and less firm.	4
	8 Cutting	Some, intermittently at outcures and constrictions. Raw banks may be up to 12"	6
BOTTOM	9 Deposition	Some new bar increase, mostly from coarse gravel.	8
	10 Rock Angularity	Rounded corners and edges, surfaces smooth, flat.	2
	11 Water Brightness	Mostly dull, but may have < 35% bright surfaces.	2
	12 Consolidation of Particles	Moderately packed with some overlapping.	4
	13 Bottom Size Distribution	Distribution shift light. Stable material 50-80%	8
	14 Scouring and Deposition	5-30% affected. Scour at constrictions and where grades steepen. Some deposition in pools.	12
	15 Aquatic Vegetation	Common. Algae forms in low velocity and pool areas. Moss here too.	2
SUM			30
Category	FAIR		Score
UPPER BANKS	1 Landform Slope	Bank Height Ratio approximately 1.45	6
	2 Mass Wasting	Frequent or large, causing sediment nearly year long.	9
	3 Debris Jam Potential	Moderate to heavy amounts, mostly larger sizes.	6
	4 Vegetative Bank Protection	<50-70% density. Lower vigor and fewer species from a shallow, discontinuous root mass.	9
LOWER BANKS	5 Channel Capacity	Barely contains present peaks. Occasional overbank floods. W/D ratio 15 to 25.	3
	6 Bank Rock Content	20-40% with most in the 3-6" diameter class.	6
	7 Obstructions to Flow	Moderately frequent, unstable obstructions move with high flows causing bank cutting and pool filling.	6
	8 Cutting	Significant. Cuts 12-24" high. Root mat overhangs and sloughing evident.	12
BOTTOM	9 Deposition	Moderate deposition of new gravel and coarse sand on old and some new bars.	12
	10 Rock Angularity	Corners and edges well rounded in two dimensions.	3
	11 Water Brightness	Mixture dull and bright, i.e. 35-65% mixture range.	3
	12 Consolidation of Particles	Mostly loose assortment with no apparent overlap.	6
	13 Bottom Size Distribution	Moderate change in sizes. Stable materials 20-50%.	12
	14 Scouring and Deposition	30-50% affected. Deposits and scour at obstructions, constrictions, and bends. Some filling of pools.	18
	15 Aquatic Vegetation	Present but spotty, mostly in backwater. Seasonal algae growth makes rocks slick.	3
SUM			45
Category	POOR		Score
UPPER BANKS	1 Landform Slope	Bank Height Ratio approximately 1.63	8
	2 Mass Wasting	Frequent or large causing sediment supply nearly year long or imminent danger of same.	12
	3 Debris Jam Potential	Moderate to heavy amounts, predominantly larger sizes.	8
	4 Vegetative Bank Protection	<50% density, fewer species and less vigor indicate poor, discontinuous and shallow root mass.	12
LOWER BANKS	5 Channel Capacity	Inadequate. Overbank flows common. W/D ratio > 25.	4
	6 Bank Rock Content	<20% rock fragments of gravel sizes, 1-3" or less.	8
	7 Obstructions to Flow	Sediment traps full, channel migration occurring.	8
	8 Cutting	Almost continuous cuts, some over 24" high. Failure of overhangs frequent.	16
BOTTOM	9 Deposition	Extensive deposits of predominantly fine particles. Accelerated bar development.	16
	10 Rock Angularity	Well rounded in all dimensions, surfaces smooth.	4
	11 Water Brightness	Predominantly bright, 65%+ exposed or scoured surface.	4
	12 Consolidation of Particles	No packing evident. Loose assortment easily moved.	8
	13 Bottom Size Distribution	Marked distribution change. Stable materials 0-20%.	16
	14 Scouring and Deposition	More than 50% of the bottom in a state of flux or change nearly year long.	24
	15 Aquatic Vegetation	Perennial types scarce or absent. Yellow-green, short term bloom may be present.	4
SUM			4
TOTAL			91

Table 4.25b. Modified Pfankuch Channel Stability Evaluation for Batesville (RM 299.00).

PFANKUCH'S CHANNEL STABILITY EVALUATION							
Stream Width	499.03 ft	X avg. depth	15.71 ft	X mean velocity	2.70 ft/s	Reach Gradient	0.0001
Stream Order	5th	Sinuosity	1.65	Widthfp	4948 ft	Depthbkf	19.23 ft
W/D Ratio	35.00	Discharge	18747.65 cfs	Drainage Area	1785.12 Sq. mi.	Belt Width	14695 ft
Stream Length	15762 ft	Entrenchment Ratio	9.91	Meander Length	11153.87 ft	Mobility Index	approx. 10.50

Sediment Supply Extreme _____ Very High _____ High _____ Moderate _____ Low <input checked="" type="checkbox"/>	Width/Depth Ratio Condition Normal _____ High _____ Very High <input checked="" type="checkbox"/> POOR TOTAL SCORE $E_{12} + G_{30} + F_{45} + P_4 =$	<div style="border: 1px solid black; padding: 5px; margin-bottom: 10px;">C4C-</div> <div style="border: 1px solid black; padding: 5px; margin-bottom: 10px;">91</div> <div style="border: 1px solid black; padding: 5px;">FAIR</div>
Remarks Clearer water suggests moderate to low sediment supply.		Stream Type Pfankuch Rating Reach Condition

HJULSTROM CURVE

Velocity (cm/sec)

Size (mm)

Erosion

Transportation

Sedimentation

Erosion velocity

Fall velocity

Remarks The diagram indicates velocities inadequate to move coarse gravel materials. The Mobility Index suggests very low erosive power. The banks erodibility potential is estimated to be moderate. The width/depth ratio is very high although the channel/width is structurally controlled by bedrock. The Pfankuch rating indicates a fair channel condition overall. The channel rating also suggests a system sensitivity to potential change associated with channel disturbance.

Table 4.26a. Modified Pfankuch Channel Stability Evaluation for Newport (RM 258.94).

PFANKUCH'S CHANNEL STABILITY EVALUATION			
Reach Location	NEWPORT (RM 258.94)	Date	8/27/2010
Stream Type	C5C-	Observers	Linh & Virak
Category	EXCELLENT		Score
UPPER BANKS	1 Landform Slope	Bank Height Ratio approximately 1.0	2
	2 Mass Wasting	No evidence of past or future mass wasting.	3
	3 Debris Jam Potential	Essential absent from immediate channel area.	2
	4 Vegetative Bank Protection	90%+ plant density. Vigor and variety suggest a deep dense soil binding root mass.	3
LOWER BANKS	5 Channel Capacity	Ample for present plus some increases. Peak flows contained. W/D ratio < 7.	1
	6 Bank Rock Content	65%+ with large angular boulders. 12" + common.	2
	7 Obstructions to Flow	Rocks and logs firmly imbedded. Flow pattern without cutting or deposition.	2
	8 Cutting	Little or none. Infreq. Raw banks less than 6".	4
BOTTOM	9 Deposition	Little or no enlargement of channel or point bars.	4
	10 Rock Angularity	Sharp edges and corners. Plane surfaces rough.	1
	11 Water Brightness	Surface dull, dark or stained. Generally not bright.	1
	12 Consolidation of Particles	Assorted sizes tightly packed or overlapping.	2
	13 Bottom Size Distribution	No size change evident. Stable material 80-100%	4
	14 Scouring and Deposition	<5% of bottom affected by scour or deposition.	6
	15 Aquatic Vegetation	Abundant Growth moss-like, dark green perennial. In swift water too.	1
SUM			2
Category	GOOD		Score
UPPER BANKS	1 Landform Slope	Bank Height Ratio approximately 1.1	4
	2 Mass Wasting	Infrequent. Mostly healed over. Low future potential.	6
	3 Debris Jam Potential	Present, but mostly small twigs and limbs.	4
	4 Vegetative Bank Protection	70-90% density. Fewer species or less vigor suggest less dense or deep root mass.	6
LOWER BANKS	5 Channel Capacity	Adequate, Bank overflows rare. W/D ratio 8-15	2
	6 Bank Rock Content	40-65%. Mostly small boulders to cobbles 6-12"	4
	7 Obstructions to Flow	Some present causing erosive cross currents and minor pool filling. Obstr. newer and less firm.	4
	8 Cutting	Some, intermittently at outcures and constrictions. Raw banks may be up to 12"	6
BOTTOM	9 Deposition	Some new bar increase, mostly from coarse gravel.	8
	10 Rock Angularity	Rounded corners and edges, surfaces smooth, flat.	2
	11 Water Brightness	Mostly dull, but may have < 35% bright surfaces.	2
	12 Consolidation of Particles	Moderately packed with some overlapping.	4
	13 Bottom Size Distribution	Distribution shift light. Stable material 50-80%	8
	14 Scouring and Deposition	5-30% affected. Scour at constrictions and where grades steepen. Some deposition in pools.	12
	15 Aquatic Vegetation	Common. Algae forms in low velocity and pool areas. Moss here too.	2
SUM			12
Category	FAIR		Score
UPPER BANKS	1 Landform Slope	Bank Height Ratio approximately 1.45	6
	2 Mass Wasting	Frequent or large, causing sediment nearly year long.	9
	3 Debris Jam Potential	Moderate to heavy amounts, mostly larger sizes.	6
	4 Vegetative Bank Protection	<50-70% density. Lower vigor and fewer species from a shallow, discontinuous root mass.	9
LOWER BANKS	5 Channel Capacity	Barely contains present peaks. Occasional overbank floods. W/D ratio 15 to 25.	3
	6 Bank Rock Content	20-40% with most in the 3-6" diameter class.	6
	7 Obstructions to Flow	Moderately frequent, unstable obstructions move with high flows causing bank cutting and pool filling.	6
	8 Cutting	Significant. Cuts 12-24" high. Root mat overhangs and sloughing evident.	12
BOTTOM	9 Deposition	Moderate deposition of new gravel and coarse sand on old and some new bars.	12
	10 Rock Angularity	Corners and edges well rounded in two dimensions.	3
	11 Water Brightness	Mixture dull and bright, i.e. 35-65% mixture range.	3
	12 Consolidation of Particles	Mostly loose assortment with no apparent overlap.	6
	13 Bottom Size Distribution	Moderate change in sizes. Stable materials 20-50%.	12
	14 Scouring and Deposition	30-50% affected. Deposits and scour at obstructions, constrictions, and bends. Some filling of pools.	18
	15 Aquatic Vegetation	Present but spotty, mostly in backwater. Seasonal algae growth makes rocks slick.	3
SUM			75
Category	POOR		Score
UPPER BANKS	1 Landform Slope	Bank Height Ratio approximately 1.63	8
	2 Mass Wasting	Frequent or large causing sediment supply nearly year long or imminent danger of same.	12
	3 Debris Jam Potential	Moderate to heavy amounts, predominantly larger sizes.	8
	4 Vegetative Bank Protection	<50% density, fewer species and less vigor indicate poor, discontinuous and shallow root mass.	12
LOWER BANKS	5 Channel Capacity	Inadequate. Overbank flows common. W/D ratio > 25.	4
	6 Bank Rock Content	<20% rock fragments of gravel sizes, 1-3" or less.	8
	7 Obstructions to Flow	Sediment traps full, channel migration occurring.	8
	8 Cutting	Almost continuous cuts, some over 24" high. Failure of overhangs frequent.	16
BOTTOM	9 Deposition	Extensive deposits of predominantly fine particles. Accelerated bar development.	16
	10 Rock Angularity	Well rounded in all dimensions, surfaces smooth.	4
	11 Water Brightness	Predominantly bright. 65%+ exposed or scoured surface.	4
	12 Consolidation of Particles	No packing evident. Loose assortment easily moved.	8
	13 Bottom Size Distribution	Marked distribution change. Stable materials 0-20%.	16
	14 Scouring and Deposition	More than 50% of the bottom in a state of flux or change nearly year long.	24
	15 Aquatic Vegetation	Perennial types scarce or absent. Yellow-green, short term bloom may be present.	4
SUM			12
TOTAL			101

Table 4.26b. Modified Pfankuch Channel Stability Evaluation for Newport (RM 258.94).

PFANKUCH'S CHANNEL STABILITY EVALUATION							
Stream Width	579.16 ft	X avg. depth	26.80 ft	X mean velocity	2.25 ft/s	Reach Gradient	0.00008
Stream Order	7th	Simuosity	1.43	Widthfp	61000 ft	Depthbkf	28.26 ft
W/D Ratio	32.00	Discharge	23485 cfs	Drainage Area	981.02 Sq. mi.	Belt Width	21273 ft
Stream Length	14462 ft	Entrenchment Ratio	105.50	Meander Length	7704 ft	Mobility Index	150.36

Sediment Supply Extreme _____ Very High _____ High <input checked="" type="checkbox"/> Moderate _____ Low _____	Width/Depth Ratio Condition Normal _____ High _____ Very High <input checked="" type="checkbox"/> POOR TOTAL SCORE $E_{2} + G_{12} + F_{75} + P_{12} =$	<div style="border: 1px solid black; padding: 5px; margin-bottom: 10px;">C5C-</div> Stream Type <div style="border: 1px solid black; padding: 5px; margin-bottom: 10px;">101</div> Pfankuch Rating <div style="border: 1px solid black; padding: 5px;">FAIR</div> Reach Condition
---	---	---

Remarks High sediment supply due to high erosion rate of noncohesive bank.

HJULSTROM CURVE

Remarks The diagram indicates velocities well within the erosion range. The banks are highly erodible and may contribute to high sediment supply. The width/depth ratio is very high and may contribute to channel migration. The Mobility Index or erosive power of the bed is significant and allows sediment transportation. The stability rating indicates a fair channel condition sensitive to disturbance.

Table 4.27a. Modified Pfankuch Channel Stability Evaluation for Augusta (RM 200.30).

PFANKUCH'S CHANNEL STABILITY EVALUATION							
Reach Location		AUGUSTA (RM 200.30)		Date	9/04/2010	Observers	Linh & Virak
Stream Type		C5C-					
Category		EXCELLENT				Score	
UPPER BANKS	1 Landform Slope	Bank Height Ratio approximately 1.0				2	
	2 Mass Wasting	No evidence of past or future mass wasting.				3	
	3 Debris Jam Potential	Essential absent from immediate channel area.				2	
	4 Vegetative Bank Protection	90%+ plant density. Vigor and variety suggest a deep dense soil binding root mass.				3	
LOWER BANKS	5 Channel Capacity	Ample for present plus some increases. Peak flows contained. W/D ratio < 7.				1	
	6 Bank Rock Content	65%+ with large angular boulders. 12" + common.				2	
	7 Obstructions to Flow	Rocks and logs firmly imbedded. Flow pattern without cutting or deposition.				2	
	8 Cutting	Little or none. Infreq. Raw banks less than 6".				4	
BOTTOM	9 Deposition	Little or no enlargement of channel or point bars.				4	
	10 Rock Angularity	Sharp edges and corners. Plane surfaces rough.				1	
	11 Water Brightness	Surface dull, dark or stained. Generally not bright.				1	
	12 Consolidation of Particles	Assorted sizes tightly packed or overlapping.				2	
	13 Bottom Size Distribution	No size change evident. Stable material 80-100%				4	
	14 Scouring and Deposition	<5% of bottom affected by scour or deposition.				6	
	15 Aquatic Vegetation	Abundant Growth moss-like, dark green perennial. In swift water too.				1	
					SUM	15	
Category		GOOD				Score	
UPPER BANKS	1 Landform Slope	Bank Height Ratio approximately 1.1				4	
	2 Mass Wasting	Infrequent. Mostly healed over. Low future potential.				6	
	3 Debris Jam Potential	Present, but mostly small twigs and limbs.				4	
	4 Vegetative Bank Protection	70-90% density. Fewer species or less vigor suggest less dense or deep root mass.				6	
LOWER BANKS	5 Channel Capacity	Adequate, Bank overflows rare. W/D ratio 8-15				2	
	6 Bank Rock Content	40-65%. Mostly small boulders to cobbles 6-12"				4	
	7 Obstructions to Flow	Some present causing erosive cross currents and minor pool filling. Obstr. newer and less firm.				4	
	8 Cutting	Some, intermittently at outcures and constrictions. Raw banks may be up to 12"				6	
BOTTOM	9 Deposition	Some new bar increase, mostly from coarse gravel.				8	
	10 Rock Angularity	Rounded corners and edges, surfaces smooth, flat.				2	
	11 Water Brightness	Mostly dull, but may have < 35% bright surfaces.				2	
	12 Consolidation of Particles	Moderately packed with some overlapping.				4	
	13 Bottom Size Distribution	Distribution shift light. Stable material 50-80%				8	
	14 Scouring and Deposition	5-30% affected. Scour at constrictions and where grades steepen. Some deposition in pools.				12	
	15 Aquatic Vegetation	Common. Algae forms in low velocity and pool areas. Moss here too.				2	
					SUM	18	
Category		FAIR				Score	
UPPER BANKS	1 Landform Slope	Bank Height Ratio approximately 1.45				6	
	2 Mass Wasting	Frequent or large, causing sediment nearly year long.				9	
	3 Debris Jam Potential	Moderate to heavy amounts, mostly larger sizes.				6	
	4 Vegetative Bank Protection	<50-70% density. Lower vigor and fewer species from a shallow, discontinuous root mass.				9	
LOWER BANKS	5 Channel Capacity	Barely contains present peaks. Occasional overbank floods. W/D ratio 15 to 25.				3	
	6 Bank Rock Content	20-40% with most in the 3-6" diameter class.				6	
	7 Obstructions to Flow	Moderately frequent, unstable obstructions move with high flows causing bank cutting and pool filling.				6	
	8 Cutting	Significant. Cuts 12-24" high. Root mat overhangs and sloughing evident.				12	
BOTTOM	9 Deposition	Moderate deposition of new gravel and coarse sand on old and some new bars.				12	
	10 Rock Angularity	Corners and edges well rounded in two dimensions.				3	
	11 Water Brightness	Mixture dull and bright, i.e. 35-65% mixture range.				3	
	12 Consolidation of Particles	Mostly loose assortment with no apparent overlap.				6	
	13 Bottom Size Distribution	Moderate change in sizes. Stable materials 20-50%.				12	
	14 Scouring and Deposition	30-50% affected. Deposits and scour at obstructions, constrictions, and bends. Some filling of pools.				18	
	15 Aquatic Vegetation	Present but spotty, mostly in backwater. Seasonal algae growth makes rocks slick.				3	
					SUM	27	
Category		POOR				Score	
UPPER BANKS	1 Landform Slope	Bank Height Ratio approximately 1.63				8	
	2 Mass Wasting	Frequent or large causing sediment supply nearly year long or imminent danger of same.				12	
	3 Debris Jam Potential	Moderate to heavy amounts, predominantly larger sizes.				8	
	4 Vegetative Bank Protection	<50% density, fewer species and less vigor indicate poor, discontinuous and shallow root mass.				12	
LOWER BANKS	5 Channel Capacity	Inadequate. Overbank flows common. W/D ratio > 25.				4	
	6 Bank Rock Content	<20% rock fragments of gravel sizes, 1-3" or less.				8	
	7 Obstructions to Flow	Sediment traps full, channel migration occurring.				8	
	8 Cutting	Almost continuous cuts, some over 24" high. Failure of overhangs frequent.				16	
BOTTOM	9 Deposition	Extensive deposits of predominantly fine particles. Accelerated bar development.				16	
	10 Rock Angularity	Well rounded in all dimensions, surfaces smooth.				4	
	11 Water Brightness	Predominantly bright, 65%+ exposed or scoured surface.				4	
	12 Consolidation of Particles	No packing evident. Loose assortment easily moved.				8	
	13 Bottom Size Distribution	Marked distribution change. Stable materials 0-20%.				16	
	14 Scouring and Deposition	More than 50% of the bottom in a state of flux or change nearly year long.				24	
	15 Aquatic Vegetation	Perennial types scarce or absent. Yellow-green, short term bloom may be present.				4	
					SUM	12	
					TOTAL	72	

Table 4.27b. Modified Pfankuch Channel Stability Evaluation for Augusta (RM 200.30).

PFANKUCH'S CHANNEL STABILITY EVALUATION							
Stream Width	535.71 ft	X avg. depth	26.15 ft	X mean velocity	2.12 ft/s	Reach Gradient	0.00002
Stream Order	7th	Sinuosity	1.36	Width/bp	35000 ft	Depth/bkf	31.34 ft
W/D Ratio	27.70	Discharge	21315 cfs	Drainage Area	981.02 Sq.mi.	Belt Width	16712 ft
Stream Length	18253 ft	Entrenchment Ratio	65.60	Meander Length	6309.60 ft	Mobility Index	50.71
<div style="display: flex; justify-content: space-between;"> <div style="width: 45%;"> <p>Sediment Supply</p> <p>Extreme _____</p> <p>Very High _____</p> <p>High _____</p> <p>Moderate <input checked="" type="checkbox"/></p> <p>Low _____</p> </div> <div style="width: 45%;"> <p>Width/Depth Ratio Condition</p> <p>Normal _____</p> <p>High _____</p> <p>Very High <input checked="" type="checkbox"/> POOR</p> <p>TOTAL SCORE $E_{15} + G_{18} + F_{27} + P_{12} =$</p> </div> </div> <div style="display: flex; justify-content: space-between; margin-top: 10px;"> <div style="width: 45%;"> <p>Remarks Banks are moderately stable contributing to moderate sediment feed.</p> </div> <div style="width: 10%; text-align: center;"> <p>from table</p> </div> <div style="width: 40%;"> <div style="border: 1px solid black; padding: 5px; width: fit-content; margin: 0 auto;">C5C-</div> <p>Stream Type</p> <div style="border: 1px solid black; padding: 5px; width: fit-content; margin: 0 auto;">72</div> <p>Pfankuch Rating</p> <div style="border: 1px solid black; padding: 5px; width: fit-content; margin: 0 auto;">GOOD</div> <p>Reach Condition</p> </div> </div>							
HJULSTROM CURVE							
<p>Remarks The diagram indicates bedform susceptible to erosion and transportation of D50 materials. The Mobility Index, however, indicates moderately low erosive power. The banks are moderately erodible at various locations and are stable at other locations. The width/depth ratio is very high and could contribute to accelerated bank erosion and sediment supply depending on the magnitude of stress near the bank. The Pfankuch rating indicates a good channel condition overall. The channel rating also suggests a system sensitivity to potential change associated with channel disturbance.</p>							

Table 4.28a. Modified Pfankuch Channel Stability Evaluation for Des Arc (RM 148.03).

PFANKUCH'S CHANNEL STABILITY EVALUATION				
Reach Location	DES ARC (RM 148.03)	Date	9/01/2010	Observers
Stream Type	C5C-			Linh & Virak
Category	EXCELLENT			Score
UPPER BANKS	1 Landform Slope	Bank Height Ratio approximately 1.0		2
	2 Mass Wasting	No evidence of past or future mass wasting.		3
	3 Debris Jam Potential	Essential absent from immediate channel area.		2
	4 Vegetative Bank Protection	90%+ plant density. Vigor and variety suggest a deep dense soil binding root mass.		3
LOWER BANKS	5 Channel Capacity	Ample for present plus some increases. Peak flows contained. W/D ratio < 7.		1
	6 Bank Rock Content	65%+ with large angular boulders. 12" + common.		2
	7 Obstructions to Flow	Rocks and logs firmly imbedded. Flow pattern without cutting or deposition.		2
	8 Cutting	Little or none. Infreq. Raw banks less than 6".		4
BOTTOM	9 Deposition	Little or no enlargement of channel or point bars.		4
	10 Rock Angularity	Sharp edges and corners. Plane surfaces rough.		1
	11 Water Brightness	Surface dull, dark or stained. Generally not bright.		1
	12 Consolidation of Particles	Assorted sizes tightly packed or overlapping.		2
	13 Bottom Size Distribution	No size change evident. Stable material 80-100%		4
	14 Scouring and Deposition	<5% of bottom affected by scour or deposition.		6
	15 Aquatic Vegetation	Abundant Growth moss-like, dark green perennial. In swift water too.		1
SUM				0
Category	GOOD			Score
UPPER BANKS	1 Landform Slope	Bank Height Ratio approximately 1.1		4
	2 Mass Wasting	Infrequent. Mostly healed over. Low future potential.		6
	3 Debris Jam Potential	Present, but mostly small twigs and limbs.		4
	4 Vegetative Bank Protection	70-90% density. Fewer species or less vigor suggest less dense or deep root mass.		6
LOWER BANKS	5 Channel Capacity	Adequate, Bank overflows rare. W/D ratio 8-15		2
	6 Bank Rock Content	40-65%. Mostly small boulders to cobbles 6-12"		4
	7 Obstructions to Flow	Some present causing erosive cross currents and minor pool filling. Obstr. newer and less firm.		4
	8 Cutting	Some, intermittently at outcures and constrictions. Raw banks may be up to 12"		6
BOTTOM	9 Deposition	Some new bar increase, mostly from coarse gravel.		8
	10 Rock Angularity	Rounded corners and edges, surfaces smooth, flat.		2
	11 Water Brightness	Mostly dull, but may have < 35% bright surfaces.		2
	12 Consolidation of Particles	Moderately packed with some overlapping.		4
	13 Bottom Size Distribution	Distribution shift light. Stable material 50-80%		8
	14 Scouring and Deposition	5-30% affected. Scour at constrictions and where grades steepen. Some deposition in pools.		12
	15 Aquatic Vegetation	Common. Algae forms in low velocity and pool areas. Moss here too.		2
SUM				20
Category	FAIR			Score
UPPER BANKS	1 Landform Slope	Bank Height Ratio approximately 1.45		6
	2 Mass Wasting	Frequent or large, causing sediment nearly year long.		9
	3 Debris Jam Potential	Moderate to heavy amounts, mostly larger sizes.		6
	4 Vegetative Bank Protection	<50-70% density. Lower vigor and fewer species from a shallow, discontinuous root mass.		9
LOWER BANKS	5 Channel Capacity	Barely contains present peaks. Occasional overbank floods. W/D ratio 15 to 25.		3
	6 Bank Rock Content	20-40% with most in the 3-6" diameter class.		6
	7 Obstructions to Flow	Moderately frequent, unstable obstructions move with high flows causing bank cutting and pool filling.		6
	8 Cutting	Significant. Cuts 12-24" high. Root mat overhangs and sloughing evident.		12
BOTTOM	9 Deposition	Moderate deposition of new gravel and coarse sand on old and some new bars.		12
	10 Rock Angularity	Corners and edges well rounded in two dimensions.		3
	11 Water Brightness	Mixture dull and bright, i.e. 35-65% mixture range.		3
	12 Consolidation of Particles	Mostly loose assortment with no apparent overlap.		6
	13 Bottom Size Distribution	Moderate change in sizes. Stable materials 20-50%.		12
	14 Scouring and Deposition	30-50% affected. Deposits and scour at obstructions, constrictions, and bends. Some filling of pools.		18
	15 Aquatic Vegetation	Present but spotty, mostly in backwater. Seasonal algae growth makes rocks slick.		3
SUM				27
Category	POOR			Score
UPPER BANKS	1 Landform Slope	Bank Height Ratio approximately 1.63		8
	2 Mass Wasting	Frequent or large causing sediment supply nearly year long or imminent danger of same.		12
	3 Debris Jam Potential	Moderate to heavy amounts, predominantly larger sizes.		8
	4 Vegetative Bank Protection	<50% density, fewer species and less vigor indicate poor, discontinuous and shallow root mass.		12
LOWER BANKS	5 Channel Capacity	Inadequate. Overbank flows common. W/D ratio > 25.		4
	6 Bank Rock Content	<20% rock fragments of gravel sizes, 1-3" or less.		8
	7 Obstructions to Flow	Sediment traps full, channel migration occurring.		8
	8 Cutting	Almost continuous cuts, some over 24" high. Failure of overhangs frequent.		16
BOTTOM	9 Deposition	Extensive deposits of predominantly fine particles. Accelerated bar development.		16
	10 Rock Angularity	Well rounded in all dimensions, surfaces smooth.		4
	11 Water Brightness	Predominantly bright, 65%+ exposed or scoured surface.		4
	12 Consolidation of Particles	No packing evident. Loose assortment easily moved.		8
	13 Bottom Size Distribution	Marked distribution change. Stable materials 0-20%.		16
	14 Scouring and Deposition	More than 50% of the bottom in a state of flux or change nearly year long.		24
	15 Aquatic Vegetation	Perennial types scarce or absent. Yellow-green, short term bloom may be present.		4
SUM				64
TOTAL				111

Table 4.28b. Modified Pfankuch Channel Stability Evaluation for Des Arc (RM 148.03).

PFANKUCH'S CHANNEL STABILITY EVALUATION							
Stream Width	613.52 ft	X avg. depth	30.25 ft	X mean velocity	3.05 ft/s	Reach Gradient	0.00008
Stream Order	7th	Sinuosity	1.37	Width/bp	34000 ft	Depth/bkf	35.24 ft
W/D Ratio	37.50	Discharge	29774 cfs	Drainage Area	1357.95 Sq. mi.	Belt Width	16971 ft
Stream Length	11491 ft	Entrenchment Ratio	55.10	Meander Length	7860.58 ft	Mobility Index	240
<div style="display: flex; justify-content: space-between;"> <div style="width: 45%;"> <p>Sediment Supply</p> <p>Extreme <input checked="" type="checkbox"/></p> <p>Very High <input type="checkbox"/></p> <p>High <input type="checkbox"/></p> <p>Moderate <input type="checkbox"/></p> <p>Low <input type="checkbox"/></p> <p>Remarks <u>Extremely high sediment supply possibly from unstable banks.</u></p> </div> <div style="width: 45%;"> <p>Width/Depth Ratio Condition</p> <p>Normal <input type="checkbox"/></p> <p>High <input type="checkbox"/></p> <p>Very High <input checked="" type="checkbox"/> POOR</p> <p>TOTAL SCORE $E_{0} + G_{20} + F_{27} + P_{64} =$</p> </div> <div style="width: 10%; text-align: center;"> <div style="border: 1px solid black; padding: 5px; margin-bottom: 10px;">C5C-</div> <div style="border: 1px solid black; padding: 5px; margin-bottom: 10px;">111</div> <div style="border: 1px solid black; padding: 5px;">POOR</div> </div> <div style="width: 10%;"> <p>Stream Type</p> <p>Pfankuch Rating</p> <p>Reach Condition</p> </div> </div>							

HJULSTROM CURVE

Velocity (cm/sec)

Size (mm)

Erosion

Transportation

Sedimentation

Fall velocity

Erosion velocity

Remarks The diagram indicates velocities well within the erosion range. The banks are expected to be extremely erodible and should contribute to extremely high sediment supply. The width/depth ratio is very high and may result in channel aggradation, increased lateral extension, and migration. The overall channel condition is poor indicating a departure from stable conditions.

Table 4.29a. Pfankuch Channel Stability Evaluation for Devalls Bluff (RM 124.35).

PFANKUCH'S CHANNEL STABILITY EVALUATION				
Reach Location	DEVALLS BLUFF (RM 124.35)	Date	9/03/2010	Observers
Stream Type	C5C-			Linh & Virak
Category	EXCELLENT			Score
UPPER BANKS	1 Landform Slope	Bank Height Ratio approximately 1.0		[2]
	2 Mass Wasting	No evidence of past or future mass wasting.		3
	3 Debris Jam Potential	Essential absent from immediate channel area.		2
	4 Vegetative Bank Protection	90%+ plant density. Vigor and variety suggest a deep dense soil binding root mass.		3
LOWER BANKS	5 Channel Capacity	Ample for present plus some increases. Peak flows contained. W/D ratio < 7.		1
	6 Bank Rock Content	65%+ with large angular boulders. 12" + common.		2
	7 Obstructions to Flow	Rocks and logs firmly imbedded. Flow pattern without cutting or deposition.		2
	8 Cutting	Little or none. Infreq. Raw banks less than 6".		4
BOTTOM	9 Deposition	Little or no enlargement of channel or point bars.		4
	10 Rock Angularity	Sharp edges and corners. Plane surfaces rough.		1
	11 Water Brightness	Surface dull, dark or stained. Generally not bright.		1
	12 Consolidation of Particles	Assorted sizes tightly packed or overlapping.		2
	13 Bottom Size Distribution	No size change evident. Stable material 80-100%		4
	14 Scouring and Deposition	<5% of bottom affected by scour or deposition.		6
	15 Aquatic Vegetation	Abundant Growth moss-like, dark green perennial. In swift water too.		1
SUM				2
Category	GOOD			Score
UPPER BANKS	1 Landform Slope	Bank Height Ratio approximately 1.1		4
	2 Mass Wasting	Infrequent. Mostly healed over. Low future potential.		[6]
	3 Debris Jam Potential	Present, but mostly small twigs and limbs.		[4]
	4 Vegetative Bank Protection	70-90% density. Fewer species or less vigor suggest less dense or deep root mass.		6
LOWER BANKS	5 Channel Capacity	Adequate, Bank overflows rare. W/D ratio 8-15		2
	6 Bank Rock Content	40-65%. Mostly small boulders to cobbles 6-12"		4
	7 Obstructions to Flow	Some present causing erosive cross currents and minor pool filling. Obstr. newer and less firm.		4
	8 Cutting	Some, intermittently at outcures and constrictions. Raw banks may be up to 12"		6
BOTTOM	9 Deposition	Some new bar increase, mostly from coarse gravel.		8
	10 Rock Angularity	Rounded corners and edges, surfaces smooth, flat.		2
	11 Water Brightness	Mostly dull, but may have < 35% bright surfaces.		2
	12 Consolidation of Particles	Moderately packed with some overlapping.		4
	13 Bottom Size Distribution	Distribution shift light. Stable material 50-80%		8
	14 Scouring and Deposition	5-30% affected. Scour at constrictions and where grades steepen. Some deposition in pools.		12
	15 Aquatic Vegetation	Common. Algae forms in low velocity and pool areas. Moss here too.		2
SUM				10
Category	FAIR			Score
UPPER BANKS	1 Landform Slope	Bank Height Ratio approximately 1.45		6
	2 Mass Wasting	Frequent or large, causing sediment nearly year long.		9
	3 Debris Jam Potential	Moderate to heavy amounts, mostly larger sizes.		6
	4 Vegetative Bank Protection	<50-70% density. Lower vigor and fewer species from a shallow, discontinuous root mass.		[9]
LOWER BANKS	5 Channel Capacity	Barely contains present peaks. Occasional overbank floods. W/D ratio 15 to 25.		[3]
	6 Bank Rock Content	20-40% with most in the 3-6" diameter class.		6
	7 Obstructions to Flow	Moderately frequent, unstable obstructions move with high flows causing bank cutting and pool filling.		6
	8 Cutting	Significant. Cuts 12-24" high. Root mat overhangs and sloughing evident.		[12]
BOTTOM	9 Deposition	Moderate deposition of new gravel and coarse sand on old and some new bars.		[12]
	10 Rock Angularity	Corners and edges well rounded in two dimensions.		3
	11 Water Brightness	Mixture dull and bright, i.e. 35-65% mixture range.		[3]
	12 Consolidation of Particles	Mostly loose assortment with no apparent overlap.		[6]
	13 Bottom Size Distribution	Moderate change in sizes. Stable materials 20-50%.		[12]
	14 Scouring and Deposition	30-50% affected. Deposits and scour at obstructions, constrictions, and bends. Some filling of pools.		[18]
	15 Aquatic Vegetation	Present but spotty, mostly in backwater. Seasonal algae growth makes rocks slick.		3
SUM				75
Category	POOR			Score
UPPER BANKS	1 Landform Slope	Bank Height Ratio approximately 1.63		8
	2 Mass Wasting	Frequent or large causing sediment supply nearly year long or imminent danger of same.		12
	3 Debris Jam Potential	Moderate to heavy amounts, predominantly larger sizes.		8
	4 Vegetative Bank Protection	<50% density, fewer species and less vigor indicate poor, discontinuous and shallow root mass.		12
LOWER BANKS	5 Channel Capacity	Inadequate. Overbank flows common. W/D ratio > 25.		4
	6 Bank Rock Content	<20% rock fragments of gravel sizes, 1-3" or less.		[8]
	7 Obstructions to Flow	Sediment traps full, channel migration occurring.		8
	8 Cutting	Almost continuous cuts, some over 24" high. Failure of overhangs frequent.		16
BOTTOM	9 Deposition	Extensive deposits of predominantly fine particles. Accelerated bar development.		16
	10 Rock Angularity	Well rounded in all dimensions, surfaces smooth.		4
	11 Water Brightness	Predominantly bright, 65%+ exposed or scoured surface.		4
	12 Consolidation of Particles	No packing evident. Loose assortment easily moved.		8
	13 Bottom Size Distribution	Marked distribution change. Stable materials 0-20%.		16
	14 Scouring and Deposition	More than 50% of the bottom in a state of flux or change nearly year long.		24
	15 Aquatic Vegetation	Perennial types scarce or absent. Yellow-green, short term bloom may be present.		4
SUM				8
TOTAL				95

Table 4.29b. Pfankuch Channel Stability Evaluation for Devalls Bluff (RM 124.35).

PFANKUCH'S CHANNEL STABILITY EVALUATION							
Stream Width	509.27 ft	X avg. depth	35.12 ft	X mean velocity	2.68 ft/s	Reach Gradient	0.00003
Stream Order	7th	Sinuosity	1.31	Width:fp	8000 ft	Depth:bkf	35.67 ft
W/D Ratio	22.35	Discharge	30045 cfs	Drainage Area	1357.95 Sq. mi.	Belt Width	14500 ft
Stream Length	10417 ft	Entrenchment Ratio	15.50	Meander Length	6574.61 ft	Mobility Index	63.78
<div style="display: flex; justify-content: space-between;"> <div style="width: 45%;"> <p>Sediment Supply</p> <p>Extreme _____</p> <p>Very High _____</p> <p>High _____</p> <p>Moderate <input checked="" type="checkbox"/></p> <p>Low _____</p> </div> <div style="width: 45%;"> <p>Width/Depth Ratio Condition</p> <p>Normal _____</p> <p>High <input checked="" type="checkbox"/> FAIR</p> <p>Very High _____</p> <p>TOTAL SCORE <u>E_2</u> + <u>G_10</u> + <u>F_75</u> + <u>P_8</u> =</p> </div> <div style="width: 10%; text-align: center;"> <div style="border: 1px solid black; padding: 5px; margin-bottom: 10px;">C5C-</div> <div style="border: 1px solid black; padding: 5px; margin-bottom: 10px;">95</div> <div style="border: 1px solid black; padding: 5px;">FAIR</div> </div> <div style="width: 10%;"> <p>Stream Type</p> <p>Pfankuch Rating</p> <p>Reach Condition</p> </div> </div> <p>Remarks <u>Moderate sediment supply. Moderate bank stability is expected.</u></p>							
HJULSTROM CURVE							
<p>Remarks <u>The diagram indicates velocities adequate for erosion and transportation of D50 materials. The Mobility Index also indicates fair erosive power or fair scouring and deposition of the bed. A relatively high width/depth ratio suggests possible reduction in the channel's ability to transport sediment. The overall channel condition is fair with a Pfankuch rating value suggesting sensitivity to potential change associated with channel disturbance.</u></p>							

Table 4.30a. Pfankuch Channel Stability Evaluation for Clarendon (RM 100.38).

PFANKUCH'S CHANNEL STABILITY EVALUATION			
Reach Location	CLARENDON (RM 100.38)	Date	9/02/2010
Stream Type	C5C-/C6C-	Observers	Linh & Virak
Category	EXCELLENT		Score
UPPER BANKS	1 Landform Slope	Bank Height Ratio approximately 1.0	2
	2 Mass Wasting	No evidence of past or future mass wasting.	3
	3 Debris Jam Potential	Essential absent from immediate channel area.	2
	4 Vegetative Bank Protection	90%+ plant density. Vigor and variety suggest a deep dense soil binding root mass.	3
LOWER BANKS	5 Channel Capacity	Ample for present plus some increases. Peak flows contained. W/D ratio < 7.	1
	6 Bank Rock Content	65%+ with large angular boulders. 12" + common.	2
	7 Obstructions to Flow	Rocks and logs firmly imbedded. Flow pattern without cutting or deposition.	2
	8 Cutting	Little or none. Infreq. Raw banks less than 6".	4
BOTTOM	9 Deposition	Little or no enlargement of channel or point bars.	4
	10 Rock Angularity	Sharp edges and corners. Plane surfaces rough.	1
	11 Water Brightness	Surface dull, dark or stained. Generally not bright.	1
	12 Consolidation of Particles	Assorted sizes tightly packed or overlapping.	2
	13 Bottom Size Distribution	No size change evident. Stable material 80-100%	4
	14 Scouring and Deposition	<5% of bottom affected by scour or deposition.	6
	15 Aquatic Vegetation	Abundant Growth moss-like, dark green perennial. In swift water too.	1
SUM			0
Category	GOOD		Score
UPPER BANKS	1 Landform Slope	Bank Height Ratio approximately 1.1	4
	2 Mass Wasting	Infrequent. Mostly healed over. Low future potential.	6
	3 Debris Jam Potential	Present, but mostly small twigs and limbs.	4
	4 Vegetative Bank Protection	70-90% density. Fewer species or less vigor suggest less dense or deep root mass.	6
LOWER BANKS	5 Channel Capacity	Adequate, Bank overflows rare. W/D ratio 8-15	2
	6 Bank Rock Content	40-65%. Mostly small boulders to cobbles 6-12"	4
	7 Obstructions to Flow	Some present causing erosive cross currents and minor pool filling. Obstr. newer and less firm.	4
	8 Cutting	Some, intermittently at outcurves and constrictions. Raw banks may be up to 12"	6
BOTTOM	9 Deposition	Some new bar increase, mostly from coarse gravel.	8
	10 Rock Angularity	Rounded corners and edges, surfaces smooth, flat.	2
	11 Water Brightness	Mostly dull, but may have < 35% bright surfaces.	2
	12 Consolidation of Particles	Moderately packed with some overlapping.	4
	13 Bottom Size Distribution	Distribution shift light. Stable material 50-80%	8
	14 Scouring and Deposition	5-30% affected. Scour at constrictions and where grades steepen. Some deposition in pools.	12
	15 Aquatic Vegetation	Common. Algae forms in low velocity and pool areas. Moss here too.	2
SUM			6
Category	FAIR		Score
UPPER BANKS	1 Landform Slope	Bank Height Ratio approximately 1.45	6
	2 Mass Wasting	Frequent or large, causing sediment nearly year long.	9
	3 Debris Jam Potential	Moderate to heavy amounts, mostly larger sizes.	6
	4 Vegetative Bank Protection	<50-70% density. Lower vigor and fewer species from a shallow, discontinuous root mass.	9
LOWER BANKS	5 Channel Capacity	Barely contains present peaks. Occasional overbank floods. W/D ratio 15 to 25.	3
	6 Bank Rock Content	20-40% with most in the 3-6" diameter class.	6
	7 Obstructions to Flow	Moderately frequent, unstable obstructions move with high flows causing bank cutting and pool filling.	6
	8 Cutting	Significant. Cuts 12-24" high. Root mat overhangs and sloughing evident.	12
BOTTOM	9 Deposition	Moderate deposition of new gravel and coarse sand on old and some new bars.	12
	10 Rock Angularity	Corners and edges well rounded in two dimensions.	3
	11 Water Brightness	Mixture dull and bright, i.e. 35-65% mixture range.	3
	12 Consolidation of Particles	Mostly loose assortment with no apparent overlap.	6
	13 Bottom Size Distribution	Moderate change in sizes. Stable materials 20-50%.	12
	14 Scouring and Deposition	30-50% affected. Deposits and scour at obstructions, constrictions, and bends. Some filling of pools.	18
	15 Aquatic Vegetation	Present but spotty, mostly in backwater. Seasonal algae growth makes rocks slick.	3
SUM			63
Category	POOR		Score
UPPER BANKS	1 Landform Slope	Bank Height Ratio approximately 1.63	8
	2 Mass Wasting	Frequent or large causing sediment nearly year long or imminent danger of same.	12
	3 Debris Jam Potential	Moderate to heavy amounts, predominantly larger sizes.	8
	4 Vegetative Bank Protection	<50% density, fewer species and less vigor indicate poor, discontinuous and shallow root mass.	12
LOWER BANKS	5 Channel Capacity	Inadequate. Overbank flows common. W/D ratio > 25.	4
	6 Bank Rock Content	<20% rock fragments of gravel sizes, 1-3" or less.	8
	7 Obstructions to Flow	Sediment traps full, channel migration occurring.	8
	8 Cutting	Almost continuous cuts, some over 24" high. Failure of overhangs frequent.	16
BOTTOM	9 Deposition	Extensive deposits of predominantly fine particles. Accelerated bar development.	16
	10 Rock Angularity	Well rounded in all dimensions, surfaces smooth.	4
	11 Water Brightness	Predominantly bright, 65%+ exposed or scoured surface.	4
	12 Consolidation of Particles	No packing evident. Loose assortment easily moved.	8
	13 Bottom Size Distribution	Marked distribution change. Stable materials 0-20%.	16
	14 Scouring and Deposition	More than 50% of the bottom in a state of flux or change nearly year long.	24
	15 Aquatic Vegetation	Perennial types scarce or absent. Yellow-green, short term bloom may be present.	4
SUM			48
TOTAL			117

Table 4.30b. Pfankuch Channel Stability Evaluation for Clarendon (RM 100.38).

PFANKUCH'S CHANNEL STABILITY EVALUATION							
Stream Width	524.71 ft	X avg. depth	26.59 ft	X mean velocity	1.95 ft/s	Reach Gradient	0.00006
Stream Order	7th	Sinuosity	2.17	Widthfp	16000 ft	Depthbkf	27.15 ft
W/D Ratio	24.18	Discharge	22443 cfs	Drainage Area	1357.95 Sq.mi.	Belt Width	17929 ft
Stream Length	10325 ft	Entrenchment Ratio	30.16	Meander Length	4855.14 ft	Mobility Index	156 - 191.7

Sediment Supply Extreme _____ Very High _____ High <input checked="" type="checkbox"/> Moderate _____ Low _____	Width/Depth Ratio Condition Normal _____ High <input checked="" type="checkbox"/> FAIR Very High _____ TOTAL SCORE E 0 + G 6 + F 63 + P 48 =	Stream Type <div style="border: 1px solid black; padding: 2px; text-align: center;">C5C-/C6C-</div> Pfankuch Rating <div style="border: 1px solid black; padding: 2px; text-align: center;">117</div> Reach Condition <div style="border: 1px solid black; padding: 2px; text-align: center;">POOR</div>
---	---	---

Remarks High sediment supply originating from the Cache River and upstream reaches as well as bank erosion.

HJULSTROM CURVE

Velocity (cm/sec)

Size (mm)

Erosion

Transportation

Sedimentation

Fall velocity

Erosion velocity

Remarks The diagram indicates velocities adequate for erosion and transportation of D50 materials. The banks are highly erodible and may contribute to high sediment supply. A relatively high width/depth ratio could contribute to a sharp reduction in the channel's ability to transport sediment. An increase in width/depth ratio would result in accelerated bank erosion and sediment feed, which can cause aggradation and lateral extension of the channel within its valley. The overall channel condition is poor, and the Pfankuch rating greater than 111 indicates a departure to channel instability.

Table 4.31a. Modified Pfankuch Channel Stability Evaluation for St. Charles (RM 56.57).

PFANKUCH'S CHANNEL STABILITY EVALUATION			
Reach Location	ST. CHARLES (RM 56.57)	Date	9/12/2010
Stream Type	C5C-	Observers	Linh & Vince
Category	EXCELLENT		Score
UPPER BANKS	1 Landform Slope	Bank Height Ratio approximately 1.0	2
	2 Mass Wasting	No evidence of past or future mass wasting.	3
	3 Debris Jam Potential	Essential absent from immediate channel area.	2
	4 Vegetative Bank Protection	90%+ plant density. Vigor and variety suggest a deep dense soil binding root mass.	3
LOWER BANKS	5 Channel Capacity	Ample for present plus some increases. Peak flows contained. W/D ratio < 7.	1
	6 Bank Rock Content	65%+ with large angular boulders. 12" + common.	2
	7 Obstructions to Flow	Rocks and logs firmly imbedded. Flow pattern without cutting or deposition.	2
	8 Cutting	Little or none. Infreq. Raw banks less than 6".	4
BOTTOM	9 Deposition	Little or no enlargement of channel or point bars.	4
	10 Rock Angularity	Sharp edges and corners. Plane surfaces rough.	1
	11 Water Brightness	Surface dull, dark or stained. Generally not bright.	1
	12 Consolidation of Particles	Assorted sizes tightly packed or overlapping.	2
	13 Bottom Size Distribution	No size change evident. Stable material 80-100%	4
	14 Scouring and Deposition	<5% of bottom affected by scour or deposition.	6
	15 Aquatic Vegetation	Abundant Growth moss-like, dark green perennial. In swift water too.	1
SUM			0
Category	GOOD		Score
UPPER BANKS	1 Landform Slope	Bank Height Ratio approximately 1.1	4
	2 Mass Wasting	Infrequent. Mostly healed over. Low future potential.	6
	3 Debris Jam Potential	Present, but mostly small twigs and limbs.	4
	4 Vegetative Bank Protection	70-90% density. Fewer species or less vigor suggest less dense or deep root mass.	6
LOWER BANKS	5 Channel Capacity	Adequate, Bank overflows rare. W/D ratio 8-15	2
	6 Bank Rock Content	40-65%. Mostly small boulders to cobbles 6-12"	4
	7 Obstructions to Flow	Some present causing erosive cross currents and minor pool filling. Obstr. newer and less firm.	4
	8 Cutting	Some, intermittently at outcures and constrictions. Raw banks may be up to 12"	6
BOTTOM	9 Deposition	Some new bar increase, mostly from coarse gravel.	8
	10 Rock Angularity	Rounded corners and edges, surfaces smooth, flat.	2
	11 Water Brightness	Mostly dull, but may have < 35% bright surfaces.	2
	12 Consolidation of Particles	Moderately packed with some overlapping.	4
	13 Bottom Size Distribution	Distribution shift light. Stable material 50-80%	8
	14 Scouring and Deposition	5-30% affected. Scour at constrictions and where grades steepen. Some deposition in pools.	12
	15 Aquatic Vegetation	Common. Algae forms in low velocity and pool areas. Moss here too.	2
SUM			10
Category	FAIR		Score
UPPER BANKS	1 Landform Slope	Bank Height Ratio approximately 1.45	6
	2 Mass Wasting	Frequent or large, causing sediment nearly year long.	9
	3 Debris Jam Potential	Moderate to heavy amounts, mostly larger sizes.	6
	4 Vegetative Bank Protection	<50-70% density. Lower vigor and fewer species from a shallow, discontinuous root mass.	9
LOWER BANKS	5 Channel Capacity	Barely contains present peaks. Occasional overbank floods. W/D ratio 15 to 25.	3
	6 Bank Rock Content	20-40% with most in the 3-6" diameter class.	6
	7 Obstructions to Flow	Moderately frequent, unstable obstructions move with high flows causing bank cutting and pool filling.	6
	8 Cutting	Significant. Cuts 12-24" high. Root mat overhangs and sloughing evident.	12
BOTTOM	9 Deposition	Moderate deposition of new gravel and coarse sand on old and some new bars.	12
	10 Rock Angularity	Corners and edges well rounded in two dimensions.	3
	11 Water Brightness	Mixture dull and bright, i.e. 35-65% mixture range.	3
	12 Consolidation of Particles	Mostly loose assortment with no apparent overlap.	6
	13 Bottom Size Distribution	Moderate change in sizes. Stable materials 20-50%.	12
	14 Scouring and Deposition	30-50% affected. Deposits and scour at obstructions, constrictions, and bends. Some filling of pools.	18
	15 Aquatic Vegetation	Present but spotty, mostly in backwater. Seasonal algae growth makes rocks slick.	3
SUM			78
Category	POOR		Score
UPPER BANKS	1 Landform Slope	Bank Height Ratio approximately 1.63	8
	2 Mass Wasting	Frequent or large causing sediment supply nearly year long or imminent danger of same.	12
	3 Debris Jam Potential	Moderate to heavy amounts, predominantly larger sizes.	8
	4 Vegetative Bank Protection	<50% density, fewer species and less vigor indicate poor, discontinuous and shallow root mass.	12
LOWER BANKS	5 Channel Capacity	Inadequate. Overbank flows common. W/D ratio > 25.	4
	6 Bank Rock Content	<20% rock fragments of gravel sizes, 1-3" or less.	8
	7 Obstructions to Flow	Sediment traps full, channel migration occurring.	8
	8 Cutting	Almost continuous cuts, some over 24" high. Failure of overhangs frequent.	16
BOTTOM	9 Deposition	Extensive deposits of predominantly fine particles. Accelerated bar development.	16
	10 Rock Angularity	Well rounded in all dimensions, surfaces smooth.	4
	11 Water Brightness	Predominantly bright, 65%+ exposed or scoured surface.	4
	12 Consolidation of Particles	No packing evident. Loose assortment easily moved.	8
	13 Bottom Size Distribution	Marked distribution change. Stable materials 0-20%.	16
	14 Scouring and Deposition	More than 50% of the bottom in a state of flux or change nearly year long.	24
	15 Aquatic Vegetation	Perennial types scarce or absent. Yellow-green, short term bloom may be present.	4
SUM			20
TOTAL			108

Table 4.31b. Modified Pfankuch Channel Stability Evaluation for St. Charles (RM 56.57).

PFANKUCH'S CHANNEL STABILITY EVALUATION							
Stream Width	558.75 ft	X avg. depth	22.66 ft	X mean velocity	2.02 ft/s	Reach Gradient	0.00006
Stream Order	7th	Sinuosity	1.09	Width:dp	21500 ft	Depth:bkf	24.45 ft
W/D Ratio	29.84	Discharge	21045 cfs	Drainage Area	1684.85 Sq. mi.	Belt Width	16775 ft
Stream Length	10727 ft	Entrenchment Ratio	38.60	Meander Length	7580 ft	Mobility Index	177.90
<div style="display: flex; justify-content: space-between;"> <div style="width: 45%;"> <p>Sediment Supply</p> <p>Extreme _____</p> <p>Very High _____</p> <p>High _____</p> <p>Moderate <input checked="" type="checkbox"/></p> <p>Low _____</p> </div> <div style="width: 45%;"> <p>Width/Depth Ratio Condition</p> <p>Normal _____</p> <p>High _____</p> <p>Very High <input checked="" type="checkbox"/> POOR</p> <p>TOTAL SCORE $E_0 + G_{10} + F_{78} + P_{20} =$</p> </div> </div> <div style="display: flex; justify-content: space-between; margin-top: 10px;"> <div style="width: 60%;"> <p>Remarks Moderate sediment supply and moderate bank stability.</p> </div> <div style="width: 35%; text-align: center;"> <p>from table</p> </div> </div>							
				C5C-	Stream Type		
				108	Pfankuch Rating		
				FAIR	Reach Condition		

HJULSTROM CURVE

The Hjulstrom Curve graph plots Velocity (cm/sec) on the y-axis (log scale from 0.1 to 1000) against Size (mm) on the x-axis (log scale from 0.001 to 1000). The graph is divided into three regions: Erosion (top), Transportation (middle), and Sedimentation (bottom). A shaded band represents the 'Erosion velocity' range, and a solid line represents the 'Fall velocity' line. Two red stars mark the intersection of the erosion velocity band and the fall velocity line at approximately 0.1 mm size and 30 cm/sec velocity.

Remarks The diagram indicates velocities adequate for erosion and transportation of D50 materials. The banks are moderately erodible and may contribute to moderate sediment supply. A very high width/depth ratio suggests susceptibility to changes in sediment feed, which can accelerate bank erosion resulting in migration of the channel. The overall channel condition is fair with a high Mobility Index or erosive power suggesting an onset of channel departure to instability.

Table 4.32. Bank Erosion Potential for Batesville (RM 299.00).

BANK EROSION HAZARD INDEX FORM

STREAM: WHITE RIVER	REACH: BATESVILLE, AR	CROSS SECTION: 299.00
	DATE: 9/15/2010	CREW: LINH & VINCE

BANK EROSION HAZARD INDEX

BANK EROSION POTENTIAL

		V. Low	Low	Mod.	High	V. High	Extr.
Bank Ht./ Bkt Ht.	Value	1-1.1	1.1-1.2	1.2-1.5	1.6-2	2.1-2.8	>2.8
	Index	1-1.9	2-3.9	4-5.9	6-7.9	8-9	10
Rt. Depth/ Bank Ht.	Value	1-.9	.89-.5	.49-.3	.29-.15	.14-.05	<.05
	Index	1-1.9	2-3.9	4-5.9	6-7.9	8-9	10
Rt. Density (%)	Value	80-100	55-79	30-54	15-29	5-14	<5.0
	Index	1-1.9	2-3.9	4-5.9	6-7.9	8-9	10
Bk. Angle (deg)	Value	0-20	21-60	61-80	81-90	91-119	>119
	Index	1-1.9	2-3.9	4-5.9	6-7.9	8-9	10
Surface Prot.(%)	Value	80-100	55-79	30-54	15-29	10-15	<10
	Index	1-1.9	2-3.9	4-5.9	6-7.9	8-9	10

ERODIBILITY VARIABLE

Bank Materials

Bedrock (Bedrock banks have very low bank erosion potential)
 Boulders (Banks composed of boulders have low bank erosion potential)
 Cobble (Subtract 10 points. If sand/gravel matrix greater than 50% of bank material, then do not adjust.
 Gravel (Add 5-10 points depending on percentage of bank material that is composed of sand)
 Sand (Add 10 points)
 Silt/Clay (No adjustment)

Stratification

Add 5-10 points depending on position of unstable layers in relation to bankfull stage.

Total Score	<i>Very Low</i>	<i>Low</i>	<i>Moderate</i>	<i>High</i>	<i>Very High</i>	<i>Extreme</i>
5-9.5	10-19.5	20-29.5	30-39.5	40-45	46-50	

Erodibility Variable/Value	Index	Bank Erosion Potential
<i>Bank Height/Bankfull Height</i>		
Bank Height (ft) A	3.9	Low
Bankfull Height (ft) B		
A/B		
<i>Root Depth/Bank Height</i>		
Root Depth (ft) C	7.9	High
C/A		
2 - 5		
<i>Root Density</i>		
Root Density (%) D	4	Mod.
30		
<i>Bank Angle</i>		
Bank Angle (degrees)	3.9	Low
39		
<i>Surface Protection</i>		
Surface Protection (%)	3.9	Low
mid 70s		
<i>Materials: Upper-sandy loam. Lower-gravel with sand matrix</i>		
0		
<i>Stratification: Boundary between sandy loam and gravel</i>		
5.0		
TOTAL SCORE:	28.6	Moderate

Table 4.33. Bank Erosion Potential for Newport (RM 258.94).

BANK EROSION HAZARD INDEX FORM				
STREAM: WHITE RIVER	REACH: NEWPORT, AR	CROSS SECTION: 258.94	DATE: 8/27/2010	CREW: LINH & VIRAK

BANK EROSION HAZARD INDEX							
BANK EROSION POTENTIAL							
Bank Ht./Bkf Ht.	Value Index	V. Low 1-1.1 1-1.9	Low 1.1-1.2 2-3.9	Mod. 1.2-1.5 4-5.9	High 1.6-2 6-7.9	V. High 2.1-2.8 8-9	Extr. >2.8 10
Rt. Depth/Bank Ht.	Value Index	1-1.9 1-1.9	.89-.5 2.3-3.9	.49-.3 4-5.9	.29-.15 6-7.9	.14-.05 8-9	<.05 10
Rt. Density (%)	Value Index	80-100 1-1.9	55-79 2-3.9	30-54 4-5.9	15-29 6-7.9	5-14 8-9	<5.0 10
Bk. Angle (deg)	Value Index	0-20 1-1.9	21-60 2-3.9	61-80 4-5.9	81-90 6-7.9	91-119 8-9	>119 10
Surface Prot. (%)	Value Index	80-100 1-1.9	55-79 2-3.9	30-54 4-5.9	15-29 6-7.9	10-15 8-9	<10 10

Erodibility Variable/Value	Index	Bank Erosion Potential
Bank Height/Bankfull Height Bank Height (ft) A Bankfull Height (ft) B A/B 29.87 / 28.34 = 1.05	1.5	V. Low
Root Depth/Bank Height Root Depth (ft) C Bank Height (ft) A C/A 2 - 5 / 0.06 - 0.17 = 9	9	V. High
Root Density Root Density (%) D 30	4	Mod.
Bank Angle Bank Angle (degrees) 39	3.9	Low
Surface Protection Surface Protection (%) mid 70s	3.9	Low
Materials: Upper-sandy loam. Lower-gravel with sand matrix	0	
Stratification: Boundary between sandy loam and gravel	7.5	
TOTAL SCORE:	30.2	High

Bank Materials

Bedrock (Bedrock banks have very low bank erosion potential)

Boulders (Banks composed of boulders have low bank erosion potential)

Cobble (Subtract 10 points. If sand/gravel matrix greater than 50% of bank material, then do not adjust.)

Gravel (Add 5-10 points depending on percentage of bank material that is composed of sand)

Sand (Add 10 points)

Silt/Clay (No adjustment)

Stratification

Add 5-10 points depending on position of unstable layers in relation to bankfull stage.

Total Score	Very Low	Low	Moderate	High	Very High	Extreme
5-9.5	10-19.5	20-29.5	30-39.5	40-45	46-50	

BANK EROSION HAZARD INDEX FORM

REACH: AUGUSTA, AR

CROSS SECTION: 200.30

DATE: 9/04/2010

CREW: LINH & VIRAK

Stream: WHITE RIVER

Bank Erosion Hazard Index

Bank Erosion Potential

Erodibility Variable/Value

Index

Bank Erosion Potential

Bank Height/Bankfull Height

Bank Height (ft) A

Bankfull Height (ft) B

A/B

32.77 / 31.36 = 1.05

Root Depth/Bank Height

Root Depth (ft) C

C/A

4.6 / 0.18 = 25.56

Root Density

Root Density (%) D

30 - 50

Bank Angle

Bank Angle (degrees)

62

Surface Protection

Surface Protection (%)

90+

1.5

7.9

5.9

5.9

1.0

0

5

27.6

V. Low

High

Mod.

Mod.

V. Low

Materials: Upper-sandy loam.
Lower-gravel with sand matrix

Stratification: Boundary between sandy loam and gravel

TOTAL SCORE:

Moderate

Bank Height/Bankfull Height

Bank Height (ft) A

Bankfull Height (ft) B

A/B

32.77 / 31.36 = 1.05

Root Depth/Bank Height

Root Depth (ft) C

C/A

4.6 / 0.18 = 25.56

Root Density

Root Density (%) D

30 - 50

Bank Angle

Bank Angle (degrees)

62

Surface Protection

Surface Protection (%)

90+

1.5

7.9

5.9

5.9

1.0

0

5

27.6

V. Low

High

Mod.

Mod.

V. Low

Materials: Upper-sandy loam.
Lower-gravel with sand matrix

Stratification: Boundary between sandy loam and gravel

TOTAL SCORE:

Moderate

Table 4.35. Bank Erosion Potential for Des Arc (RM 148.03).

<h2 style="margin: 0;">BANK EROSION HAZARD INDEX FORM</h2>				
STREAM: WHITE RIVER	REACH: DES ARC, AR	CROSS SECTION: 148.03	DATE: 9/01/2010	CREW: LINH & VIRAK
BANK EROSION HAZARD INDEX				
BANK EROSION POTENTIAL				
ERODIBILITY VARIABLE				
Bank Ht./Bkf Ht.	Value	Index	V. Low	Low
			1-1.1	1.1-1.2
			1-1.9	2-3.9
			1-1.9	.89-.5
			1-1.9	2.3-3.9
			1-1.9	.49-.3
			1-1.9	4-5.9
			1-1.9	6-7.9
			1-1.9	8-9
			1-1.9	10-15
			1-1.9	15-29
			1-1.9	30-54
			1-1.9	6-7.9
			1-1.9	8-9
			1-1.9	10-15
			1-1.9	15-29
			1-1.9	30-54
			1-1.9	6-7.9
			1-1.9	8-9
			1-1.9	10-15
			1-1.9	15-29
			1-1.9	30-54
			1-1.9	6-7.9
			1-1.9	8-9
			1-1.9	10-15
			1-1.9	15-29
			1-1.9	30-54
			1-1.9	6-7.9
			1-1.9	8-9
			1-1.9	10-15
			1-1.9	15-29
			1-1.9	30-54
			1-1.9	6-7.9
			1-1.9	8-9
			1-1.9	10-15
			1-1.9	15-29
			1-1.9	30-54
			1-1.9	6-7.9
			1-1.9	8-9
			1-1.9	10-15
			1-1.9	15-29
			1-1.9	30-54
			1-1.9	6-7.9
			1-1.9	8-9
			1-1.9	10-15
			1-1.9	15-29
			1-1.9	30-54
			1-1.9	6-7.9
			1-1.9	8-9
			1-1.9	10-15
			1-1.9	15-29
			1-1.9	30-54
			1-1.9	6-7.9
			1-1.9	8-9
			1-1.9	10-15
			1-1.9	15-29
			1-1.9	30-54
			1-1.9	6-7.9
			1-1.9	8-9
			1-1.9	10-15
			1-1.9	15-29
			1-1.9	30-54
			1-1.9	6-7.9
			1-1.9	8-9
			1-1.9	10-15
			1-1.9	15-29
			1-1.9	30-54
			1-1.9	6-7.9
			1-1.9	8-9
			1-1.9	10-15
			1-1.9	15-29
			1-1.9	30-54
			1-1.9	6-7.9
			1-1.9	8-9
			1-1.9	10-15
			1-1.9	15-29
			1-1.9	30-54
			1-1.9	6-7.9
			1-1.9	8-9
			1-1.9	10-15
			1-1.9	15-29
			1-1.9	30-54
			1-1.9	6-7.9
			1-1.9	8-9
			1-1.9	10-15
			1-1.9	15-29
			1-1.9	30-54
			1-1.9	6-7.9
			1-1.9	8-9
			1-1.9	10-15
			1-1.9	15-29
			1-1.9	30-54
			1-1.9	6-7.9
			1-1.9	8-9
			1-1.9	10-15
			1-1.9	15-29
			1-1.9	30-54
			1-1.9	6-7.9
			1-1.9	8-9
			1-1.9	10-15
			1-1.9	15-29
			1-1.9	30-54
			1-1.9	6-7.9
			1-1.9	8-9
			1-1.9	10-15
			1-1.9	15-29
			1-1.9	30-54
			1-1.9	6-7.9
			1-1.9	8-9
			1-1.9	10-15
			1-1.9	15-29
			1-1.9	30-54
			1-1.9	6-7.9
			1-1.9	8-9
			1-1.9	10-15
			1-1.9	15-29
			1-1.9	30-54
			1-1.9	6-7.9
			1-1.9	8-9
			1-1.9	10-15
			1-1.9	15-29
			1-1.9	30-54
			1-1.9	6-7.9
			1-1.9	8-9
			1-1.9	10-15
			1-1.9	15-29
			1-1.9	30-54
			1-1.9	6-7.9
			1-1.9	8-9
			1-1.9	10-15
			1-1.9	15-29
			1-1.9	30-54
			1-1.9	6-7.9
			1-1.9	8-9
			1-1.9	10-15
			1-1.9	15-29
			1-1.9	30-54
			1-1.9	6-7.9
			1-1.9	8-9
			1-1.9	10-15
			1-1.9	15-29
			1-1.9	30-54
			1-1.9	6-7.9
			1-1.9	8-9
			1-1.9	10-15
			1-1.9	15-29
			1-1.9	30-54
			1-1.9	6-7.9
			1-1.9	8-9
			1-1.9	10-15
			1-1.9	15-29
			1-1.9	30-54
			1-1.9	6-7.9
			1-1.9	8-9
			1-1.9	10-15
			1-1.9	15-29
			1-1.9	30-54
			1-1.9	6-7.9
			1-1.9	8-9
			1-1.9	10-15
			1-1.9	15-29
			1-1.9	30-54
			1-1.9	6-7.9
			1-1.9	8-9
			1-1.9	10-15
			1-1.9	15-29
			1-1.9	30-54
			1-1.9	6-7.9
			1-1.9	8-9
			1-1.9	10-15
			1-1.9	15-29
			1-1.9	30-54
			1-1.9	6-7.9
			1-1.9	8-9
			1-1.9	10-15
			1-1.9	15-29
			1-1.9	30-54
			1-1.9	6-7.9
			1-1.9	8-9
			1-1.9	10-15
			1-1.9	15-29
			1-1.9	30-54
			1-1.9	6-7.9
			1-1.9	8-9
			1-1.9	10-15
			1-1.9	15-29
			1-1.9	30-54
			1-1.9	6-7.9
			1-1.9	8-9
			1-1.9	10-15
			1-1.9	15-29
			1-1.9	30-54
			1-1.9	6-7.9
			1-1.9	8-9
			1-1.9	10-15
			1-1.9	15-29
			1-1.9	30-54
			1-1.9	6-7.9
			1-1.9	8-9
			1-1.9	10-15
			1-1.9	15-29
			1-1.9	30-54
			1-1.9	6-7.9
			1-1.9	8-9
			1-1.9	10-15
			1-1.9	15-29
			1-1.9	30-54
			1-1.9	6-7.9
			1-1.9	8-9
			1-1.9	10-15
			1-1.9	15-29
			1-1.9	30-54
			1-1.9	6-7.9
			1-1.9	8-9
			1-1.9	10-15
			1-1.9	15-29
			1-1.9	30-54
			1-1.9	6-7.9
			1-1.9	8-9
			1-1.9	10-15
			1-1.9	15-29
			1-1.9	30-54
			1-1.9	6-7.9
			1-1.9	8-9
			1-1.9	10-15
			1-1.9	15-29
			1-1.9	30-54
			1-1.9	6-7.9
			1-1.9	8-9
			1-1.9	10-15
			1-1.9	15-29
			1-1.9	30-54
			1-1.9	6-7.9
			1-1.9	8-9
			1-1.9	10-15
			1-1.9	15-29
			1-1.9	30-54
			1-1.9	6-7.9
			1-1.9	8-9
			1-1.9	10-15
			1-1.9	15-29
			1-1.9	30-54
			1-1.9	6-7.9
			1-1.9	8-9
			1-1.9	10-15
			1-1.9	15-29
			1-1.9	30-54
			1-1.9	6-7.9
			1-1.9	8-9
			1-1.9	10-15
			1-1.9	15-29
			1-1.9	30-54
			1-1.9	6-7.9
			1-1.9	8-9
			1-1.9	10-15
			1-1.9	15-29
			1-1.9	30-54
			1-1.9	6-7.9
			1-1.9	8-9
			1-1.9	10-15
			1-1.9	15-29
			1-1.9	30-54
			1-1.9	6-7.9
			1-1.9	8-9
			1-1.9	10-15
			1-1.9	15-29
			1-1.9	30-54
			1-1.9	6-7.9
			1-1.9	8-9
			1-1.9	10-15
			1-1.9	15-29
			1-1.9	30-54
			1-1.9	6-7.9

Table 4.36. Bank Erosion Potential for Devalls Bluff (RM 124.35).

<h2 style="margin: 0;">BANK EROSION HAZARD INDEX FORM</h2>				
STREAM: WHITE RIVER	REACH: DEVALLS BLUFF, AR	CROSS SECTION: 124.35	DATE: 9/03/2010	CREW: LINH & VIRAK
BANK EROSION HAZARD INDEX				
BANK EROSION POTENTIAL				
ERODIBILITY VARIABLE				
Bank Ht./Bkf Ht.	Value	V. Low	Low	Mod.
	Index	1-1.1	1.1-1.2	1.2-1.5
Rt. Depth/Bank Ht.	Value	1-1.9	2-3.9	4-5.9
	Index	1-1.9	.89-.5	.49-.3
Rt. Density (%)	Value	80-100	55-79	30-54
	Index	1-1.9	2-3.9	4-5.9
Bk. Angle (deg)	Value	0-20	21-60	61-80
	Index	1-1.9	2-3.9	4-5.9
Surface	Value	80-100	55-79	30-54
	Index	1-1.9	2-3.9	4-5.9
Prot. (%)	Value	0-20	21-60	61-80
	Index	1-1.9	2-3.9	4-5.9
Bank Materials				
Bedrock (Bedrock banks have very low bank erosion potential)				
Boulders (Banks composed of boulders have low bank erosion potential)				
Cobble (Subtract 10 points. If sand/gravel matrix greater than 50% of bank material, then do not adjust.)				
Gravel (Add 5-10 points depending on percentage of bank material that is composed of sand)				
Sand (Add 10 points)				
Silt/Clay (No adjustment)				
Stratification				
Add 5-10 points depending on position of unstable layers in relation to bankfull stage.				
Total Score				
Very Low	Low	Moderate	High	Extreme
5-9.5	10-19.5	20-29.5	30-39.5	40-45
TOTAL SCORE:				
34.1				

Erodibility Variable/Value	Index	Bank Erosion Potential
Bank Height/Bankfull Height		
Bank Height (ft) A		
Bankfull Height (ft) B		
A/B	1.0	V. Low
35.81 / 35.7		
Root Depth/Bank Height		
Root Depth (ft) C		
C/A	7.9	High
4 - 6 / 0.11 - 0.17		
Root Density		
Root Density (%) D		
20 - 30	7.9	High
Bank Angle		
Bank Angle (degrees)		
22	3.9	Low
Surface Protection		
Surface Protection (%)		
appr. 50+	5.9	Mod.
Materials: Upper-sandy loam. Lower-gravel with sand matrix		
Stratification: Boundary between sandy loam and gravel	0	
	7.5	
TOTAL SCORE:		
34.1		

Table 4.37. Bank Erosion Potential for Clarendon (RM 100.38).

BANK EROSION HAZARD INDEX FORM				
STREAM: WHITE RIVER	REACH: CLARENDON, AR	CROSS SECTION: 100.38	DATE: 9/02/2010	CREW: LINH & VIRAK

BANK EROSION HAZARD INDEX									
BANK EROSION POTENTIAL									
Bank Ht./Bkf Ht.	Value Index	V. Low 1-1.1	Low 1.1-1.2	Mod. 1.2-1.5	High 1.6-2	V. High 2.1-2.8	Extr. >2.8		
Rt. Depth/Bank Ht.	Value Index	1-1.9	2-3.9	4-5.9	6-7.9	8-9	10		
Rt. Density (%)	Value Index	1-1.9	2-3.9	4-5.9	6-7.9	8-9	10		
Bk. Angle (deg)	Value Index	1-1.9	2-3.9	4-5.9	6-7.9	8-9	10		
Surface Prot. (%)	Value Index	1-1.9	2-3.9	4-5.9	6-7.9	8-9	10		

ERODIBILITY VARIABLE	
Bank Materials Bedrock (Bedrock banks have very low bank erosion potential) Boulders (Banks composed of boulders have low bank erosion potential) Cobble (Subtract 10 points. If sand/gravel matrix greater than 50% of bank material, then do not adjust.) Gravel (Add 5-10 points depending on percentage of bank material that is composed of sand) Sand (Add 10 points) Silt/Clay (No adjustment)	

Stratification	
Add 5-10 points depending on position of unstable layers in relation to bankfull stage.	

Total Score	
Very Low 5-9.5	Low 10-19.5
	Moderate 20-29.5
	High 30-39.5
	Very High 40-45
	Extreme 46-50

Erodibility Variable/Value	Index	Bank Erosion Potential
Bank Height/Bankfull Height		
Bank Height (ft) A/B	6	High
44.38 / 27.23	1.63	
Root Depth/Bank Height		
Root Depth (ft) C/A	9	V. High
4 / 0.09		
Root Density		
Root Density (%) D	7.9	High
10 - 20		
Bank Angle		
Bank Angle (degrees)	5.9	Mod.
70		
Surface Protection		
Surface Protection (%) mid 70s	3.9	Low
Materials: Upper-sandy loam. Lower-gravel with sand matrix		
Stratification: Boundary between sandy loam and gravel	0	
7.5		
TOTAL SCORE:	40.2	Very High

Table 4.38. Bank Erosion Potential for St. Charles (RM 56.57).

BANK EROSION HAZARD INDEX FORM			
STREAM: WHITE RIVER	REACH: ST. CHARLES, AR	CROSS SECTION: 56.57	DATE: 9/12/2010 CREW: LINH & VINCE

BANK EROSION HAZARD INDEX									
BANK EROSION POTENTIAL									
Bank Ht./Bkf Ht.	Value	Index	V. Low	Low	Mod.	High	V. High	Extr.	
			1-1.1	1.1-1.2	1.2-1.5	1.6-2	2.1-2.8	>2.8	
Rt. Depth/Bank Ht.	Value	Index	1-1.9	2-3.9	4-5.9	6-7.9	8-9	10	
			1-1.9	.89-.5	.49-.3	.29-.15	.14-.05	<.05	
Rt. Density (%)	Value	Index	1-1.9	2-3-3.9	4-5.9	6-7.9	8-9	10	
			80-100	55-79	30-54	15-29	5-14	<5.0	
Bk. Angle (deg)	Value	Index	1-1.9	2-3.9	4-5.9	6-7.9	8-9	10	
			0-20	21-60	61-80	81-90	91-119	>119	
Surface Prot. (%)	Value	Index	1-1.9	2-3.9	4-5.9	6-7.9	8-9	10	
			80-100	55-79	30-54	15-29	10-15	<10	
	Value	Index	1-1.9	2-3.9	4-5.9	6-7.9	8-9	10	

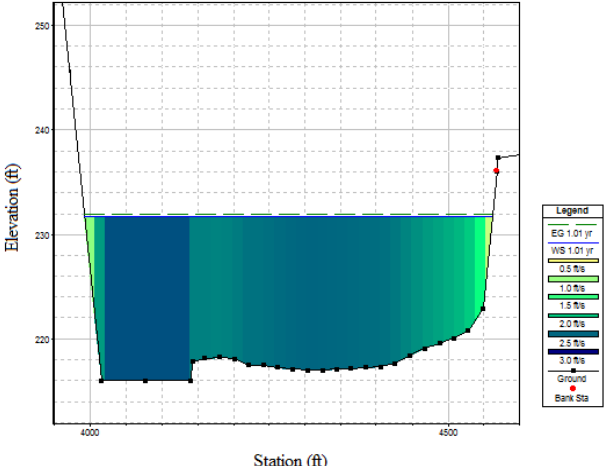
ERODIBILITY VARIABLE	
Bank Materials	Bedrock (Bedrock banks have very low bank erosion potential)
	Boulders (Banks composed of boulders have low bank erosion potential)
	Cobble (Subtract 10 points. If sand/gravel matrix greater than 50% of bank material, then do not adjust.)
	Gravel (Add 5-10 points depending on percentage of bank material that is composed of sand)
	Sand (Add 10 points)
	Silt/Clay (No adjustment)

Stratification	
Add 5-10 points depending on position of unstable layers in relation to bankfull stage.	

Total Score	
Very Low	Extreme
5-9.5	46-50
10-19.5	40-45
20-29.5	30-39.5
30-39.5	High
40-45	Very High
46-50	Extreme

Erodibility Variable/Value	Index	Bank Erosion Potential
Bank Height/Bankfull Height		
Bank Height (ft) A		
Bankfull Height (ft) B		
A/B	3.9	Low
1.19		
Root Depth/Bank Height		
Root Depth (ft) C		
C/A	6.0	High
10.15 - 0.19		
Root Density		
Root Density (%) D		
5.9		Mod.
30 - 40		
Bank Angle		
Bank Angle (degrees)		
3.9		Low
31		
Surface Protection		
Surface Protection (%)		
3.9		Low
mid 70s		
Materials: Upper-sandy loam. Lower-gravel with sand matrix		
0		
Stratification: Boundary between sandy loam and gravel		
5.0		
TOTAL SCORE:		Moderate
		28.6

Table 4.39. Near Bank Stress Rating for Batesville (RM 295.27).

Estimating Near-Bank Stress (NBS)									
Stream: WHITE RIVER		Location: BATESVILLE (RM 295.27)			Date: 9/15/2010				
Crew: Linh & Vince									
Methods for Estimating Near-Bank Stress									
(1) Transverse bar or split channel/central bar creating NBS/high velocity gradient: Level I - Reconnaissance.									
(2) Channel pattern (R_c/W): Level II - General Prediction.									
(3) Ratio of pool slope to average water surface slope (S_p/S): Level II - General Prediction.									
(4) Ratio of pool slope to riffle slope (S_p/S_{rif}): Level II - General Prediction.									
(5) Ratio of near-bank maximum depth to bankfull mean depth (d_{nb}/d_{bkf}): Level III - Detailed Prediction.									
(6) Ratio of near-bank area to bankfull area (a_{nb}/a_{bkf}): Level III - Detailed Prediction/Level IV - Validation.									
(7) Velocity profiles/Isovels/Velocity gradient: Level IV - Validation.									
Transverse and/or central bars - short and/or discontinuous. NBS = High/Very High									
(1) Extensive deposition (continuous, cross channel). NBS = Extreme									
Chute cutoffs, down-valley meander migration, converging flow (Figure X). NBS = Extreme									
(2)	Radius of Curvature R_c (feet)	Bankfull Width W_{bkf} (feet)	Ratio R_c/W	<div>VELOCITY DISTRIBUTION River Cross-Section 295.27</div> 					
(3)	Pool Slope S_p	Average Slope S	Ratio S_p/S						
(4)	Pool Slope S_p	Riffle Slope S_{rif}	Ratio S_p/S_{rif}						
(5)	Near-Bank Max Depth d_{nb} (feet)	Mean Depth d (feet)	Ratio d_{nb}/d						
(6)	Near-Bank Area A_{nb} (feet)	Bankfull Area A_{bkf} (feet)	Ratio A_{nb}/A_{bkf}						
	2829.00	7781.81	0.36						
(7)	Velocity Gradient (ft/s/ft)						Note: The stream width was divided into thirds to apportion the shear stress in the near-bank (one third width) and compared to the bankfull stress of the entire channel.		

Converting Values to a Near-Bank Stress Rating							
Near-Bank Stress Rating	Method Number						
	(1)	(2)	(3)	(4)	(5)	(6)	(7)
Very Low	N/A	>3.0	< 0.20	< 0.4	<1.0	N/A	<1.0
Low		2.21 - 3.0	0.20 - 0.40	0.41 - 0.60	1.0 - 1.5	< 0.33	1.0 - 1.2
Moderate		2.01 - 2.2	0.41 - 0.60	0.61 - 0.80	1.51 - 1.8	0.33 - 0.41	1.21 - 1.6
High	See (1) Above	1.81 - 2.0	0.61 - 0.80	0.81 - 1.0	1.81 - 2.5	0.42 - 0.45	1.61 - 2.0
Very High		1.5 - 1.8	0.81 - 1.0	1.01 - 1.2	2.51 - 3.0	0.46 - 0.50	2.01 - 2.3
Extreme		< 1.5	> 1.0	> 1.2	> 3.0	> 0.50	> 2.3

	Overall Near-Bank Stress Rating
	MODERATE

Table 4.40. Near Bank Stress Rating for Newport (RM 258.94).

Estimating Near-Bank Stress (NBS)											
Stream: WHITE RIVER		Location: NEWPORT (RM 258.94)			Date: 8/27/2010		Crew: Linh & Virak				
Methods for Estimating Near-Bank Stress											
(1) Transverse bar or split channel/central bar creating NBS/high velocity gradient: Level I - Reconnaissance. (2) Channel pattern (R_c/W): Level II - General Prediction. (3) Ratio of pool slope to average water surface slope (S_p/S): Level II - General Prediction. (4) Ratio of pool slope to riffle slope (S_p/S_{rif}): Level II - General Prediction. (5) Ratio of near-bank maximum depth to bankfull mean depth (d_{nb}/d_{bkf}): Level III - Detailed Prediction. (6) Ratio of near-bank area to bankfull area (A_{nb}/A_{bkf}): Level III - Detailed Prediction/Level IV - Validation. (7) Velocity profiles/Isovels/Velocity gradient: Level IV - Validation.											
Transverse and/or central bars - short and/or discontinuous. NBS = High/Very High (1) Extensive deposition (continuous, cross channel). NBS = Extreme Chute cutoffs, down-valley meander migration, converging flow (Figure X). NBS = Extreme											
(2)	Radius of Curvature R_c (feet)	Bankfull Width W_{bkf} (feet)	Ratio R_c/W	<div style="text-align: center;"> VELOCITY DISTRIBUTION River Cross-Section 258.94 </div>							
(3)	Pool Slope S_p	Average Slope S	Ratio S_p/S								
(4)	Pool Slope S_p	Riffle Slope S_{rif}	Ratio S_p/S_{rif}								
(5)	Near-Bank Max Depth d_{nb} (feet)	Mean Depth d (feet)	Ratio d_{nb}/d								
(6)	Near-Bank Area A_{nb} (feet)	Bankfull Area A_{bkf} (feet)	Ratio A_{nb}/A_{bkf}								
	4493.75	10506.51	0.42								
(7)	Velocity Gradient (ft/s/ft)		Note: The stream width was divided into thirds to apportion the shear stress in the near-bank (one third width) and compared to the bankfull stress of the entire channel.								
Converting Values to a Near-Bank Stress Rating											
Near-Bank Stress Rating	Method Number										
	(1)	(2)	(3)	(4)	(5)	(6)	(7)				
Very Low	N/A	> 3.0	< 0.20	< 0.4	< 1.0	N/A	< 1.0				
Low		2.21 - 3.0	0.20 - 0.40	0.41 - 0.60	1.0 - 1.5	< 0.33	1.0 - 1.2				
Moderate		2.01 - 2.2	0.41 - 0.60	0.61 - 0.80	1.51 - 1.8	0.33 - 0.41	1.21 - 1.6				
High	See (1) Above	1.81 - 2.0	0.61 - 0.80	0.81 - 1.0	1.81 - 2.5	0.42 - 0.45	1.61 - 2.0				
Very High		1.5 - 1.8	0.81 - 1.0	1.01 - 1.2	2.51 - 3.0	0.46 - 0.50	2.01 - 2.3				
Extreme		< 1.5	> 1.0	> 1.2	> 3.0	> 0.50	> 2.3				
						Overall Near-Bank Stress Rating					
						HIGH					

Table 4.41. Near Bank Stress Rating for Augusta (RM 200.30).

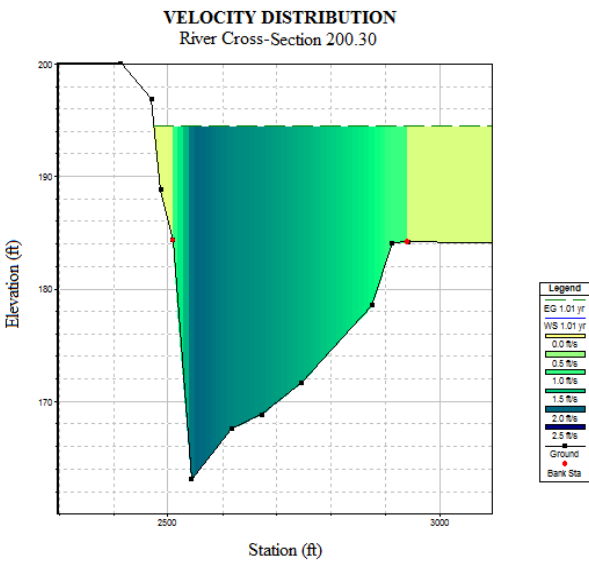
Estimating Near-Bank Stress (NBS)											
Stream: WHITE RIVER		Location: AUGUSTA (RM 200.30)			Date: 9/04/2010		Crew: Linh & Virak				
Methods for Estimating Near-Bank Stress											
(1) Transverse bar or split channel/central bar creating NBS/high velocity gradient: Level I - Reconnaissance.											
(2) Channel pattern (R_c/W): Level II - General Prediction.											
(3) Ratio of pool slope to average water surface slope (S_p/S): Level II - General Prediction.											
(4) Ratio of pool slope to riffle slope (S_p/S_{rif}): Level II - General Prediction.											
(5) Ratio of near-bank maximum depth to bankfull mean depth (d_{nb}/d_{bkf}): Level III - Detailed Prediction.											
(6) Ratio of near-bank area to bankfull area (A_{nb}/A_{bkf}): Level III - Detailed Prediction/Level IV - Validation.											
(7) Velocity profiles/Isovels/Velocity gradient: Level IV - Validation.											
(1) Transverse and/or central bars - short and/or discontinuous. NBS = High/Very High											
(1) Extensive deposition (continuous, cross channel). NBS = Extreme											
Chute cutoffs, down-valley meander migration, converging flow (Figure X). NBS = Extreme											
(2)	Radius of Curvature R_c (feet)	Bankfull Width W_{bkf} (feet)	Ratio R_c/W								
(3)	Pool Slope S_p	Average Slope S	Ratio S_p/S								
(4)	Pool Slope S_p	Riffle Slope S_{rif}	Ratio S_p/S_{rif}								
(5)	Near-Bank Max Depth d_{nb} (feet)	Mean Depth d (feet)	Ratio d_{nb}/d								
(6)	Near-Bank Area A_{nb} (feet)	Bankfull Area A_{bkf} (feet)	Ratio A_{nb}/A_{bkf}								
	3175.33	9391.05	0.34								
(7)	Velocity Gradient (ft/s/ft)		Note: The stream width was divided into thirds to apportion the shear stress in the near-bank (one third width) and compared to the bankfull stress of the entire channel.								
Converting Values to a Near-Bank Stress Rating											
Near-Bank Stress Rating		Method Number									
		(1)	(2)	(3)	(4)	(5)	(6)	(7)			
Very Low		N/A	>3.0	< 0.20	< 0.4	<1.0	N/A	<1.0			
Low			2.21 - 3.0	0.20 - 0.40	0.41 - 0.60	1.0 - 1.5	< 0.33	1.0 - 1.2			
Moderate			2.01 - 2.2	0.41 - 0.60	0.61 - 0.80	1.51 - 1.8	0.33 - 0.41	1.21 - 1.6			
High		See (1) Above	1.81 - 2.0	0.61 - 0.80	0.81 - 1.0	1.81 - 2.5	0.42 - 0.45	1.61 - 2.0			
Very High			1.5 - 1.8	0.81 - 1.0	1.01 - 1.2	2.51 - 3.0	0.46 - 0.50	2.01 - 2.3			
Extreme			< 1.5	> 1.0	> 1.2	> 3.0	> 0.50	> 2.3			
						Overall Near-Bank Stress Rating					
						MODERATE					

Table 4.42. Near Bank Stress Rating for Des Arc (RM 148.03).

Estimating Near-Bank Stress (NBS)

Stream: WHITE RIVER

Location: DES ARC (RM 148.03) Date: 9/01/2010

Crew: Linh & Virak

Methods for Estimating Near-Bank Stress

- (1) Transverse bar or split channel/central bar creating NBS/high velocity gradient: **Level I - Reconnaissance.**
- (2) Channel pattern (R_c/W): **Level II - General Prediction.**
- (3) Ratio of pool slope to average water surface slope (S_p/S): **Level II - General Prediction.**
- (4) Ratio of pool slope to riffle slope (S_p/S_{rif}): **Level II - General Prediction.**
- (5) Ratio of near-bank maximum depth to bankfull mean depth (d_{nb}/d_{bkf}): **Level III - Detailed Prediction.**
- (6) Ratio of near-bank area to bankfull area (a_{nb}/a_{bkf}): **Level III - Detailed Prediction/Level IV - Validation.**
- (7) Velocity profiles/Isovels/Velocity gradient: **Level IV - Validation.**

Transverse and/or central bars - short and/or discontinuous. NBS = High/Very High			
(1) Extensive deposition (continuous, cross channel). NBS = Extreme			
Chute cutoffs, down-valley meander migration, converging flow (Figure X). NBS = Extreme			
(2)	Radius of Curvature R_c (feet)	Bankfull Width W_{bkf} (feet)	Ratio R_c/W
(3)	Pool Slope S_p	Average Slope S	Ratio S_p/S
(4)	Pool Slope S_p	Riffle Slope S_{rif}	Ratio S_p/S_{rif}
(5)	Near-Bank Max Depth d_{nb} (feet)	Mean Depth d (feet)	Ratio d_{nb}/d
(6)	Near-Bank Area A_{nb} (feet)	Bankfull Area A_{bkf} (feet)	Ratio A_{nb}/A_{bkf}
	4900.00	8113.84	0.60
(7)	Velocity Gradient (ft/s/ft)		

VELOCITY DISTRIBUTION
River Cross-Section 148.03

Note: The stream width was divided into thirds to apportion the shear stress in the near-bank (one third width) and compared to the bankfull stress of the entire channel.

Converting Values to a Near-Bank Stress Rating

Near-Bank Stress Rating	Method Number						
	(1)	(2)	(3)	(4)	(5)	(6)	(7)
Very Low	N/A	>3.0	< 0.20	< 0.4	<1.0	N/A	<1.0
Low		2.21 - 3.0	0.20 - 0.40	0.41 - 0.60	1.0 - 1.5	< 0.33	1.0 - 1.2
Moderate		2.01 - 2.2	0.41 - 0.60	0.61 - 0.80	1.51 - 1.8	0.33 - 0.41	1.21 - 1.6
High	See (1) Above	1.81 - 2.0	0.61 - 0.80	0.81 - 1.0	1.81 - 2.5	0.42 - 0.45	1.61 - 2.0
Very High		1.5 - 1.8	0.81 - 1.0	1.01 - 1.2	2.51 - 3.0	0.46 - 0.50	2.01 - 2.3
Extreme		< 1.5	> 1.0	> 1.2	> 3.0	> 0.50	> 2.3

Overall Near-Bank Stress Rating

EXTREME

Table 4.43. Near Bank Stress Rating for Devalls Bluff (RM 124.35).

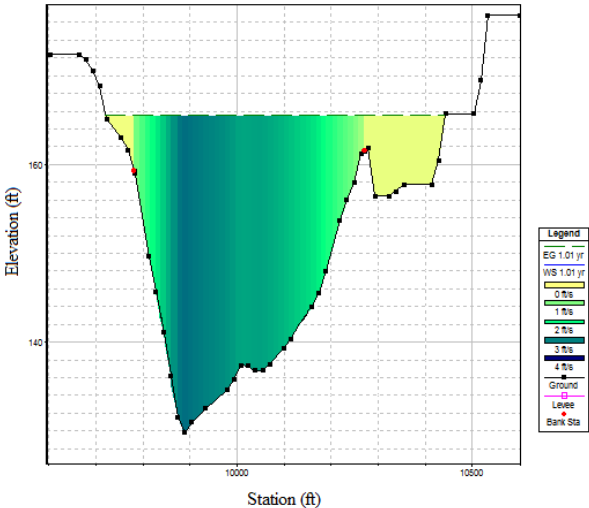
Estimating Near-Bank Stress (NBS)							
Stream: WHITE RIVER		Location: DEVALLS BLUFF (RM 124.35)		Date: 9/03/2010		Crew: Linh & Virak	
Methods for Estimating Near-Bank Stress							
(1) Transverse bar or split channel/central bar creating NBS/high velocity gradient: Level I - Reconnaissance.							
(2) Channel pattern (R_c/W): Level II - General Prediction.							
(3) Ratio of pool slope to average water surface slope (S_p/S): Level II - General Prediction.							
(4) Ratio of pool slope to riffle slope (S_p/S_{rif}): Level II - General Prediction.							
(5) Ratio of near-bank maximum depth to bankfull mean depth (d_{nb}/d_{bkf}): Level III - Detailed Prediction.							
(6) Ratio of near-bank area to bankfull area (a_{nb}/a_{bkf}): Level III - Detailed Prediction/Level IV - Validation.							
(7) Velocity profiles/Isovels/Velocity gradient: Level IV - Validation.							
Transverse and/or central bars - short and/or discontinuous. NBS = High/Very High							
(1) Extensive deposition (continuous, cross channel). NBS = Extreme							
Chute cutoffs, down-valley meander migration, converging flow (Figure X). NBS = Extreme							
(2)	Radius of Curvature R_c (feet)	Bankfull Width W_{bkf} (feet)	Ratio R_c/W				
(3)	Pool Slope S_p	Average Slope S	Ratio S_p/S				
(4)	Pool Slope S_p	Riffle Slope S_{rif}	Ratio S_p/S_{rif}				
(5)	Near-Bank Max Depth d_{nb} (feet)	Mean Depth d (feet)	Ratio d_{nb}/d				
(6)	Near-Bank Area A_{nb} (feet)	Bankfull Area A_{bkf} (feet)	Ratio A_{nb}/A_{bkf}				
	4725.00	11601.33	0.41				
(7)	Velocity Gradient (ft/s/ft)	Note: The stream width was divided into thirds to apportion the shear stress in the near-bank (one third width) and compared to the bankfull stress of the entire channel.					
Converting Values to a Near-Bank Stress Rating							
Near-Bank Stress Rating	Method Number						
	(1)	(2)	(3)	(4)	(5)	(6)	(7)
Very Low	N/A	>3.0	< 0.20	< 0.4	<1.0	N/A	<1.0
Low		2.21 - 3.0	0.20 - 0.40	0.41 - 0.60	1.0 - 1.5	< 0.33	1.0 - 1.2
Moderate	See (1) Above	2.01 - 2.2	0.41 - 0.60	0.61 - 0.80	1.51 - 1.8	0.33 - 0.41	1.21 - 1.6
High		1.81 - 2.0	0.61 - 0.80	0.81 - 1.0	1.81 - 2.5	0.42 - 0.45	1.61 - 2.0
Very High		1.5 - 1.8	0.81 - 1.0	1.01 - 1.2	2.51 - 3.0	0.46 - 0.50	2.01 - 2.3
Extreme		< 1.5	> 1.0	> 1.2	> 3.0	> 0.50	> 2.3
						Overall Near-Bank Stress Rating	
						MODERATE	

Table 4.44. Near Bank Stress Rating for Clarendon (RM 100.38).

Estimating Near-Bank Stress (NBS)							
Stream: WHITE RIVER		Location: CLARENDON(RM 100.38)			Date: 9/02/2010		Crew: Linh & Virak
Methods for Estimating Near-Bank Stress							
(1) Transverse bar or split channel/central bar creating NBS/high velocity gradient: Level I - Reconnaissance.							
(2) Channel pattern (R_c/W): Level II - General Prediction.							
(3) Ratio of pool slope to average water surface slope (S_p/S): Level II - General Prediction.							
(4) Ratio of pool slope to riffle slope (S_p/S_{rif}): Level II - General Prediction.							
(5) Ratio of near-bank maximum depth to bankfull mean depth (d_{nb}/d_{bkf}): Level III - Detailed Prediction.							
(6) Ratio of near-bank area to bankfull area (A_{nb}/A_{bkf}): Level III - Detailed Prediction/Level IV - Validation.							
(7) Velocity profiles/Isovels/Velocity gradient: Level IV - Validation.							
Transverse and/or central bars - short and/or discontinuous. NBS = High/Very High							
(1) Extensive deposition (continuous, cross channel). NBS = Extreme							
Chute cutoffs, down-valley meander migration, converging flow (Figure X). NBS = Extreme							
(2)	Radius of Curvature R_c (feet)	Bankfull Width W_{bkf} (feet)	Ratio R_c/W				
(3)	Pool Slope S_p	Average Slope S	Ratio S_p/S				
(4)	Pool Slope S_p	Riffle Slope S_{rif}	Ratio S_p/S_{rif}				
(5)	Near-Bank Max Depth d_{nb} (feet)	Mean Depth d (feet)	Ratio d_{nb}/d				
(6)	Near-Bank Area A_{nb} (feet)	Bankfull Area A_{bkf} (feet)	Ratio A_{nb}/A_{bkf}				
	4882.00	11450.51	0.43				
(7)	Velocity Gradient (ft/s/ft)						
<p style="text-align: center;">VELOCITY DISTRIBUTION River Cross-Section 100.38</p>							
<p>Note: The stream width was divided into thirds to apportion the shear stress in the near-bank (one third width) and compared to the bankfull stress of the entire channel.</p>							
Converting Values to a Near-Bank Stress Rating							
Near-Bank Stress Rating	Method Number						
	(1)	(2)	(3)	(4)	(5)	(6)	(7)
Very Low	N/A	>3.0	< 0.20	< 0.4	<1.0	N/A	<1.0
Low		2.21 - 3.0	0.20 - 0.40	0.41 - 0.60	1.0 - 1.5	< 0.33	1.0 - 1.2
Moderate		2.01 - 2.2	0.41 - 0.60	0.61 - 0.80	1.51 - 1.8	0.33 - 0.41	1.21 - 1.6
High	See (1) Above	1.81 - 2.0	0.61 - 0.80	0.81 - 1.0	1.81 - 2.5	0.42 - 0.45	1.61 - 2.0
Very High		1.5 - 1.8	0.81 - 1.0	1.01 - 1.2	2.51 - 3.0	0.46 - 0.50	2.01 - 2.3
Extreme		< 1.5	> 1.0	> 1.2	> 3.0	> 0.50	> 2.3
						Overall Near-Bank Stress Rating	
						HIGH	

Table 4.45. Near Bank Stress Rating for St. Charles (RM 56.57).

Estimating Near-Bank Stress (NBS)							
Stream: WHITE RIVER		Location: ST. CHARLES (RM 56.57)		Date: 9/12/2010		Crew: Linh & Vince	
Methods for Estimating Near-Bank Stress							
(1) Transverse bar or split channel/central bar creating NBS/high velocity gradient: Level I - Reconnaissance. (2) Channel pattern (R_c/W): Level II - General Prediction. (3) Ratio of pool slope to average water surface slope (S_p/S): Level II - General Prediction. (4) Ratio of pool slope to riffle slope (S_p/S_{rif}): Level II - General Prediction. (5) Ratio of near-bank maximum depth to bankfull mean depth (d_{nb}/d_{bkf}): Level III - Detailed Prediction. (6) Ratio of near-bank area to bankfull area (A_{nb}/A_{bkf}): Level III - Detailed Prediction / Level IV - Validation. (7) Velocity profiles/Isovels/Velocity gradient: Level IV - Validation.							
Transverse and/or central bars - short and/or discontinuous. NBS = High/Very High (1) Extensive deposition (continuous, cross channel). NBS = Extreme Chute cutoffs, down-valley meander migration, converging flow (Figure X). NBS = Extreme							
(2)	Radius of Curvature R_c (feet)	Bankfull Width W_{bkf} (feet)	Ratio R_c/W	<div style="text-align: center;"> VELOCITY DISTRIBUTION River Cross-Section 56.57 </div>			
(3)	Pool Slope S_p	Average Slope S	Ratio S_p/S				
(4)	Pool Slope S_p	Riffle Slope S_{rif}	Ratio S_p/S_{rif}				
(5)	Near-Bank Max Depth d_{nb} (feet)	Mean Depth d (feet)	Ratio d_{nb}/d				
(6)	Near-Bank Area A_{nb} (feet)	Bankfull Area A_{bkf} (feet)	Ratio A_{nb}/A_{bkf}				
	3787.50	10111.72	0.37				
(7)	Velocity Gradient (ft/s/ft)			Note: The stream width was divided into thirds to apportion the shear stress in the near-bank (one third width) and compared to the bankfull stress of the entire channel.			
Converting Values to a Near-Bank Stress Rating							
Near-Bank Stress Rating	Method Number						
	(1)	(2)	(3)	(4)	(5)	(6)	(7)
Very Low	N/A	>3.0	< 0.20	< 0.4	<1.0	N/A	<1.0
Low		2.21 - 3.0	0.20 - 0.40	0.41 - 0.60	1.0 - 1.5	< 0.33	1.0 - 1.2
Moderate		2.01 - 2.2	0.41 - 0.60	0.61 - 0.80	1.51 - 1.8	0.33 - 0.41	1.21 - 1.6
High	See (1) Above	1.81 - 2.0	0.61 - 0.80	0.81 - 1.0	1.81 - 2.5	0.42 - 0.45	1.61 - 2.0
Very High		1.5 - 1.8	0.81 - 1.0	1.01 - 1.2	2.51 - 3.0	0.46 - 0.50	2.01 - 2.3
Extreme		< 1.5	> 1.0	> 1.2	> 3.0	> 0.50	> 2.3
						Overall Near-Bank Stress Rating	
						MODERATE	

Table 4.46. Results of Potential and Stability Assessments.

Section	River Mile	Size and Order	Dep. Features	Meander Patterns	Flow Regime	Vegetation	Near Bank Stress	Erosion Potential	Stability Adjective Rating
1	295.27 - 293.21	S-11(5)	B-1	M-1	P:2,7,8	M,3b,6a,5a,1,F	High	Moderate	FAIR
2	293.21 - 291.27	S-11(5)	B-1	M-1	P:2,7,8	M,3b,6a,5a,1,F	Moderate	Moderate	FAIR
3	290.54 - 287.90	S-11(5)	B-4	M-3	P:2,7,8	L,3a,,6a,5a,1,F	Moderate	Moderate	FAIR
4	286.54 - 285.34	S-12(5)	B-7	M-3	P:2,7,8	L,3a,,6a,5a,1,F	Moderate	Moderate	GOOD
5	285.34 - 283.60	S-11(5)	B-1	M-3	P:2,7,8	L,3a,,6a,5a,1,F	High	Moderate	POOR
6	281.04 - 280.00	S-11(5)	B-1	M-3	P:2,7,8	L,3a,,6a,5a,1,F	Low	Low	EXCELLENT
7	280.00 - 276.57	S-12(5)	B-2	M-2	P:2,7,8	L,3a,,6a,5a,1,F	Low	Moderate	FAIR
8	276.57	S-11(5)	B-1	M-2	P:2,7,8	L,3a,,6a,5a,1,F	Low	High	POOR
9	276.57 - 274.71	S-11(5)	B-2	M-2	P:2,7,8	L,3a,,6a,5a,1,F	Low	High	FAIR
10	270.75	S-11(5)	B-2	M-2	P:2,7,8	L,3a,,6a,5a,1,F	Extreme	Very High	POOR
11	270.75 - 268.78	S-12(5)	B-1	M-2	P:2,7,8	L,3a,,6a,5a,1,F	Extreme	Moderate	FAIR
12	268.78 - 266.28	S-11(5)	B-1	M-2	P:2,7,8	L,3a,,6a,5a,1,F	Very High	Moderate	FAIR
13	266.28 - 262.47	S-12(5)	B-4	M-1	P:2,7,8	L,3a,,6a,5a,1,F	Very High	Moderate	FAIR
14	262.47 - 260.98	S-11(5)	B-7	M-1	P:2,7,8	M,3b,6a,5a,1,F	Very High	Moderate	FAIR
15	260.98 - 258.72	S-12(5)	B-1	M-1	P:2,7,8	M,3b,6a,5a,1,F	Extreme	Moderate	POOR
16	258.72 - 257.25	S-12(5)	B-1	M-1	P:2,7,8	M,3b,6a,5a,1,F	Extreme	Moderate	FAIR
17	258.94 - 256.89	S-12(7)	B-4	M-7	P:2,7,8	M,3b,6a,5a,1,F	High	High	FAIR
18	256.89 - 253.08	S-12(7)	B-4	M-7	P:2,8	L,3a,,6a,5a,1,F	Very High	High	FAIR
19	253.08 - 248.95	S-12(7)	B-4	M-7	P:2,8	L,3a,,6a,5a,1,F	High	High	FAIR
20	247.80 - 240.36	S-12(7)	N/A	M-7*	P:2,8	M,3b,,6a,5a,1,12a,F	Moderate	Moderate	GOOD
21	240.36 - 238.48	S-12(7)	B-1	M-3*	P:2,8	L,3a,,6a,5a,1,F	Extreme	High	FAIR
22	238.48 - 234.98	S-12(7)	B-4	M-3*	P:2,8	L,3a,,6a,5a,1,F	High	High	POOR
23	234.98 - 234.22	S-12(7)	N/A	M-3*	P:2,8	L,3a,,6a,5a,1,F	Very High	Moderate	GOOD
24	232.55 - 231.45	S-12(7)	N/A	M-3*	P:2,8	L,3a,,6a,5a,1,F	Very High	High	POOR
25	231.45 - 228.89	S-11(7)	B-4	M-3	P:2,8	L,3a,,6a,5a,1,F	Extreme	Moderate	GOOD
26	228.89 - 227.78	S-11(7)	B-4	M-3	P:2,8	L,3a,,6a,5a,1,F	Very High	Moderate	FAIR
27	227.78 - 226.14	S-12(7)	B-4	M-3	P:2,8	L,3a,,6a,5a,1,F	Extreme	Moderate	GOOD
28	226.14	S-12(7)	B-4	M-7	P:2,8	M,3b,5a,6a,1,F	Extreme	Moderate	FAIR
29	223.9 - 221.53	S-11(7)	B-1	M-7	P:2,8	M,3b,5a,6a,1,F	Extreme	Moderate	FAIR
30	221.53	S-12(7)	B-1	M-7	P:2,8	M,3b,5a,6a,1,F	Moderate	High	FAIR
31	219.41	S-12(7)	B-1	M-7	P:2,8	M,3b,5a,6a,1,F	Very High	Very High	POOR
32	219.41 - 216.97	S-11(7)	B-1	M-7	P:2,8	M,3b,5a,6a,1,F	Extreme	High	FAIR
33	216.97 - 215.33	S-11(7)	B-1	M-7	P:2,8	M,3b,5a,6a,1,F	Extreme	High	POOR
34	215.33 - 213.33	S-11(7)	B-1	M-6	P:2,8	L,8a,5a,6b,3b,F	High	High	FAIR
35	213.33 - 207.17	S-11(7)	B-1	M-6	P:2,8	M,5a,6b,3b,1,F	Moderate	High	FAIR
36	207.17 - 203.71	S-11(7)	B-1	M-6	P:2,8	L,8a,5a,3b,1,F	High	High	FAIR
37	201.56 - 201.01	S-12(7)	B-1	M-6	P:2,8	M,8b,5b,3b,1,12a,F	Moderate	High	POOR
38	201.01 - 197.27	S-12(7)	B-4	M-6	P:2,8	M,8b,5b,3b,1,12a,F	Moderate	Moderate	GOOD
39	197.27 - 195.01	S-12(7)	B-1	M-6	P:2,8	L,8a,5a,3b,1,12a,F	Very High	High	FAIR
40	195.01 - 192.68	S-12(7)	B-4	M-6	P:2,8	M,8b,5b,3b,1,12a,F	Very High	High	GOOD
41	192.68 - 191.64	S-12(7)	B-1	M-7	P:2,8	L,8a,5a,3b,1,12a,F	Moderate	High	FAIR
42	191.64 - 189.95	S-12(7)	B-1	M-7	P:2,8	L,8a,5a,3b,1,12a,F	Moderate	Very High	POOR
43	189.95 - 188.59	S-11(7)	B-1	M-7	P:2,8	M,8b,5b,3b,1,12a,F	Very High	Very High	POOR
44	188.59 - 187.55	S-12(7)	B-1	M-7	P:2,8	M,8b,5b,3b,1,12a,F	Extreme	High	FAIR
45	187.55 - 186.26	S-12(7)	B-1	M-7*	P:2,8	M,8b,5b,3b,1,12a,F	Extreme	Very High	POOR
46	186.26 - 181.29	S-12(7)	B-4	M-7*	P:2,8	M,8b,5b,3b,1,12a,F	Moderate	Moderate	GOOD
47	181.29 - 177.81	S-11(7)	B-1	M-7*	P:2,8	M,8b,5a,12a,F	Low	Very High	POOR
48	177.81 - 176.00	S-12(7)	B-4	M-3*	P:2,8	M,8b,5b,3b,1,12a,F	Moderate	High	FAIR
49	175.50 - 172.65	S-12(7)	B-4	M-3*	P:2,8	M,8b,5b,3b,1,12a,F	Extreme	High	FAIR
50	172.65 - 169.52	S-12(7)	B-1	M-3*	P:2,8	L,8a,5b,3b,1,12a,F	Extreme	High	POOR
51	169.52 - 167.08	S-12(7)	B-4	M-3*	P:2,8	M,8b,5b,3b,1,12a,F	Very High	Very High	POOR
52	167.08 - 166.08	S-12(7)	B-4	M-3*	P:2,8	M,8b,5b,3b,1,12a,F	Extreme	High	FAIR
53	166.08 - 164.39	S-11(7)	B-4	M-3*	P:2,8	M,8b,5b,3b,1,12a,F	High	High	FAIR
54	164.39 - 163.40	S-11(7)	B-4	M-3*	P:2,8	M,8b,5b,3b,1,12a,F	High	High	FAIR
55	163.40 - 161.91	S-12(7)	B-4	M-3*	P:2,8	M,8b,5b,3b,1,12a,F	High	Very High	POOR
56	161.91 - 161.23	S-12(7)	B-4	M-3*	P:2,8	M,8b,5b,3b,1,12a,F	Very High	Very High	POOR
57	161.23 - 158.63	S-12(7)	B-1	M-3*	P:2,8	M,8b,5b,3b,1,12a,F	High	Moderate	GOOD
58	158.63	S-12(7)	B-1	M-3*	P:2,8	M,8b,5b,3b,1,12a,F	High	High	FAIR
59	155.71 - 155.04	S-12(7)	B-1	M-3*	P:2,8	M,8b,5b,3b,1,12a,F	Moderate	Moderate	GOOD
60	155.04 - 152.68	S-12(7)	B-1	M-3	P:2,8	M,8b,5b,3b,12a,F	Moderate	Very High	POOR
61	152.68 - 149.03	S-12(7)	B-1	M-1	P:2,8	L,8a,5b,3b,1,12a,F	High	Very High	POOR
62	149.03 - 147.19	S-12(7)	B-4	M-1	P:2,8	L,8a,5b,3b,1,12a,F	Extreme	High	POOR
63	147.19 - 145.72	S-12(7)	B-1	M-1	P:2,8	L,8a,5b,3b,1,12a,F	Moderate	Very High	POOR
64	145.72 - 143.75	S-12(7)	B-4	M-1	P:2,8	L,8a,5b,3b,1,12a,F	High	Moderate	GOOD
65	143.75 - 141.78	S-12(7)	B-2	M-1	P:2,8	L,8a,5b,3b,1,12a,F	Extreme	Very High	POOR
66	141.78 - 140.39	S-12(7)	B-1	M-1	P:2,8	L,8a,5b,3b,1,12a,F	Extreme	Very High	POOR
67	140.39 - 139.21	S-12(7)	B-4	M-1	P:2,8	M,8b,5b, 6b,3b,1,12a,F	Extreme	High	FAIR
68	139.21 - 138.01	S-12(7)	B-1	M-1	P:2,8	M,8b,5b, 6b,3b,1,12a,F	Extreme	Very High	POOR
69	138.01 - 136.03	S-12(7)	B-4	M-1	P:2,8	L,8a,5b,3b,1,12a,F	Extreme	Very High	POOR
70	136.03 - 135.16	S-12(7)	B-1	M-1	P:2,8	L,8a,5b,3b,1,12a,F	Very High	Very High	POOR

Table 4.46(Continued...). Results of Potential and Stability Assessments.

Section	River Mile	Size and Order	Dep. Features	Meander Patterns	Flow Regime	Vegetation	Near Bank Stress	Erosion Potential	Stability Adjective Rating
71	133.65 - 132.61	S-12(7)	B-1	M-1	P:2,8	L,8a,5b,3b,1,12a,F	Extreme	Very High	POOR
72	132.61 - 130.54	S-11(7)	B-4	M-1	P:2,8	M,8b,5b, 6b,3b,1,12a,F	Extreme	Very High	POOR
73	130.54 - 128.70	S-12(7)	B-4	M-1	P:2,8	M,8b,5b,3b,1,12a,F	Extreme	High	FAIR
74	128.70 - 124.33	S-12(7)	B-4	M-1	P:2,8	M,8b,5b,3b,1,12a,F	Extreme	High	FAIR
75	124.33 - 122.36	S-12(7)	B-7	M-8	P:2,8	M,8b,5b,3b,1,12a,F	High	Very High	POOR
76	122.36 - 118.19	S-11(7)	B-1	M-8	P:2,8	M,8b,5b,3b,1,12a,F	Very High	High	POOR
77	118.19 - 116.4	S-12(7)	B-1	M-8	P:2,8	M,8b,5b,12a,F	Extreme	Very High	POOR
78	116.4 - 114.53	S-12(7)	B-4	M-8	P:2,8	M,8b,5b,12a,F	Extreme	Very High	POOR
79	114.53 - 112.77	S-12(7)	B-1	M-8	P:2,8	M,8b,5b,12a,F	Extreme	Very High	POOR
80	111.34	S-12(7)	B-1	M-8	P:2,8	M,8b,5b,3b,12a,F	Low	Very High	POOR
81	109.77 - 108.75	S-12(7)	B-1	M-8	P:2,8	M,8b,5b,3b,12a,F	Very High	Moderate	GOOD
82	108.75 - 107.67	S-11(7)	B-1	M-8	P:2,8	L,8a,5b, 3b,6b,1,12a,F	Extreme	Very High	POOR
83	107.67	S-11(7)	B-1	M-8	P:2,8	M,8b,5b,3b,12a,F	Extreme	Very High	POOR
84	107.67 - 103.51	S-12(7)	B-1	M-8	P:2,8	M,8b,5b,3b,12a,F	Extreme	Very High	POOR
85	104.31 - 103.51	S-11(7)	B-1	M-8	P:2,8	M,8b,5b,3b,1,12a,F	Extreme	Moderate	FAIR
86	103.51 - 102.25	S-11(7)	B-1	M-8	P:2,8	M,8b,5b,3b,1,12a,F	Extreme	High	POOR
87	102.25 - 101.14	S-11(7)	N/A	M-8	P:2,8	M,8b,5b,12a,F	Extreme	High	POOR
88	101.14 - 100.34	S-12(7)	B-1	M-8	P:2,8	M,8b,5b, 3b,6b,1,12a,F	Extreme	Very High	POOR
89	100.34 - 98.48	S-12(7)	B-1	M-1	P:2,8	L,8a,5b, 3b,6b,1,12a,F	Moderate	High	FAIR
90	98.48 - 96.72	S-12(7)	B-1	M-1	P:2,8	M,8b,5b, 6b,12a,F	Very High	Very High	POOR
91	96.72 - 94.57	S-12(7)	B-1	M-1	P:2,8	M,8b,5b, 6b,12a,F	Very High	Moderate	FAIR
92	94.57 - 92.42	S-12(7)	B-1	M-3	P:2,8	M,8b,5b, 6b,1,12a,F	High	High	FAIR
93	89.46 - 87.41	S-12(7)	B-1	M-3	P:2,8	M,8b,5b, 6b,1,12a,F	High	Very High	POOR
94	87.41 - 84.62	S-12(7)	B-1	M-3	P:2,8	H,8c,5b, 6b,1,12a,F	Extreme	Low	EXCELLENT
95	84.62 - 81.65	S-12(7)	B-1	M-3	P:2,8	H,8a,5b,12a,F	Extreme	Low	EXCELLENT
96	80.31 - 78.89	S-12(7)	B-4	M-1	P:2,8	M,8b,5b,12a,F	Extreme	High	FAIR
97	78.89	S-12(7)	B-1	M-1	P:2,8	M,8b,5b,12a,F	Extreme	High	POOR
98	76.87 - 75.73	S-12(7)	B-4	M-1	P:2,8	H,8c,5b,12a,F	Extreme	High	POOR
99	75.73 - 73.62	S-12(7)	B-4	M-1	P:2,8	H,8c,5b,12a,F	Extreme	Moderate	FAIR
100	75.73 - 68.51	S-12(7)	N/A	M-3	P:2,8	H,8c,5b,12a,F	Very High	Moderate	FAIR
101	71.59 - 68.51	S-12(7)	B-1	M-3	P:2,8	M,8b,5b,12a,F	Moderate	High	POOR
102	68.51 - 67.21	S-12(7)	N/A	M-3	P:2,8	M,8b,5b,12a,F	Very High	Low	GOOD
103	67.21 - 64.72	S-12(7)	B-1	M-3	P:2,8	M,8b,5b,12a,F	High	High	POOR
104	64.72	S-12(7)	B-4	M-3	P:2,8	M,8b,5b,12a,F	Low	Very High	POOR
105	64.72 - 60.12	S-11(7)	B-1	M-3	P:2,8	H,8c,5b,6b,12a,F	Low	High	POOR
106	62.7 - 60.12	S-12(7)	B-4	M-3	P:2,8	H,8c,5b,6b,12a,F	Moderate	Very High	POOR
107	60.12 - 58.79	S-11(7)	B-4	M-3	P:2,8	H,8c,5b,6b,12a,F	Moderate	High	POOR
108	58.79 - 57.61	S-12(7)	B-4	M-1	P:2,8	M,8b,5b,6b,12a,F	Extreme	High	POOR
109	57.61 - 55.30	S-12(7)	B-4	M-1	P:2,8	M,8b,5b,6b,1,12a,F	Very High	Moderate	FAIR
110	55.30 - 54.33	S-12(7)	B-1	M-1	P:2,8	H,8c,5b,12a,F	Very High	High	FAIR
111	54.33 - 53.38	S-11(7)	B-1	M-1	P:2,8	H,8c,5b,12a,F	Extreme	High	FAIR
112	54.33 - 51.45	S-11(7)	B-4	M-5	P:2,8	H,8c,5b,12a,F	Extreme	Very High	POOR
113	51.45	S-11(7)	B-4	M-5	P:2,8	H,8c,5b,12a,F	Extreme	Very High	POOR
114	49.77 - 49.08	S-12(7)	B-4	M-5	P:2,8	H,8c,5b,12a,F	Moderate	Moderate	FAIR
115	49.08 - 47.19	S-11(7)	B-1	M-7	P:2,8	H,8c,5b,12a,F	Moderate	Very High	POOR
116	47.19	S-11(7)	B-4	M-7*	P:2,8	H,8c,5b,12a,F	Moderate	High	FAIR
117	45.31	S-11(7)	B-1	M-7*	P:2,8	H,8c,5b,12a,F	Very High	Low	GOOD
118	45.31 - 42.00	S-11(7)	B-1	M-7*	P:2,8	H,8c,5b,12a,F	Very High	Very High	POOR
119	42.00 - 40.52	S-11(7)	B-4	M-7*	P:2,8	H,8c,5b,12a,F	High	High	FAIR
120	40.52	S-11(7)	B-1	M-7*	P:2,8	H,8c,3b,5b,12a,12b,F	Moderate	High	FAIR
121	40.52 - 38.69	S-11(7)	B-1	M-7*	P:2,8	H,8c,3b,5b,12a,12b,F	Moderate	Very High	POOR
122	38.69	S-12(7)	B-1	M-7*	P:2,8	H,8c,3b,5b,12a,12b,F	Moderate	Very High	POOR
123	36	S-12(7)	B-4	M-1*	P:2,8	H,8c,3b,5b,12a,F	Extreme	High	FAIR
124	36	S-12(7)	B-1	M-1*	P:2,8	H,8c,3b,5b,12a,F	Extreme	Moderate	GOOD
125	34.42 - 32.81	S-12(7)	B-1	M-1*	P:2,8	H,8c,3b,5b,12a,F	Extreme	Moderate	GOOD
126	30.88 - 29.74	S-12(7)	B-4	M-1*	P:2,8	H,8c,3b,5b,12a,F	Extreme	Moderate	FAIR
127	29.74 - 29.13	S-12(7)	B-1	M-1*	P:2,8	H,8c,3c,5b,12a,F	Extreme	Very High	POOR
128	29.13 - 26.38	S-12(7)	B-4	M-1*	P:2,8	H,8c,3c,5b,12a,F	Extreme	High	POOR
129	26.38 - 24.47	S-12(7)	B-4	M-5	P:2,8	H,8c,3b,5b,F	Extreme	High	POOR
130	24.47	S-12(7)	B-1	M-5	P:2,8	H,8c,3b,5b,12c,F	Extreme	Very High	POOR
131	22.01	S-11(7)	B-4	M-5	P:2,8	H,8c,3b,5b,F	High	Moderate	GOOD
132	22.01 - 17.64	S-11(7)	B-4	M-5	P:2,8	H,8c,3b,5b,F	Very High	High	POOR
133	17.64	S-11(7)	B-1	M-5	P:2,8	H,8c,3b,5b,F	Very High	Moderate	FAIR
134	14.01	S-12(7)	N/A	M-5	P:2,8	H,8c,3b,5b,F	Very High	Low	GOOD
135	14.01 - 11.80	S-12(7)	B-1	M-5	P:2,8	H,8c,3b,5b,F	Very High	Very High	POOR
136	11.8	S-12(7)	N/A	M-5	P:2,8	H,8c,3b,5b,1,F	Very High	Moderate	GOOD
137	9.97 - 6.92	S-12(7)	B-1	M-5	P:2,8	H,8c,3b,5b,1,F	Moderate	Very High	POOR
138	6.92 - 5.32	S-12(7)	B-4	M-5	P:2,8	H,8c,3b,5b,6c,F	Moderate	Low	GOOD
139	4.31 - 3.26	S-12(7)	B-4	M-5	P:2,8	M,8b,4b,F	Very High	High	FAIR
140	3.26 - 1.36	S-12(7)	B-4	M-1	P:2,8	M,8b,3b,4b,6c,F	Extreme	Moderate	FAIR
141	1.36 - 0.00	S-12(7)	B-4	M-1	P:2,8	M,8b,3b,4b,6c,F	Extreme	Moderate	FAIR

*Meander patterns induced by lateral confinement of nearby levee.

CHAPTER 5: SEDIMENT ANALYSES

Introduction

The assessments of the stability and morphology of a fluvial system are frequently associated with the apprehension of the intrinsic characteristic of sediment regime. Understanding the patterns of sediment conveyance and entrainment within the flow of a fluvial system not only explicate uncertainty colligated with the conjecture as to the manner and way by which the channel attains its present configuration, but also provides concrete validation of channel processes, stability, and morphology inherent to the system as it responds to disturbances. Validation of channel processes, bed and bank stability, and the morphology of a fluvial system that generally mandate extensive sediment analyses emphasizing field measurements of suspended and bed-load sediment discharges are often considered uneconomical. Therefore, in most scenarios, sediment data are predicted by utilizing methodologies available in the literature, albeit a dearth of actual channel particle size, rather than field measured. In the case pertaining to the White River, however, sediment analyses performed by implementing several of these methodologies are contingent on the dominant bed material, or the median grain size bed material, attained from particle size distribution curves developed from sieve analyses of field data. The field data collected consists of approximately seven hundred soil samples obtained from a Modified Wolman Pebble Count scheme for various 'reference' reaches of the river. Additional core samples collected from the mid-sections of depositional point bar features and bend apexes via open bucket are also antecedently expressed in a preceding chapter as particle size distribution curves representative of expected bed-load sizes being transported and deposited at bankfull stage or normal high flow. The

dominant bed material, derived explicitly from the Modified Wolman Pebble Count samples, are then utilized in several sediment analysis methodologies to compute the bed-load and suspended-load transported within the reference reaches of the White River by identifying the threshold of sediment movements; to illustrate the process attributable to the formation of bedforms at various reaches of the White River by identifying the threshold of sediment movements; to obtain the total sediment supply and sediment trend within the various sections of the White River; to determine the empirical relationships of bed-load, suspended-load, and total load to fluvial and geomorphological parameters; to elaborate and explicate erosional and depositional magnitudes, patterns, and processes inherent to the White River channel; and to ascertain the significance of each component to the meandering/shifting, dynamic equilibrium, and overall stability of the White River.

Sediment Transport Mechanisms

Since the sediment regime in an alluvial system is largely responsible for the stability of its bed and banks, various methods are conducted to predict the stability conditions of the bed and banks of the White River by identifying the threshold of sediment movement. The definition of the threshold of sediment movement, often expressed “in terms of a critical shear stress or a critical velocity at which the forces or moments resisting motion of an individual grain are overcome” (Sturm, 2001, p. 380), generally depicts the mechanisms of sediment motion within a fluvial system. Initially when the threshold of incipient movement is exceeded, sediment particles begin to roll, slide, and jump along the bed thus defining the bed-load transport discharge. As the stream power of a fluvial system increases (i.e. slope and discharge increase), a higher threshold of sediment movement allows the sediment particles to be entrained and

transported by the flow resulting in the suspended-load transport discharge. The total sediment discharge is the summation of the bed-load and suspended-load discharges. Based on the flow data extracted from the HEC-RAS Model and the dominant median particle size obtained from laboratory sieve analyses of soil samples collected from the sites, sediment analyses are conducted to determine the sediment transport mechanisms and the bedforms manifested from the flow and sediment regimes. The results of the sediment analyses, conducted by implementing the equations of Van Rijn, Yang, Karim-Kennedy, and Kennedy, verified the conjecture that the sediment transport mechanism of the White River is best classified as “mixed-load” having characteristics of both bed-load and suspended-load. Overall, the results indicate that suspended-load is the dominant transport mechanism in the White River. A closer inspection of the resulting data reveals that bed-load transport is the dominant mechanism for the segment from Batesville to Newport. The primary contributor to sediment load for the segments from Augusta to Des Arc, Clarendon to St. Charles, and St. Charles to the Lower Mississippi River are suspended-loads while segments with equivalent or near equivalent components of both bed-load and suspended-load (i.e., mixed-load) discharges are Devalls Bluff to Clarendon as well as the transitions from Newport to Augusta and Clarendon to St. Charles. The numerical quantities of bed-load and suspended-load discharges, acquired from implementing the methodologies of Van Rijn, Karim-Kennedy, Kennedy, and Yang for various reaches of the White River are tabulated as shown by **Table 5.1**.

Bedforms

Bedforms, irregular bed features of a natural fluvial system that are formulated by the motion of flow, are commonly classified as ripples, dunes, flats, and antidunes,

Table 5.1. Numerical Quantities of Various Sediment Load types.

Sections (RM 299.00 – 0.00)	Van Rijn Method			Karim- Kennedy Method			Kennedy Method			Yang Method		
	g _b	g _s	g _t	g _b	g _s	g _t	g _b	g _s	g _t	g _b	g _s	g _t
	(tons/day)			(tons/day)			(tons/day)			(tons/day)		
Batesville-Newport	61	5	66	15	4	19	15	3	18	--	--	6
Newport-Augusta	1	2	3	1	4	5	1	6	7	1	1	2
Augusta-Des Arc	1	12	13	2	33	35	1	82	83	1	7	8
Des Arc-Devalls Bluff	1	13	14	1	42	43	1	97	98	1	9	10
Devalls Bluff-Clarendon	1	3	4	1	5	6	1	12	13	1	1	2
Clarendon-St. Charles	1	37	38	3	27	30	3	133	136	3	5	8
St. Charles-LMR	10	36	46	9	13	22	9	7	16	3	1	4

*Sediment load expressed as tons per day per unit width.

each with a distinct physical origin. Ripples and dunes are the lower regime bedforms in that they are generally seen in static conditions or subcritical flow, while antidunes and flats are the upper regime bedforms in that they are observable only in dynamic conditions at or near supercritical flow (Sturm, 2001). The progression of the bedforms usually involved various flow regimes and is evident with velocity augmentation. Initially when the magnitude of the velocity is small, the bed of the channel remains relatively flat as no quantity of sediment is moved. When the velocity exceeds the critical threshold for sediment motion, ripples, triangular (or sometimes sinusoidal) in shape patterns with relatively flat, long upstream slopes followed by subsequent steep slopes equivalent to the sediment's angles of repose, are formed. As the velocity increases, a transition zone consisting of ripple and dune bedforms occurs simultaneously at various locations of the bed. Further increases in velocity result in the absence of ripples and the formation of well-developed dunes exhibiting a larger-in-scale triangular in shape patterns with larger amplitudes and wavelengths. Additional enhancement of the magnitude of velocity results in the washing out of dunes to form an upper-regime flat bed with a dominant

mechanism of suspended sediment transport followed by a subsequent formation of antidunes. “Ripples, dunes, and antidunes are undular (wavelike) features [possessing] a wavelength and wave height that scale with the flow depth”(Garcia, 2008, p. 81), are the products of the flow and sediment transport regimes, and conversely the constituents that have a profound influence on the flow and sediment regimes within an alluvial channel. Characteristics inherent to ripples and dunes are that they both share similar triangular shapes with pronounced slip faces and migrate only in the downstream direction. Ripple forms, however, are dependent on the sediment particle diameter while dunes forms are dependent exclusively on the flow conditions (Sturm, 2001). Ripples distinctively form in the presence of a viscous sublayer under a condition with higher flow resistance, and may also occur on the upstream slopes of dunes. Dunes have significant effects on the variation of the water surface while ripples have little effect on the water surface. Unlike ripples, when dunes invariably migrate downstream bed-load sediment are always deposited on the slip surfaces. In contrast to ripples and dunes which are the results of discontinuities of the bed and disturbances due to turbulent flows, antidunes are caused by the standing waves that occur when the Froude Number approaches unity (Garcia, 2008). Dunes and antidunes are similar in the aspect that they both contribute to the water surface and bed undulations. However, the distinguishing features that separate antidunes from dunes are that antidunes’ water surface undulations are in phase with the bed, and that antidunes may migrate upstream, downstream, or remain stationary (Sturm, 2001). The schematic of the aforementioned bedforms are shown in **Figure 5.1**.

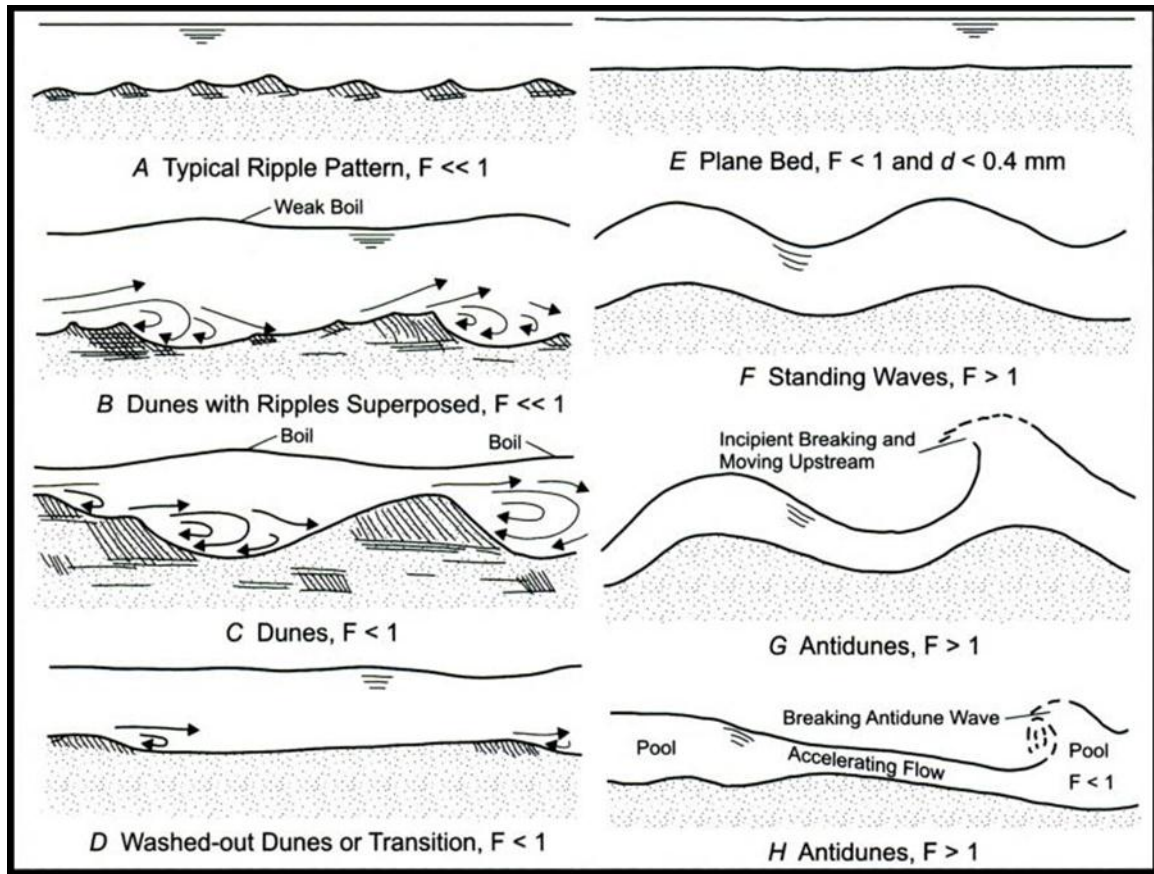


Figure 5.1. The Schematic of Different Bedforms (Garcia, 2008).

Computations and results for sediment analyses as shown in **Appendix C** and tabulated in **Table E.2**, respectively, also provide variables beneficial to the prediction of the bedforms within various sections of the White River. The correlations between the dimensionless particle diameter d_* and the transport parameter T based on Van Rijn's criteria as well as Engelund's dimensionless shear stress τ_* versus Shields dimensionless critical shear stress parameter τ'_* (due to grain resistance) clearly indicate that flat beds and antidunes are expected to be the common bedforms for the segment from Batesville to Newport while ripples are predominant for the segments from Devalls Bluff to Clarendon. The plotted relationships also show that dunes are dominant bed features for

the segments from Newport to Augusta, Augusta to Des Arc, Des Arc to Devalls Bluff, and Clarendon to St. Charles. Dunes are expected to be well-developed for Clarendon to St. Charles, Augusta to Des Arc, and Des Arc to Devalls Bluff, and less-developed for Newport to Augusta as it falls within the lower range of lower regime bedforms. The presence of ripples with variabilities in wavelengths and wave heights are also anticipated for the segment from Newport to Augusta as the results exhibit a great dispersion in the transport parameters and shear stresses. The bedforms for the segment from St. Charles to LMR vary from ripples to antidunes as it falls within both the lower regime bedform and upper regime bedform regions. In addition, sediment analyses results also shows that the transition zone between the lower regime bedforms and the upper regime bedforms occurs primarily in the upper portion between St. Charles and the Lower Mississippi River.

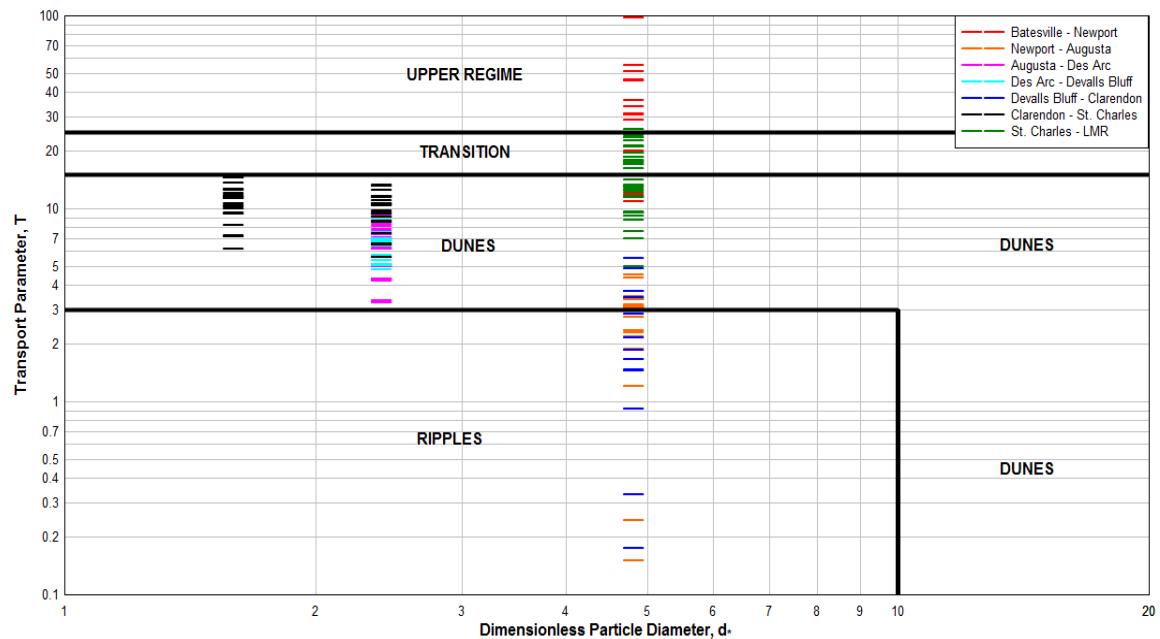


Figure 5.2. Prediction of the White River's Bedforms from Transport Parameter, T , and Dimensionless Particle Diameter, d_* (Van Rijn, 1984c)

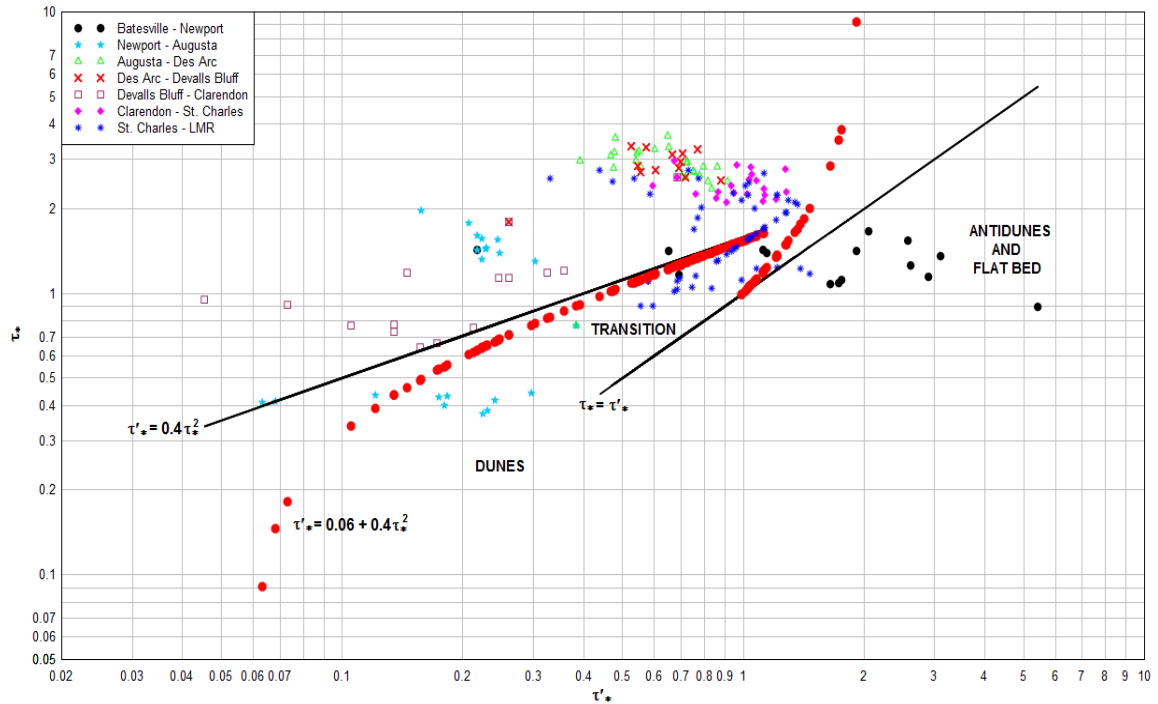


Figure 5.3. Prediction of the White River's Bedforms from Engelund's Dimensionless Shields Parameters Diagram (Engelund & Hansen, 1967; Engelund, 1967).

Sediment Transport and Supply

Sediment rating curves and sediment concentration profiles are also plotted for various sections of the White River to determine the trends in sediment supply and sediment transport within the channel of each individual segment. With the exception of the segments from Batesville to Newport and Devalls Bluff to Clarendon, the sediment rating curves show a general correlation of sediment transport augmentation to discharge augmentation. The sediment rating curve and the sediment concentration profile depict a decrease in sediment transport with respect to an increase in discharge and a decrease in sediment supply from Batesville to Newport, respectively. The implication is that for the segment from Batesville to Newport, the banks exhibit an exceptional magnitude of stability or a moderate banks erodibility potential while velocities are adequate to filter

sediment through the system. The rating curve also indicates a dominant sediment transport mechanism in the form of bed-load which contradicts with the upper regime bed forms, such as flats and antidunes, that are observable only in dynamic conditions where suspended-loads dominate. One explanation is that despite the high velocities that washed out the ripples and dunes of finer materials to produce a flat bed with a larger value of suspended sediment transport, the channel bed itself is composed primarily of gravel-size materials that constitute a fully rough turbulent boundary where the critical shear stress is constant or proportional to the grain diameter (see Shields parameter versus dimensionless particle curve in **Appendix C**). For this reason, the critical shear stress is never exceeded for the gravel-size materials signifying that the movement of particles is primarily along the bed, which is also verified by the particle's position on the Hjulström Curve as well as the transparency of the water seen in the channel during a field investigation at the site. The segment from Newport to Augusta is characterized by an increase in sediment transport corresponding to an increase in discharge, and exhibits an overall pattern of sediment supply diminishment. The steepness of the sediment trend curve suggests that at Newport the banks and bed erodibility potential is significantly higher than at Augusta. Erosion of the banks and scouring of the beds are responsible for the formations of dune bedforms from Newport to Augusta. The dunes are expected to decrease in size from Newport to Augusta. The sediment rating curve also indicates a converging pattern from a dominant suspended-load transport to a mixed-load transport as the channel approaches Augusta. Sediment transport and sediment supply enhancements are apparent for the segment from Augusta to Des Arc. Suspended-load is the primary transport mechanism, dunes are expected to be well-developed, and the banks

are expected to be highly erodible and should contribute to high sediment supply as shown by the high sediment concentration in the profile plot. The sediment rating and the sediment trend curves show a slight increase in the rate of sediment transport and a respective decrease in the total sediment concentration from Des Arc to Devalls Bluff. High bank erosion potentials, as well as scouring and deposition of the bed are expected as the sediment supply is significantly high. Dunes are expected to be well-developed while the flat decreasing slope of the sediment concentration trend implies a reduction in the channel's ability to supply and transport suspended sediment. The sediment rating curve also indicates a slight reduction in the channel's ability to transport sediment for the segment from Devalls Bluff to Clarendon. The significant decline in the total sediment denotes a transformation to a lower regime bedform, where deformation of the bed contributes to the progression of discontinuities on the bed responsible for the formation of ripple patterns. The steep rate of enhancement in the total sediment concentration in conjunction with the constant rate of sediment transport indicate that for the segment from Devalls Bluff to Clarendon, sediment supply competency preponderates sediment transport capacity, a prerequisite for bed aggradation as well as lateral extension. In the case pertaining to the segment from Clarendon to St. Charles, sediment transport follows an increasing pattern in association with discharge enhancement while sediment supply declines as the channel approaches St. Charles. Suspended-load is the predominant transport mechanism and dunes are expected to be well-developed as they fall very close to the transition zone of bedform regimes. High sediment concentration in the profile graph affirms that the banks and the beds are highly erodible and should contribute to high sediment supplies, which may include washed

loads from upstream. The general diminishment in the sediment concentration trend conveys a progressive decrease in sediment supply as the channel traverses southward toward St. Charles. From St. Charles to the Lower Mississippi River, the sediment rating curve suggests a divergent from mixed-load to suspended-load, and an overall augmentation in sediment transport accompanying an enhancement in discharge values. The total sediment concentration trend, however, does not exhibit the same level of agreement among the various sediment analysis methodologies implemented. The justification is that the presence of a variety of bedforms ranging from ripples to antidunes may have contributed to the discrepancies between the methods implemented to predict the sediment supplies, which are possibly derived based on the assumption of uniform bed form conditions. If the increasing trend in sediment concentration is adopted, as denoted by three of the four methods, then the total sediment supplies, hence the bank and bed erodibility potentials, are anticipated to increase as the White River amalgamates to the Lower Mississippi River.

Correlations Between Fluvial/Morphological Parameters and Sediment Discharges

To comprehend the patterns of sediment conveyance and entrainment within the reaches of the White River, various fluvial and morphological parameters are plotted with bed-load discharges, suspended-load discharges, and total sediment concentrations derived from sediment analyses. Since a multitude of parameters may permit many relationships with the modes of sediment conveyance and entrainment, only apposite correlations that depict a reasonable level of agreement or a definite trend in data are presented, and briefly discussed. Implications of controls imparted by individual parameters to sediment supply and transport are also concisely explicated subsequently.

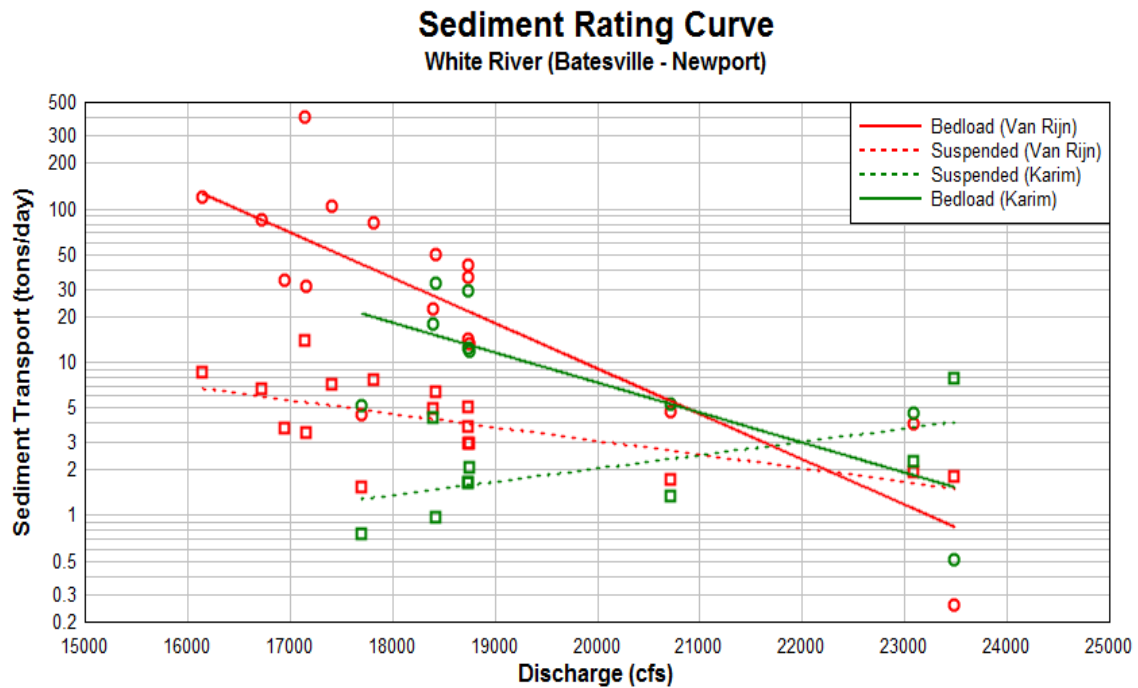


Figure 5.4. Sediment Rating Curve for Batesville to Newport (RM 299.00 - 258.94).

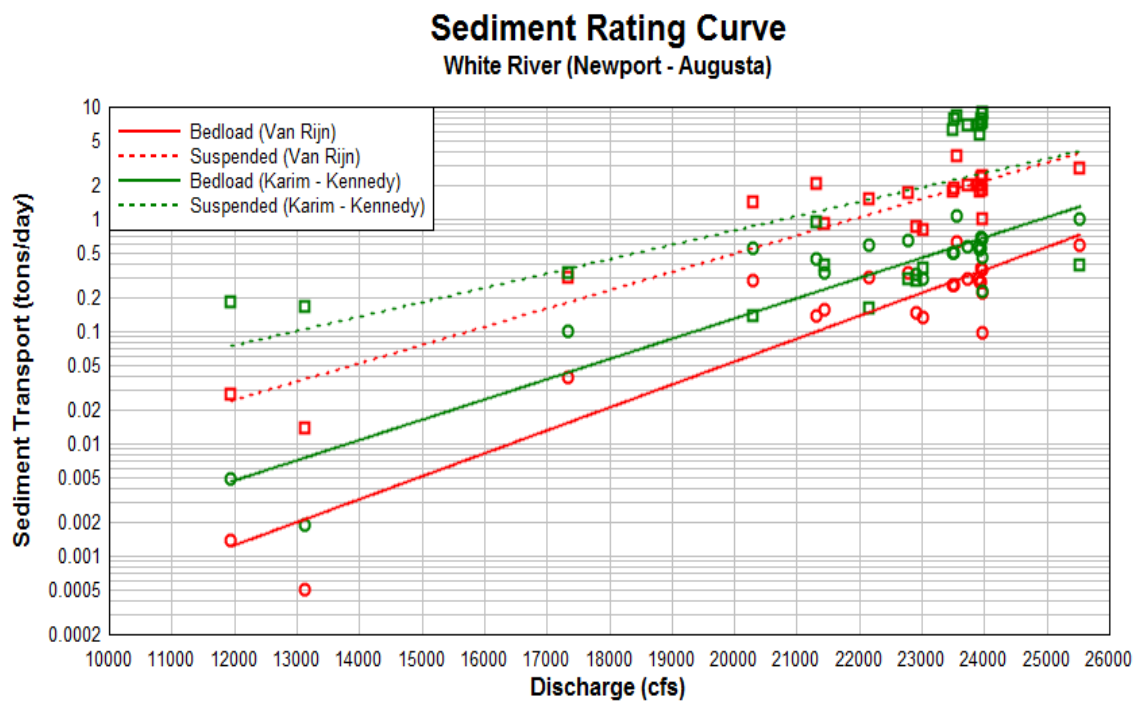


Figure 5.5. Sediment Rating Curve for Newport to Augusta (RM 258.94 - 200.30).

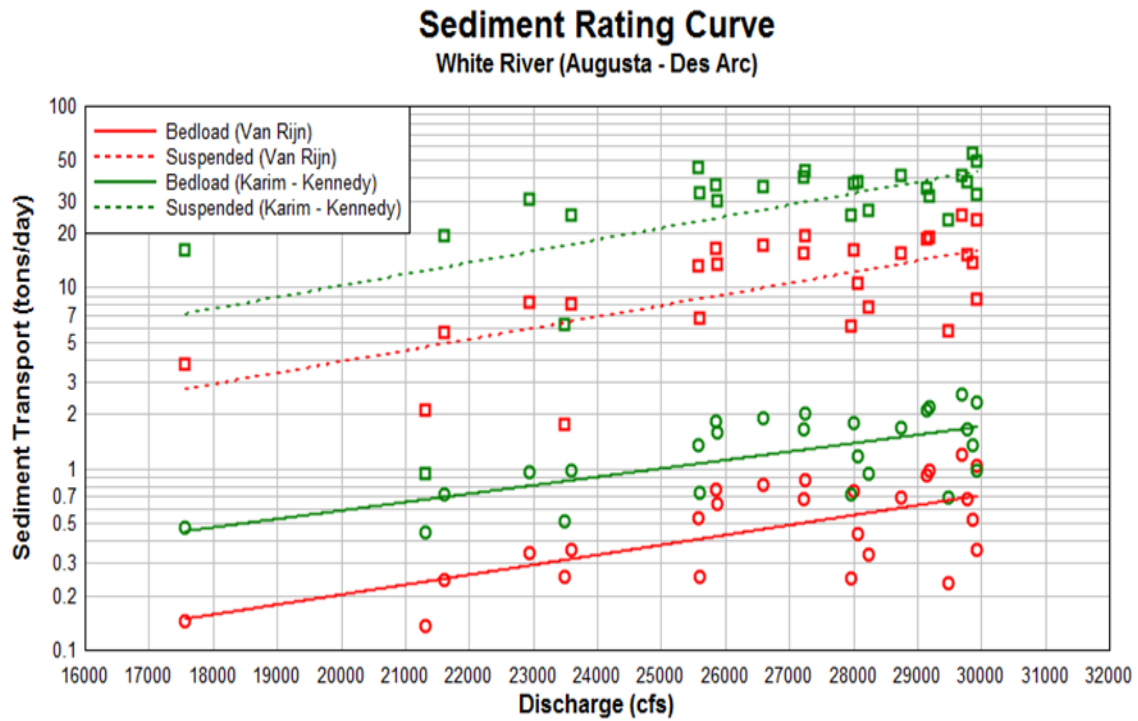


Figure 5.6. Sediment Rating Curve for Augusta to Des Arc (RM 200.30 - 148.03).

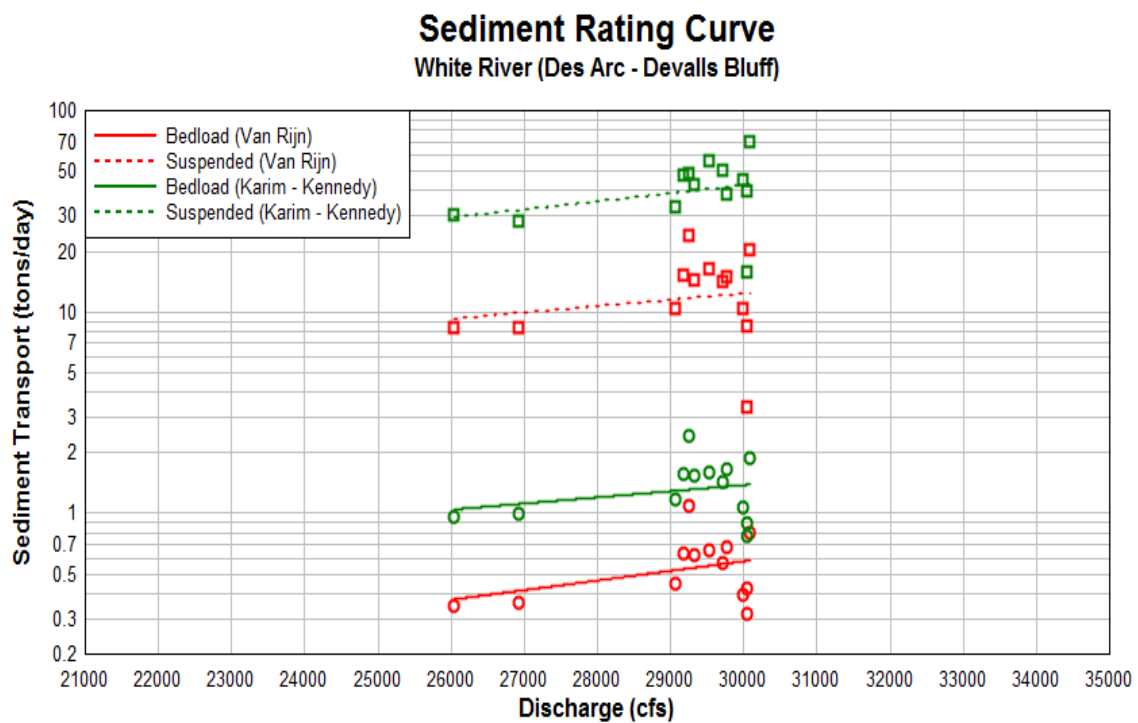


Figure 5.7. Sediment Rating Curve for Des Arc to Devalls Bluff (RM 148.03 - 124.35).

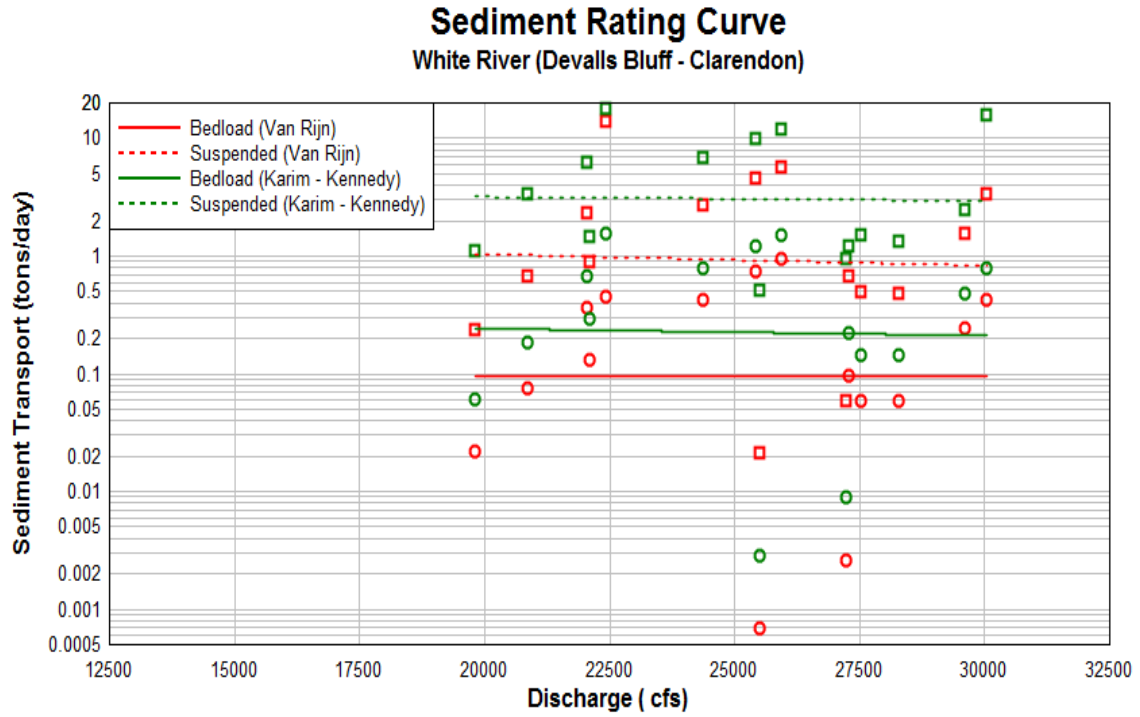


Figure 5.8. Sediment Rating Curve for Devalls Bluff to Clarendon (RM 124.35 - 100.38).

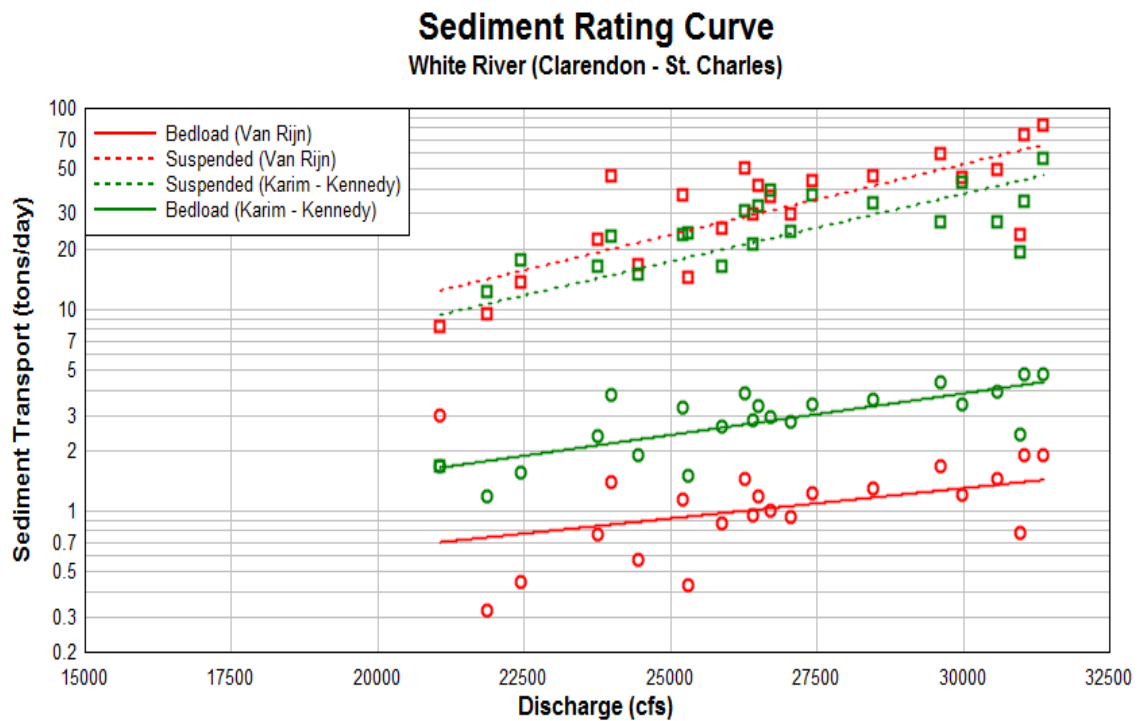


Figure 5.9. Sediment Rating Curve for Clarendon to St. Charles (RM 100.38 -56.57).

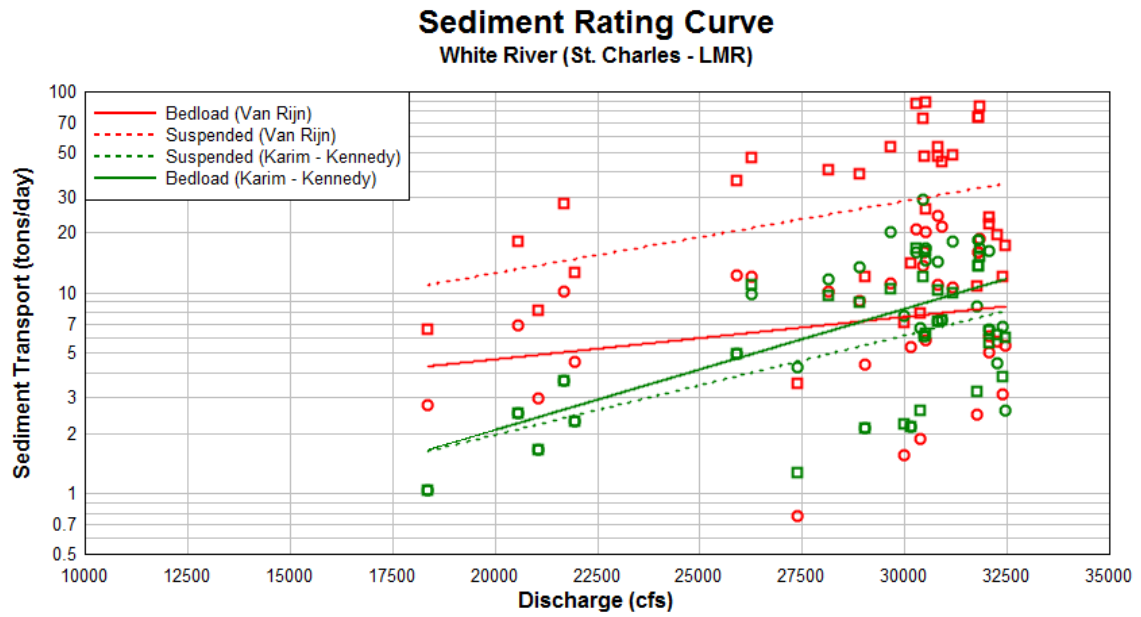


Figure 5.10. Sediment Rating Curve for St. Charles to LMR (RM 56.57 – 0.00).

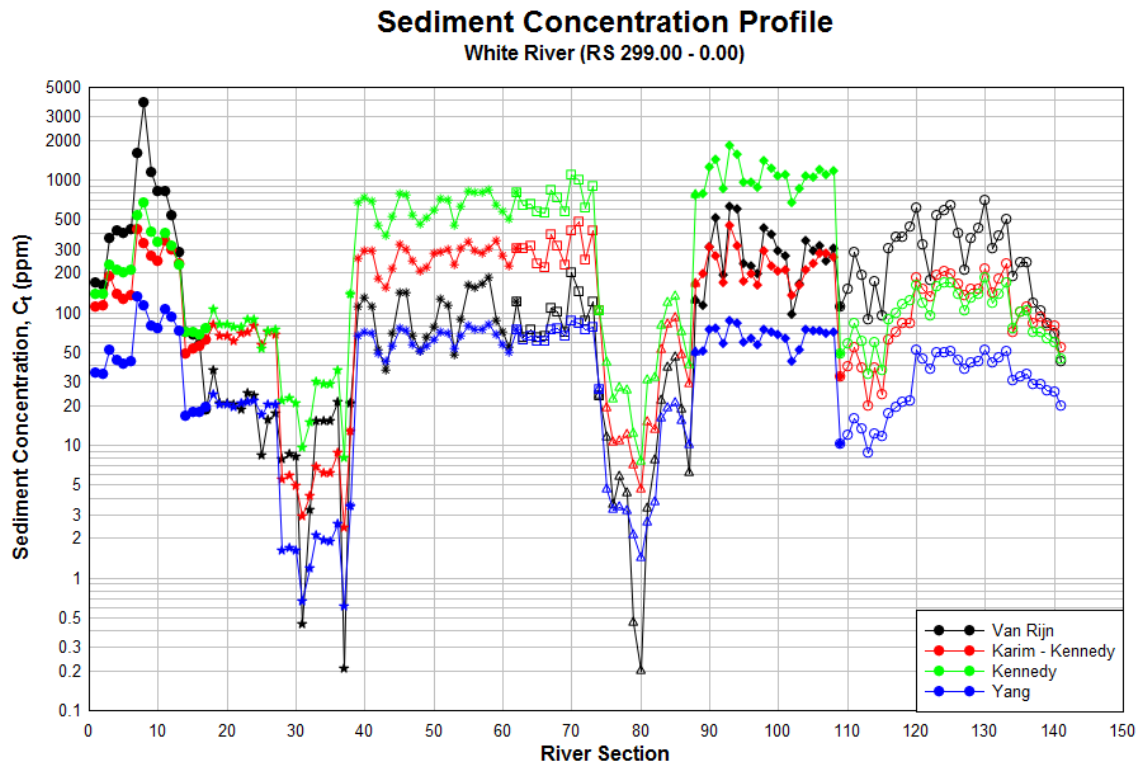


Figure 5.11. Total sediment Concentration for Batesville to LMR (RM 299.00 – 0.00).

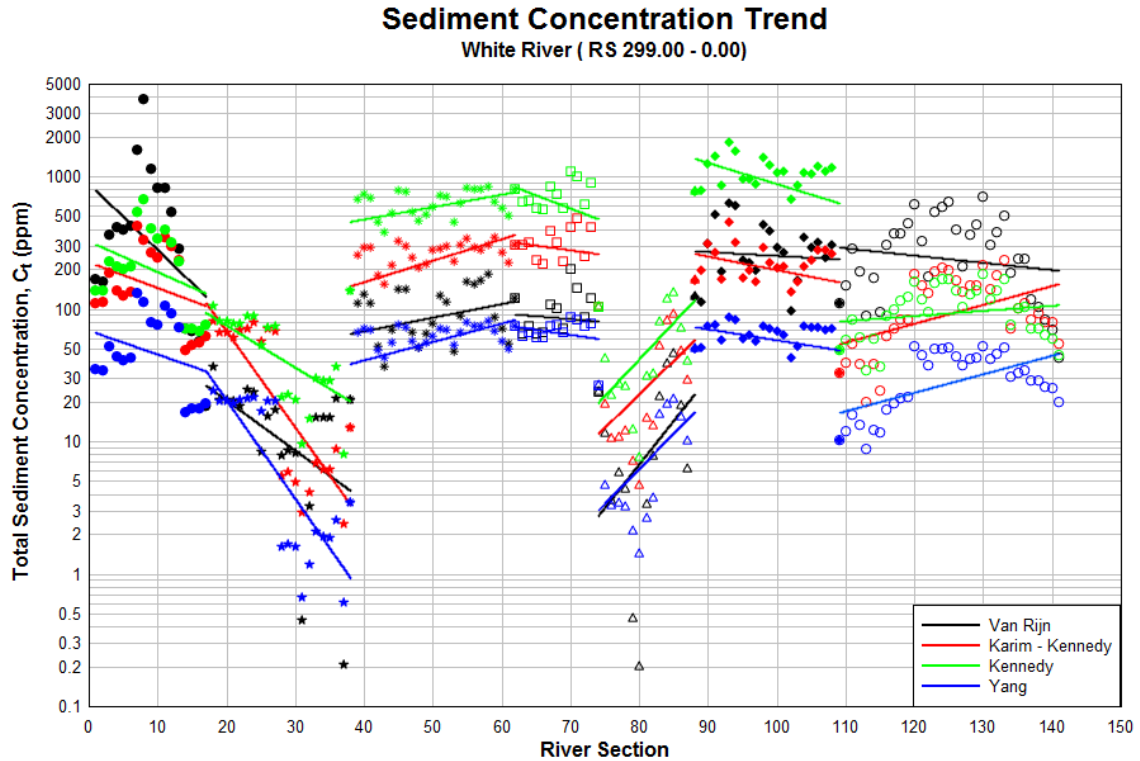


Figure 5.12. Sediment Concentration Trends for Various Sections from Batesville to LMR (RM 299.00 – 0.00).

Width to depth ratio versus bed-load and suspended-load discharges. When the products of bed-load and suspended-load discharges attained from the sediment analysis methods of Van Rijn and Kennedy are plotted against W/D ratio, the resulting correlations are shown in **Figure 5.13** and **Figure 5.14**. The bed-load discharge and W/D ratio clearly indicate an exponential growth relationship. The segments from Batesville to Newport and St. Charles to LMR appear to fall within the upper limits of W/D ratios and bed-load discharges while the segments from Newport to Augusta and Devalls Bluff to Clarendon appear to exhibit low magnitudes of W/D ratios and bed-load discharges as anticipated. The results of the sediment analyses, specifically the correlations between the dimensionless particle diameter d_* and the transport parameter T , suggest that the

segments from Batesville to Newport and St. Charles to LMR may be characterized by upper regime bedforms while the segments from Newport to Augusta and Devalls Bluff to Clarendon may be characterized by lower regime bedforms. The only conflicting attribute is that the segment from St. Charles to LMR, characterized by both lower and upper regime bedforms, only displays bed-load discharges within the upper limits of the W/D ratio versus the bed-load discharge correlation plot. Bed-load augmentation and a corresponding W/D ratio augmentation as indicated by the correlation plot suggest that high magnitudes of erosional activities of the banks contribute to much of the bed-load sediment load as the channel widens and loses its ability to entrain sediment. The suspended-load discharge versus the W/D ratio correlation plot indicates an increase in suspended-load until a critical W/D quantity of approximately 27.5, beyond which suspended sediment decreases rapidly. If the W/D ratio versus suspended-load correlation is legitimate regardless of longitudinal gradient, then from the Kennedy results substantial enhancements of W/D ratios for Clarendon to St. Charles would result in the settling of sediment and ultimately bed aggradation, and from the Van Rijn results further augmentations of W/D ratios for Clarendon to St. Charles and St. Charles to LMR would lead to similar outcomes. The correlation between suspended-load discharge to W/D ratio for both the Kennedy and Van Rijn methods reveal a considerable degree of sensitivity to the impact of W/D augmentations for the segments from Clarendon to St. Charles, and an inconsiderable degree of sensitivity for the segments from Batesville to Newport and Newport to Augusta. If the conjecture that high degrees of sensitivity in W/D augmentations connote high bank erodibility potentials is formulated, then a definite conclusion that the banks of the segments from Clarendon to St. Charles are highly

unstable could be made. It should also be noted that since high magnitudes of both bed-load and suspended-load discharges are shown in **Figure 5.13** and **Figure 5.14** for Clarendon to St. Charles, the potentials for bed aggradation (i.e., high sediment supplies) as well as lateral extension are significantly great for this segment. Furthermore, the demarcation line that defines the initial threshold when the channel begins to lose its ability to carry suspended sediment is represented by a critical W/D ratio of approximately 27.5, which could be perceived by the rapid diminishments of suspended-load and the dispersions of bed-load data points on the W/D ratio versus Bed-load discharge and W/D ratio versus Suspended-load discharge correlation plots, respectively.

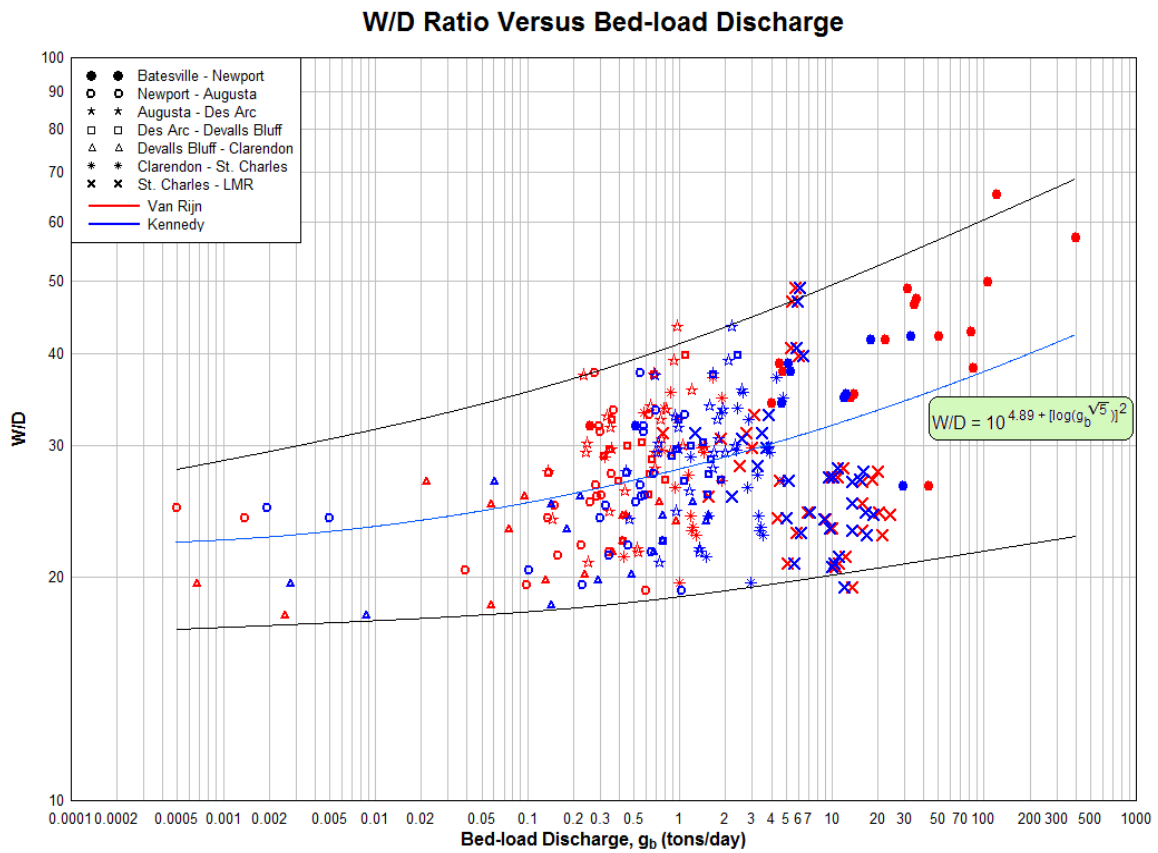


Figure 5.13. Correlation Plot of W/D Ratio Versus Bed-load Discharge.

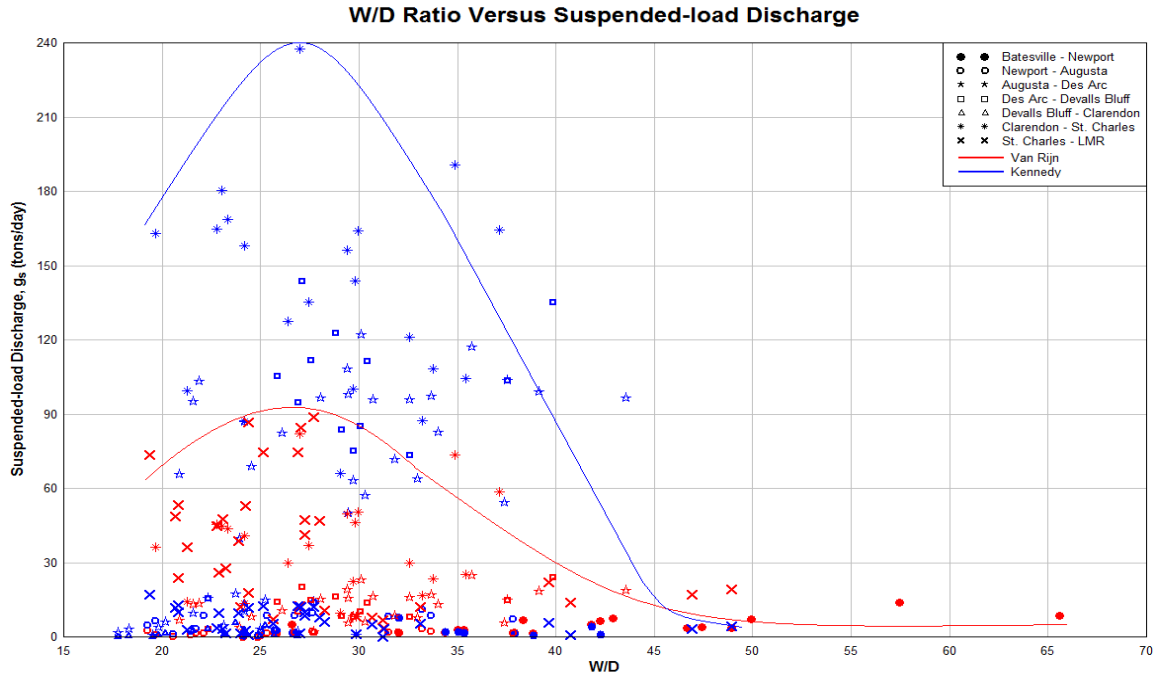


Figure 5.14. Correlation Plot of W/D Ratio Versus Suspended-load Discharge.

Channel dimensions versus sediment loads. Despite possessing differing levels of agreement regarding bed-load, suspended-load, and total load discharges to channel dimensions, a common theme evident from the correlation plots of sediment load types versus channel width, depth, and flow area is the high quantities of sediment within the reach from Clarendon to St. Charles. Irrespective of the sediment analysis methodologies implemented and the mild longitudinal gradient associated with the reach from Clarendon to St. Charles, channel width, depth, and flow area of this reach appear to promote significantly high quantities of bed-load, suspended-load, and total load. The correlation of channel width to suspended-load discharge indicates that high magnitudes of suspended-load fall within a channel width interval of approximately 450 to 675 feet. The Gaussian-like envelope curve that represents the trend of suspended-load with respect to the dispersion of channel width values also shows that optimum quantities of

suspended-load tend to cluster around a mean channel width interval of approximately 540 to 570 feet. The implication is that since this interval most likely signifies the threshold that separates the width range where the flow could sustain suspended sediments from the width range where suspended sediments begin to settle, the preponderance of width values within this critical interval implies that the banks and the bed of Clarendon to St. Charles are highly erodible, and should contribute to much of the suspended sediment entrained and conveyed within the channel. This conjecture is also confirmed by the high sediment concentration in the sediment profile plot as well as the velocity versus sediment concentration plots, which imply that high boundary susceptibility to change in velocity may result in substantial enhancement in sediment conveyance. Unlike the Gaussian-like curve for suspended-load, the envelope curves that represent the trend of bed-load within the reaches of the White River exhibit irregular patterns of fluctuation and attenuation in reaction to augmentations in channel width. One common theme is that, similar to the correlation plot of suspended-load versus channel width, the segment from Clarendon to St. Charles also exhibits substantially high amounts of bed-load sediment. The correlation plot, however, indicates several critical width intervals in colligation to high quantities of bed-load. The first critical width interval comprises widths ranging from 450 to 480 feet while the second critical width interval comprises widths ranging from 525 to 550 feet. The apexes of the magnitude of bed-load sediment not only occurred within these intervals solely for the segment from Clarendon to St. Charles, but also the segment from St. Charles to LMR. Since "bed-load [sediment] is more often associated with an energy limitation rather than a supply limitation" (Rosgen & Silvey, 1996, p. 7-3), great quantities of bed-load within the

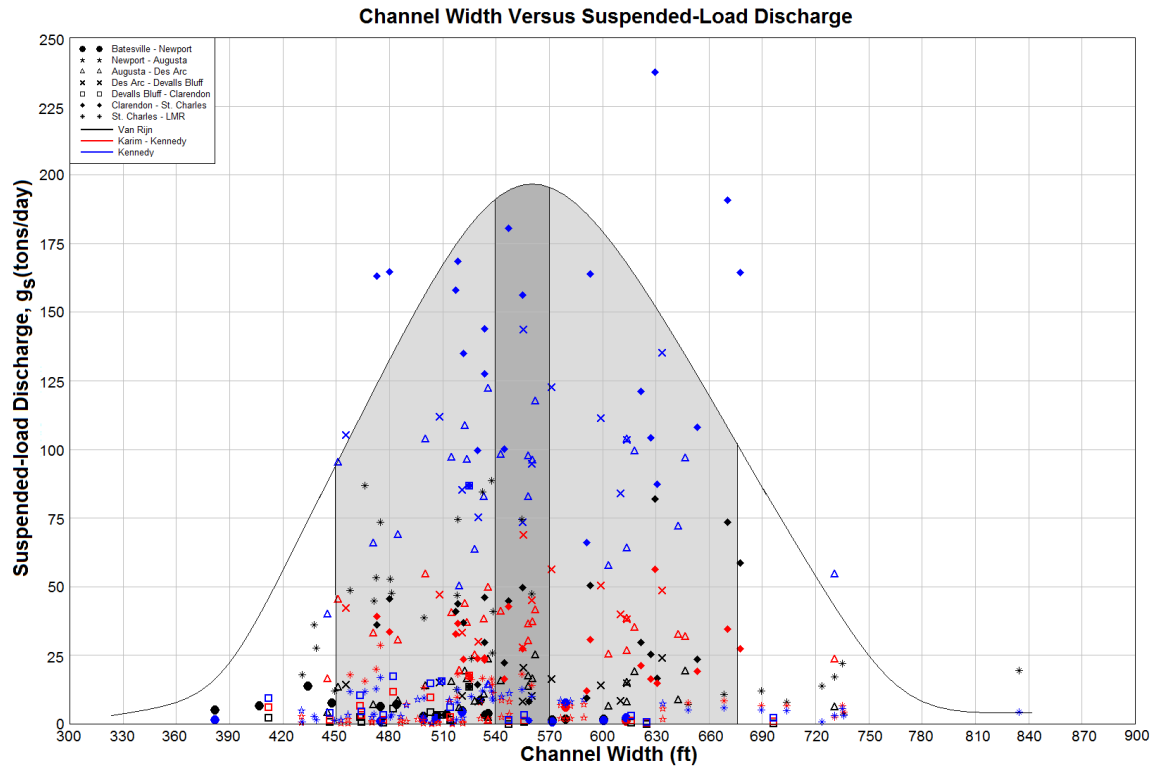


Figure 5.15. Correlation Plot of Channel Width Versus Suspended-load Discharge.

critical intervals of the aforementioned reaches indicate that these reaches lack the bed tractive force and stream power mandatory for the entrainment of finer and cohesive sediment particles supplied from bank erosion. The gentle longitudinal gradient and flow velocity identified with the reach from Clarendon to St. Charles corroborate the lack in strength of tractive force and stream power. It is certain that within this reach, an energy limitation would indicate an intermittent transport mechanism of fine sediment particles along the bed by sliding, rolling, and saltation. Extremely high amounts of bed-load and modest amounts of suspended-load for the reach from St. Charles to LMR, however, may be attributed to the tailwater influence from the Lower Mississippi River. The product of the longitudinal gradient and velocity, or stream power, is adequate to keep non-cohesive sediment particles suspended while the tailwater effect limits the transportation and

entrainment of finer cohesive particles within the flow. Contrary to the presumption that high quantities of bed-load would correspond to low quantities of suspended-load and vice versa, virtually identical critical width intervals for high magnitudes of bed-load and suspended-load suggest that the reach from Clarendon to St. Charles may be characterized by both intermittent mechanism of fine grain movement and continuous mechanism of coarse grain movement. In simple terms, highly erodible banks and inadequate stream power within the reach from Clarendon to St. Charles constitute high bed-load discharges of fine cohesive materials and high suspended-load discharges of non-cohesive materials. Therefore, optimum magnitude of the total sediment load is also observable for Clarendon to St. Charles in the channel width versus total sediment discharge plot as well as the sediment profiles.

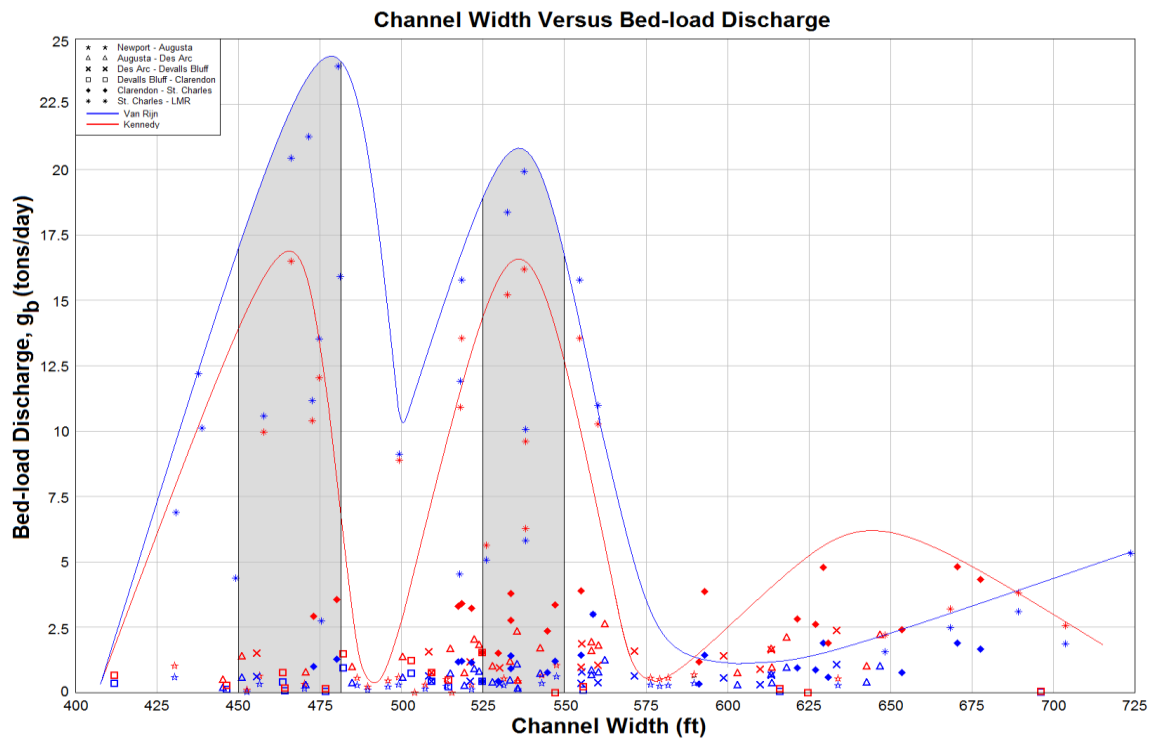


Figure 5.16. Correlation of Channel Width Versus Bed-load Discharge.

The correlations of maximum channel depth to suspended-load discharge and maximum channel depth to bed-load discharge also reveal high quantities of sediment load for the reaches extending from Clarendon to St. Charles and St. Charles to LMR. A Gaussian-like envelope curve that represents the correlation between channel depth and suspended-load depicts optimum magnitudes within a depth interval of approximately 27 to 33 feet. Since higher depth values correspond to greater shear stresses exerted on the surface areas of the channel boundary, specifically the left and right banks of the channel, the critical channel depth interval of 27 to 33 feet likely symbolizes the instances when near bank stresses exceed the bank flow resistance capability, thus resulting in erosion of the banks. The threshold is also speculated to represent the instance when velocity, hence stream power, is maximum. Beyond this range on either side, attenuations in the suspended-load discharge are visible. Irrespective of channel materials that make up the banks and the width of the channel, the reach from Clarendon to St. Charles clearly exhibits the highest frequency of depth values that fall within this range. Unlike the Gaussian-like curve that represents the correlation of channel depth and suspended-load, the curves that represent the relationship between channel depth and bed-load possess a diminishing pattern accompanying an augmentation in channel depth values. The reach from Clarendon to St. Charles still demonstrates a significant amount of bed-load with respect to channel depth although not quite as profound as St. Charles to LMR. Due to the presence of extremely high amounts of bed-load and modest amounts of suspended load within the critical depth interval of 27 to 33 feet and high longitudinal gradient and velocity characteristic of the reach, the conjecture made in regard to the tailwater influence from the Lower Mississippi River is further proof that explicate the limitations

induced on the transportation and entrainment of materials eroded from the banks of St. Charles to LMR.

Flow area versus bed-load discharge, suspended-load discharge, and total load discharge appear to match the curves associated with the relationships among depth and width to said sediment load types. Disregarding the influence of the longitudinal gradient and radius of curvature, a common theme shown by various correlation curves is the promotion of high sediment loads and high bed-loads by the dimensions associated with the reach from Clarendon to St. Charles and St. Charles to LMR, respectively. A critical flow area of approximately 10,000 to 12,000 square feet appears to depict optimum quantities of bed-load, suspended-load, and ultimately the total sediment load. One perceptible feature is a jump in the total sediment discharge for the flow area equivalent

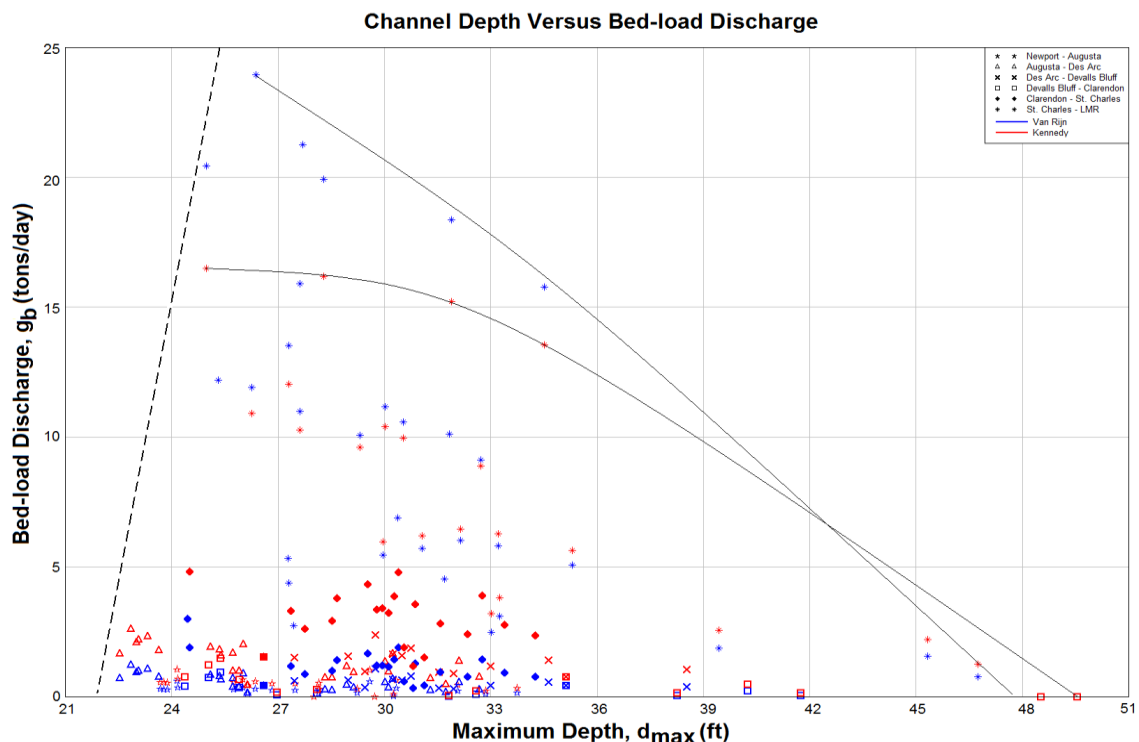


Figure 5.17. Correlation of Maximum Channel Depth Versus Bed-load Discharge.

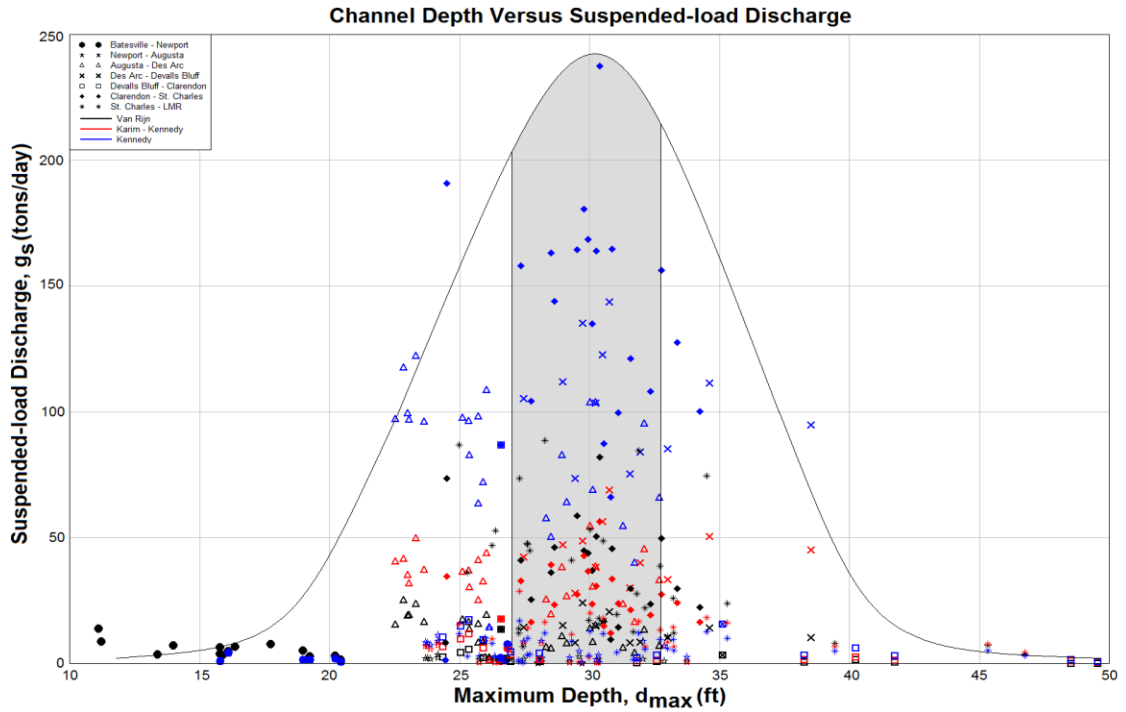


Figure 5.18. Correlation of Maximum Channel Depth Versus Suspended-load Discharge.

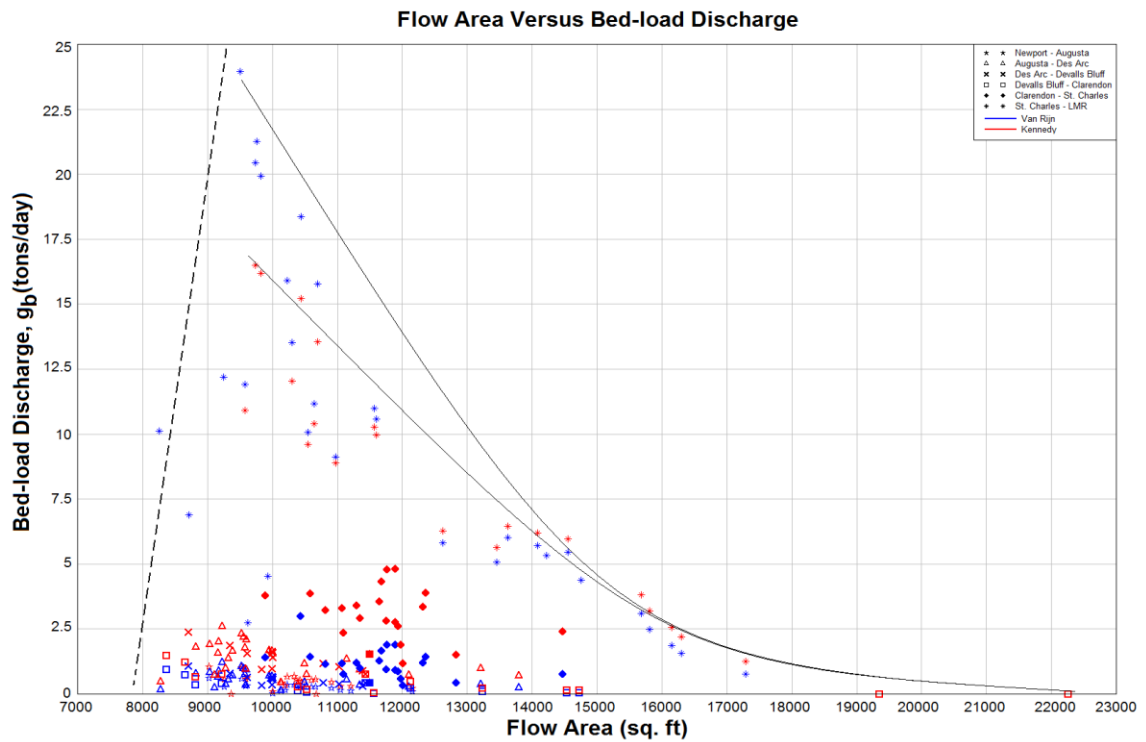


Figure 5.19. Correlation of Flow Area Versus Bed-load Discharge.

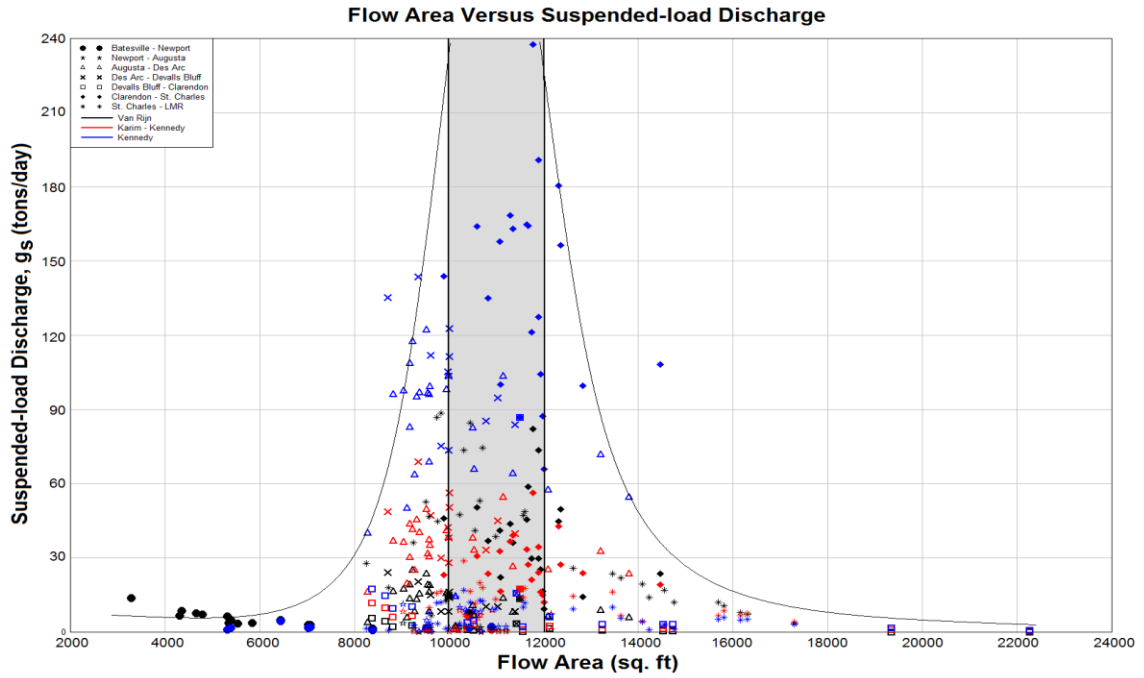


Figure 5.20. Correlation of Flow Area Versus Suspended-load Discharge.

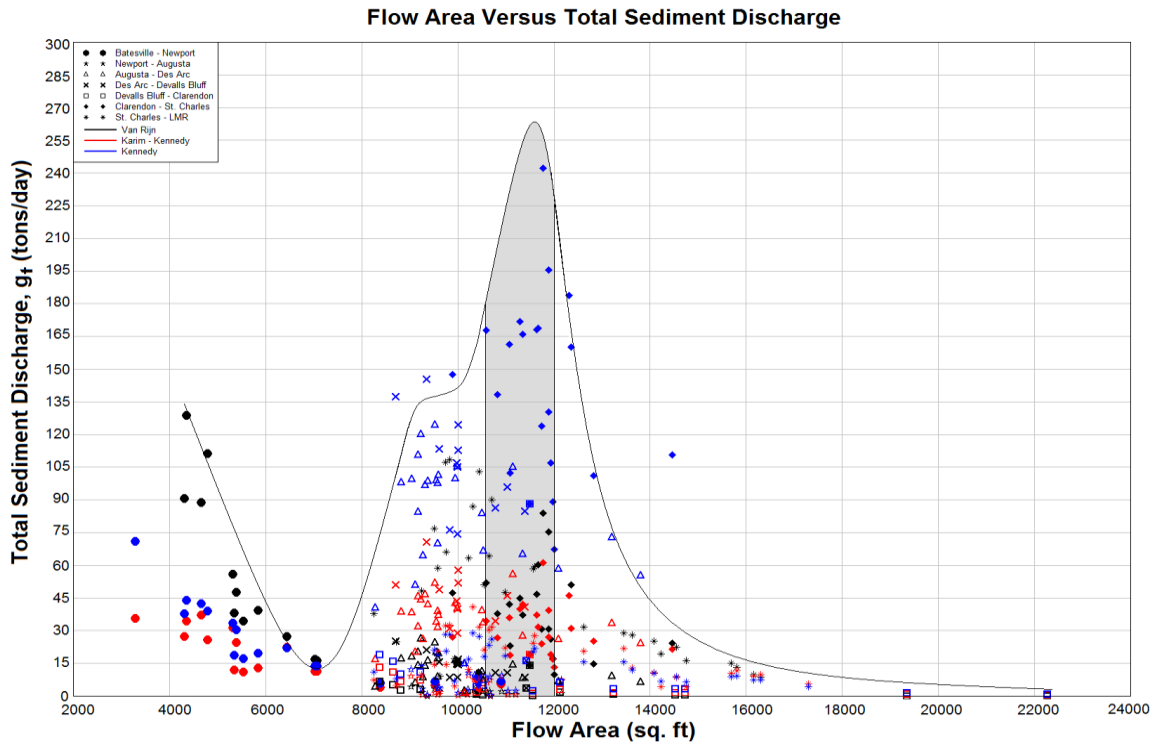


Figure 5.21. Correlation of Flow Area Versus Total Sediment Discharge.

to 9,000 square feet. It is speculated that this jump represents a sudden change in the longitudinal gradient at Clarendon, which may be attributed to deposition of sediment eroded and transported from the Cache River.

Curvature versus total sediment concentration. The confirmation that optimum magnitudes of sinuosity and lateral migration tend to fall within a specific radius of curvature interval of approximately 1500 to 2000 feet is further reinforced by correlating radius of curvature to the total sediment concentration obtained from various sediment analysis methodologies. The average curve of all methodologies implemented, such as Van Rijn, Yang, Karim-Kennedy, and Kennedy, shows that substantial quantities of sediment load occur within a radius of curvature interval of 1000 to 1800 feet. Beyond this range on either side, attenuations in the total sediment concentration are visible. Since the majority of radii of curvature that fall within the demarcation lines of this interval are associated with the reaches from St. Charles to LMR, Devalls Bluff to Clarendon, and Batesville to Newport, which were previously discovered to exhibit highest frequencies of sinuosity quantities above 1.5, their boundaries must generally exhibit high degrees of susceptibility to variations in flow and velocity. Quantities of total sediment concentration that reflect channel boundary sensitivity to non-uniform circulation that directs rapid flowing water to the concave bank and sluggish water to the convex bank may be attributable primarily to the angle by which the advancing circulation makes with the concave bank, or the angle by which the undulating thalweg makes with the concave bank. It is speculated that, for the radii of curvature that occupy the range from 1000 to 1800 feet, the angle by which the advancing circulation makes with the concave bank may represent the critical value at which boundary resistance is

minimal or that the exerting outer-bank radial force is optimal, thus resulting in high quantities of total sediment concentration shown for the aforementioned reaches. Because high quantities of total sediment concentrations are derived from the channel boundary and that they signify high frequencies and magnitudes of erosion and deposition, discrepancies in channel dimensions for the reaches from St. Charles to LMR, Devalls Bluff to Clarendon, and Batesville to Newport are also anticipated. The deviation of channel dimensions from the radius of curvature versus channel dimensions (i.e., the cross-sectional area, the channel width, and the mean depth) plot in **Figure 3.20** verified the previous speculation. Specifically, and in conjunction to the results of sediment analyses as shown by the sediment rating curves, high quantities of total sediment concentration for the reach from Batesville to Newport consist predominantly of gravel bed-load while high quantities of total sediment concentration for the reaches from Devalls Bluff to Clarendon and St. Charles to LMR consist predominantly of suspended-load discharge and mixed-load discharge, respectively. The implication is that for the section from Batesville to Newport, where the banks exhibit an overall moderate erodibility potential, channel dimension discrepancies are not solely attributable to bank or bed instability but rather a turbulent crooked flow and a structurally controlled boundary. Conversely, for the segments from Devalls Bluff to Clarendon and St. Charles to LMR, where sediment supply competency preponderates sediment transport capacity, channel dimension discrepancies are attributable to high bank erodibility potential, most of which contribute to the high sediment concentrations shown within the critical radius of curvature interval of **Figure 5.22**.

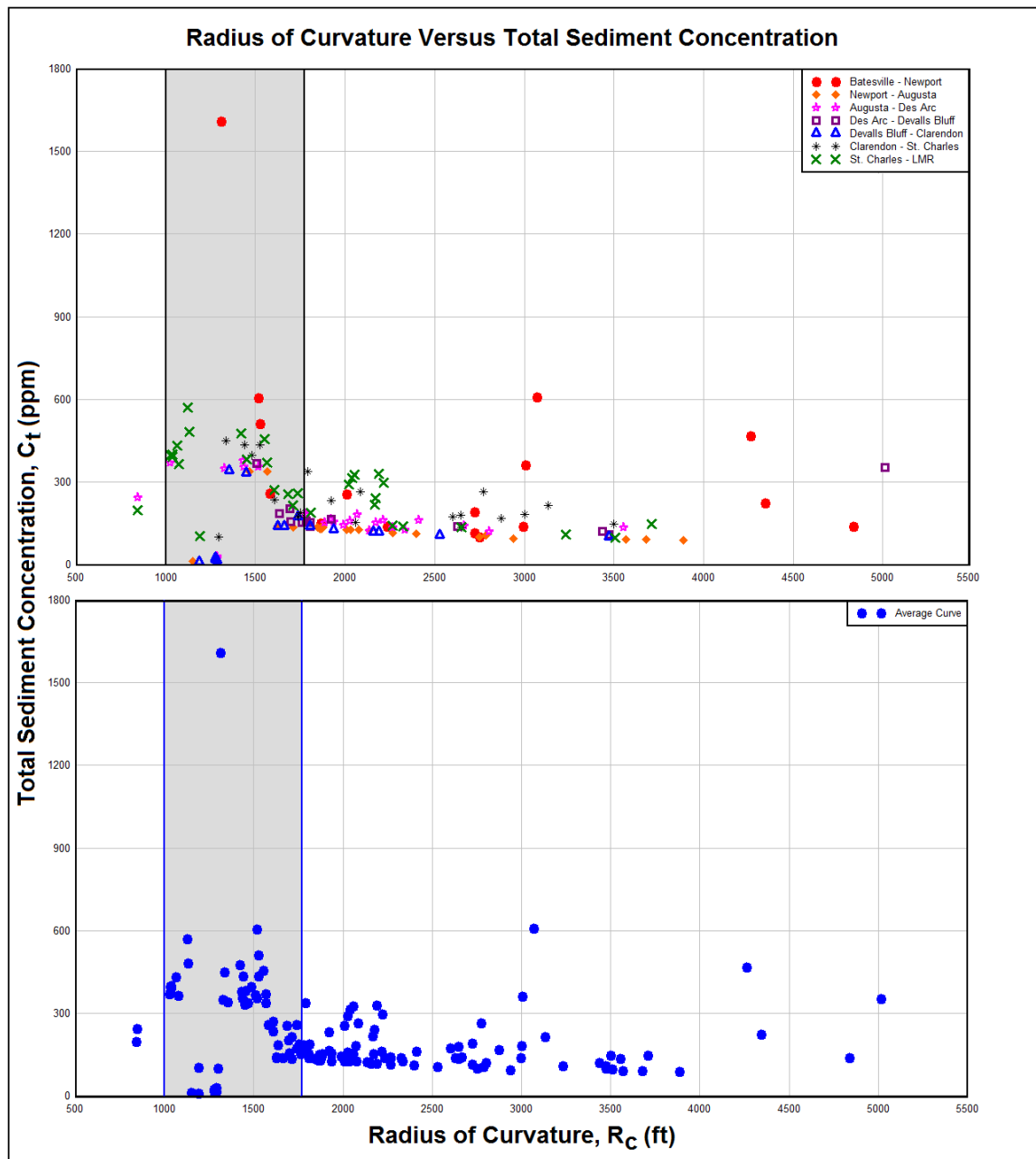


Figure 5.22. Correlation of Radius of Curvature Versus Total Sediment Concentration.

Velocity versus total sediment discharge. Since the augmentations of erosional and depositional activities are often colligated with velocity, the amount of sediment loads transported or entrained in a fluvial system must also conform to fluctuations of

velocity within various localities of the system. The correlations of the total sediment discharges attained from the methodologies of Van Rijn and Kennedy and the velocity data exported from simulations of the HEC-RAS Model indicate functions in which the total sediment loads, denoted as g_b , are proportional to powers of the velocities. The power function relationships apparent for various reaches of the White River not only provide concrete evidence that velocity augmentation complements sediment discharge enhancement, but also the degree of susceptibility to velocity alteration. Although the level of agreement regarding sediment load susceptibility to velocity alteration may vary between the subsequent plots, which are derived from utilizing the results of two separate sediment analysis methodologies, it is evident from both correlation plots that the reaches from Clarendon to St. Charles and Devalls Bluff to Clarendon exhibit highest and lowest sensitivity to changes in velocity, respectively. The implication is that for the reach from Clarendon to St. Charles, a modest alteration in velocity can trigger a considerable change in the total sediment amount conveyed within the channel. The justification is that for this particular segment, the banks and bed are highly unstable that any increase in velocity can result in a substantial enhancement in sediment conveyance, significant amounts of which may include sediment loads migrated from upstream as well as sediments contributed by the Cache River. High sediment concentration in the sediment profile also affirms the high erodibility potential of the bed and the banks within this segment. Conversely, for the reach from Devalls Bluff to Clarendon, velocity alteration contributes to an insignificant change in the quantity of sediment conveyed within the channel. Seemingly conflicting discoveries that arose from examining the velocity versus total sediment discharge correlation plots and the meander area histograms for the section

from Devalls Bluff to Clarendon are (1) velocity has little significance on sediment loads and (2) optimum rate of erosion and deposition occurred within this section. One explanation is that the banks are dominant and frequent contributors of sediment supply while the bed, in conjunction with an extremely flat longitudinal gradient, are undergoing aggradation. A prerequisite for bed aggradation is tantamount to the preponderancy of sediment supply competency over sediment transport capacity as illustrated previously by the sediment rating curve and the sediment concentration trend. A reduction in the channel's ability to transport sediment in addition to a mild gradient and excessive bank erosion, therefore, explicate the notion that within the channel of this section the effect of velocity on total sediment load is negligible despite the channel possessing high magnitudes of erosion and deposition. A similar, yet simplistic, explanation is that the static flow conditions responsible for the formation of ripple patterns, are inadequate to filter much of the excessive sediments eroded from the banks, thus resulting in settling of the sediments to the channel bed. Verification of this conclusion can be perceived from the transport parameter versus dimensionless particle diameter plot, the sediment rating and sediment trend curves, and the plots of W/D ratio versus bed-load and suspended-load discharges. The most convincing validation involves the relatively low magnitudes of W/D ratios as well as the lack of a dominant particle size within the bed (i.e., from the particle size distribution curve) of this section. In addition, the lack of a dominant particle size within the bed also signifies that although the channel exhibits a higher suspended-load discharge, an abundant amount of sediments that settles to the bed are composed of cohesive materials such as silts and clays. Furthermore, the verifiable truth that silts and clays require a greater velocity to be entrained into the flow (because of their cohesive

characteristics) enhances the probability that the section from Devalls Bluff to Clarendon is actually experiencing bed aggradation. Finally, it should be noted that, in many studies, a lack of a dominant particle size has also been linked to high sinuosity ratios and lateral extensions.

Shear force versus total sediment concentration. Derived based on the principle of conservation of momentum, shear stress is a parameter that represents the force exerted on the boundary of a channel by fluid in motion. The consideration of such force on the banks and the bed of the channel makes shear force a viable predictor for erosion potential. Shear force, therefore, is subsequently plotted against the total sediment concentration to affirm the sensitivity of the banks and bed to moving water for various reaches of the White River. Although the level of agreement regarding sediment concentration to shear stress enhancement may differ between the various sediment analysis methodologies implemented, a common theme evident from the correlation plot is the high and low degrees of channel boundary sensitivity for the reaches from Clarendon to St. Charles and Devalls Bluff to Clarendon, respectively. The steepness of the correlation plot indicates that for the reach from Clarendon to St. Charles, where the shear stress exerted on the channel boundary likely exceeds the resisting critical shear stress that the boundary possessed, the augmentations of erosional and depositional tendencies are highly probable. Previously, a high degree of instability in the banks and bed within this reach had also been confirmed by the high magnitude of sediment concentration in the sediment profile plot as well as the acute responsiveness in sediment load discharge to velocity enhancement. As for the reach from Devalls Bluff to Clarendon, where a reduction in the ability to transport sediment is apparent and the

Velocity Versus Total Sediment Discharge Van Rijn Results

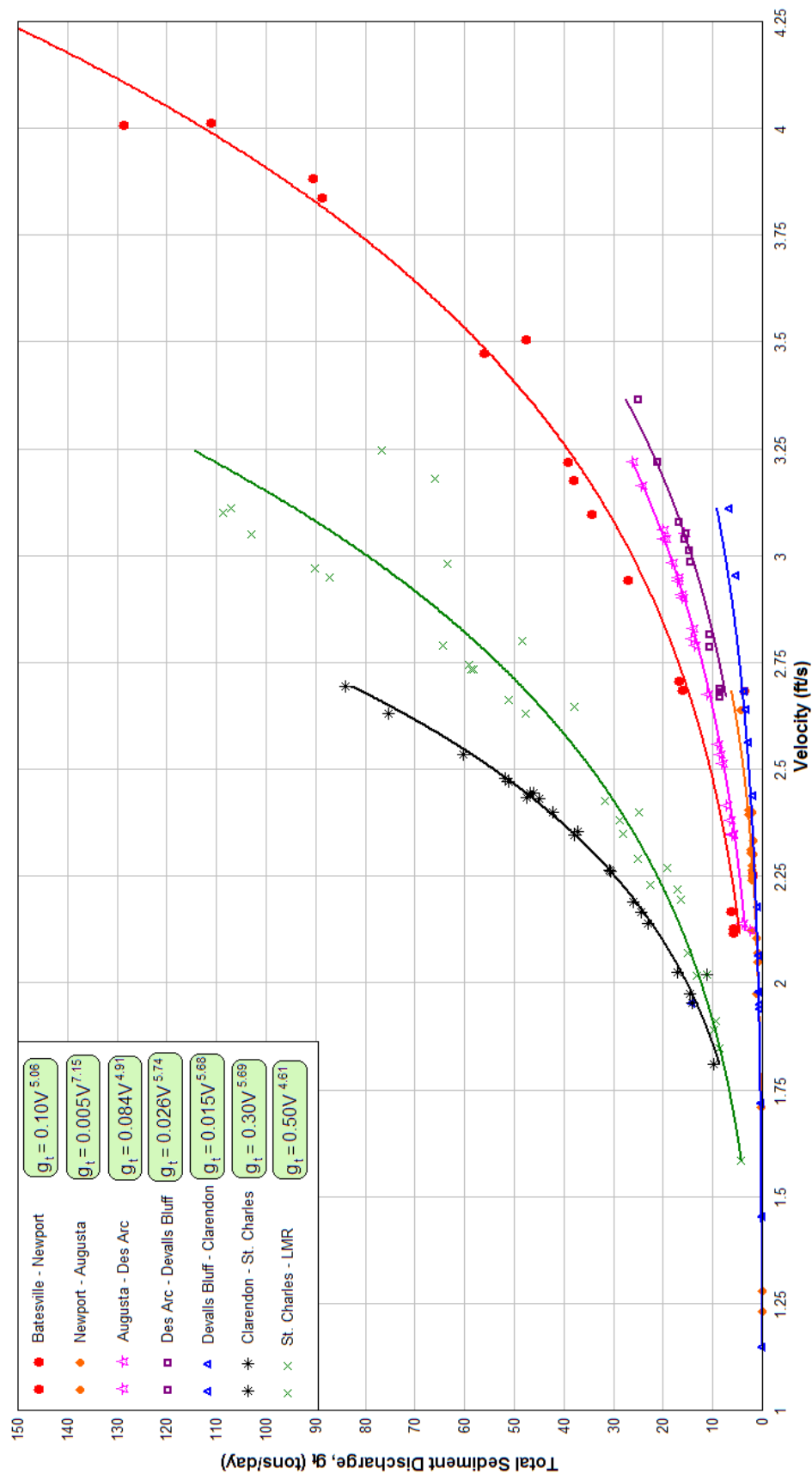


Figure 5.23. Correlation of Velocity Versus Total Sediment Discharge (Van Rijn Results).

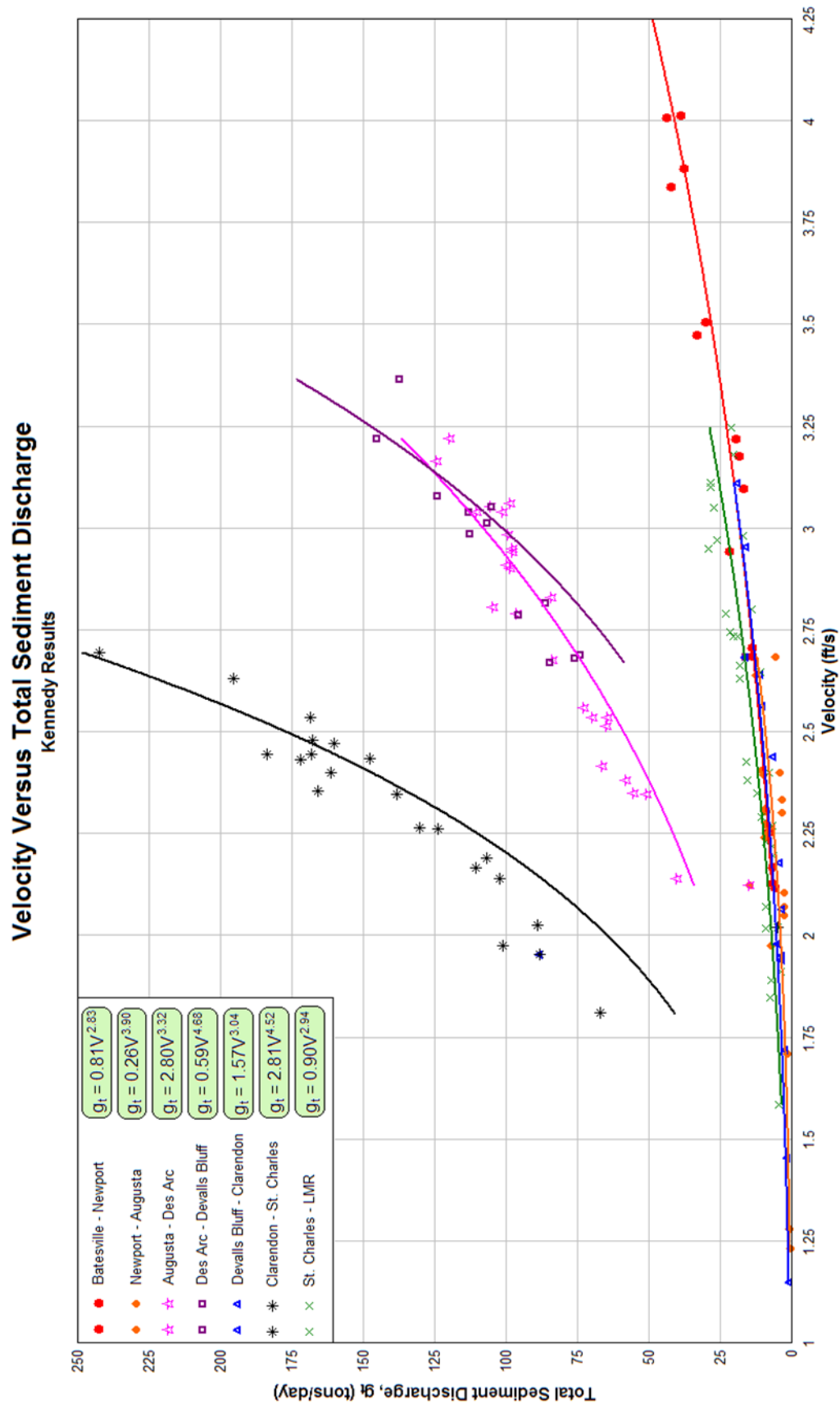


Figure 5.24. Correlation of Velocity Versus Total Sediment Discharge (Kennedy Results).

velocity in the channel has been shown to be indifferent to erosion and deposition, the total sediment concentration's unresponsiveness to shear stress alteration are primarily attributable to a mild longitudinal gradient and low stream power. Despite possessing an overall insusceptibility to shear stress fluctuation, much of the high magnitudes of erosion and deposition within this section as shown by the meander area histograms are derived from sediment eroded from the banks. Since exhibiting a low longitudinal gradient and stream power, the primary mechanism of excess energy dissipation for the section from Devalls Bluff to Clarendon involves undulation of the flow. The wavelike motion of the flow, analogous to the principle of centrifugal force, allows the channel to dissipate excess energy by directing higher shear stresses toward the outside of the bend. This form of energy dissipation, although not exuberant, is responsible for the highly tortuous planform (i.e., sinuosity) that the section exhibits. As the sinuosity increases or the radius of curvature diminishes, contributed partly due to the preponderancy of sediment supply competency over sediment transport capacity or bed aggradation in addition to undulating flow, the effect of the shear stress exerted on the outer bank is further enhanced. In a simplistic context, as the bend becomes sharper the friction between the water and the outer river banks reduces, thus increasing the velocity and shear stress effects on the outer banks. Specialized bank erosion potentials and near bank shear stresses for various reaches of the White River are included in the third hierarchical level of the Rosgen Stream Classification System and are presented in chapter 4.

Sediment Load Rankings and Their Implications

Since the sediment analysis methodologies are derived from different data, conditions, and assumptions, the magnitudes of bed-load, suspended-load, and total load

Shear Force Versus Total Sediment Concentration

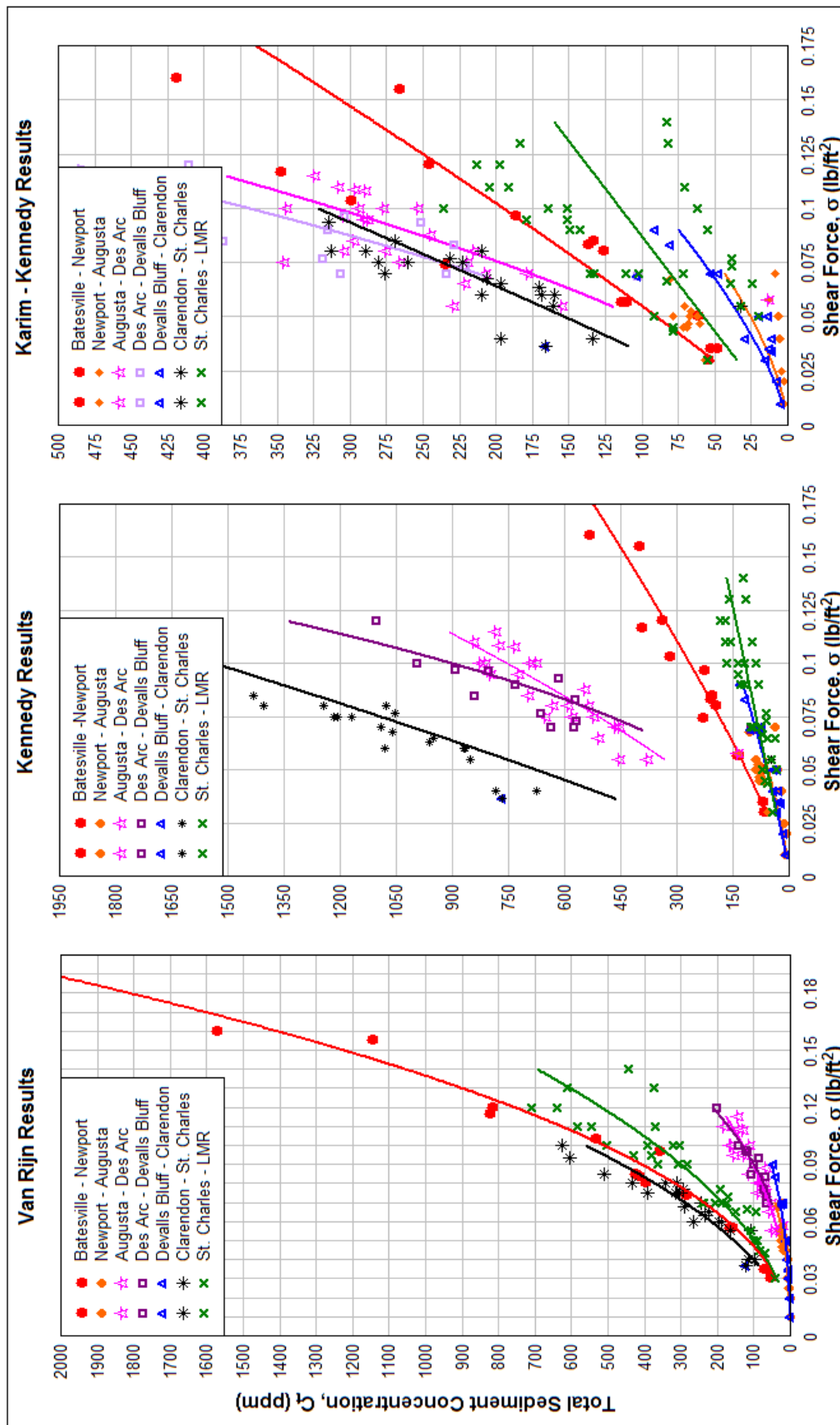


Figure 5.25. Correlation of Shear Force Versus Total Sediment Concentration.

discharges resulting from the implementations of these methodologies are marked by dissimilarities. Rankings of the sediment loads for various reaches of the White River reveal that the highest quantities of bed-load, suspended-load, and total-load do not always occur within the reaches from Clarendon to St. Charles nor St. Charles to LMR for the various methodologies implemented. For example, bed-load and total-load for the reaches from Des Arc to Devalls Bluff and Augusta to Des Arc from Karim-Kennedy and Kennedy methods ranks first and second, respectively, in comparison to other reaches. Because of the divergence among the ranks and magnitudes of sediment load types of various methodologies, the correlation plots of channel dimensions versus sediment quantities may appear to imply that reaches like Batesville to Newport, Augusta to Des Arc, or Des Arc to Devalls Bluff possess sediment loads equivalent to or greater than Clarendon to St. Charles and St. Charles to LMR. This misconception is countered by averaging the ranks among the methodologies to determine an overall rank representative of individual reaches. From this ranking scheme, the two reaches that possess the greatest amounts of sediments for all methodologies are Clarendon to St. Charles and St. Charles to LMR. In addition to what is shown by the correlation plots between channel dimensions and sediment load types as well as the sediment profile and trend plots, the cumulative ranking of the results obtained from various methodologies also reveal a generally high amount of sediment for the reach from Des Arc to Devalls Bluff. Since the mean channel width value of this reach is equivalent to the median of the critical width interval depicting optimum suspended-load, sediment transported and entrained within this reach is considered purely width-related. As for the reaches from Clarendon to St. Charles and St. Charles to LMR which exhibit an average depth and

width proximal to the median of the critical suspended-load width interval and the critical channel depth interval, sediment conveyance within these reaches is deemed width-related and depth-related, respectively. The confirmation that the channel dimensions of Clarendon to St. Charles, St. Charles to LMR, and Des Arc to Devalls Bluff promote significantly high quantities of bed-load, suspended-load, and ultimately total load are reinforced by these findings.

Table 5.2. Rankings of Bed-load, Suspended-load, and Total Sediment Discharges for Various Reaches of the White River.

Section (RM 299.90 – 0.00)	Van Rijn Method			Karim-Kennedy Method			Kennedy Method		
	g_b	g_s	g_t	g_b	g_s	g_t	g_b	g_s	g_t
	(rank)			(rank)			(rank)		
Batesville-Newport	1st	5th	1st	1st	7th	5th	1st	7th	4th
Newport-Augusta	3rd	7th	7th	7th	6th	7th	7th	6th	7th
Augusta-Des Arc	4th	4th	5th	4th	2nd	2nd	4th	3rd	3rd
Des Arc-Devalls Bluff	5th	3rd	4th	5th	1st	1st	5th	2nd	2nd
Devalls Bluff-Clarendon	6th	6th	6th	6th	5th	6th	6th	4th	6th
Clarendon-St. Charles	3rd	1st	3rd	3rd	3rd	3rd	3rd	1st	1st
St. Charles-LMR	2nd	2nd	2nd	2nd	4th	4th	2nd	5th	5th

Erosional and Depositional Activities

Albeit a dearth of quantitative information on the lateral migration rates, the physical manifestations of erosional and depositional activities within the meander bends of the White River are connected to sinuosity augmentations and lateral migrations perceived through the superimposition of aerial photographs on quadrangle maps. Meander areas are determined via ArcGIS by drawing and attributing polygons of the areas formed when the channel expands, constricts, or migrates laterally. Approximately 600 polygons are drawn and areas computed to represent the erosion and deposition of

sediment particles transported by the flow. The net eroded areas and deposited areas are tabulated, and subsequently plotted as bar histograms, to represent individual sinuosity sections. The examination of the meander histograms reveal an overall dominance of erosional activities within various reaches of the White River. The maximum values of eroded and deposited areas, hence optimum degree or rate of erosion and deposition, appear to occur from Des Arc to Devalls Bluff and Devalls Bluff to Clarendon. It is indubitable that, for the reach from Devalls Bluff to Clarendon, the maximum extent of erosion dominance is manifested in the disparities between eroded meander areas and deposited meander areas. The reaches from Augusta to Des Arc and Clarendon to St. Charles, despite displaying lower magnitudes of eroded and deposited areas, also exhibit disparities nearly equivalent and comparable to the segment from Devalls Bluff to Clarendon. Disparities in meander areas for the reaches are indicators of an imbalance or disequilibrium in the mechanisms of erosional and depositional activities. The primary constituent responsible for the disequilibrium of erosional and depositional activities is speculated to be bank instability. The reaches that exhibit higher degrees of balance between erosion and deposition include St. Charles to LMR and Newport to Augusta. Higher frequencies of deposition dominance are also seen in several sections within these reaches. For the upper portion of the reach from Newport to Augusta that possesses multiple sections exhibiting a dominant characteristic of deposition, it is suspected that a substantial quantity of sediment is contributed by the Black River. As the White River abruptly changes into a lowland river near the confluence with the Black River, an abrupt diminishment in the longitudinal gradient suggests a deduction in the ability to transport sediment, thus resulting in deposition of sediments from upstream. A dominant

characteristic of deposition for various sections along the lower portion of St. Charles to LMR are attributable to the tailwater of the Lower Mississippi River. Significant disparities between deposition and erosion meander areas for an individual section also denote changes in width. Specifically, a section exhibiting a high erosion histogram and a low deposition histogram is anticipated to be undergoing channel widening, a section possessing a low erosion histogram and a high deposition histogram is likely undergoing channel narrowing, and a section with nearly equivalent erosion and deposition histograms likely possess stability of width.

Table 5.3. Ranking of Erosional and Depositional Magnitudes of Various Reaches.

Sections	Erosion (yd²)	Rank	Deposition (yd²)	Rank	$\Delta(E-D)$ (yd²)	Rank
Batesville-Newport	102268	4th	74668	4th	27600	4th
Newport-Augusta	86403	7th	72334	5th	14069	6th
Augusta-Des Arc	109606	3rd	57859	6th	51747	2nd
Des Arc-Devalls Bluff	120022	2nd	94088	1st	25934	5th
Devalls Bluff-Clarendon	141572	1st	83056	2nd	58516	1st
Clarendon-St. Charles	90312	6th	53775	7th	36537	3rd
St. Charles-LMR	90685	5th	79917	3rd	10768	7th

Specific energy versus erosion and deposition and lateral migrations. The confirmation that high total flow energy is tantamount to highly sinuous meandering bends is further reinforced by correlating mean specific energy to the magnitudes of lateral migrations and erosional and depositional activities attained from the superimpositions of aerial photographs on quadrangle maps through ArcGIS data attributing and extraction processes. Similar to the relationship between mean specific energy and average sinuosity that yields a wavelike pattern forming a cubic polynomial

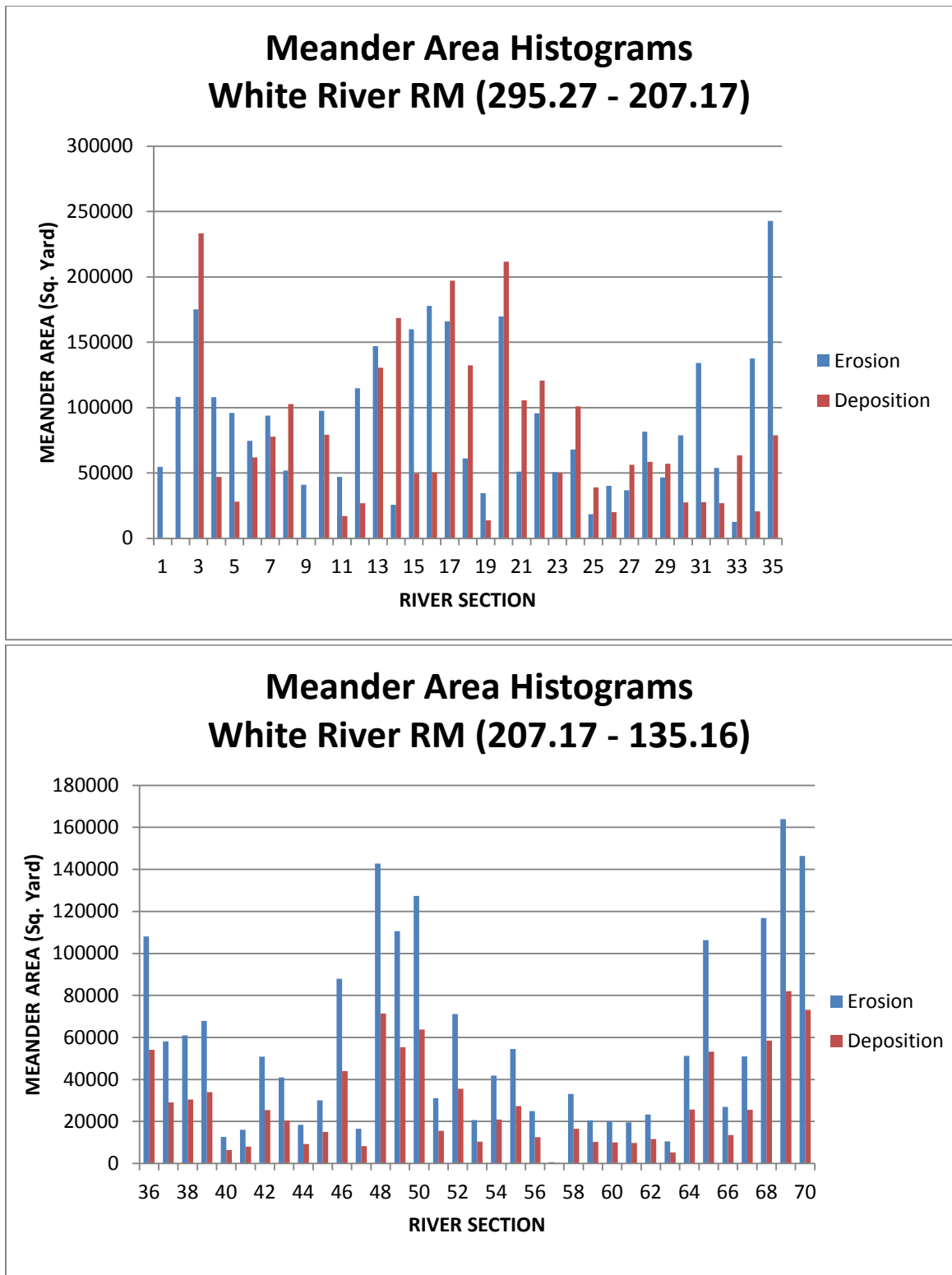


Figure 5.26. Meander Area Histograms (RM 295.27 – 135.16).

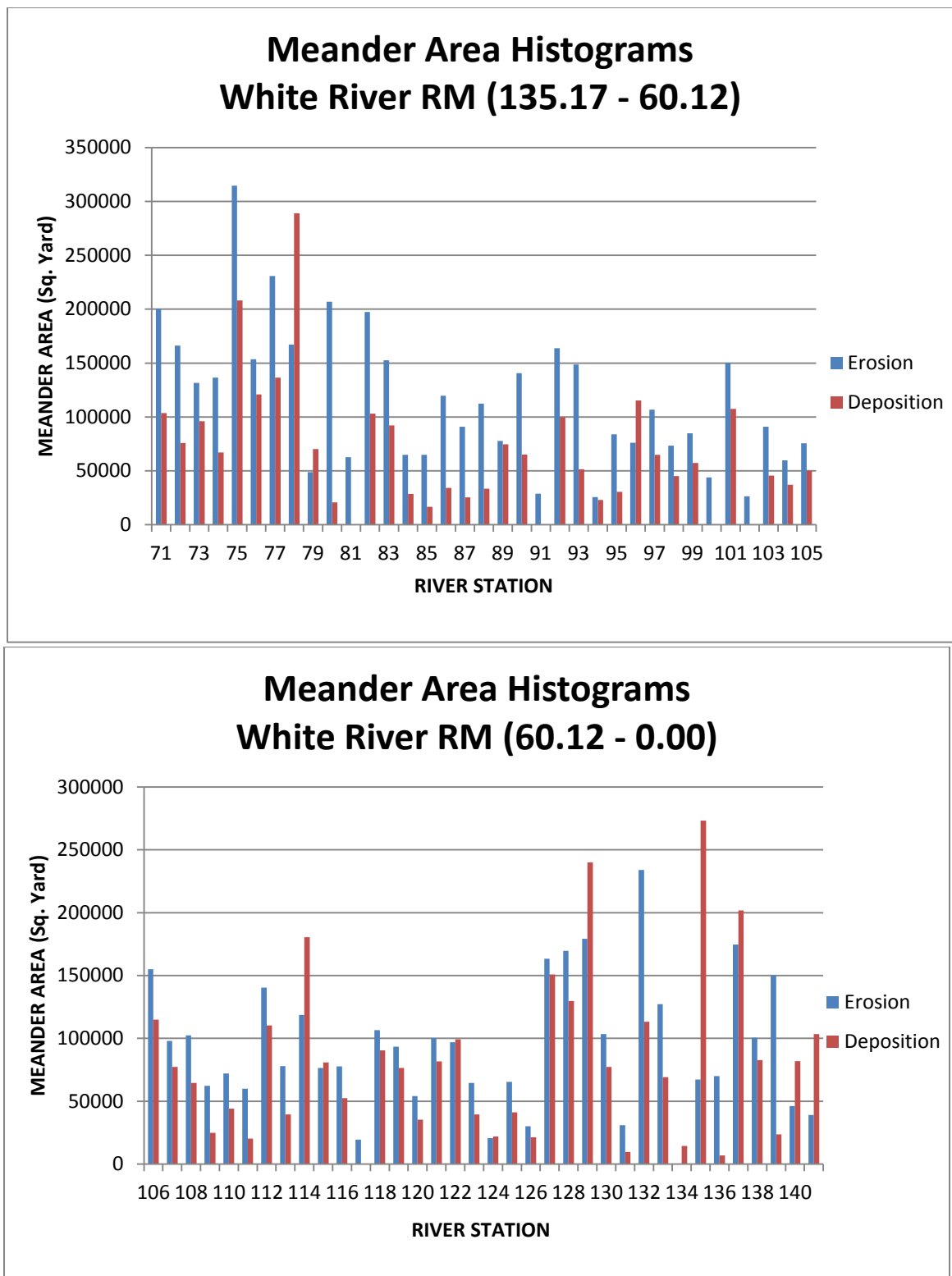


Figure 5.27. Meander Area Histograms (RM 135.16 – 0.00).

function, the correlations involving specific energy and lateral bank retreats and specific energy and erosion and deposition of sediment particles are also characterized by cubic functions illustrating prevalent trends denoting significant augmentations in lateral channel migrations and erosion and deposition proclivities as the mean specific energy increases. The steep acclivities associated with alluvial reaches possessing high magnitudes of mean specific energy and substantial magnitudes of migrations and sediment particle displacements, or reaches downstream of Des Arc that reside within the swamp lands of the alluvial floodplain, appear to reflect the distributions of potential and kinetic energy within the channel of these reaches. Since the channel of the reaches that occupy the swamp lands of the Mississippi Alluvial Plain physiographic region generally possess higher average depth or mean depth exceeding upstream reaches, which subsequently implies a preponderance of potential energy over kinetic energy within the context of total flow energy or specific energy, a product of the sum of a potential energy term and a kinetic energy term, these reaches, therefore, likely feature a dearth of an effective and exuberant mode of excess energy dissipation and, thus, energy expenditure by means of thalweg undulation or flow vacillation and bedform oscillations are inherent. Implications of this inference are especially apparent for the channels of reaches occupying the regions extending from Des Arc to Devalls Bluff and Devalls Bluff to Clarendon as these sections are distinguished by very high maximum depths representing low channel bed datum elevation or a high degree of incision within the floodplain, and thus also connote a high probability for flooding and a high susceptibility to fluctuations in the water level during and after inundation episodes. In view of the fact that the rise and fall in water levels promote conveyance, entrainment, and settling of sediment

particles within the channel and near the channel boundaries, the channels of alluvial reaches prone to inundation would experience frequent erosion and deposition activities and other planform changing phenomena that promote augmentations in sinuosity and, in conjunction with the vacillating flow pattern, instigate frequent bank advancements and bank retreats in a lateral direction. This explains why reaches secernated by high specific energy or high channel depths (most notably reaches extending from Des Arc to Devalls Bluff and Devalls Bluff to Clarendon) are typically accompanied by high sinuosity as well as high degrees of channel migrations and high frequencies of erosion and deposition. In simple terms, high specific energy within the channels of the reaches comprising the White River represents high flood potentials and high inclinations for planform alterations or deformations.

Channel Processes, Boundary Stability, and Morphology

The intrinsic characteristic of sediment entrainment and conveyance within the flows of various reaches of the White River is imprinted in the numerical patterns associated with sediment analysis results and their correlations to fluvial and geomorphological parameters. The results of sediment analyses distinctively evinced percipience into the transport mechanisms, bedforms, trends of sediment supply and transport, and erosional and depositional patterns of the channel while the correlations between sediment regime and fluvial and geomorphological parameters permit insights into the channel boundary stability, the influence of channel dimensions to sediment movements, the interaction between channel boundaries and flow regimes, and the impact induced on the flow regimes by channel dimensions and configurations and vice versa. The extraction of the data and findings colligated with sediment analyses and

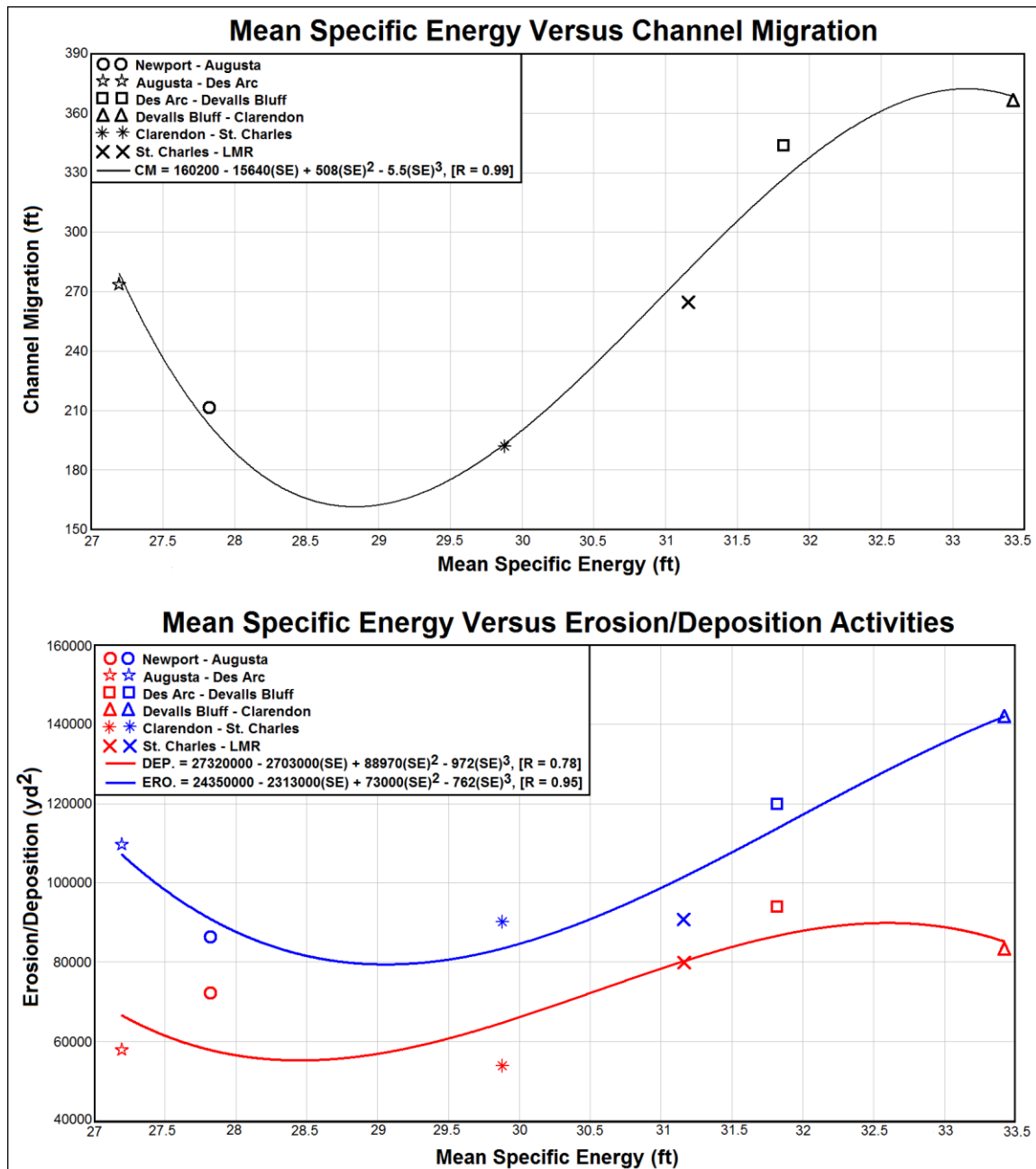


Figure 5.28. Correlations of Mean Specific Energy Versus Erosion and Deposition Activities and Lateral Migrations.

correlations ascertained the significance of each previously mentioned factor to the meandering/shifting, dynamic equilibrium, and overall stability of specific reaches of the White River. The results emanating from sediment analyses and parametric correlations

indicate that the White River's reach from Batesville to Newport, distinguished by a dominant intermittent transport mechanism of gravel-sized materials along its bed and a recessive continuous transport mechanism of finer materials within its flow, is characterized by high regime bedforms prevalent with flats and antidunes and an exuberant turbulent flow strength that permits incision into bedrock and facilitation of sediment through the system. Since the majority of the bends within the section from Batesville to Newport also exhibit radii of curvature that occupy the range from 1000 to 1800 feet, the angles by which the advancing circulations make with the concave bank promote optimum outer-bank radial forces responsible for the erosion of the banks, thus contributing to the high total sediment concentration within this section. The implication that the radius of curvature promotes high sediment supply does not, however, imply instability of the channel boundaries, specifically the banks, but rather an energetic mode of excess energy dissipation constituted by a crooked, turbulent flow. The majority of the reaches from Batesville to Newport also appear to maintain high W/D ratios in conjunction to unusually low depths and cross-sectional areas. Highest frequencies of sinuosity quantities above 1.5 are associated with bends notable for having channel dimension discrepancies and boundaries that display the highest degrees of susceptibility to variations in flow and velocity. Meander area histograms, which represent the physical manifestation of erosional and depositional activities responsible for channel expansion, constriction, lateral migration, and sinuosity augmentation, indicate a slight preponderance of erosional activities over depositional activities. The sediment rating curve and sediment concentration profile also depict a diminishment in sediment transport and supply with respect to an augmentation of discharge as the channel

approaches Newport. For the reach from Batesville to Newport, which consists of a number of bends or sections with wide point bar features and an accompanying relatively high quantity of total sediment concentration, the banks exhibit an exceptional magnitude of stability or a moderate erodibility potential and the channel possesses an overall fair stability adjective rating. Sediment analyses conducted by implementing various methodologies show that the reach from Newport to Augusta is distinguished by a mixed sediment regime composed of nearly equivalent quantities of bed-load transported intermittently along the bed and suspended-load transported continuously within the flow, respectively, and less developed dune and ripple bedforms with variability in wavelengths and wave heights. The sediment rating curve and the sediment concentration profile denote that an augmentation in sediment transport complements an enhancement in discharge and an overall diminishment in sediment supply. The reach from Newport to Augusta also emphasizes low to moderate W/D ratios in conjunction to low bed-load and suspended-load discharges, and also asseverates an inconsiderable degree of sensitivity of suspended-load sediments to the impact of W/D augmentations. The sharp inclination ascribable to the sediment trend and the perceivable pattern of sediment attenuation (toward Augusta) insinuate that at Newport the banks and bed erodibility potential is significantly greater than at Augusta. Contribution of sediment load from the Black River to the confluence with the White River at Newport also elucidate the high-level of sediment concentration at the upper portion of this reach. Erosional and depositional activities attributable to the frequency of bends exhibiting close-to-cutoff configurations and width expansions for the 'reference' reach, however, exhibit an overall degree of balance tantamount to equilibrium. Low total sediment concentrations, moderate erosion

potential, and a fair stability adjective rating enhance the implications of dynamic equilibrium for the segment from Newport to Augusta. The recurrences of well-developed dune bedforms and the dominance of a continuous transport mechanism in the form of suspended-load are inherently connected to the segment from Augusta to Des Arc. A gradual augmentation in the quantities of sediment transport and sediment supply coincident with an enhancement in discharge and width is apparent as the White River approaches Des Arc. For this reason and in addition to the steady sequence of hydraulic depth amplification, it is indisputable that sediment supply augmentations conform to a pattern of bank erosion acceleration particularly in the locality proximal to Des Arc. Distinctive patterns of erosional and depositional animations, causative of lateral shifts, channel widenings, and the frequency of near chute cut-off bends within this reach, display a definitive preponderance of erosional activities over depositional activities. Meander area histograms appear to reflect the channel expansions and lateral shifts existing at various bends of this section while the non-uniformity in discharge and the availability of radii of curvature within the interval of 1500 to 2000 feet appear to reflect the frequency of near cut-off bends within this section. The discernible dominance of erosional activities shown on the meander area histograms for the reach from Augusta to Des Arc indicates that the banks possessed high erosion potential. Overall, the channel also exhibits a fair stability adjective rating. Several attributives representative of the reach from Des Arc to Devalls Bluff are the noticeable prevalence of suspended sediment load and the presence of well-developed dune bedforms within the channel. The reach from Des Arc to Devalls Bluff, although displaying a higher longitudinal gradient in comparison to the upstream alluvial reaches, is also marked by a gradual pattern of

augmentation in the rate of sediment transport and a gentle pattern of diminishment in the rate of sediment supply. Contrary to the overall high sediment concentration and cumulative optimum magnitudes of eroded and deposited meander areas that this reach exhibits, the gentle slopes associated with the patterns of sediment supply and transport appear to suggest a reduction in the channel's ability to sustain suspended-load within the flow. The implication is that despite possessing very highly erodible banks and a more inclined longitudinal gradient, hence greater stream power adequate for the promotion of bed scouring, the sediment transported and entrained within this reach, specifically suspended-load, is controlled by channel width, the average of which occupied the median value of the critical suspended-load width interval that facilitates optimal magnitudes of suspended sediment. Attenuations in channel width with steady accompanying augmentations in channel hydraulic depth toward Devalls Bluff, which also connote a reduction in W/D ratio, appear to coincide with the gradual reduction in suspended-load as shown by the sediment concentration trend plot. Since the longitudinal gradient does not indicate a perceivable vicissitude in value, the gradual diminishment in sediment supply may also be attributable to an enhancement in bank stability as the channel approaches Devalls Bluff. Extremely high magnitudes of eroded and deposited areas, or very high erosion and deposition potential for the bends that occupy the reach from Des Arc to Devalls Bluff, indicate sensitivity to disturbance and departure to channel instability. Therefore, the existence of channel expansions and lateral shifts at various bends from Des Arc to Devalls Bluff strengthens the validation that this reach carries a poor stability adjective rating. In the case pertaining to the reach from Devalls Bluff to Clarendon, where the flat longitudinal gradient conveys a mechanism of excess

energy expenditure involving bends and meanders, the radii of curvature appear to promote high sediment concentration encompassing equivalent components of both bed-load and suspended-load. Sediment analysis results indicate lower regime bedforms of ripples and less-developed dunes, and a general correlation of sediment transport constancy to discharge augmentation. The steep rate of enhancement in sediment supply, as shown by the sediment concentration trend, in conjunction with the nearly constant rate of sediment transport, as shown by the sediment rating curve, indicate that for the segment from Devalls Bluff to Clarendon, sediment supply competency not only preponderates sediment transport capacity, but also signifies an overall reduction in the channel's ability to transport sediment. It is speculated that since the reach exhibits extremely high channel depths, corresponding low W/D ratios, and very high cross-sectional flow areas, such discrepancies in channel dimension are attributable to high bank erodibility potential, which contributes to the high sediment supply that the channel retains. However, the parametric correlations between velocity and total sediment discharge and shear force and total sediment concentration denote low degrees of sensitivity to changes in velocity and low degrees of the channel boundary susceptibility to vicissitudes in shear stress, respectively. One explanation is that since higher depth values correspond to greater shear stresses exerted on the surface areas of the channel boundary, specifically the left and right banks of the channel, the low longitudinal gradient, velocity, and stream power are inadequate for exuberant energy dissipation so the flow, hence thalweg, has to oscillate to dissipate energy gradually. The wavelike motion of the flow, analogous to the principle of centrifugal force, allows the channel to dissipate excess energy by directing higher shear stresses toward the outside of the bend,

thus altering the configuration of the river and increasing its sinuosity. An accompanying explanation is that the undulating flow is producing an effect that causes the banks to supply an enormous amount of sediment to the channel while the bed is slowly undergoing aggradation due to a lack of tractive force to transport cohesive sediment proximal to the channel bottom. Extremely high magnitudes of erosion and deposition within the bends of Devalls Bluff to Clarendon as shown by the meander area histograms in addition to the frequency of near cut-off bends, excessive lateral shifts or extensions, and high sinuosity ratios within this section asseverate the poor stability adjective rating that it possesses. Furthermore, the maximum extent of erosion dominance manifested in the indubitable disparities between eroded meander areas and deposited meander areas provide irrefutable evidence of dynamic imbalance or disequilibrium within the reach from Devalls Bluff to Clarendon. Despite possessing differing levels of agreement between the quantities of sediment attained from various methodologies, a common theme evident from the sediment analysis results is the high magnitudes of cumulative or composite sediment within the reach from Clarendon to St. Charles. The array of sediment data acquired by implementing these sediment analysis methodologies reveals that for Clarendon to St. Charles, where the bedforms are characterized by well-developed dunes with vicissitudes in wavelengths and wave heights, numerical patterns of sediment conveyance enhancement and sediment supply diminishment accompany an augmentation in discharge downstream. The sharp inclination ascribable to the sediment trend and the perceivable pattern of sediment attenuation toward St. Charles insinuate that at Clarendon the banks and beds are more critical to the mechanism of sediment conveyance and entrainment. Since parametric correlations between sediment regimes

and channel dimensions illustrate a composite sediment load in excess of upstream 'reference' reaches and highest frequencies of width, depth, and cross-sectional area values within the critical intervals of 540 to 570 feet, 27 to 33 feet, and 10000 to 12000 square feet, respectively, it is inferred that the promotion of high suspended-loads and bed-loads within the bends of Clarendon to St. Charles is controlled by channel dimensions. The complementary relationship between sediment regimes and channel dimensions are also affirmed by the W/D ratio versus sediment regime correlation plots which connote that high magnitudes of both bed-loads and suspended-loads are the resultants of channel boundaries susceptibility to the impact of W/D augmentations. If the conjecture that high degrees of sensitivity to W/D augmentations constitute high bank erodibility potential is formulated, then a definite conclusion that the banks of the reach from Clarendon to St. Charles are highly unstable could be made. The corroboration of such an assumption is depicted by the slope of the relationship between total sediment concentration and velocity, where the steep inclination in trend is representative of the substantial rate of sediment enhancement in response to an inconsequential augmentation in velocity. The implication is that for the reach from Clarendon to St. Charles, which has been shown to possess maximum quantities of sediment for all implemented methodologies and in comparison to upstream reaches, a modest alteration in velocity may activate a considerable change in the total sediment amount conveyed within the channel. Extremely high boundary perceptibility to shear force exerted by the flow, as shown by the parametric relationship between shear force and total sediment concentration, appears to imply not only the significance of velocity to contribution of sediment quantities, but also the level of departure to instability for the reach from

Clarendon to St. Charles. Meander area histograms representative of the manifestations of erosional and depositional activities also illustrate a high extent of erosion dominance for various bends from Clarendon to St. Charles. The highest and lowest magnitudes of disparity between eroded areas and deposited areas proximal to Clarendon and St. Charles provide evidence of channel bed aggradation and a reduction in the channel's ability to transport sediment load, respectively. Irrespective of the moderately mild longitudinal gradient associated with Clarendon to St. Charles, which only possess adequate stream power to promote continuous entrainment and conveyance of non-cohesive particles within the flow and to a less extent intermittent transport of cohesive sediment near the channel's bed, extremely high quantities of silt-clay content contributed by the Cache River as well as the banks proximal to Clarendon may be the catalysts responsible for bed aggradations, channel expansions, and lateral shifts seen within the bends of this reference reach. Therefore, in its entirety, the reach from Clarendon to St. Charles is classified with a poor stability adjective rating signifying dynamic disequilibrium or a departure to channel instability. Albeit a dearth of extensive or dynamically varied sediment data mandated for the comprehension of the erosion process and its innate characteristics for fluvial systems residing within the lower portion of the Mississippi Alluvial Plain, characteristics inherent to the final reach of the White River, extending from St. Charles to the confluence with the Lower Mississippi River, encompasses sediment transport mechanisms in the form of suspended-loads and mixed loads, transiences of lower and upper regime bedforms ranging from ripples to antidunes, and high quantities of sediment that comply to an overall perceptual structure or pattern of particle transport and supply augmentations in colligation to an enhancement in

discharge. The perceivable pattern illustrating the conversion from a mixed-load transport near St. Charles to a suspended-load transport near the Lower Mississippi River is synchronous to the W/D ratio augmentation that connotes high quantities of bed-load sediments. Exhibition of high magnitudes of bed-load sediment within the upper limits of the W/D ratio range, as shown by the W/D ratio versus bed-load discharge correlation plot, indicates a depletion in the capacity of the channel to entrain sediments that arise from erosional activities involving the banks. It is speculated that since “bed-load [sediment] is more often associated with an energy limitation rather than a supply limitation” (Rosgen & Silvey, 1996, p. 7-3) , since bed-loads are manifested in the critical width and depth intervals of the parametric correlation plots depicting the relationship between sediment discharge and channel dimensions, and that since optimum magnitudes of bed-loads are evident in the region proximal to the Lower Mississippi River, such a depletion in the ability of the channel to convey and sustain sediment particles, particularly finer cohesive particles, within the flow is the resultant of the combinations of bank stability, or lack thereof, channel dimension anomalies, and the tailwater effect induced by the Lower Mississippi River. The corroboration of this conjecture is affirmed by adducing factual and observable evidence of channel expansions (or W/D ratio enhancements) in bends proximal to the Lower Mississippi River, sediment competency preponderance over sediment transport capacity as illustrated by the meander area histograms (which signifies an increasing occurrence of deposition for various reaches along the lower portion of St. Charles to LMR), and high frequencies and magnitudes of erosion and deposition implicated by the meander area histograms as well as high quantities of total sediment concentrations resulting from sediment analyses.

Discrepancies in channel dimensions, complementing high bank erodibility potential within the bends of St. Charles to LMR, are also discovered to be correlated to radii of curvature, the majority of which fall within the 1000 to 1800 feet interval that represents the critical point where boundary resistance is minimal. For this reason, the bends within this reach that display the highest channel discrepancies are also the bends that possess sinuosity quantities exceeding 1.5. Despite possessing very high quantities of total sediment concentrations among all sediment analysis methodologies implemented and in comparison to upstream reaches, the reach from St. Charles to LMR possesses an overall fair stability adjective rating because, as a whole, it exhibits a higher degree of balance between erosional and depositional activities. Specifically it should be noted that although the reach from St. Charles to LMR maintains an overall fair stability rating, W/D augmentations, channel dimension discrepancies, and critical radii of curvature in proximity to LMR provide irrefutable proof that the bends within the lower portion of this reach exhibit high boundary susceptibility to variations in flow and may be subjected to bed degradation. As for the upper portion representing the transition region from Clarendon to St. Charles to LMR, apexes of the magnitude of bed-load sediment and the occurrences of lateral shift phenomena are indicative of the enhanced accumulation of sediment, specifically finer cohesive materials derived from the banks and from upstream, to the channel bottom, otherwise known as bed aggradation.

Comparison of Sediment Analysis Methodologies

An issue that has remained prevalent in predicting quantities of sediment within the channel of a fluvial system has been the importance of selecting sediment transport formulas that produce reliable results. Due to the abundance of sediment discharge

formulas present in the literature, the initial selection then elimination of sediment transport equations must in some way reflect the constituents such as the longitudinal gradient, velocity, and stream power that the fluvial system exhibits. Generally, it is recommended that a multitude of sediment transport formulas be implemented and compared whenever possible to obtain a level of consistency that enables the investigator to draw conclusions about the accuracy of the methods in describing sediment conveyance and entrainment within the channel of the fluvial system. In the case pertaining to the White River, a multitude of sediment transport formulas including those of Einstein-Brown, Engelund-Hansen, Yang, Kennedy, Karim-Kennedy, Van Rijn, and Meyer-Peter and Muller were initially selected for sediment analysis. Since field data obtained from a Modified Wolman Pebble Count and static and dynamic attributes from the HEC-HAS Model are accountable for the formulation of the conjectures that (a) the sediment transport mechanism is best classified as a mixed-load having characteristics of both bed-load and suspended-load and (b) that the alluvial sections in general lack the stream power mandated for continuous entrainment of cohesive particles within the flow, yet adequate for the entrainment and conveyance of coarse particles within the flow and along the channel bottom, sediment transport formulae of Einstein-Brown, Engelund-Hansen, and Meyer-Peter and Muller were excluded from the actual analyses in that they were discovered to be efficient when appreciable bed material was carried along the bed, for sand transport purely in the lower regime, and for coarse material primarily in bed-load transport, respectively. Utilizing the dominant bed materials derived explicitly from the Modified Wolman Pebble Count samples with sediment transport equations of Van Rijn, Yang, Kennedy, and Karim-Kennedy for sediment analyses produce numerical data

that distinctively and collectively formed similar patterns illustrating a sediment concentration profile and a sediment concentration trend. The resulting patterns representative of total sediment loads being transported within specific reaches or sections of the White River, however, depict differing degrees of agreement in sediment quantities among various implemented methodologies. The Yang sediment transport equation, which is derived from a multiple regression analysis consisting of 463 sets of laboratory data, yielded unusually low quantities of total sediment for all sections while the Van Rijn transport equation, which is derived from laboratory and field data, appears to overestimate and underestimate sediment concentrations for the reference reaches from Batesville to Newport and Devalls Bluff to Clarendon, respectively. With the exception of the reach extending from St. Charles to LMR, the sediment discharge equations of Kennedy and Karim-Kennedy, which are derived from a nonlinear regression analysis using the same data set comprising 339 river flows and 608 flume flows, yield similar magnitudes of sediments for all reference reaches. Both the Karim-Kennedy and Kennedy formulae distinctively resulted in the highest quantities of total sediment discharge within the reach from Clarendon to St. Charles. Because the Kennedy transport equation takes into account the partial armoring factor, or “portions of the [channel bottom] that [remained intact] and unavailable for transport”, and the partial covering factor, or “the sheltering effect of larger grains on smaller grains” (Sturm, 2001, p. 418), the results from this equation consistently show higher total sediment discharges than the results from implementing the Karim-Kennedy equation. Since the methodologies of Yang, Karim-Kennedy, and Kennedy determine the total sediment discharge without distinguishing between bed-load and suspended-load, the Ashida-Michiue formulation is

implemented to determine the bed-load discharge, which is then subtracted from the total sediment discharge to obtain the suspended sediment discharge. The employment of the Ashida-Michiue formulation with the aforementioned sediment analysis methodologies equate to identical bed-load discharges for Kennedy and Karim-Kennedy results and extremely low magnitudes of bed-load discharge for Yang results. Extremely low sediment quantities acquired from implementing the Yang methodology insinuate that it may not be a viable option to produce reliable results for the White River system. It is speculated that since the Yang sediment transport equation, developed by emphasizing the concept of unit stream power, is based on data for which the flow depths are in order of one-tenth of a foot to one foot, it may be suitable only for small fluvial systems; thus explicating the apparent underestimation of sediment discharge for various reaches of the much larger White River fluvial system. For this reason, the Yang results are not utilized for parametric correlations between sediment regime and fluvial and geomorphological parameters. The rankings of sediment discharges for various reaches of the White River indicate that although the Van Rijn, Kennedy, and Karim-Kennedy results yield differing quantities of bed-load sediment, the order of magnitudes for bed-load discharge is identical among the reference reaches and methodologies. For example, rankings indicate that all three methodologies predict the highest magnitude of bed-load discharge for the reach from Batesville to Newport and sixth lowest rank for bed-load transportation within Devalls to Clarendon. Inspection of the magnitudes and ranks of sediment discharges, as shown by **Figure 5.12** and **Table 5.2**, also reveal distinctive overestimations of sediment concentrations from the Van Rijn methodology for the reaches from Batesville to Newport and St. Charles to LMR. The overestimations of total sediment concentrations

for the reaches from Batesville to Newport and St. Charles to LMR, both of which possess more inclined longitudinal gradients, appear to reflect Julien's suggestion that the Van Rijn formula is ineffective in predicting the upper sediment regime for very large rivers (Julien, 1995). The derivation of the Van Rijn equation based on "bed-load transport of sediment as affected by the specific gravity of the [particle]" (Sturm, 2001) and a transport parameter emphasizing the Shield parameter for grain shear stress and critical value of the Shield dimensionless parameter suggest that the poor prediction of the total sediment concentration for upper regime may be contributed by the limitation of this methodology to produce reliable quantities of suspended-load discharge or sand particles in suspension. Induction of the overestimations of bed-load discharge for the reach from Newport to Augusta and suspended-load from St. Charles to the confluence with the Lower Mississippi River provide evidence verifying this limitation. Sediment concentration trend plots also depict a slight departure in the overall pattern or slope of sediment transport within the reaches from Newport to Augusta and St. Charles to LMR. The similarities manifested from the comparison of the Kennedy and Karim-Kennedy results involve high quantities of suspended sediment within the reaches from Augusta to Des Arc, Des Arc to Devalls Bluff, and Clarendon to St. Charles. One distinctive dissimilarity manifested from the comparison of the Kennedy to Karim-Kennedy results is the excessively high magnitude of suspended-load discharges exhibited by the reach from Clarendon to St. Charles when implementing the Kennedy sediment transport equation. The inclusion of the previously mentioned partial bed armoring and hiding factors into the Kennedy formulation possibly permit sediments contributed by the Cache River into computations. Corroboration of this assumption is explicated by the fulminant

jump in the sediment concentration trend proximal to Clarendon. It is possible, however, that this jump may just represent an abrupt change in the longitudinal gradient at Clarendon, which may be contributed by ongoing deposition of sediment eroded and transported from the boundaries of the Cache River. Among the four sediment analysis methodologies implemented, the Kennedy sediment transport equation appears to provide the most reliable results because it is derived on the basis of a large set of data comprising both flume and actual river flows, it takes into account the sheltering and armoring effects of varied particle sizes, and its sediment discharge ranking closely resembles the ranking of erosional activities represented by the ARCGIS meander area polygons.

Table 5.4. Results of Sediment Analyses.

Section	Van Rijn's Method						Karim-Kennedy's Method						Kennedy's Method								
	q_b (ft^2/s)	q_s (ft^2/s)	q_t (ft^2/s)	R_b (tons/day)	R_s (tons/day)	R_t (tons/day)	C_t (ppm)	q_b (ft^2/s)	q_s (ft^2/s)	q_t (ft^2/s)	R_b (tons/day)	R_s (tons/day)	R_t (tons/day)	C_t (ppm)	q_b (ft^2/s)	q_s (ft^2/s)	q_t (ft^2/s)	R_b (tons/day)	R_s (tons/day)	R_t (tons/day)	C_t (ppm)
1	0.00195	0.00041	0.00236	13.918	2.944	16.862	166.504	N/A	N/A	0.00157	N/A	N/A	11.22447	110.83436	0.00172	0.00023	0.00195	12.30490	1.62339	13.92829	137.53280
2	0.00185	0.00041	0.00227	13.227	2.958	16.184	162.107	N/A	N/A	0.00159	N/A	N/A	11.38979	114.08422	0.00166	0.00028	0.00194	11.83340	2.02423	13.85763	138.80290
3	0.00597	0.00070	0.00667	42.626	5.036	47.661	360.014	N/A	N/A	0.00346	N/A	N/A	24.71548	186.69043	0.00403	0.00022	0.00426	28.81822	1.60446	30.42269	229.80029
4	0.00498	0.00053	0.00551	35.578	3.797	39.376	417.345	N/A	N/A	0.00182	N/A	N/A	12.97458	137.51835	N/A	N/A	0.00277	N/A	N/A	19.79802	209.84043
5	0.00433	0.00048	0.00481	30.950	3.434	34.385	396.952	N/A	N/A	0.00154	N/A	N/A	10.97285	126.67514	N/A	N/A	0.00241	N/A	N/A	17.21332	198.71793
6	0.00482	0.00051	0.00533	34.410	3.652	38.061	426.547	N/A	N/A	0.00167	N/A	N/A	11.92275	133.61595	N/A	N/A	0.00261	N/A	N/A	18.64995	209.00646
7	0.01684	0.00121	0.01804	120.267	8.608	128.876	1572.929	N/A	N/A	0.00481	N/A	N/A	34.37337	419.52717	N/A	N/A	0.00615	N/A	N/A	43.91849	536.02539
8	0.05517	0.00192	0.05709	394.089	13.737	407.826	3829.875	N/A	N/A	0.00498	N/A	N/A	35.56595	333.99845	N/A	N/A	0.00994	N/A	N/A	70.98958	666.66055
9	0.01457	0.00099	0.01557	104.117	7.079	111.196	1147.098	N/A	N/A	0.00362	N/A	N/A	25.84820	266.65040	N/A	N/A	0.00545	N/A	N/A	38.93019	401.60437
10	0.01175	0.00093	0.01268	83.967	6.647	90.614	817.058	N/A	N/A	0.00383	N/A	N/A	27.37106	246.80105	N/A	N/A	0.00528	N/A	N/A	37.73382	390.24059
11	0.01136	0.00106	0.01242	81.154	7.590	88.744	826.516	N/A	N/A	0.00373	N/A	N/A	27.33747	347.74047	N/A	N/A	0.00594	N/A	N/A	42.45307	395.38427
12	0.00697	0.00088	0.00785	49.803	6.291	56.093	536.073	N/A	N/A	0.00439	N/A	N/A	31.33055	299.41943	0.00454	0.00014	0.00467	32.40553	0.96549	33.37102	318.91702
13	0.00312	0.00069	0.00381	22.295	4.935	27.231	285.976	N/A	N/A	0.00314	N/A	N/A	22.41809	235.43536	0.00247	0.00061	0.00308	17.63487	4.35907	21.99304	230.98098
14	0.00663	0.00021	0.00684	4.487	1.512	5.999	71.878	N/A	N/A	0.00058	N/A	N/A	4.10933	49.23642	0.00072	0.00010	0.00083	5.12533	0.75021	5.87554	70.39859
15	0.00666	0.00024	0.00690	4.702	1.693	6.395	68.757	N/A	N/A	0.00069	N/A	N/A	4.93096	53.01716	0.00074	0.00019	0.00093	5.31622	1.33504	6.65126	71.51368
16	0.00055	0.00026	0.00082	3.946	1.893	5.839	57.538	0.00065	0.00014	0.00079	4.63530	0.97501	5.61051	55.28553	0.00065	0.00010	0.00096	4.63550	2.24398	6.87948	67.79884
17	0.00004	0.00025	0.00028	0.255	1.763	2.018	18.459	0.00007	0.00008	0.00005	0.50713	6.26148	6.76861	61.92003	0.00007	0.00018	0.00015	0.50713	7.70932	8.21644	75.16500
18	0.00009	0.00051	0.00059	0.624	3.608	4.232	36.484	0.00015	0.00116	0.00131	1.06271	8.28775	9.35046	80.61120	0.00015	0.00158	0.00172	1.06271	11.25169	12.31440	106.16364
19	0.00004	0.00028	0.00032	0.290	1.975	2.266	20.607	0.00008	0.00095	0.00103	0.56580	6.77514	7.34094	66.76270	0.00008	0.00116	0.00124	0.56580	8.30286	8.88666	80.65668
20	0.00004	0.00028	0.00032	0.295	2.008	2.302	20.590	0.00008	0.00097	0.00105	0.57289	6.90547	7.47836	66.87978	0.00008	0.00118	0.00126	0.57289	8.41968	8.99257	80.42153
21	0.00004	0.00025	0.00029	0.274	1.790	2.064	20.288	0.00008	0.00078	0.00086	0.53864	6.13424	60.29826	0.00008	0.00103	0.00111	0.53864	7.37655	7.91517	77.80455	
22	0.00004	0.00028	0.00032	0.276	1.999	2.275	18.720	0.00008	0.00110	0.00118	0.54176	7.86454	8.40630	69.17101	0.00008	0.00125	0.00132	0.54176	8.89804	9.43980	77.67515
23	0.00005	0.00033	0.00038	0.365	2.344	2.708	24.736	0.00010	0.00099	0.00109	0.68540	7.07829	7.76189	70.89436	0.00010	0.00126	0.00135	0.68540	9.98944	10.67303	88.33006
24	0.00005	0.00034	0.00039	0.352	2.440	2.792	23.465	0.00009	0.00123	0.00132	0.66401	8.73483	9.39884	78.98279	0.00009	0.00140	0.00149	0.66401	9.98797	10.65159	89.51352
25	0.00001	0.00014	0.00016	0.097	1.015	1.113	8.432	0.00003	0.00102	0.00105	0.22538	2.27372	7.50270	56.86111	0.00003	0.00096	0.00099	0.22538	6.85025	7.07563	53.62446
26	0.00003	0.00025	0.00028	0.222	1.805	2.027	15.557	0.00006	0.00124	0.00130	0.45173	8.86750	9.31923	71.52130	0.00006	0.00127	0.00133	0.45173	9.04863	9.50036	73.91140
27	0.00004	0.00026	0.00030	0.254	1.893	2.146	17.392	0.00007	0.00110	0.00117	0.50575	7.86171	8.36746	67.80167	0.00007	0.00120	0.00129	0.50575	8.72837	9.23412	74.82422
28	0.00002	0.00011	0.00013	0.124	0.795	0.929	7.809	0.00004	0.00005	0.00009	0.29534	0.36136	5.52057	0.00004	0.00032	0.00036	0.29534	2.69605	2.56499	21.56265	
29	0.00002	0.00013	0.00015	0.156	0.904	1.060	8.623	0.00005	0.00005	0.00010	0.38608	0.72208	5.87639	0.00005	0.00035	0.00039	0.38608	2.49963	2.80496	23.82720	
30	0.00002	0.00012	0.00014	0.147	0.848	0.995	8.174	0.00004	0.00004	0.00008	0.32004	0.27293	5.59927	4.92245	0.00004	0.00031	0.00035	0.32004	2.19963	2.5196	20.69676
31	0.00000	0.00000	0.00000	0.001	0.027	0.028	0.445	0.00000	0.00003	0.00003	0.00490	0.18041	0.18531	2.89896	0.00000	0.00009	0.00009	0.00490	0.61324	0.61814	9.70312
32	0.00001	0.00004	0.00005	0.038	0.298	0.337	3.258	0.00001	0.00005	0.00006	0.10072	0.32677	0.42749	4.13841	0.00001	0.00020	0.00021	0.10072	1.52018	1.41946	14.71649
33	0.00005	0.00024	0.00029	0.337	1.708	2.044	15.191	0.00009	0.00004	0.00013	0.63966	0.29602	0.93568	6.95260	0.00009	0.00047	0.00056	0.63966	3.37570	4.01536	29.83623
34	0.00004	0.00021	0.00026	0.301	1.527	1.828	15.266	0.00008	0.00002	0.00010	0.58300	0.15976	0.74276	6.20369	0.00008	0.00040	0.00049	0.58300	2.88920	3.47220	29.90677
35	0.00004	0.00020	0.00024	0.281	1.435	1.716	15.260	0.00008	0.00002	0.00010	0.50569	0.13603	0.68683	6.10744	0.00008	0.00038	0.00046	0.50569	2.72291	3.27370	29.11063
36	0.00008	0.00039	0.00048	0.588	2.814	3.402	21.273	0.00014	0.00005	0.00020	1.01270	0.39010	1.40277	8.77115	0.00014	0.00068	0.00082	1.01266	4.83866	5.85132	36.58696
37	0.00000	0.00000	0.00000	0.000	0.014	0.014	0.207	0.00000	0.00002	0.00002	0.04519	0.16315	0.16505	2.40282	0.00000	0.00008	0.00008	0.00000	0.54387	0.54577	7.94554
38	0.00002	0.00029	0.00031	0.136	2.090	2.227	20.760	0.00006	0.00013	0.00019	0.93177	1.37696	12.83802	0.00006	0.00096	0.00108	0.93177	14.16996	14.61517	136.26421	
39	0.00009	0.00185	0.00194	6.338	13.217	13.855	110.892	0.00022	0.00421	0.00443	1.56464	30.08174	31.64637	253.29689	0.00022	0.01156	0.01178	1.56464	82.56287	84.12750	673.34742
40	0.00011	0.00227	0.00238	16.243	17.006	127.777	107.777	0.00025	0.00514	0.00540	8.03338	36.73973	38.54311	289.60272	0.00025	0.01343	0.01369	8.03338	95.97600	97.73797	734.64780
41	0.00010	0.00213	0.00223	0.682	15.222	15.904	111.639	0.00023	0.00563	0.00586	1.64941	40.18653	41.83593	293.67011	0.00023	0.01354	0.01377	1.64941	96.51501	98.36443	690.47562
42	0.00003	0.00078	0.00082	0.242	5.587	5.829	51.942	0.00010	0.00270	0.00280	0.71385	19.39137	20.02302	178.42430	0.00010	0.00700	0.00710	0.71385	50.07392	50.75177	452.24694
43	0.00002	0.00053	0.00055	0.145	3.758	3.903	36.683	0.00007	0.00224	0.00231	0.46819	16.02987	16.49806	155.07489	0.00007	0.00557	0.00563	0.46819	39.77042	40.23861	378.22620
44	0.00005	0.00112	0.00117	0.358	7.994	8.353	69.316	0.00014	0.00349	0.00362	0.98429	24.91085	25.89379	214.88776	0.00014	0.00887	0.00891	0.98429	63.36829	64.35123	534.03887
45	0.00012	0.00267	0.00279	0.866	19.049	19.916	141.647	0.00028	0.00611	0.00639	1.99634	43.63502	45.63136	324.54667	0.00028	0.01517	0.01545	1.99634	108.38022	110.37656	785.03785
46	0.00011	0.00240	0.00252	0.818	17.150	17.968	139.858	0.00027	0.00506	0.00533	1.90791	36.15939	38.06730	296.30686	0.00027	0.01364	0.01390	1.90791	97.41060	99.31850	773.07178
47	0.00005	0.00115	0.00119	0.341	8.192	8.533	66.885	0.00013	0.00424	0.00437	0.94565	30.25723	31.20289								

Table 5.4(Continued...). Results of sediment analyses.

Location	Section	Van Rijn's Method						Karrim-Kennedy's Method						Kennedy's Method								
		q _b (t ² /s)	q _s (t ² /s)	q _s (t ² /s)	R _s (tons/day)	R _s (tons/day)	C _t (ppm)	q _b (t ² /s)	q _s (t ² /s)	q _s (t ² /s)	R _s (tons/day)	R _s (tons/day)	C _t (ppm)	q _b (t ² /s)	q _s (t ² /s)	q _s (t ² /s)	R _s (tons/day)	R _s (tons/day)	C _t (ppm)			
CLARENDON	89	0.00006	0.00200	0.00206	0.431	14.262	14.693	114.130	0.00021	0.00334	0.00355	1.49969	23.84316	25.34284	196.85024	0.00021	0.01394	0.01415	1.49969	99.54767	101.04736	784.88411
	90	0.00017	0.00627	0.00644	1.200	44.823	46.023	311.339	0.00047	0.00600	0.00647	3.36348	42.86790	46.23138	312.74688	0.00047	0.02526	0.02573	3.36348	180.46650	183.82997	1243.57649
	91	0.00023	0.00822	0.00845	1.663	58.698	60.360	512.131	0.00061	0.00383	0.00444	4.33532	27.36480	31.70013	268.96201	0.00061	0.02301	0.02361	4.33532	164.34806	168.68339	1431.20636
	92	0.00011	0.00330	0.00341	0.781	23.556	24.337	190.426	0.00034	0.00269	0.00302	2.40126	19.18710	21.58836	168.91639	0.00034	0.01514	0.01548	2.40125	108.15350	110.55475	865.02701
	93	0.00026	0.01149	0.01175	1.884	82.068	83.952	625.023	0.00067	0.00790	0.00857	4.77770	56.41509	61.19280	455.57842	0.00067	0.03326	0.03392	4.77770	237.56251	242.34021	1804.21518
	94	0.00027	0.01028	0.01054	1.899	73.421	75.319	603.338	0.00067	0.00483	0.00551	4.80565	34.52999	39.33564	315.09481	0.00067	0.02671	0.02738	4.80565	190.81784	195.62349	1567.02526
	95	0.00012	0.00353	0.00366	0.869	25.248	26.117	234.794	0.00037	0.00229	0.00265	2.61135	16.34089	18.95224	170.38165	0.00037	0.01460	0.01494	2.61135	104.27857	106.88992	960.94635
	96	0.00013	0.00417	0.00430	0.933	29.810	30.743	224.905	0.00039	0.00338	0.00377	2.76207	24.14089	26.90296	196.81285	0.00039	0.01784	0.01823	2.76207	127.44025	130.20232	952.51568
	97	0.00011	0.00311	0.00321	0.763	22.195	22.959	195.224	0.00033	0.00230	0.00263	2.35788	16.45088	18.80877	159.93604	0.00033	0.01401	0.01434	2.35788	100.07006	102.42793	870.97259
	98	0.00020	0.00706	0.00726	1.431	50.402	51.833	434.138	0.00054	0.00429	0.00483	3.85757	30.64943	34.50700	289.01854	0.00054	0.02296	0.02350	3.85757	164.01047	167.86804	1406.00379
	99	0.00020	0.00645	0.00664	1.402	46.048	47.450	391.365	0.00053	0.00325	0.00378	3.79707	23.18287	26.97995	222.52962	0.00053	0.02014	0.02067	3.79707	143.85659	147.65366	1217.84196
	100	0.00016	0.00515	0.00531	1.143	36.786	37.930	291.084	0.00045	0.00331	0.00376	3.23844	23.62197	26.86041	206.13321	0.00045	0.01891	0.01937	3.23844	135.11295	138.35139	1061.74155
	101	0.00013	0.00416	0.00429	0.958	29.691	30.649	267.427	0.00039	0.00297	0.00336	2.81948	21.19249	24.01196	209.51293	0.00039	0.01696	0.01735	2.81947	121.15373	123.97320	1081.71039
	102	0.00005	0.00132	0.00136	0.322	9.414	9.736	97.684	0.00017	0.00170	0.00187	1.86441	12.16561	13.35202	133.96169	0.00017	0.00924	0.00941	1.86441	66.00888	67.19529	674.17475
	103	0.00008	0.00232	0.00240	0.577	16.559	17.136	163.975	0.00026	0.00209	0.00236	1.88881	14.93674	16.82555	161.00518	0.00026	0.01222	0.01248	1.88881	87.25993	89.14874	853.07207
	104	0.00020	0.00695	0.00715	1.447	49.651	51.098	343.987	0.00054	0.00382	0.00436	3.89097	27.28951	31.18048	209.90404	0.00054	0.02188	0.02243	3.89096	156.30717	160.19813	1078.43886
	105	0.00018	0.00638	0.00656	1.286	45.573	46.859	293.094	0.00050	0.00469	0.00519	3.54949	33.49875	37.04824	231.72919	0.00050	0.02306	0.02355	3.54949	164.70757	168.25706	1052.41372
	106	0.00017	0.00612	0.00629	1.216	43.742	44.957	315.306	0.00048	0.00513	0.00561	3.39683	36.64299	40.03982	280.81831	0.00048	0.02358	0.02406	3.39683	168.47669	171.87352	1205.43072
	107	0.00014	0.00505	0.00520	1.003	36.109	37.112	243.806	0.00041	0.00547	0.00588	2.92215	39.06530	41.98744	275.83827	0.00041	0.02384	0.02425	2.92215	163.31951	166.05410	1090.89947
	108	0.00016	0.00573	0.00590	1.174	40.954	42.128	305.025	0.00046	0.00457	0.00504	3.30677	32.66690	35.97367	260.46505	0.00046	0.02212	0.02258	3.30677	157.98870	161.29548	1167.84950
	ST. CHARLES	109	0.00042	0.00173	0.00156	2.988	8.187	11.471	109.981	N/A	N/A	0.00046	N/A	N/A	3.31730	32.65814	0.00053	0.00017	0.00069	3.30677	2.1908	4.94088
110		0.00064	0.00176	0.00239	4.538	12.547	17.085	149.376	N/A	N/A	0.00063	N/A	N/A	4.53429	39.64452	0.00072	0.00017	0.00093	4.53429	4.0355	6.74748	58.35278
111		0.00041	0.00388	0.00529	10.106	27.714	37.821	283.872	N/A	N/A	0.00102	N/A	N/A	7.32078	54.94801	0.00135	0.00021	0.00155	7.32078	1.47275	11.09491	83.25751
112		0.00096	0.00251	0.00347	6.886	17.898	24.785	192.551	N/A	N/A	0.00070	N/A	N/A	4.97080	38.61774	0.00100	0.00011	0.00111	5.62166	0.76135	7.91495	61.49051
113		0.00038	0.00092	0.00130	2.728	6.580	9.308	89.419	N/A	N/A	0.00029	N/A	N/A	2.05608	19.75171	0.00049	0.00002	0.00050	3.46793	0.13360	3.60153	34.59799
114		0.00075	0.00195	0.00270	5.329	13.937	19.266	171.436	N/A	N/A	0.00060	N/A	N/A	4.28184	38.10077	0.00082	0.00012	0.00094	5.86118	0.87882	6.74000	59.97404
115		0.00061	0.00167	0.00229	4.388	11.940	16.328	93.688	N/A	N/A	0.00059	N/A	N/A	4.22920	24.26629	0.00071	0.00018	0.00089	5.03686	1.30606	6.34292	36.39431
116		0.00171	0.00506	0.00677	12.195	36.150	48.345	302.872	N/A	N/A	0.00139	N/A	N/A	9.94471	62.30130	0.00156	0.00040	0.00196	11.1848	28.8334	14.00182	87.71813
117		0.00223	0.00668	0.00888	15.911	47.526	63.437	371.385	N/A	N/A	0.00170	N/A	N/A	12.16060	71.19320	0.00191	0.00047	0.00238	13.63257	3.36558	16.99815	99.51419
118		0.00298	0.00626	0.00924	21.264	44.753	66.017	373.443	N/A	N/A	0.00203	N/A	N/A	14.52023	82.13807	0.00238	0.00049	0.00287	17.01021	3.49943	20.50964	116.01896
119		0.00335	0.00738	0.01074	23.960	52.732	76.691	443.702	N/A	N/A	0.00201	N/A	N/A	14.34249	82.97932	0.00261	0.00035	0.00296	18.62759	2.48699	21.11458	122.15971
120		0.00286	0.01214	0.01500	20.442	86.740	107.183	612.122	0.00231	0.00220	0.00451	16.50713	15.70921	32.21634	183.98769	0.00231	0.00165	0.00396	16.50713	11.78183	28.28897	161.55841
121		0.00148	0.00680	0.00828	10.570	48.607	59.177	322.418	0.00139	0.00249	0.00389	9.96051	17.81671	27.77212	151.34135	0.00139	0.00165	0.00305	9.96051	11.81186	21.72737	118.62451
122		0.00071	0.00332	0.00403	5.067	23.699	28.766	175.031	0.00079	0.00226	0.00305	5.63516	16.13970	21.77486	132.49389	0.00079	0.00140	0.00219	5.63516	10.03480	15.66996	95.34728
123		0.00221	0.01042	0.01263	15.784	74.427	90.210	545.462	0.00190	0.00253	0.00443	13.54893	18.06964	31.61857	191.18393	0.00190	0.00176	0.00365	13.54893	12.55004	26.09897	157.80930
124		0.00221	0.01042	0.01263	15.784	74.427	90.210	583.749	0.00190	0.00253	0.00443	13.54893	18.06964	31.61857	204.60326	0.00190	0.00176	0.00365	13.54893	12.55004	26.09897	168.88604
125		0.00257	0.01184	0.01440	18.369	84.519	102.888	638.194	0.00213	0.00232	0.00445	15.21440	16.58994	31.80434	197.27522	0.00213	0.00169	0.00382	15.21440	12.06188	27.27628	169.18870
126		0.00154	0.00662	0.00816	10.994	47.314	58.308	393.206	0.00144	0.00198	0.00342	10.26643	14.13424	24.40067	164.55000	0.00144	0.00142	0.00285	10.26643	10.11410	20.38053	137.43952
127		0.00081	0.00362	0.00444	5.813	25.873	31.686	207.170	0.00088	0.00202	0.00290	6.27190	14.41298	20.68488	135.24102	0.00088	0.00132	0.00220	6.27190	9.44930	15.72121	102.78774
128		0.00141	0.00574	0.00715	10.068	41.026	51.094	362.262	0.00134	0.00161	0.00296	5.94222	11.52000	21.11422	149.70160	0.00134	0.00122	0.00250	5.94222	8.69277	18.26699	129.65636
129		0.00167	0.00655	0.00821	11.900	46.779	58.679	428.980	0.00153	0.00136	0.00289	10.91135	9.74713	20.65847	151.02607	0.00153	0.00111	0.00264	10.91135	7.94449	18.85584	137.84770
130		0.00279	0.01241	0.01520	19.933	88.635	108.567	709.764	0.00227	0.00231	0.00458	16.19238	16.48986	32.68224	213.66187	0.00227	0.00170	0.00397	16.19238	12.13902	28.33141	185.21804
131		0.00128	0.00541	0.00669	9.128	38.628	47.756	306.095	0.00125	0.00186	0.00310	8.89596	13.27988	22.17584	142.13731	0.00125	0.00132	0.00257	8.89597	9.46101	18.35698	117.66007

CHAPTER 6: RESULTS AND SOLUTIONS

Introduction

A multitude of activities ranging from the measurements, quantifications, computations, and correlations of fluvial and morphological parameters via ArcGIS and the HEC-RAS Model; to the utilizations of the Rosgen Stream Classification system, the Rosgen's bank erodibility hazard rating procedures, and the modified Pfankuch's Channel Stability Evaluation methodology by means of field observation, monitoring, and data extraction; to the implementations of various sediment analysis methodologies given the laboratory-derived dominant bed materials were undertaken in order to achieve an air of verisimilitude to the research conducted to establish the stability conditions of various White River reaches that extend from Batesville to the confluence with the Lower Mississippi River. The assemblages of fluvial and morphological parameters and the correlations between parameters acquired through extensive applications of the HEC-RAS Model and ArcGIS served not only as the initial interpretation of the entities that instigate planform metamorphoses and lateral migrations, but also the degree of influence induced by each parameter to the meandering and shifting propensities, dynamic equilibrium, and overall stability of the White River. The collection of data obtained from on-site observation and investigation, which include landform slope, mass wasting, debris accumulation, riparian vegetation cover, rooting depth and density, depositional patterns, and channel particle size distribution, for RSC classification, BEHI assessment, and Pfankuch's Channel Stability Evaluation characterized the geomorphology of the White River fluvial system, provided numerical indices and adjective ratings to the initial interpretation of channel and channel boundary stability,

and averred the dynamic equilibrium and overall stability inferred from parametric correlations of significant fluvial and morphological constituents. The numerical patterns associated with sediment analyses results permitted percipience into the transport mechanisms, bedforms, trends of sediment supply and transport, and erosional and depositional patterns of the channel while the correlations between sediment regime and various fluvial and geomorphological parameters further reinforced inferences formulated prior to the development of the particle size distribution curves in regard to dynamic equilibrium and overall stability of the channel. In view of the fact that a multitude of activities or components are mandated for a legitimate conclusion of channel stability, or lack thereof, for various reference reaches, which has resulted in their separations into several chapters, a clear and concise condensation is essential. Therefore, the culmination of the explicit effort to address the contributions of hydraulic components, geomorphic parameters, and field constituents to the meandering and shifting proclivities, sediment entrainment and conveyance processes, dynamic equilibrium, and overall stability of the White River's alluvial reaches is summarized in this chapter. Additional objectives include brief discussions of the geologic processes that shaped the patterns of the White River and the way its tributaries amalgamate to its main stem, concise discourses of the geomorphology parameter that imparts the greatest influence to the excessive meandering/shifting and occurrences of channel cut-off, constriction and expansion that define particular sections of the White River, and short expositions on sections destitute of dynamic equilibrium or stability and on the stream restoration solutions that may assist in diminishing channel sinuosity and bringing about a new dynamic equilibrium to these sections.

Fluvial and Morphological Contributions and Correlations

On the basis of a collection of fluvial and morphological parameters measured and extracted from the HEC-RAS Model and ArcGIS, final inferences made regarding the weight of influence warranted by each parameter to the dynamic equilibrium and stability of the White River are addressed herewith. Comparisons of static and dynamic fluvial parameters and morphological parameters distinctively permitted percipience into the intrinsic attributes that defined the alluvial river and detailed the internal processes occurring within its reaches. In particular, the highly sinuous planform and changes in planform perceived from the superimposition of aerial photographs to quadrangle maps confirmed the supposition that fluvial parameters encompassing the longitudinal gradient, velocity, and stream power conveyed a dominant mechanism of energy dissipation via bends and meanders. Inspection of the surrounding floodplain revealed that of the sub-basins through which the White River traversed, the sub-basins exhibiting high optimum width dimensions also displayed bends characterized with high sinuosity values and vice versa. High sinuosity values were discovered to be highly and monotonically colligated with sub-basin width values especially in bends occupying sub-basins with optimum width dimensions in excess of 140,000 feet; thus showing that sub-basin width played an important role in channel planform development in a lateral direction. Variability in the values of parameters including the meander belt width, flood-prone width, meander amplitude, meander wavelength, and sinuosity all denoted that meander developments are controlled primarily by heterogeneity in lenses and strata of resistant materials and irregular mechanisms of erosion and deposition. Variation in meander belt widths, amplitudes, and wavelengths to a less extent was also imputed to fault positions and

bedform structures or patterns. A morphological parameter such as entrenchment ratio inferred that the White River reach extending from Batesville to the confluence with the Lower Mississippi River is slightly entrenched in its valley floor and insinuated that flows exceeding the bankfull discharge frequently extend onto its low-energy cohesive floodplain while width to depth ratio permitted visual assessments of the channel cross-sectional shape and the distribution of energy available in the channel and depicted channel sensitivity to variations in discharge. An average width to depth ratio numerical quantity of approximately 29.5 for the White River, which implied that the channel is too wide and shallow, also emphasized the significant amount of stress exerted on the channel boundary and strengthened the notion that its channel lacked the capacity to maintain the flow; thus further reinforcing the illation of frequent overbank flows. Radius of curvature and channel curvature, which possessed a complex linkage to a multitude of parameters and activities including sinuosity, flow pattern, bedform, channel dimension, lateral migration, and other anomalous planform metamorphosis phenomena, were discovered to be directly accountable for the asymmetry in velocity, or flow, and shear stress distributions, the formation of helicoidal circulation, and the creation and spacing of riffle and pool features within the White River channel. The function of the radius of curvature in forcing changes to velocity and shear stress distributions, as shown by its relationship with the width to depth ratio, also appeared to influence channel shape and planform stability. The correlation plot between the two parameters revealed that low width to depth ratios correspond to large sinuosity values and high percentages of silt-clay contents within the channel while high width to depth ratios insinuate bank instability and attenuation in the power mandated for sediment transport. Reaches

secernated by extremely high magnitudes of sinuosity, hence high degree of instability, were also discovered to be coincident to the channel dimension discrepancies as shown by various correlation plots, the most notable of which included the flow area versus radius of curvature plot, the width versus radius of curvature plot, and the depth versus radius of curvature plot. The discovery provided concrete evidence that both excessively high and excessively low dimensions with respect to a particular radii of curvature represent potential offsets in dynamic equilibrium. Metamorphoses in channel configuration (i.e., lateral migration, channel cut-off, channel expansion and constriction) initiated by the natural propensity for flowing fluid to meander and accelerated by the non-uniformity in velocity and boundary shear stress distributions in response to curvature effects enhanced the weight of contributions effectuated by radii of curvature and channel curvatures. These anomalous phenomena were distinctively evinced by the correlation between radius of curvature and sinuosity and the correlation between channel curvature and sinuosity, which denoted that large sinuosity values frequently occupied the radius of curvature and channel curvature intervals of 1250 to 2000 feet and 2.75 to 3.75, respectively, and are confirmed by substantial magnitudes of lateral migrations and channel expansions visible from the superimposition of aerial photographs to quadrangle maps for various bends possessing sinuosity values exceeding 1.3 and curvature values within the said ranges. The findings also concurred with the inveterate and often promulgated unanimity, as formulated and elucidated in terms of flow convergence and divergence by many investigators, that rapid rate of bank erosions and optimum rate of channel migration occurred within the channel curvature range of 2 to 3 for all alluvial bends; a critical range distinguished by concave and convex bank flow convergence and

divergence activities resulting in intense flow turbulence that instigates rapid bank erosions, accelerated lateral migrations, and escalated energy losses. Thus, it is confirmed with certainty that the most profound indicator that planform development, dynamic equilibrium, and channel stability, or lack thereof, all pivoted around channel curvature is manifested in the high sinuosity values consistently observed in bends possessing channel curvature values of 2.75 to 3.75; substantial augmentations in sinuosity generally perceived through the superimposition of aerial photographs to quadrangle maps for bends with channel curvature ranging from 2.75 to 3.75; and high occurrences of lateral migration, channel cut-off, or channel constriction and expansion characteristic of bends maintaining curvature values between 2.75 and 3.75. On the whole, the key results distinctively imparted concrete evidence that channel curvature contributed to planform metamorphosis phenomena, dynamic processes and activities, and overall stability more so than other fluvial and morphological parameters although the correlations existing between these parameters in unity provided legitimate assessments of lateral migration tendencies, flow convergence and divergence activities, boundary shear stress and velocity distributions, and ultimately overall channel condition. Sediment analyses and field observation, monitoring, and data extraction also verified the inference made regarding the significance of channel curvature, and will be explicated in detail subsequently.

Table 6.1. Results of Fluvial and Morphological Correlations.

<i>Results by Sections</i>	<i>Batesville to Newport</i>	<i>Newport to Augusta</i>	<i>Augusta to Des Arc</i>	<i>Des Arc to Devalls Bluff</i>	<i>Devalls Bluff to Clarendon</i>	<i>Clarendon to St. Charles</i>	<i>St. Charles to LMR</i>
<i>Vertical Containment</i>	Not Entrenched	Not Entrenched	Slightly Entrenched	Slightly Entrenched	Slightly Entrenched	Slightly Entrenched	Slightly Entrenched
<i>Horizontal Containment /Channel Capacity</i>	Inadequate	Inadequate	Inadequate	Inadequate	Inadequate	Inadequate	Inadequate
<i>Channel Curvature</i>	Above critical range	Above critical range	Within critical range	Near critical range	Within critical range	Near critical range	Within critical range
<i>Energy Dissipation Mechanisms</i>	Turbulent and crooked flow	Bends and meanders	Bends and Meanders	Bends and Meanders	Bends and Meanders	Bends and Meanders	Bends and Meanders
<i>Sinuosity Enhancements</i>	High	High	Very Low	Very High	Very High	High	High
<i>Wavelength Dispersion</i>	High	Very High	Moderate	Low	Moderate	High	High
<i>Sub-basin Width: Sinuosity</i>	High	Moderately High	Moderate	Low	High	High	Low
<i>Channel Dimensions: Radius of Curvature</i>	Low widths, depths, and flow areas	No perceivable discrepancies	No perceivable discrepancies	No perceivable discrepancies	High depths and flow areas	No Perceivable discrepancies	Low widths, depths, and flow areas
<i>W/D ratio: Radius of Curvature</i>	High W/D ratios	No perceivable discrepancies	No perceivable discrepancies	No perceivable discrepancies	Low W/D ratios	No perceivable discrepancies	High W/D ratios
<i>Water Surface Angles: Boundary Shear Stresses</i>	Low inclinations for erosion and migration	Low inclinations for erosion and migration	No perceivable discrepancies	No perceivable discrepancies	High inclinations for erosion and migration	High inclinations for erosion and migration	High inclinations for erosion and migration
<i>Water Surface Angles: Hydraulic Depths</i>	No implications of aggradations/degradations	No implications of aggradations/degradations	No implications of aggradations/degradations	Slight implications of bed aggradations	Implications of bed aggradations	Implications of bed aggradations	Implications of bed degradations
<i>Anomalous Planform Deformations</i>	Occasional expansions	Frequent channel cut-offs and expansions	Frequent channel cut-offs and expansions	Frequent channel expansions/ High lateral migrations	Frequent channel cut-offs and expansions/ High lateral migrations	Frequent channel expansions	Frequent channel expansions
<i>Classification</i>	Stable	Stable	Stable	Stable (at risk)	Unstable	Unstable	Unstable

Results of Rosgen Stream Classifications

The utilization of the hierarchical Rosgen Stream Classification System to characterize the geomorphology of the White River fluvial system and to assess its stability condition were contingent on fluvial and morphological parameters extracted from the HEC-RAS Model and aerial photographs, on field activities and data collection performed for specific “reference” reaches, on extrapolations of the assemblages of data

attained from the “reference” reaches to regions with similar landform arrangements and fluvial features, and on conversions of these data into applicable numerical indices. The White River system at the delineation level exhibited highly sinuous planforms, low relief profiles, and an extensively developed floodplain typically associated with a Rosgen Type “C” stream. The geomorphic characterization of Level I, involving the implementation of geomorphic parameters for classification purposes, specifically depicted a fluvial system characterized by a deprivation in vertical containment as the mean entrenchment ratio exceeded the 20 plus range, a planform marked by a meandering river’s tortuosity ratio exceeding 1.3, a high exertion of hydraulic stress against the banks with width to depth ratio exceeding the often adduced high range of 12, and a dominant channel material ranging from very fine to fine sand. Geomorphic characterization also depicted a valley distinguished by a very gentle longitudinal gradient of approximately 0.00007, a high meandering boundary limit on the order of 17,000 feet or a meander belt width ratio of roughly 30, and an extensively developed low-energy cohesive floodplain constructed with alluvium from accretion activities. These prominent attributes strongly confirmed that the White River fitted the description of a type “C” river, and its basin a type “X” valley. The “C” stream type channel was often discovered to be highly susceptible to significant alteration and rapid destabilization “when the effects of imposed changes in bank stability, watershed condition, [and] flow regime [combined promoted] an exceedance of a channel stability threshold” while the channel’s aggradation/degradation and lateral extension proclivities were shown to be “inherently dependent on the natural stability of streambanks, the existing upstream watershed conditions and flow and sediment regime” (Rosgen & Silvey, 1996, p. 4-8).

Properties of the Type “X” valley included landforms such as coastal plains, alluvial flats, and expansive wetlands that were constructed with “alluvial materials originating from both riverine and lacustrine deposition processes” (Rosgen & Silvey, 1996, p. 4-16), of which alluvial flats and expansive wetlands were commonly encountered in the Mississippi Alluvial Plain physiographic region. Reach-specific morphological description conducted for Level II classification showed a multitude of “reference” reaches classified as “C5c-” stream types with stream banks and bed materials composed predominantly of sandy materials, and a diversified riparian habitats consisting of hard hardwoods such as oaks, hickories, sycamores, maples and clusters of clambering plants, herbaceous monocots and dicots encompassing mulberries, wild grapes, greenbriers, Mississippi Hackberries, and grasses lining the upper streambanks. Riparian vegetations, most notably smaller shrubs and bushes, in addition to the natural recruitment of hardwood and softwood debris appeared to influence the rate of lateral adjustment and stream-bed stability, respectively, while point bars and other depositional features associated with the “C5c-” White River “reference” reaches illustrated susceptibility “to shifts in both the lateral and vertical stability [catalyzed] by direct channel disturbance and changes in the flow and sediment regimes of the contributing watershed” (Rosgen & Silvey, 1996, p. 5-100). Reference reaches marked by an indistinct zonation and perceivable a dearth in river flora diversity, most notably reaches extending from Des Arc to the proximity of St. Charles, showed signs implicating greater bank instability and higher lateral migration tendencies. In contrast to the reach-specific morphological description presented as Level II classification and the extrapolations of data obtained from the “reference” reaches to areas having similar landforms and fluvial features,

which provided significant physical attributes and slight indications of stability for the remaining stream sections, the Level III analysis provided a “base datum of normality” depicting hydrologic, biological, ecological, and human factors influential to the conditions or “state” of these sections as they pertain to stability, potential, and function. By incorporating these additional factors as an overlay to the basic physical or morphological stream template of Level II classification, the Level III analysis process permitted a quantitative assessment of stream condition and departure from an accepted range of morphological values validated for “C” stream types by further analyzing factors that impact stream condition. Factors including riparian vegetation, streamflow regime, stream size and order, depositional patterns, meander patterns, and near bank stresses, some of which were acquired through aerial photographs, the HEC-RAS Model, or field inspections, were then converted to applicable numerical indices and adjective ratings denoting overall channel stability, condition and departure, and hazard potential. Results distinctively showed an almost complete unanimity on the issues of stream size and order, flow regime, and depositional patterns which specifically classified various reaches of the White River as size 12 and 7th order perennial streams with streamflows dominated by runoffs and altered by developments and point bars and sidebars as the prevalent depositional features at or near bend apices. The presence of meander patterns encompassing regular meanders (M-1), tortuous meanders (M-2), irregular meanders (M-3), unconfined meander scrolls (M-5), confined meander scrolls (M-6), distorted meander loops (M-7), and irregular meanders with oxbows and oxbow cutoffs (M-8), however, varied from reach to reach; thus indicating irregular mechanisms of erosion and deposition controlled primarily by heterogeneity in lenses and strata of resistant sub-

surface materials. Since riparian vegetation often defines existing stream morphology, function, water quality, and stability more so for type “C” streams, their influence on these constituents were closely examined by detecting changes in vegetative composition, vigor, and density along the river. A riparian vegetation inventory/condition survey to identify the composition, vigor, density, and potential of current riparian communities along the White River revealed low to moderately dense fragmented forests with brush and grass understories and lentic/lotic wetland areas in functional-at-risk conditions. Bare soil and low density grass covers with high and low brushes or forbs were common for regions above Augusta while wetland vegetation communities and moderately dense overstories with low brush, grass, and forb understories were common for areas below Des Arc. The native riparian forests composed of flood adaptable ethylene producing hardwoods, and wetland areas composed of bog, fen, and marsh, encountered along various sections of the White River have diminished in size and vigor over the past 80 years and have, for the most part, been altered by human activities; therefore the river currently functions at considerable risks. The estimation of Near Bank Stress values by determining the ratios of near-bank area to bankfull area and converting these values to adjective NBS ratings yielded high to extreme streambank stresses for the majority of alluvial reaches along the White River. The results also directly denoted very high sinuosity values for “reference” reaches secernated by extreme Near Bank Stresses. Similarly, the conversions of riparian vegetation rooting depth and density, streambank area and angle, and bank surface protection into numerical indices representing stream bank stabilities or Bank Erosion Hazard Indices have resulted in high to very high erodibility potentials for streambanks of reaches extending from Newport to the

confluence with the Lower Mississippi River. Very high BEHIs were also distinguished for “reference” reaches possessing high sinuosity ratios, which reaffirmed their contribution to planform metamorphoses. The modified Pfankuch’s Channel Stability Evaluation method, utilized to quantitatively and qualitatively assess the overall condition of the White River’s reaches by applying numerical and adjective ratings to measureable and observable vegetative, geomorphic/geotechnical, and hydrologic categories such as landform slope, mass wasting, debris potential, vegetative protection, depositional patterns, particle size distribution, debris jam potential, and water brightness to name a few, evinced channel stability ratings tantamount to values ranging from 98 points to 112 points or from “fair” to “poor” conditions. Unstable reaches or reaches exhibiting “poor” Pfankuch adjective ratings were discovered to possess not only very high Bank Erosion Potentials and very high to extreme Near Bank Stresses, but also high sinuosity ratios with transported mixed channel materials. Final illations made regarding the overall stability condition of various White River reaches generally mandated thorough investigations of in-stream sediment entrainment and conveyance to determine aggradation and degradation potentials, and therefore will be covered extensively in the following sediment analysis section.

Sediment Analyses and Parametric Correlations

Since further assessments of stability and morphology of a fluvial system often mandated comprehending the patterns of sediment conveyance and entrainment within its channel, sediment analyses were conducted for alluvial reaches of the White River by implementing established sediment transport formulae of Van Rijn, Yang, Karim-Kennedy, and Kennedy. The dominant median particle sizes attained from laboratory

Table 6.2. Results of RSC Classifications and Assessments.

<i>Results by Sections(RSC Classification)</i>	<i>Batesville to Newport (1-17)</i>	<i>Newport to Augusta (18-38)</i>	<i>Augusta to Des Arc (39-62)</i>	<i>Des Arc to Devalls Bluff (63-74)</i>	<i>Devalls Bluff to Clarendon (75-88)</i>	<i>Clarendon to St.Charles (89-109)</i>	<i>St. Charles to LMR (110-141)</i>
<i>Station RM</i>	295.27 to 256.89	256.89 to 197.27	197.27to 147.19	147.19 to 124.33	124.33 to 100.34	100.34 to 55.30	55.30 to 0.00
<i>Slope</i>	0.000112	0.00005	0.000078	0.00008	0.000045	0.00006	0.000093
<i>Sinuosity</i>	1.65	1.59	1.49	1.60	1.72	1.57	1.51
<i>Entrenchment Ratio</i>	66.15	60.00	47.75	25.44	49.48	43.24	42.35
<i>W/D Ratio</i>	42.43	26.43	30.48	29.83	22.50	28.36	27.82
<i>Meander Width Ratio</i>	36.54	34.37	31.81	28.42	32.33	32.11	28.98
<i>D50/Channel Material</i>	Gravel (32 mm)	F Sand (0.1875 mm)	VF Sand (0.0935 mm)	VF Sand (0.0935 mm)	Mixed (0.062 mm) & (0.187 mm)	Mixed (0.062 mm) & (0.0935 mm)	F Sand (0.1875 mm)
<i>Stream Type</i>	C4c-	C5c-	C5c-	C5c-	C5c-	C5c-/C6c-	C5c-
<i>Valley Type</i>	V*/X	X	X	X	X	X	X
<i>Stream Size and Order</i>	S – 11 (5 th)	S – 12 (7 th)	S – 12 (7 th)	S – 12 (7 th)	S – 12 (7 th)	S – 12 (7 th)	S – 12 (7 th)
<i>Depositional Features</i>	B – 1 (Point Bars)	B – 4 / B – 1 (Side and Point Bars)	B – 1 / B – 4 (Point and Side Bars)	B – 4 / B – 1 (Side and Point Bars)	B – 1 (Point Bars)	B – 1 / B – 4 (Point and Side Bars)	B – 4 / B – 1 (Side and Point Bars)
<i>Meander Patterns</i>	M-1,M-2,M-3	M-1,M-7, M-6	M-3,M-7	M-1	M-8	M-3,M-1	M-5,M-1, M-7
<i>Flow Regime</i>	P;1,7,8	P;1,8	P;1,8	P;1,8	P;1,8	P;1,8	P;1,8
<i>Riparian Vegetation</i>	L,3a,6a,5a,1,F	M,3a,6a,5a, 1,F	M,8b,5b, 3b,1,12a,F	L,8a,5b,1, 12a,F	M,8b,5b,3b, 12a,F	M,8b,5b, 6b,12a,F	H,8c,3b, 5b,12a,F
<i>Near Bank Stress</i>	High (0.45)	Very High (0.47)	High (0.45)	Extreme (0.56)	Extreme (0.53)	Very High (0.47)	Very High (0.51)
<i>BEHI (Bank Erosion Potential)</i>	Moderate (29.4)	High (31.39)	High (36.20)	Very High (40.10)	Very High (40.51)	High (32.56)	High (33.42)
<i>Pfankuch Stability Rating</i>	Fair (98.85 pts.)	Fair (97.89 pts.)	Fair (100.70 pts.)	Poor (111 pts.)	Poor (112 pts.)	Poor (109.2 pts.)	Fair (101.57 pts.)

sieve analyses of soil samples collected from the sites were employed as the primary input data for sediment analyses while static and dynamic fluvial parameters including the longitudinal gradient, velocity, hydraulic depth, discharge, and maximum width were utilized as complementary data during analyses. The numerical sequences of sediment analyses results distinctively permitted percipience into the transport mechanisms, bedforms, trends of sediment transport and supply, and erosional and depositional patterns prevalent in the White River reaches while their correlations to fluvial and

geomorphological parameters in unison provided additional insights into the channel boundary stability conditions, the colligations among channel dimensions and sediment mobility, and the interactions between channel boundaries and flow regimes. Final illations made regarding the meandering and shifting proclivity and dynamic stability for various alluvial reaches relied heavily and extensively on these reciprocally related revelations. Even though a mixed-load consisting of equivalent or near equivalent bed-load discharge and suspended-load discharge was initially anticipated as the dominant sediment transport mechanism within the White River channel, sediment analyses resulting data revealed that suspended-load discharge of non-cohesive particles is the primary mode of sediment movement. Dunes with significant variability in wavelengths and wave heights were discovered to be the dominant bedforms although transiencies of lower and upper regime bedforms ranging from well-developed ripples to antidunes and flats were identified at various sections exhibiting substantially low and high longitudinal gradients and stream powers. Meticulous examinations of the sediment transport analyses resulting data, most notably the results of implementing the Van Rijn and Karim-Kennedy equations, insinuated an overall perceptual structure or pattern of particle transport augmentation in colligation to an enhancement in discharge. Sediment supply, however, did not consistently conform to discharge variation in that it diminished in several instances at various locations in response to discharge augmentation. Enhancements in bank stability and an efficient mobility of sediment through the system were attributed as the primary factors accountable for the attenuations in the rate of sediment supply as the reaches proceeded downstream. Conversely, reductions in the capability to filter sediment through the system in accompaniment to high bank erosion

potentials were verified as the constituents responsible for tremendous increases in sediment supply downstream. Width to depth ratios, for various sections of the White River that extend from Batesville to the confluence with the Lower Mississippi River, were discovered to be highly influential to the quantities of sediment loads transported intermittently along the bed and sediment loads transported continuously within the flows. The demarcation line that defined the initial threshold when the channel began to lose its ability to entrain sediment or the critical point signifying high boundary susceptibility to the impact of W/D augmentations was represented by a width to depth ratio value of approximately 27.5, which could be perceived by the rapid diminishments of suspended-load and the dispersions of bed-load data points on the respective W/D versus sediment load correlation plots. Similarly, channel dimensions encompassing width, depth, and flow area also facilitated substantial magnitudes of bed-load discharge and suspended-load discharge within reaches secernated by the critical width intervals of 450 to 480 feet and 540 to 570 feet, the pivotal depth range of 27 to 33 feet, and the crucial flow area interval of 10,000 to 12,000 square feet. It was elaborated (in chapter 3) that since higher depth values corresponded to greater extents of shear stresses exerted on the surface areas of the channel boundary, specifically the left and right banks of the channel, the pivotal depth range of 27 to 33 feet symbolized the instances when the impact contributed by velocity on the channel boundary is maximum or where near bank stresses exceeded the bank flow resistance capability, thus resulting in erosions of the banks and supplements of sediments to the channel. Likewise and under the inference of energy limitation, the critical intervals of 450 to 480 feet and 540 to 570 feet epitomized a dearth in bed tractive force and stream power mandatory for the entrainment of

cohesive particles supplied from bank erosion. As for the crucial flow area intervals of 10,000 to 12,000 square feet, high quantities of sediment supply that the channel retained are attributable to high boundary erodibility potentials that the reaches sustained. The majority of reaches possessing channel dimensions within the critical width, depth, and flow area intervals that promoted bed-load and suspended-load conveyance were also confirmed to be highly susceptible to velocity fluctuations. Power functions generated for the correlations of the total sediment concentration and velocity justified the notion that within these reaches that possessed critical channel dimensions, modest enhancements in velocity may subsequently produce substantial changes in the total sediment amounts conveyed within the channel or specifically the highest perceivable rates of sediment load augmentations. The physical manifestations of erosional and depositional activities represented by the meander area histograms, which were quantified from the areas formed when the channel expanded, constricted, and migrated laterally over the course of approximately 20 years, illustrated an overall preponderance of erosional activities within the White River system. High imbalances in erosion and deposition, or disequilibrium of erosional and depositional activities, shown for alluvial reaches maintaining critical dimensions further reinforced the conception that the quantities of sediment loads introduced into the channel must directly conform to the velocity's impact on the channel boundary. Significant disparities between erosion and deposition meander areas, therefore, also insinuated high degrees of bank instability as well as high potentials for anomalous planform deformations encompassing channel expansion, constriction, and lateral migration. Radius of curvature, previously considered a viable prognosticator of channel boundary stability and dynamic equilibrium due to its inherent connectivity to a

multitude of fluvial and morphological parameters and other anomalous planform metamorphosis phenomena, was not only confirmed to be highly correlated to optimum magnitudes of sinuosity and lateral migration within a specific interval of 1000 to 1800 feet, but also to high quantities of total sediment concentration. Because the manifestations that the critical radius of curvature promoted high sediment load indubitably pertain to the mutual interactions between velocity and curvature, which were antecedently explicated in terms of flow convergence and divergence that jointly operated as an agent catalyzing rapid bank erosions, lateral migration, and energy losses, a radius of curvature value of 1000 to 1800 feet, therefore, also epitomized the instances when boundary resistance became negligible, when the outer-bank radial force exerted on the boundary became insurmountable, or when a minimum in the energy losses generated by the bend is achieved; thus characterizing form and dynamic instability. The exhibitions of high sinuosity values, perceivable channel expansions and constrictions, excessive lateral migrations, and finally high magnitudes of total sediment loads for bends residing within the aforementioned critical curvature range solidified channel curvature or radius of curvature as the morphological parameter that imparted the greatest influence on planform development, dynamic equilibrium, and overall stability of the reaches that defined the White River fluvial system. Implications of channel aggradation and degradation potentials for these alluvial reaches were also identified from the results of sediment analyses and their correlations to fluvial and morphological parameters.

Table 6.3. Results of Sediment Analyses and Parametric Correlations.

Results by Sections	Batesville to Newport	Newport to Augusta	Augusta to Des Arc	Des Arc to Devalls Bluff	Devalls Bluff to Clarendon	Clarendon to St. Charles	St. Charles to LMR
<i>Sediment Transport Mechanism</i>	Bed-load	Mixed-load	Suspended-load	Suspended-load	Mixed-load	Suspended-load	Suspended-load/Mixed-load*
<i>Bedforms</i>	Antidunes and Flats	Dunes and Ripples	Dunes (well developed)	Dunes (well developed)	Ripples	Dunes (well developed)	Transient bedforms
<i>Sediment Transport</i>	Decreases with discharge augmentation	Increases with discharge augmentation	Increases with discharge augmentation	Increases with discharge augmentation	Remains constant with discharge augmentation	Increases with discharge augmentation	Increases with discharge augmentation
<i>Sediment Supply</i>	Decreases with discharge augmentation	Decreases with discharge augmentation	Increases with discharge augmentation	Decreases with discharge augmentation	Increases with discharge augmentation	Decreases with discharge augmentation	Increases with discharge augmentation
<i>W/D Ratio: Bed-load Discharge</i>	In the high range	In the low range	In the mid-range	In the mid-range	In the low range	In the mid-range	In the high range
<i>W/D Ratio: Suspended-load Discharge</i>	Insensitive to W/D augmentation	Insensitive to W/D augmentation	Mildly sensitive to W/D augmentation	Mildly sensitive to W/D augmentation	Insensitive to W/D augmentation	Extremely sensitive to W/D augmentation	Sensitive to W/D augmentation
<i>Channel Dimensions: Bed-load Discharge</i>	Dimensions do not facilitate bed-load discharge	Dimensions do not facilitate bed-load discharge	Dimensions do not facilitate bed-load discharge	Dimensions do not facilitate bed-load discharge	Dimensions do not facilitate bed-load discharge	Within critical width, depth, and flow area intervals that facilitate bed-load	Within critical width, depth, and flow area intervals that facilitate bed-load
<i>Channel Dimensions: Suspended-load Discharge</i>	Dimensions do not facilitate suspended-load discharge	Dimensions do not facilitate suspended-load discharge	Within critical width and cross-sectional area intervals that facilitate suspended-load	Within critical width, depth, and flow area intervals that facilitate suspended-load	Dimensions do not facilitate suspended-load discharge	Within critical width, depth, and flow area intervals that facilitate suspended-load	Within critical depth and flow area intervals that facilitate suspended-load (Van Rijn)
<i>Radius of Curvature: Total Sediment Concentration</i>	Within critical curvature range that promotes high total sediment concentration	Not within critical curvature range that promotes high total sediment concentration	Not within critical curvature range that promotes high total sediment concentration	Within critical curvature range that promotes high total sediment concentration	Within critical curvature range that promotes high total sediment concentration	Within critical curvature range that promotes high total sediment concentration	Within critical curvature range that promotes high total sediment concentration
<i>Velocity: Total Sediment Concentration</i>	TSC sensitive to velocity augmentation (Van Rijn)	TSC insensitive to velocity augmentation	TSC sensitive to velocity augmentation (Kennedy)	TSC sensitive to velocity augmentation (Kennedy)	TSC insensitive to velocity augmentation	TSC sensitive to velocity augmentation	TSC sensitive to velocity augmentation (Van Rijn)
<i>Shear Stress: Total Sediment Concentration</i>	Inconclusive	TSC insensitive to increase in boundary shear stress	Inconclusive	Inconclusive	TSC insensitive to increase in boundary shear stress	TSC sensitive to increase in boundary shear stress	Inconclusive
<i>Δ(Erosion - Deposition)</i>	Imbalance in erosion and deposition	Slight imbalance in erosion and deposition	Extreme imbalance in erosion and deposition	Imbalance in erosion and deposition (High E & D)	Extreme imbalance in erosion and deposition	Imbalance in erosion and deposition	Slight imbalance in erosion and deposition
<i>Anomalous Boundary Deformations</i>	High bank erodibility potential (due to turbulent and crooked flow)	No implications of boundary instability	High bank erodibility potential	High bank erodibility potential	High bed aggradation, bank erodibility, and lateral extension potentials	High bed aggradation, bank erodibility, and lateral extension potentials	High bed degradation, bank erodibility, and lateral extension potentials
<i>Classification</i>	Stable	Stable	Stable	Unstable	Unstable	Unstable	At risk

Drainage Patterns and Tectonic Influences

Due to a lack of concrete data detailing the specific geologic processes accountable for the drainage patterns encountered within the White River Basin, a generalized classification of stream patterns through simple observations were conducted for easier interpretation of the evolution of the landscape. Dendritic and subdendritic drainage patterns resembling branches of trees were identified for streams or tributaries residing within the Mississippi Alluvial Plain physiographic region while trellis patterns were established for streams in the Ozark Plateaus physiographic region. Since dendritic drainage patterns were discovered to develop in regions secerated by uniformly dipping bedrock or regions where eroded rocks offered uniform lateral resistance, as in “flat-lying beds of plains and plateaus and in massive crystalline rocks” where horizontal folded sedimentary rocks, massive igneous rocks, or complex metamorphic possibly epitomized the structural conditions, the bountiful presence of these types of drainage patterns within the lower regions of the White River denoted a “[dearth] of marked structural control” (Zernitz, 1932, p. 500). Tributaries of these dendritic drainage patterns also joined larger streams at angles approximately less than ninety degrees and seemed to follow the gradient of the terrain. In contrast, trellis drainage patterns usually occurred in regions with tilted strata “where rocks have been folded and bent into long folds and eroded into resistant ridges and valleys (AGS, 2009, p. 23), and the channel structurally-controlled as in highland streams in the Ozark Plateaus where the main channels aligned “themselves parallel to structures in the bedrock with minor tributaries [connecting at ninety degree angles]” (Pidwirny, 2006, para. 3). Reaches such as the Little Red River, the White River directly upstream of Newport, the Strawberry River,

and the Spring River, which connected perpendicularly to the main channel (i.e., the White River and the Black River at Newport) that aligned itself to the Grand Prairie Ridge and the Ozark Escarpment, exemplified trellis drainage patterns and, in addition, insinuated that it may be semi-confined and structurally-controlled. The overall irregular and highly sinuous patterns of the White River and its tributaries, however, may be attributed to the fact that they epitomized underfit streams occupying an abandoned and larger Mississippi River meander belt (R. Cox, personal communication, 2010; Spitz & Schumm, 1997). Irregular and anomalous drainage patterns of the White River and its surrounding tributaries also appeared to reflect tectonic influences. In view of the fact that drainage channels possessed the inclinations to develop in regions where surface runoff is augmented and earth materials provided minimal resistance to erosion, the presence of a series of parallel or near parallel northeast-trending faults encompassing the Western Rift Margin Fault, the Eastern Rift Margin Faults, the inferred Howe and Thompson Fault, and the inferred Big Creek Fault, and northwest-trending fault zones including the White River Fault Zone and the Bolivar-Mansfield Tectonic Zone all constituted weak planes along which erosion progressed; thus altering the stream patterns and explicating disruption or anomalous behavior in the planforms of major tributary streams as they intersected or extended close to these tectonic features. Specifically, anomalous northwest trends in the tributaries of the Bayou de View and the White River near Newport, and in the tributary streams near Crowley's Ridge illustrated the influence of the White River Fault Zones. The WRFZ also appeared to possess significant control over the course of the White River from Batesville to Newport as illustrated by the sharp change of direction and the abrupt change in the channel longitudinal gradient near

Newport. The steeper longitudinal gradient was also detected for the reach occupying the WRFZ, which suggested that it may in fact be coincident to the WRFZ or that its valley gradient steepened along the WRFZ. A large anomalous bend in the Bayou de View and a convexity in the Cache River within the WRFZ suggested that significant downstream steepening began at the southwestern margin of the WRFZ; a location that once represented “the northern limit of an abandoned White River meanderbelt” (Spitz & Schumm, 1997, p. 277). Anomalous drainage pattern shifts from a southward trend to a southeast trend were also identified for tributary streams at locations where the Eastern Rift Margin Faults crossed the Mississippi Alluvial Plain. Anomalous course changes were also observed for the Black and Cache Rivers in proximity to the Bolivar-Mansfield Tectonic Zone. Tributaries including the Strawberry River, the Spring River, and the White River at Newport, which amalgamated perpendicularly to the Black River to form trellis drainage patterns, also exhibited orientations parallel to the BMTZ; thus solidifying the notion that faulting may exert significant control over the course of tributary streams. Since the White River and its major tributary streams all indicated anomalous behaviors and gradient variations in proximity to tectonic features, variations in channel patterns from low sinuosity to high sinuosity and vice versa may also reflect subsidence and uplift axes. The analysis of planform geometry for the White River and its surrounding tributaries showed that when the rivers crossed uplift or subsidence axes, changes from low to high sinuosity and high to low sinuosity occurred, respectively. Tectonic influence on the sinuosity of the White River was also justified when the alluvial sections plotted well within the range of self-organizing meandering of the discharge versus slope discriminant diagram. The findings presented in this section suggested that the Western

Rift Margin Fault, the Eastern Rift Margin Faults, the White River Fault Zone, the Bolivar-Mansfield Tectonic Zone, and other inferred faults contributed to the drainage patterns encountered within the White River Basin. The sinuosity values of the White River and its tributary streams to some extent were also discovered to be colligated with the position of fault and uplift and subsidence anomalies.

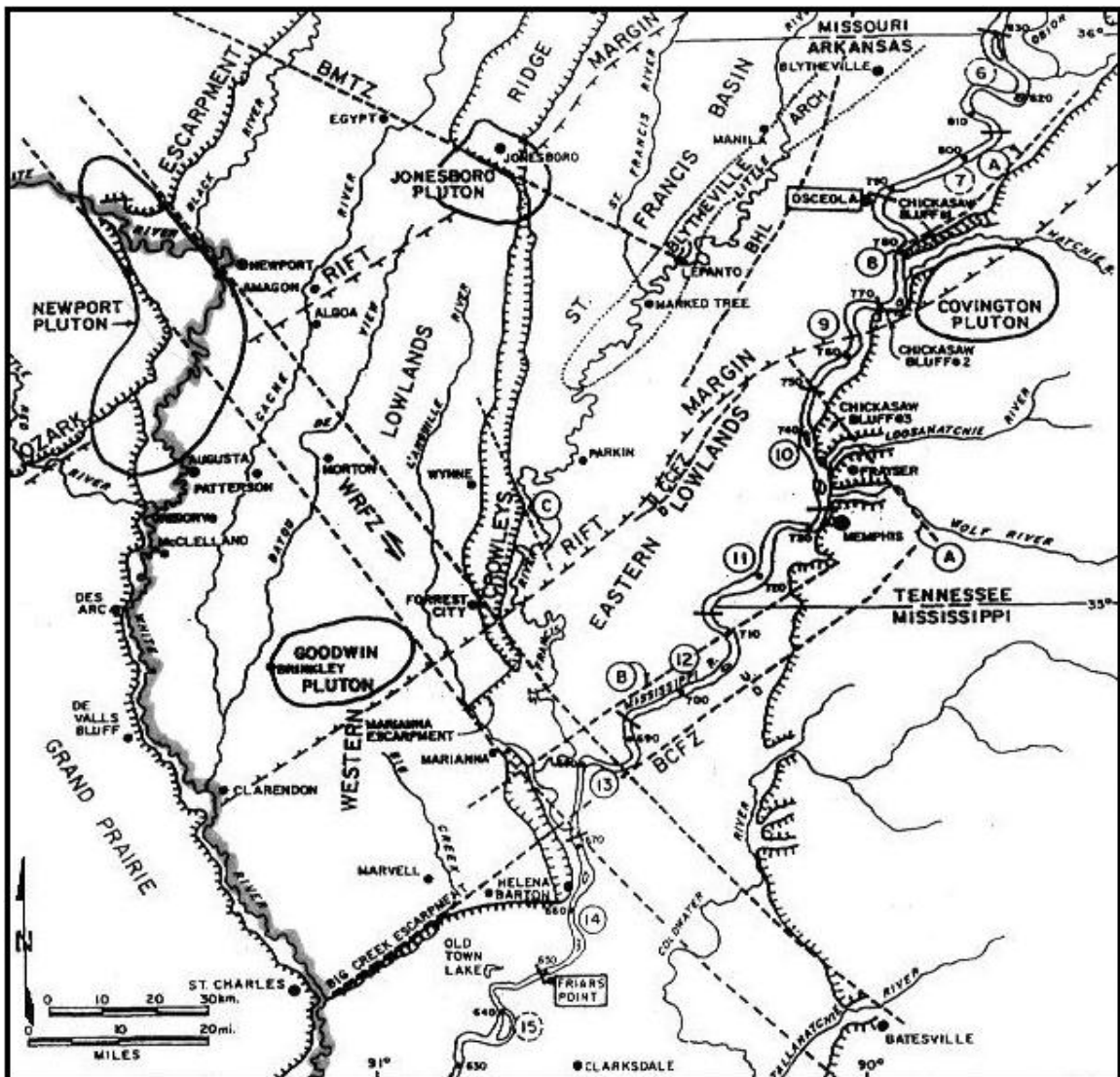


Figure 6.1. Faults and Tectonic Zones of the Mississippi Alluvial Plain (Spitz & Schumm, 1997).

Significance of Fluvial and Morphological Parameters

On the basis of an assemblage of fluvial and morphological parameters obtained via the HEC-RAS Model and ArcGIS, final inferences made regarding the weight of influence warranted by each parameter to the dynamic and stability of the White River fluvial system are briefly addressed in this section. Assessments of static and dynamic fluvial parameters including the longitudinal gradient, velocity, discharge, and stream power explicitly connoted a prevalent mode of energy dissipation by means of bends and meanders for this fluvial system. Variability in the magnitudes of morphological parameters encompassing the meander belt width, flood-prone width, meander amplitude, meander wavelength, and sinuosity asseverated an irregular meander development imputed to heterogeneity in lenses and strata of resistant subsurface materials, imbalances in erosional and depositional activities, positions and orientations of local fault lines or tectonic zones, and sizes and patterns of bed structures. Extremely high width to depth ratio and entrenchment ratio values regularly detected for the alluvial sections of the White River strengthened the illations of frequent overbank flows for this system and affirmed channel boundary susceptibility to varying discharges. Substantial width to depth ratios at various sections also signified attenuations in the capability to entrain and transport sediment while modest width to depth ratios indicated significant flow-induced shear stresses on the channel banks and high silt and clay contents on the channel bed. Sub-basin widths were also discovered to be monotonically correlated and highly influential to planform development in the lateral direction. Radius of curvature and channel curvature were confirmed to be directly accountable for asymmetric velocity and shear stress distributions, helical flow formations and stalling, pool and riffle sequence

spacings, and internal flow turbulence within various sections of the alluvial river.

The function of curvature in generating changes in velocity and shear stress distributions, to a great extent, also influenced its channel shape and planform stability. Perceivable lateral migrations, channel cut-offs, channel expansions and constrictions within various reaches of the White River that displayed high to extremely high sinuosity values were discovered to be firmly colligated with a radius of curvature interval and a channel curvature interval of 1250 to 1000 feet and 2.75 to 3.75, respectively. High to very high bank erosion potentials, very high to extreme near bank stresses, high to very high total sediment concentrations, and strong implications of bed aggradation and degradation tendencies were also shown for sections secernated by curvature values within the aforementioned critical ranges. Even though the multifarious empirical relationships were formulated to predict channel instability if the arrays of data collected from a particular fluvial system deviated from the trendlines of such empirical equations, as in the case of meander wavelength and width where high dispersions from the linear empirical line implied higher degree of instability or dynamic disequilibrium, none of these relationships were as efficient as the correlations involving radius of curvature and channel curvature in detecting the stability condition, or lack thereof, and departure from the stability condition for alluvial reaches composing the White River channel. Thus, it was confirmed with certainty that the most viable predictor of planform development, dynamic equilibrium, and channel stability of the White River all pivoted around curvature. In view of the fact that channel curvature may be easily altered by mechanical means, it may also yield the most practical stream restoration solutions for bends destitute of stability.

Stream Restoration Solutions

The determination of sections destitute of dynamic equilibrium as shown by **Table 6.4** are dependent primarily on parametric correlations involving channel curvature, which has been discovered to exert the greatest influence on sinuosity, sediment concentration, channel migration, and other planform metamorphoses, and on Near Bank Stress computations, Bank Erosion Hazard Index assessments, and Pfankuch's Channel Stability evaluations conducted in chapter 4 as recommended by the hierarchical Rosgen Stream Classification (RSC) system. Since it has been antecedently established that, on an engineering time scale, adjustments in channel form are impacted more so by imbalances in the inflow and outflow sediment discharges otherwise known as temporal aggradation and degradation than external influences elicited by human activities, the stream restoration solutions suggested for each bend classified as unstable must then be applicable purely to an engineering perspective. In view of the fact that solutions involving revetment, dike, artificial cut-offs, dredging, channel cutting and realignment are often considered to be the most reliable and practical methods to neutralize boundary stresses contributed by a curvature-induced vacillating flow, these methods are proposed for the diminishment of channel sinuosity and the reattainment of dynamic equilibrium for sections secerated by considerable near bank stresses, significant erosion potentials, and poor adjective ratings. Specifically, it should be noted that due to implications of bed aggradation or attenuation in the capability to entrain and convey sediment within the flow, dredging in accompaniment with the construction of a dike and revetment system are suitable for reaches extending from Des Arc to Devalls Bluff. As for the reaches extending from Devalls Bluff to Clarendon, which are veritably distinguished by extreme

near bank stresses, extreme erosion potentials, occupations well within the critical channel curvature range of optimal migration rate, and implications of channel aggradation, channel cutting or alignment to reduce channel curvature in addition to dredging and the construction of a dike and revetment system are viable options for the neutralization of such critical and anomalous phenomena. Dredging, construction of a dike and revetment system, and channel cutting all appear to be necessities for reaches proximal to Clarendon due to the frequent exhibitions of excessive boundary stresses, very high erosion potentials, channel curvature values within the critical range of maximum migration rate, large sediment accumulations to the channel bed, and consistently poor stability ratings manifested within these reaches. Stream restoration via dredging is especially important for bends in proximity to Clarendon considering that significant amounts of sediment contributed by the Cache River, which contain extremely high quantities of silt-clay contents requiring substantial magnitude of velocity to be entrained into the flow, contribute to much of the sediment accumulation that takes place near the channel bottom. Dike and revetment systems of large angular rocks are adequate for most situations to neutralize boundary stresses while channel cutting is a critical method for bends possessing curvature values close to 3. Stream restoration solutions such as artificial cut-offs, or forcing the river to take a shorter path downstream by directing flows across depositional bars or necks of meanders, may be implemented as an alternative to decrease channel meandering and to promote sediment outflow for bends close to chute or neck cut-offs.

Table 6.4. Stream Restoration Solutions.

Location			Section No.	Channel Curvature	Sinuosity ratio	Near Bank Stress	Erosion Potential	Stability Rating	Proposed Solution
BATESVILLE to NEWPORT	24% of bends are classified as "UNSTABLE".	24% of bends occupy critical range of Re/W and display "POOR" adjective ratings	5	3.76	2.86	High (0.42)	Moderate (+2)	Poor (+4)	Dike and revetment system.
			8	3.02	2.99	Low (0.24)	High (+3)	Poor (+4)	Revetment of large angular rocks.
			10	3.73	2.39	Extreme (0.70)	Very High (+4)	Poor (+4)	Dike and revetment system.
			15	3.10	1.61	Extreme (0.59)	Moderate (+2)	Poor (+4)	Revetment of large angular rocks at bend apices.
NEWPORT to AUGUSTA	24% of bends are classified as "UNSTABLE".	24% of bends occupy critical range of Re/W and display "POOR" adjective ratings	22	2.76	2.17	High (0.46)	High (+3)	Poor (+4)	Revetment of large angular rocks at bend apices.
			24	3.40	2.40	Very High (0.50)	High (+3)	Poor (+4)	Artificial Cut-off.
			31	3.69	1.36	Very High (0.48)	Very High (+4)	Poor (+4)	Artificial Cut-off.
			33	3.43	1.29	Extreme (0.64)	High (+3)	Poor (+4)	Revetment of large angular rocks at bend apices.
			37	3.62	1.71	Moderate (0.34)	High (+3)	Poor (+4)	Nothing, cut-off is imminent.
			42	2.55	1.18	Moderate (0.34)	Very High (+4)	Poor (+4)	Revetment of crushed rocks at bend apices
			43	2.89	1.18	Very High (0.48)	Very High (+4)	Poor (+4)	Revetment of crushed rocks at bend.
AUGUSTA to DES ARC	46% of bends are classified as "UNSTABLE". 17% of bends ONLY display "POOR" adjective ratings.	29% of bends occupy critical range of Re/W and display "POOR" adjective ratings	45	2.74	1.35	Extreme (0.54)	Very High (+4)	Poor (+4)	Revetment of crushed rocks at lower bend.
			47	2.96	1.80	Low (0.32)	Very High (+4)	Poor (+4)	Artificial Cut-off for bends at mid-span.
			50	3.53	2.33	Extreme (0.52)	High (+3)	Poor (+4)	Revetment of large angular rocks.
			51	3.17	1.16	Very High (0.48)	Very High (+4)	Poor (+4)	Revetment of large angular rocks.
			55	3.33	1.42	High (0.43)	Very High (+4)	Poor (+4)	Revetment of crushed rocks at bend apices.
			56	5.75	1.92	Very High (0.49)	Very High (+4)	Poor (+4)	Dike and revetment system at bend apex.
			60	3.52	1.05	Moderate (0.35)	Very High (+4)	Poor (+4)	Artificial Cut-off.
			61	1.76	1.98	High (0.45)	Very High (+4)	Poor (+4)	Revetment of crushed rocks.
			62	3.13	1.37	Extreme (0.50)	High (+3)	Poor (+4)	Revetment of crushed rocks.
			63	2.78	1.74	Moderate (0.41)	Very High (+4)	Poor (+4)	Revetment of crushed rocks.
			65	3.32	2.63	Extreme (0.64)	Very High (+4)	Poor (+4)	Dike and revetment system at lower bend apex.
DES ARC to DEVALLS BLUFF	67% of bends are classified as "UNSTABLE". 17% of bends ONLY display "POOR" adjective ratings.	50% of bends occupy critical range of Re/W and display "POOR" adjective ratings	66	3.25	1.58	Extreme (0.66)	Very High (+4)	Poor (+4)	Dredging, Dike and revetment system at lower bend apex.
			68	2.97	1.54	Extreme (0.67)	Very High (+4)	Poor (+4)	Dredging, Dike and revetment system at lower bend apex.
			69	6.67	1.24	Extreme (0.62)	Very High (+4)	Poor (+4)	Revetment of crushed rocks.
			70	2.67	1.37	Very High (0.49)	Very High (+4)	Poor (+4)	Dredging, Dike and revetment system at bend apices.
			71	2.94	2.86	Extreme (0.57)	Very High (+4)	Poor (+4)	Revetment of large angular rocks at lower bend apex.
			72	3.91	1.99	Extreme (0.53)	Very High (+4)	Poor (+4)	Dredging, Dike and revetment system at lower bend apex.
			75	4.91	1.30	High (0.43)	Very High (+4)	Poor (+4)	Revetment of large angular rocks.
			76	3.49	1.66	Very High (0.50)	High (+3)	Poor (+4)	Cutting to reduce radius of curvature. Dike and revetment system.
DEVALLS BLUFF to CLARENDON	86% of bends are classified as "UNSTABLE". 36% of bends ONLY display "POOR" adjective ratings.	50% of bends occupy critical range of Re/W and display "POOR" adjective ratings	77	3.94	2.09	Extreme (0.55)	Very High (+4)	Poor (+4)	Artificial Cut-off.
			78	3.14	2.05	Extreme (0.52)	Very High (+4)	Poor (+4)	Dredging, Channel realignment to reduce curvature. Dike and revetment system of large angular rocks.
			79	2.17	2.31	Extreme (0.52)	Very High (+4)	Poor (+4)	Dredging, Channel realignment to reduce curvature. Dike and revetment system of large angular rocks.
			80	2.32	1.88	Low (0.22)	Very High (+4)	Poor (+4)	Channel realignment.
			82	2.88	1.80	Extreme (0.60)	Very High (+4)	Poor (+4)	Dredging, Cutting to reduce channel curvature. Dike and revetment system.
			83	2.92	1.32	Extreme (0.70)	Very High (+4)	Poor (+4)	Dredging, Cutting to reduce channel curvature. Dike and revetment system.
			84	2.53	1.27	Extreme (0.61)	Very High (+4)	Poor (+4)	Artificial Cut-off. Dike and revetment system.
			86	3.10	2.73	Extreme (0.52)	High (+3)	Poor (+4)	Dredging, Cutting to reduce channel curvature. Dike and revetment system.
			87	3.50	1.32	Extreme (0.71)	High (+3)	Poor (+4)	Dredging, Channel realignment. Dike and revetment system.
			88	3.31	2.17	Extreme (0.52)	Very High (+4)	Poor (+4)	Dredging, Cutting to reduce channel curvature. Dike and revetment system.
			90	2.79	2.02	Very High (0.49)	Very High (+4)	Poor (+4)	Dredging, Cutting to reduce channel curvature. Dike and revetment system.
			93	2.84	2.77	High (0.44)	Very High (+4)	Poor (+4)	Dredging, Dike and revetment system at bend apices.
CLARENDON to ST. CHARLES	48% of bends are classified as "UNSTABLE". 10% of bends ONLY display "POOR" adjective ratings.	38% of bends occupy critical range of Re/W and display "POOR" adjective ratings	97	2.72	1.77	Extreme (0.71)	High (+3)	Poor (+4)	Dredging, Cutting to reduce channel curvature. Dike and revetment system at bend apices.
			98	3.52	1.36	Extreme (0.52)	High (+3)	Poor (+4)	Dredging, Dike and revetment system at bend apices.
			101	2.09	2.54	Moderate (0.39)	High (+3)	Poor (+4)	Revetment of large angular rocks at bend apices.
			103	2.78	1.87	High (0.42)	High (+3)	Poor (+4)	Revetment of large angular rocks at bend apices.
			105	3.34	1.68	Low (0.30)	High (+3)	Poor (+4)	Revetment of large angular rocks at bend apex.
			106	3.71	2.06	Moderate (0.31)	Very High (+4)	Poor (+4)	Revetment of large angular rocks at bend apex.
			107	5.59	1.10	Moderate (0.37)	High (+3)	Poor (+4)	Nothing.
			108	2.78	1.32	Extreme (0.66)	High (+3)	Poor (+4)	Revetment of large angular rocks at bend apex.
			112	2.39	1.45	Extreme (0.69)	Very High (+4)	Poor (+4)	Dike and revetment system.
			113	4.76	1.14	Extreme (0.81)	Very High (+4)	Poor (+4)	Dike and revetment system.
ST. CHARLES to LMR	41% of bends are classified as "UNSTABLE". 28% of bends ONLY display "POOR" adjective ratings.	13% of bends occupy critical range of Re/W and display "POOR" adjective ratings	115	2.39	2.40	Moderate (0.41)	Very High (+4)	Poor (+4)	Revetment of large angular rocks at bend apex.
			118	3.29	3.06	Very High (0.50)	Very High (+4)	Poor (+4)	Dike and revetment system.
			121	1.84	1.82	Moderate (0.36)	Very High (+4)	Poor (+4)	Dike and revetment system.
			122	1.97	1.99	Moderate (0.39)	Very High (+4)	Poor (+4)	Revetment of large angular rocks at sharp bend apices.
			127	1.92	1.82	Extreme (0.59)	Very High (+4)	Poor (+4)	Dike and revetment system.
			128	3.13	1.36	Extreme (0.51)	High (+3)	Poor (+4)	Revetment of large angular rocks at lower bend apices.
			129	2.74	1.71	Extreme (0.52)	High (+3)	Poor (+4)	Revetment of large angular rocks at bend apices.
			130	2.09	1.73	Extreme (0.54)	Very High (+4)	Poor (+4)	Revetment of large angular rocks at bend apices.
			132	3.68	1.86	Very High (0.47)	High (+3)	Poor (+4)	Revetment of large angular rocks at bend apices.
			135	2.05	1.63	Very High (0.47)	Very High (+4)	Poor (+4)	Dike and revetment system.
			137	2.27	1.38	Moderate (0.38)	Very High (+4)	Poor (+4)	Revetment of large angular rocks at bend apices.

Note: Shaded cells indicate bends with "POOR" adjective ratings and Re/W values outside of the critical interval of 2.75 and 3.75.

Final Adjective and Numerical Ratings

There is strong observational evidence that from a macrocosmic perspective of the myriad of parameters and parametric correlations established for this research, there exists an apparent yet temporary obnubilation in regard to the level of contribution imparted by individual parameters on the overall condition of the White River at various localities. When this problem is rectified by applying numerical and adjective ratings to specified ranges within which data at various localities may occupy, the final products are two concise tables indicating the weights of influence contributed by individual parameters to specific reference reaches. Results of prior assessments conducted to address bank erosion hazards, bank erosion potential, sediment concentration and mobility, and overall stability are also included in **Table 6.6** and **Table 6.7** for comparison and tallying purposes. In these tables, final adjective ratings for the reference reaches are expressed as either stable or aggrading/degrading while the total numerical ratings specifically denote high degrees of instability with high rating values and vice versa. Adjective and numerical ratings indicate high and distinct implications of control exerted by various morphological parameters for alluvial reaches residing south of Des Arc, where the majority of these contributing parameters also range from poor to very poor in colligation with high to extreme bank instability. It is therefore befitting that reaches extending from Des Arc to Devalls Bluff, Devalls Bluff to Clarendon, and Clarendon to St. Charles are secernated by substantially high total numerical rating values and are all characterized as aggrading streams adjectively. Inspecting the total numerical rating values among unstable alluvial reaches reveals that the reaches extending from Devalls Bluff to Clarendon, Clarendon to St. Charles, and Des Arc to

Table 6.5. Criteria for the Conversions of Data into Adjective and Numerical Ratings.

	Range	Condition	Value		Range	Condition	Value
Sinuosity	Less than 1.4	Excellent	+1	Mobility Index	Less than 60	Excellent	+1
	1.4 - 1.5	Good	+2		61 - 120	Good	+2
	1.5 - 1.6	Fair	+3		120 - 180	Fair	+3
	1.6 - 1.7	Poor	+4		181 - 240	Poor	+4
	Greater than 1.7	Very Poor	+5		Greater than 240	Very Poor	+5
Width/Depth Ratio	Less than 12	Excellent	+1	Total Energy Slope	Less than 21	Good	+1
	12 - 24	Good	+2		21 - 28	Fair	+2
	24 - 36	Fair	+3		28 - 35	Poor	+3
	36 - 48	Poor	+4		Greater than 35	Very Poor	+4
	Greater than 48	Very Poor	+5		Less than 320	Low	+1
Entrenchment Ratio	Less than 25	Excellent	+1	Total Sediment Concentration	320 - 630	Moderate	+2
	25 - 33	Good	+2		630 - 940	High	+3
	33 - 42	Fair	+3		Greater than 940	Very High	+4
	42 - 50	Poor	+4	Bank Erosion Hazard Index	10 - 29.5	Low	+1
	Greater than 50	Very Poor	+5		20 - 29.5	Moderate	+2
Channel Curvature	Greater than 4.8	Excellent	+1		30 - 39.5	High	+3
	3.8 - 4.8	Good	+2		40 - 45.0	Very High	+4
	Less than 2.8	Fair	+3	Near Bank Stress	Less than 0.33	Low	+1
	2.8 - 3.8	Poor	+4		0.33 - 0.41	Moderate	+2
	Approximately 3.3	Very Poor	+5		0.42 - 0.45	High	+3
Wavelength	Greater than 7100	Excellent	+1		0.46 - 0.50	Very High	+4
	6600 - 7100	Good	+2		Greater than 0.5	Extreme	+5
	6100 - 6600	Fair	+3	Pfrankuch Adjective Rating	Less than 70	Excellent	+1
	5600 - 6100	Poor	+4		70 - 90	Good	+2
	Less than 5600	Very Poor	+5		91 - 110	Fair	+3
Meander Width Ratio	Less than 20	Excellent	+1		Greater than 111	Poor	+4
	20 - 26	Good	+2				
	26 - 32	Fair	+3				
	32 - 38	Poor	+4				
	Greater than 38	Very Poor	+5				

Devalls Bluff in descending order exemplify extreme to high departure from stability. It should be noted that the maximum total numerical rating observed for the section extending from Devalls Bluff to Clarendon ostensibly reflect and match many of the discoveries detected antecedently; such discoveries include the definitive inferences that this alluvial reach is characterized by channel curvatures within the critical range of maximum lateral migration activity and high total sediment concentration instigations, that this section is distinguished by high sinuosity augmentations and numerous anomalous planform deformations (i.e., channel cut-offs, migrations, and expansions), that this section is secernated by a mixed-load composed of cohesive and non-cohesive materials, and that this segment is marked by high sub-basin width, dimension disparity, depth and stress, and extreme imbalance in erosion and deposition. Similarly, high total numerical ratings shown for sections encompassing Des Arc to Devalls Bluff and Clarendon to St. Charles also reflect preceding illations of critical channel curvatures, high total sediment concentrations within the critical curvature interval, high sinuosity augmentations, considerable imbalances in erosion and deposition, and frequent anomalous planform deformations formulated during parametric correlations and planform assessments. In term of contributions among individual parameters to the conditions of the alluvial reaches, channel curvature is once again justified as the most profound prognosticator of channel development, dynamic equilibrium, and channel stability, or lack thereof, as a result of its easily perceived or perspicuous correlations to Bank Erosion Hazard Indices, Near Bank Stresses, and Pfankuch Adjective Stability Ratings for reaches deemed destitute of stability. An alternate theme evident from the inspections of the resulting tables includes the obvious connections between the total

energy slope and Bank Erosion Hazard Index, the total energy slope and Near Bank Stress, and the total energy slope and Pfankuch Adjective Stability Rating, which affirmed that the total energy slope also exerts an extremely high degree of control over the stability of the channel boundaries or the inductions of sediments into the river channel, and the overall condition of the White River fluvial system and its alluvial reaches. The rating tables also indicated that for sections destitute of stability or reaches exemplifying high degrees of departure from stability, such as the cases of reaches extending from Des Arc to Devalls Bluff, Devalls Bluff to Clarendon, and Clarendon to St. Charles, low width to depth ratios distinctively entail high sinuosity values and likewise high mobility indices promote high total sediment conveyances and vice versa. The levels of contribution imparted by the remaining parameters are not as easily distinguishable from reach to reach as adjective and numerical values exhibit substantial vicissitudes with no discernible patterns. Their contributions to various reference reaches, however, have resulted in and are inherent to the composite final adjective and numerical ratings shown in these tables. Final conclusions regarding the contribution warranted by each parameter to the dynamic stability of the White River fluvial system are also addressed in greater detail in the section *Significance of Fluvial and Morphological Parameters*.

In summary, the key findings hither corroborates the fact that reaches below Des Arc are extremely unstable and indicated that these reaches are highly susceptible to influences exerted by various morphological parameters. Overall, the reach extending from Devalls Bluff to Clarendon is discovered to exhibit highest departure from stability followed closely by sections extending from Clarendon to St. Charles and Des Arc to

Devalls Bluff, respectively. Findings also show concrete evidence that channel curvature personifies the most viable prognosticator of meander developments, planform metamorphoses, flow patterns, sediment concentrations, and dynamic stability for the White River fluvial system. Sub-basin widths and total energy slopes, to a lesser extent, are also discovered to be significant predictors of lateral meander and planform developments as well as dynamic stability. Other fluvial and morphological parameters, and the multifarious correlations existing between these parameters, together also provide a sound interpretation of planform metamorphosis, lateral migration, flow patterns, boundary shear stress and erosion potential, and the overall stability condition of the White River channel. The basis of this interpretation is manifested by the weights of influence permitted by these parameters to alluvial reaches composing the White River; all of which are shown by the two composite rating tables. Finally, it should also be mentioned that nowhere are the connections between channel curvature, total energy slope, sinuosity and Bank Erosion Hazard Index, Near Bank Stress, Pfankuch Adjective Stability Rating more apparent than within these subsequent tables that articulate numerical and adjective ratings.

Table 6.6. Final Adjective Ratings.

Section	Station	Sinuosity	W/D ratio	Entrenchment Ratio	Channel Curvature	Wave-length	Total Energy Slope	Meander Width Ratio	Mobility Index	Total Sediment	Bank Erosion Hazard Index	Near Bank Stress	Pfankuch Adjective Stability Rating	Condition/ Anomaly
Batesville to Newport	295.27 through 256.89	Poor	Poor	Poor	Excellent	Good	Good	Poor	Excellent	Low	Moderate	High	Fair	Stable
Newport to Augusta	256.89 through 197.27	Fair	Fair	Poor	Good	Fair	Fair	Poor	Good	Low	High	Very High	Fair	Stable
Augusta to Des Arc	197.27 through 147.19	Good	Fair	Fair	Very Poor	Fair	Fair	Fair	Poor	High	High	High	Fair	Stable
Des Arc to Devalls Bluff	147.19 through 124.33	Poor	Fair	Good	Poor	Poor	Poor	Fair	Poor	High	Very High	Extreme	Poor	Aggrading
Devalls Bluff to Clarendon	124.33 through 100.34	Very Poor	Good	Poor	Very Poor	Poor	Poor	Poor	Good	Low	Very High	Extreme	Poor	Aggrading
Clarendon to St. Charles	100.34 through 55.30	Poor	Fair	Poor	Poor	Fair	Poor	Poor	Poor	Very High	High	Very High	Poor	Aggrading
St. Charles to LMR	55.30 through 0.00	Fair	Fair	Poor	Very Poor	Poor	Poor	Fair	Poor	Low	High	Very High	Fair	Degrading slightly

Table 6.7. Final Numerical Ratings.

Section	Station	Sinuosity	W/D ratio	Entrenchment Ratio	Channel Curvature	Wave-length	Total Energy Slope	Meander Width Ratio	Mobility Index	Total Sediment	Bank Erosion Hazard Index	Near Bank Stress	Pfankuch Adjective Stability Rating	Total Numerical Rating
Batesville to Newport	295.27 through 256.89	+3.50	+3.94	+3.65	+1.00	+2.47	+1.17	+4.18	+1.11	+1.35	+2.24	+3.00	+3.06	+31/60
Newport to Augusta	256.89 through 197.27	+2.90	+2.76	+4.10	+1.54	+2.90	+2.47	+3.81	+1.95	+1.00	+2.67	+3.67	+3.00	+33/60
Augusta to Des Arc	197.27 through 147.19	+1.90	+3.00	+3.42	+4.66	+3.46	+2.46	+3.46	+4.13	+2.58	+3.25	+3.38	+3.29	+39/60
Des Arc to Devalls Bluff	147.19 through 124.33	+4.00	+3.00	+1.50	+3.99	+4.08	+3.08	+2.83	+4.17	+2.66	+3.58	+4.50	+3.70	+41/60
Devalls Bluff to Clarendon	124.33 through 100.34	+5.00	+2.43	+4.14	+4.66	+4.21	+2.93	+3.57	+1.86	+1.14	+3.50	+4.69	+3.79	+42/60
Clarendon to St. Charles	100.34 through 55.30	+4.00	+2.81	+3.81	+3.99	+3.29	+2.81	+3.57	+3.86	+3.62	+2.89	+3.52	+3.53	+42/60
St. Charles to LMR	55.30 through 0.00	+2.10	+2.84	+3.50	+5.00	+3.59	+2.78	+3.06	+3.81	+1.00	+2.84	+3.84	+3.19	+37/60

CHAPTER 7: SUMMARY, CONCLUSIONS, AND RECOMMENDATIONS

Summary

An analysis of a multitude of fluvial and morphological parameters was conducted to determine empirical relationships that may permit percipience into the current conditions of various White River sections (RM 299.00 – RM 0.00) and to accentuate the contributions imparted by these parameters to the dynamic equilibrium and stability of these sections. Extractions and computations of pertinent variables through applications of the HEC-RAS Model and ArcGIS were executed as the initial step in the efforts to address the connectivity between fluvial/morphological parameters and planform deformation phenomena, i.e., channel meanderings, expansions, constrictions, migrations, and cut-offs. Computations of fluvial and morphological parameters, such as the longitudinal gradient, the entrenchment ratio, the width to depth ratio, sinuosity, and the meander belt width, also assisted in the characterization of the geomorphology and the classification of the White River during utilizations of the Rosgen Stream Classification System. The level-by-level assessments featured in the RSC system, a method for classifying streams and rivers by implementing a hierarchical inventory approach based on common characteristics inherent to channel morphology, were established upon assumptions that stream morphology is prevalently reliant on landform arrangements (Rosgen & Silvey, 1996). The four inventory levels associated with the RSC assessments of the White River reaches include Geomorphic Characterization which depicts broad-level classification of the entire White River (RM 299.00 through RM 0.00) based upon overall vertical containment, channel slope, and stream configuration and shape determined via the HEC-RAS Model and Aerial

Photographs in ArcGIS; Morphological Description which personifies reach-specific classifications of selected ‘reference’ reaches, e.g., reaches in the vicinity of Batesville (RM 299.00), Newport (RM 258.94), Augusta (RM 200.30), Des Arc (RM 148.03), Devalls Bluff (RM 124.35), Clarendon (RM 100.38), and St. Charles (RM 56.57), given ArcGIS/HEC-RAS-derived data and data retrieved from the field; Assessment of Stream Condition and Departure which denotes in-depth classifications of stream conditions and quantitative assessments of stream departure (from an accepted range of morphological values validated for different Rosgen stream types) by taking into considerations riparian vegetation, streamflow regime(s), stream size and order, depositional features and meander patterns, streambank stability or erosion potential, and features colligated with Pfankuch adjective stability ratings attained from a combination of on-site investigations and investigations conducted with the assistance of the HEC-RAS Model and ArcGIS; and Field Data Verification which conveys the confirmation of stream condition, stream potential, and stream stability through data obtained at each of the lower levels in addition to sediment size distribution (at or near bankfull discharge) data derived from soil samples collected from depositional point bars and the apices of banks. The dominant bed materials D_{50s} or the median grain size bed materials attained from the particle size distribution curves, which were explicitly developed from sieve analyses of approximately seven hundred soil samples collected from the channel and banks of various ‘reference’ reaches by means of a Modified Wolman Pebble Count Scheme, were then input into several sediment analysis methodologies encompassing Van Rijn, Yang, Karim-Kennedy, and Kennedy sediment transport functions to compute sediment loads being transported within the channel at the normal flow condition. During the procedures

involved in sediment analyses, the critical threshold of sediment movements were also identified to predict channel bedforms and the dominant sediment transport mechanisms, i.e., suspended-load discharge, bed-load discharge, and mixed-load discharge, of various sections. The arrays of data representing the results of sediment analyses were employed and plotted to determine the sediment supply and sediment trend within various reaches of the alluvial White River. The sediment analyses resulting data were also plotted with a number of fluvial and morphological parameters to determine empirical correlations that may permit further insights into the contributions imparted by these parameters to the sediment entrainment and conveyance processes, to the erosion and deposition patterns, and to the magnitudes of sediment supplements introduced into the channel. Parametric correlations formulated during this stage served not only as the step taken to reinforce the connection between fluvial/morphological parameters and planform deformation phenomena, but also to ascertain the implications of channel bed aggradation and degradation at reaches antecedently classified as unstable or destitute of dynamic stability during RSC assessments. The collections of fluvial and morphological parameters and related assessments were then converted into numerical and adjective ratings, and assembled, to confirm final stability conditions for individual reaches and validate the significance of each parameter to the meandering/shifting and total dynamic stability of the White River. The final results are two concise rating tables (**Table 6.6** and **Table 6.7**) illustrating the culmination of all assessments and activities conducted for this research.

Conclusions

The first objective of this research was to identify fluvial and morphological parameters accountable for the channel planform developments and the planform

metamorphosis phenomena perceived at various localities of the White River (RM 299.00 – RM 0.00) when aerial photographs (2003) were superimposed on quadrangle maps (1984). The results of the analyses conducted for these purposes elicited concrete evidence that individual static and dynamic fluvial parameters and morphological parameters (e.g., longitudinal gradient, channel dimensions, stream power, discharge, velocity, fluid shear force, sub-basin width, total energy slope, entrenchment ratio, width to depth ratio, sinuosity, meander belt width, meander wavelength, and radius of curvature) imparted differing levels of influence on the White River fluvial system and the processes inherent to its channel, as a consequence, prompting changes to the planforms of various reaches and bends. These fluvial and morphological parameters and the multifarious correlations existing between these parameters together provided a sound interpretation of flow patterns, boundary stability and erosion potential, and the overall stability condition of alluvial reaches comprising the White River. In terms of the magnitudes of contributions furnished by individual constituents, the findings indicated that channel curvature, which possessed a firm connectivity to a multitude of fluvial and morphological parameters and other anomalous planform deformation phenomena, imposed the highest degree of influence on the White River system and its channel. Since channel curvature was also confirmed to be highly influential to velocity and boundary shear stress distributions, highly correlated with optimum magnitudes of sinuosity and lateral migrations, and highly colligated with large quantities of sediment loads or concentrations for various meandering bends, most notably bends secernated by curvature values ranging from 2.75 to 3.75, it was concluded with certainty that the most viable prognosticator of meander developments, planform metamorphoses, flow

divergence and convergence patterns, channel boundary stability, sediment conveyance and entrainment, and dynamic stability of the White River channel all pivoted around channel curvature. Sub-basin widths and total energy slopes, to slightly lesser extents, were also discovered to be significant predictors of later migrations, planform developments, and dynamic stability. Specific and final inferences made regarding the contributions warranted by the remaining parameters to the dynamic and stability of the White River fluvial system were addressed explicitly within **Section 6.6**; however, the levels of contribution imparted by these parameters were not as easily distinguishable from reach to reach. The basis of this interpretation is manifested in the conversions of fluvial and morphological parameters, and related stability assessments, to adjective and numerical ratings; all of which were tabulated, tallied, and articulated by **Table 6.6** and **Table 6.7** of chapter 6.

The second objective of this research was to pinpoint factors influential to the shape and configuration of the White River, the ways its tributaries amalgamated to its main stem, and the drainage patterns encountered within the White River Basin. The general consensus is that heterogeneity in lenses and strata of resistant subsurface materials, an imbalance in erosional and depositional activities, and an abundance of parallel and perpendicular fault lines, tectonic zones, and inferred faults all contributed to the present configurations of the White River and its tributaries and to the drainage patterns visible on its floodplain. High degrees of disparity between the meander wavelength values of various bends, as measured and quantified from aerial photographs via ArcGIS, confirmed the heterogeneity of boundary materials and corroborated an irregular mechanism of erosion and deposition. Substantial vicissitudes in the array of

meander wavelength quantities without a discernible pattern also indicated diverse and simultaneous waveforms in bed topography and planform, which were considered interrelated with the vacillating flow patterns that induced metamorphoses in channel forms, and insinuated asymmetry in velocity and shear stress distributions within the channel and at its boundary, respectively; all of which were actuated by curvature effects, or the natural propensity of flowing fluid to meander, to dissipate excess energy.

Irregular, anomalous behaviors and gradient variations detected for the White River and its major tributaries in proximity to tectonic features validated the conception that variations in channel patterns from low sinuosity to high sinuosity and vice versa reflect tectonic controls or subsidence and uplift axes of faults. Analyses of planform geometry for the White River and its surrounding tributary streams distinctively showed that when these channels crossed uplift and subsidence axes, changes from low sinuosity to high sinuosity and high sinuosity to low sinuosity transpired, respectively. This discovery showed irrefutable proof that the sinuosity of the White River and its tributary streams to certain extents were strongly colligated with the positions of fault and subsidence anomalies. Alternately, it had been stated that the overall irregular and highly sinuous patterns of the White River and its tributaries may also be attributed to the fact that these underfit streams currently occupied an abandoned and larger Mississippi River meander belt (R. Cox, personal communication, 2010; Spitz & Schumm, 1997). As for the general processes attributable to the formations of drainage patterns encountered on the White River floodplain, flows over uniformly dipping bedrock or eroded rocks offering uniform lateral resistance have resulted in the dendritic and subdendritic drainage patterns seen on the Mississippi Alluvial Plain physiographic region while flows over tilted rocks or tilted

strata have resulted in the trellis drainage patterns identified for the Ozark Plateaus physiographic region. Since drainage channels tend to develop in regions where surface runoff is augmented and earth materials provided minimal resistance to erosion, the manner by which tributary streams amalgamated to the White River reflect the position and orientation of faults, which constituted weak planes along which erosion may progress.

The third objective of this study was to determine whether river sections distinguished by high sinuosity ratios and/or excessive lateral migrations were dynamically stable or destitute of dynamic stability. Results of fluvial and morphological correlations (performed in chapter 3) insisted that for the majority of bends extending from Des Arc to Devalls Bluff, Devalls Bluff to Clarendon, and Clarendon to St. Charles, channel expansions and lateral migrations frequently accompanied sinuosity enhancements. Assessments conducted during RSC classification of the White River fluvial system distinctively denoted very high sinuosity values for bends secernated by very high to extreme Near Bank Stresses, high to very high Bank Erosion Hazard Indices, and 'POOR' Pfankuch stability ratings. The majority of bends classified as unstable by Pfankuch Channel Stability Evaluations also appeared to occupy regions extending from Des Arc to Devalls Bluff, Devalls Bluff to Clarendon, and Clarendon to St. Charles, and their channels apparently possessed a dearth of specific dominant bed materials or median grain size bed materials. Thorough investigations of in-stream sediment entrainment and conveyance by means of various widely known sediment transport formulae (i.e., those of Van Rijn, Yang, Karim-Kennedy, and Kennedy) also indicated high implications of channel aggradations for bends composing the reaches from Des Arc

to Devalls Bluff, Devalls Bluff to Clarendon, and Clarendon to St. Charles. The majority of ‘unstable’ bends within these reaches were also characterized by imbalances in erosion and deposition as well as channel curvature values within the critical interval (2.75 to 3.75) promoting high sediment concentrations and maximum lateral migrations. These findings confirmed that high sinuosity and excessive lateral migrations are often colligated with, but not limited to, high NBSs, high BEHIs, high supplements of sediments to the channel, and ‘POOR’ Pfankuch stability ratings. Since the reaches extending from Des Arc to Devalls Bluff, Devalls Bluff to Clarendon, and Clarendon to St. Charles prevalently and frequently possessed the aforementioned features, or combinations of these features, they were, therefore, definitively classified as dynamically unstable. For numerical and adjective ratings of the bends (RM 299.00 – RM 0.00), please refer to **Table 4.47** and **Table 6.4**.

The fourth objective of this study was to provide stream restoration solutions for the diminishment of sinuosity ratios and the reattainment of dynamic equilibrium for sections classified as ‘unstable’. Solutions involving revetment, dike, artificial cut-offs, dredging, channel cutting and realignment were proposed as reliable and practical options to limit sinuosity augmentations and lateral migrations, to reduce sediment accumulations within the channel, and to neutralize boundary stresses contributed by a curvature-induced vacillating flow. Specifically, due to implications of bed aggradation and attenuation in the power to entrain and convey sediment within the flow, dredging accompanying the construction of a dike and revetment system was considered adequate for reaches/sections extending from Des Arc to Devalls Bluff. As for the reaches extending from Devalls Bluff to Clarendon, channel cutting or realignment to reduce

channel curvature in addition to dredging and the construction of a dike and revetment system was deemed a viable option for the neutralizations of high NBSs, extreme erosion potentials, large accumulations of sediment to the channel bed, and lateral migrations induced by curvature effects. Frequent exhibitions of excessive boundary stresses, very high erosion potentials, channel curvature values within the critical range of optimum migration rate, large sediment accumulations to the channel bottom, and poor stability ratings manifested within the reaches proximal to Clarendon made stream restoration solutions such as dredging, construction of a dike and revetment system, and channel cutting (to reduce curvature) mandatory. Stream restoration via dredging, especially, was considered a necessity for bends at or directly downstream of Clarendon since large amounts of sediment supplied by the Cache River, which contained extremely high quantities of cohesive materials requiring substantial magnitudes of velocity and stream power for entrainment, were responsible for much of the sediment accumulations that took place near the channel bottom. Overall, the constructions of dike and revetment systems consisting of large angular rocks were regarded as feasible solutions to neutralize boundary stresses for the unstable sections while channel cutting or alignment was conceived as an effective method to diminish curvature effects for bends possessing curvature values tantamount to or close to three. Stream restoration solutions such as artificial cut-offs, or forcing the river to take a shorter path downstream by directing flows across depositional bars or necks of meanders, may also be implemented as an alternative to decrease channel meandering and to promote sediment outflow for bends near chute or neck cut-offs. Stream restoration solutions proposed for all unstable bends are listed in **Table 6.4**.

Recommendations

Over the course of the literature search, it was discovered that there is an absence of formulae to depict the entrainment and conveyance of sediment particles within large alluvial channels. Many sediment transport functions, originating from regression analyses of field and laboratory data sets comprising actual river flows and flume flows, have been suggested for sediment analysis; however, it remains unclear whether the often promulgated methodologies are viable and practical options to predict quantities and modes of sediment particle movements within a fluvial system the size of the White River. The fact that a multitude of these sediment transport functions were derived from the bulk of data of actual rivers and flume models of smaller sizes (several orders of magnitude in size below the White River fluvial system) and that there existed no available guideline to justify their accuracy raise the question of whether or not their implementation would yield realistic results, or whether different situations would mandate the utilization of different functions in order to ensure that sediment analysis is conservative. Additionally, a dearth of sufficient sediment data from the studied river channel for comparison purposes made it quite difficult to identify the most conservative sediment transport methodology or methodologies. For these reasons, it is recommended that a sediment model be constructed for the White River to better comprehend the patterns and magnitudes of sediment entrainment, sediment transport, and sediment accumulation within its channel at various localities.

Although the analysis conducted during the Pfankuch channel stability evaluation, a methodology that had been widely used by the Forest Service, the Bureau of Land Management, and hydrologists alike, placed focus upon measurements of lateral and

vertical stability or bank and bed stability by applying specific numerical ratings to an extensive lists of measurable and observable vegetative, geomorphic/geotechnical, and hydrologic categories (including landform slope, mass wasting, debris potential, vegetative protection, depositional patterns, and particle size distribution), its utilization in the field for streambed stability condition were considered problematic for various 'reference' reaches of the White River. Extensive documentation to pinpoint locations where aggradation/degradation phenomena have raised or lowered channel bed elevation, which appeared to be an ideal streambed stability evaluation methodology, were regarded as tedious or uneconomical (because of the large dimensions associated with these reaches) and, therefore, were replaced with the Mobility Index and Hjulström Curve to determine streambed aggradation and degradation potentials. Since these alternatives are not universally accepted or held in high regard due to the degree of uncertainty involved, it is suggested that further research be conducted to formulate a less arduous and more effective option to predict streambed aggradation/degradation potentials. The recommendation involving the construction of a sediment transport model within the HEC-RAS Model may also assist in the attainment of channel bed aggradation and degradation potentials for alluvial reaches composing the White River, and may provide a template for an alternative to actual stability assessment via field monitoring or the installation of permanent longitudinal profiles with benchmarks tied into permanent cross-sections or stationing pins; an approach that is often deemed uneconomical and inconvenient.

In view of the fact that stream channel instability occurred in response to measurable and observable changes in the variables controlling river channel form, i.e.,

streamflow, riparian vegetation, and direct physical modifications, the procedures encompassing the implementation of aerial photographs and quadrangle maps, the HEC-RAS Model, and on-site investigations exemplify an excellent reference procedure that provide desirable field and photographic evidence of channel metamorphoses over time. In addition, it had been shown that simultaneous applications of the HEC-RAS Model and various aerial/quadrangle images have successfully assisted in the formulation of empirical relationships that permitted not only percipience into the intrinsic attributes of the White River and detailed the internal processes occurring within its channel, but also ascertained the contributions imparted by various parameters to the meandering/shifting propensity, dynamic equilibrium, and overall stability of its alluvial reaches. Attainment of additional aerial photographs and modifications of the HEC-RAS Model for comparison purposes, therefore, is recommended for use in further planform assessments and stability evaluations.

Finally, since riparian vegetation played an important role in boundary stability, dendrochronology represents another possible topic for future research to develop a history of flood occurrence as tree-ring data can provide additional information about the mechanisms that have contributed to extreme inundations in the past. This means that dendrochronology may also be practical for flood hazard analysis of streams residing within the White River Basin.

REFERENCES

- Abad, J.D., & Garcia, M. H. (2006). RVR meander: A toolbox for re-meandering of channelized streams. *Computers & Geosciences*, 32(1), 92-101. doi:10.1016/j.cageo.2005.05.006
- Abell, R. A., Olson, D. M., Dinerstein, E., Hurley, P. T., Diggs, J. T., Eichbaum, W., . . . Hedao, P. (2000). *Freshwater ecoregions of North America: A conservation assessment*. Washington, DC: Island Press.
- Ackers, P. (1964). Experiments on small streams in alluvium. *Journal of the Hydraulic Divisions, ASCE* 90(4), 1-37.
- Ackers, P., & Charlton, F. G. (1970a). Meander geometry arising from varying flows. *Journal of Hydrology*, 11(3), 230-252.
- Ackers, P., & Charlton, F. G. (1970b). The geometry of small meandering streams. In *Proceedings of the Institute of Civil Engineers, Supplement 12* (paper 73285), 289-317.
- Ackers, P., & Charlton, F. G. (1971). The slope and resistance of small meandering channels. In *Proceedings of the Institute of Civil Engineers, Supplement 15* (paper 73625), 349-370.
- Ackers, P., & Charlton, F. G. (1975). Theories and relationships of river channel patterns, a discussion. *Journal of Hydrology*, 26(3-4), 359-362.
- Allan, J. D., & Castillo, M. M. (2007). *Stream ecology: Structure and function of running waters* (2nd ed.). Springer.
- Arkansas Geological Survey. (2009). *Regions and Landforms in Arkansas*. Little Rock, AR: Arkansas Geological Survey. Retrieved from <http://www.geology.ar.gov/pdf/landforms%20workshop.pdf>
- Arkansas Soil and Water Conservation Commission. (2000). *White River allocation: Bull Shoals Dam to the Mississippi River, Technical Analysis*. Little Rock, AR: Arkansas Soil & Water Conservation Commission.
- Arnwine, D. H., James, R. R., & Sparks, K. J. (2003). *Regional characterization of streams in Tennessee with emphasis on diurnal dissolved oxygen, nutrients, habitat, geomorphology, and macroinvertebrates*. Nashville, TN: Tennessee Department of Environment and Conservation Division of Water Pollutant Control. Retrieved from Tennessee Department of Environment and Conservation website <http://www.tn.gov/environment/wpc/publications/>

- Ashida, K., & Michiue, M. (1972). Study on hydraulic resistance and bedload transport rate in alluvial streams. *Transactions, Japan Society of Civil Engineering*, (206), 59-69.
- Bagnold, R. A. (1960). Some aspects of the shape of river meanders. *United States Geological Survey Professional Paper 181-E*, 135-144.
- Baker, J. A., Killgore, K. J., & Kasul, R. L. (1991). Aquatic habitats of fish communities in the Lower Mississippi River. *Aquatic Science*, 3(4), 313-356.
- Bathurst, J. C., Graf, W. H., & Cao, H. H. (1987). Bed load discharge equations for steep mountain rivers. In C. R. Thorne, J. C. Bathurst, & R. D. Hey (Eds.), *Sediment transport in gravel-bed rivers* (pp. 453-491). Chichester, UK: John Wiley & Sons.
- Biedenharn, D. S., Combs, P. G., Hill, G. J., Pinkard, C. F., & Pinkston, C. B. (1989). Relationship between channel migration and radius of curvature on the Red River. In S.S.Y. Wang (Ed.), *Sediment transport modeling: Proceedings of the international symposium* (pp. 536-541). New York, NY: American Society of Civil Engineers.
- Bledsoe, B. P., & Watson, C. C. (2001). Logistic analysis of channel pattern thresholds: Meandering, braiding, and incising. *Geomorphology*, 38, 281-300. doi:10.1016/S0169-555X(00)00099-4
- Brice, J. C. (1974). Evolution of meander loops. *Geological Society of America Bulletin*, 85(4), 581-586. doi:10.1130/0016-7606(1974)85<581:EOML>2.0.CO;2
- Brice, J. C. (1982). *Stream channel stability assessment* (Report No. FHWA-RD-82-021). Washington, DC: Federal Highway Administration, U. S. Department of Transportation.
- Brook, G. A., & Luft, E. R. (1987). Channel pattern changes along the lower Oconee River, Georgia, 1805/1807 to 1949. *Physical Geography*, 8(3), 191-209.
- Brown, A. V., & Brussock, P. P. (1991). Comparisons of benthic invertebrates between riffles and pools. *Hydrobiologia*, 220(2), 99-108. doi:10.1007/BF00006542
- Brown, A. V., Brown, K. B., Jackson, D. C., & Pierson, W.K. (2005). Lower Mississippi River and its tributaries. In A. C. Benke, & C.E. Cushing (Eds.), *Rivers of North America* (pp. 231-281). Burlington, MA: Elsevier Academic Press.
- Brown, A. V., Lyttle, M. M., & Brown, K. B. (1998). Impacts of gravel mining on gravel bed streams. *Transactions of the American Fisheries Society*, 127, 979-994.

- Brownlie, W. R. (1983). Flow depth in sand-bed channels. *Journal of Hydraulic Engineering, ASCE 109*(7), 959-990. doi:10.1061/(ASCE)0733-9429(1983)109:7(959)
- Buchanan, T. M. (1997). The fish community of Indian Bayou, a coastal plain stream of remarkable species richness in the lower White River drainage of Arkansas. *Journal of the Arkansas Academy of Science, 51*, 55-65.
- Burke, T. D. (1984). Channel migration on the Kansas River. In C.M. Elliott (Ed.), *River meandering: Proceedings of the conference rivers '83* (pp. 250-258). New York, NY: American Society of Civil Engineers.
- Carlston, C. W. (1965). The relation of free meander geometry to stream discharge and its geomorphic implications. *American Journal of Science, 263*(10), 864-885. doi:10.2475/ajs.263.10.864
- Carson, M. A., & Lapointe, M. F. (1983). The inherent asymmetry of river meander planform. *Journal of Geology, 91*(1), 41-55.
- Carson, M. A. (1984a). The meandering-braided threshold: A reappraisal. *Journal of Hydrology, 73*(3-4), 315-334. doi:10.1016/0022-1694(84)90006-4
- Carson, M. A. (1984b). Observations on the meandering-braided river transition, the Canterbury Plains, New Zealand: Part I. *New Zealand Geographer, 40*(1), 12-19. doi:10.1111/j.1745-7939.1984.tb01477.x
- Carson, M. A. (1984c). Observations on the meandering-braided river transition, the Canterbury Plains, New Zealand: Part II. *New Zealand Geographer, 40*(2), 89-99. doi:10.1111/j.1745-7939.1984.tb01044.x
- Chang, H. H. (1984a). Analysis of river meanders. *Journal of Hydraulic Engineering, ASCE 110*(1), 37-50. doi:10.1061/(ASCE)0733-9429(1984)110:1(37)
- Chang, H. H. (1984b). Meandering of underfit streams. *Journal of Hydrology, 75*(1-4), 311-322. doi:10.1016/0022-1694(84)90056-8
- Chang, T. P., & Toebes, G. H. (1970). A statistical comparison of meander planforms in the Wabash Basin. *Water Resources Research, 6*(2), 557-578. doi:10.1029/WR006i002p00557
- Chang, T. P., & Toebes, G. H. (1980). Geometric parameters for alluvial rivers related to regional geology. *Proceedings International Association for Hydraulic Research Congress, 3*(14), 192-201.

- Chordas, S. W., & Harp, G. L. (1991). *The aquatic macroinvertebrates of the White River National Wildlife Refuge (Arkansas Water Resources Research Center Publication No. 154)*. Fayetteville, AR: University of Arkansas Water Resources Research Center.
- Chow, V. T. (1959). *Open channel hydraulics*. New York, NY: McGraw-Hill.
- Coleman, N. L. (1970). Flume studies of sediment transfer coefficient. *Water Resources Research*, 6(3), 801-809. doi:10.1029/WR006i003p00801
- Cserkesz-Nagy, A., Toch, T., Vajk, O., & Sztano, O. (2010). Erosional scours and meander development in response to river engineering: middle Tisza region, Hungary. *Proceedings of the Geologists' Association*, 121(2), 238-247. doi:10.1016/j.pgeola.2009.12.002
- Culbertson, D. M., Young, L. E., & Brice, J. C. (1967). *Scour and fill in alluvial channels*. Retrieved from United States Geological Survey Online Publications Directory website: <http://pubs.usgs.gov/of/1968/0068/>
- Davis, W. M. (1899). The geographical cycle. *The Geographical Journal*, 14(5), 481-504.
- Doisy, K. E., Rabeni, C. E., & Galat, D. L. (1997). The benthic insect community of the lower Jacks Fork River. *Transactions of the Missouri Academy of Sciences*, 31, 19-36.
- Dunne, T., & Leopold, L. B. (1978). *Water in environmental planning* (1st ed.). San Francisco, CA: W. H. Freeman and Company.
- Dury, G. H. (1965). *Theoretical implications of underfit streams* (USGS Professional Paper 452C). Washington, DC: Government Printing Office.
- Einstein, H. A. (1950). *The bed load function for sediment transportation in open channels* (Technical Bulletin 1026). Washington, DC: USDA Soil Conservation Service.
- Engelund, F. (1967). Closure to "Hydraulic resistance of alluvial streams". *Journal of the Hydraulics Division, ASCE* 93(HY7), 287-296.
- Engelund, F., & Hansen, E. (1967). *A monograph on sediment transport in alluvial streams*. Copenhagen, Denmark: Teknik Vorlag.
- Ferguson, R. I. (1981). Channel form and channel changes. In J. Lewin (Ed.), *British rivers* (pp. 90-125). London, UK: Allen and Unwin.

- Ferguson, R. I. (1984). The threshold between meandering and braiding. In K. V. H. Smith (Ed.), *Proceedings of the first international conference on hydraulic design in water resources engineering: Channels and channel control structures* (pp. 6-15 - 6-29). Berlin, DE: Springer-Verlag.
- Ferguson, R. I. (1987). Hydraulic and sedimentary controls of channel pattern. In K.S. Richards (Ed.), *River channels: Environment and process* (pp. 129-158). Oxford, UK: Blackwell.
- Food and Agriculture Organization of the United Nations. (1996). *Forest resources assessment 1990: Survey of tropical forest cover and change processes* (FAO forestry paper 130). Rome: FAO Forestry Department.
- Fredsoe, J. (1978). Meandering and braiding of rivers. *Journal of Fluid Mechanics*, 84(4), 609-624.
- Galay, V. J., Kellerhals, R., & Bray, D. I. (1973). Diversity of river types in Canada. In *Fluvial processes and sedimentation* (pp. 217-250). Proceedings of Hydrology Symposium, National Research Council of Canada.
- Garcia, M. H. (2008). Sediment transport and morphodynamics. In M. H. Garcia (Ed.), *Sedimentation engineering: Processes, measurements, modeling, and practice* (pp. 21-164). Reston, VA: American Society of Civil Engineers.
- Gilvear, D. J. (1999). Fluvial geomorphology and river engineering: Future roles utilizing a fluvial hydrosystems framework. *Geomorphology*, 31, 229-245. doi:10.1016/S0169-555X(99)00086-0
- Gordon, M. E., Chordas, S. W., Harp, G. L., & Brown, A. V. (1995). Aquatic mollusca of the White River National Wildlife Refuge, Arkansas, U.S.A. *Walkerana*, 7(17-18), 1-9.
- Harnischmacher, S. (2007). Thresholds in small rivers? Hypotheses developed from fluvial morphological research in western Germany. *Geomorphology*, 92, 119-133.
- Harvey, M. D. (1989). Meanderbelt dynamics of the Sacramento River. In *Proceedings of the California riparian systems conference, U.S. Department of Agriculture Forest Service TR-PSW 110*, 54-61.
- Hays, R. L., Summers, C., & Seitz, W. (1981). *Estimating wildlife habitat variables* (FWS/OBS-B1/47). Washington, DC: U.S. Department of the Interior Fish and Wildlife Service.
- Henderson, F. M. (1966). *Open channel flow*. New York, NY: Macmillan Company.

- Hey, R. D. (1976). Geometry of river meanders. *Nature*, 262, 482-484. doi:10.1038 /262482a0
- Hickin, E. J. (1974). The development of meanders in natural river channels. *American Journal of Science*, 274, 414-442.
- Hickin, E. J., & Nanson, G. C. (1975). The characteristic of channel migration on the Beaton River, northwest British Columbia, Canada. *Geological Society of America Bulletin*, 86(4), 487-494. doi:10.1130/0016-7606(1975)86<487:TCOCMO>2.0.CO;2
- Hickin, E.J., & Nanson, G. C. (1984). Lateral migration rates of river bends. *Journal of Hydraulic Engineering, ASCE* 110(11), 1557-1567.
- Hjulström, F. (1939). Transportation of debris by moving water. In P. D. Trask (Ed.), *Recent marine sediments: A symposium* (1st ed., pp. 5-32). Tulsa, OK: American Association of Petroleum Geologists.
- Hooke, J. M. (1987). Changes in Meander Morphology. In V. Gardiner (Ed.), *International Geomorphology, 1986: Proceedings of the first international conference on geomorphology* (pp. 591-609). Chichester, UK: John Wiley & Sons.
- Hooke, J. M. (2004). Cutoffs galore!: Occurrence and causes of multiple cutoffs on a meandering river. *Geomorphology*, 61, 225-238. doi:10.1016/j.geomorph.2003.12.006
- Hooke, J. M. (2007a). Complexity, self-organisation and variation in behaviour in meandering rivers. *Geomorphology*, 91, 236-258. doi:10.1016/j.geomorph.2007.04.021
- Hooke, J. M. (2007b). Spatial variability, mechanisms and propagation of change in an active meandering river. *Geomorphology*, 84, 277-296. doi:10.1016/j.geomorph.2006.06.005
- Hooke, J. M. (2008). Temporal variations in fluvial processes on an active meandering river over a 20-year period. *Geomorphology*, 100(1-2), 3-13. doi:10.1016/j.geomorph.2007.04.034
- Hudson, P. F. (2002). Pool-riffle morphology in an actively migrating alluvial channel: The lower Mississippi River. *Physical Geography*, 23(2), 154-169. doi:10.2747/0272-3646.23.2.154
- Julien, P. Y. (1995). *Erosion and sedimentation*. New York, NY: Cambridge University Press.

- Julien, P. Y., & Klaassen, G. J. (1995). Sand-dune geometry of large rivers during floods. *Journal of Hydraulic Engineering, ASCE* 125(12), 657-663. doi:10.1061/(ASCE)1234-5678(1995)121:9(657)
- Junk, W. J. (1999). The flood pulse concept of large rivers: Learning from the tropics. *Archiv Für Hydrobiologie*, 115(3), 261-280.
- Karim, F. (1988). Bed material discharge prediction for nonuniform bed sediments. *Journal of Hydraulic Engineering, ASCE* 124(6), 597-604. doi:10.1061/(ASCE)0733-9429(1998)124:6(597)
- Karim, F. (1995). Bed configuration and hydraulic resistance in alluvial-channel flows. *Journal of Hydraulic Engineering, ASCE* 121(1), 15-25. doi:10.1061/(ASCE)1234-5678 (1995)121:1(15)
- Karim, F. (1999). Bed-form geometry in sand-bed flows. *Journal of Hydraulic Engineering, ASCE* 125(12), 1253-1261. doi:10.1061/(ASCE)0733-9429(1999)125:12(1253)
- Karim, F., & Kennedy, J. F. (1990). Menu of coupled velocity and sediment discharge relations for rivers. *Journal of Hydraulic Engineering, ASCE* 116(8), 978-996. doi:10.1061/(ASCE)0733-9429(1990)116:8(978)
- Kawakami, E. (2004). The flood pulse concept and its relation to fish biology in the Pantanal[Supplemental material]. Retrieved from <http://www-heb.pac.dfompo.gc.ca/congress/2004/Advances/55ResendeFlood.pdf>
- Keller, E.A., & Brookes, A. (1984). Consideration of meandering in channelization projects: Selected observations and judgements. In C.M. Elliott (Ed.), *River meandering: Proceedings of the conference rivers '83* (pp. 384-398). New York, NY: American Society of Civil Engineers.
- Kellerhals, R., Church, M., & Bray, D. I. (1976). Classification and analysis of river processes. *Journal of the Hydraulics Division, ASCE* 102(7), 813-829.
- Kellerhals, R., Neill, C. R., & Bray, D. I. (1972). *Hydraulic and geomorphic characteristics of rivers in Alberta* (River Engineering and Surface Hydrology Report No. 72-1). Alberta, CAN: Research Council of Alberta.
- Kennedy, J. F. (1961). *Stationary waves and antidunes in alluvial channels*. (Doctoral dissertation, California Institute of Technology). Retrieved from http://thesis.library.caltech.edu/2688/1/Kennedy_jf_1960.pdf
- Kennedy, J. F. (1963). Mechanics of dunes and antidunes in erodible-bed channels. *Journal of Fluid Mechanics*, 16(4), 521-544. doi:10.1017/S0022112063000975

- Kennedy, J. F. (1995). The Albert Shields story. *Journal of Hydraulic Engineering*, ASCE 121(11), 766-772. doi:10.1061/(ASCE)0733-9429(1995)121:11(766)
- Kennedy, J. F., & Brooks, N. H. (1965). Laboratory study of an alluvial stream at constant discharge. In *Proceedings of the Federal-Agency Sedimentation Conference 1963, Miscellaneous Publications U.S. Department of Agriculture 970*, 320-330.
- Keulegan, G. H. (1938). Laws of turbulent flow in open channels. *Journal of Research of National Bureau of Standards*, RP1151(21), 707-741.
- Khan, H. R. (1971). *Laboratory studies of alluvial river channel patterns*. (Unpublished Doctoral Dissertation). Colorado State University, Fort Collins, CO.
- Kolla, V., Posamentier, H. W., & Wood, L.J. (2007). Deep-water and fluvial sinuous channels—Characteristics, similarities and dissimilarities, and modes of formation. *Marine and Petroleum Geology*, (24), 388-405.
- Laczay, I. A. (1977). Channel pattern changes of Hungarian rivers: The example of the Hernad River. In K.J. Gregory (Ed.), *River channel changes* (pp. 185-192). Chichester, UK: John Wiley & Sons.
- Lagasse, P. F., Spitz, W. J., Zevenbergen, L. W., & Zachmann, D. W. (2004a). *Handbook for predicting stream meander migration* (NCHRP Report 533). Washington, DC: Transportation Research Board of the National Academies.
- Lagasse, P. F., Zevenbergen, L. W., Spitz, W. J., & Thorne, C. R. (2004b). *NCHRP Web-Only Document 67: Methodology for predicting channel migration* (Project 24-16). Retrieved from Transportation Research Board website: <http://www.trb.org/Main/Blurbs/155132.aspx>
- Lane, E. W. (1957). *A study of the shape of channels formed by natural streams flowing in erodible materials* (MRD/SSR-9). Omaha, NE: United States Army Engineer Division, Corps of Engineers.
- Leeder, M. R., & Bridges, P. H. (1975). Flow separation in meander bends. *Nature*, 253, 338-339. doi:10.1038/253338a0
- Leopold, L. B. (1973). River channel change with time: An example. *Geological Society of America Bulletin*, 84(6), 1845-1860. doi:10.1130/0016-7606(1973)84<1845:RCCWTA>2.0.CO;2
- Leopold, L. B. (1994). *A view of the river*. Cambridge, MA: Harvard University Press.
- Leopold, L. B., & Wolman, M. G. (1957). River channel pattern: Braided, meandering and straight. *United States Geological Survey Professional Paper 282-B*, 39-85.

- Leopold, L. B., & Wolman, M. G. (1960). River meanders. *Geological Society of America Bulletin*, 71(6), 769-793. doi:10.1130/0016-7606(1960)71[769:RM]2.0.CO;2
- Leopold, L. B., Wolman, M. G., & Miller, J. P. (1964). *Fluvial processes in geomorphology*. New York, NY: Dover Earth Science Publications.
- Lewin, J. (1978). Meander development and floodplain sedimentation: A case study from mid-Wales. *Geological Journal*, 13(1), 25-36. doi:10.1002/gj.3350130104
- Lewin, J., & Brewer, P. A. (2001). Predicting channel patterns. *Geomorphology*, 40, 329-339. doi:10.1016/S0169-555X(01)00061-7
- Luchi, R., Hooke, J. M., Zolezzi, G., & Bertoldi, W. (2010). Width variations and mid-channel bar inception in meanders: River Bollin (UK). *Geomorphology*, 119, 1-8. doi:10.1016/j.geomorph.2010.01.010
- Mackin, J. H. (1948). Concept of the graded river. *Geological Society of America Bulletin*, 59(5), 463-512. doi:10.1130/0016-7606(1948)59[463:COTGR]2.0.CO;2
- Markham, A. J., & Thorne, C. R. (1992). Geomorphology of gravel-bed river bends. In P. Billi, R. D. Hey, C.R. Thorne, & P. Tacconi (Eds.), *Dynamics of gravel-bed rivers* (pp. 432-450). Chichester, UK: John Wiley & Sons.
- Matthes, G. H. (1941). Basic aspects of stream meanders. *Transactions of the American Geophysical Union*, 22, 632-636.
- Matthes, G. H. (1956). River engineering. In P.O. Abbott (Ed.), *American civil engineering practice volume II* (pp. 15-56). New York, NY: John Wiley & Sons.
- McKeown, F. A., Jones-Cecil, M., Askew, B. L., & McGrath, M. A. (1998). Analysis of stream profile data and inferred tectonic activity, eastern Ozark Mountains region. *U.S. Geological Survey Bulletin* 1807, 1-39.
- Meinzer, O.E. (1923). *Outline of ground-water hydrology with definitions: United States Geological Survey Water Supply Paper 494*. Washington, D.C: Government Printing Office.
- Melton, F. A. (1936). An empirical classification of flood-plain streams. *Geographical Review*, 26(4), 593-609.
- Miall, A. D. (1977). A review of the braided-river depositional environment. *Earth-Science Reviews*, 13(1), 1-62. doi:10.1016/0012-8252(77)90055-1

- Miller, T. K. (1988). An analysis of the relation between stream channel sinuosity and stream channel gradient. *Computers, Environment and Urban Systems*, 12(3), 197-207.
- Mollard, J. D. (1973). Air photo interpretation of fluvial features. In *Fluvial processes and sedimentation* (pp. 341-380). Proceedings of Hydrology Symposium, National Research Council of Canada.
- Nanson, G. C., & Croke, J. C. (1992). A genetic classification of floodplains. *Geomorphology*, 4(6), 459-486. doi:10.1016/0169-555X(92)90039-Q
- Nanson, G. C., & Hickin, E. J. (1983). Channel migration and incision on the Beatton River. *Journal of Hydraulic Engineering, ASCE* 109(3), 327-337.
- Nanson, G. C., & Hickin, E. J. (1986). A statistical analysis of bank erosion and channel migration in western Canada. *Geological Society of America Bulletin*, 97(4), 497-504. doi: 10.1130/0016-7606(1986)97<497:ASAOBE>2.0.CO;2
- Neill, C. R. (1984). Bank erosion versus bedload transport in a gravel river. In C.M. Elliott (Ed.), *River meandering* (pp. 204-211). New York, NY: American Society of Civil Engineers.
- Paine, D. P., & Kiser, J. D. (2003). *Aerial photography and image interpretation* (2nd ed.). Hoboken, NJ: John Wiley & Sons.
- Parish Geomorphic Ltd. (2004). *Belt width delineation procedures* (Final Report 98-023). Retrieved from http://www.sustainabletechnologies.ca/portal/alias__rainbow/lang__en/tabID__121/DesktopDefault.aspx
- Parker, G., & Anderson, A. G. (1975). Modeling of meandering and braiding in rivers. *Proceedings of the First ASCE Symposium on Modeling Techniques*, San Francisco, CA. 575-591.
- Peterson, J. T., & Rabeni, C. F. (2001). Evaluating the physical characteristics of channel units in an Ozark stream. *Transactions of the American Fisheries Society*, 130, 898-910.
- Petts, G. E., & Foster, I. (1985). *Rivers and landscape*. London, UK: Edward Arnold.
- Peurifoy, R. L., & Oberlender, G. D. (2001). *Estimating construction costs* (5th ed.). New York, NY: McGraw-Hill.
- Pfankuch, D. J. (1975). *Stream reach inventory and channel stability evaluation* (USDA Forest Service R-175-902). Washington, DC: Government Printing Office.

- Pidwirny, M. (2006). The drainage basin concept. In *Fundamental of physical Geography, 2nd edition*. Retrieved from <http://www.physicalgeography.net/fundamentals/chapter10.html>
- Rabeni, C. F. (2000). Evaluating the physical habitat integrity in relation to the biological potential of streams. *Hydrobiologia*, 422/423, 245-256. doi:10.1023/A:1017022300825
- Richards, K. (1982). *Rivers: Form and process in alluvial channels*. New York, NY: Methuen & Company.
- Ricketts, T. H., Dinerstein, E., Olson, D. M., Loucks, C. J., Eichbaum, W., DellaSalla, D., . . . Walters, S. (1999). *Terrestrial ecoregions of North America*. Washington, DC: Island Press.
- Rosgen, D. L. (1985). A stream classification system. In *Proceedings of the first North American riparian conference – Riparian ecosystem and their management: reconciling conflicting uses, U.S. Department of Agriculture Forest Service RM 120*, 91-95.
- Rosgen, D. L. (1994). A classification of natural rivers. *Catena*, 22, 169-199.
- Rosgen, D. L. (2001). A stream channel stability assessment methodology. In *Proceedings of the Seventh Federal Interagency Sedimentation Conference: Vol I* (pp. II-18–II-26). Reno, NV: The Subcommittee on Sedimentation.
- Rosgen, D. L. (2004). *River assessment and monitoring field guide*. Fort Collins, CO: Wildland Hydrology Inc.
- Rosgen, D. L., & Silvey, H. L. (1996). *Applied river morphology*. Pagosa Springs, CO: Wildland Hydrology Books.
- Rouse, H. (1937). Modern conceptions of the mechanic of fluid turbulence. *Transactions of the American Society of Civil Engineers*, 102(1965), 463-543.
- Rouse, H. (1939). *An analysis of sediment transportation in light of fluid turbulence* (SCS-T P-25). Washington, DC: United States Department of Agriculture.
- Schumm, S. A., & Khan, H. R. (1972). Experimental study of channel patterns. *Geological Society of America Bulletin*, 83(6), 1755-1770. doi:10.1130/0016-7606(1972)83[1755:ESOC]2.0.CO;2
- Schumm, S. A., & Lichty, R. W. (1963). Channel widening and floodplain construction along the Cimaron River in South Western Kansas. *United States Geological Survey Professional Paper 352-D*, 71-88.

- Schumm, S. A. (1963). *A tentative classification of alluvial river channels*. Washington, DC: United States Geological Survey Circular 477.
- Schumm, S. A. (1968). River adjustments to altered hydrologic regimen: Murrumbidgee River and paleochannels, Australia. *United States Geological Survey Professional Paper* 598, 1-65.
- Schumm, S. A. (1969). River metamorphosis. *Journal of the Hydraulics Division, ASCE* 95(HY1), 255-273.
- Schumm, S. A. (1977). *The fluvial system*. New York, NY: John Wiley & Sons.
- Schumm, S. A. (1981). Evolution and response of the fluvial system, sedimentologic implications. *Society of Economic Paleontologists and Mineralogists, Special Publication* 31, 19-29.
- Schumm, S. A. (1985). Patterns of alluvial rivers. *Annual Review of Earth and Planetary Sciences*, 13, 5-27. doi:10.1146/annurev.earth.13.050185.000253
- Selby, M. J. (1985). *Earth's changing surface: An introduction to geomorphology*. Oxford, UK: Oxford University Press.
- Shields, A., Ott, W. P., & Van Uchelen, J. C. (1936). *Application of similarity principles and turbulence research to bed-load movement*. (Doctoral dissertation translation, California Institute of Technology). Retrieved from <http://repository.tudelft.nl/view/hydro/uuid%3Aa66ea380-ffa3-449b-b59f-38a35b2c6658/>
- Spitz, W. J., & Schumm, S. A. (1997). Tectonic geomorphology of the Mississippi valley between Osceola, Arkansas, and Friars Point, Mississippi. *Engineering Geology*, 46(3), 259-280. doi:10.1016/S0013-7952(97)00006-9
- Stolum, H. H. (1996). River meandering as a self-organisation process. *Science*, 271(5256), 1710-1713. doi:10.1126/science.271.5256.1710
- Stolum, H. H. (1998). Planform geometry and dynamics of meandering rivers. *Geological Society of America Bulletin*, 110(11), 1485-1498.
- Sturm, T. W. (2001). *Open channel hydraulics* (International ed.). Boston, MA: McGraw-Hill.
- Thornbury, W. D. (1969). *Principles of geomorphology* (2nd ed.). New York, NY: John Wiley & Sons.
- Thorne, C. R., Hey, R. D., & Newson, M. D. (Eds.). (1997) *Applied fluvial geomorphology for river engineering and management*. Chichester, UK: John Wiley & Sons.

- Thorp, J. H., & Delong, M. D. (1994). The riverine productivity model: An heuristic view of carbon sources and organic processing in large river ecosystems. *Oikos*, 70(2), 305-308.
- Timar, G. (2003). Controls on channel sinuosity changes: A case study of the Tisza River, the great Hungarian Plain. *Quaternary Science Reviews*, 22(20), 2199-2207. doi:10.1016/S0277-3791(03)00145-8
- U.S. Army Corps of Engineers. (2009). *Final environmental impact statement: White River basin, Arkansas, minimum flows*. Little Rock, AR: USACE. Retrieved from http://www.swl.usace.army.mil/planning/wrminflow_pdf/a_REVISED_WRMF_FIS_010609.pdf
- U. S. Army Corps of Engineers Hydrologic Engineering Center. (1976). *HEC 6: Scour and deposition in rivers and reservoirs, User's manual* (723-X6-L202A). Davis, CA: U.S. Army Corps of Engineer.
- U.S. Army Corps of Engineers Hydrologic Engineering Center. (2000). *HEC-GeoRAS: An extension for support of HEC-RAS using ArcView, User's manual* (version 3.0). Davis, CA: U.S. Army Corps of Engineers.
- U.S. Army Corps of Engineers Hydrologic Engineering Center. (2005). *HEC-GeoRAS: GIS tools for HEC-RAS using ArcGIS, User's manual* (version 4.0 BETA). Davis, CA: U. S. Army Corps of Engineers.
- U.S. Army Corps of Engineers Hydrologic Engineering Center. (2010). *HEC-RAS: River Analysis System, User's manual* (version 4.1). Davis, CA: USACE. Retrieved from <http://www.hec.usace.army.mil/software/hecras/hecras-document.html>
- U.S. Department of Agriculture, Natural Resources Conservation Service. (2007). Chapter XII: Channel alignment and variability design. In *National engineering handbook Part 654 : Stream restoration design* (pp. 12-1 – 12-31). Washington, DC: Retrieved from <http://www.nae.usace.army.mil/Regulatory/Restoration/index.htm>
- U. S. Department of Agriculture, Soil Survey Staff. (1951). *USDA: Soil Survey Manual* (Report No.18). Washington, DC: Government Printing Office.
- U.S. Department of the Interior, Bureau of Land Management. (1998). *Riparian area management: A user guide to assessing proper functioning condition for the supporting science for lotic areas* (TR1717-15). Denver, CO: BLM Service Center. Retrieved from <ftp://ftp.blm.gov/pub/nstc/techrefs/Final%20TR%201737-15.pdf>

- U.S. Department of the Interior, Bureau of Land Management. (2005). *Riparian area management: Riparian and wetland classification* (TR 1737-21). Denver, CO: BLM Service Center. Retrieved from <ftp://ftp.blm.gov/pub/nstc/techrefs/Final%20TR%201737-21.pdf>
- U.S. Department of the Interior, Bureau of Land Management. (1994). *Riparian area management: The use of aerial photography to manage riparian-wetland areas* (TR1737-10). Denver, CO: BLM Service Center. Retrieved from <http://www.blm.gov/nstc/library/pdf/Final%20TR%201737-10.pdf>
- Van den Berg, J. H. (1995). Prediction of alluvial channel pattern of perennial rivers. *Geomorphology*, 12(4), 259-279. doi:10.1016/0169-555X(95)00014-V
- Van den Berg, J.H., & Van Gelder, A. (1993). Prediction of suspended bed material transport in flows over silt and very fine sand. *Water Resources Research*, 29(5), 1393-1404.
- Van Rijn, L. C. (1982). Equivalent roughness of alluvial bed. *Journal of the Hydraulics Division, ASCE* 108(HY10), 1215-1218.
- Van Rijn, L. C. (1984a). Sediment transport, part I: Bed load transport. *Journal of Hydraulic Engineering, ASCE* 110(10), 1431-1456.
- Van Rijn, L. C. (1984b). Sediment transport, part II: Suspended load transport. *Journal of Hydraulic Engineering, ASCE* 110(11), 1613-1641.
- Van Rijn, L. C. (1984c). Sediment transport, part III: Bed forms and alluvial roughness. *Journal of Hydraulic Engineering, ASCE* 110(12), 1733-1754.
- Ward, J. V., & Stanford, J. A. (1983). The intermediate disturbance hypothesis: An explanation for biotic diversity pattern in lotic ecosystems. In T. D. Fontaine & S. M. Bartell (Eds.), *Dynamics of lotic ecosystems* (pp. 347-356). Ann Arbor, MI: Ann Arbor Science Publishers.
- Watson, C. C., Biedenharn, D. S., & Scott, S. H. (1999). *Channel rehabilitation: processes, design, and implementation*. Vicksburg, MS: U.S. Army Engineer. Retrieved from USACE Research and Development Center website:
- Williams, G. P. (1978). Bank-full discharge of rivers. *Water Resources Research*, 14(6), 1141-1154.
<http://chl.erdc.usace.army.mil/Media/2/9/0/ChannelRehabilitation.pdf>
- Williams, G. P. (1986). River meanders and channel size. *Journal of Hydrology*, 88(1-2), 147-164. doi:10.1016/0022-1694(86)90202-7

- Wolman, M. G. (1954). A method of sampling coarse river-bed material. *Transactions of the American Geophysical Union*, 35(6), 951-956.
- Wright, S. (2000, June). Where river flows through forest-In Arkansas, some of the nation's most important bottomland hardwood forests are teeming with both wildlife and controversy. *National Wildlife Magazine*, 38(4), 38-44.
- Yalin, M. S. (1972). *Mechanics of sediment transport*. New York, NY: Pergamon Press.
- Yang, C. T. (1972). Unit stream power and sediment transport. *Journal of the Hydraulics Division, ASCE* 98(HY10), 1805-1826.
- Yang, C. T. (1973). Incipient motion and sediment transport. *Journal of the Hydraulics Division, ASCE* 99(HY10), 1679-1704.
- Yang, C. T. (1996). *Sediment transport theory and practice*. New York, NY: McGraw-Hill.
- Yen, C., & Ho, S. (1990). Bed evolution in channel bends. *Journal of Hydraulic Engineering*, 116(4), 544-562. doi:10.1061/(ASCE)0733-9429(1990)116:4(544)
- Zernitz, E. R. (1932). Drainage patterns and their significance. *The Journal of Geology*, 40(6), 498-521. doi:10.1086/623976
- Zweifel, R. D., Hayward, R. S., & Rabeni, C. F. (1999). Bioenergetics insight into black bass distribution shifts in Ozark border region streams. *National American Journal of Fisheries Management*, 19(1), 192-197. doi:10.1577/1548-8675(1999)019<0192:BIIBBD>2.0.CO;2

APPENDIX A: Procedure for Drainage Delineation

Since it is suspected that the dimensions of a sub-basin, specifically the width, may be correlated to the sinuosity, drainage delineation procedure to determine the dimensions of the White River's sub-basins are implemented as follows:

- 1.0. Run EPA Basins 4.0 to find sub-basin HUC numbers (i.e. the White River – 08010301, 08020302, 08020303, 08020304, 11010004, 11010012, 11010013, 11010014).
- 2.0. Download sub-basins DEMG.exe from http://www.epa.gov/waterscience/ftp/basins/gis_data/huc/.
- 3.0. Extract the DEMG files.
- 4.0. Add the DEM files to ArcMAP.

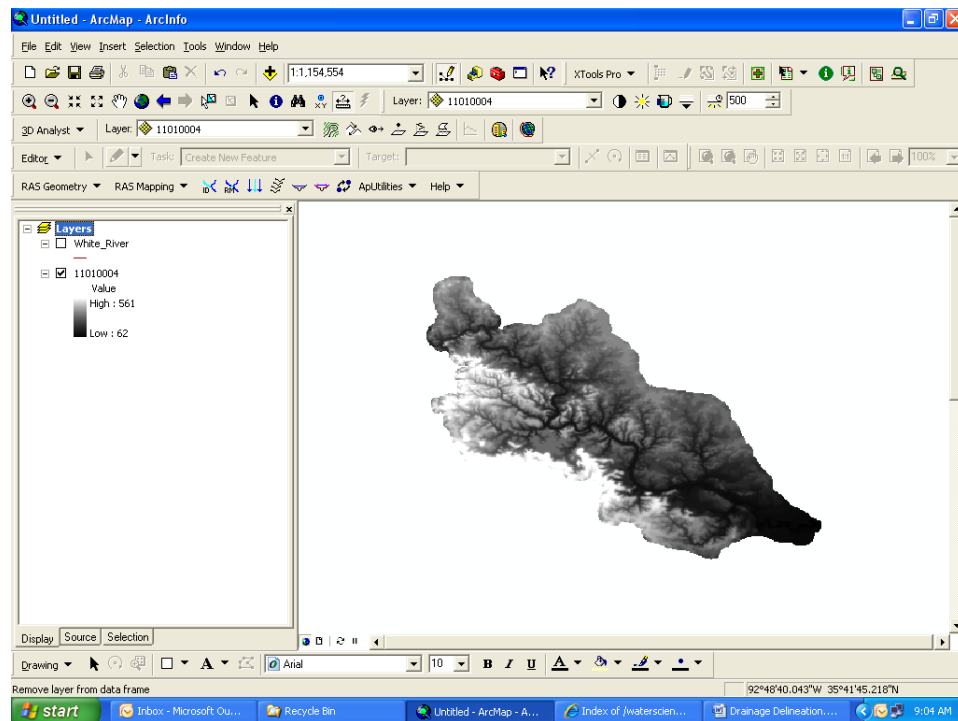


Figure A.1. Open DEM Files from ArcMAP.

- 5.0. Open Arc Toolbox > Conversion Table > From Raster > Raster to Polygon.

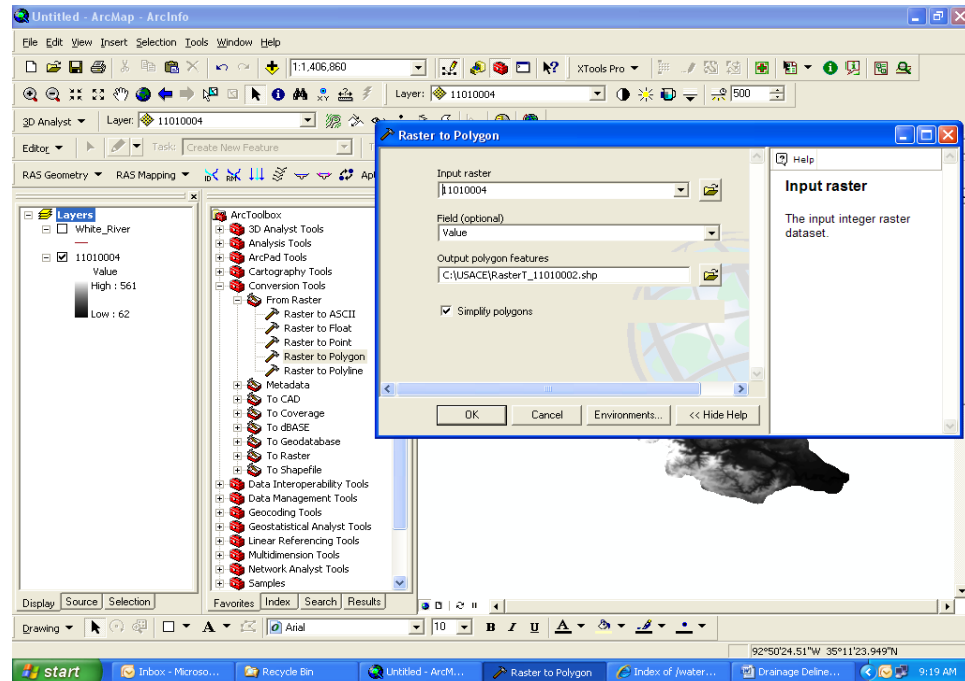


Figure A.2. Raster to Polygon Window.

6.0. Use Arc Toolbox > Data Management Tools > Generalization > Aggregate Polygon and set distance to 100 ft.

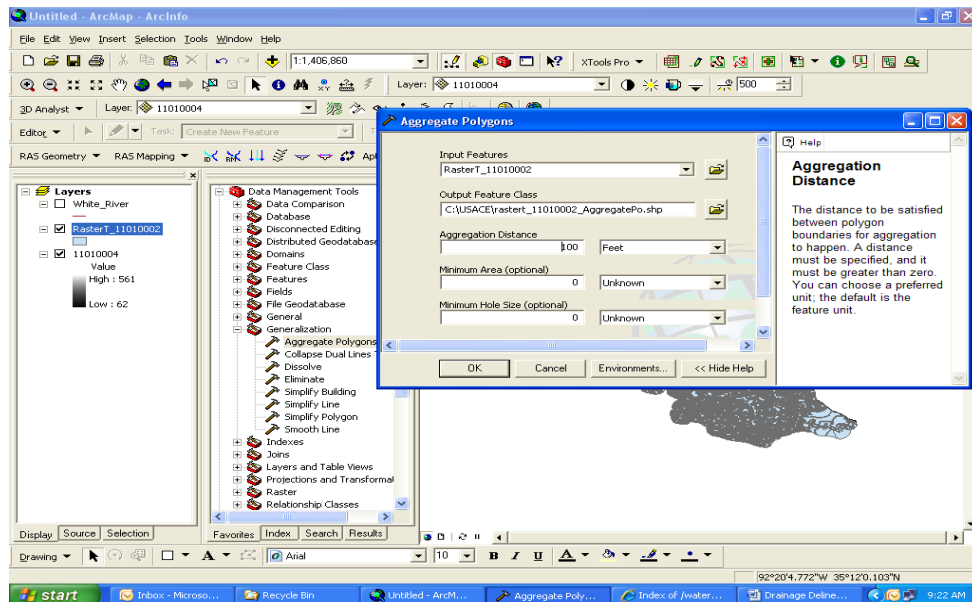


Figure A.3. Aggregate Polygon Window.

7.0. Go to Arc Toolbox > Analysis Tools > Proximity > Buffer to create sub-basin polygon.

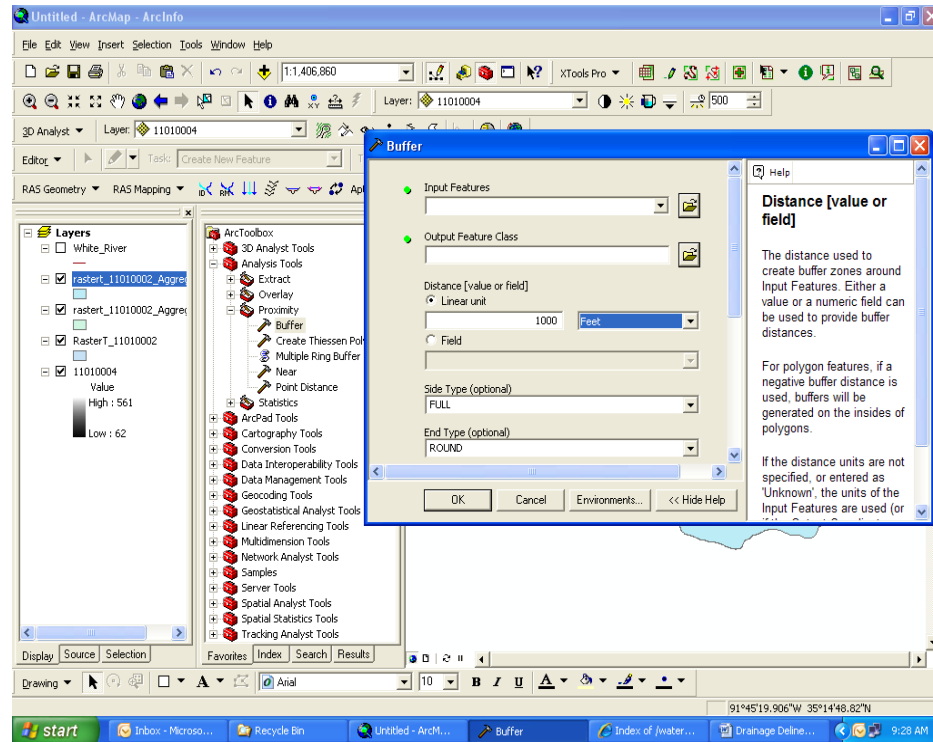


Figure A.4. Buffer Window.

8.0. Calculate the polygon area following the steps:

8.1. Click the right button of the newly created polygon > Open Attributes table.

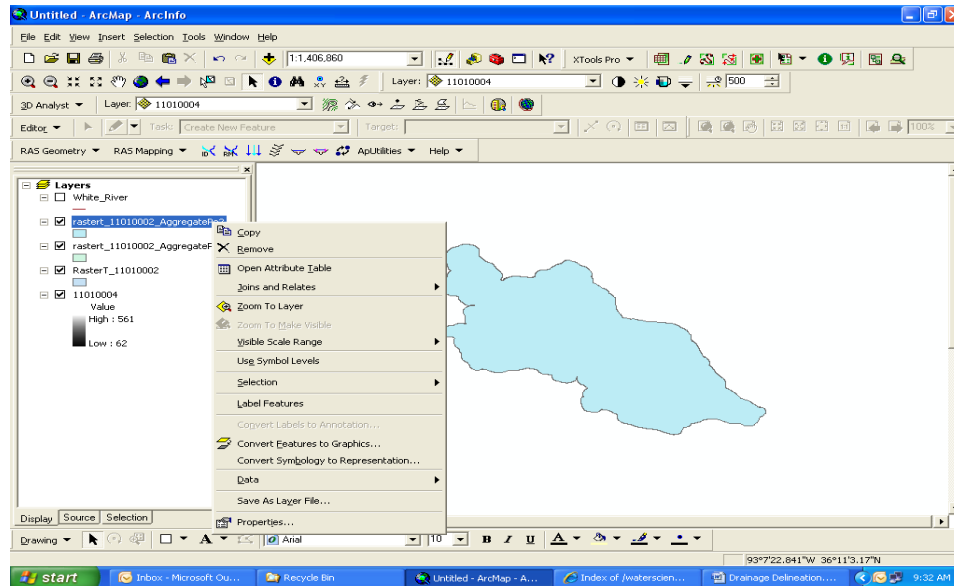


Figure A.5. Open Attributes Option.

8.2. Go to Options > Add Fields > Give a name “Poly_Area” > Type > Double.

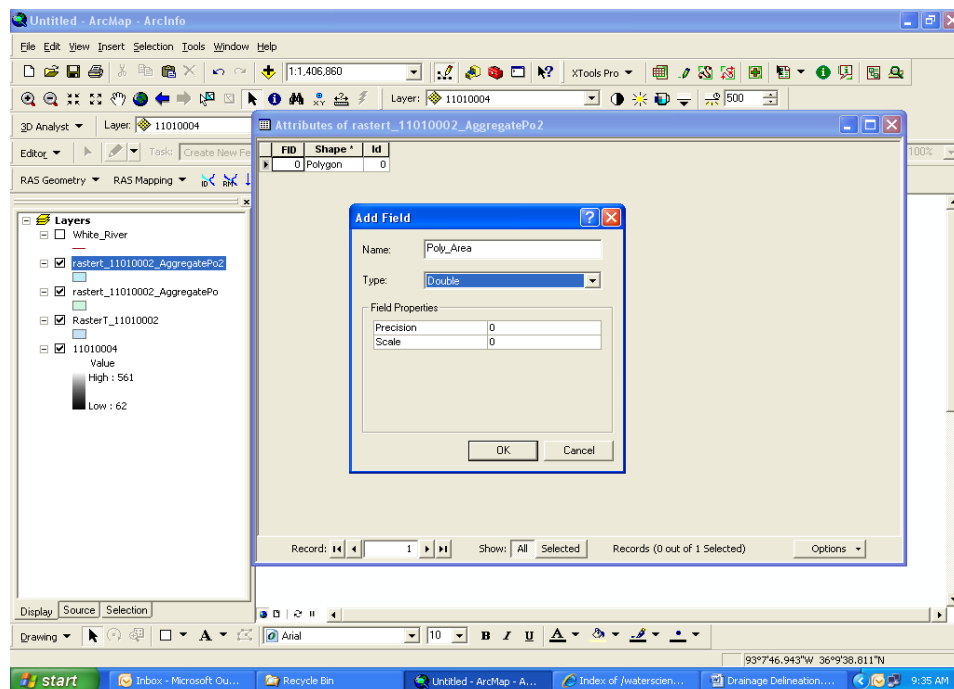


Figure A.6. Add Field Window.

8.3. Go to “Poly-Area” Title Bar and click the right button > Field Calculator.

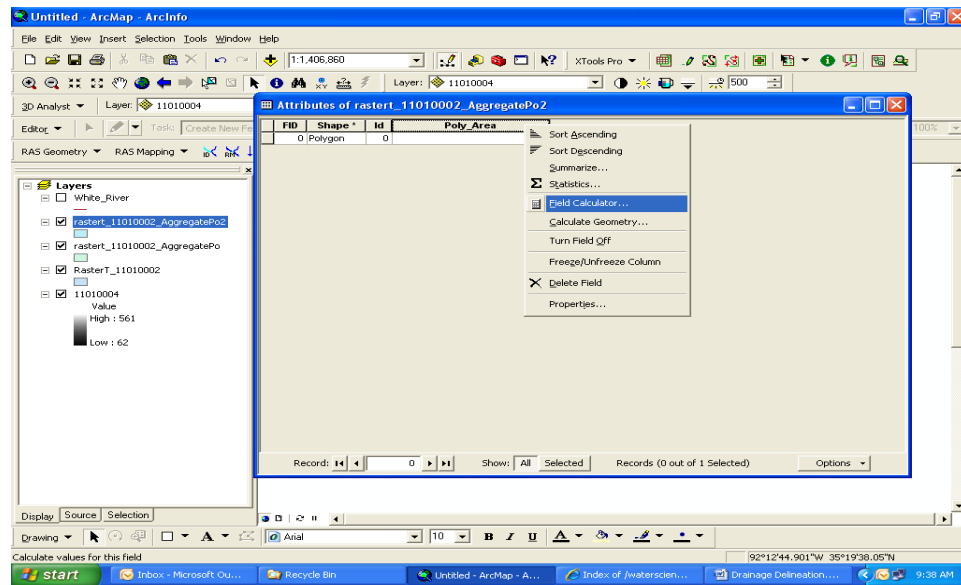


Figure A.7. Field Calculator.

8.4. Check Advanced > Click Help and find “To Calculate Area” > Copy VBA script and paste to Pre-logic VBA script code > Poly_Area = Output.

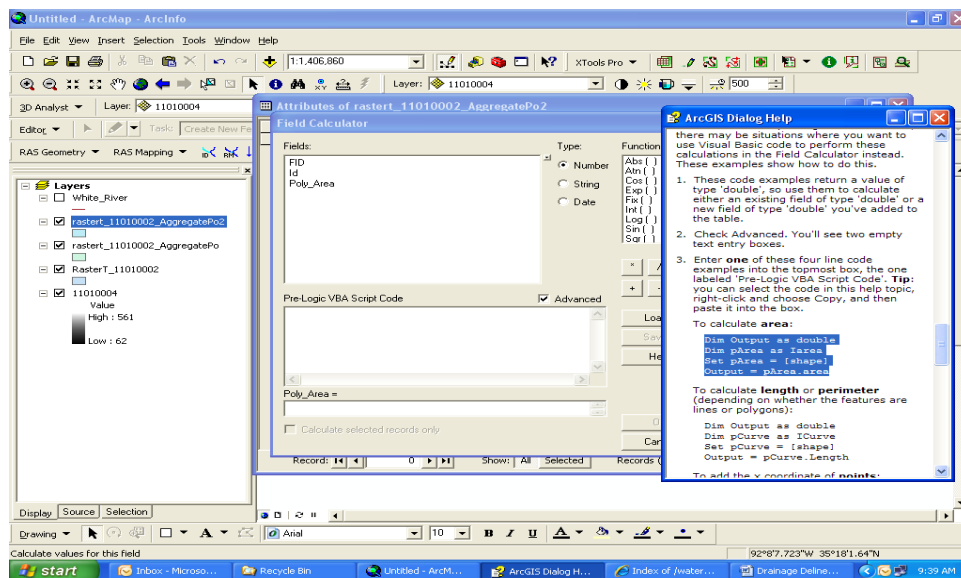


Figure A.8. VBA Script for Area Calculation.

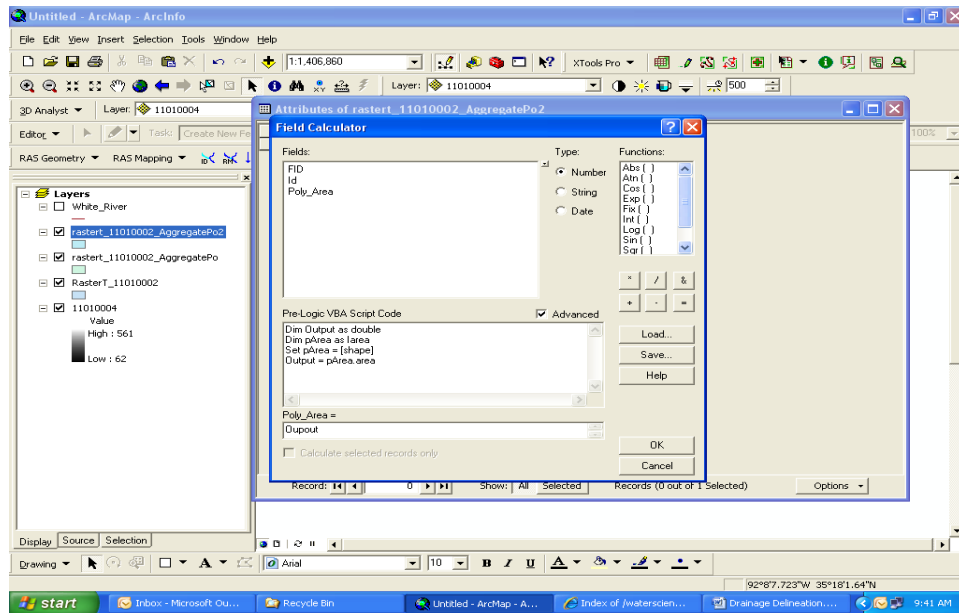


Figure A.9. Copy and Paste VBA Script to Pre-logic VBA Script Code Box.

8.5. Check the unit by right clicking the right button of “Poly_Area” > Calculate Geometry > Select “Square Miles US”.

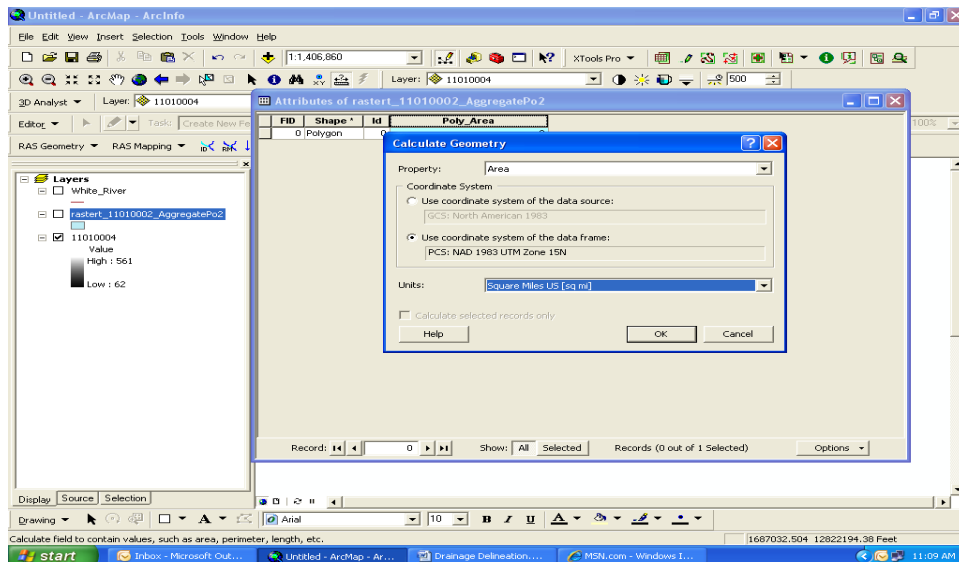


Figure A.10. Unit Selection from Calculate Geometry Window.

8.6. Finally, use Ruler tool to manually measure sub-basin width and length.

APPENDIX B: Procedure for Extracting NRCS-NCGC's SSURGO Soil Data Mart

The surface soil texture for various counties of Arkansas proximal to the White River are extracted by following the procedure shown below. The counties include Arkansas Counties (AR001), Desha County (AR041), Independence County (AR063), Jackson County (AR067), Monroe County (AR095), Phillips County (AR107), White County (AR145), Woodruff County (AR147), and Lonoke and Prairie Counties (AR680).

Obtain the Data

- 1.0. Go to the United States Department of Agriculture's National Resources Conservation Service website <http://soildatamart.nrcs.usda.gov/>.
- 2.0. Click on "Select State"> Highlight Arkansas > Select Survey Area.

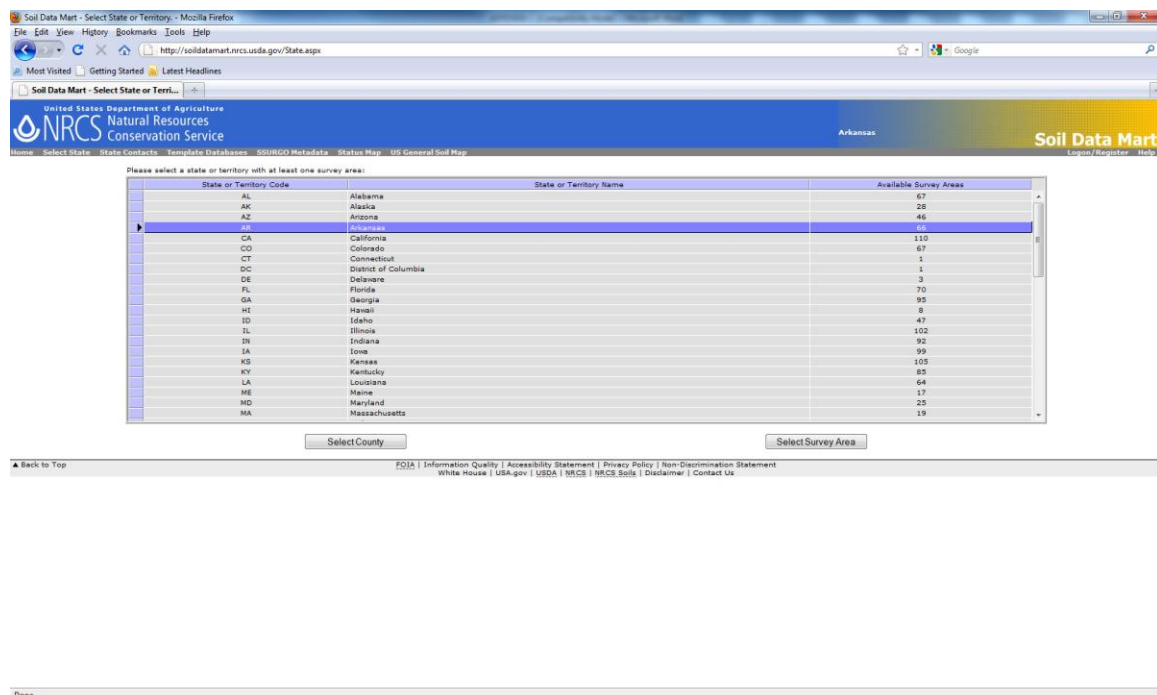


Figure B.1. Select Survey Area: Arkansas.

- 3.0. Highlight a county > Click Download Data > Select option "Tabular and Spatial Data" > Select spatial format "ArcView Shapefile" > Select coordinate system "UTM Zone 15, Northern Hemisphere (NAD83)" > Select template database "US: MS Access 2002 Version" > Enter personal email address > Click Submit Request.

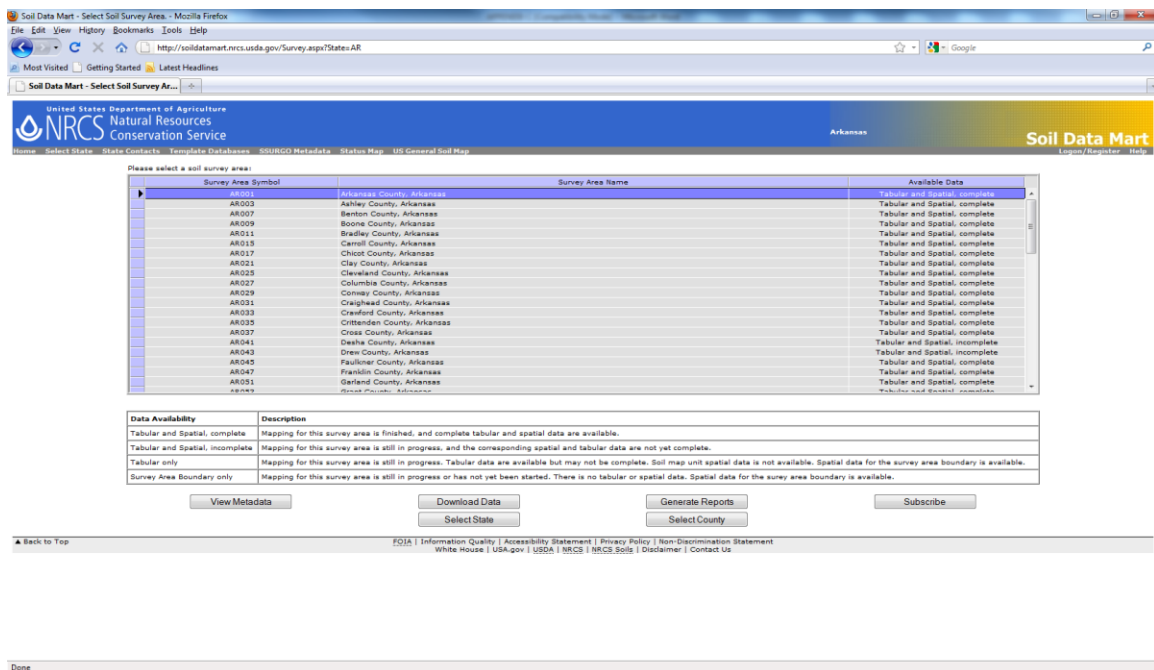


Figure B.2. Select Survey Area by County.

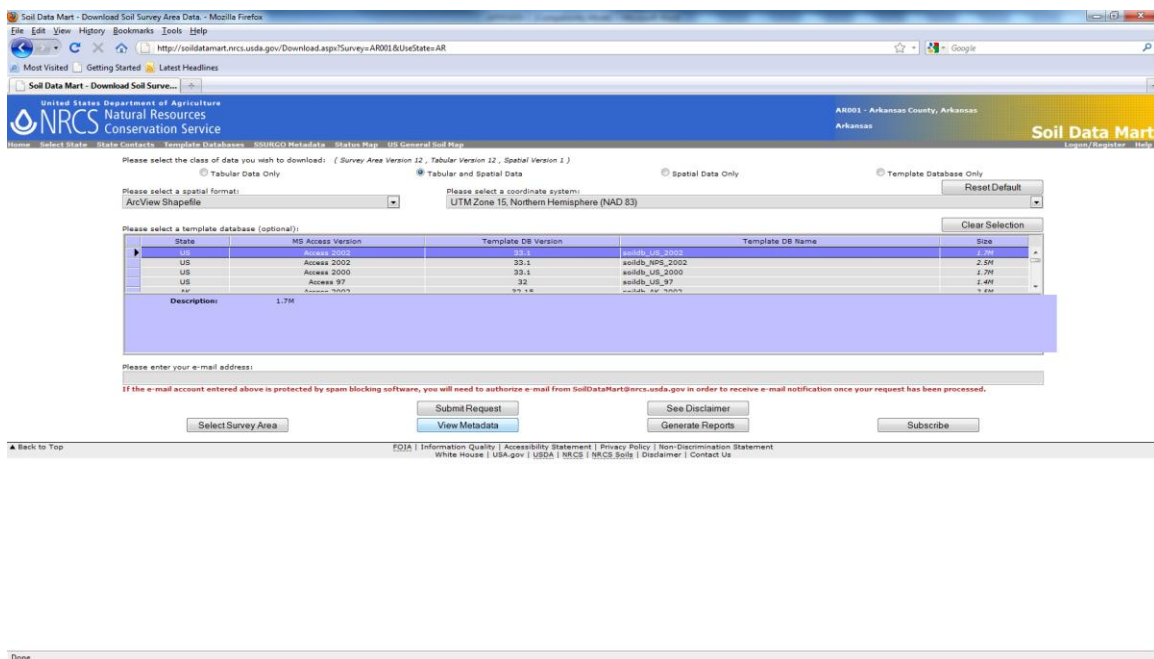


Figure B.3. Select Option/Submit Request Window.

4.0. Click on the link to download a zip file “soil_XXXXX” and extract.

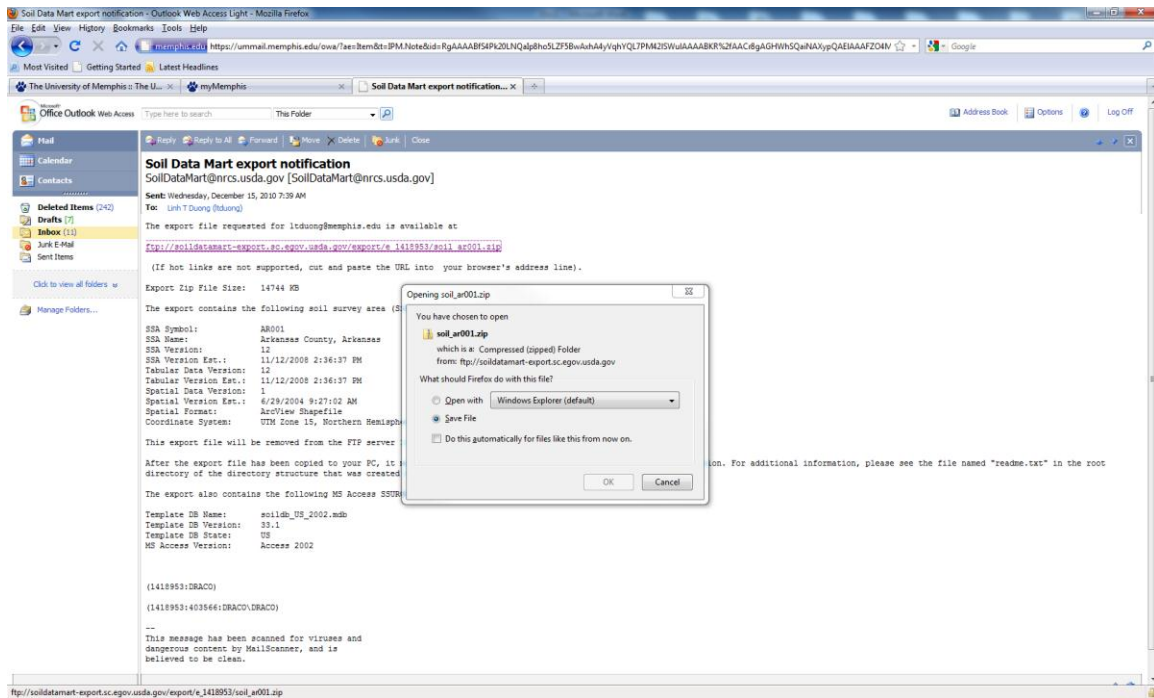


Figure B.4. Download Soil Data Mart Zip File.

Preprocess the Data

5.0. Inside this folder, there should be another zip file “soildb_US_2002”. Extract and Open the Microsoft Access database template.

6.0. The import form should appear. Enter the path to the folder containing the tabular data> Click OK > Close Microsoft Access > Launch ArcGIS.

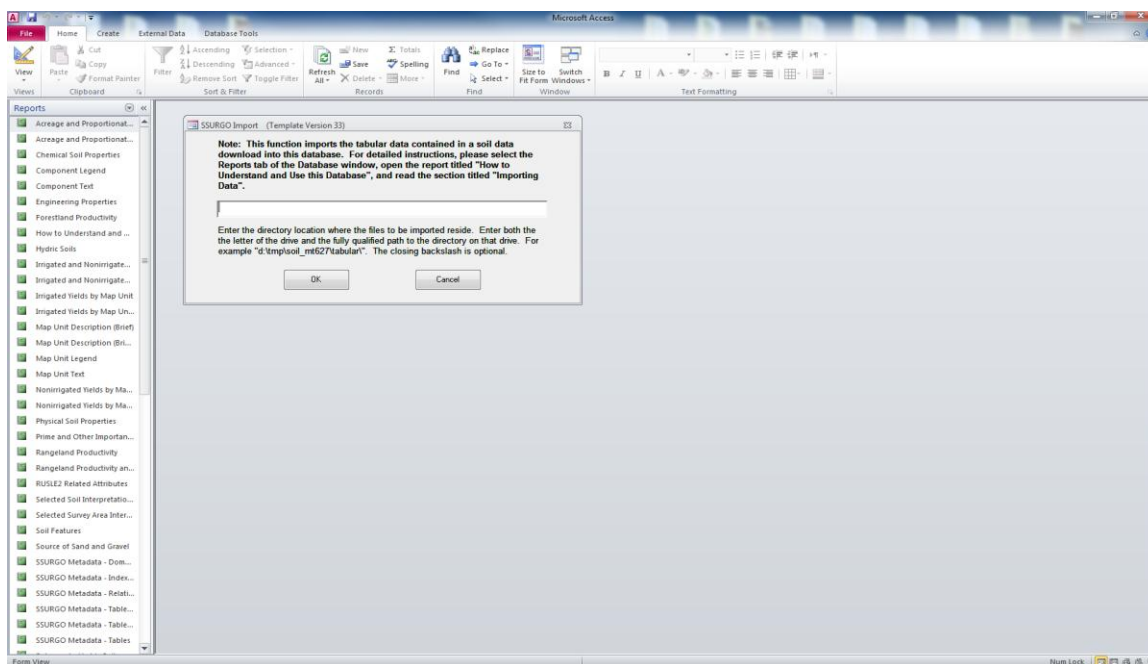


Figure B.5. SSURGO Import Window.

7.0. Add the “soilmu_a_XXXXX.shp shapefile” file from the “spatial” folder into ArcGIS (XXXX is the unique identifier for the soil file you downloaded).

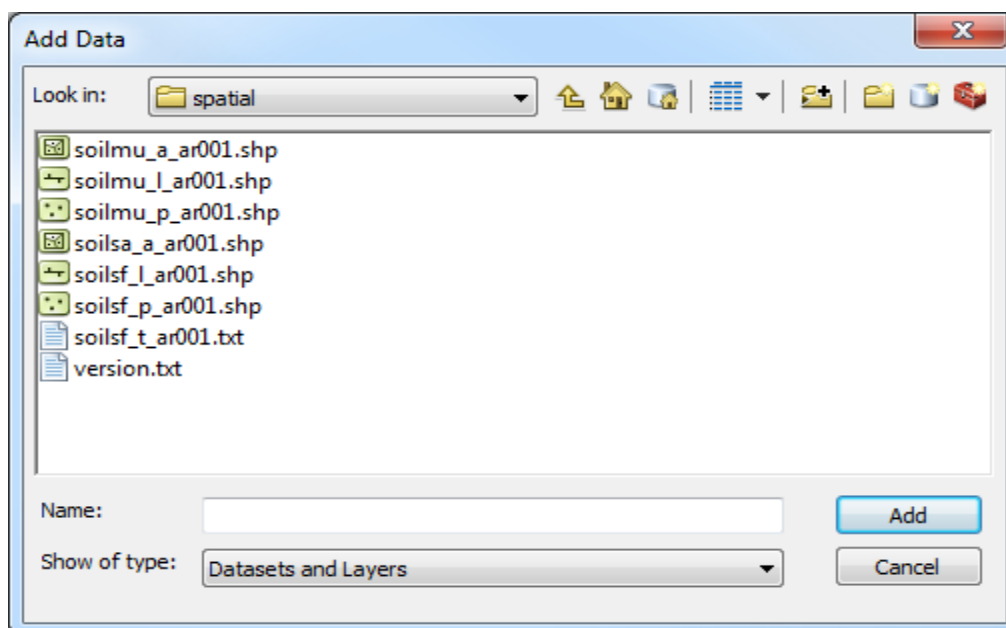


Figure B.6. Add Data Shapefile.

9.0. Join the “mapunit” table contained within the geodatabase to “soilmu_a_XXXXX.shp” using the mukey field by:

9.1. Right Clicking the “soilmu_a_XXXXX.shp” > Joins and Relates > Join > Click OK.

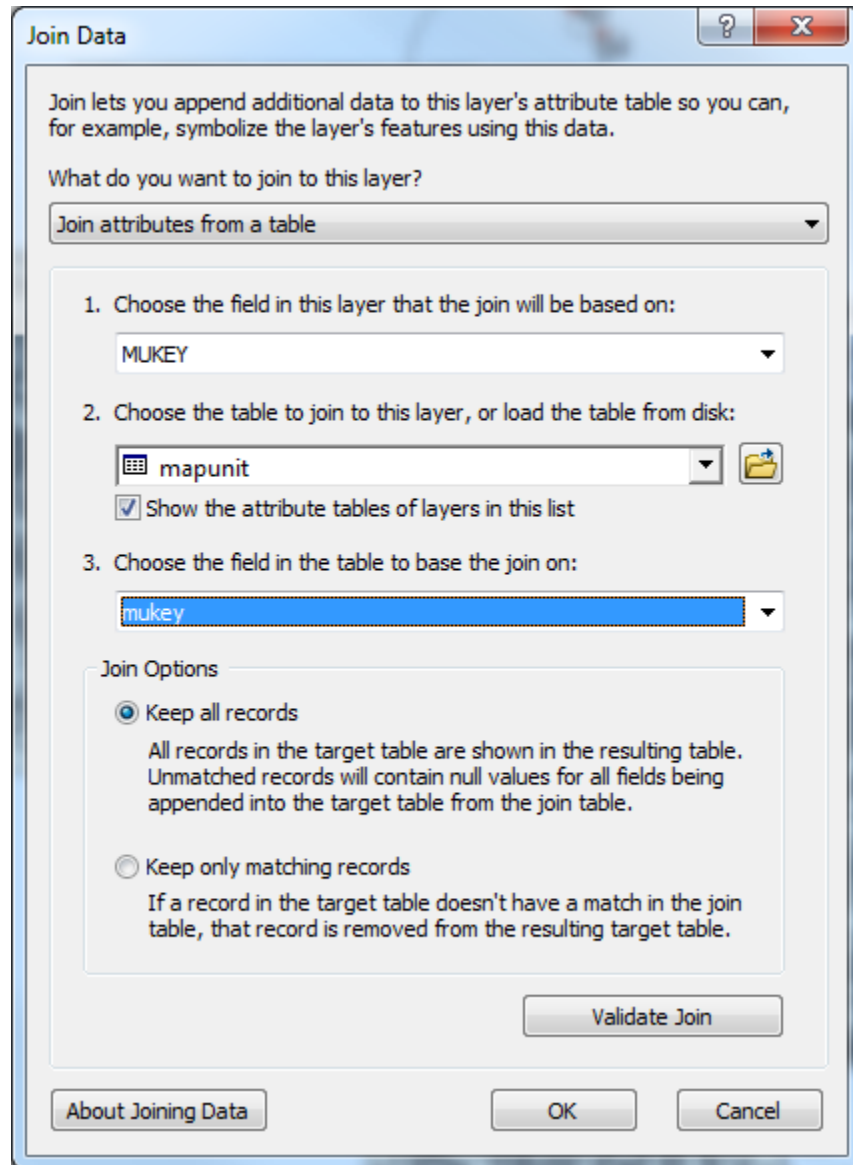


Figure B.9. Join Data Window.

9.2. Double Click on “soilmu_a_XXXXX.shp” > Select Symbolology > Categories > Value Field “muname” > Uncheck “all other values” box > Right Click “all other value” box > Property for all symbols > Select “No Color” for Outline Color.

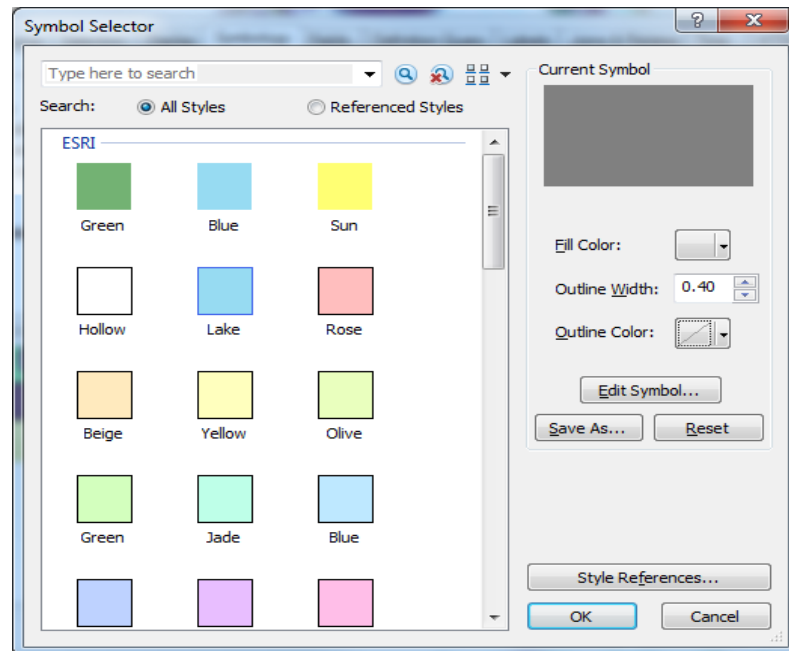


Figure B.10. Symbol Selector Window.

9.3. Click on “Add All Values”. This should assign each soil type to a specific color.

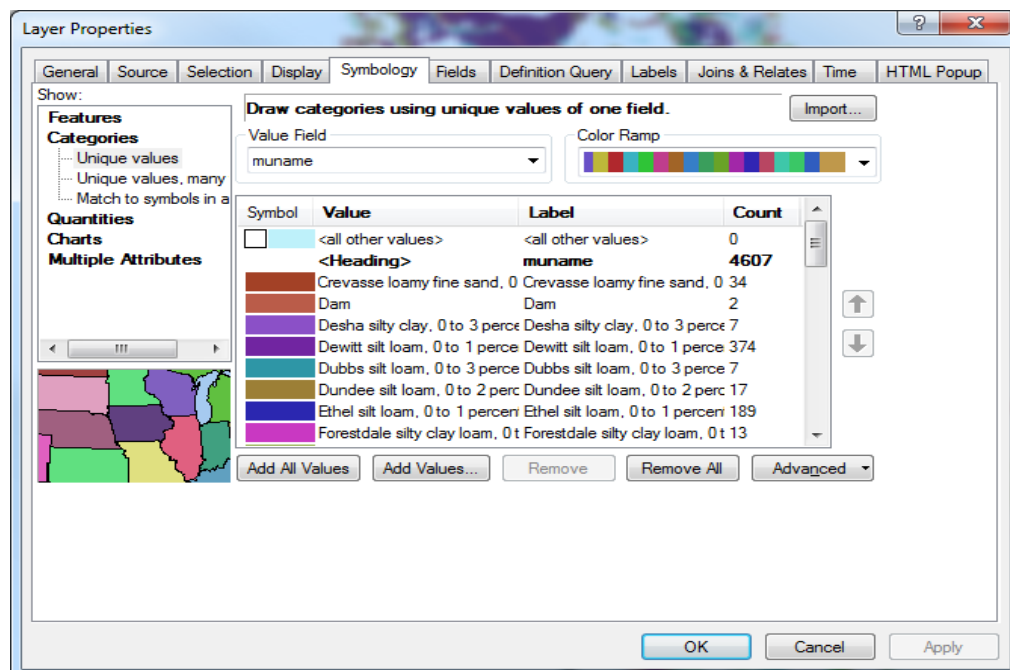


Figure B.11. Layer Properties/Symbology Window.

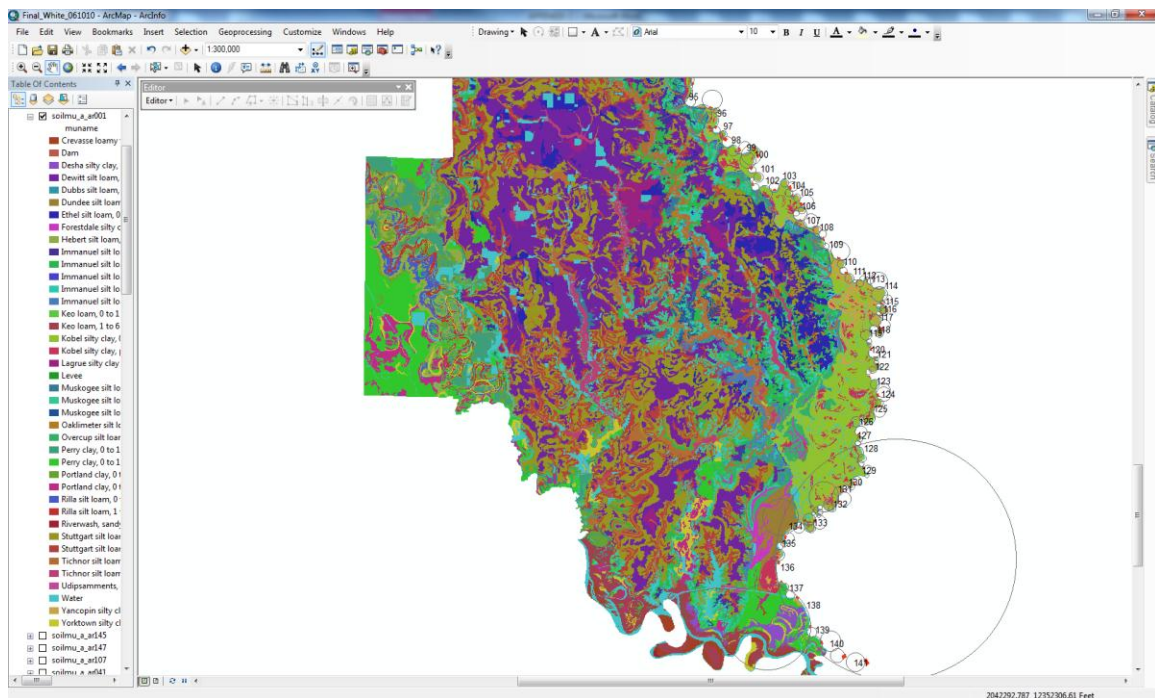


Figure B.12. Final Soil Map.

APPENDIX C : Sediment Analysis Calculations

With given quantities such as slope, hydraulic depth, median grain size particles, flow, and width via aerial photographs, the HEC-RAS Hydraulic Model and field data, calculate the total sediment discharge for the White River using Van Rijn's method, Yang's method, Karim-Kennedy's method, and Kennedy's method.

Given for Batesville, AR:

$$S_o = 0.0001$$

$$V = 2.70 \text{ ft/s}$$

$$y_o = 14.13 \text{ ft}$$

$$d_{50} = 0.000615 \text{ ft (Fine sand)}$$

$$d_{90} = 0.20997$$

$$Q = 18747.65 \text{ cfs}$$

$$W = 499.03 \text{ ft}$$

$$q = 37.57 \text{ ft}^2/\text{s}$$

$$SG = 2.65 \text{ (for sand and gravel)}$$

Solution. First determine some quantities common to all four methods. For the White River's water temperature (approximately 20°C), the kinematic viscosity $\nu = 1.052 \times 10^{-5} \text{ ft}^2/\text{s}$ and the dimensionless particle diameter d_* is obtained from

$$d_* = \left[\frac{(\gamma_s / \gamma - 1) g d_{50}^3}{\nu^2} \right]^{1/3} = \left[\frac{(SG - 1) g d_{50}^3}{\nu^2} \right]^{1/3} = \left[\frac{(2.65 - 1)(32.2)(0.000615)^3}{(1.052 \times 10^{-5})^2} \right]^{1/3} = 4.82$$

The fall velocity then is given by (Julien, 1995)

$$w_f = \frac{8\nu}{d_{50}} \left[\sqrt{1 + 0.0139 d_*^3} - 1 \right] = \frac{8(1.052 \times 10^{-5})}{0.000615} \left[\sqrt{1 + 0.0139(4.82)^3} - 1 \right] = 0.082 \text{ ft/s}$$

, and using *Figure C-1* with $d^* = 4.82$, the dimensionless critical shear stress or *Shields Parameter* τ_{*c} is approximately 0.055. The corresponding critical value of shear velocity is

$$\mu_{*c} = \sqrt{\tau_{*c}(SG-1)gd_{50}} = \sqrt{(0.055)(1.65)(32.2)(0.000615)} = 0.042 \text{ ft/s}$$

The shear velocity is

$$\mu_* = \sqrt{gy_o S_o} = \sqrt{(32.2)(14.13)(0.0001)} = 0.21 \text{ ft/s}$$

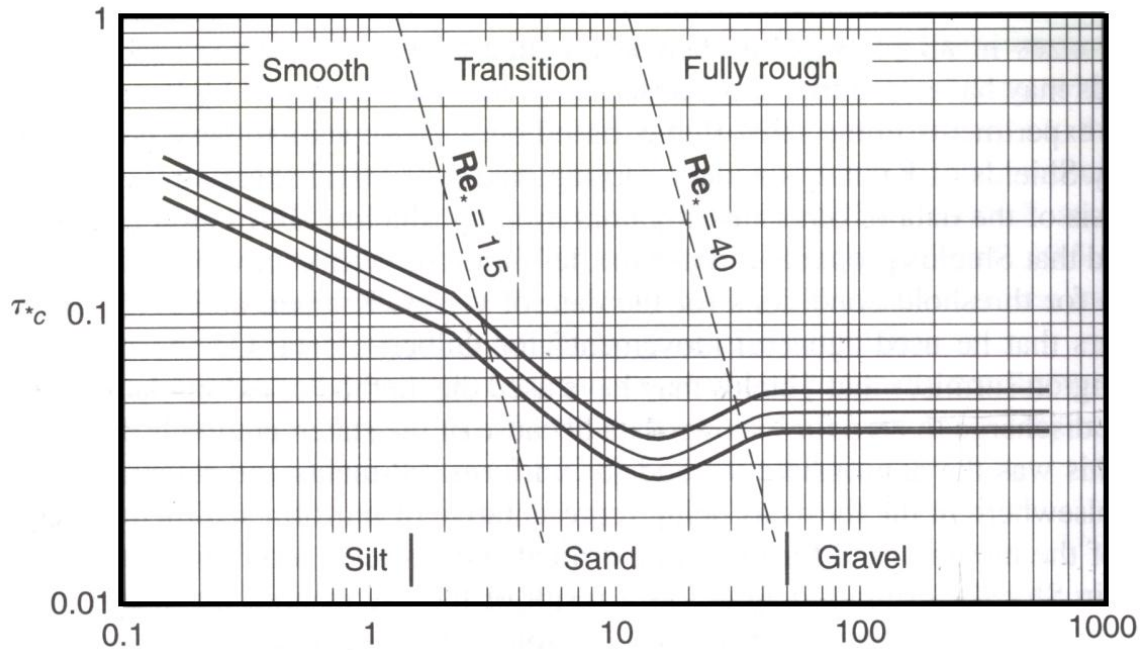


Figure C.1. Modified Shield Diagram for Direct Determination of Critical Shear Stress (after Julien, 1995).

(I) Van Rijn's Method. The value of a transport parameter T is needed, and it is dependent on the grain shear velocity μ'_* . The grain shear velocity is obtained from Keulegan's equation using the given water velocity and the equivalent sand grain roughness $k'_s = 3d_{90}$:

$$\mu'_* = \frac{V}{5.75 \log \frac{12y_o}{3d_{90}}} = \frac{2.70}{5.75 \log \frac{12(14.13)}{3(0.20997)}} = 0.19 \text{ ft/s}$$

Then, by definition the Shields parameter due to grain resistance is

$$\tau'_* = \frac{\mu'^2_*}{(SG-1)gd_{50}} = \frac{0.19^2}{1.65(32.2)(0.000615)} = 1.15$$

The resulting value of

$$T = \frac{\tau'_*}{\tau_{*c}} - 1 = \frac{1.15}{0.055} - 1 = 19.8$$

and the bed-load discharge becomes

$$q_b = 0.053 \sqrt{(SG-1)gd_{50}^3} \frac{T^{2.1}}{d_*^{0.3}} = 0.053 \sqrt{(1.65)(32.2)(0.000615)^3} \frac{19.8^{2.1}}{4.82^{0.3}} = 0.00195 \text{ ft}^2/\text{s}$$

For the suspended sediment discharge, values of sediment diffusion coefficient β , Rouse number R_o , mixing correction factor ΔR_o , the reference level a , and the reference concentration at the distance $z = a$ above the bed C_a are needed. The value of the of sediment diffusion coefficient β comes from the results of Coleman (1970):

$$\beta = 1 + 2 \left[\frac{w_f}{\mu_*} \right]^2 = 1 + 2 \left[\frac{0.082}{0.21} \right]^2 = 1.29$$

And then from the definition of Rouse number R_o with an assumed von Karman constant $k = 0.4$ for clear water :

$$R_o = \frac{w_f}{\beta k \mu_*} = \frac{0.082}{(1.29)(0.4)(0.21)} = 0.74$$

The value of C_a as a volumetric concentration is

$$C_a = 0.015 \frac{d_{50}}{a} \frac{T^{1.5}}{d_*^{0.3}} = 0.015 \frac{0.000615}{0.00123} \frac{19.8^{1.5}}{4.82^{0.3}} = 0.41$$

**Note that for Batesville through Newport the reference level a is approximately $2d_{50} = 0.00123$.

With the maximum volumetric concentration C_o taken to be 0.65, the correction to R_o follows:

$$\Delta R_o = 2.5 \left[\frac{w_f}{u_*} \right]^{0.8} \left[\frac{C_a}{C_o} \right]^{0.4} = 2.5 \left[\frac{0.082}{0.21} \right]^{0.8} \left[\frac{0.41}{0.65} \right]^{0.4} = 0.97$$

So that $R'_o = R_o + \Delta R_o = 0.74 + 0.97 = 1.71$. The integration factor I_f required for the calculation of the suspended sediment discharge is expressed as:

$$I_f = \frac{\left[\frac{a}{y_o} \right]^{R'_o} - \left[\frac{a}{y_o} \right]^{1.2}}{\left[1 - \frac{a}{y_o} \right]^{R'_o} [12 - R'_o]} = \frac{\left[\frac{0.00123}{14.13} \right]^{1.71} - \left[\frac{0.00123}{14.13} \right]^{1.2}}{\left[1 - \frac{0.00123}{14.13} \right]^{1.71} [12 - 1.71]} = 2.61 \times 10^{-5}$$

Finally, the suspended sediment discharge is given by:

$$q_s = I_f V y_o C_a = (2.61 \times 10^{-6})(2.70)(14.13)(0.41) = 0.0004 \text{ ft}^2/\text{s}$$

The total sediment discharge is the sum of the bed-load and suspended-load discharges:

$$q_t = q_b + q_s = 0.00195 + 0.0004 = 0.0023 \text{ ft}^2/\text{s}$$

Convert to tons/day,

$$g_t = \gamma_s q_t = SG \gamma_w q_t = 2.65(62.4)(0.0023)(86400/2000) = 16.86 \text{ tons/day}$$

And express as the total sand concentration by weight in ppm:

$$C_t = 10^6 \frac{\gamma_s}{\gamma} \frac{q_t}{q} = 10^6 SG \frac{q_t}{q} = 10^6 (2.65) \frac{0.0023}{37.57} = 166.5 \text{ ppm}$$

(II) Yang's Method. First the critical velocity is needed, since

$$\mu_* d_{50} / \nu = (0.21)(0.000615) / (1.052 \times 10^{-5}) = 12.50 < 70, \text{ so the critical velocity becomes}$$

$$V_c = \left[\frac{2.5}{\log(\mu_* d_{50} / \nu) - 0.06} + 0.66 \right] w_f = \left[\frac{2.5}{\log(12.50) - 0.06} + 0.66 \right] (0.082) = 0.25 \text{ ft/s}$$

A multiple regression analysis of 463 sets of laboratory for sand transport gives the following relationship for total sediment discharge (Yang, 1973):

$$\begin{aligned} \log C_t = & 5.435 - 0.286 \log \left[\frac{w_f d_{50}}{\nu} \right] - 0.457 \log \left[\frac{\mu_*}{w_f} \right] \\ & + \left(1.799 - 0.409 \log \left[\frac{w_f d_{50}}{\nu} \right] - 0.314 \log \left[\frac{\mu_*}{w_f} \right] \right) \log \left[\frac{VS}{w_f} - \frac{V_c S}{w_f} \right] \end{aligned}$$

$$\begin{aligned} \log C_t = & 5.435 - 0.286 \log \left[\frac{(0.082)(0.000615)}{1.052 \times 10^{-5}} \right] - 0.457 \log \left[\frac{0.21}{0.082} \right] \\ & + \left(1.799 - 0.409 \log \left[\frac{(0.082)(0.000615)}{1.052 \times 10^{-5}} \right] - 0.314 \log \left[\frac{0.21}{0.082} \right] \right) \\ & \log \left[\frac{(2.70)(0.0001)}{0.082} - \frac{(0.25)(0.0001)}{0.082} \right] = 1.54 \end{aligned}$$

$$C_t = 10^{1.54} = 34.85 \text{ ppm}$$

$$q_t = \frac{C_t q}{10^6 SG} = \frac{(34.85)(37.57)}{(10^6)(2.65)} = 0.00049 \text{ ft}^2/\text{s}$$

Convert to tons/day,

$$g_t = \gamma_s q_t = SG \gamma_w q_t = 2.65(62.4)(0.00049)(86400 / 2000) = 3.50 \text{ tons/day}$$

(III) Karim-Kennedy's Method. Three dimensionless parameters are required for the total sediment discharge computation:

$$\frac{V}{\sqrt{(SG-1)gd_{50}}} = \frac{2.70}{\sqrt{(1.65)(32.2)(0.000615)}} = 14.95$$

$$\frac{\mu_* - \mu_{*c}}{\sqrt{(SG-1)gd_{50}}} = \frac{0.21 - 0.042}{\sqrt{(1.65)(32.2)(0.000615)}} = 0.945$$

$$\frac{y_o}{d_{50}} = \frac{14.13}{0.000615} = 22969.70$$

$$\begin{aligned} \log \frac{q_t}{\sqrt{(SG-1)gd_{50}}^3} &= -2.279 + 2.972 \log \left[\frac{V}{\sqrt{(SG-1)gd_{50}}} \right] \\ &+ 1.060 \log \left[\frac{V}{\sqrt{(SG-1)gd_{50}}} \right] \log \left[\frac{\mu_* - \mu_{*c}}{\sqrt{(SG-1)gd_{50}}} \right] \\ &+ 0.299 \log \left(\frac{y_o}{d_{50}} \right) \log \left[\frac{\mu_* - \mu_{*c}}{\sqrt{(SG-1)gd_{50}}} \right] \end{aligned}$$

$$\log \frac{q_t}{\sqrt{(SG-1)gd_{50}^3}} = -2.279 + 2.972 \log[14.95] + 1.060 \log[14.95] \log[0.945] \\ + 0.299 \log(22969.70) \log[0.945] = 1.16$$

Finally, the total sediment discharge is given by

$$q_t = 10^{1.16} \sqrt{(SG-1)gd_{50}^3} = 10^{1.16} \sqrt{(1.65)(32.2)(0.000615)^3} = 0.00157 \text{ ft}^2/\text{s}$$

Convert to tons/day,

$$g_t = \gamma_s q_t = SG \gamma_w q_t = 2.65(62.4)(0.00157)(86400/2000) = 11.12 \text{ tons/day}$$

And express as the total sand concentration by weight in ppm:

$$C_t = 10^6 \frac{\gamma_s}{\gamma} \frac{q_t}{q} = 10^6 SG \frac{q_t}{q} = 10^6 (2.65) \frac{0.00157}{37.57} = 110.8 \text{ ppm}$$

(IV) *Kennedy's Method.*

$$q_t = 0.00139 \left[\frac{V}{\sqrt{(SG-1)gd_{50}^3}} \right]^{2.97} \left[\frac{\mu_*}{w_f} \right]^{1.47} \sqrt{(SG-1)gd_{50}^3} \\ = 0.00139 \left[\frac{2.70}{\sqrt{(1.65)(32.2)(0.000615)}} \right]^{2.97} \left[\frac{0.21}{0.082} \right]^{1.47} \sqrt{(1.65)(32.2)(0.000615)^3} \\ = 0.0019 \text{ ft}^2/\text{s}$$

Convert to tons/day,

$$g_t = \gamma_s q_t = SG \gamma_w q_t = 2.65(62.4)(0.0019)(86400/2000) = 13.57 \text{ tons/day}$$

And express as the total sand concentration by weight in ppm:

$$C_t = 10^6 \frac{\gamma_s}{\gamma} \frac{q_t}{q} = 10^6 SG \frac{q_t}{q} = 10^6 (2.65) \frac{0.0019}{37.57} = 137.50 \text{ ppm}$$

(V) For the methodologies that yield the total sediment discharge without distinguishing between bed-load and suspended-load, Ashida-Michiue formulation is implemented to determine the bed-load transport:

Ashida and Michiue's dimensionless bed-load transport (1972) is given by

$$q_b^* = 17(\tau'_* - \tau_{*c}) \left(\sqrt{\tau'_*} - \sqrt{\tau_{*c}} \right)$$

$$\begin{aligned} q_b &= 17 \sqrt{(SG-1)gd_{50}} d_{50} (\tau'_* - \tau_{*c}) \left(\sqrt{\tau'_*} - \sqrt{\tau_{*c}} \right) \\ &= 17 \sqrt{(2.65-1)(32.2)(0.000615)} (0.000615) (1.145 - 0.055) (\sqrt{1.145} - \sqrt{0.055}) \\ &= 0.0017 \text{ ft}^2/\text{s} \end{aligned}$$

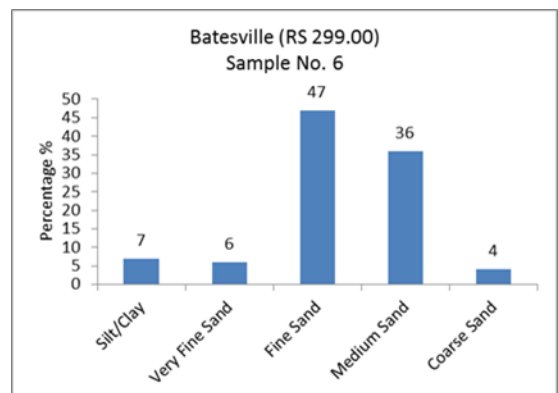
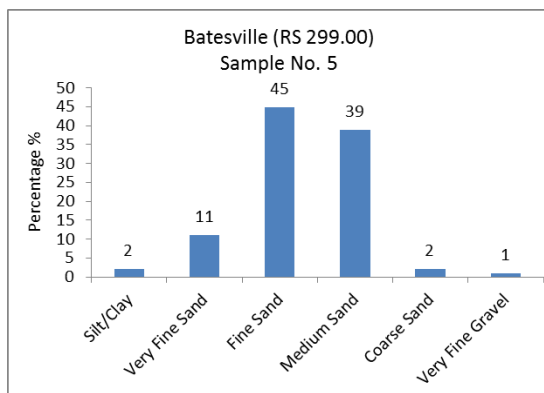
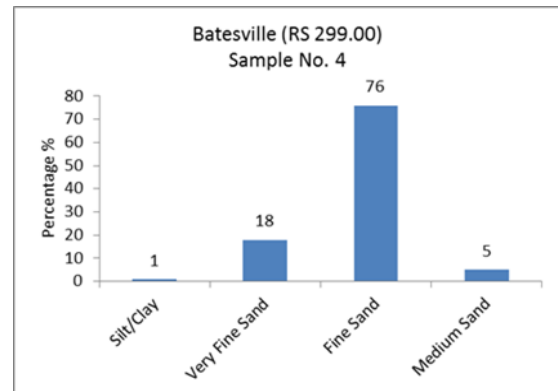
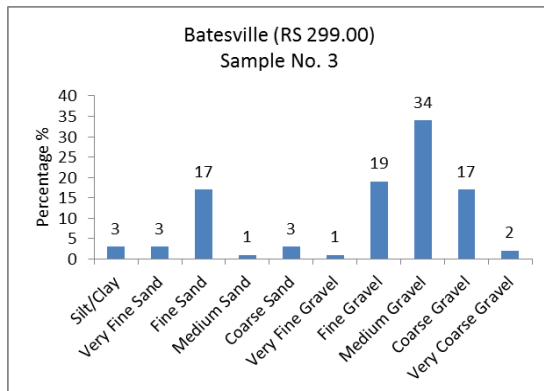
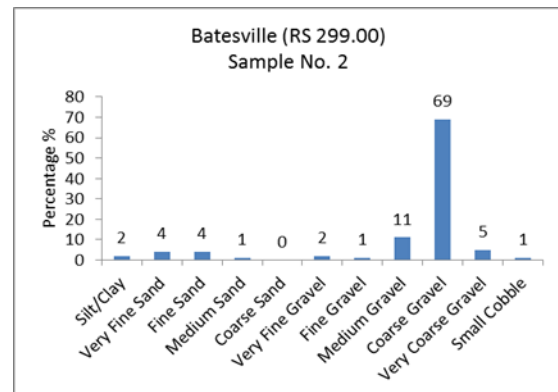
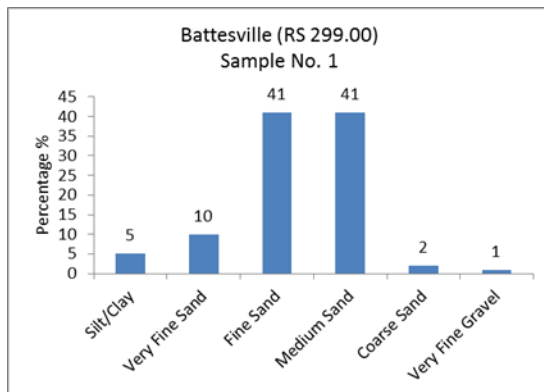
The suspended sediment discharge is the difference of the total sediment discharge and bed-load discharge. Using the total sediment discharge obtained from the Kennedy's Method, the suspended sediment discharge is:

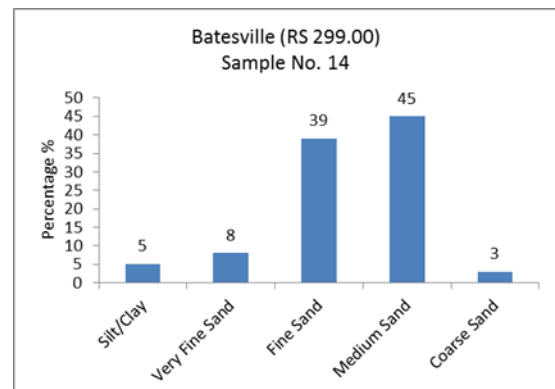
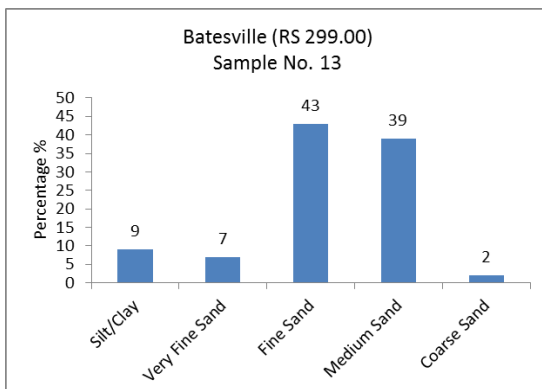
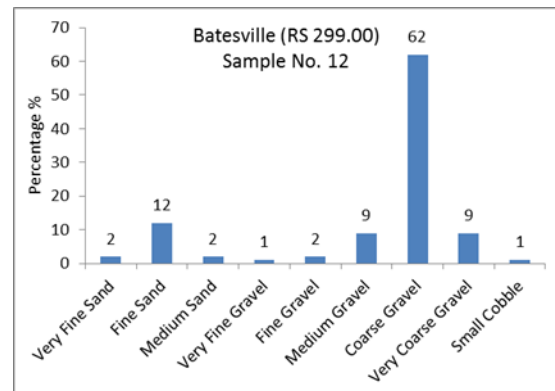
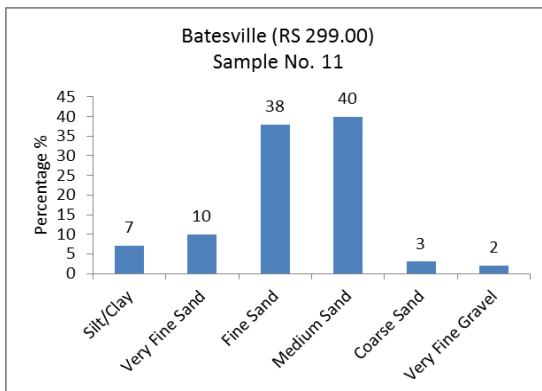
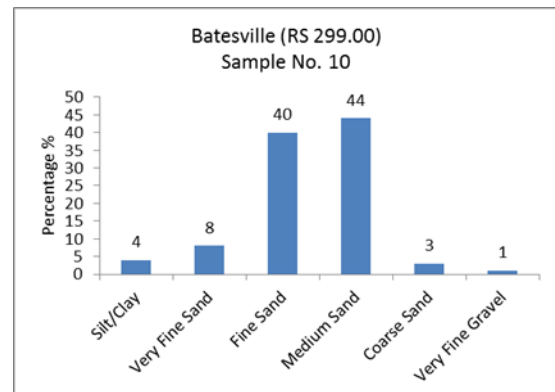
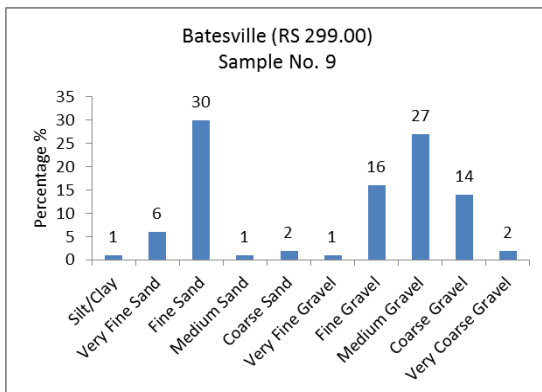
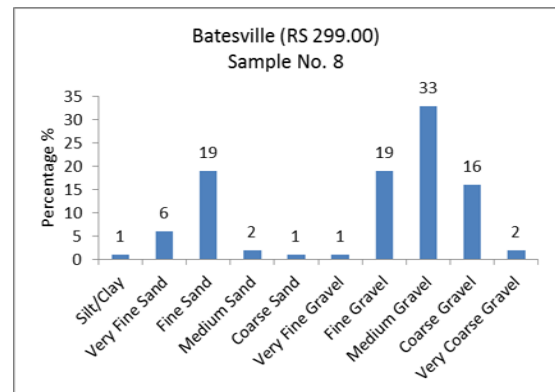
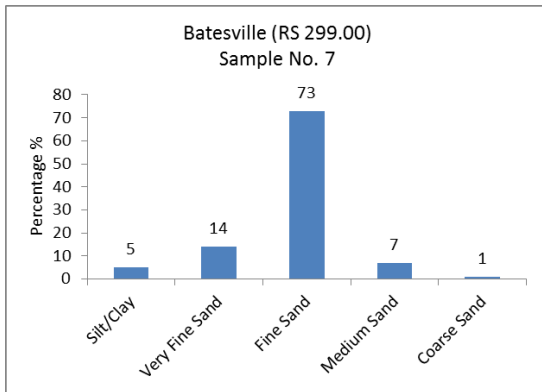
$$q_s = q_t - q_b = 0.0019 - 0.0017 = 0.0002 \text{ ft}^2/\text{s}$$

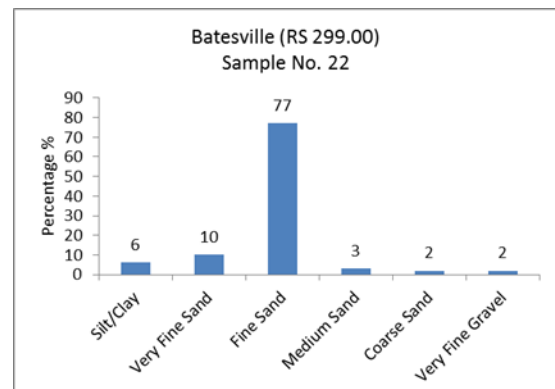
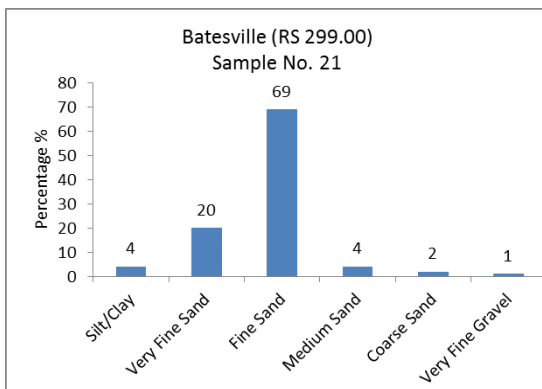
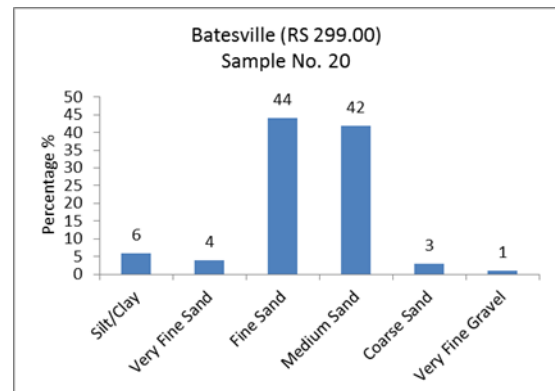
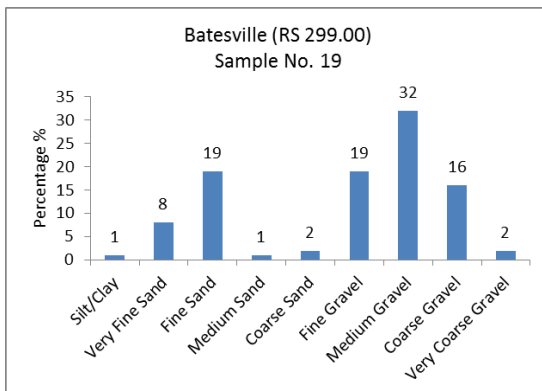
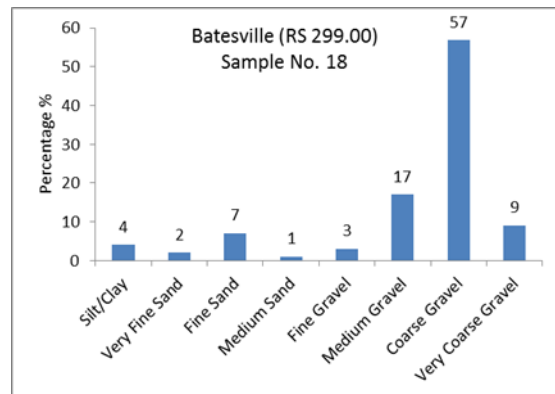
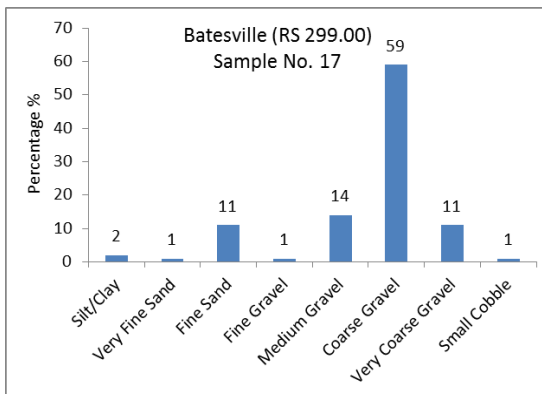
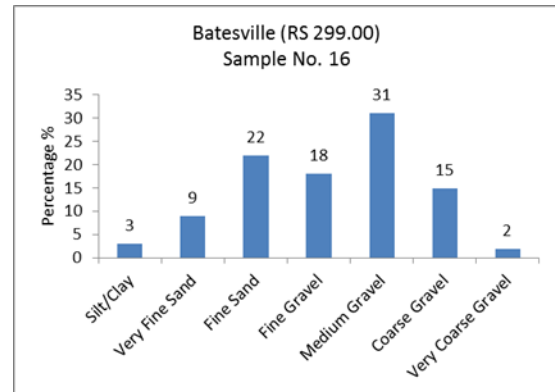
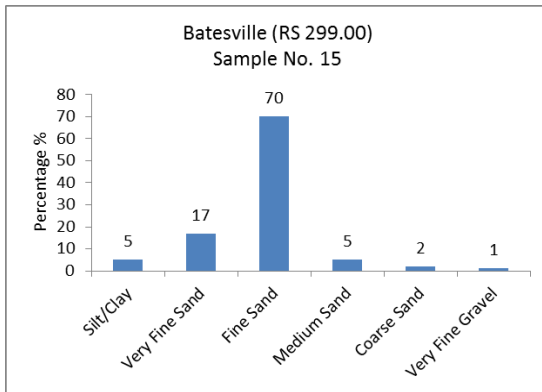
Note: If the bed-load sediment discharge obtained using Ashida-Michiue formulation is greater than the total sediment discharge, the bed-load sediment discharge is discarded.

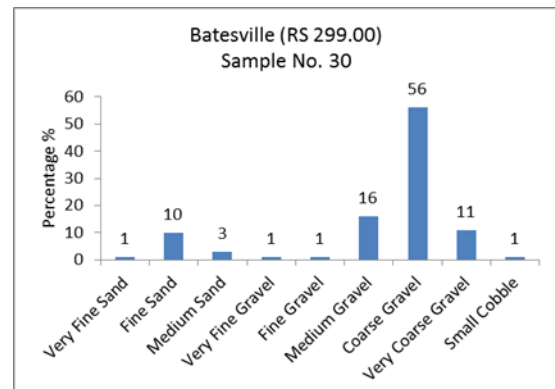
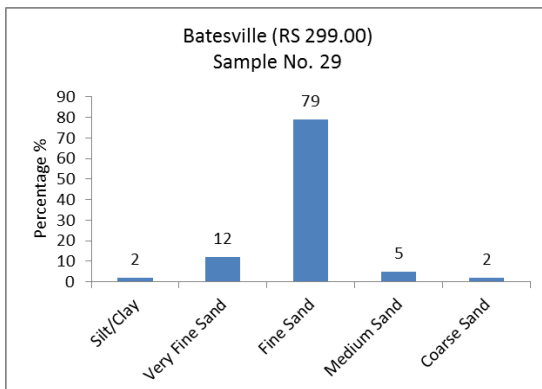
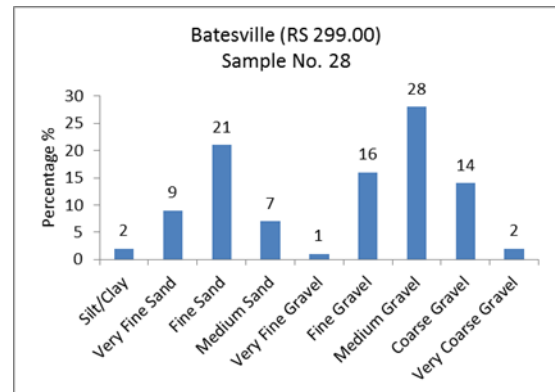
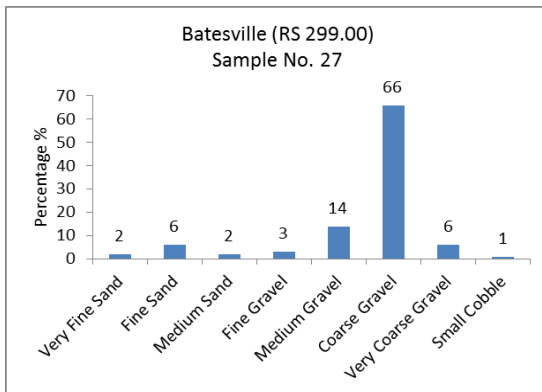
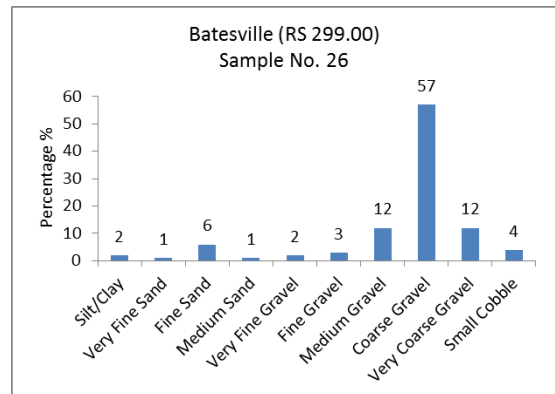
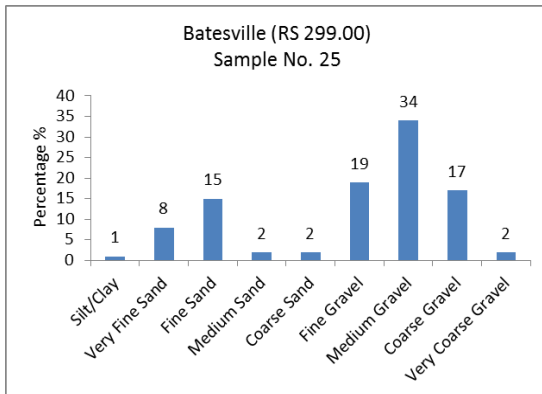
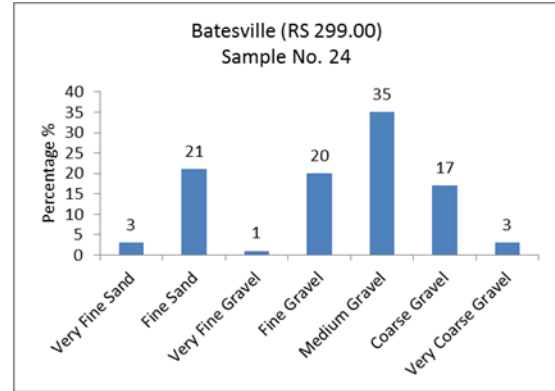
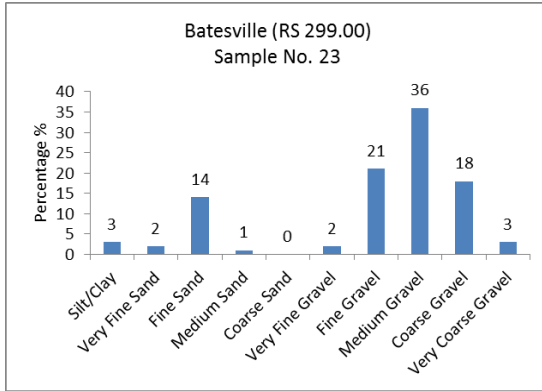
APPENDIX D: Sieve Analysis Histograms

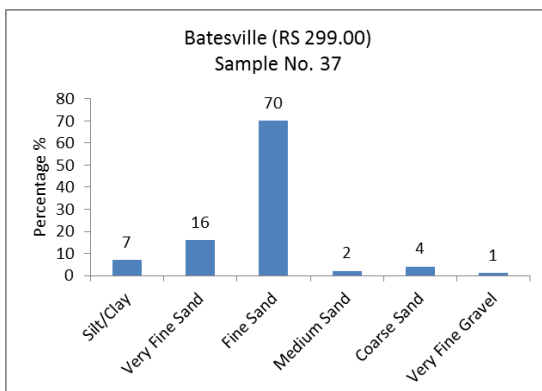
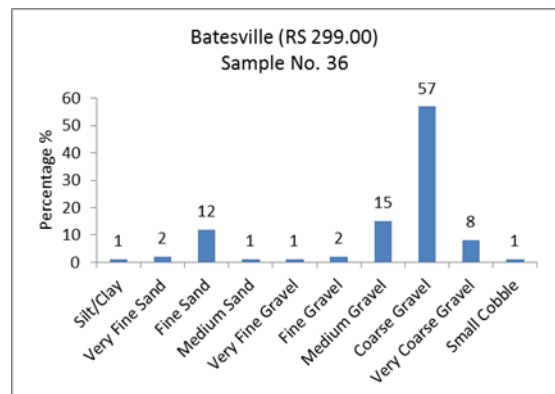
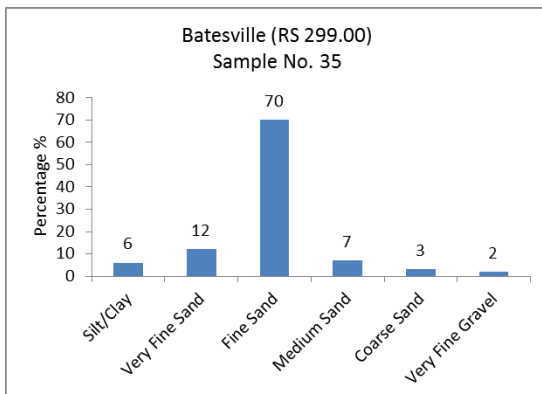
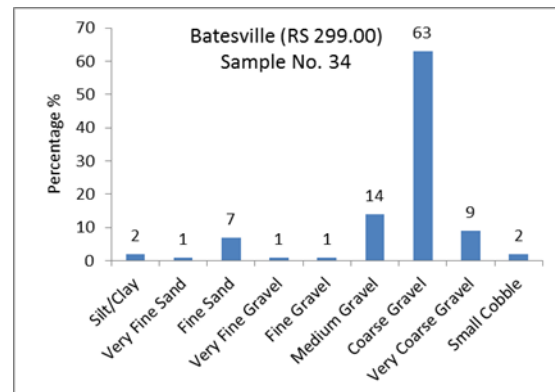
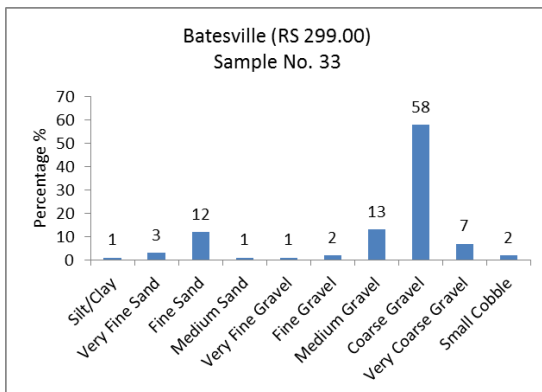
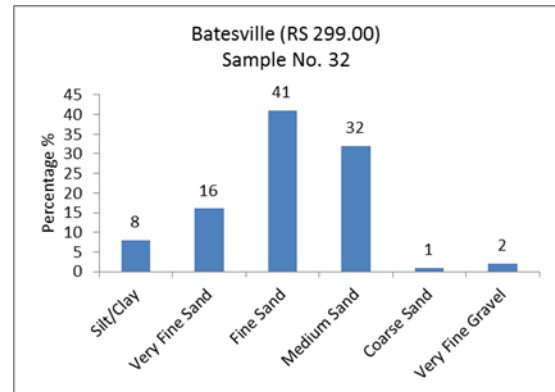
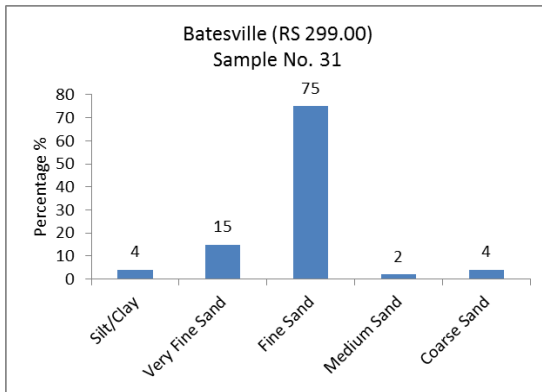
Sieve analysis results for the soil samples obtained from the reference sites are presented here as bar histograms. The U.S. standard sieve numbers used are No. 4, No. 8, No. 20, No. 40, No. 50, No. 100, and No. 200. Soil classification size ranges are based on the American Geophysical Union (AGU). Particles sizes smaller than 0.075 mm or finer than No. 200 are automatically classified as silt/clay and are not separated by hydrometer analysis.

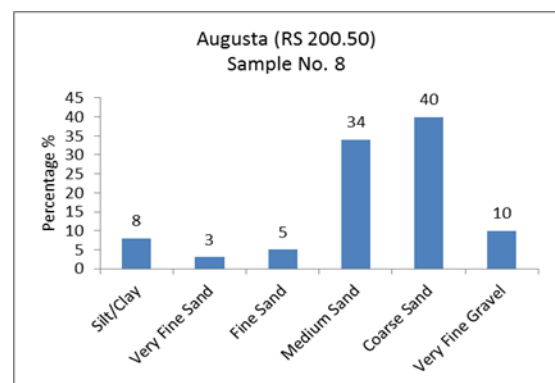
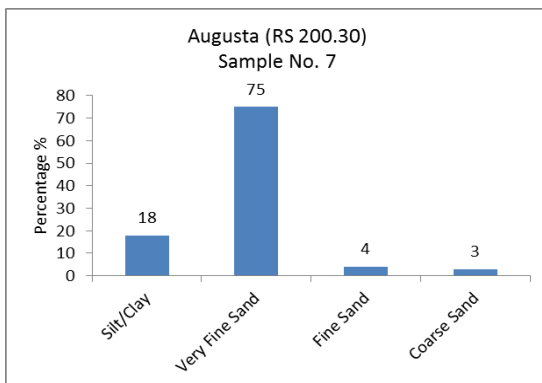
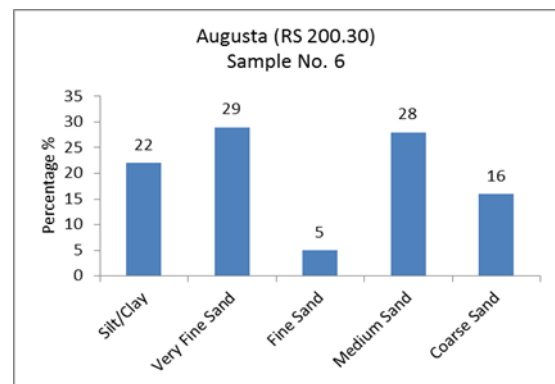
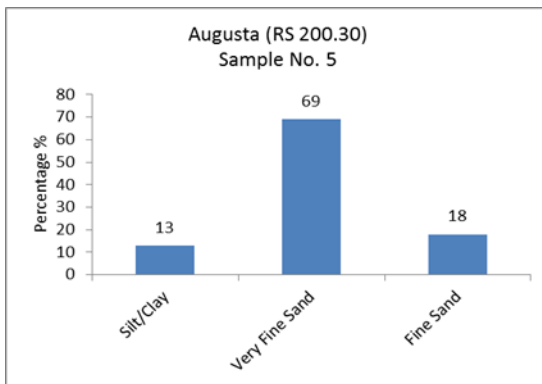
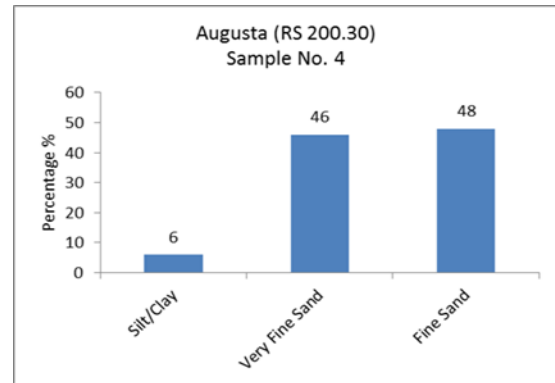
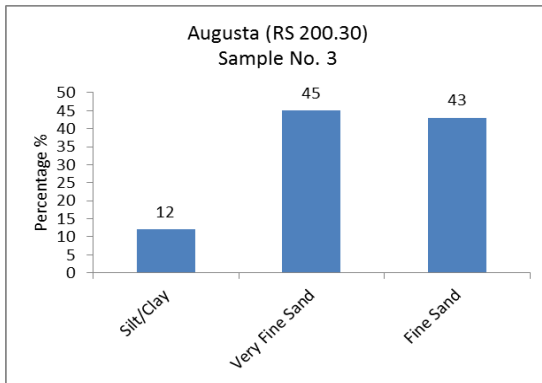
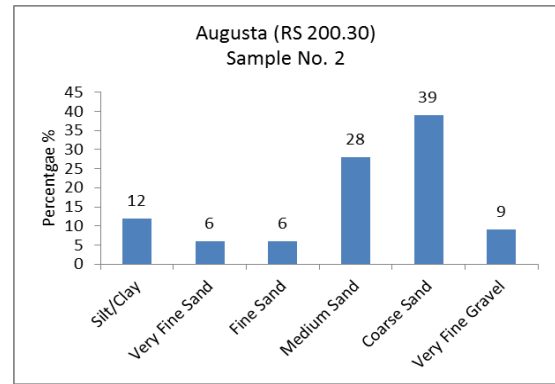
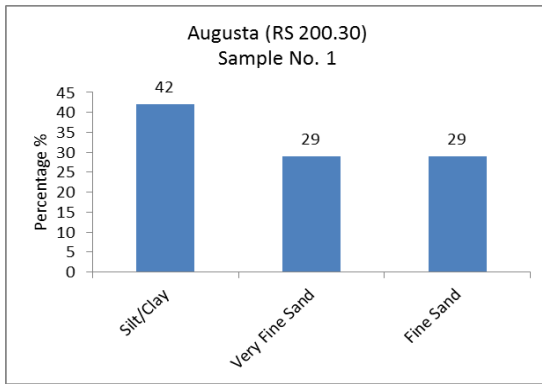


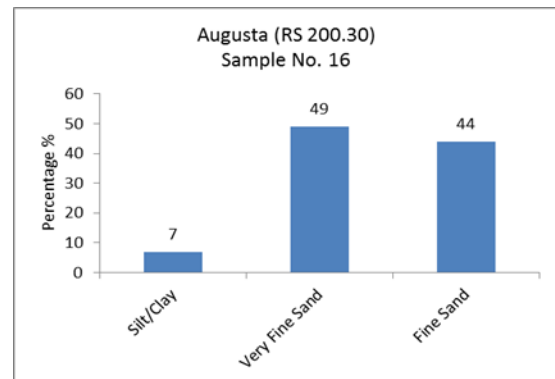
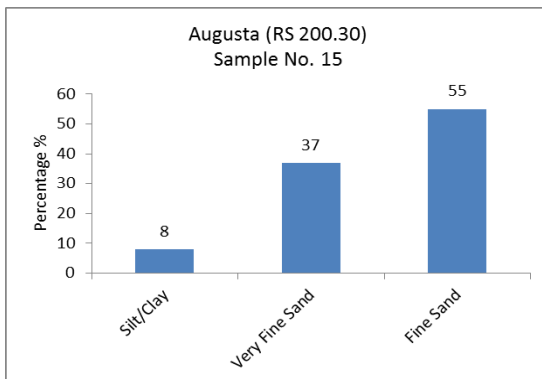
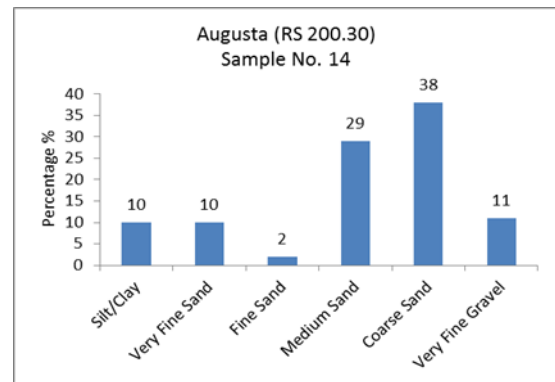
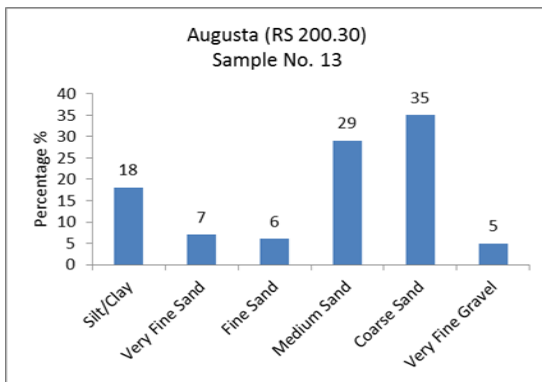
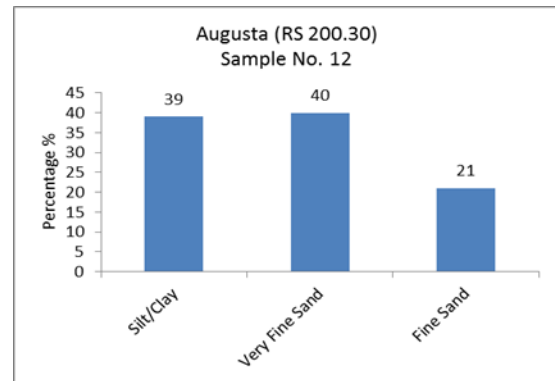
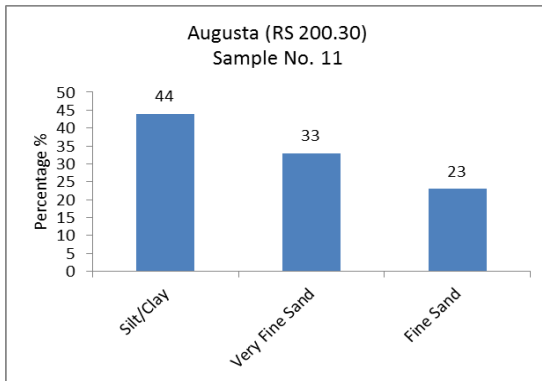
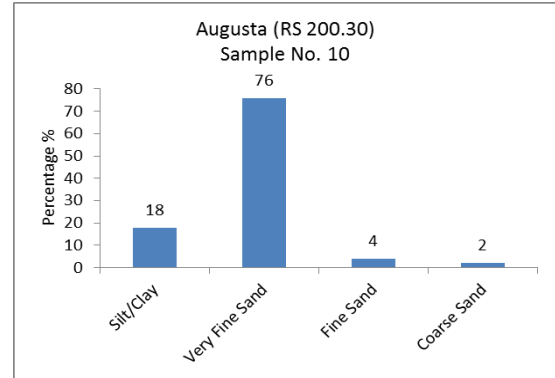
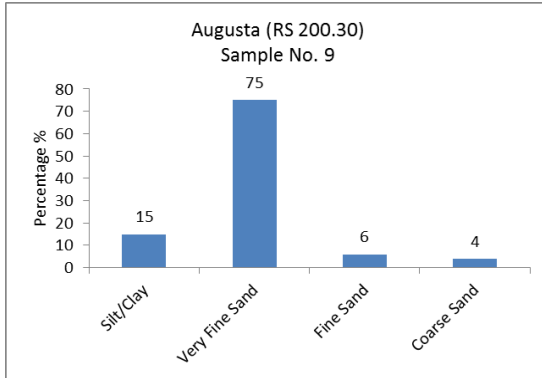


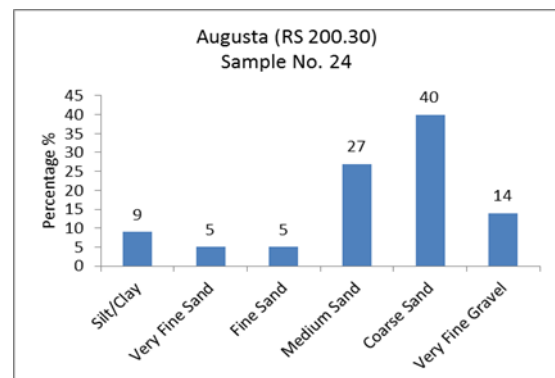
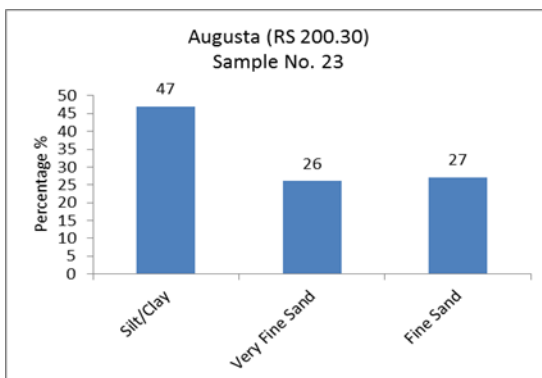
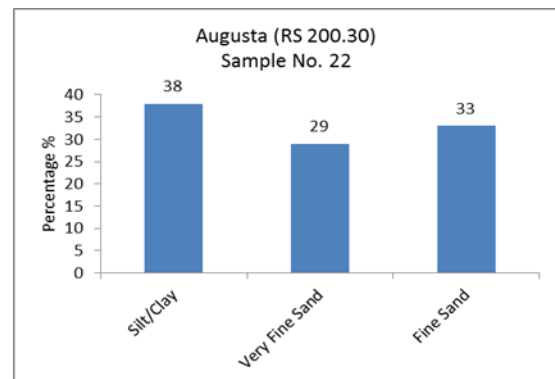
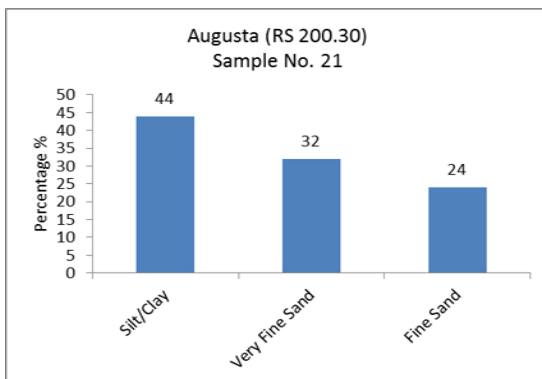
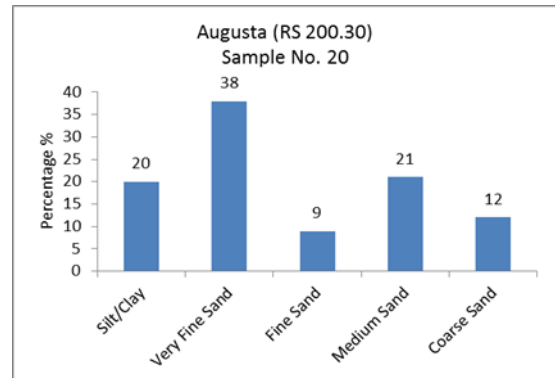
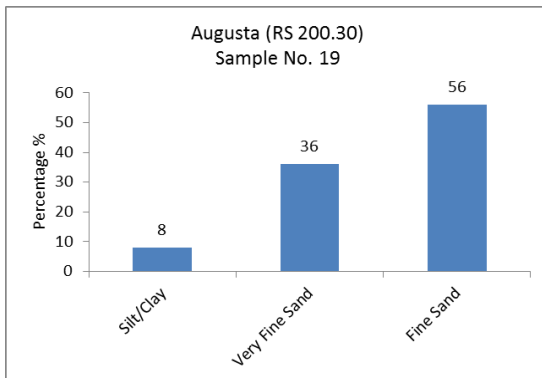
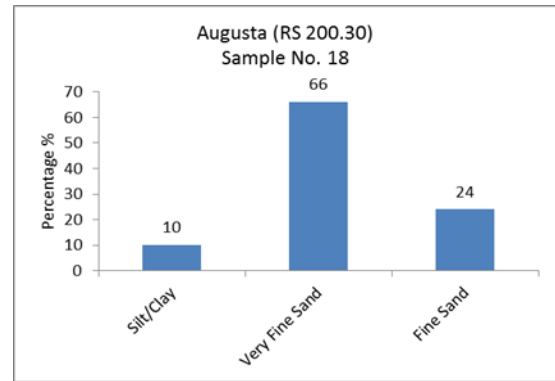
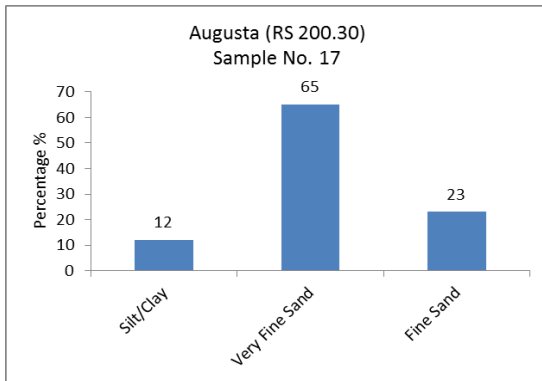


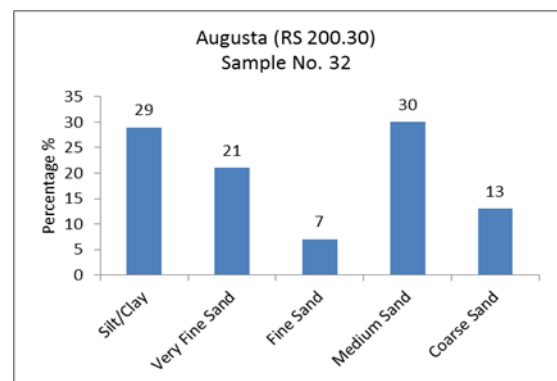
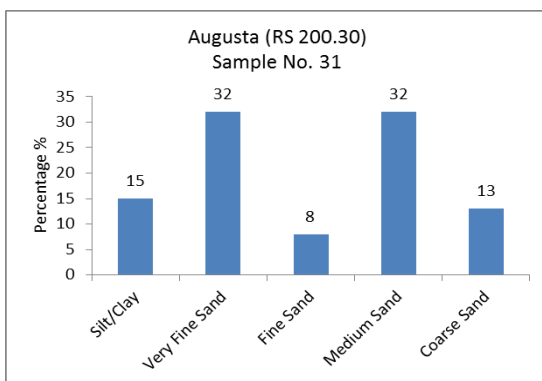
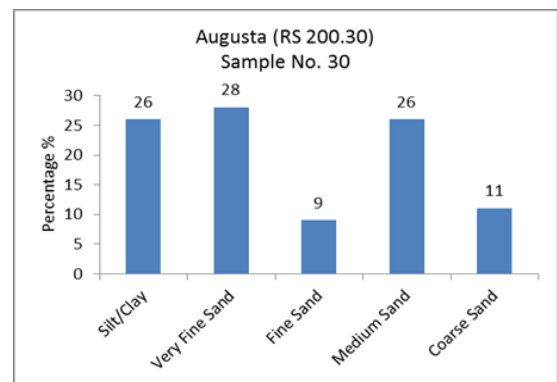
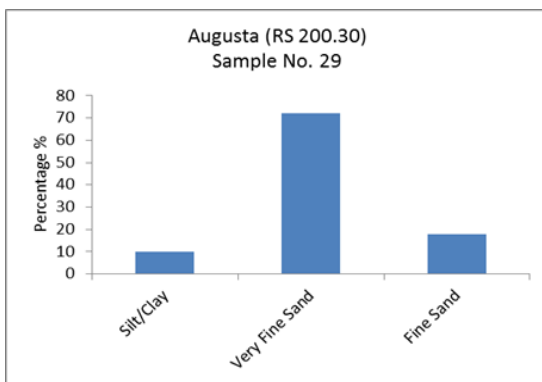
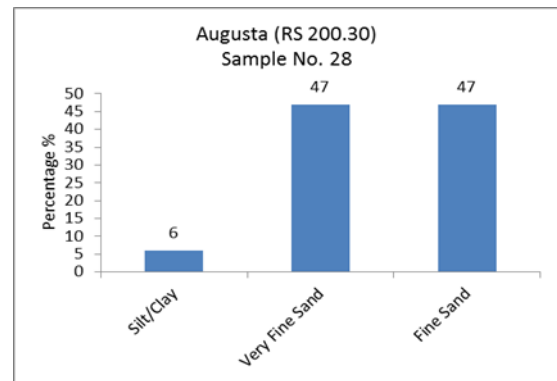
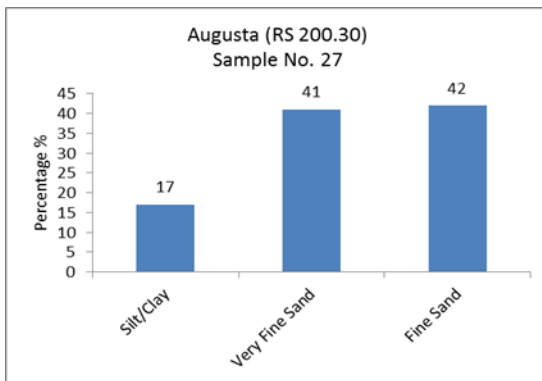
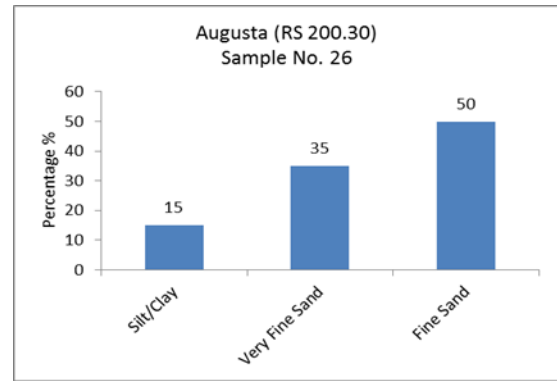
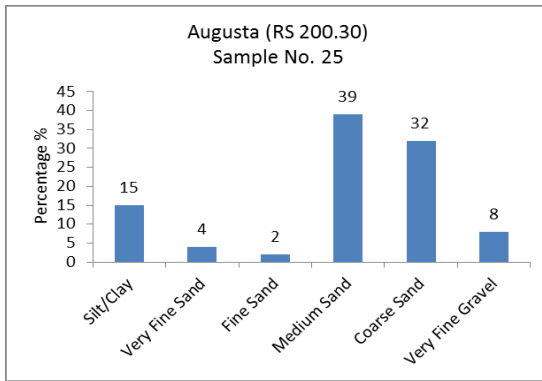


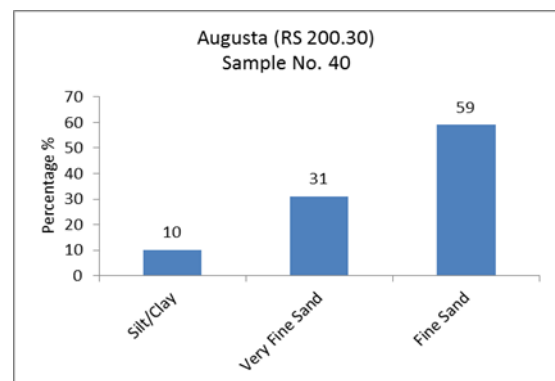
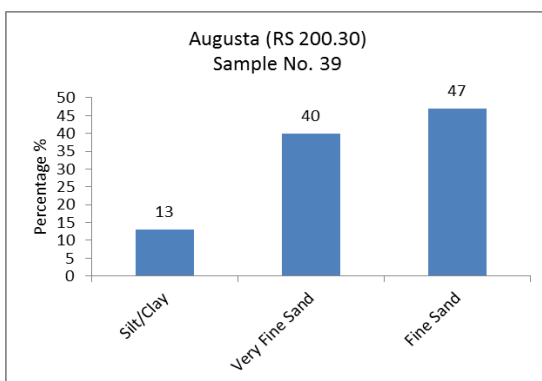
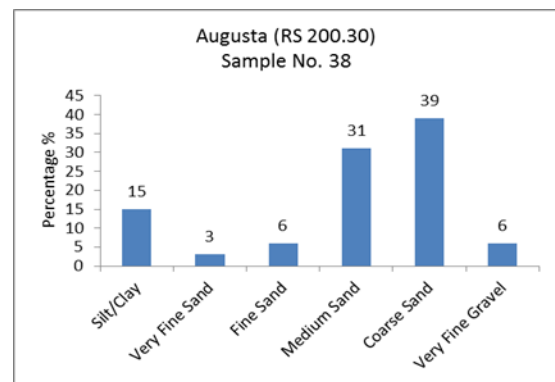
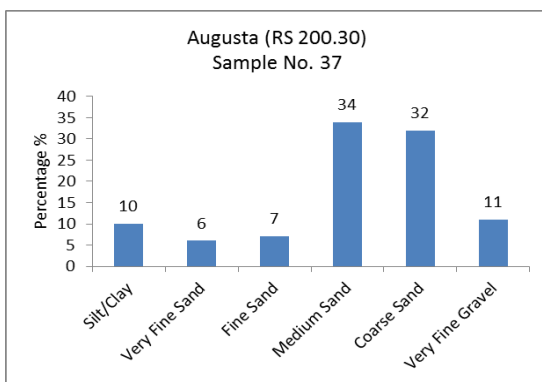
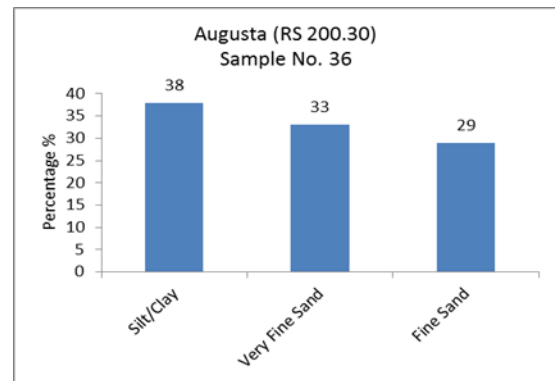
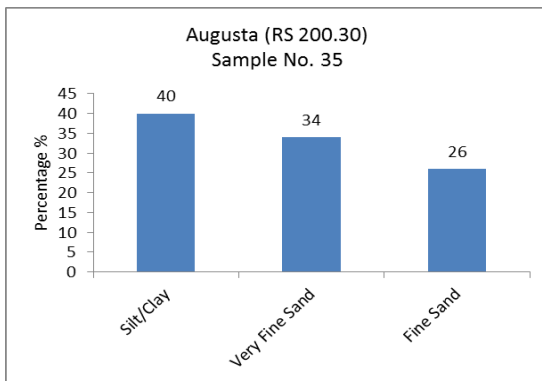
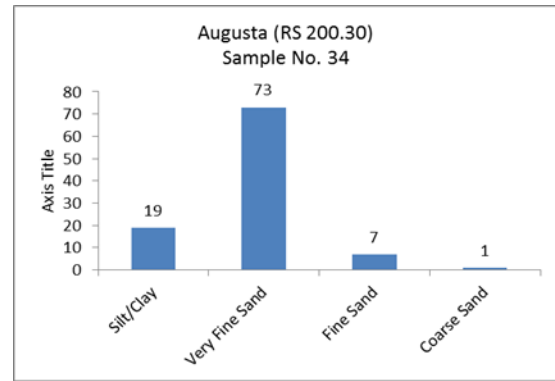
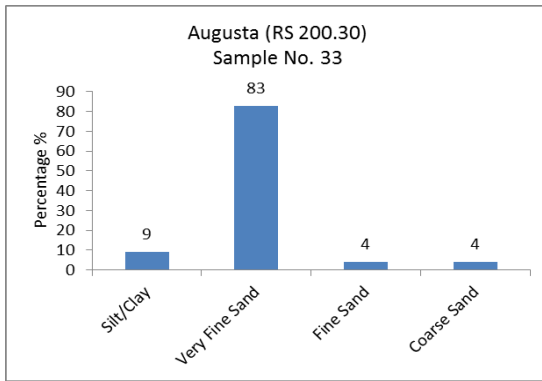


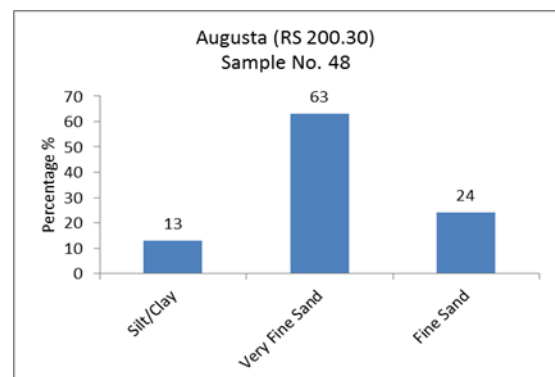
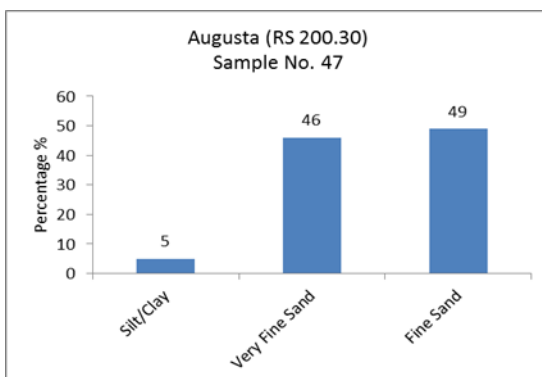
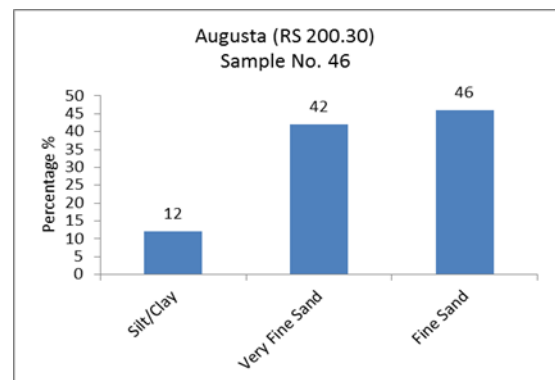
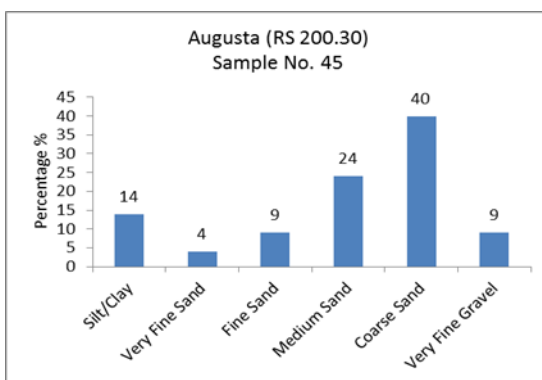
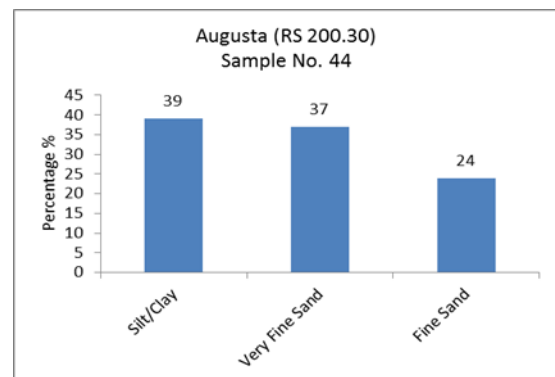
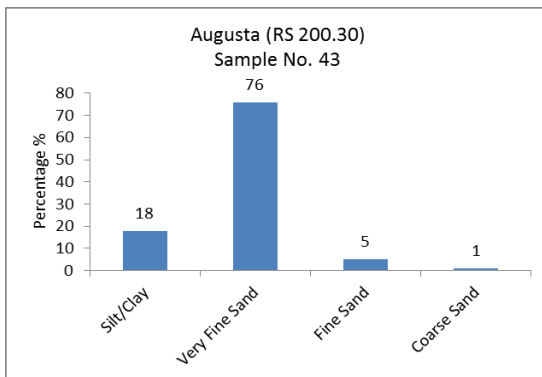
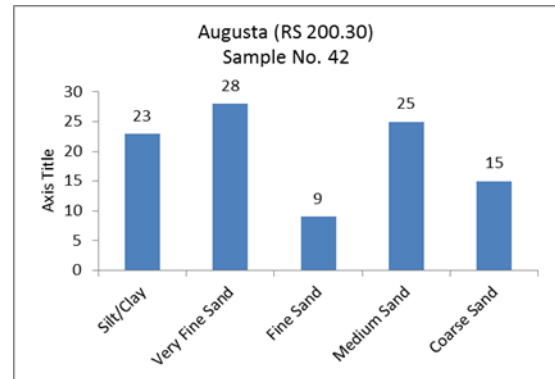
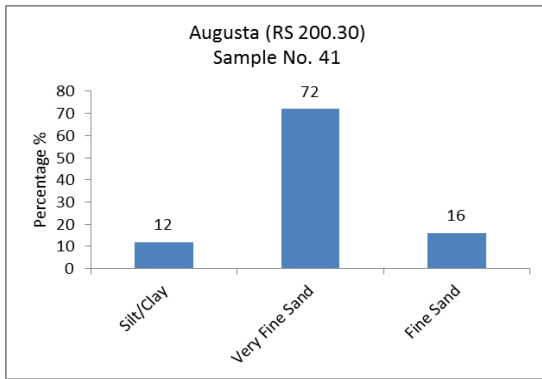


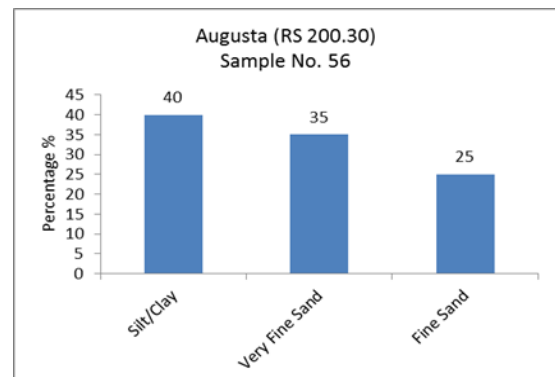
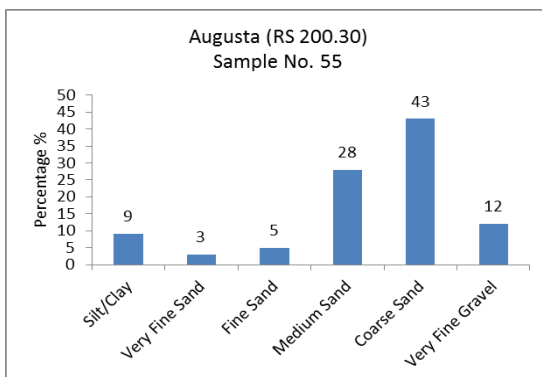
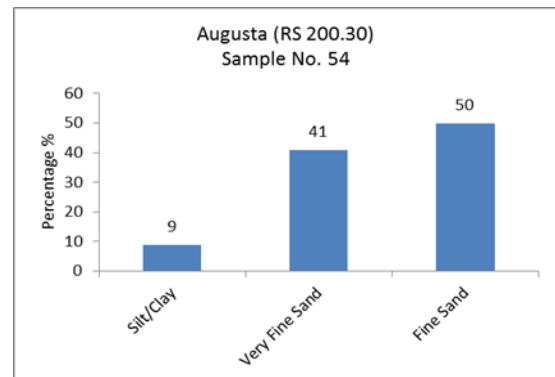
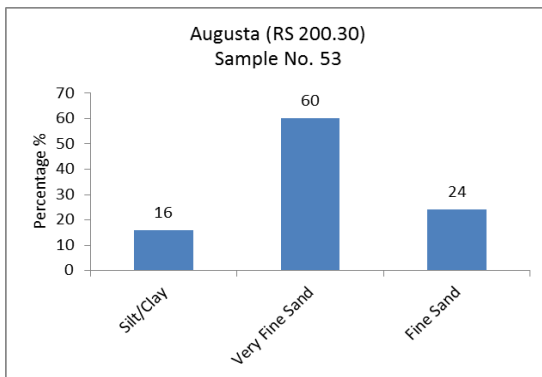
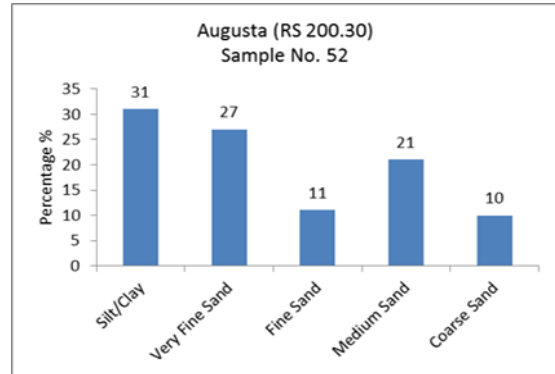
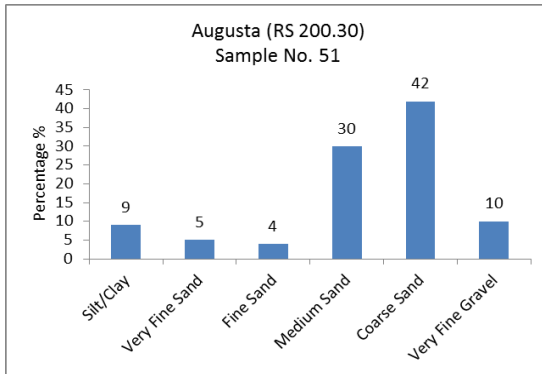
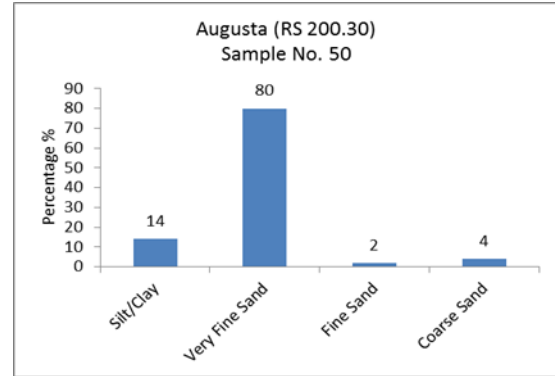
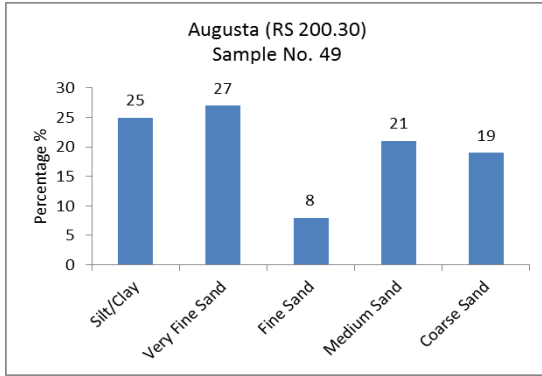


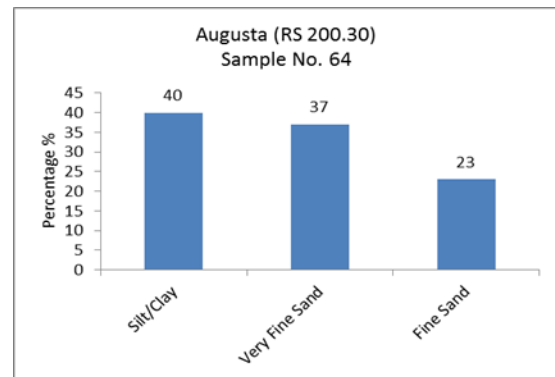
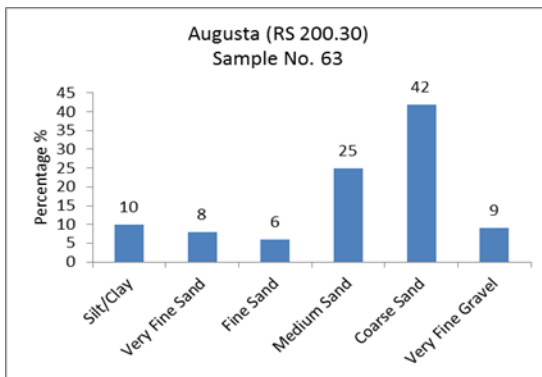
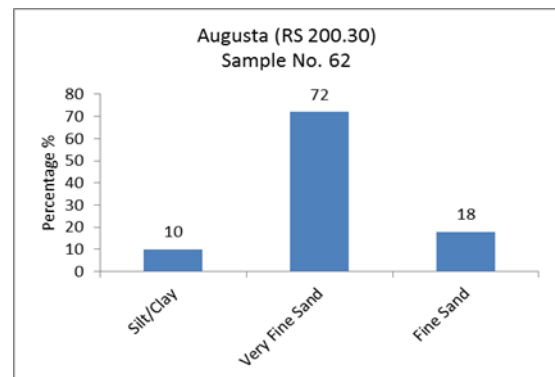
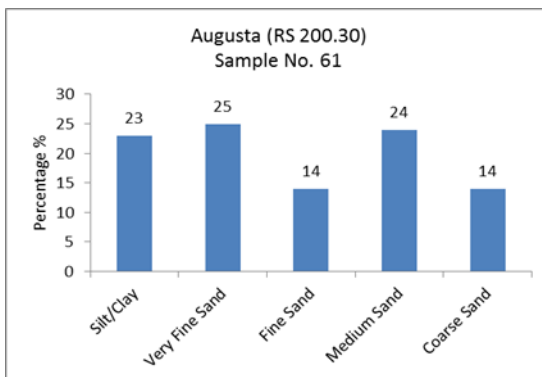
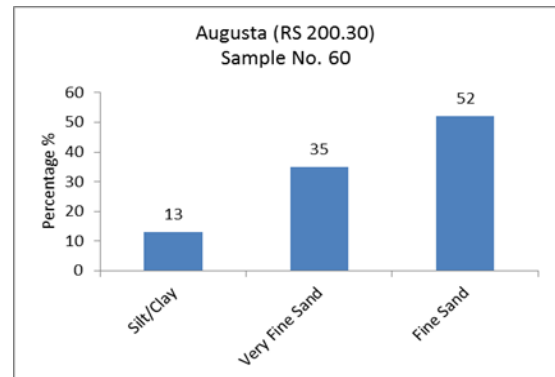
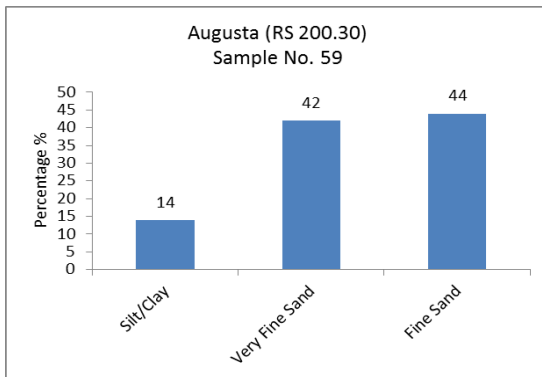
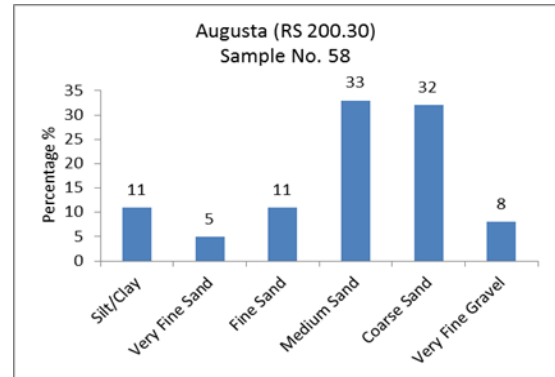
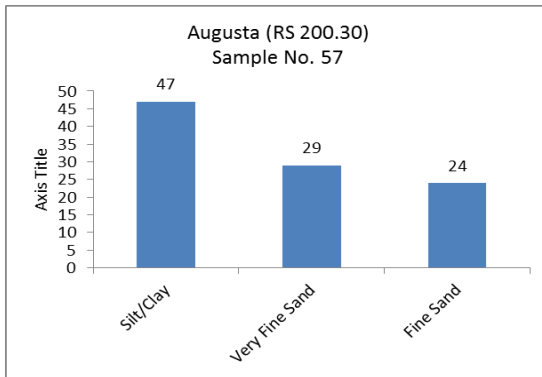


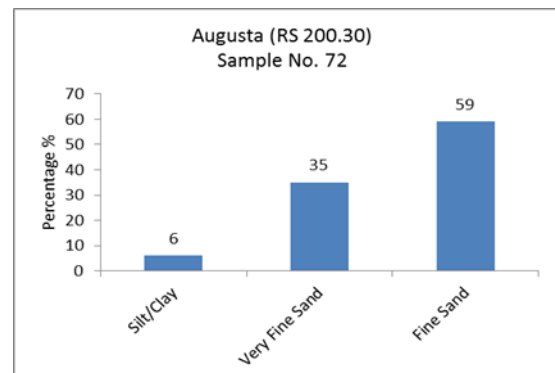
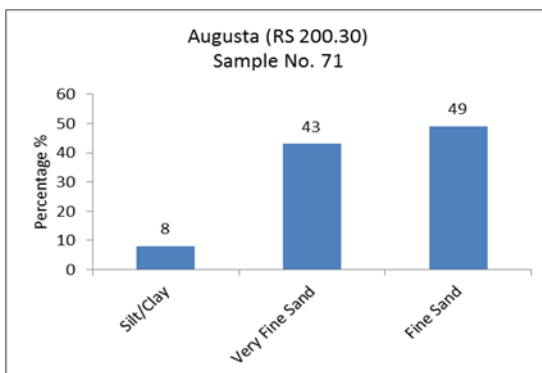
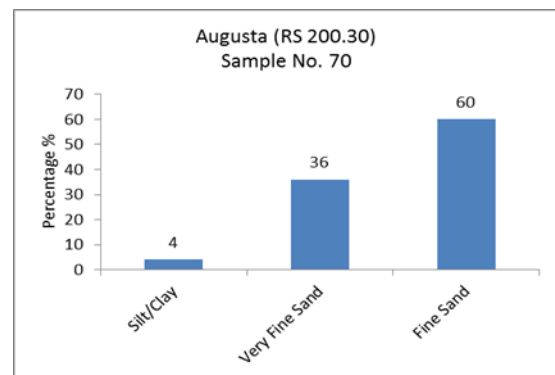
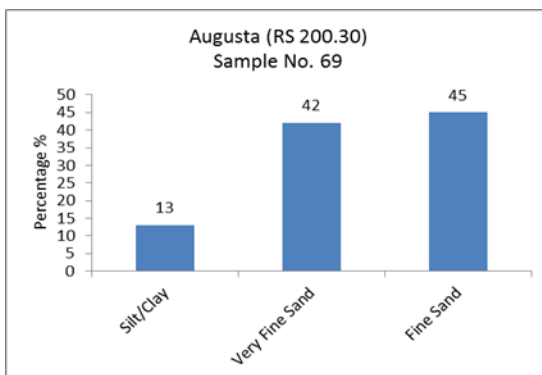
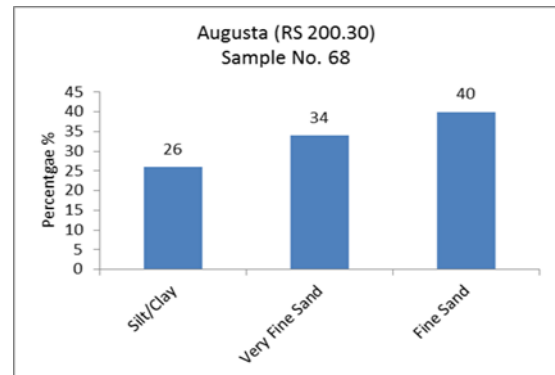
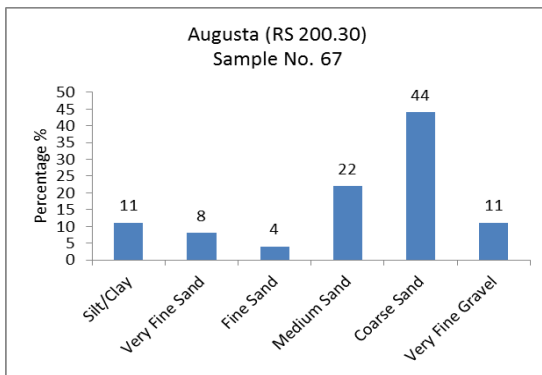
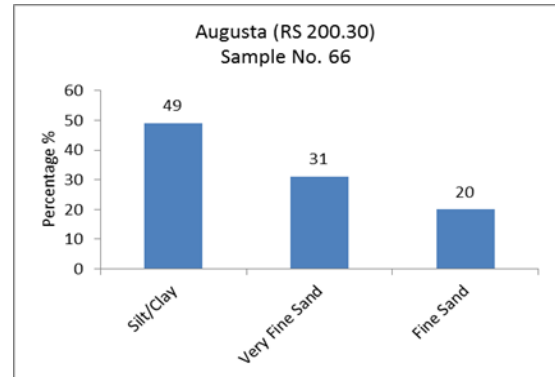
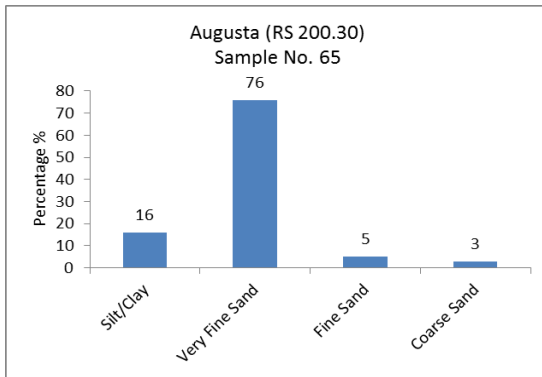


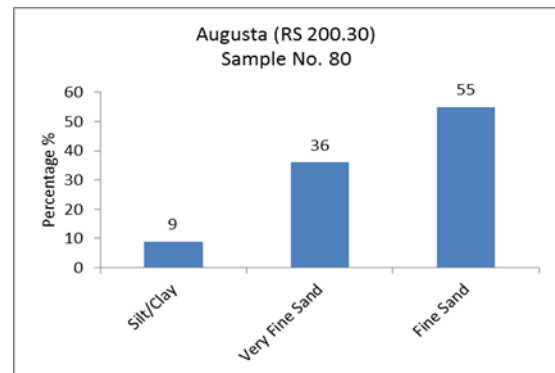
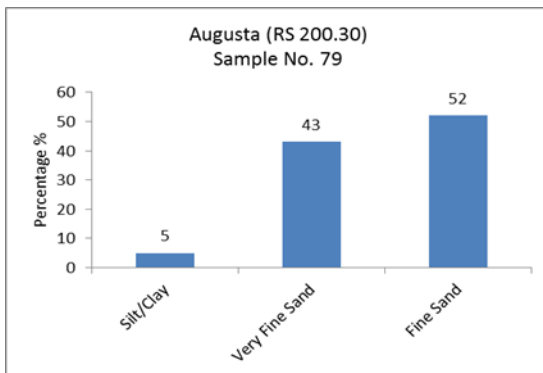
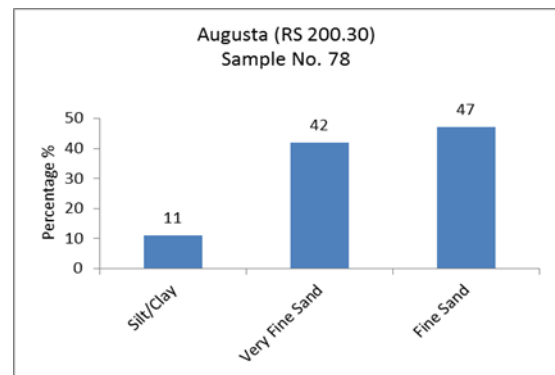
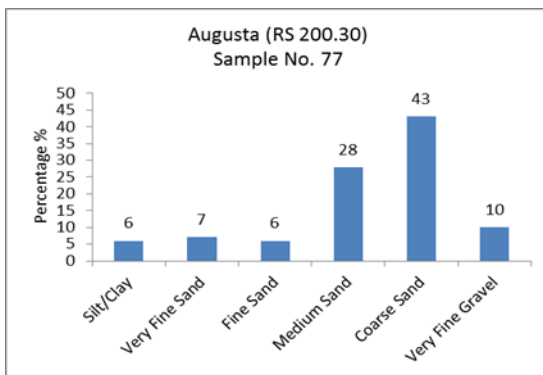
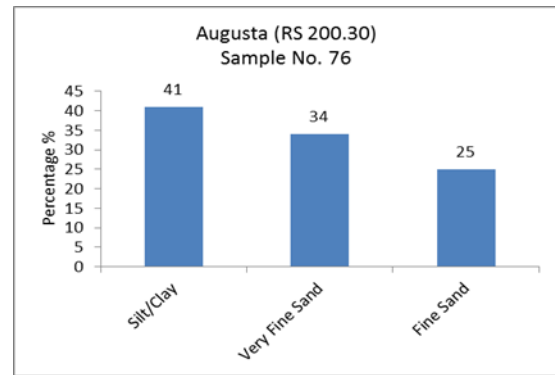
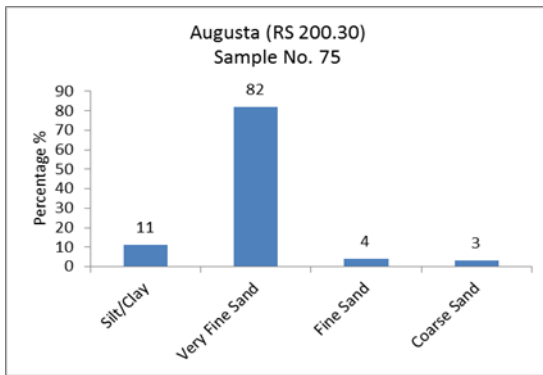
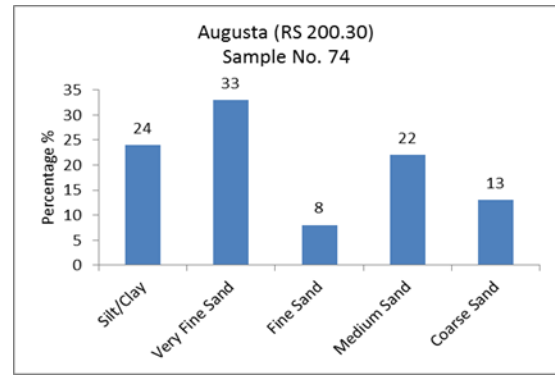
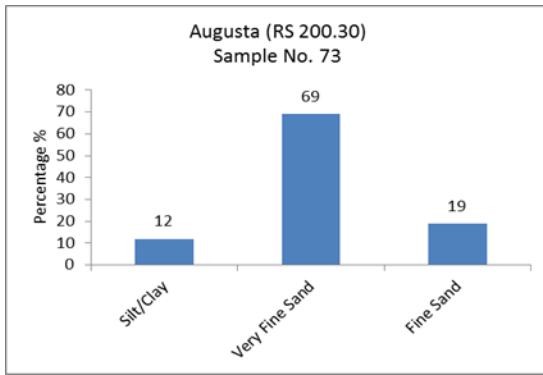


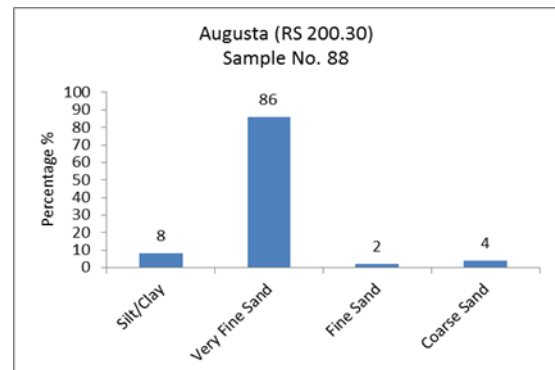
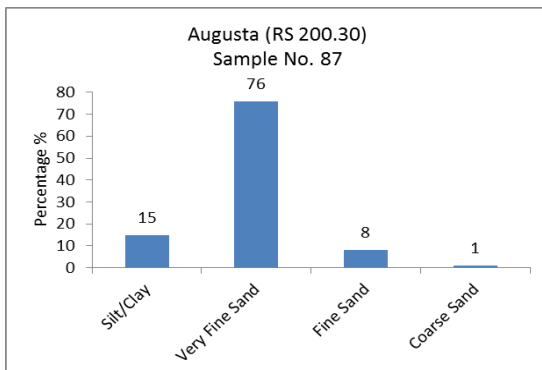
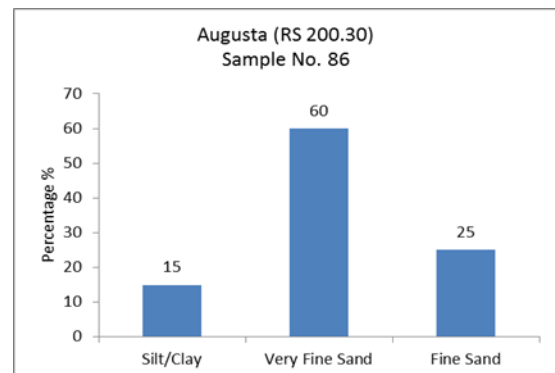
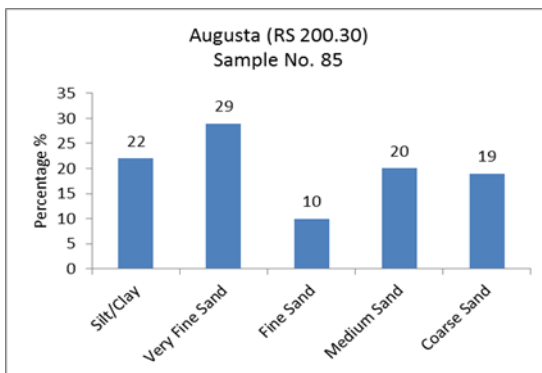
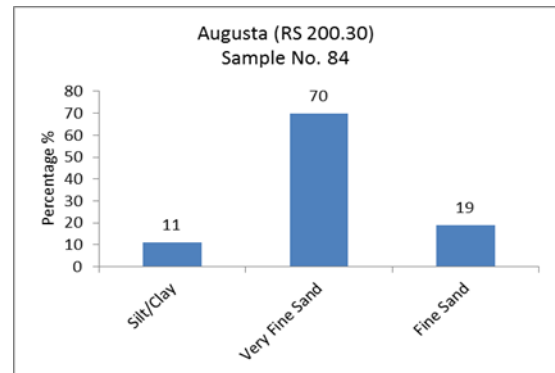
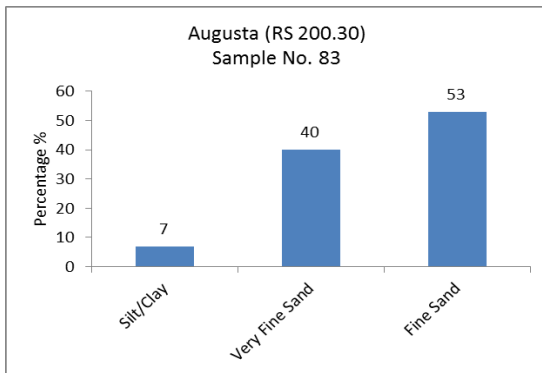
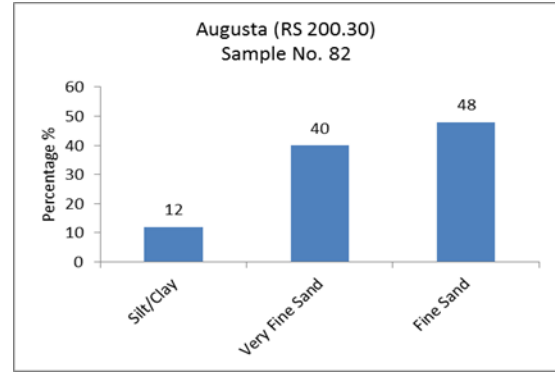
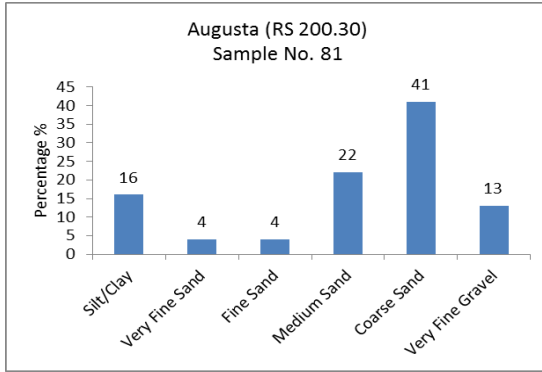


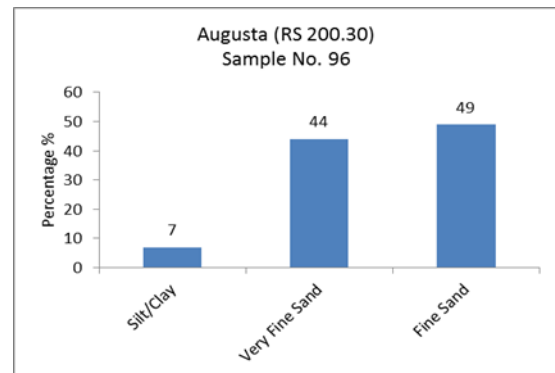
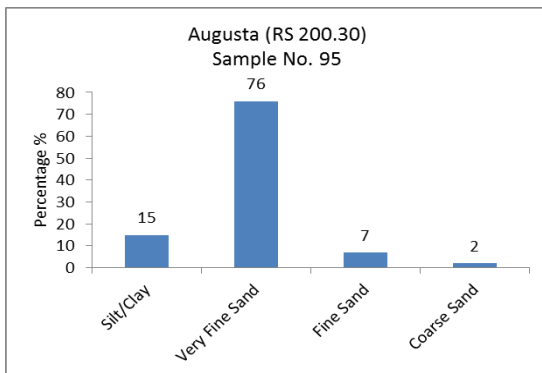
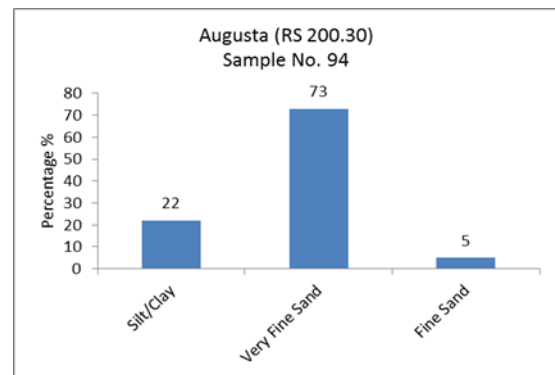
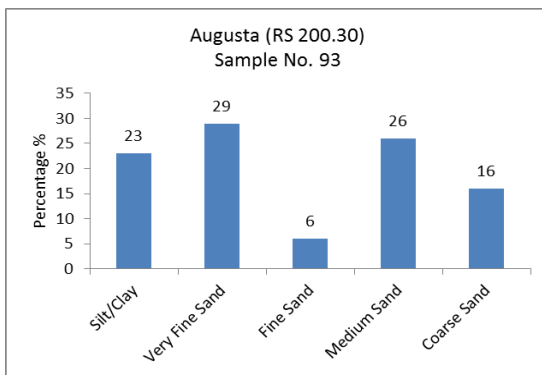
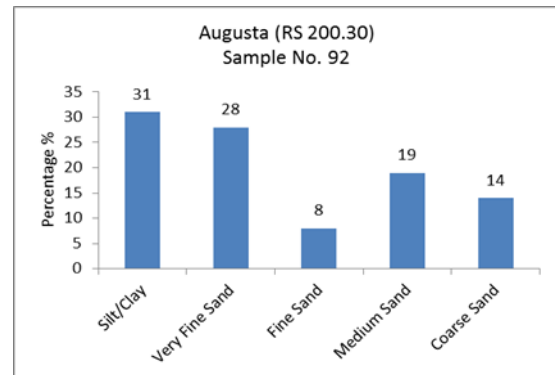
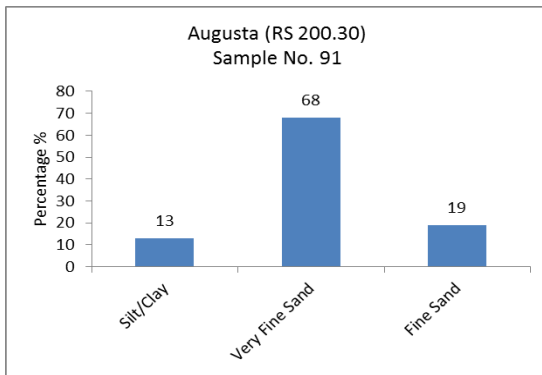
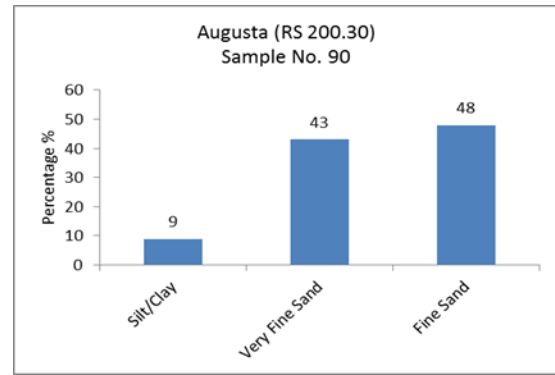
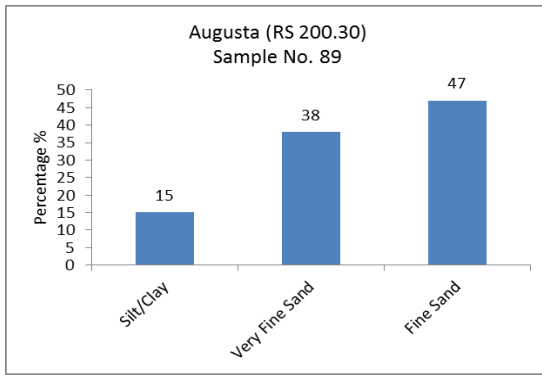


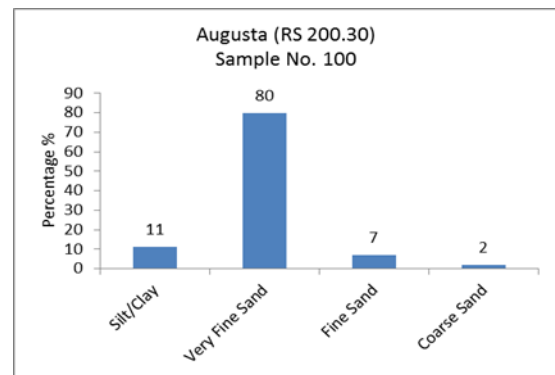
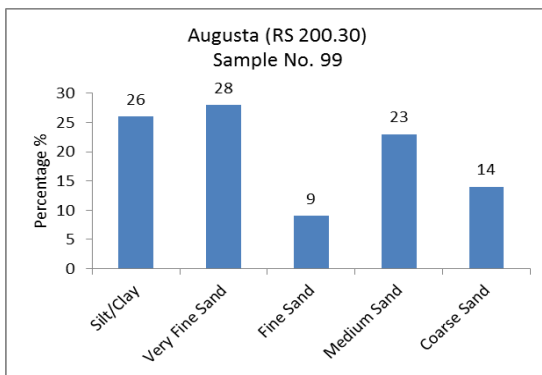
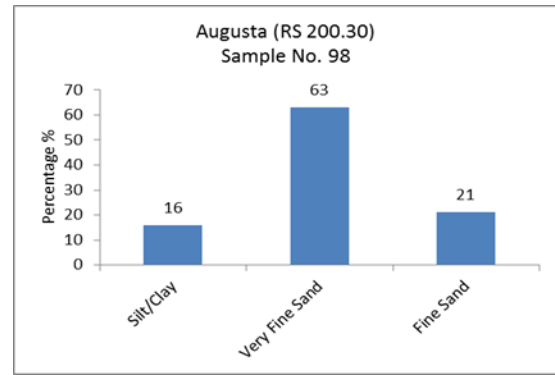
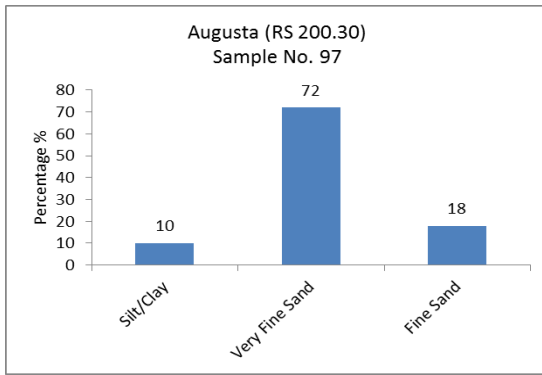


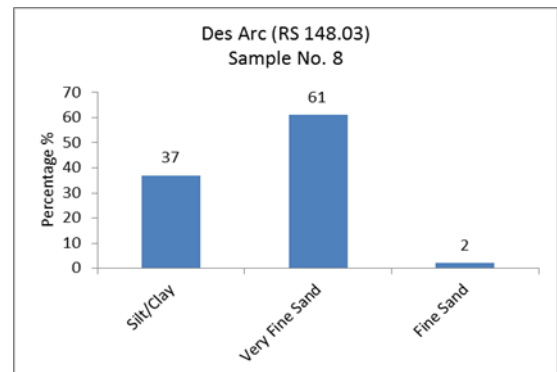
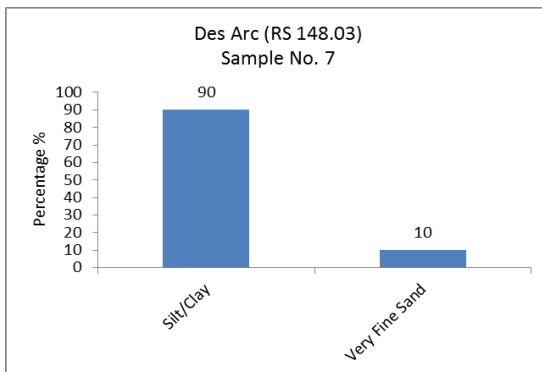
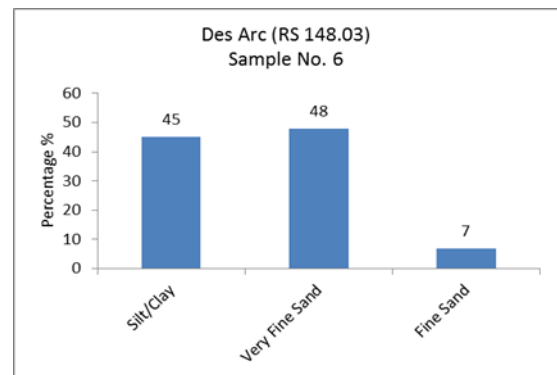
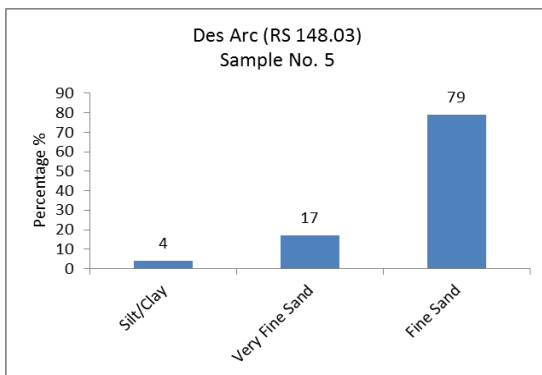
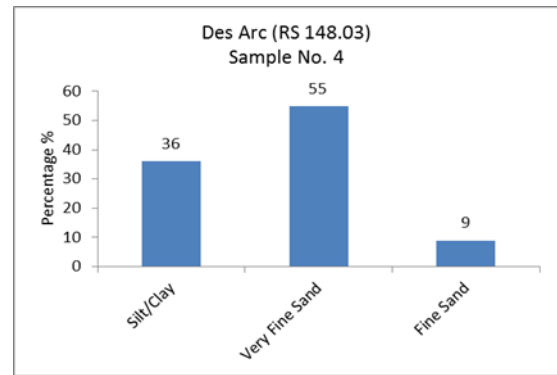
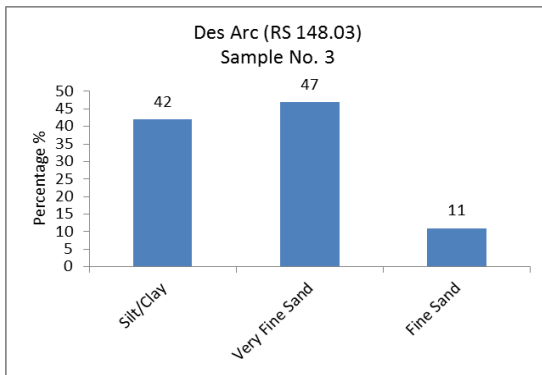
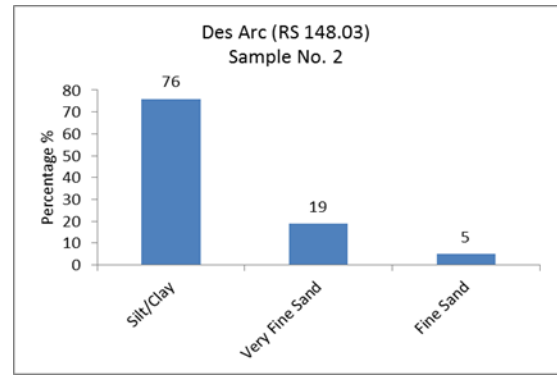
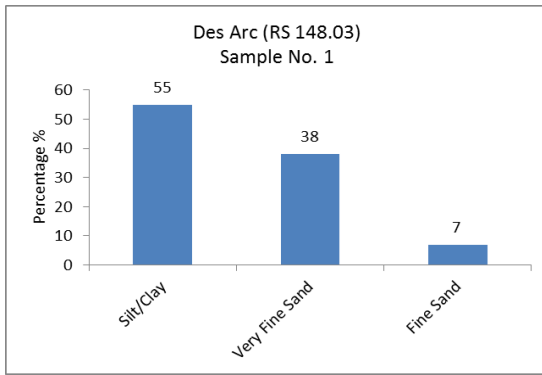


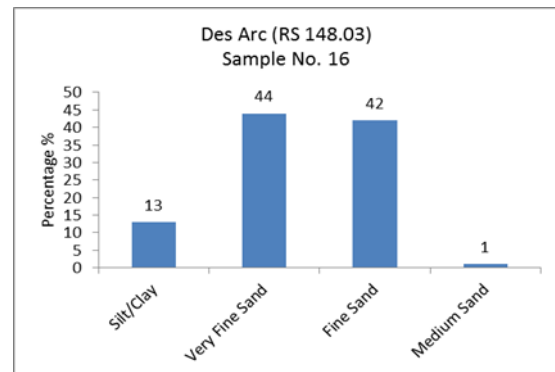
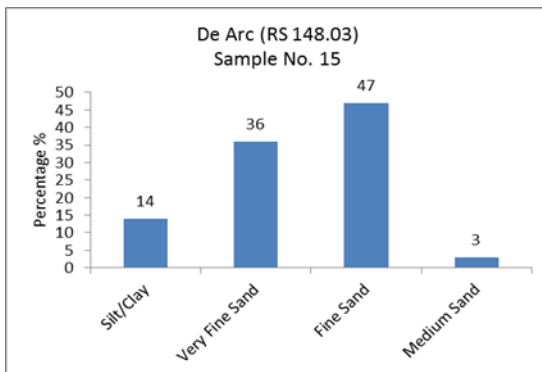
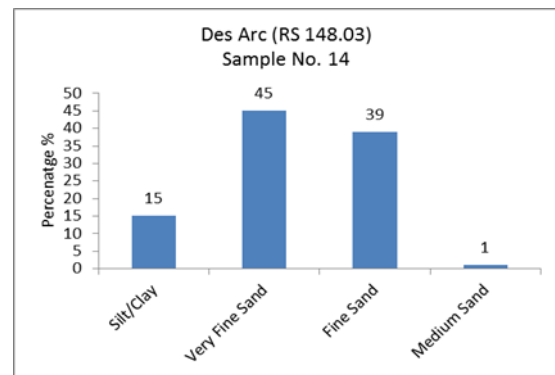
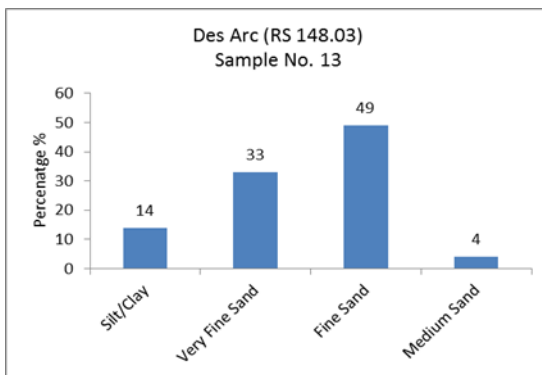
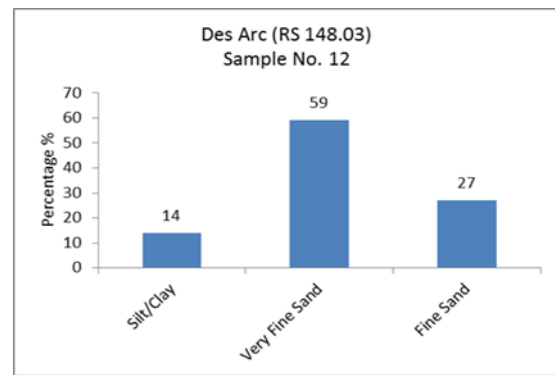
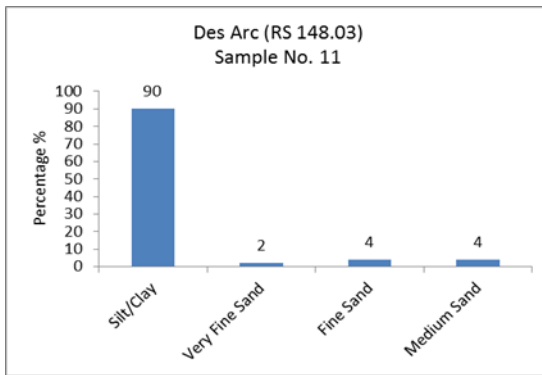
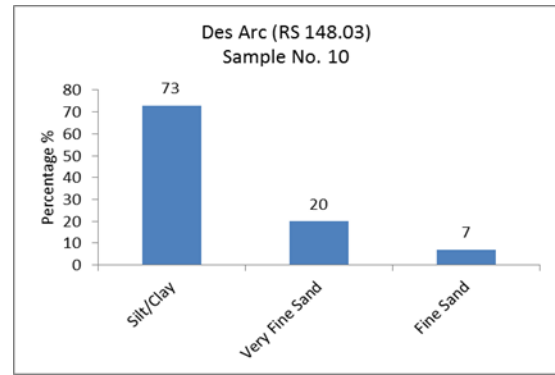
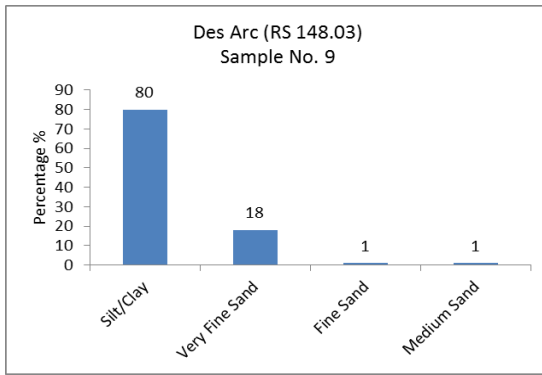


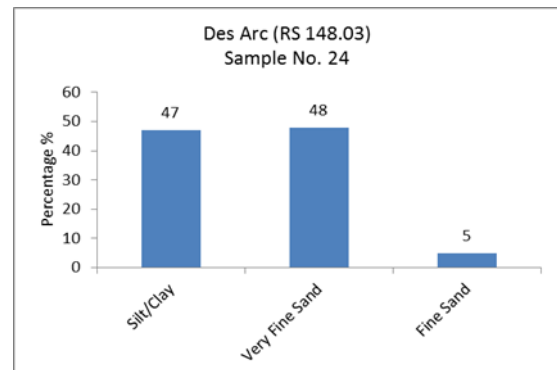
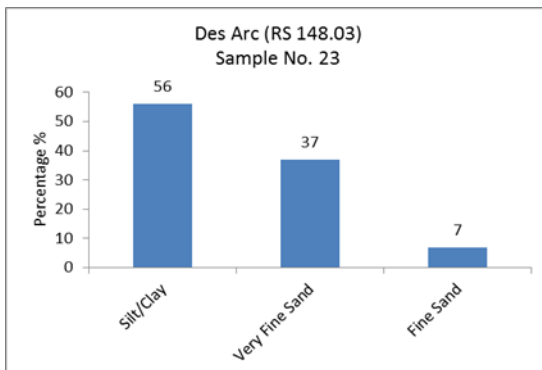
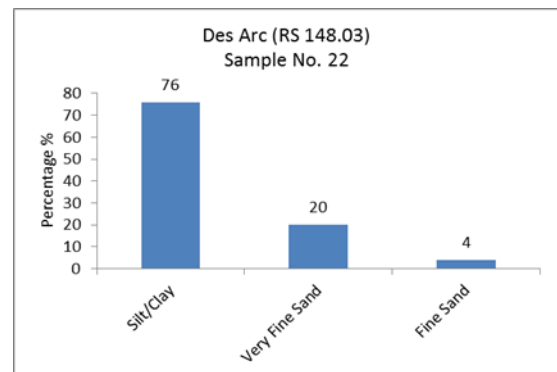
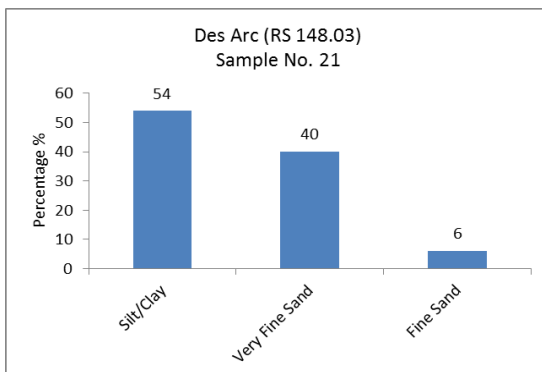
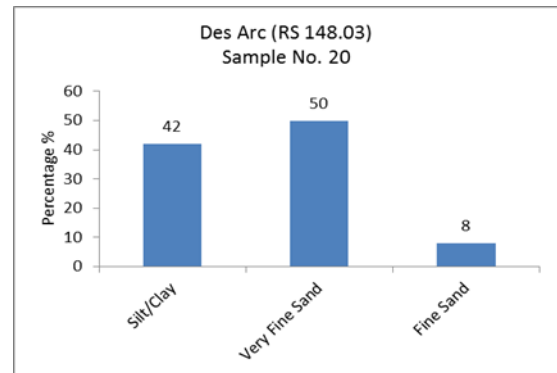
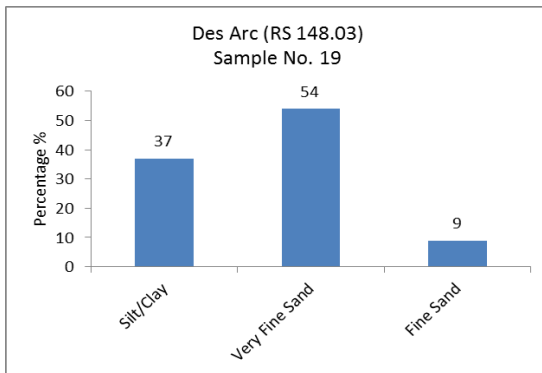
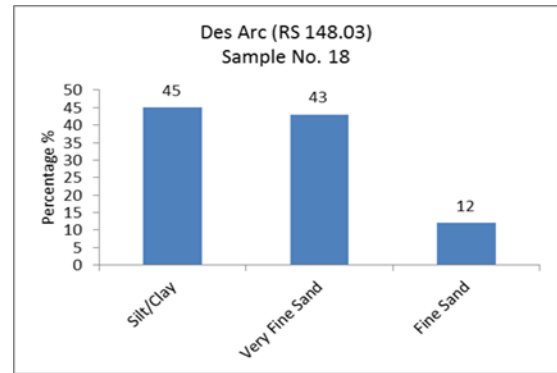
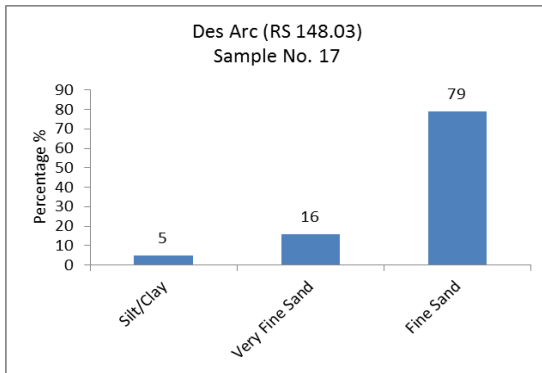


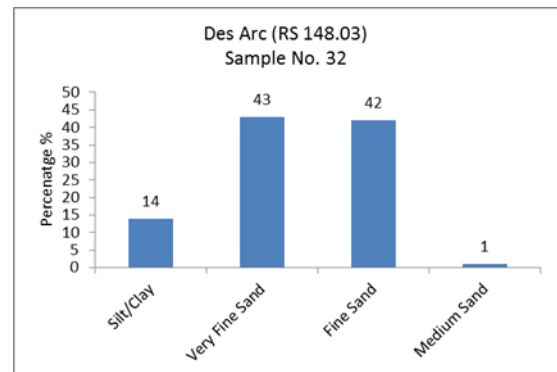
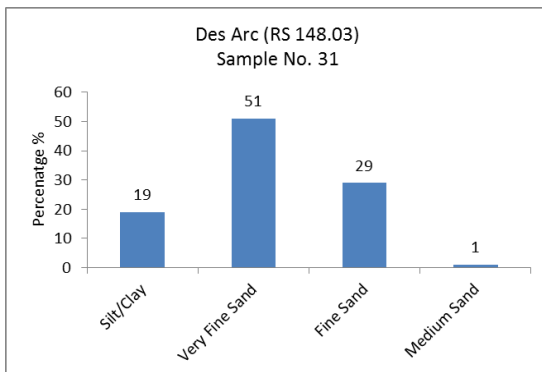
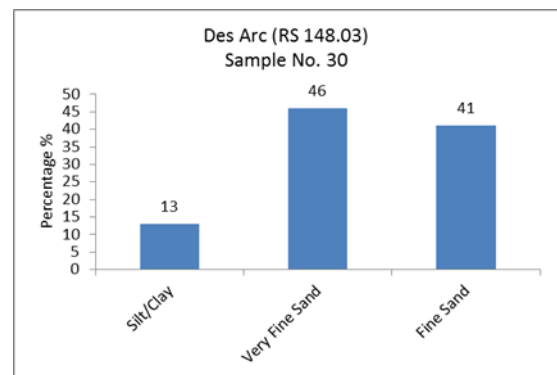
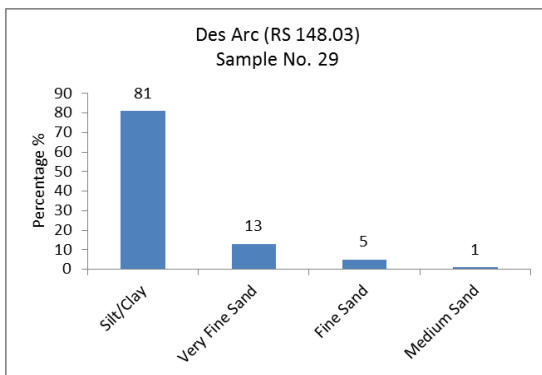
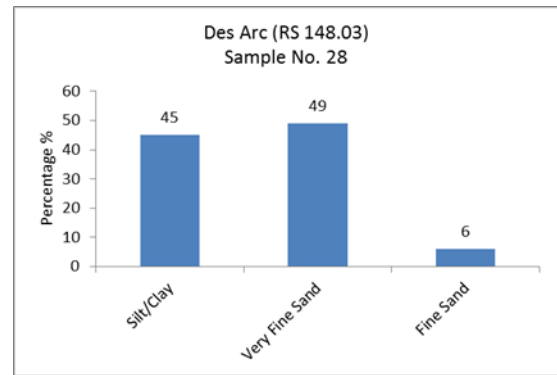
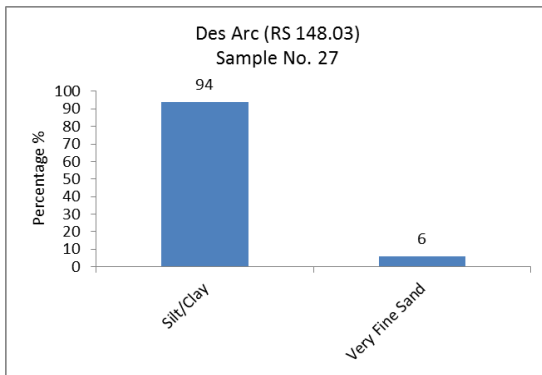
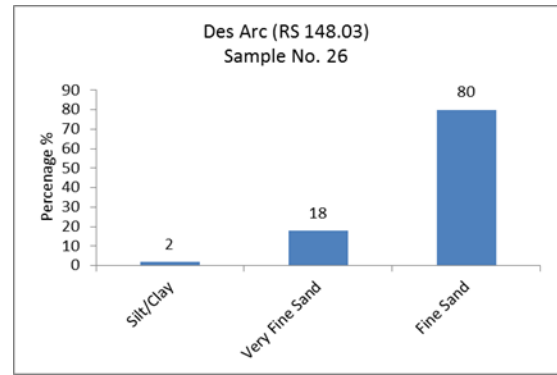
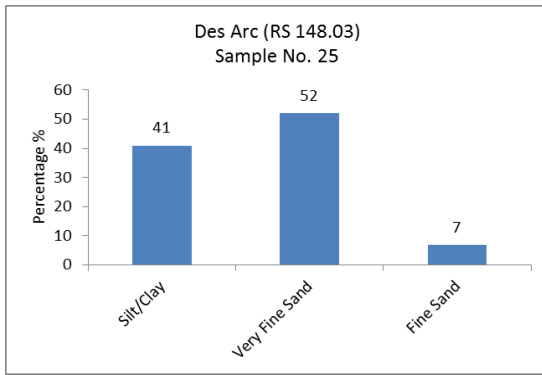


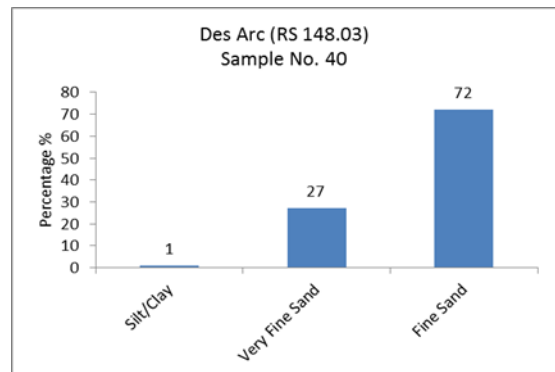
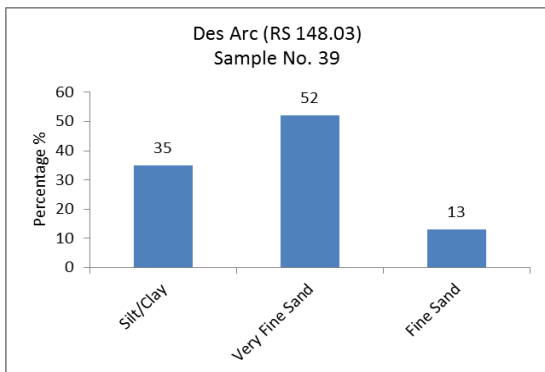
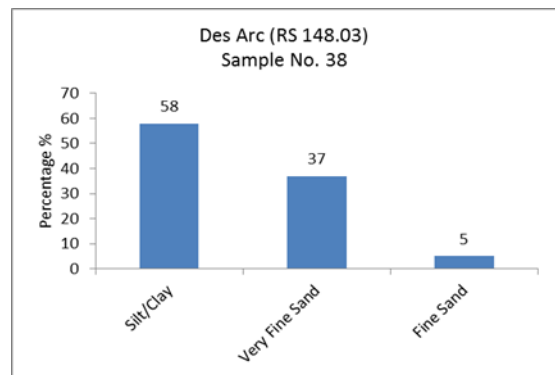
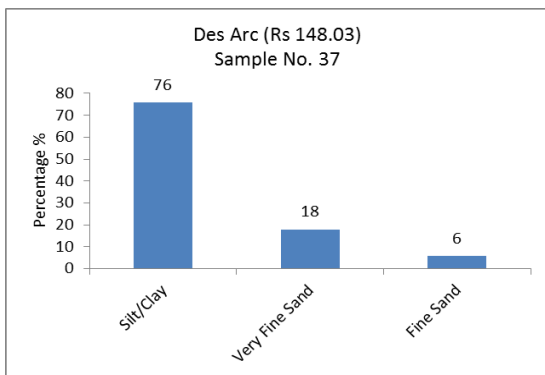
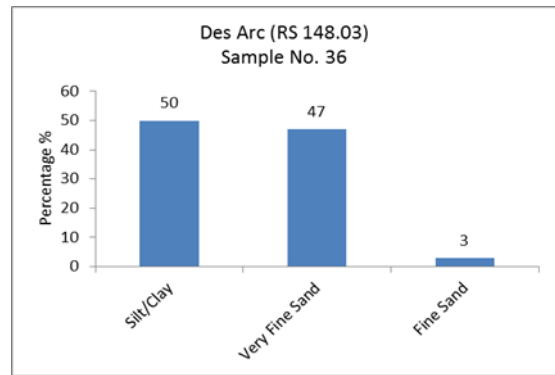
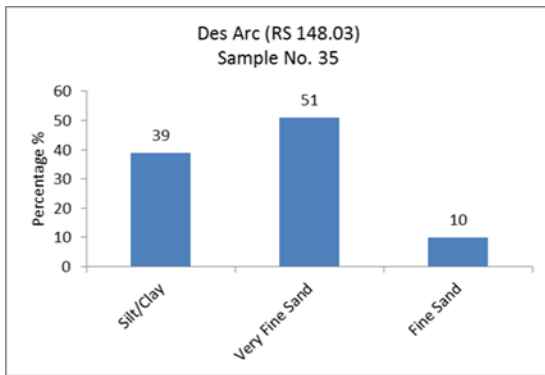
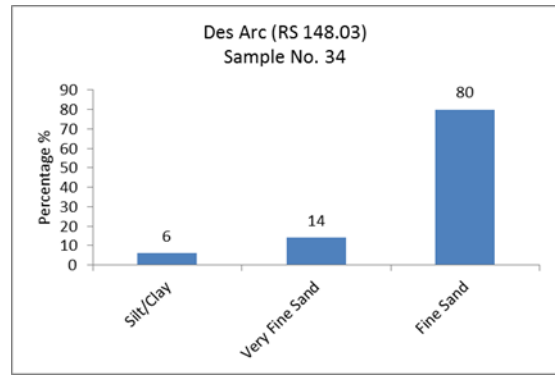
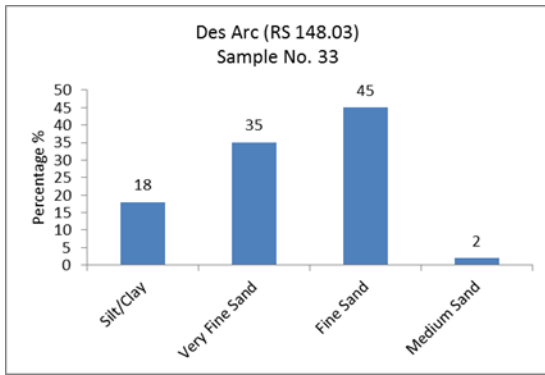


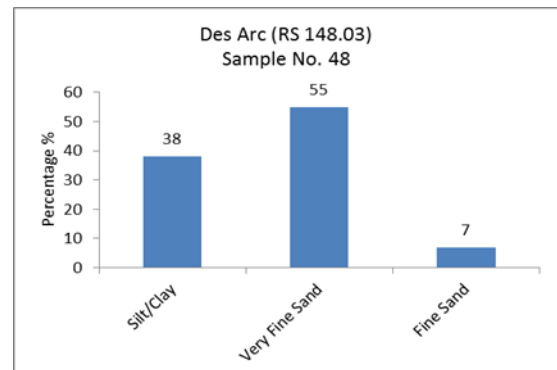
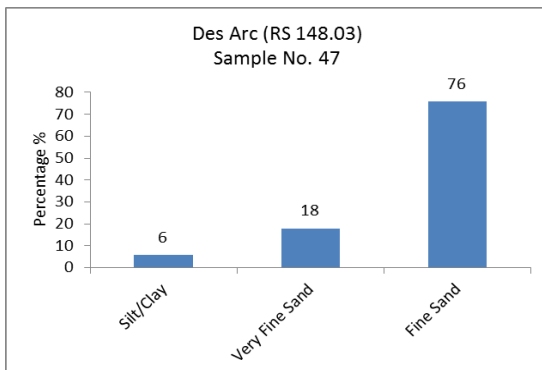
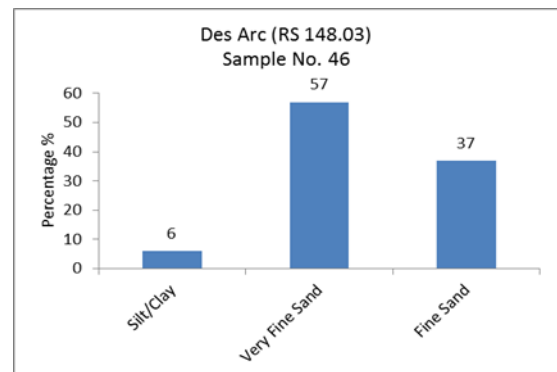
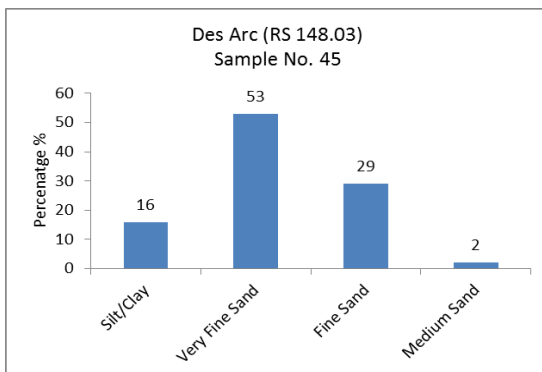
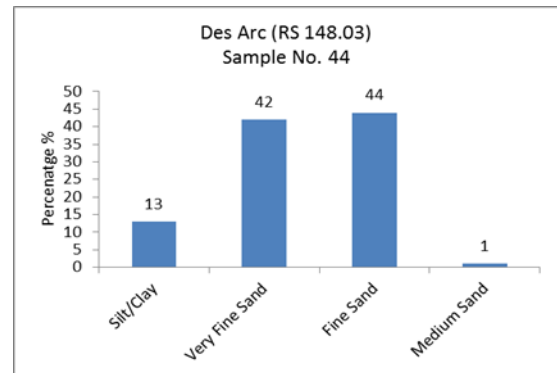
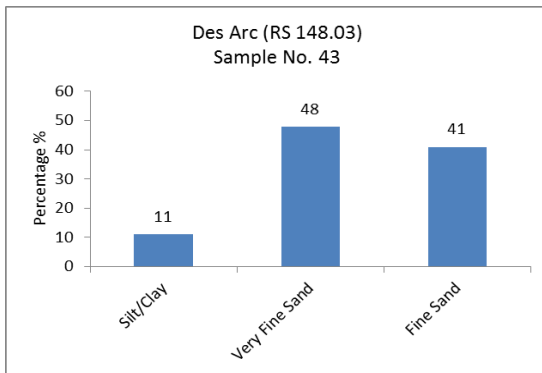
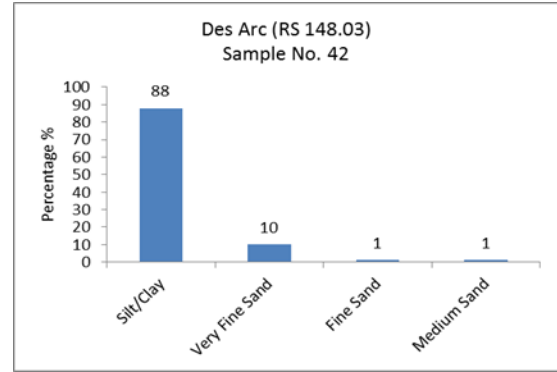
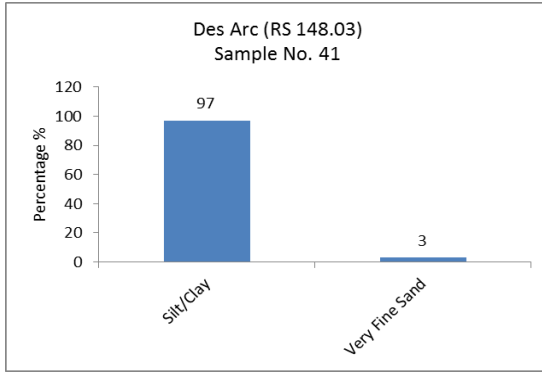


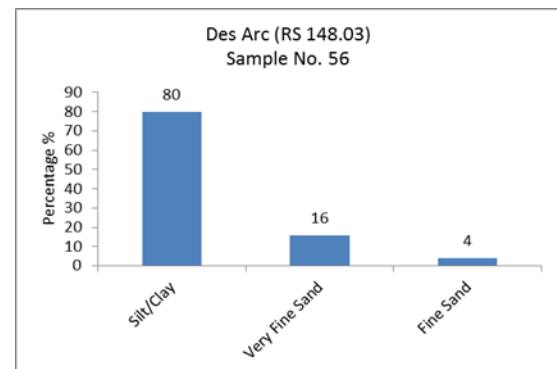
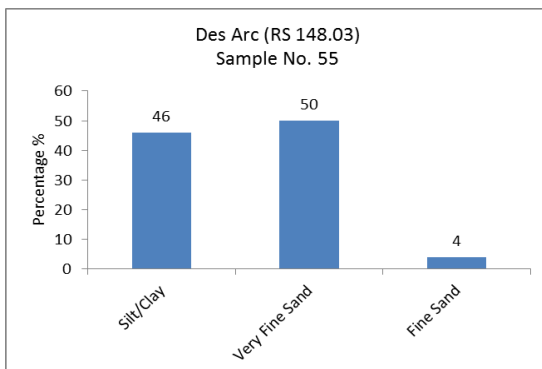
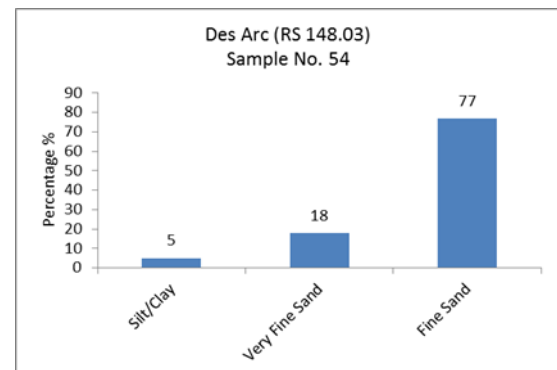
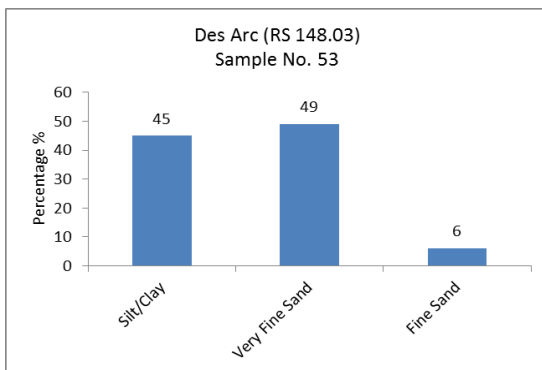
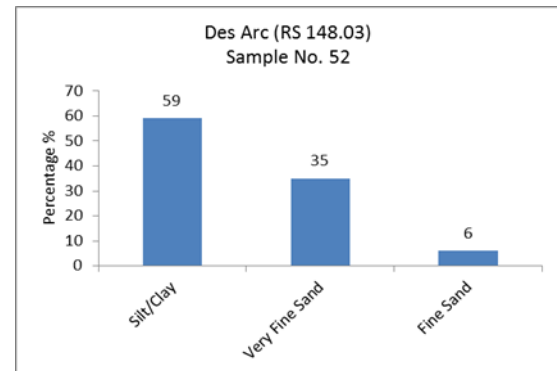
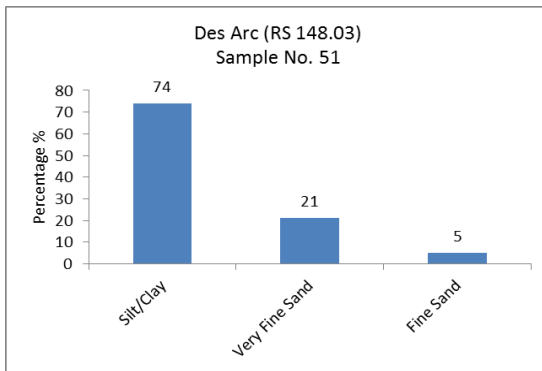
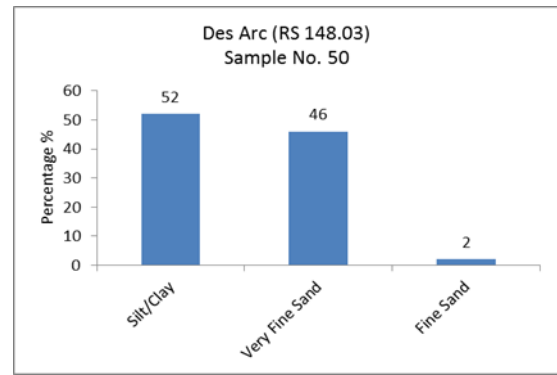
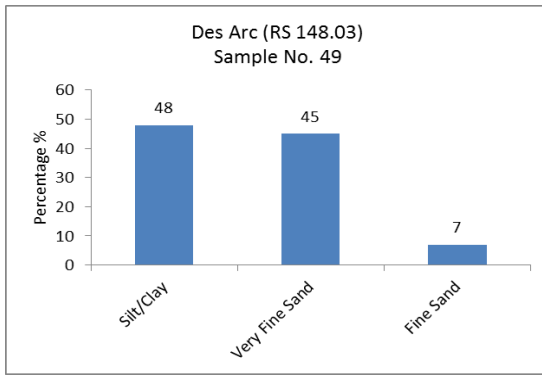


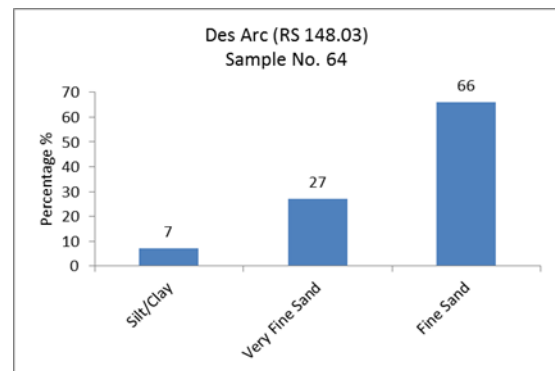
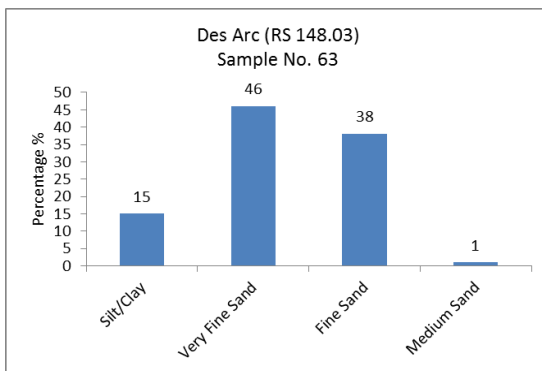
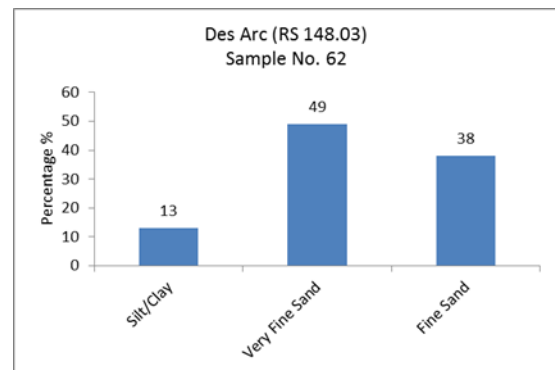
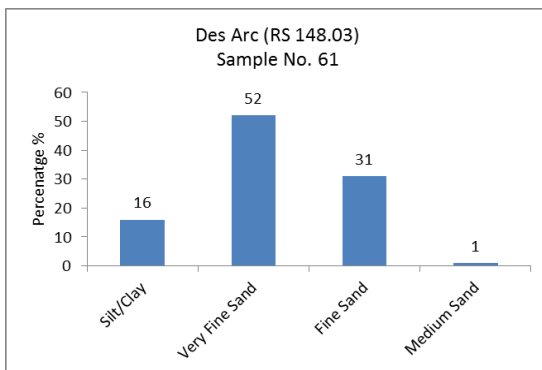
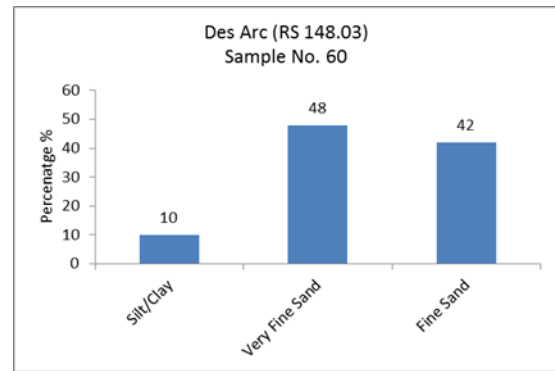
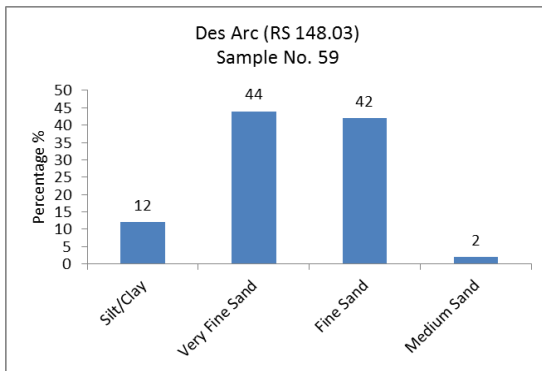
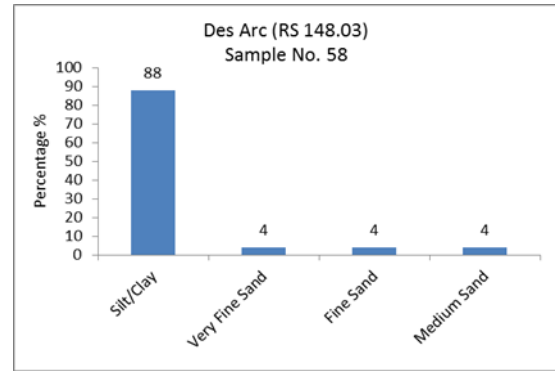
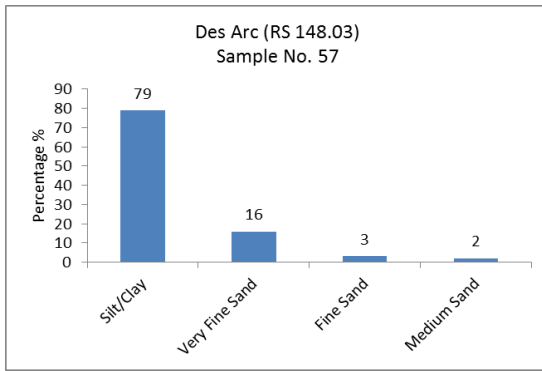


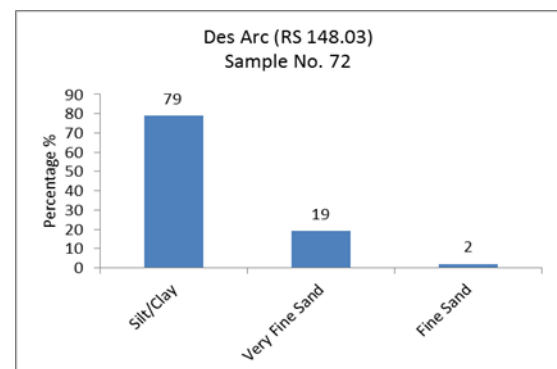
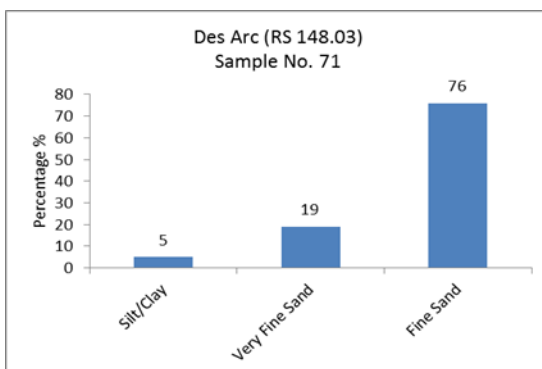
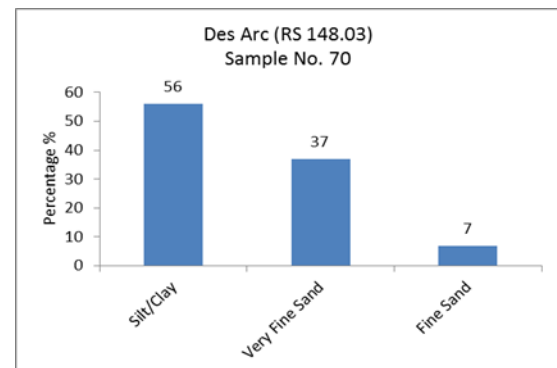
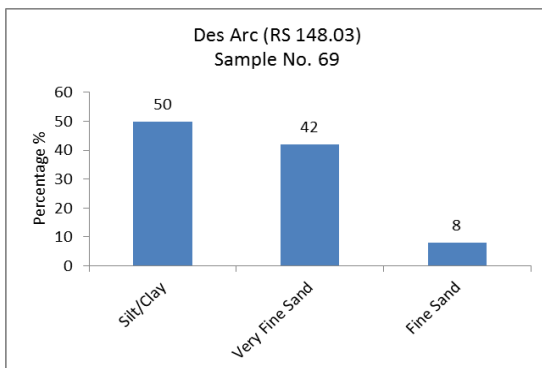
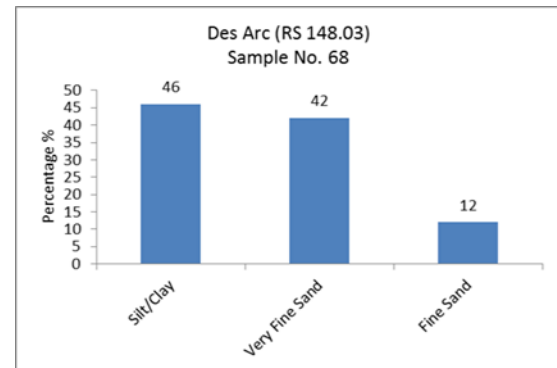
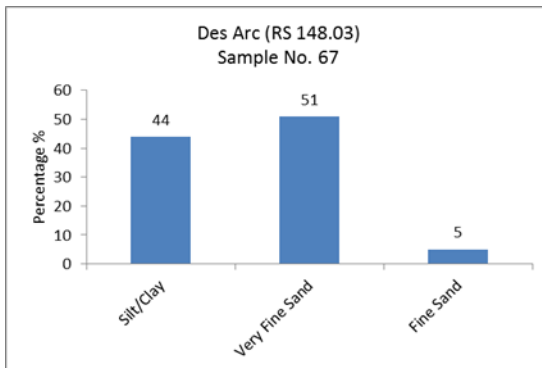
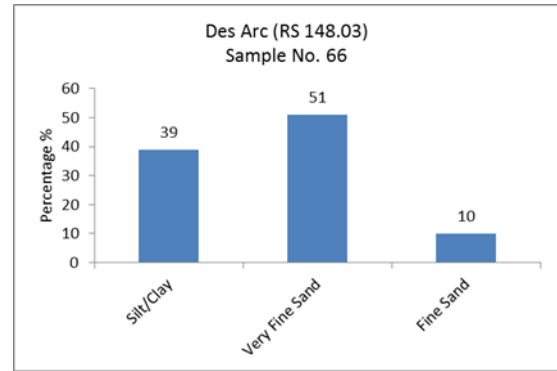
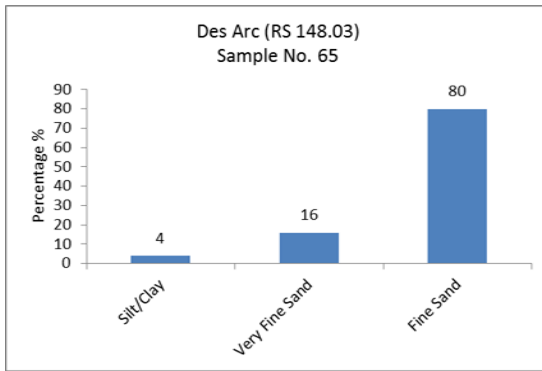


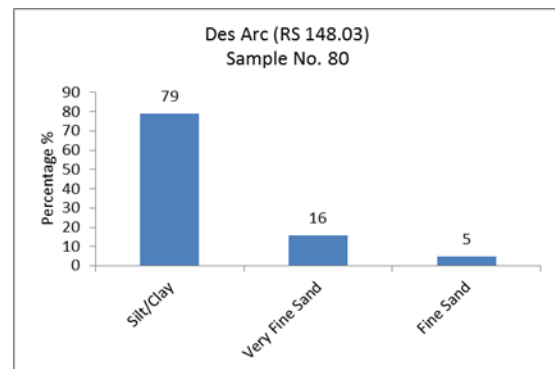
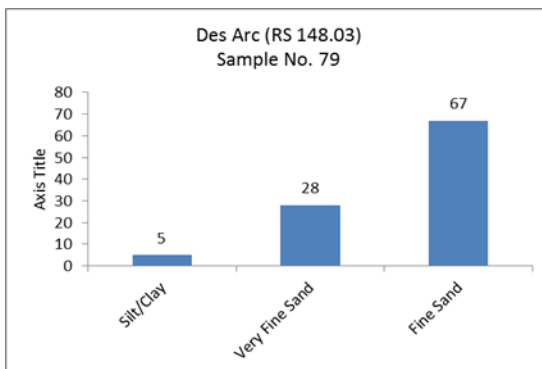
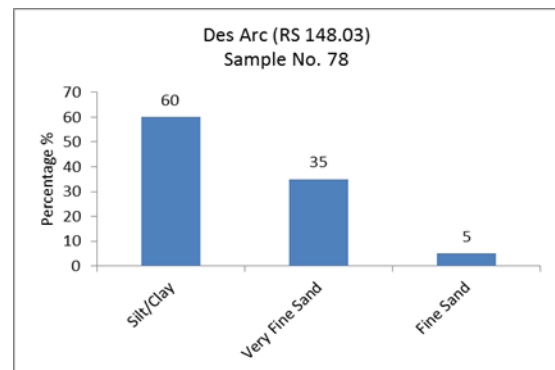
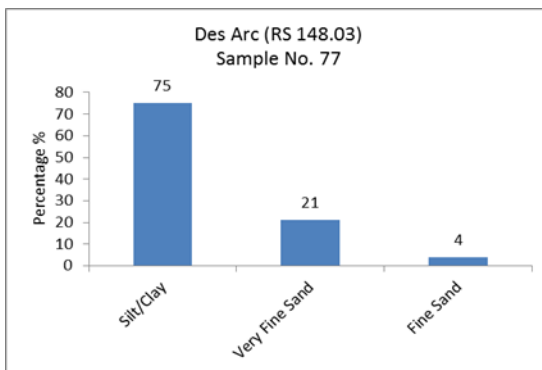
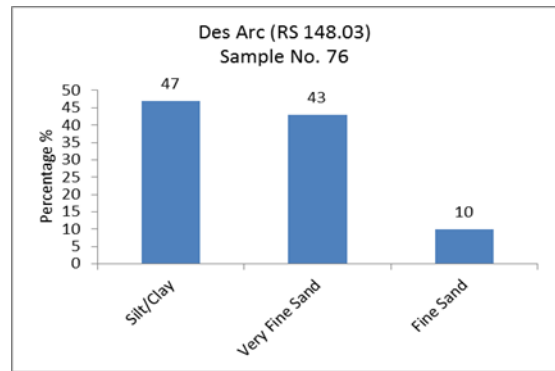
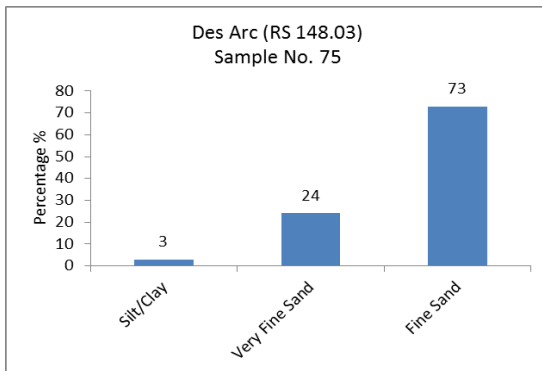
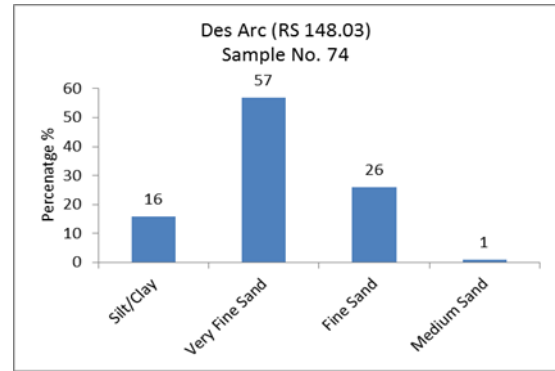
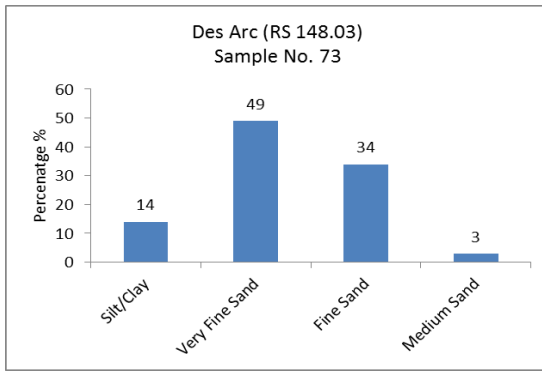


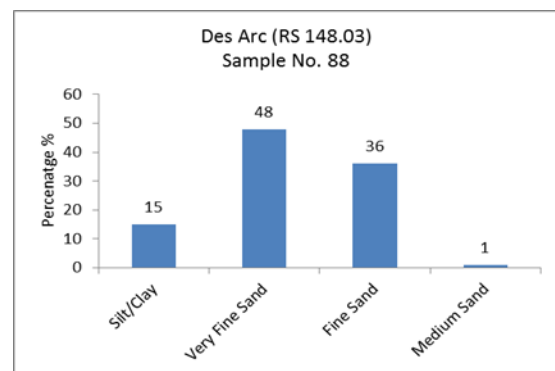
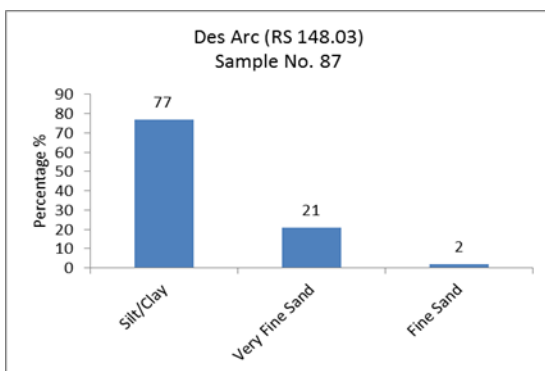
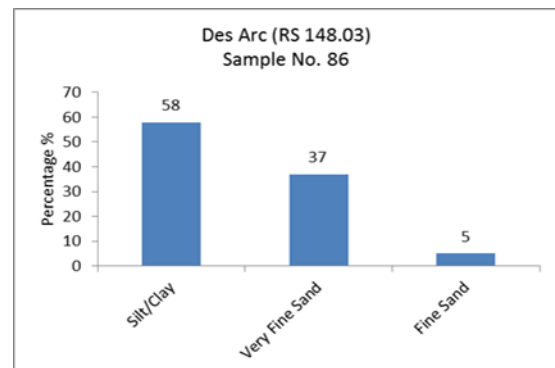
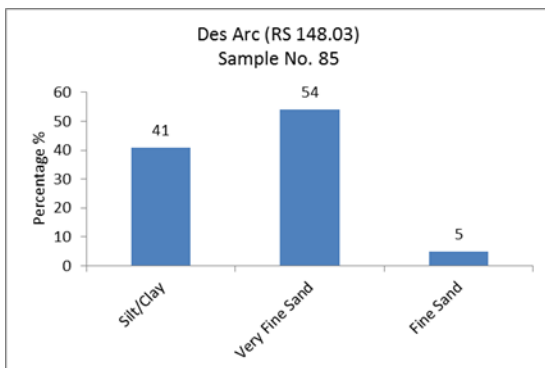
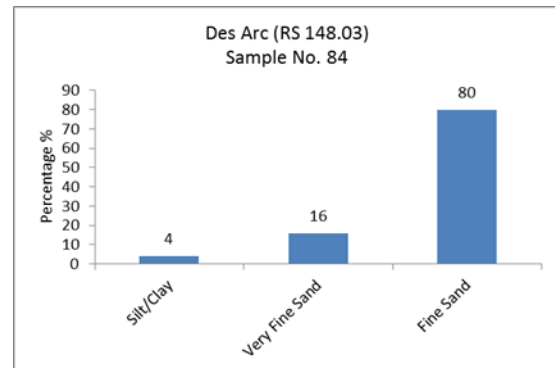
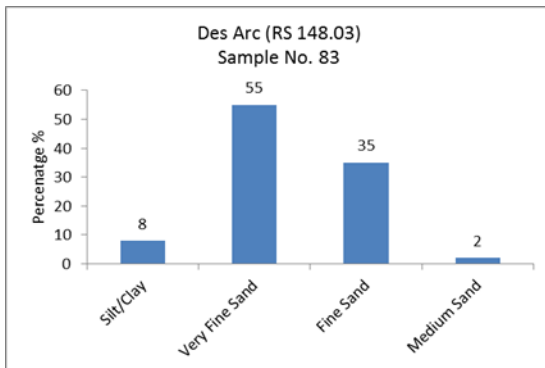
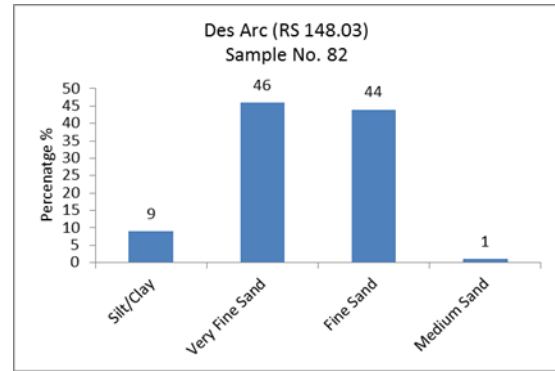
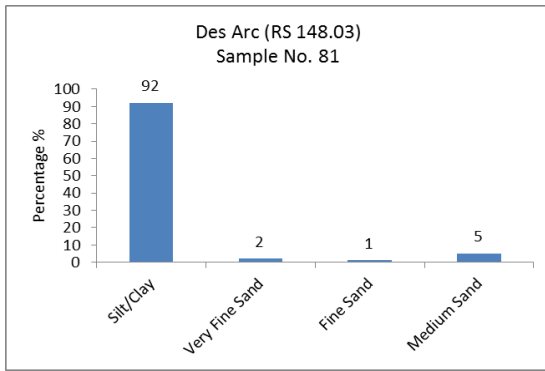


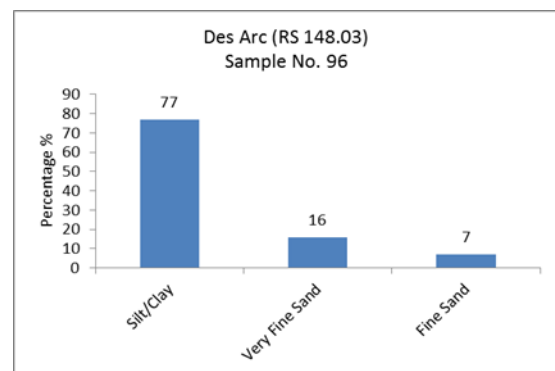
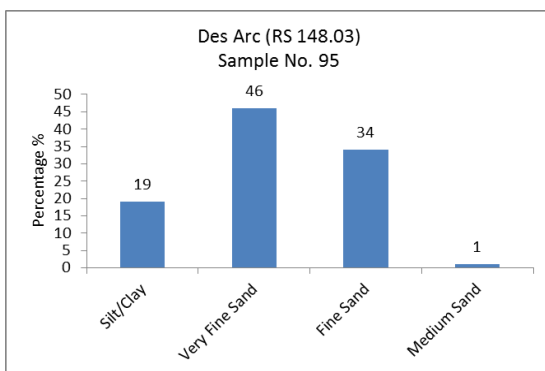
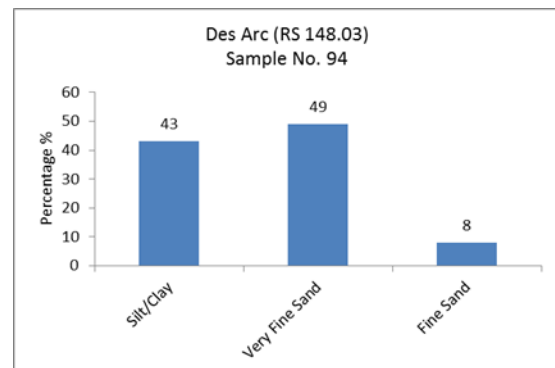
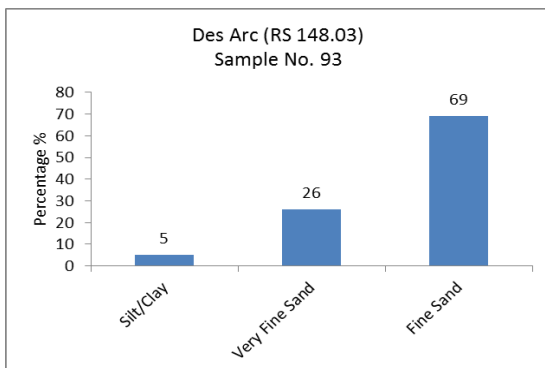
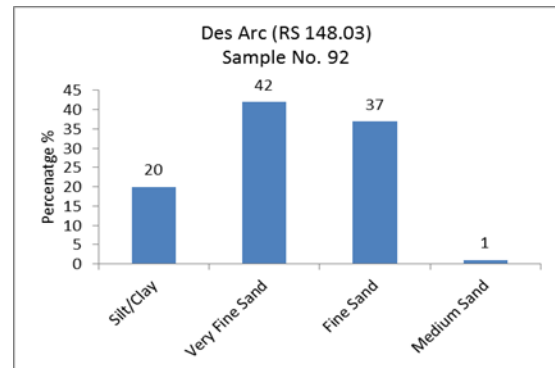
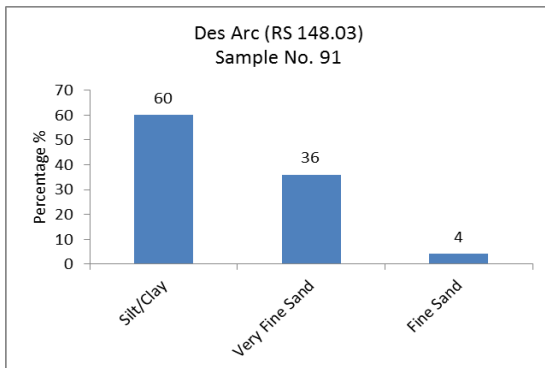
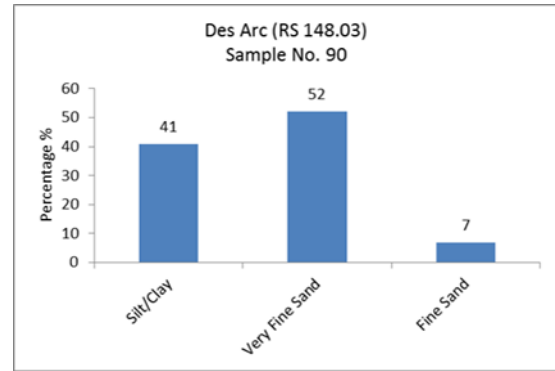
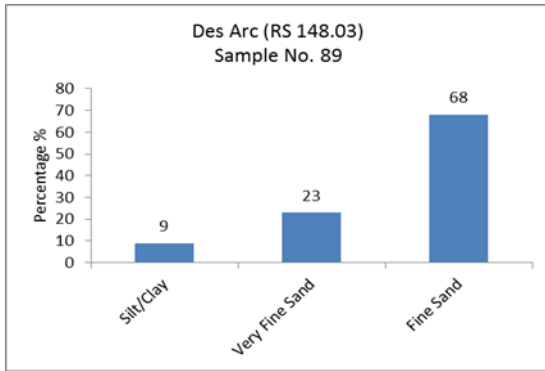


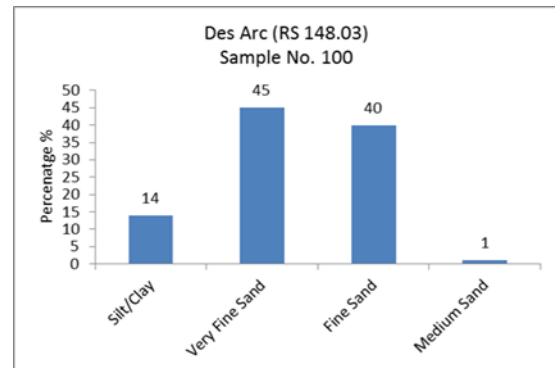
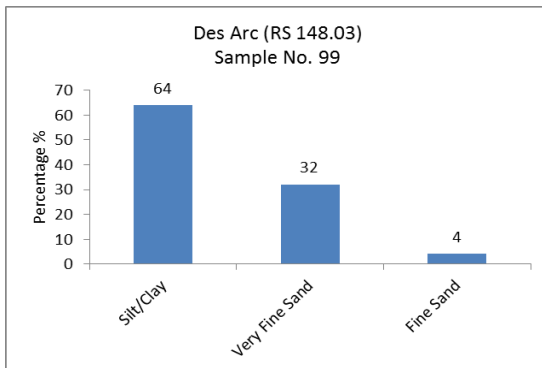
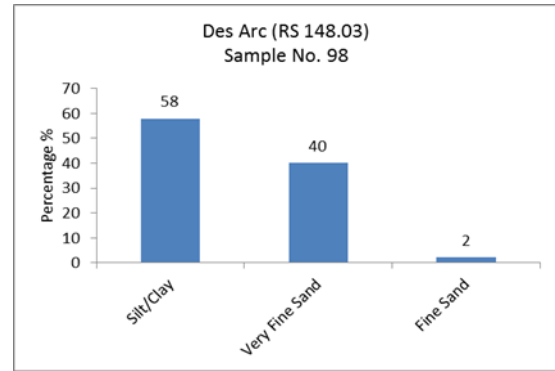
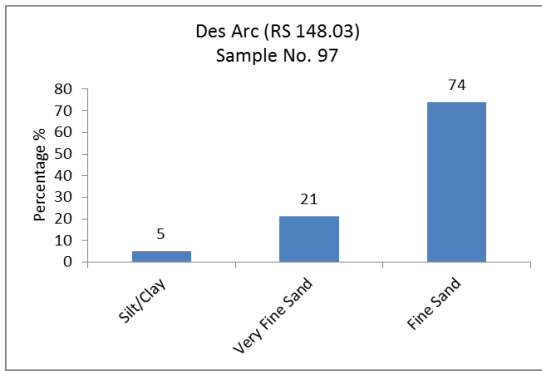


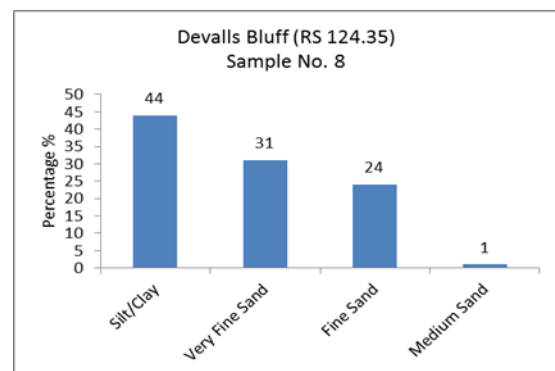
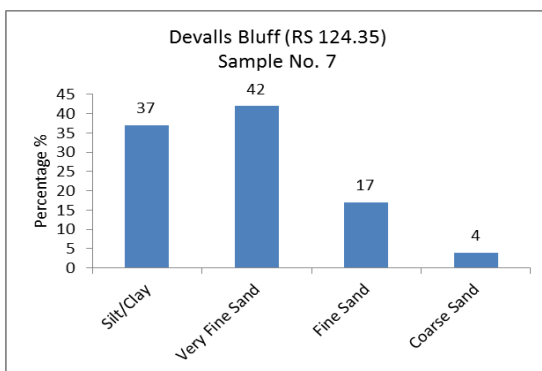
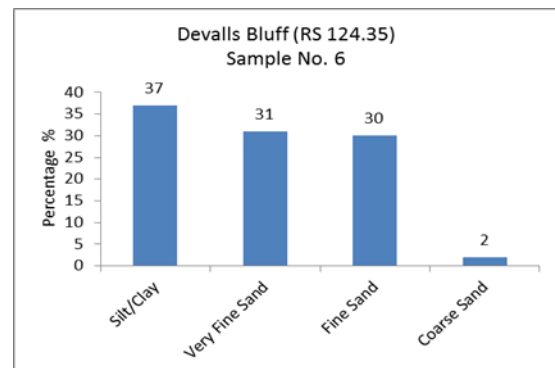
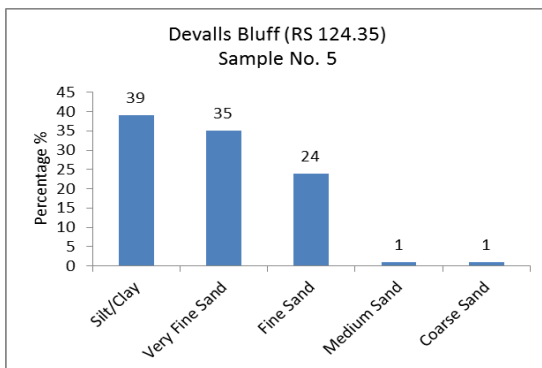
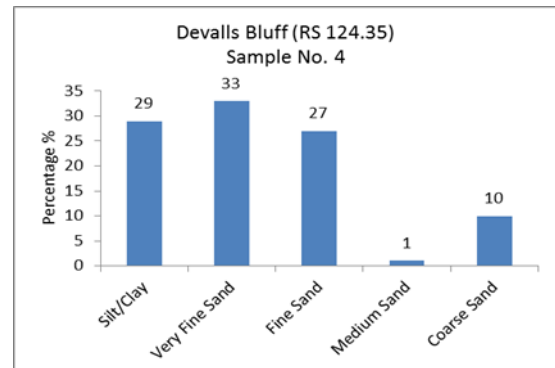
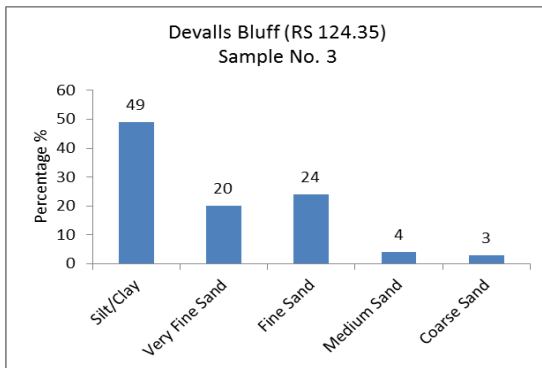
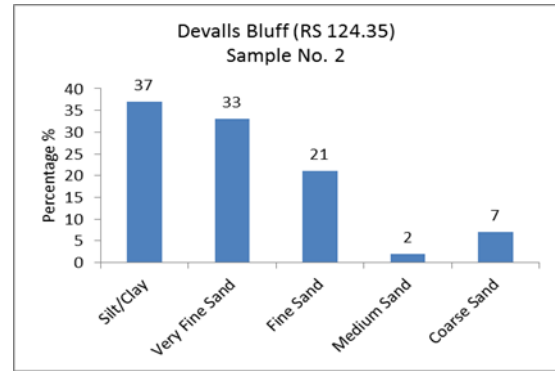
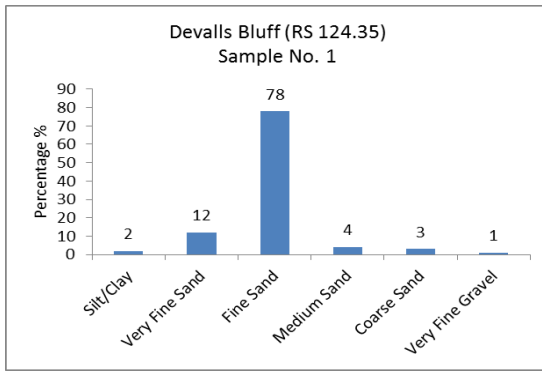


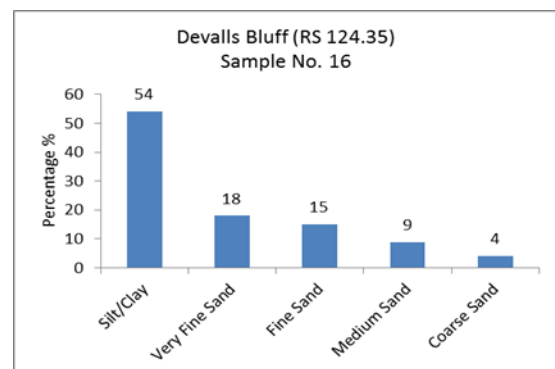
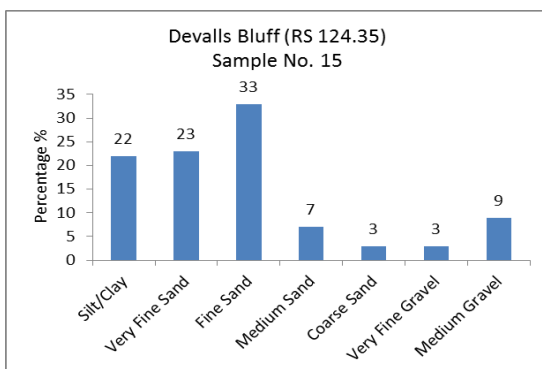
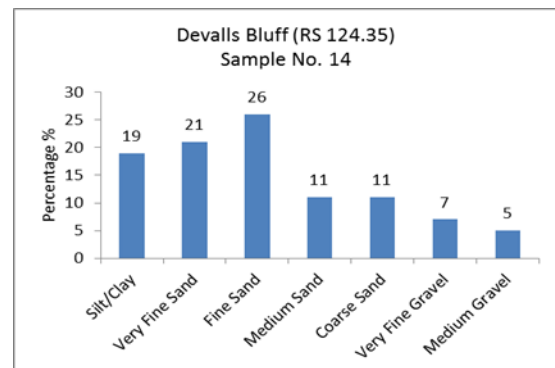
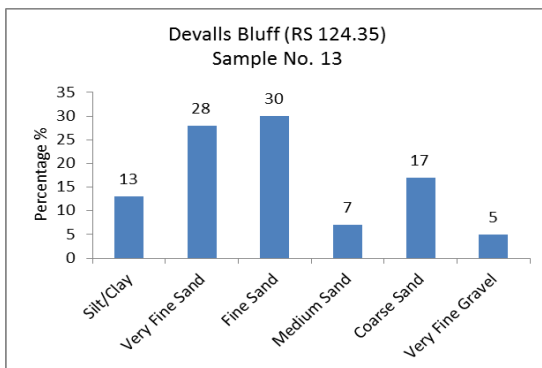
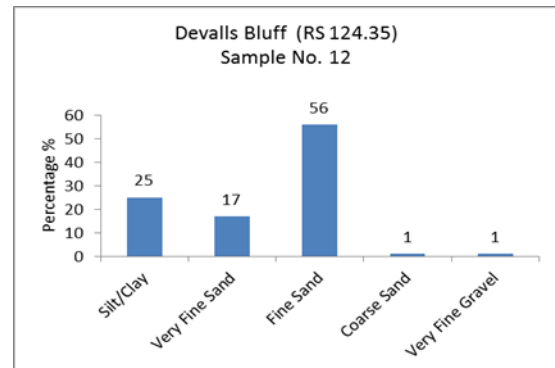
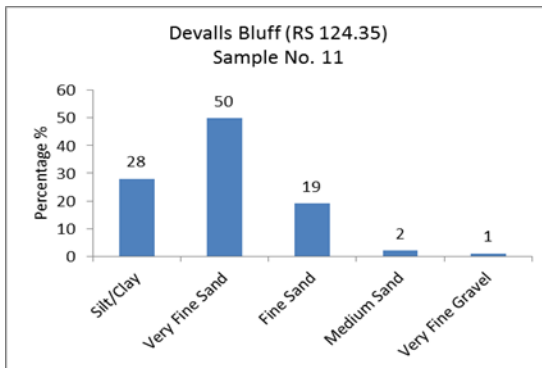
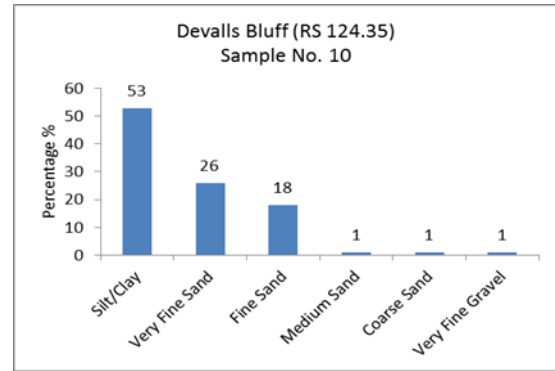
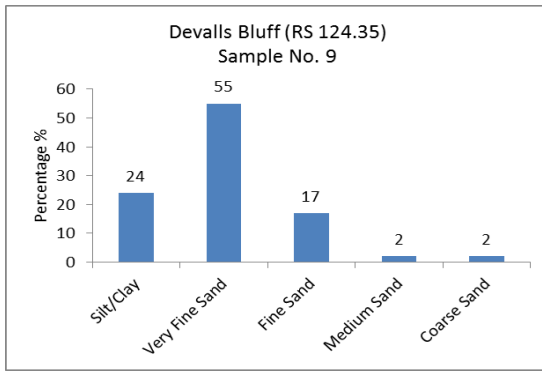


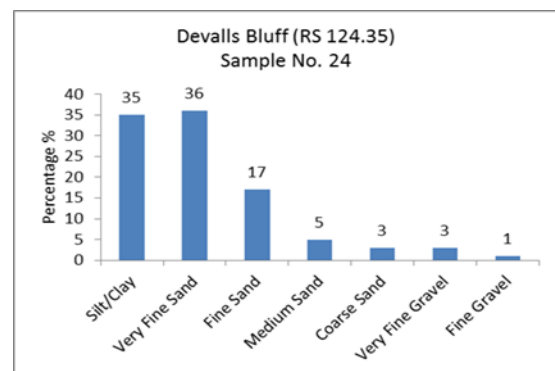
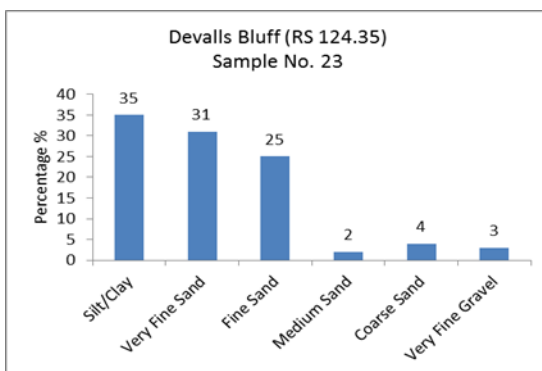
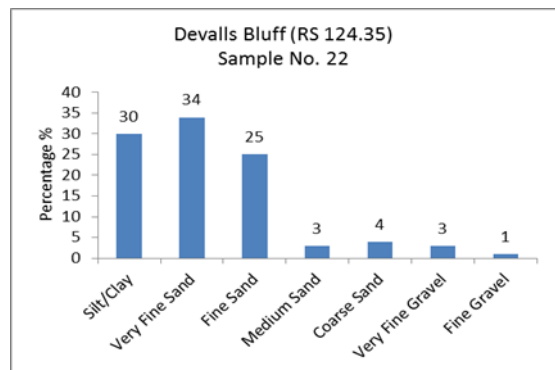
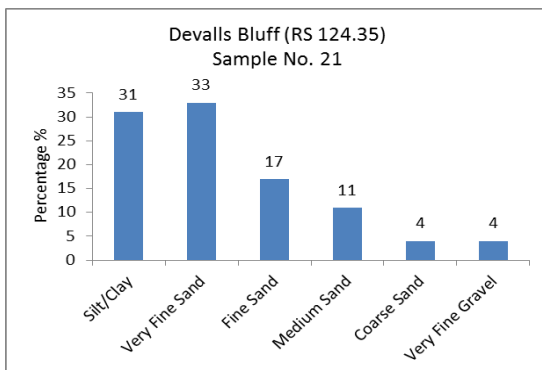
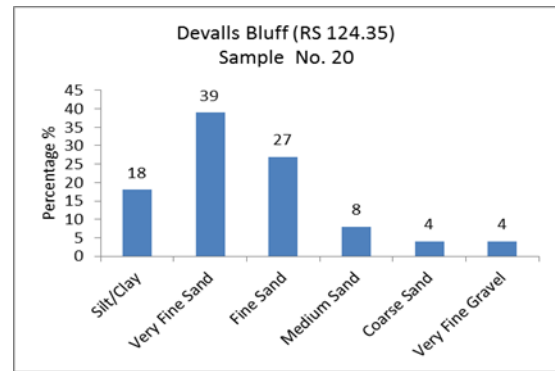
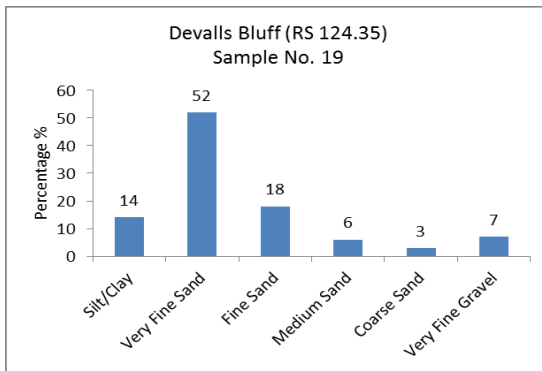
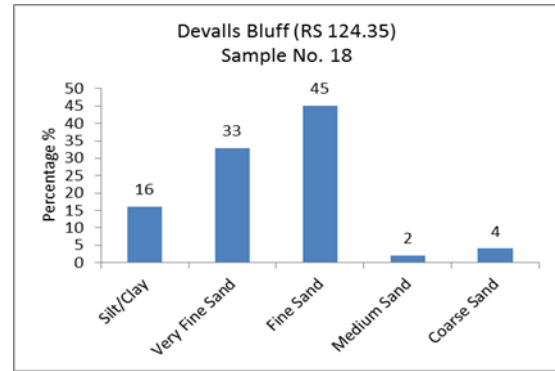
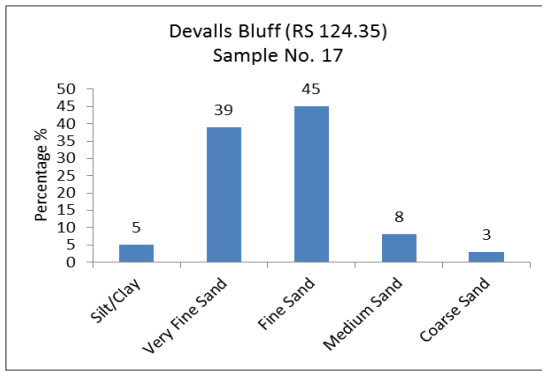


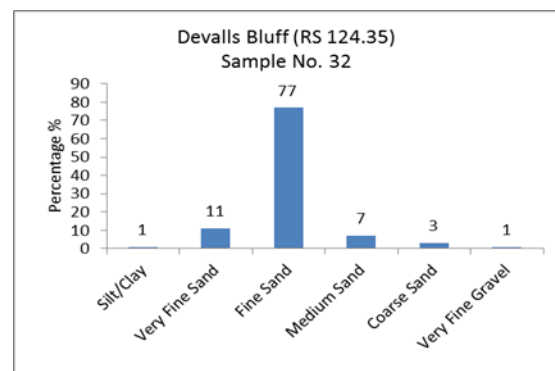
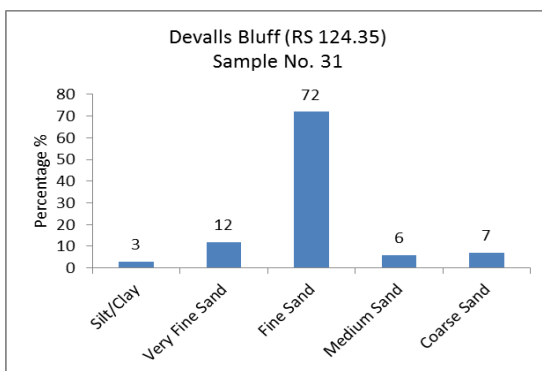
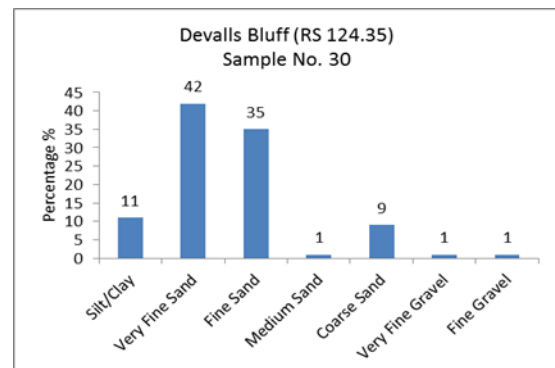
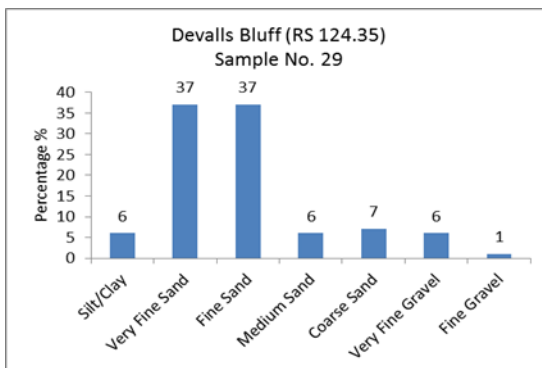
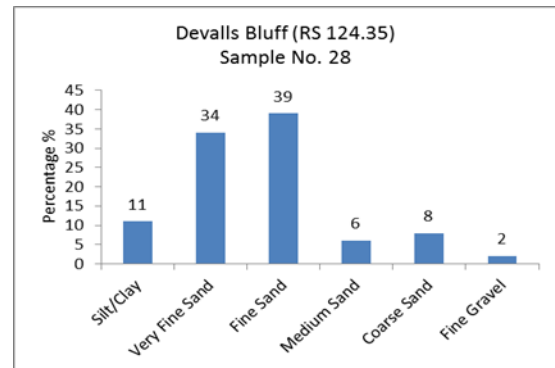
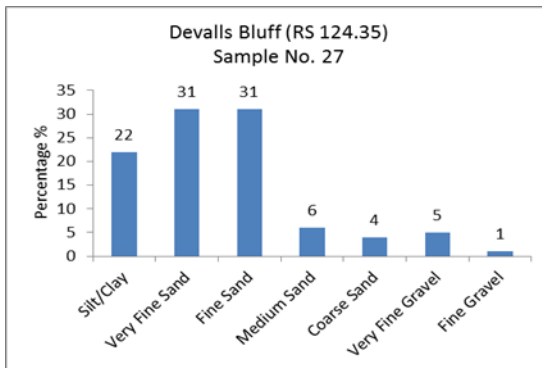
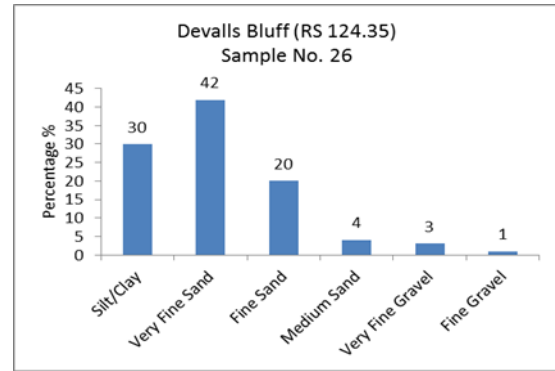
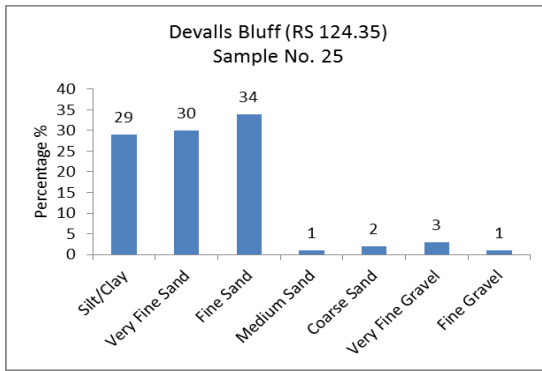


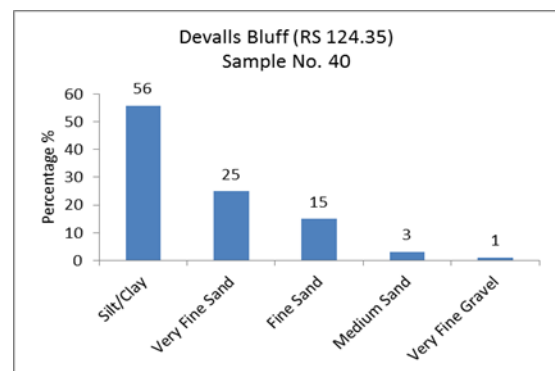
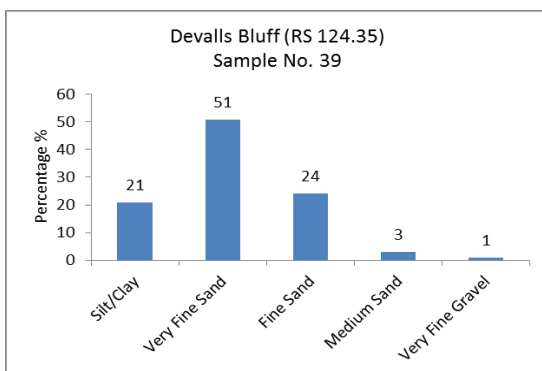
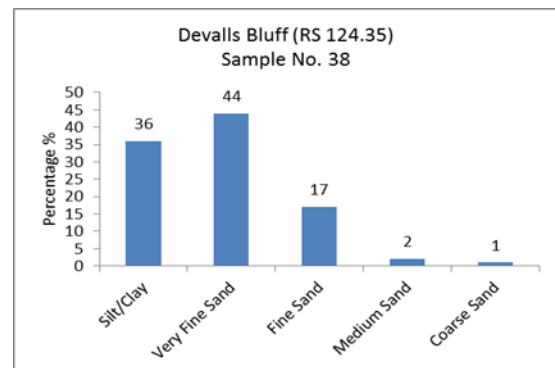
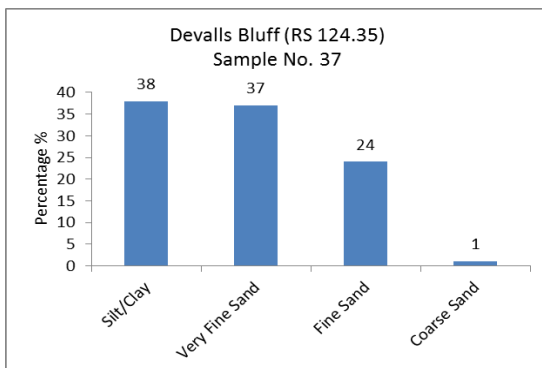
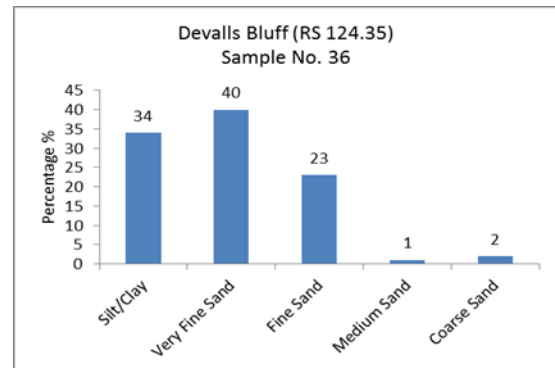
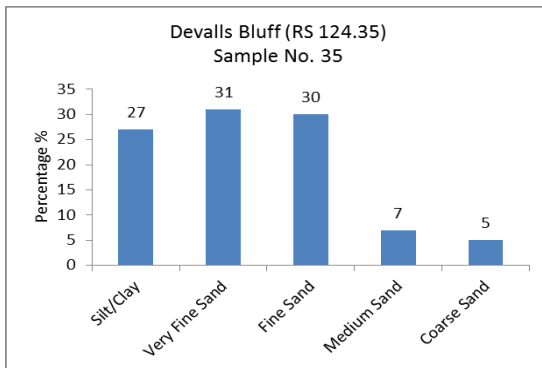
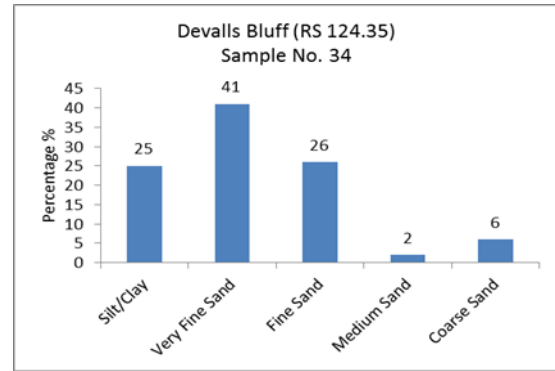
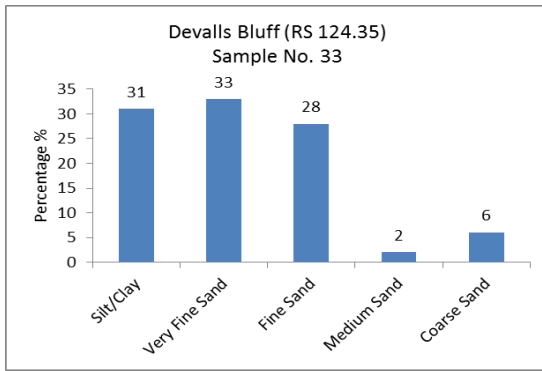


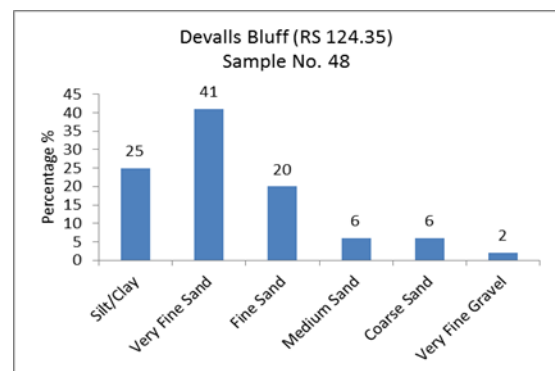
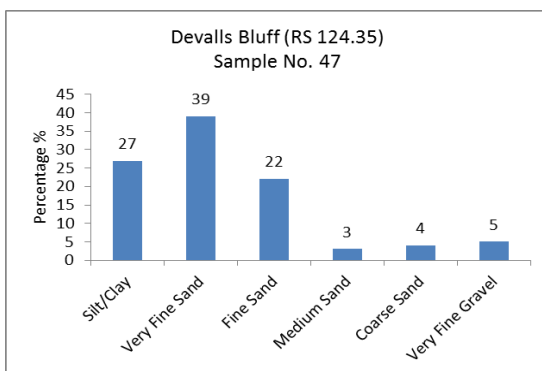
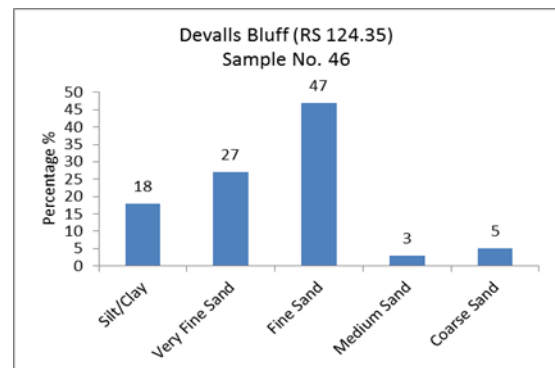
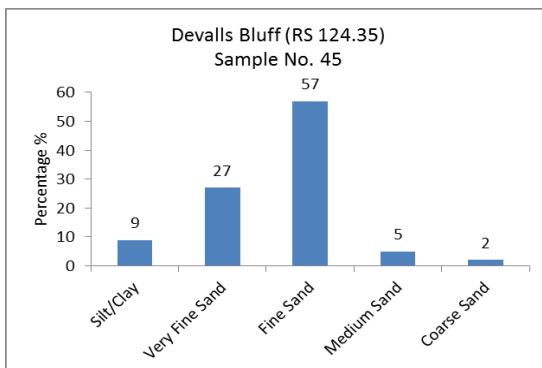
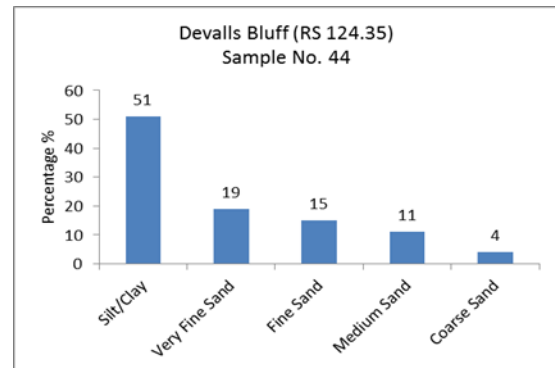
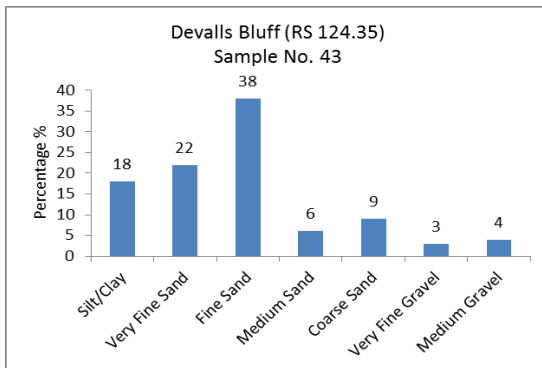
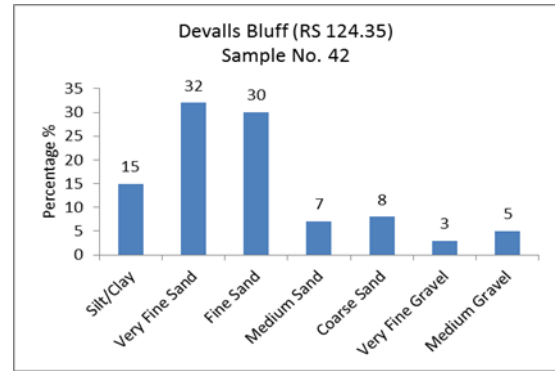
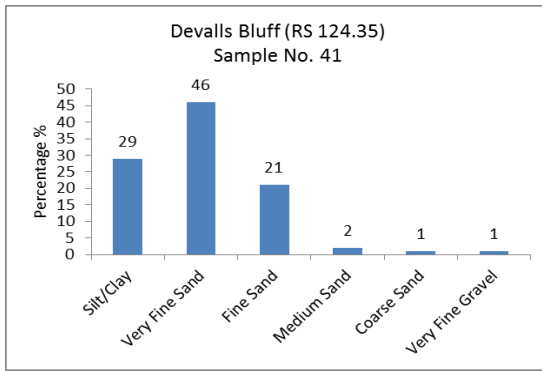


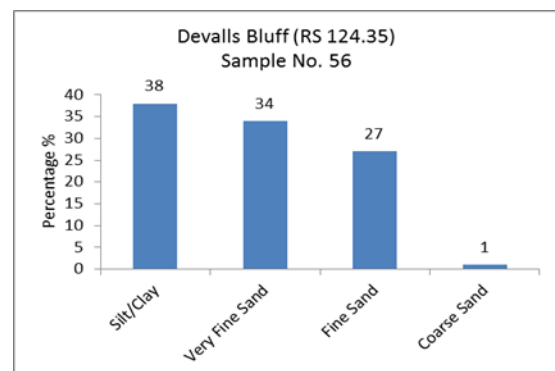
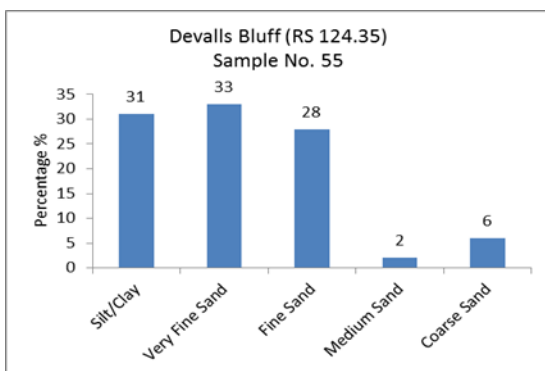
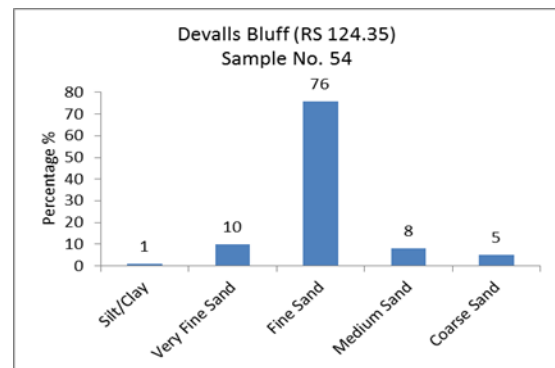
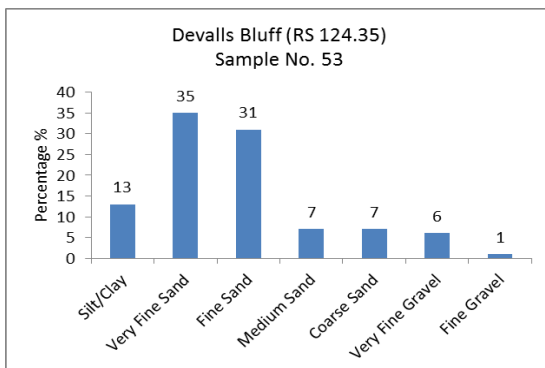
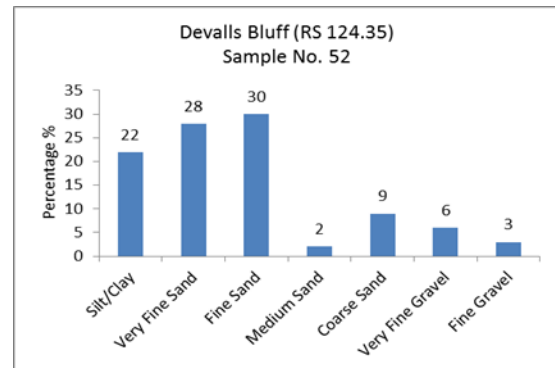
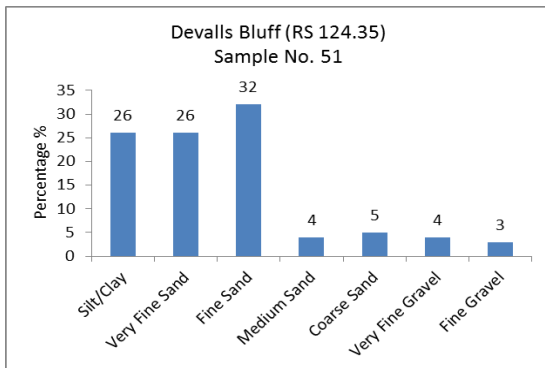
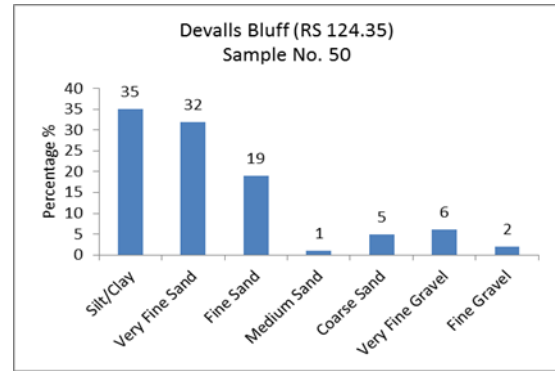
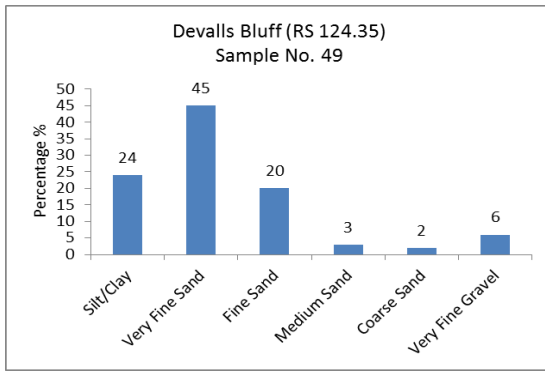


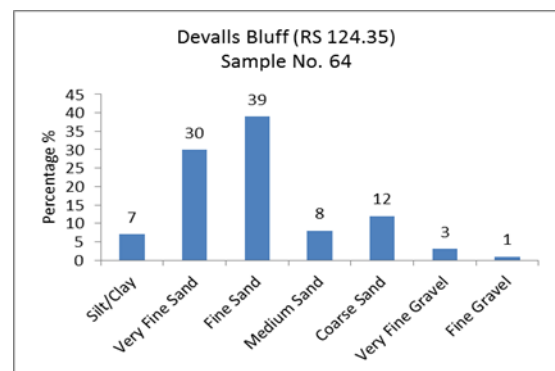
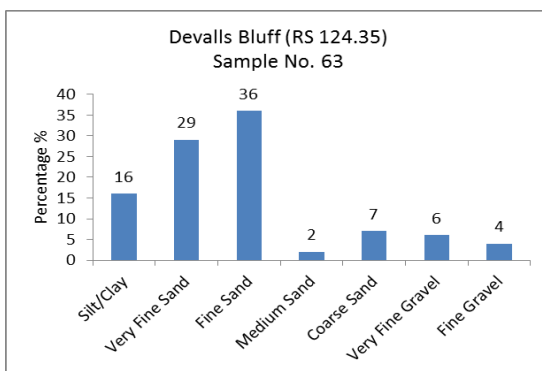
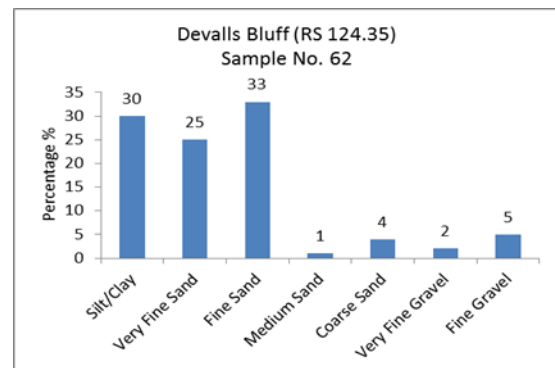
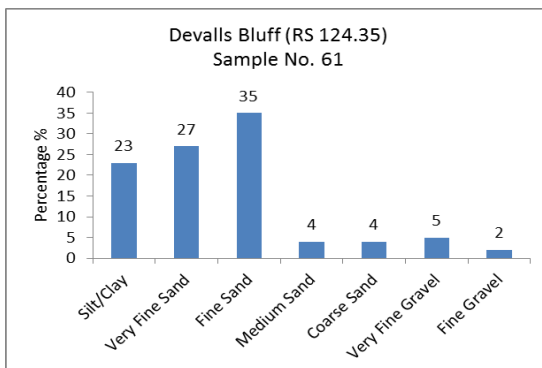
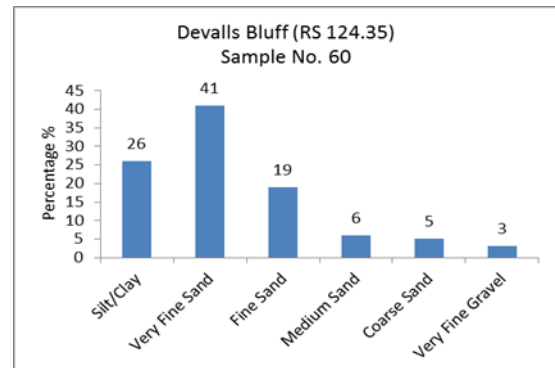
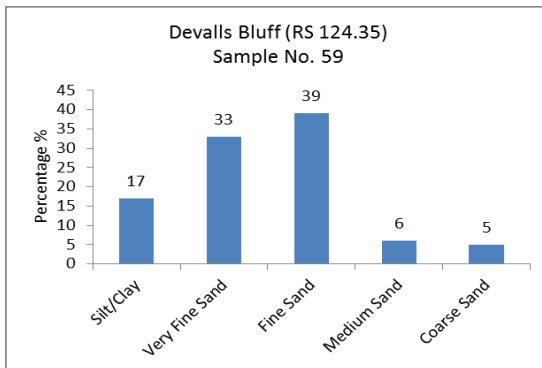
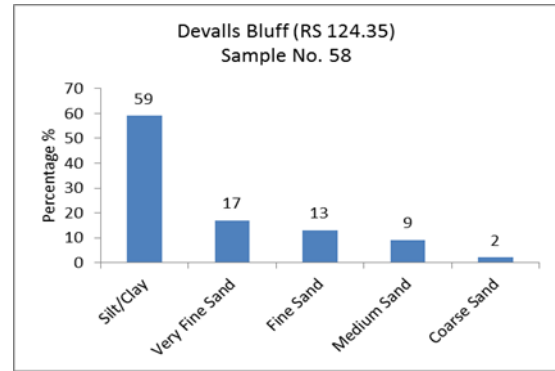
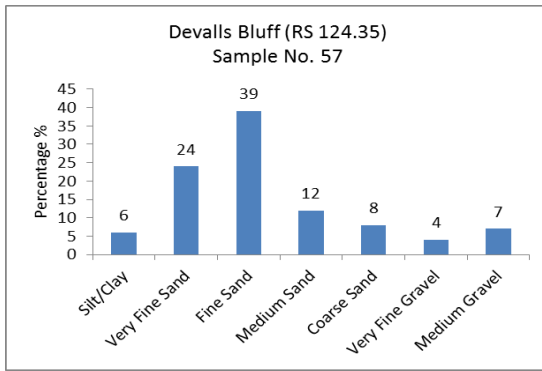


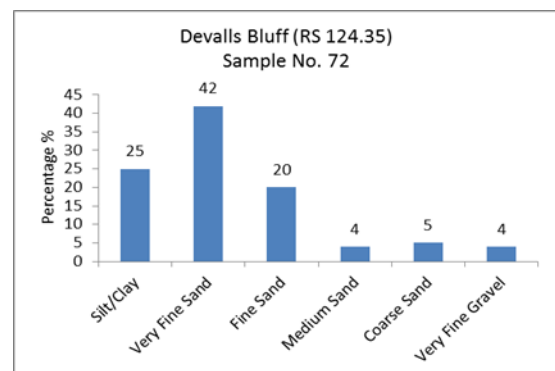
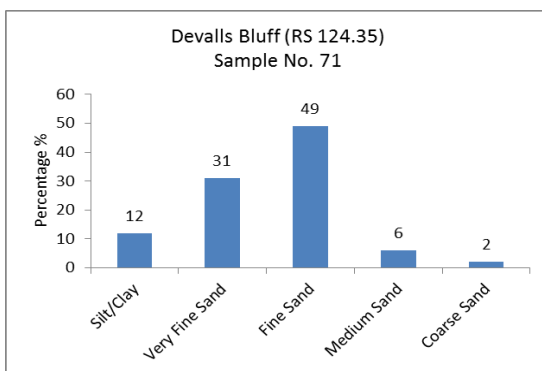
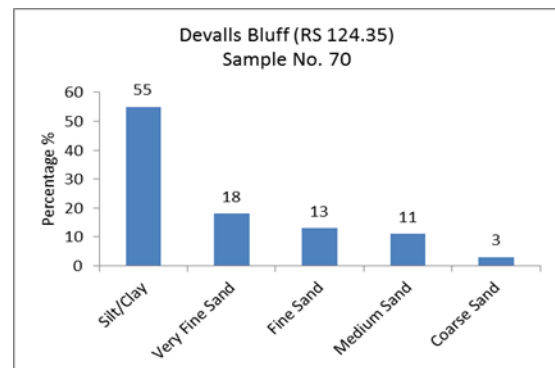
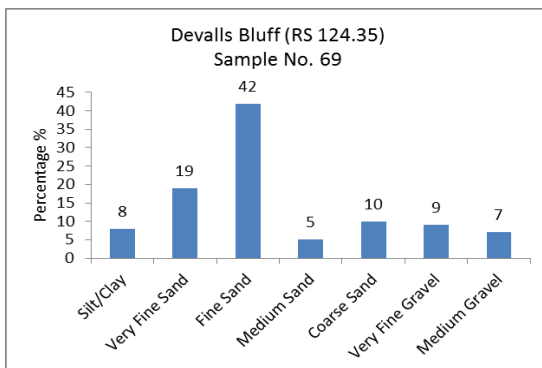
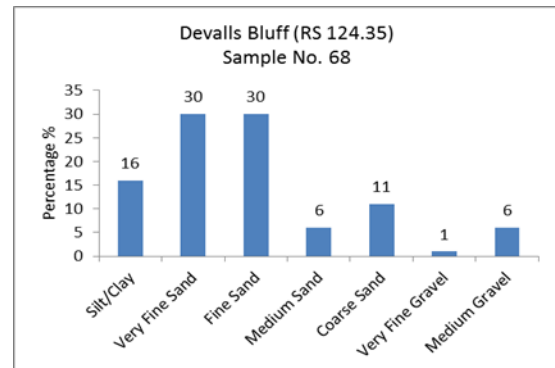
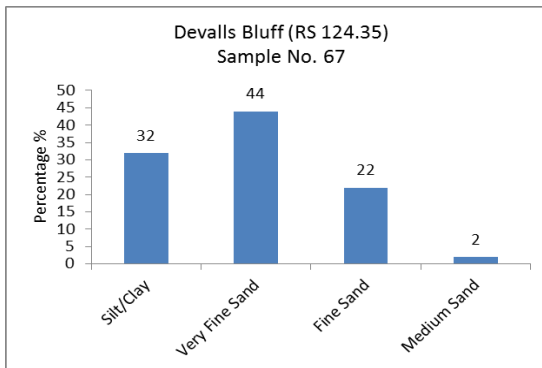
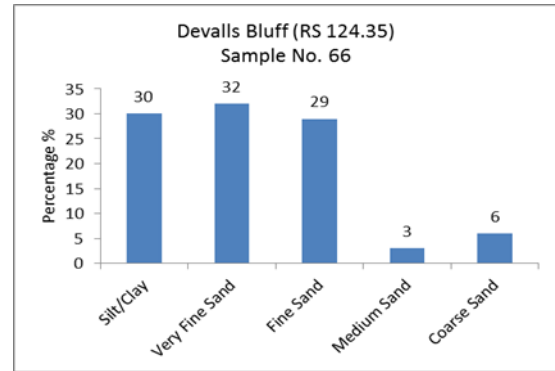
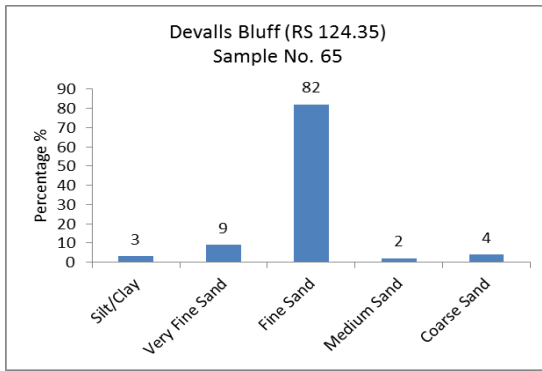


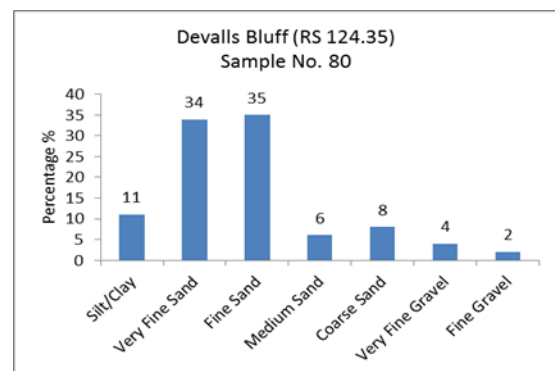
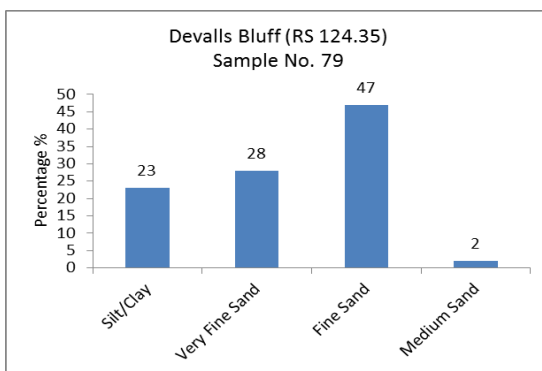
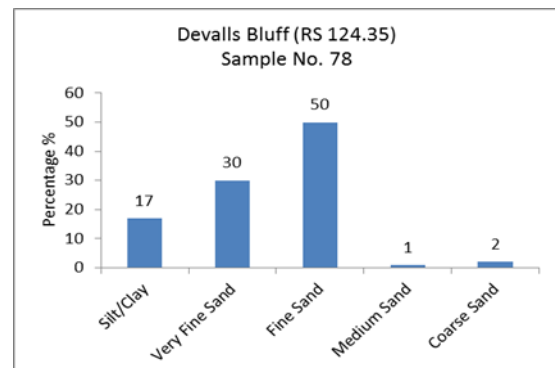
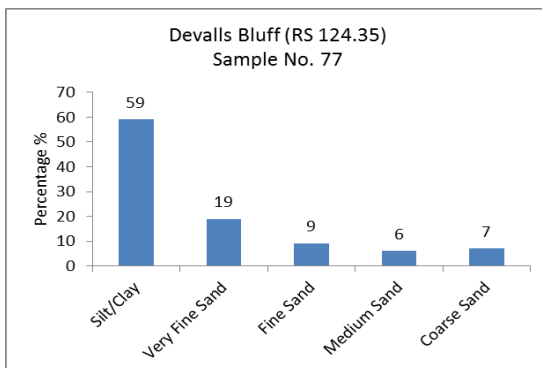
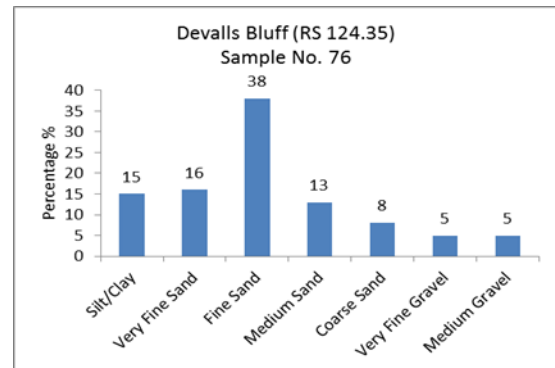
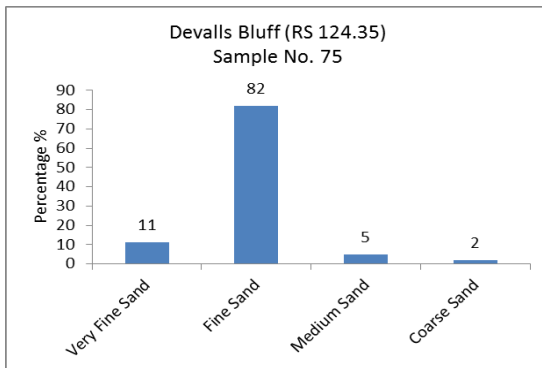
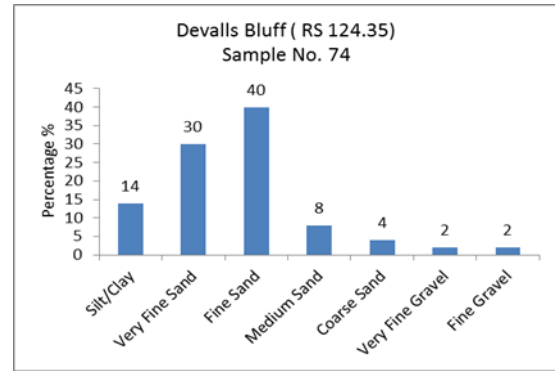
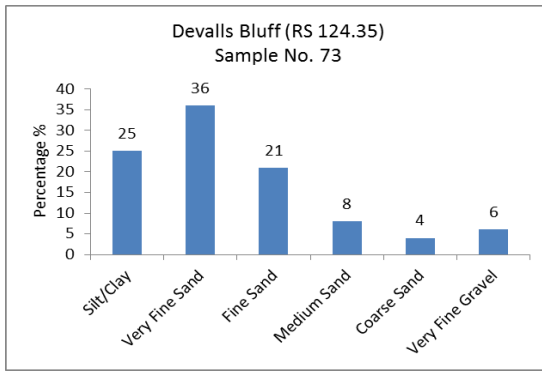


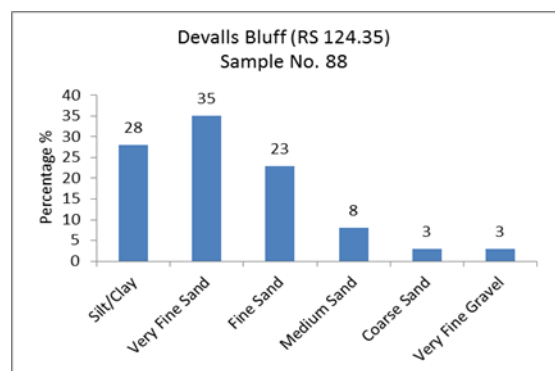
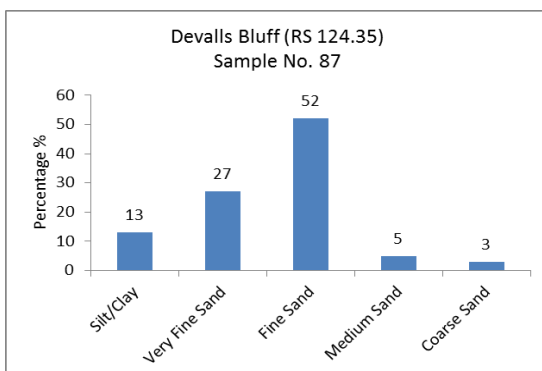
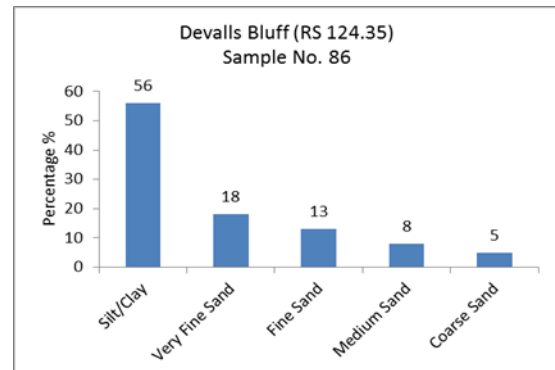
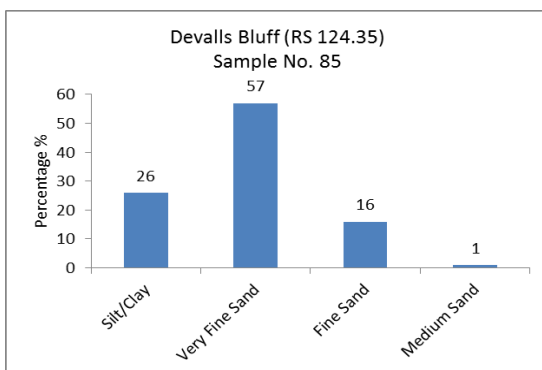
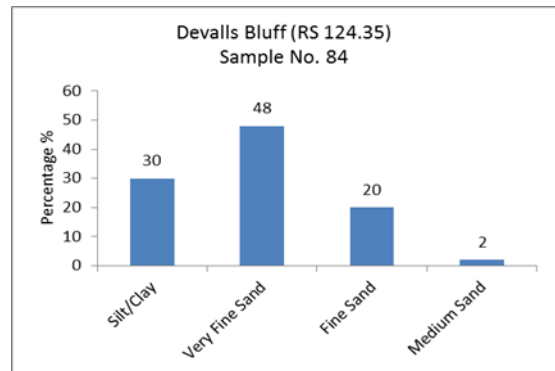
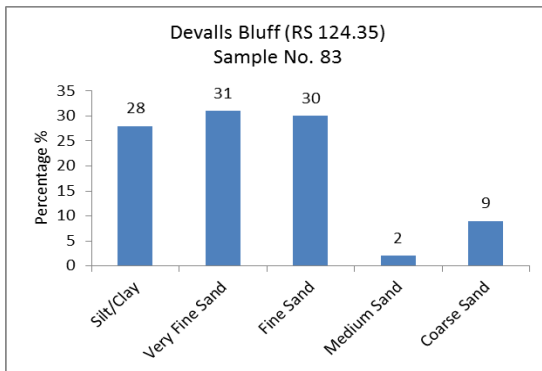
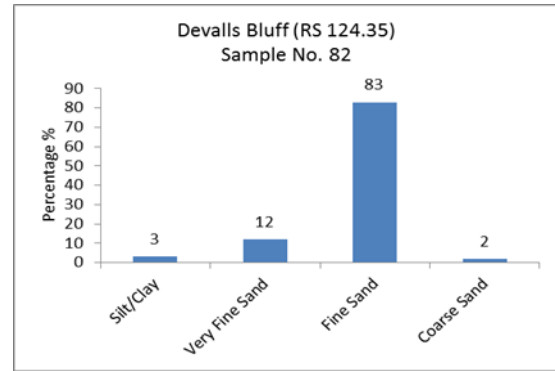
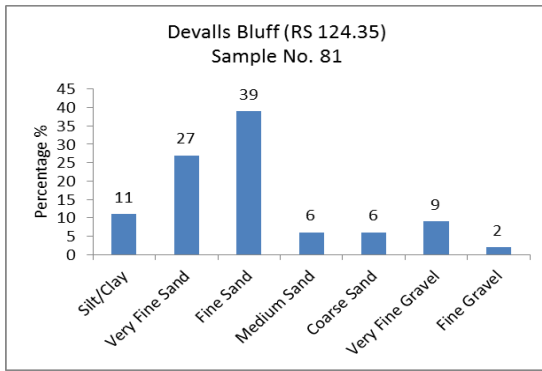


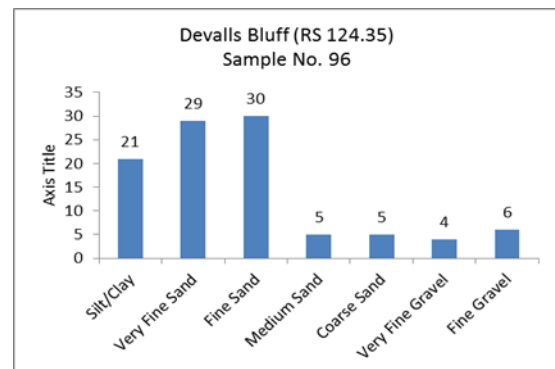
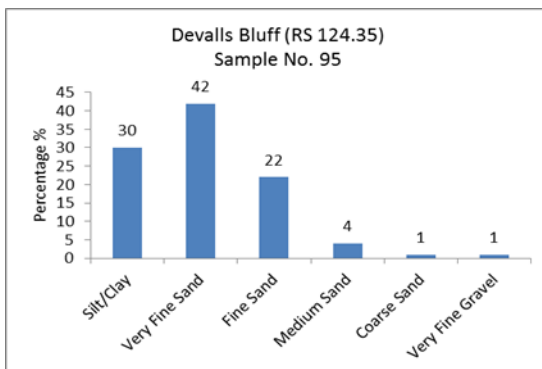
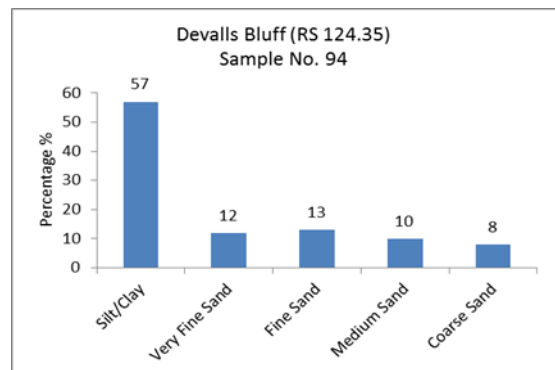
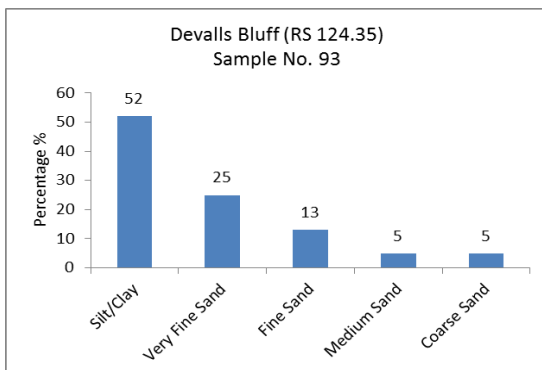
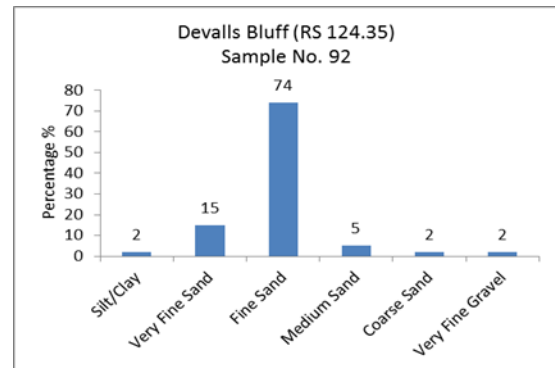
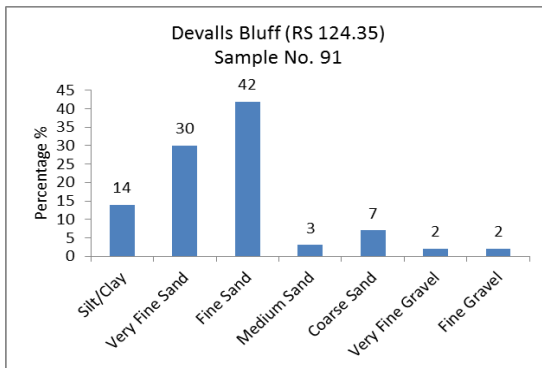
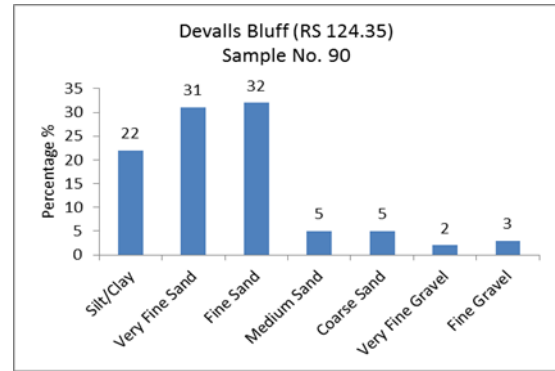
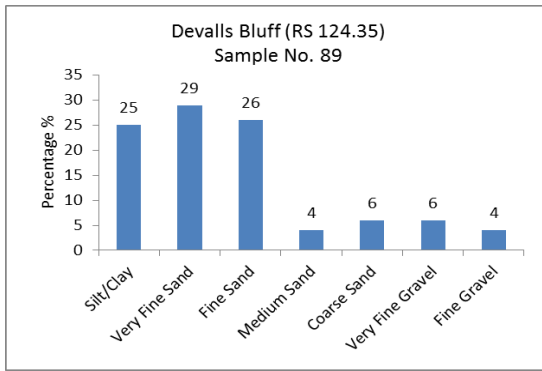


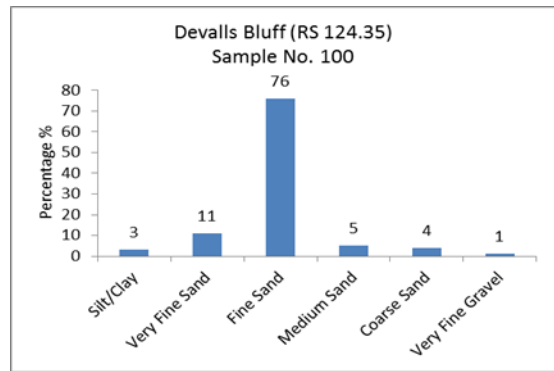
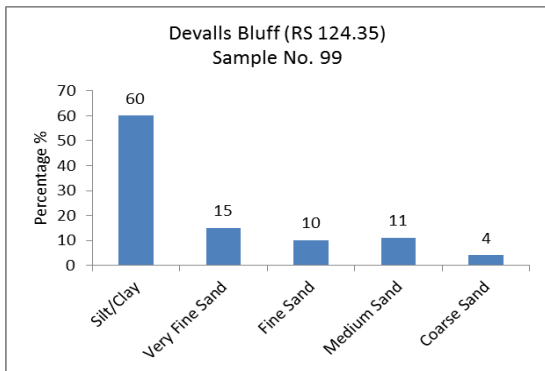
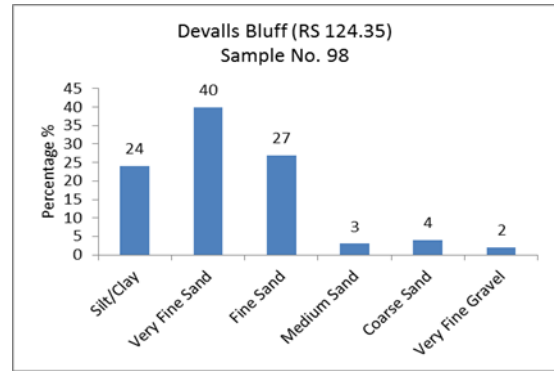
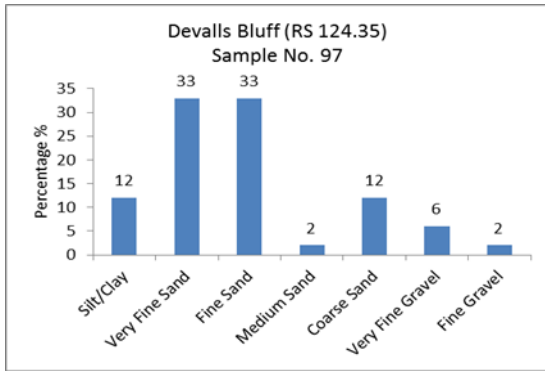


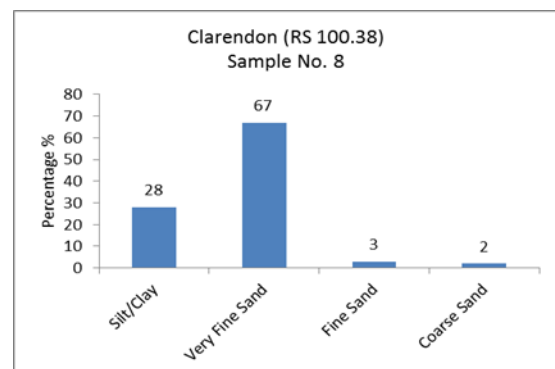
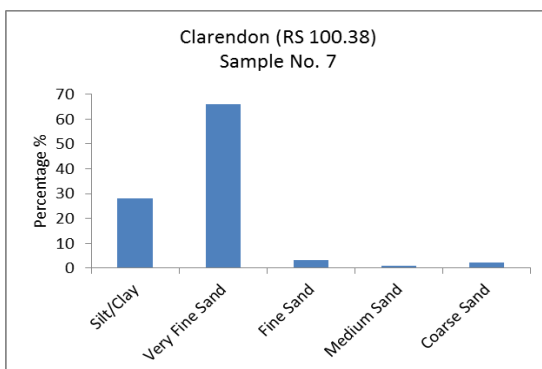
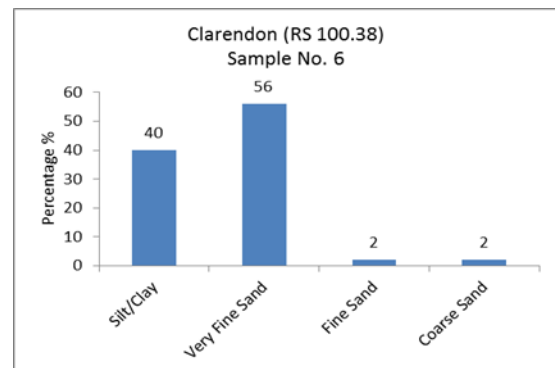
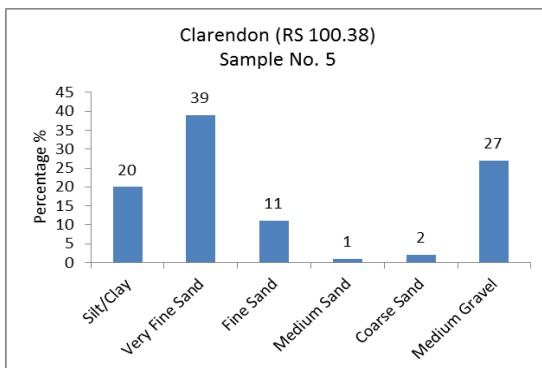
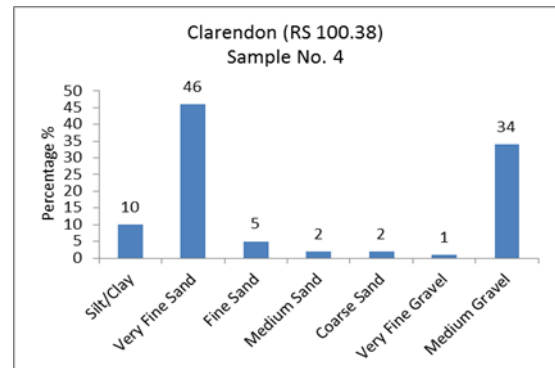
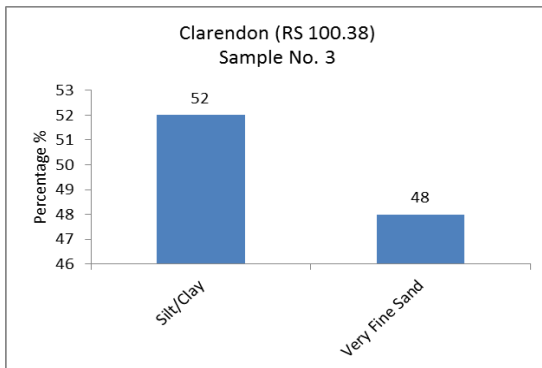
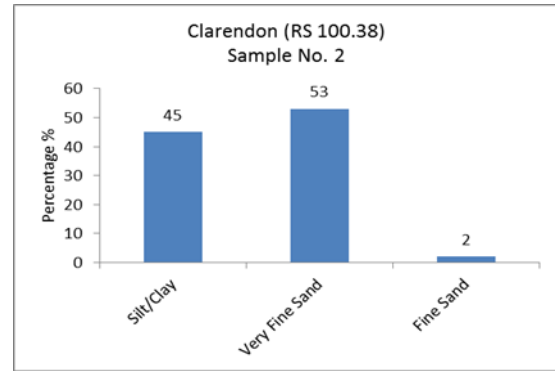
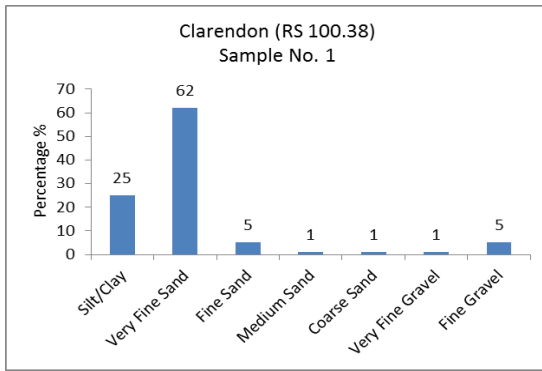


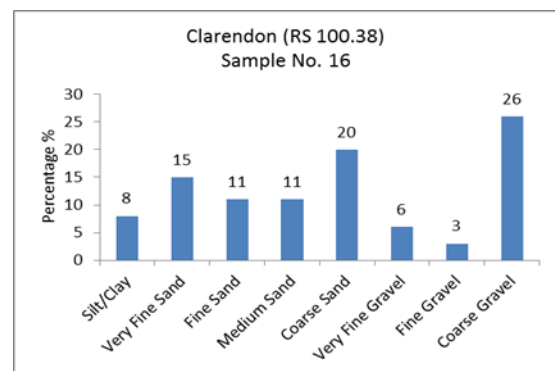
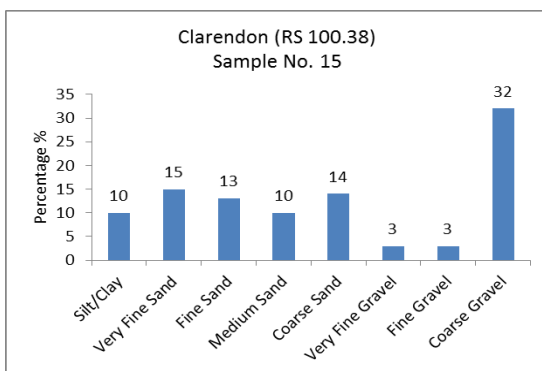
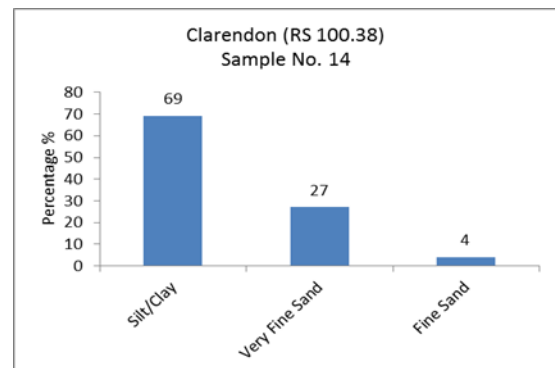
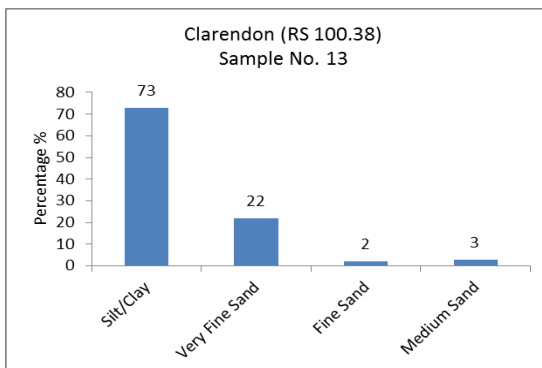
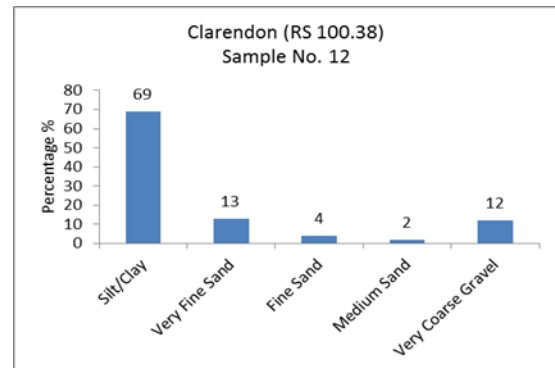
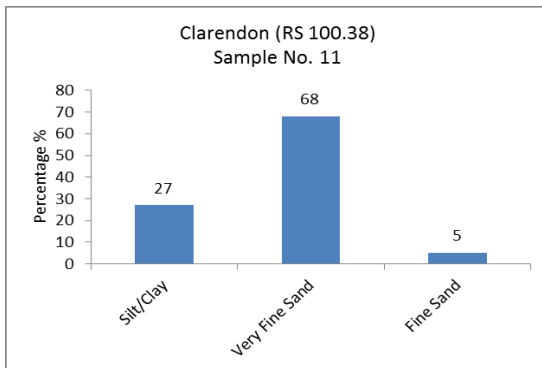
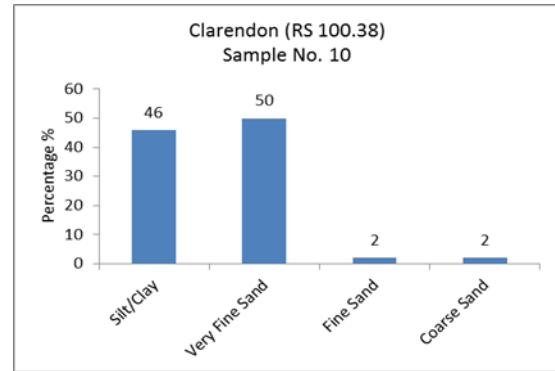
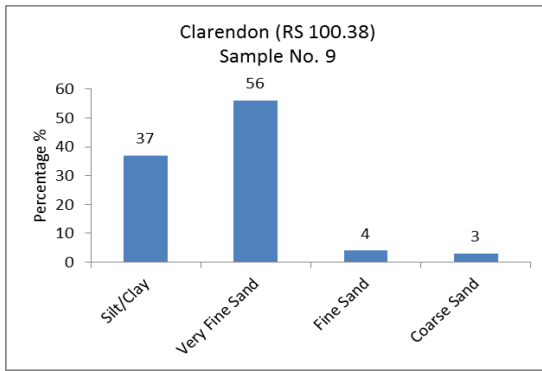


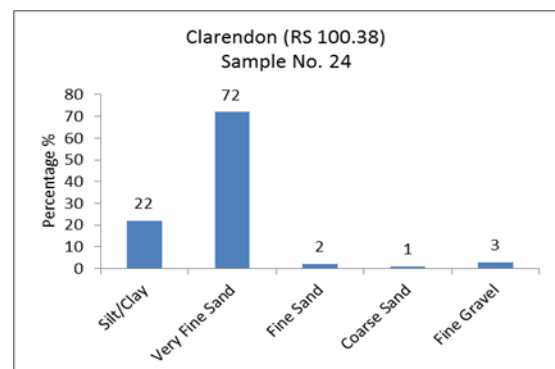
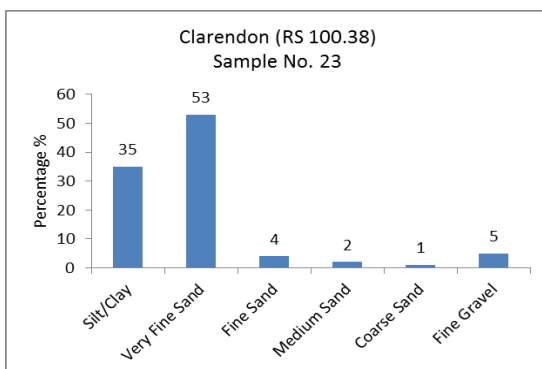
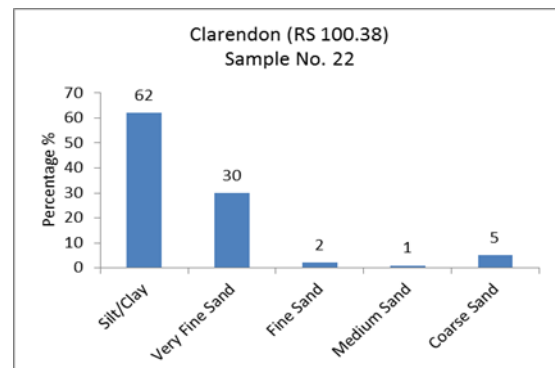
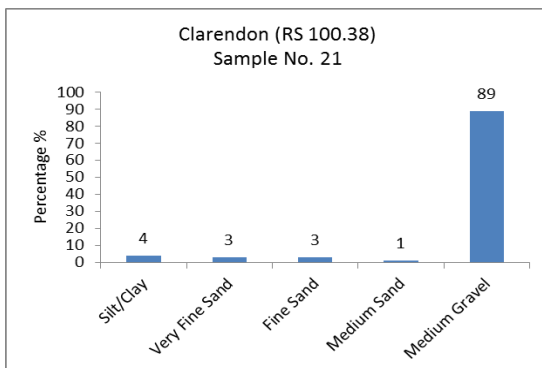
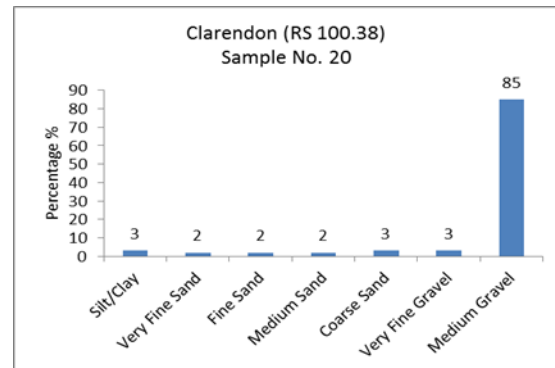
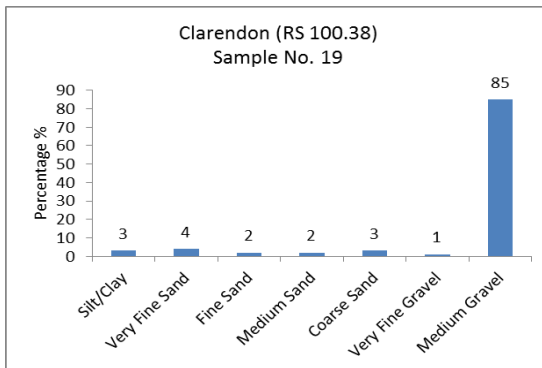
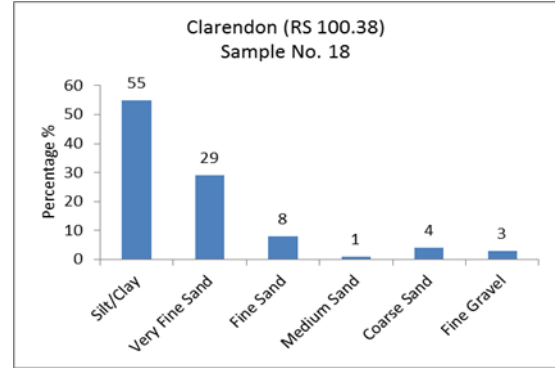
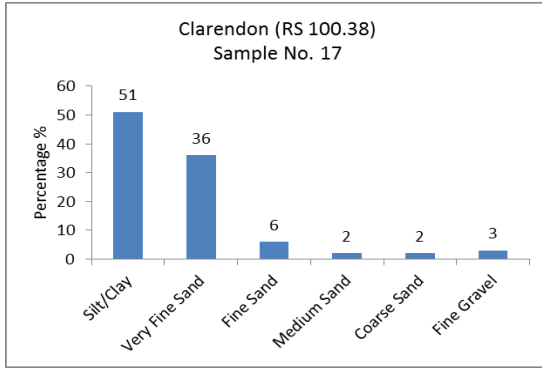


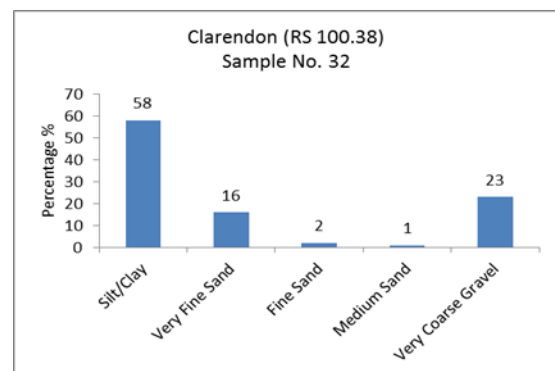
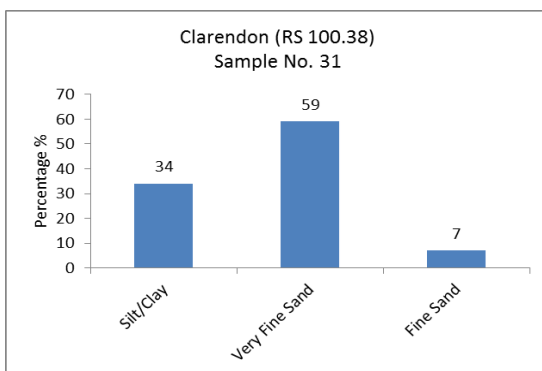
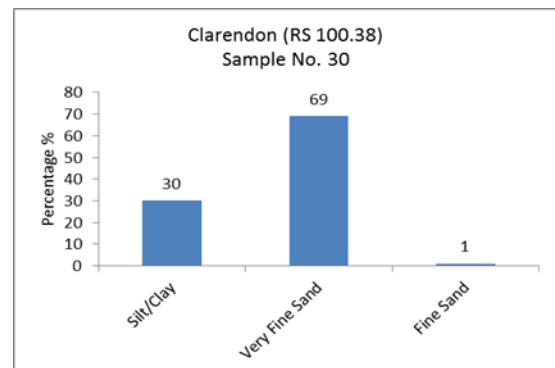
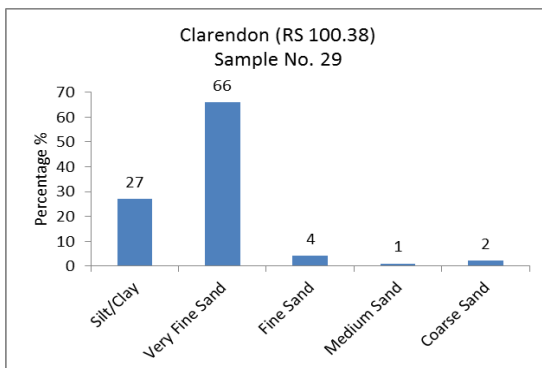
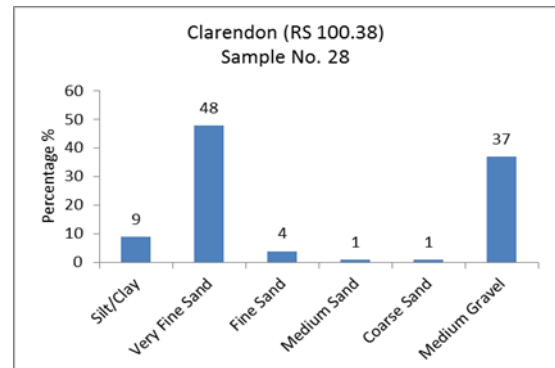
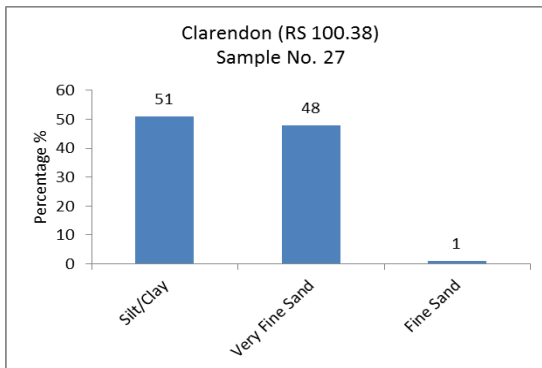
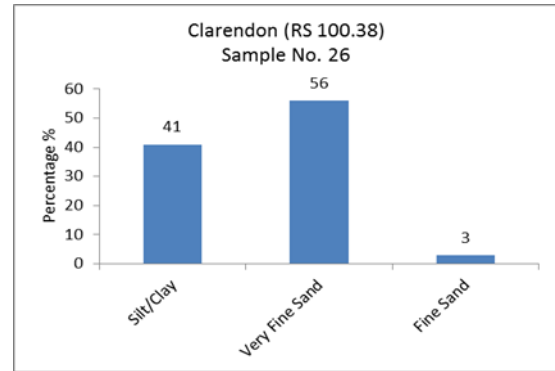
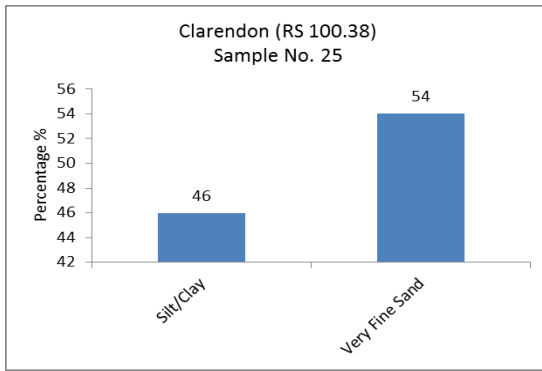


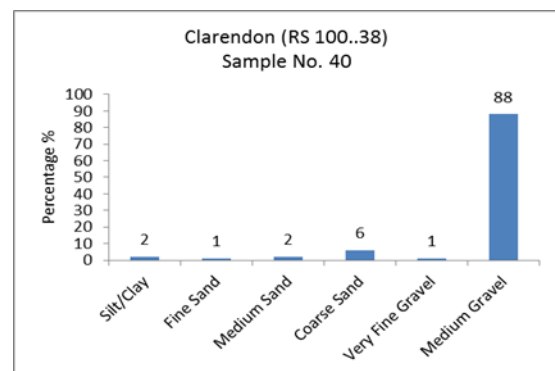
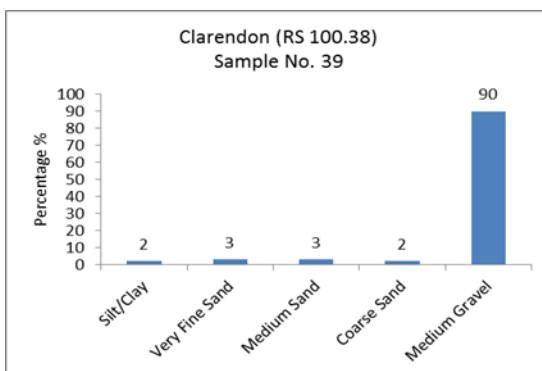
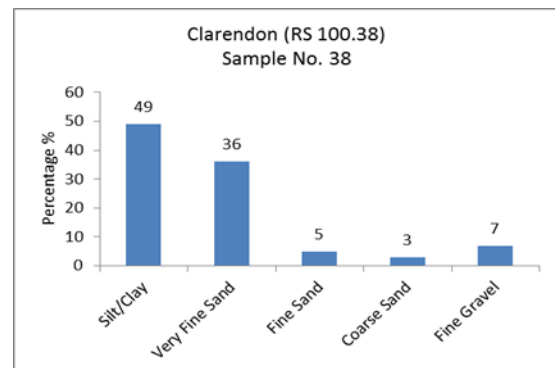
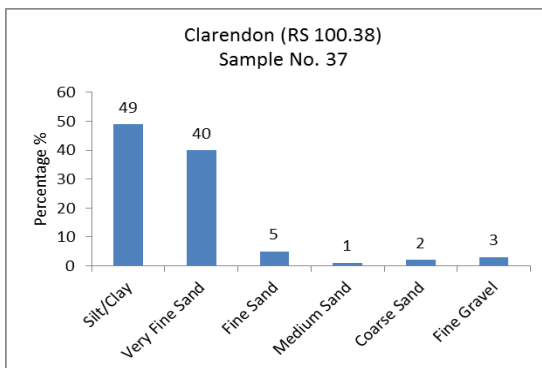
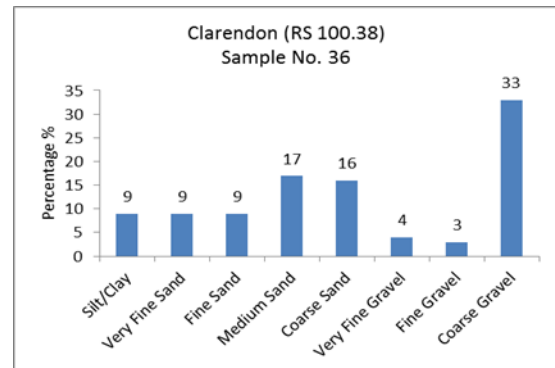
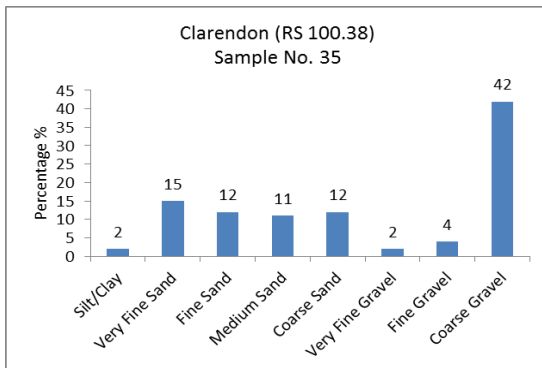
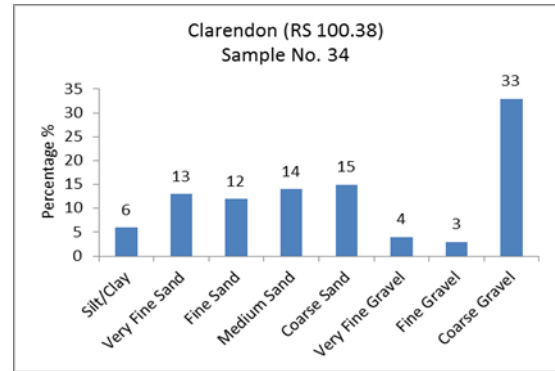
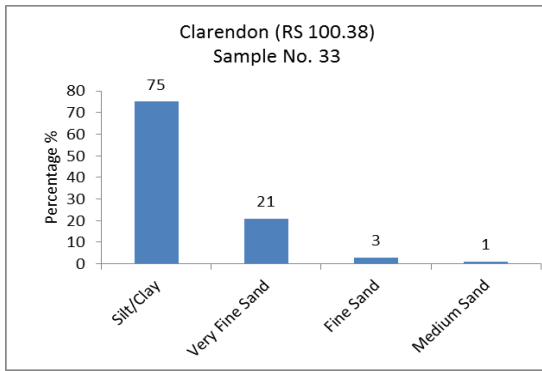


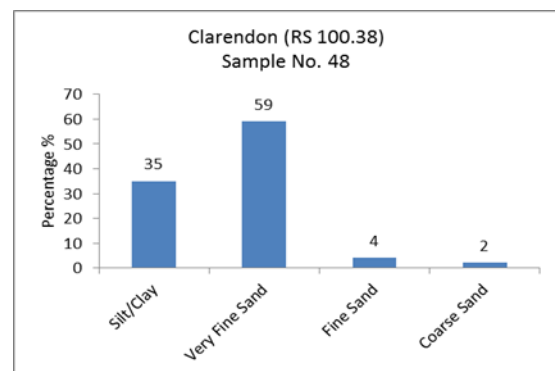
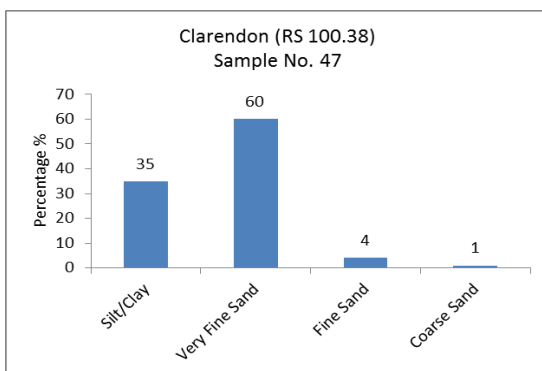
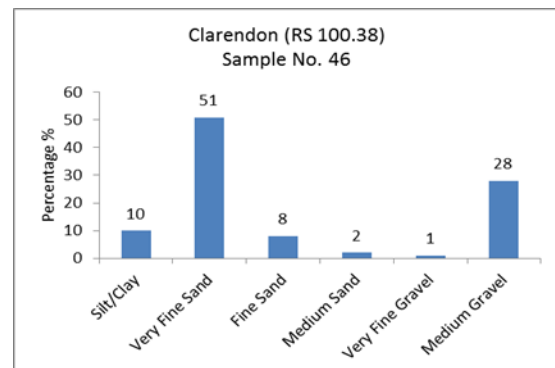
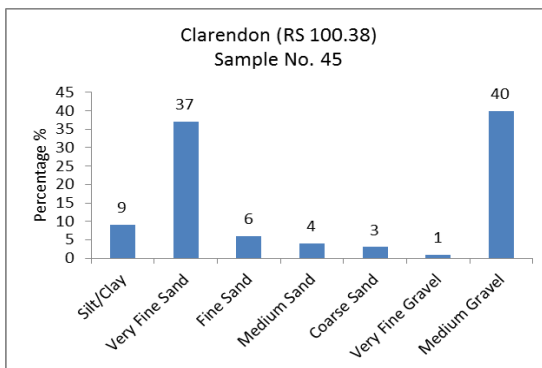
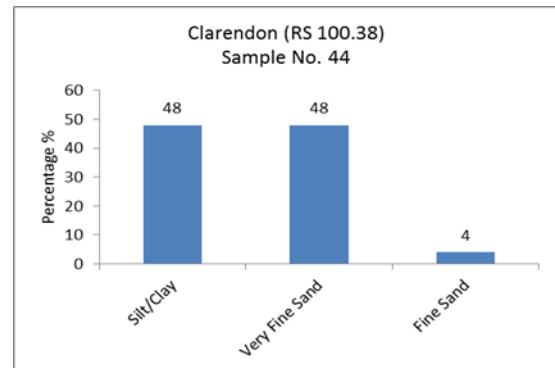
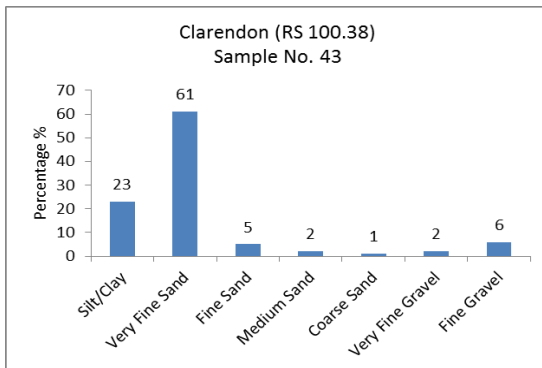
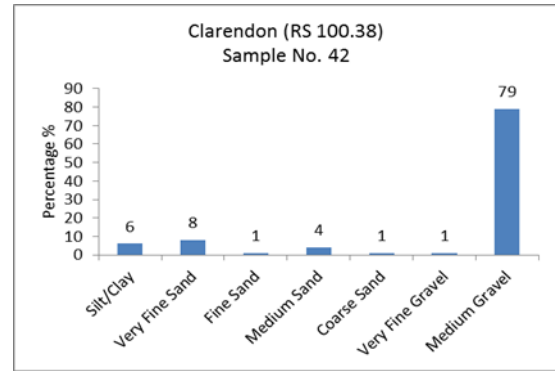
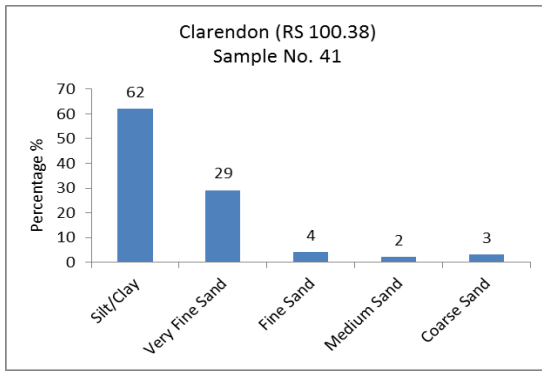


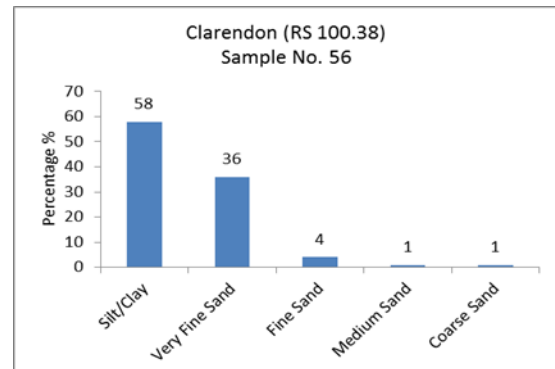
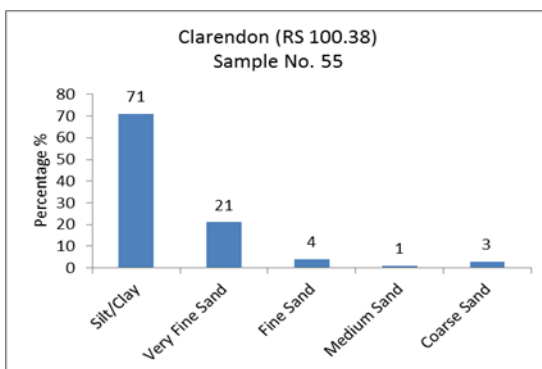
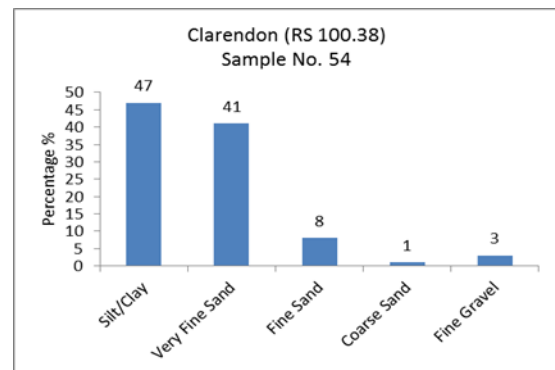
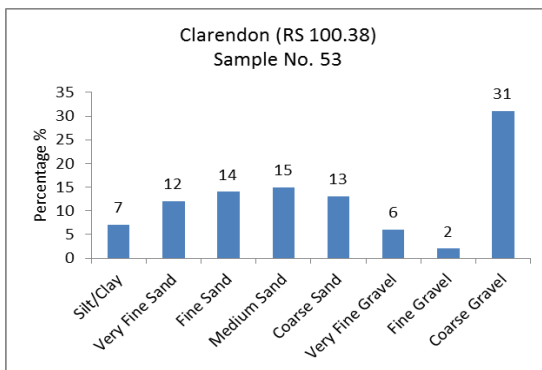
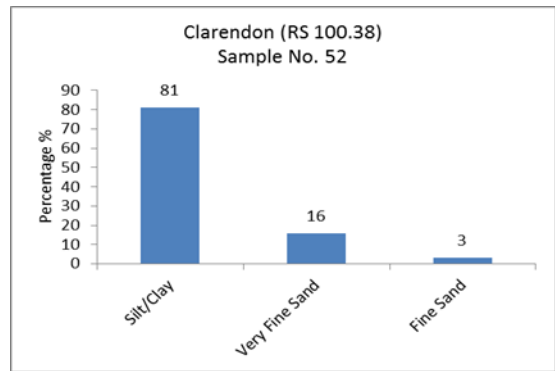
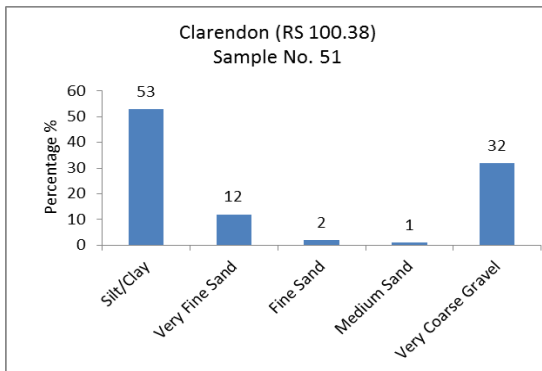
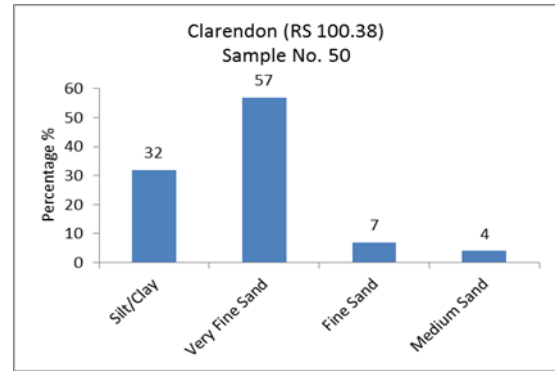
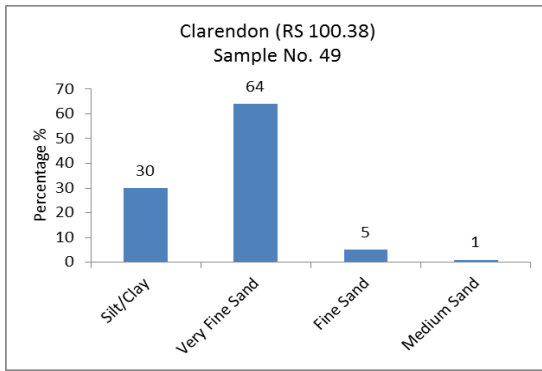


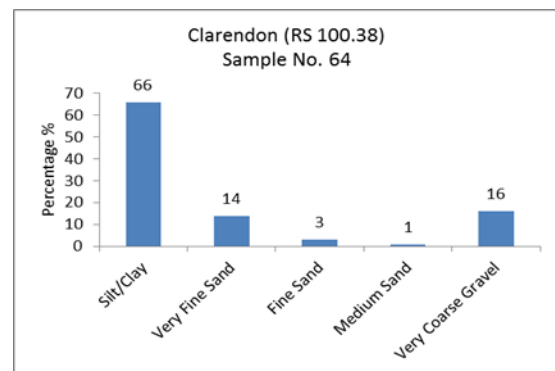
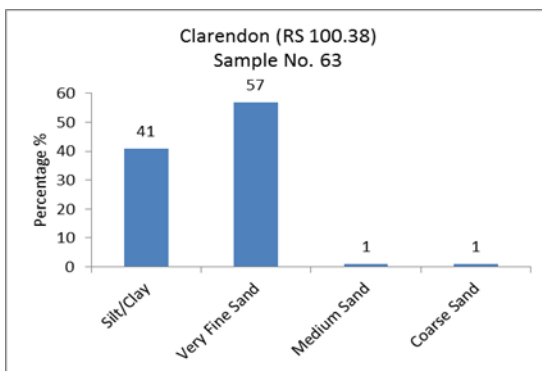
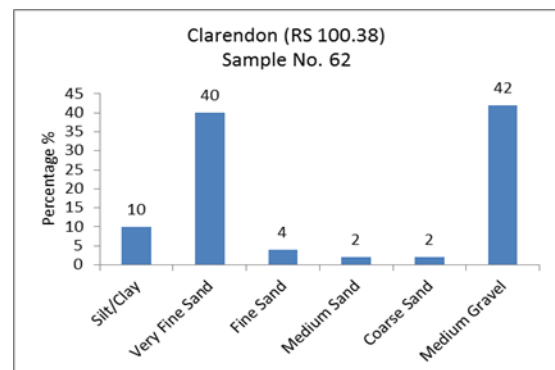
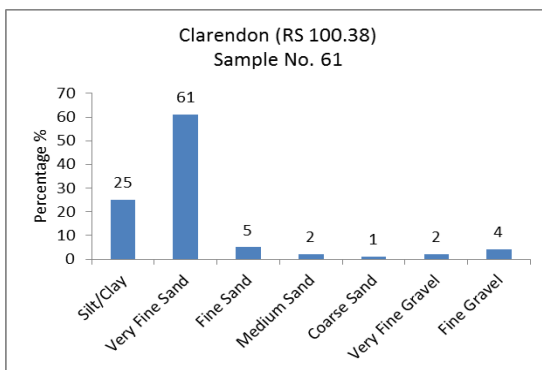
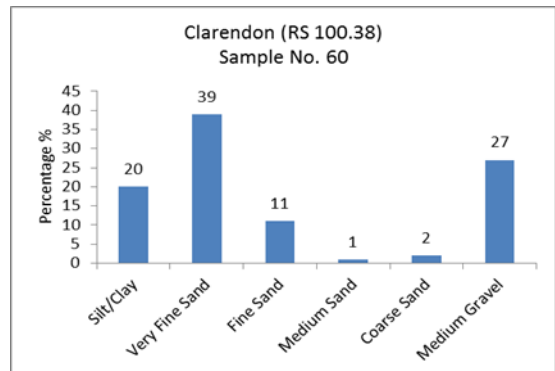
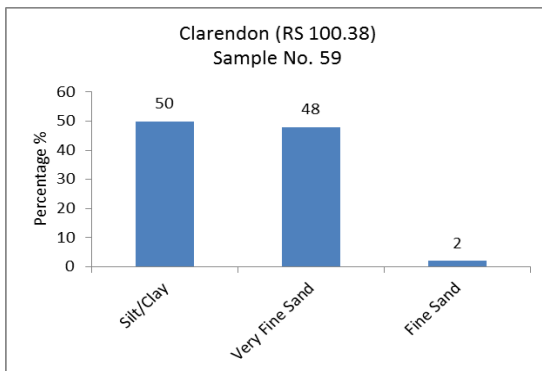
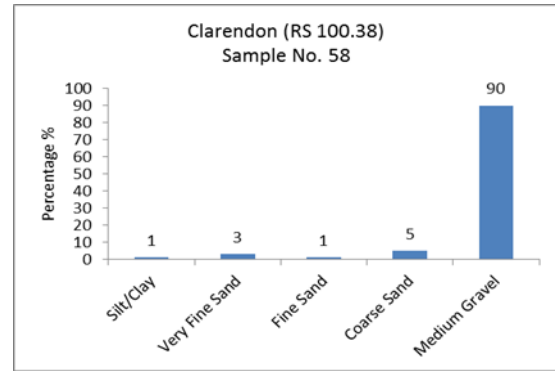
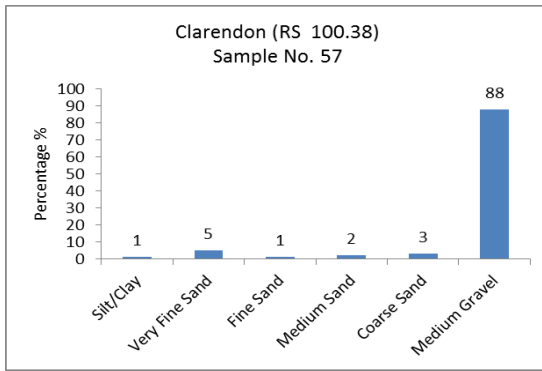


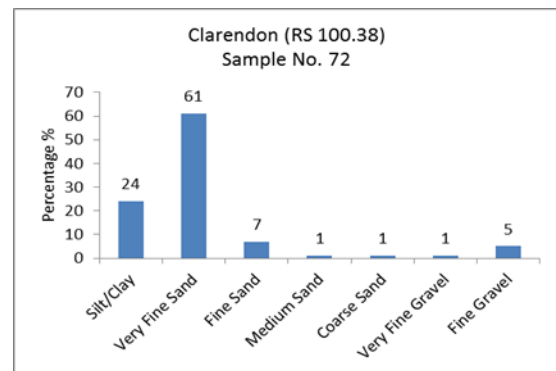
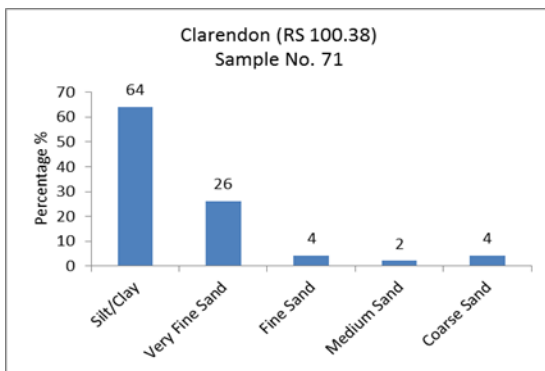
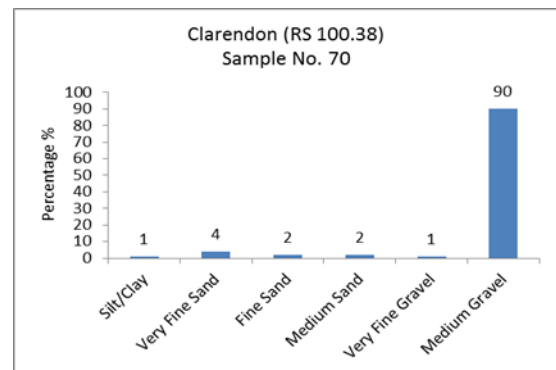
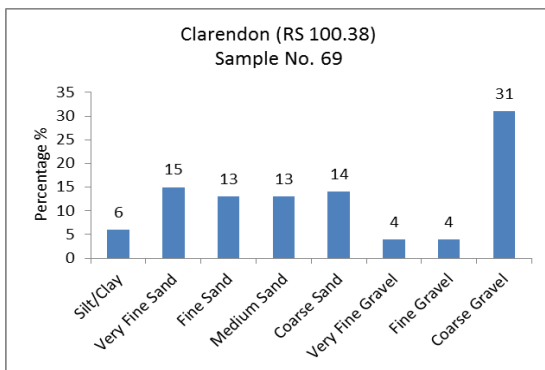
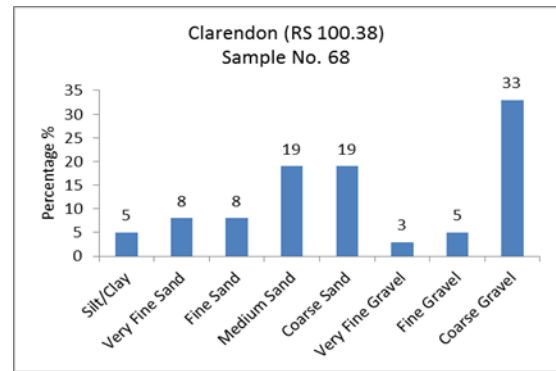
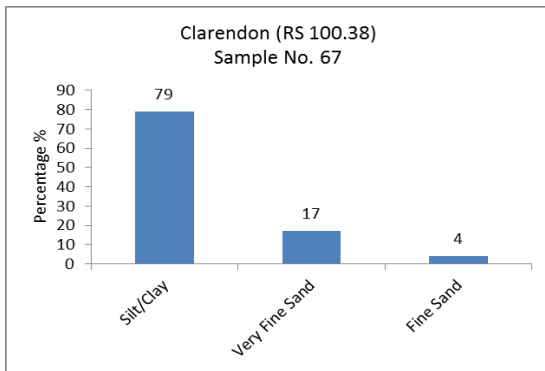
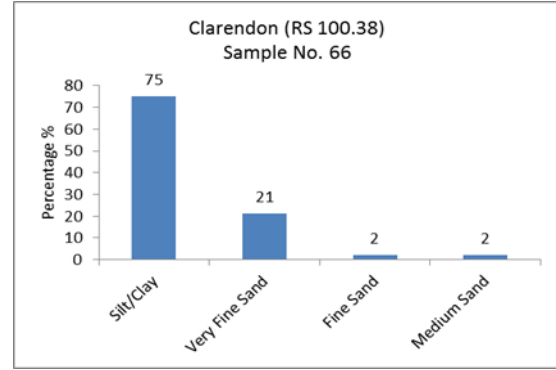
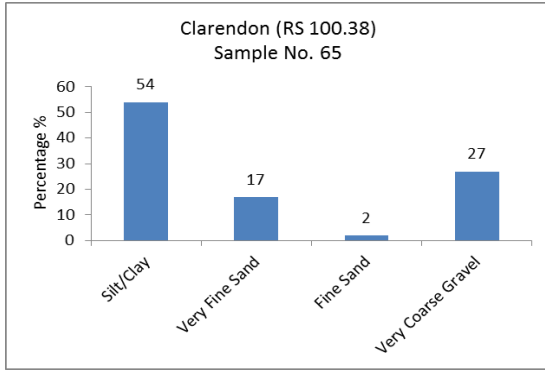


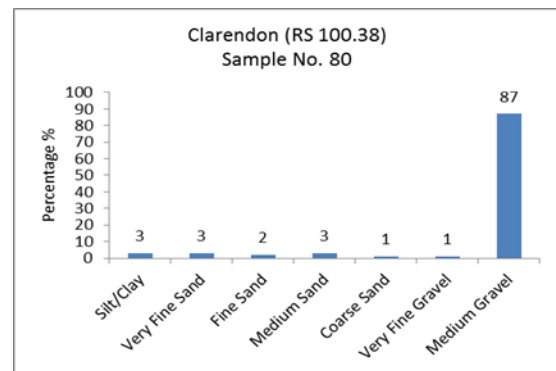
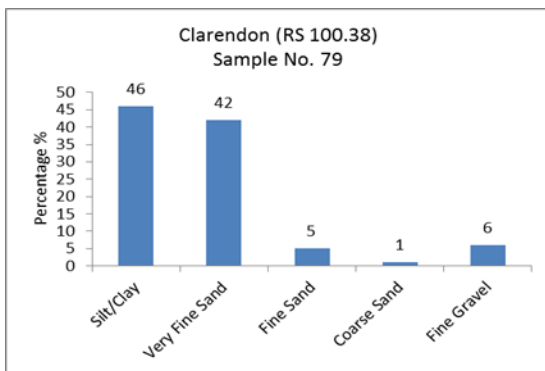
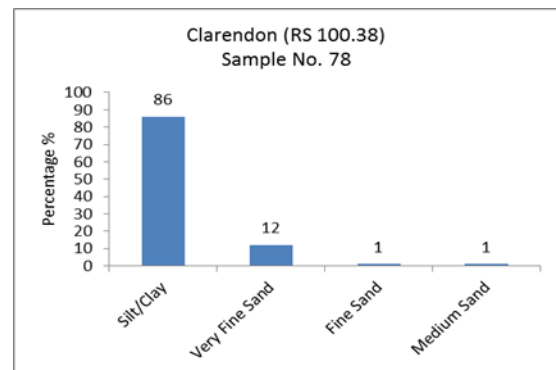
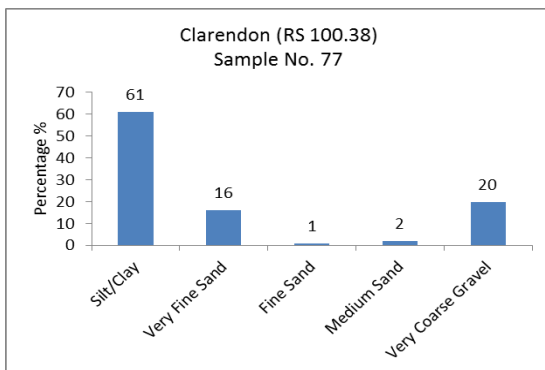
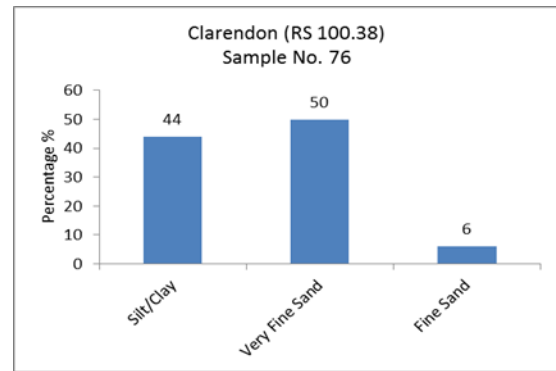
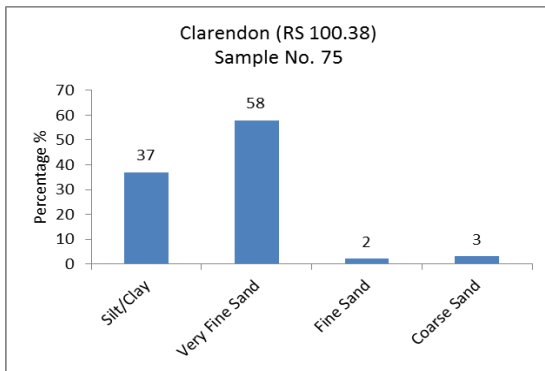
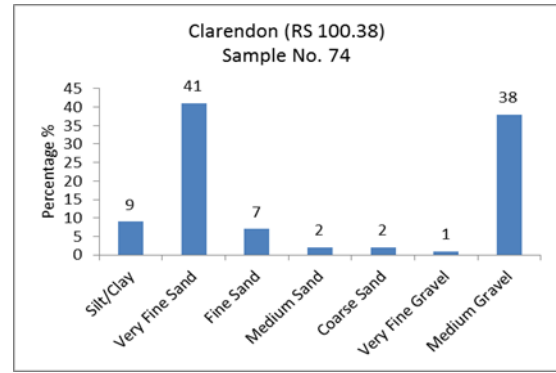
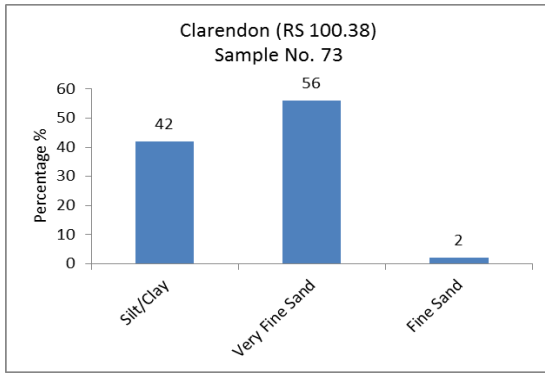


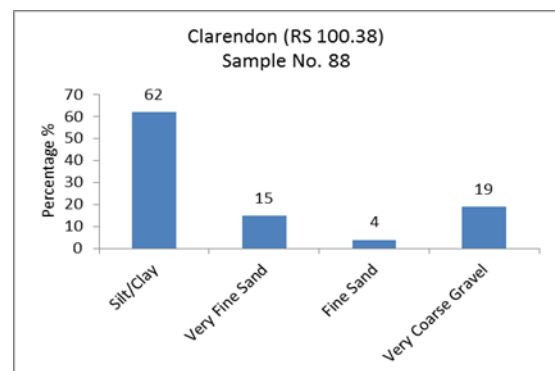
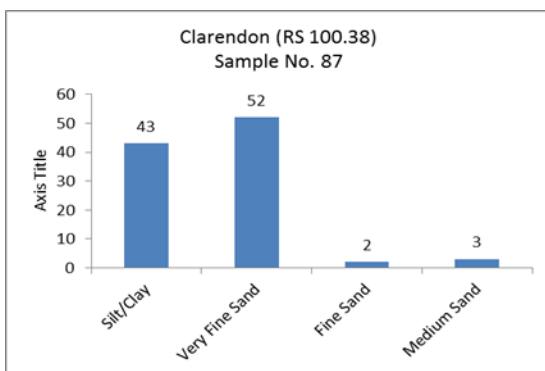
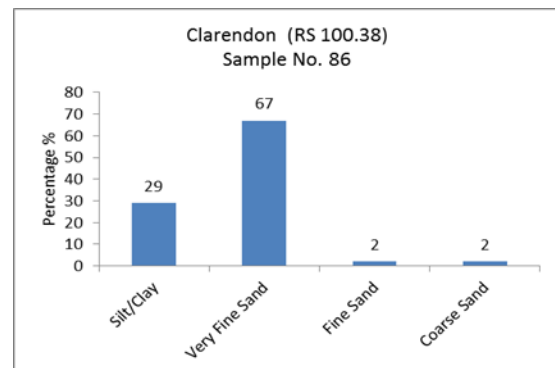
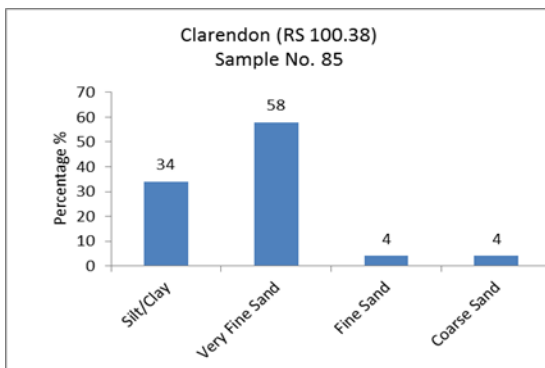
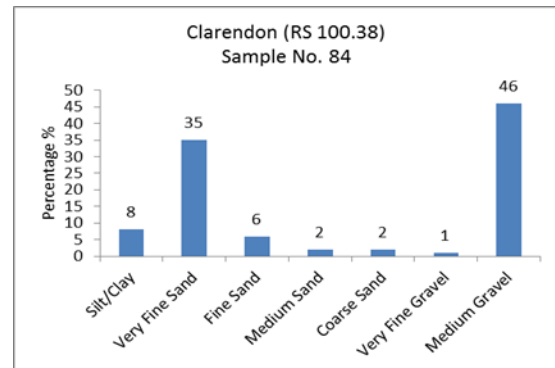
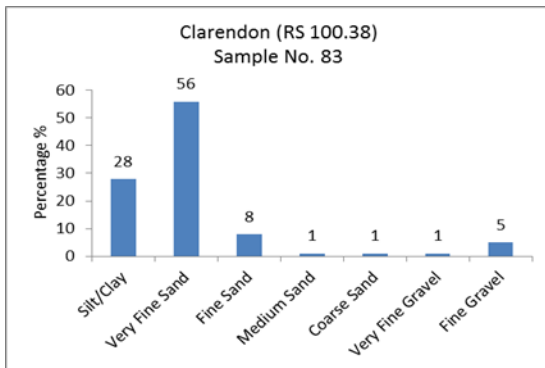
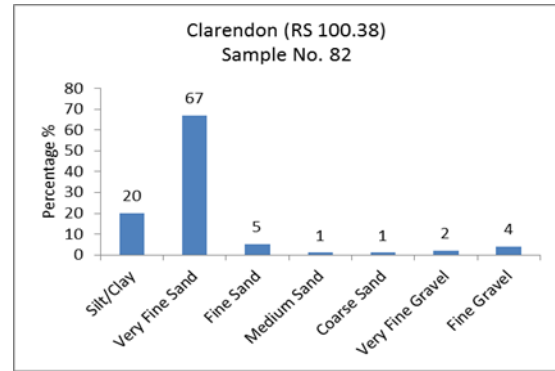
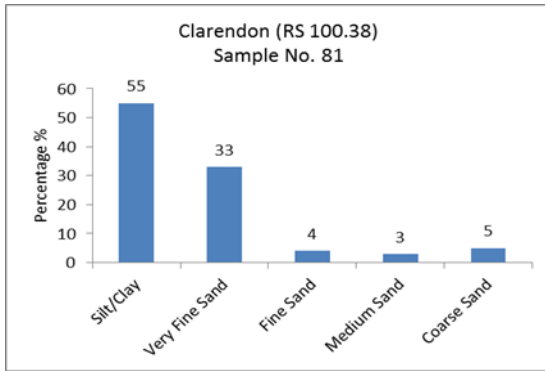


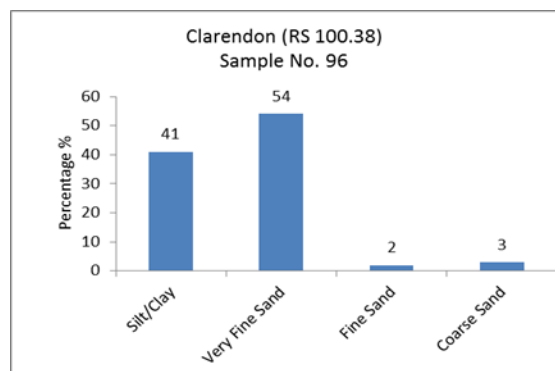
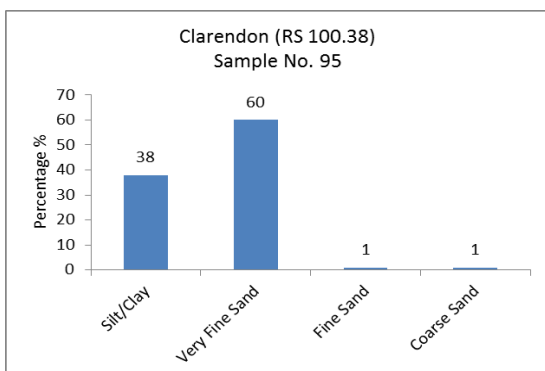
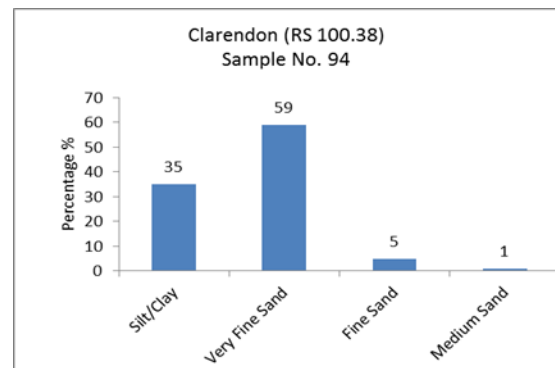
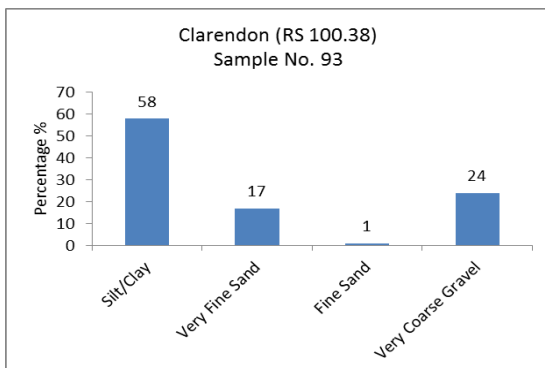
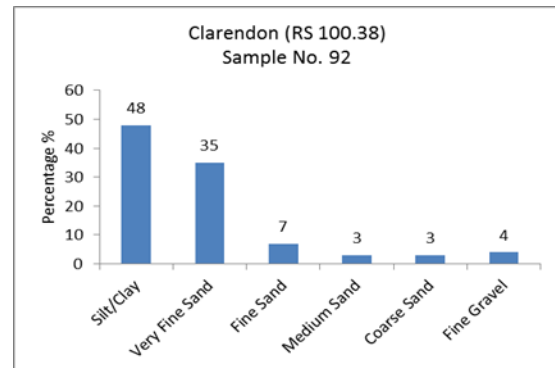
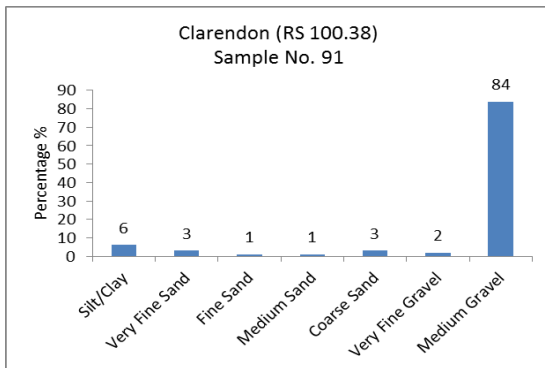
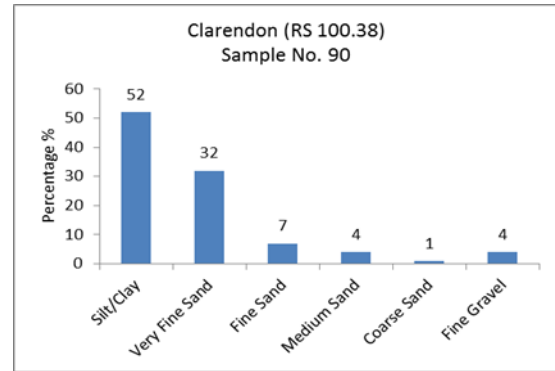
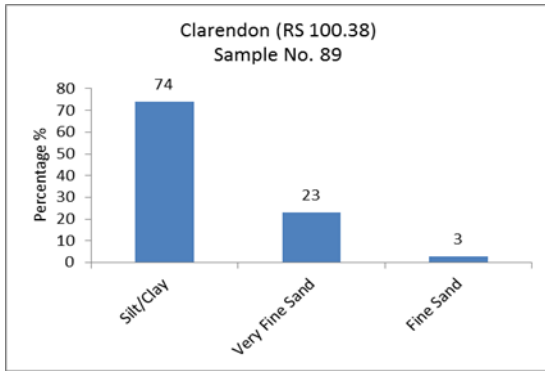


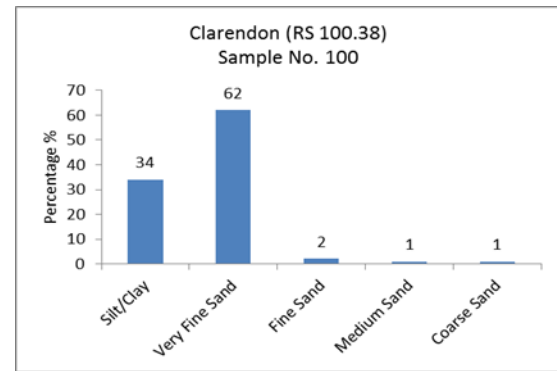
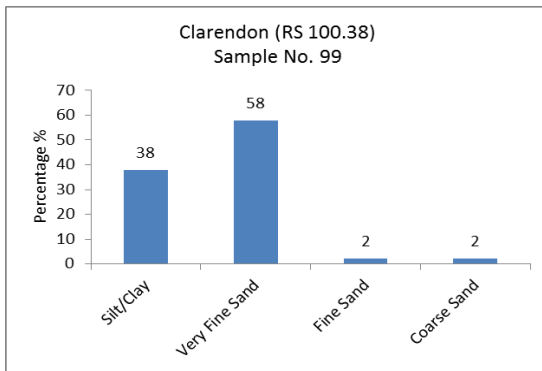
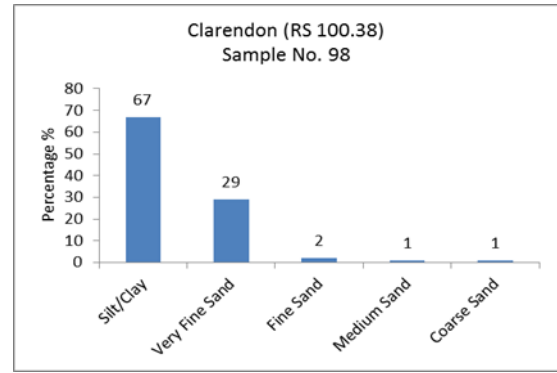
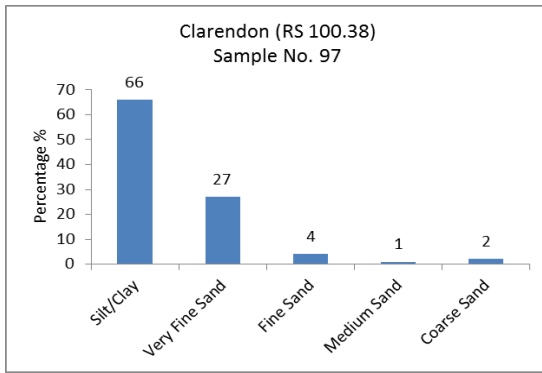


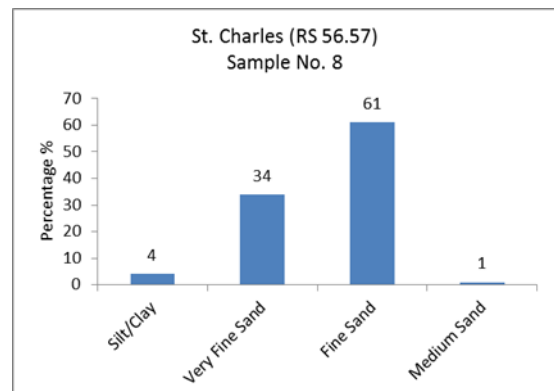
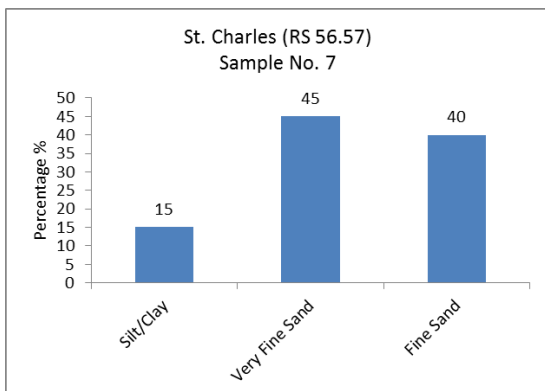
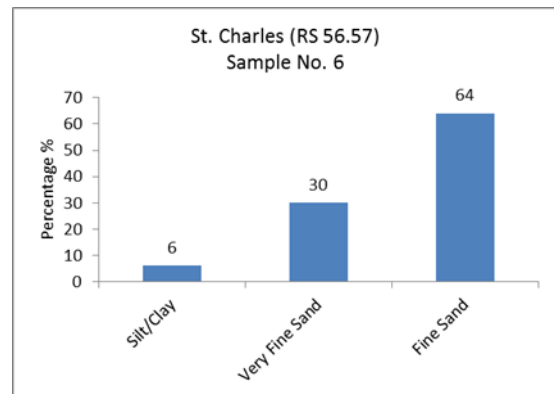
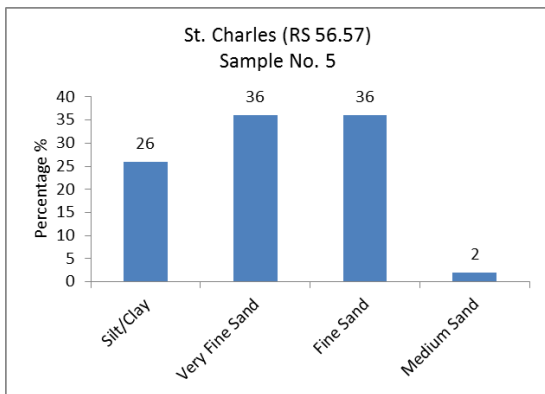
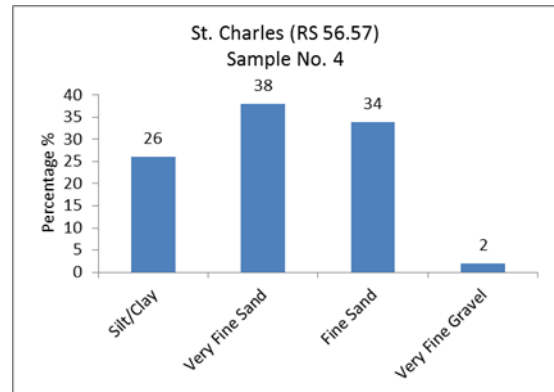
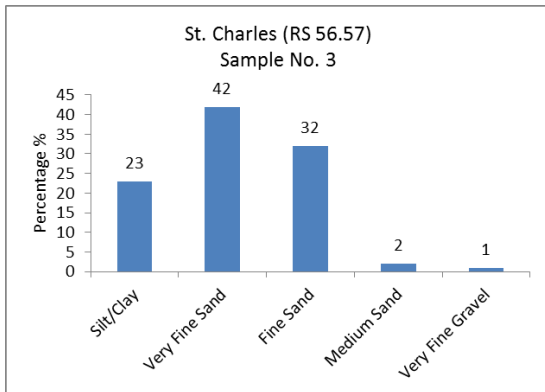
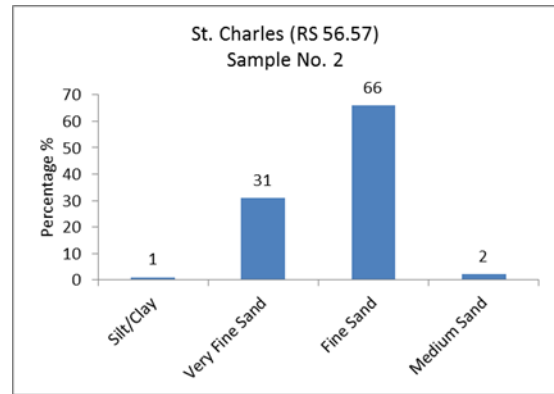
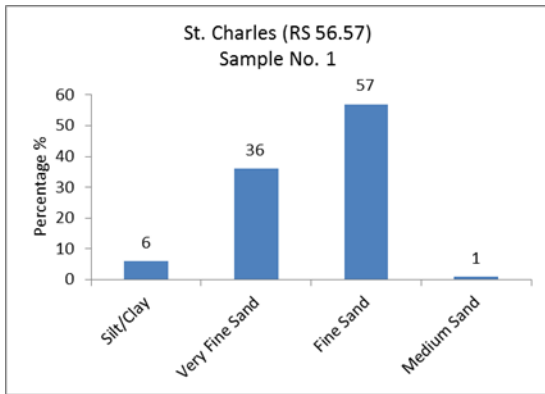


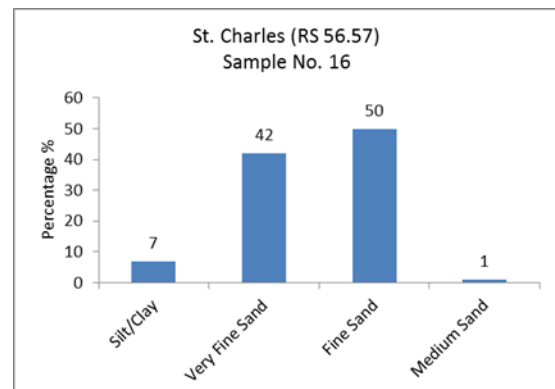
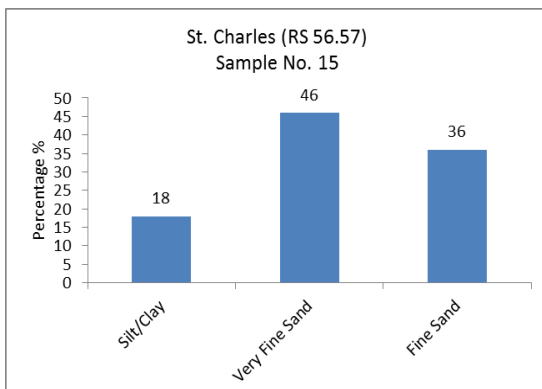
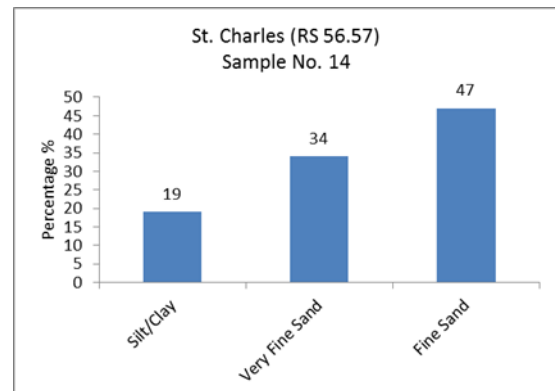
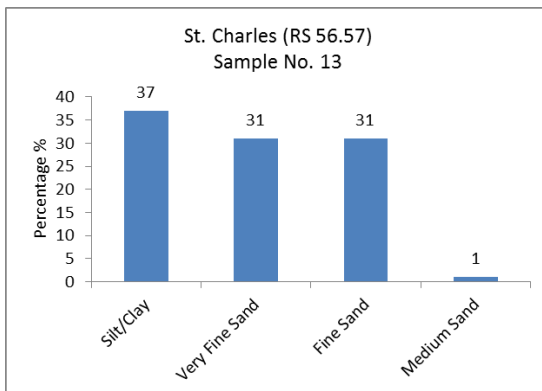
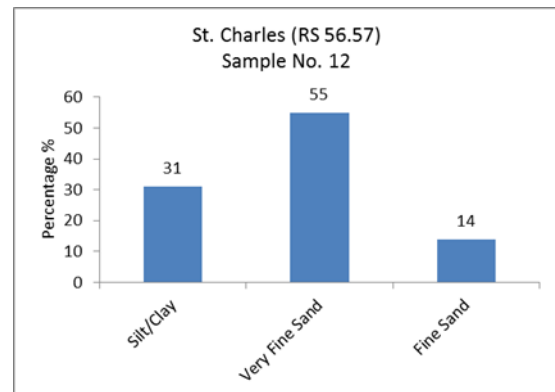
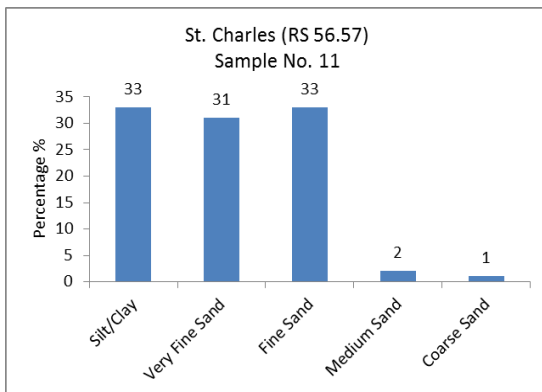
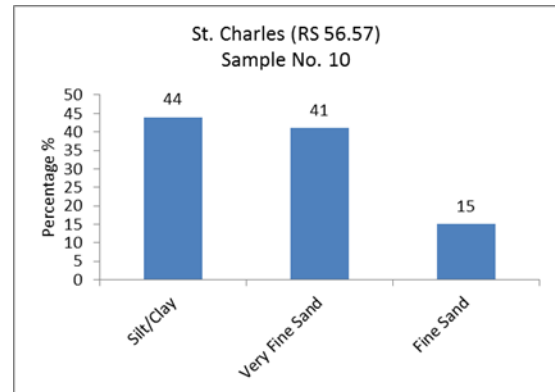
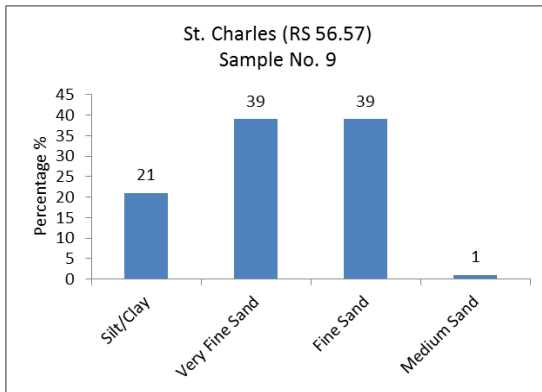


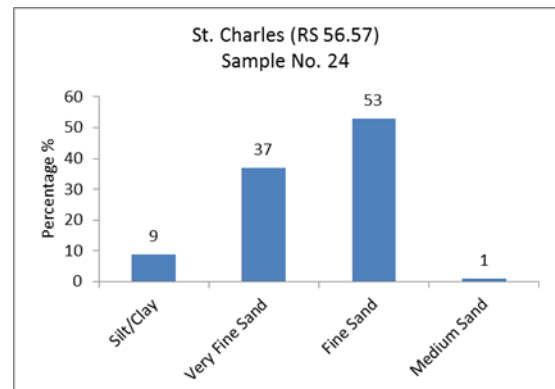
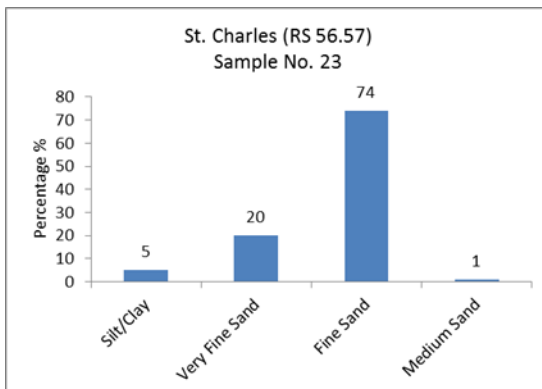
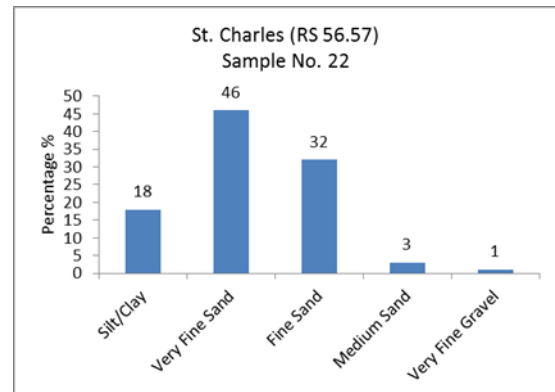
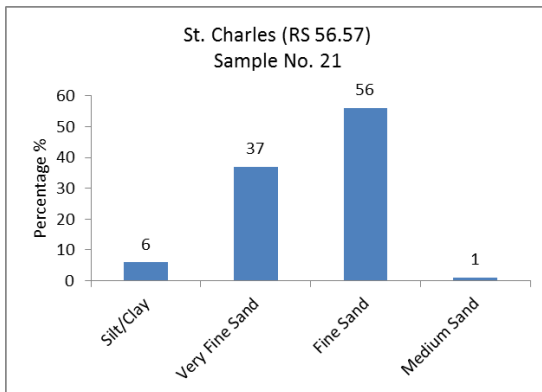
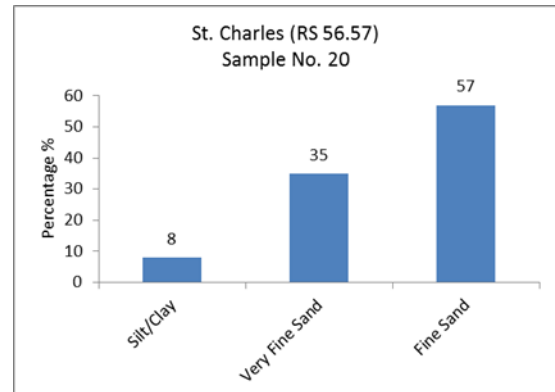
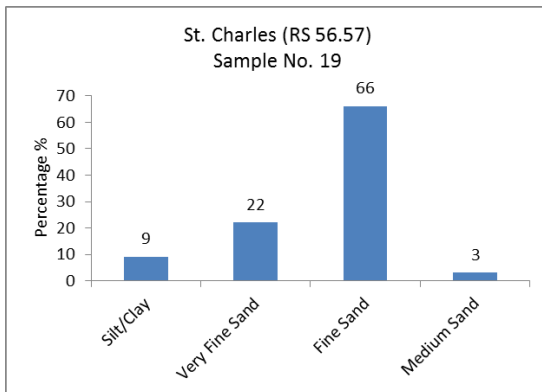
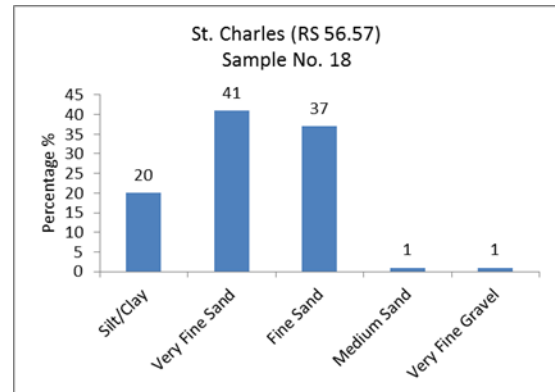
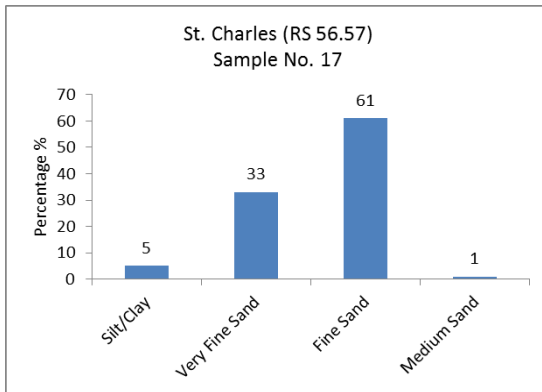


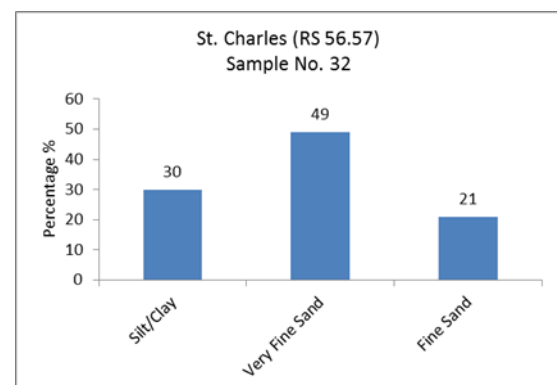
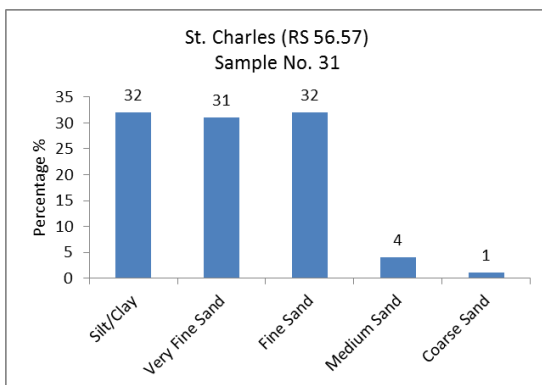
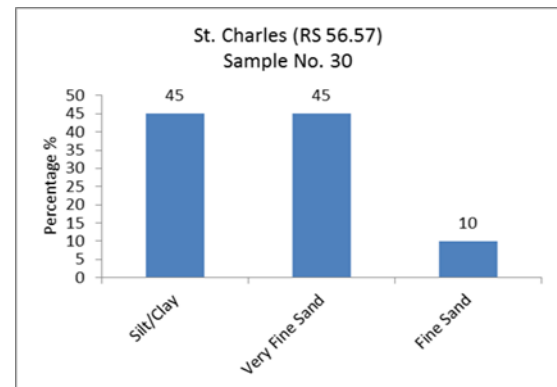
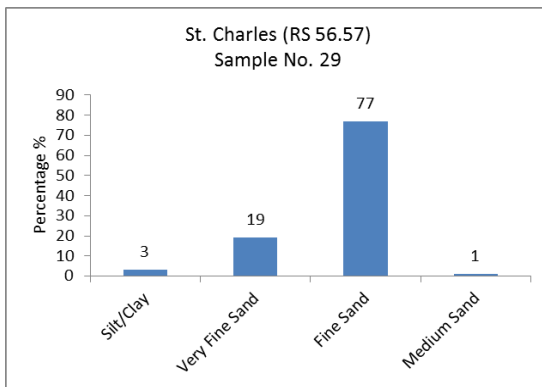
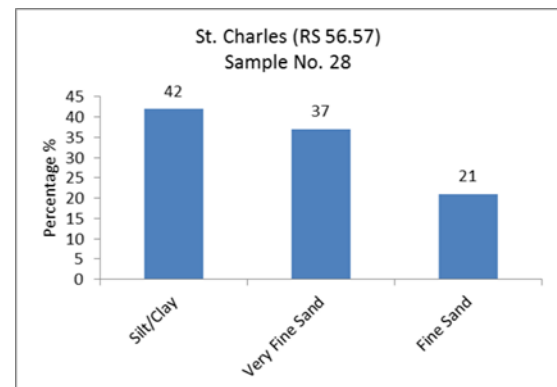
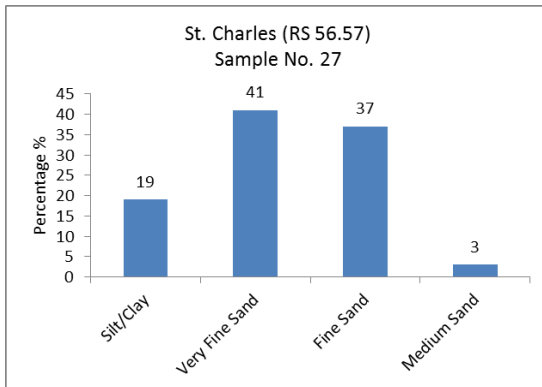
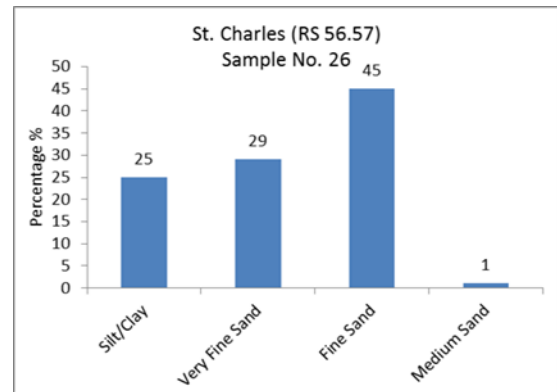
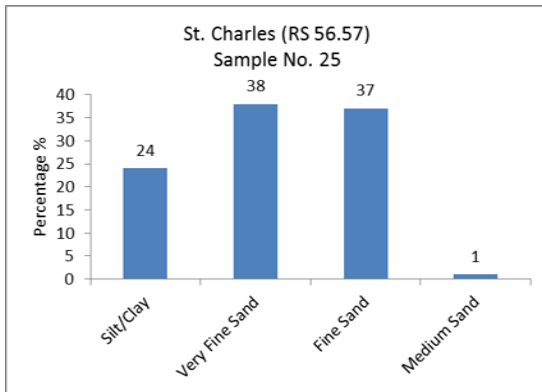


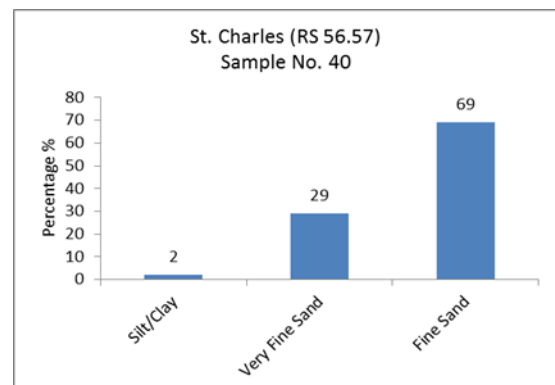
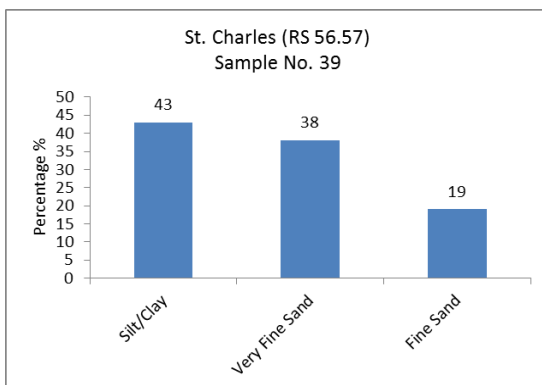
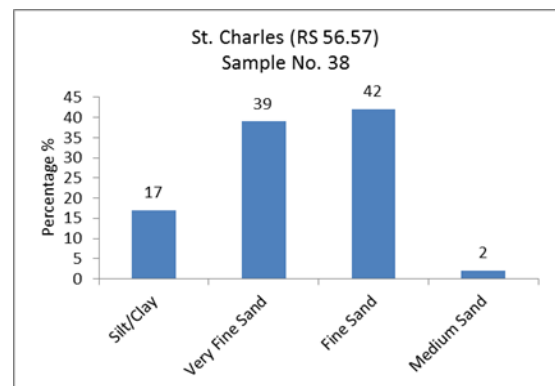
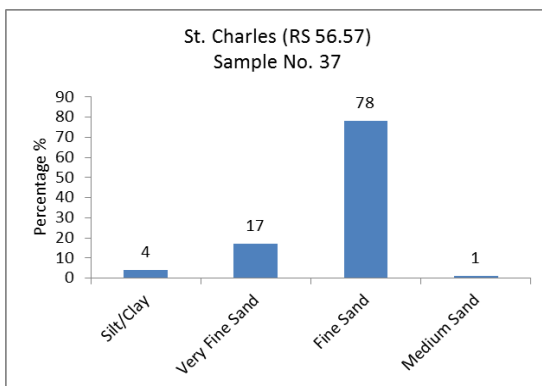
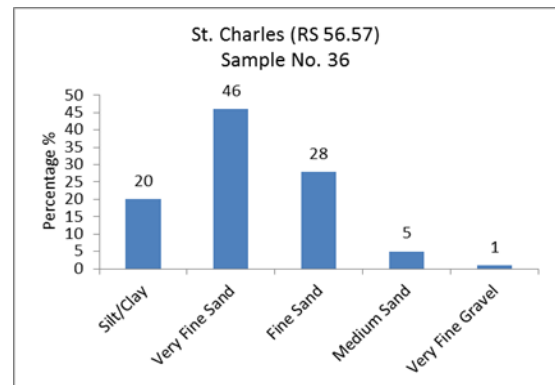
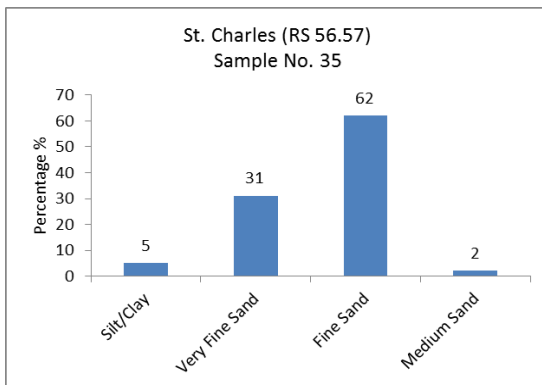
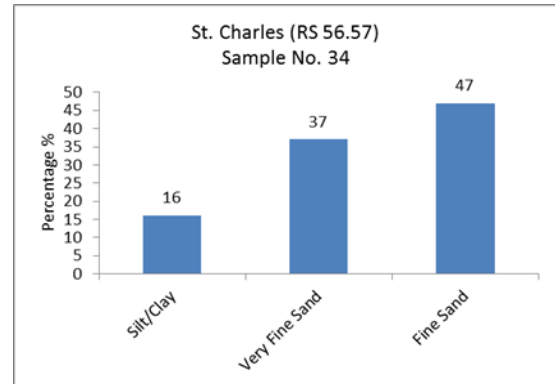
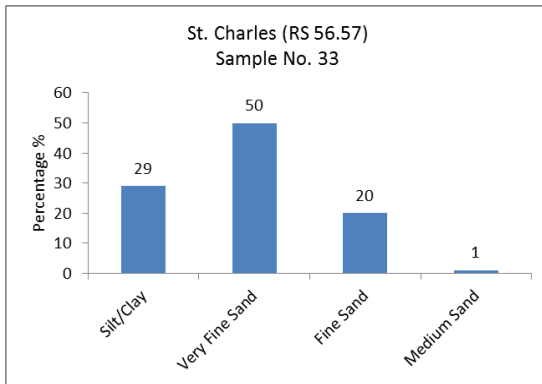


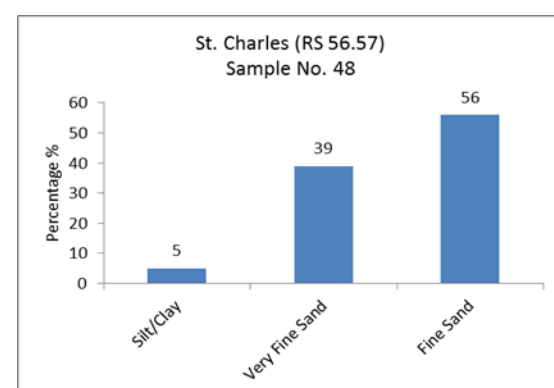
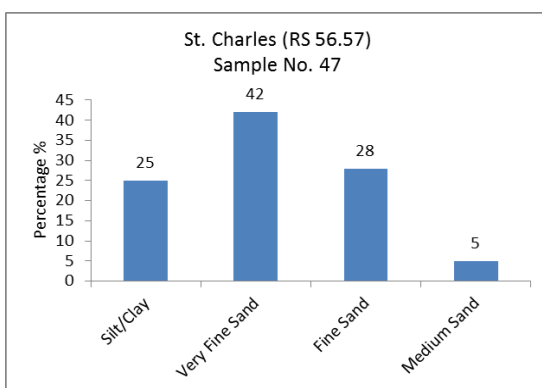
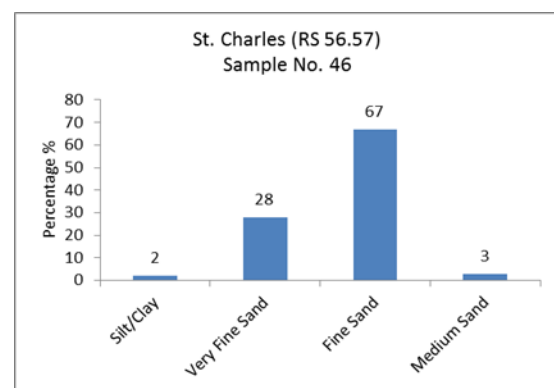
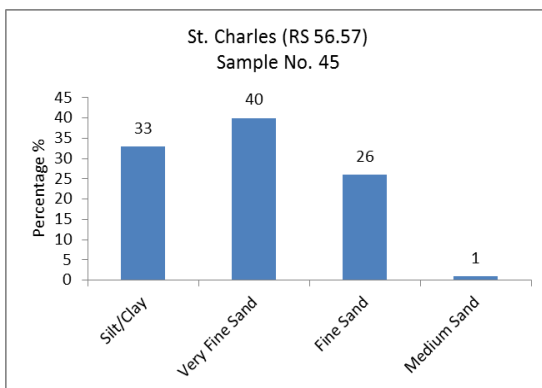
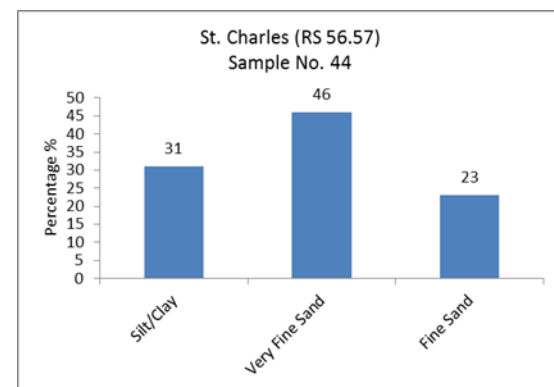
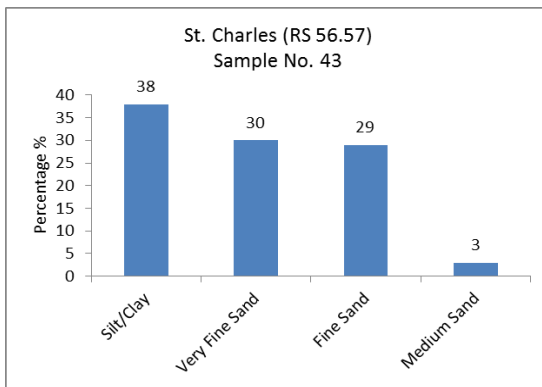
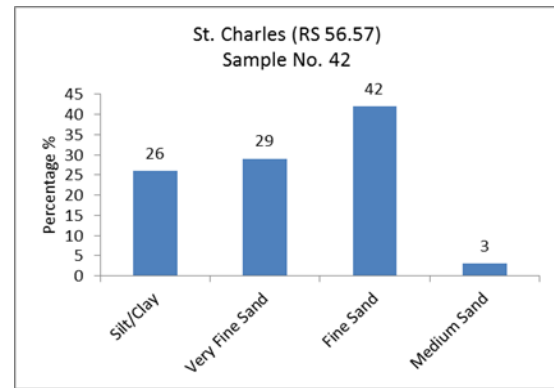
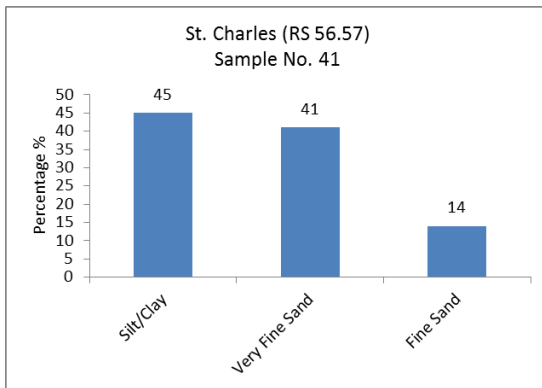


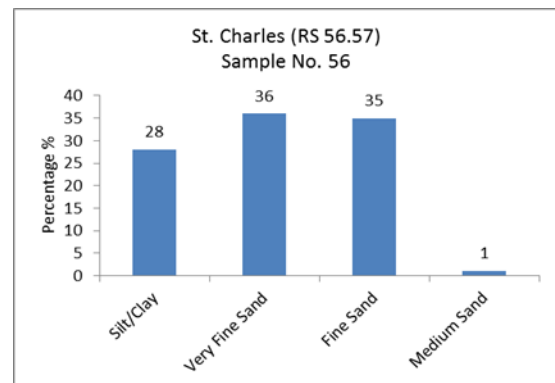
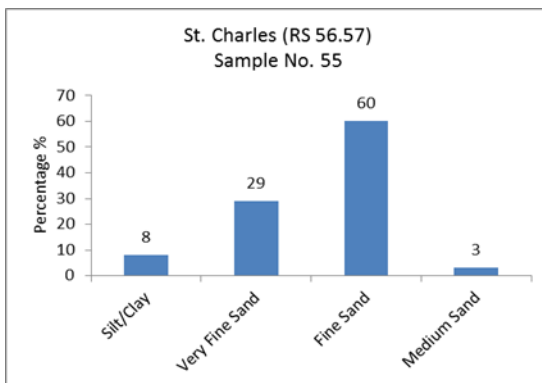
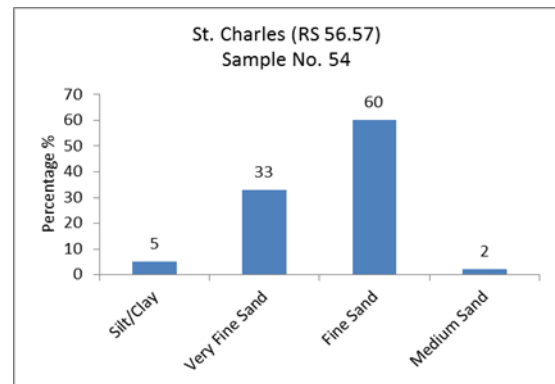
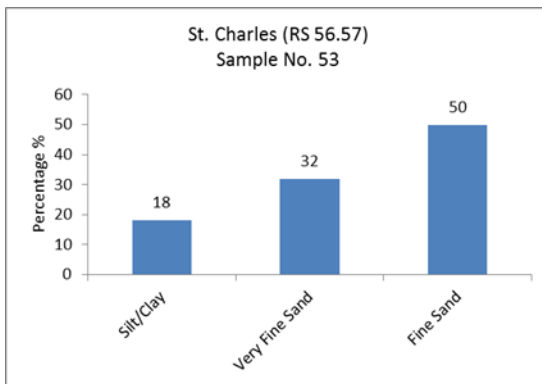
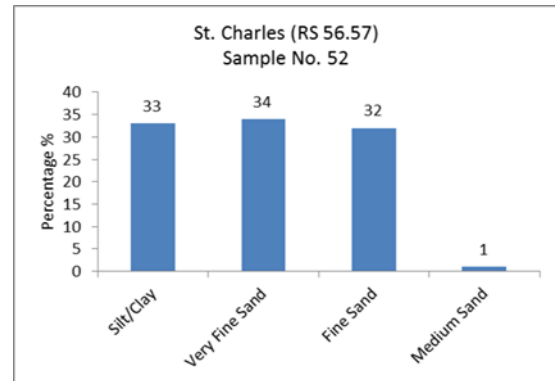
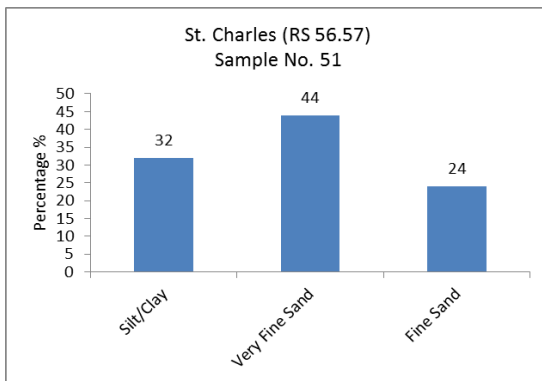
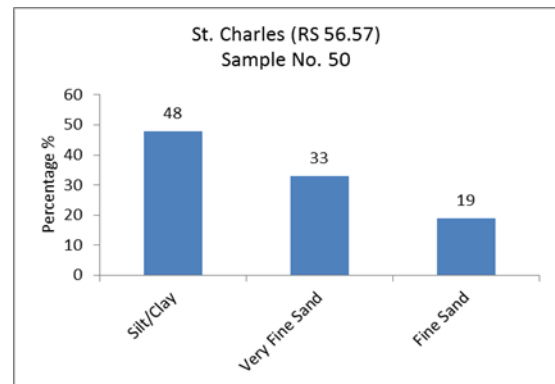
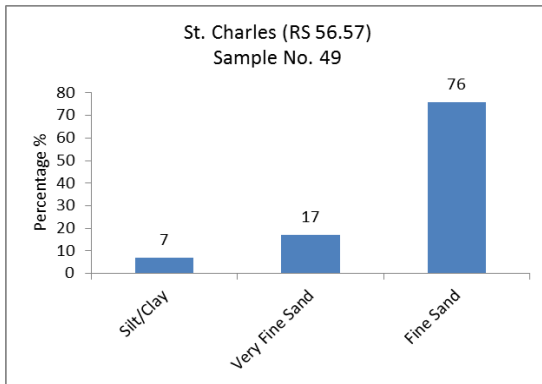


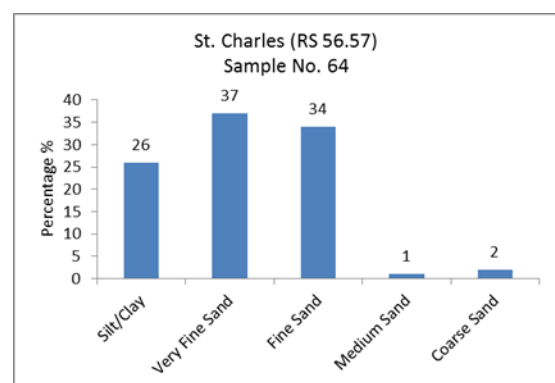
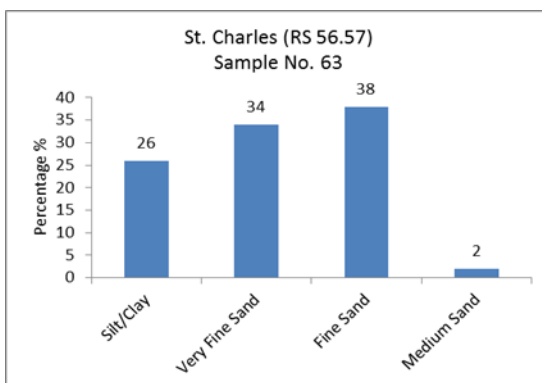
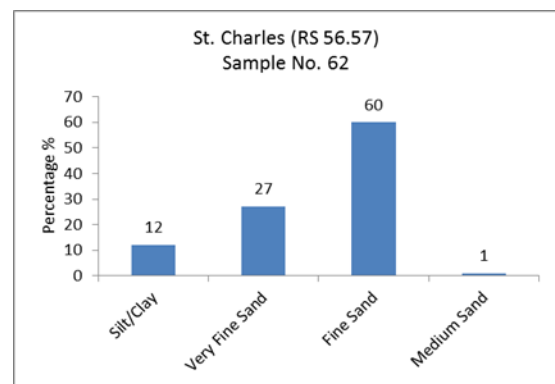
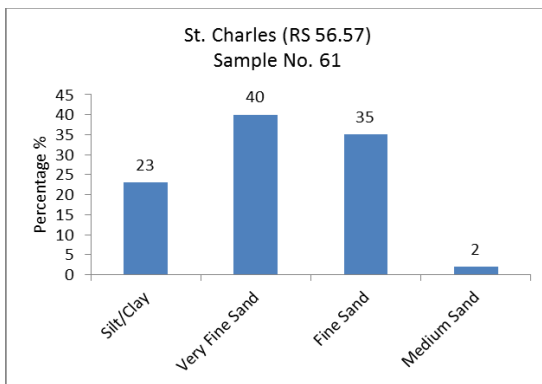
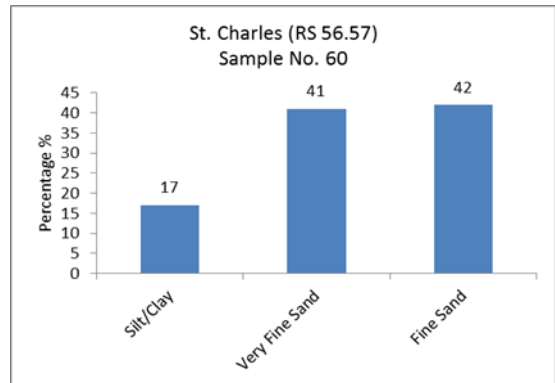
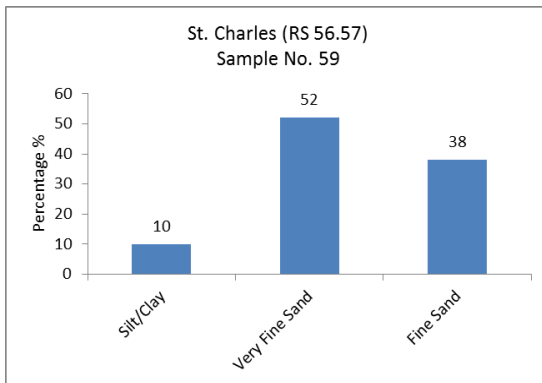
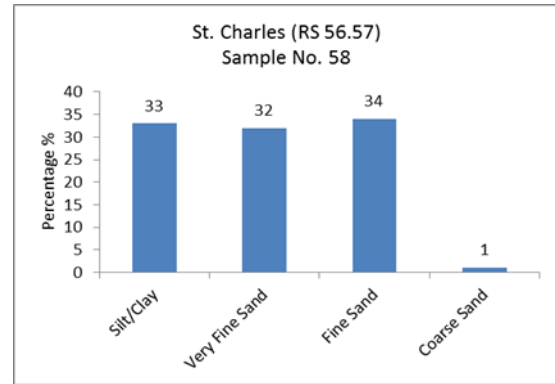
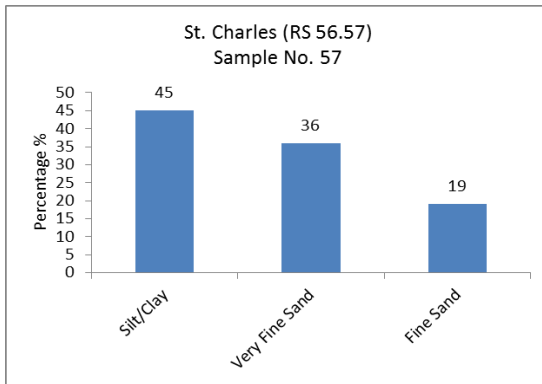


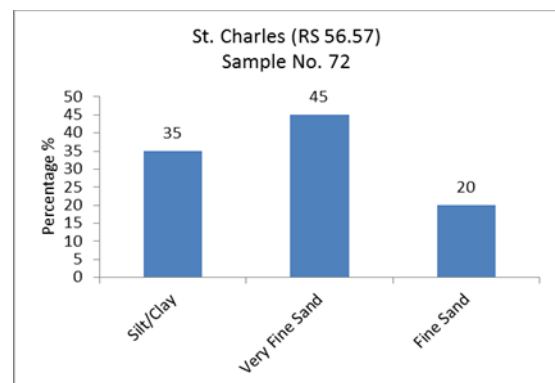
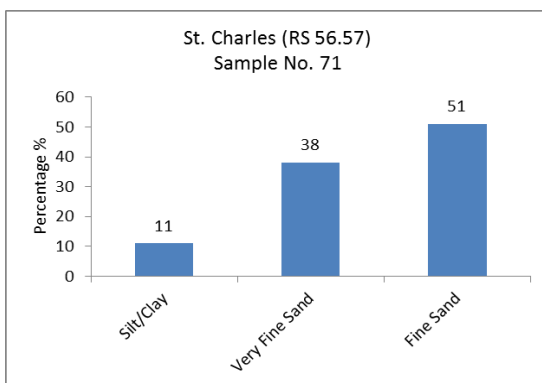
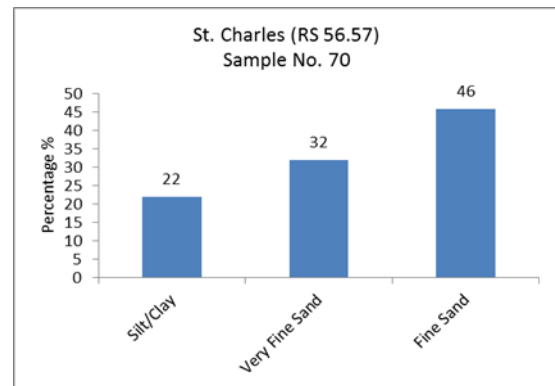
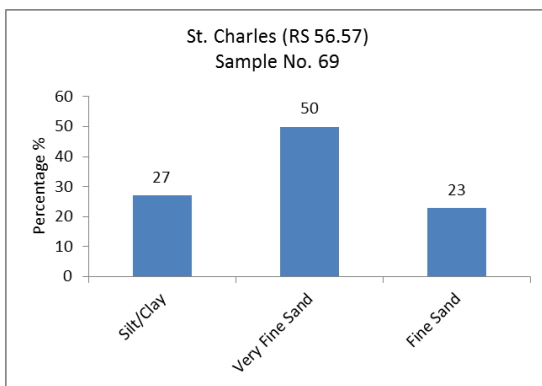
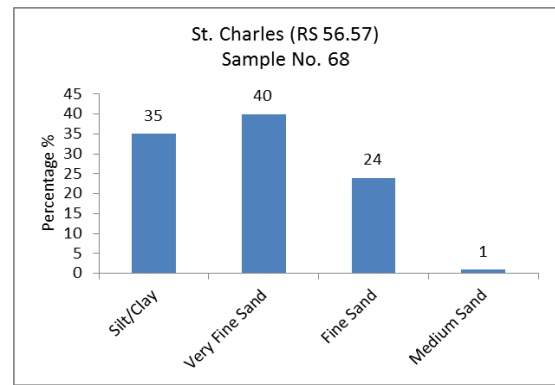
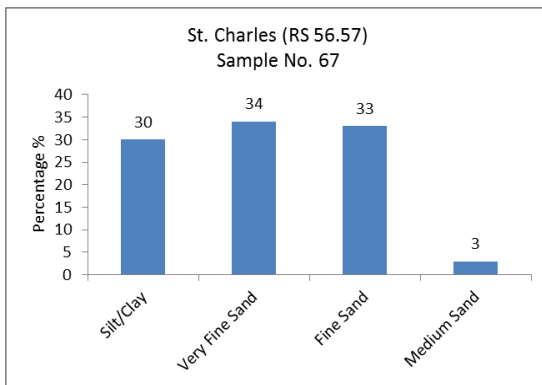
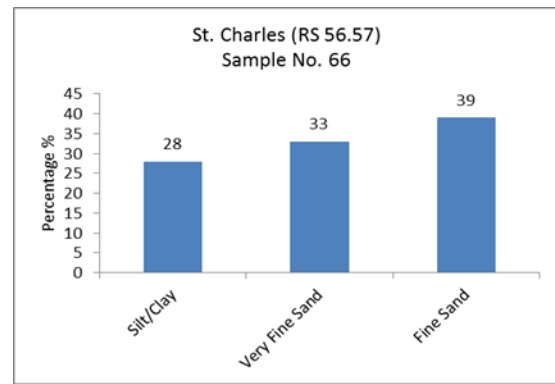
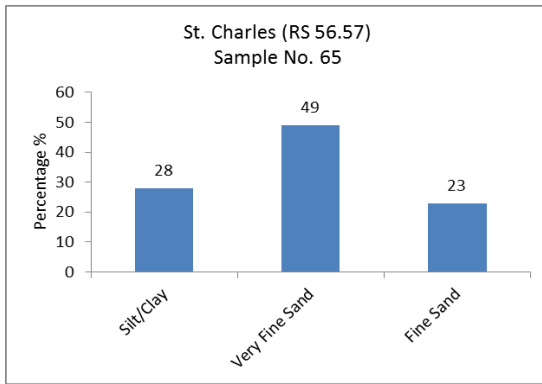


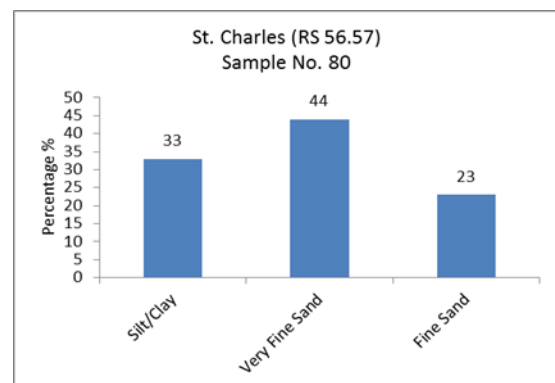
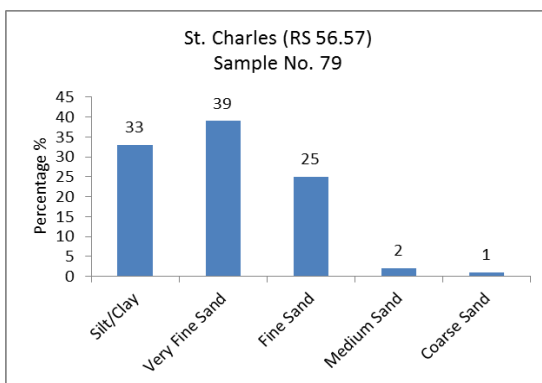
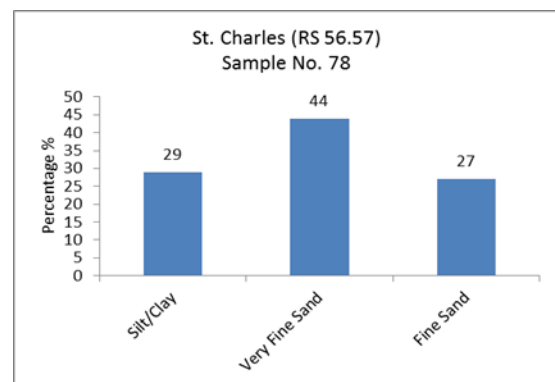
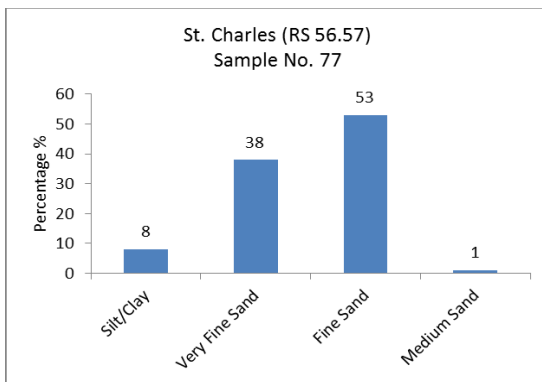
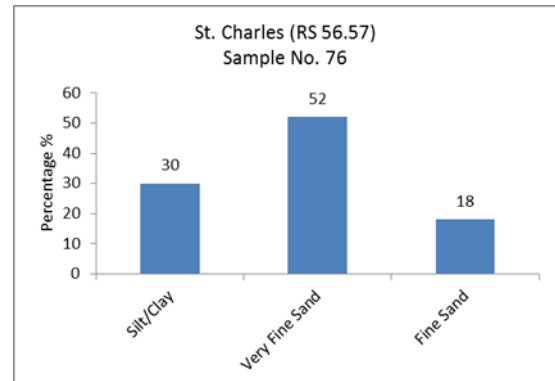
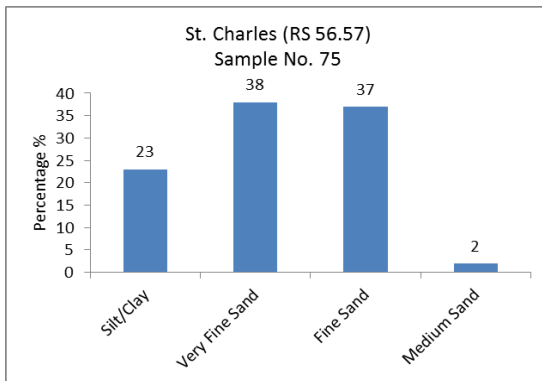
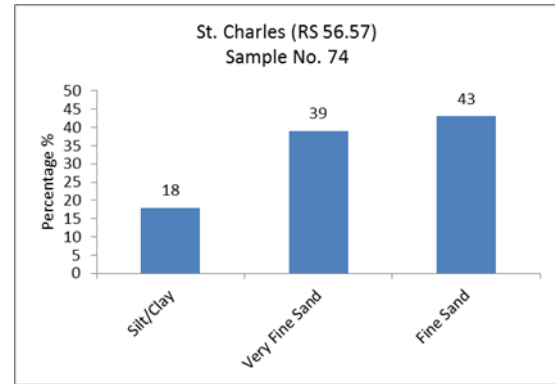
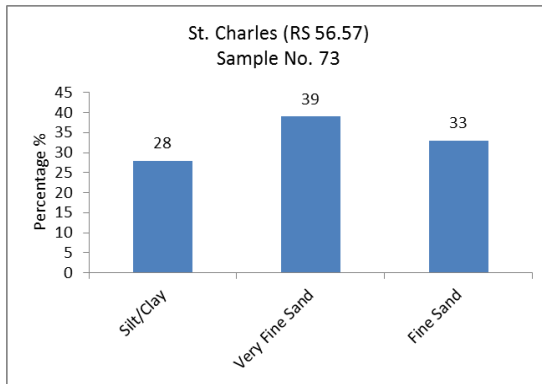












APPENDIX E: LARGE DATA TABLES.

Table E.1. The Unified Table of Data.

Location	Section	Station	Channel Slope	Width (ft)	Flood Prone Width 50-yr (ft)	Flood Prone Width 100-yr (ft)	Max Depth (ft)	Hydraulic Depth (ft)	Flow Area (sq. ft)
BATESVILLE	1	295.27 - 293.21	0.00010	499.03	4947.49	5009.44	19.23	14.13	7026.69
	2	293.21 - 291.27	0.00010	506.27	7021.71	7048.18	20.22	14.46	7073.82
	3	290.54 - 287.90	0.00010	381.69	8573.10	8668.19	18.98	14.35	5384.52
	4	286.54 - 285.34	0.00010	535.55	7063.88	7138.21	15.77	11.29	5848.78
	5	285.34 - 283.60	0.00010	534.01	13114.89	13126.28	15.88	10.91	5539.16
	6	281.04 - 280.00	0.00010	512.05	16862.29	19041.06	13.39	10.98	5348.31
	7	280.00 - 276.57	0.00017	531.38	27778.69	27861.60	11.21	8.10	4358.19
	8	276.57	0.00012	434.21	33114.95	33202.84	11.11	7.56	3283.29
	9	276.57 - 274.71	0.00012	484.03	34197.87	34308.17	13.98	9.69	4795.51
	10	270.75	0.00012	406.63	46612.99	47282.07	16.35	10.61	4313.37
	11	270.75 - 268.78	0.00015	447.53	40935.48	41328.51	17.74	10.43	4655.93
	12	268.78 - 266.28	0.00015	474.75	40782.83	41414.74	15.78	11.23	5315.53
	13	266.28 - 262.47	0.00015	520.70	50475.20	55232.60	16.10	12.46	6445.88
	14	262.47 - 260.98	0.00008	571.52	62237.30	62307.40	20.44	14.72	8384.14
	15	260.98 - 258.72	0.00008	600.64	63202.14	63269.54	26.76	15.85	9523.86
	16	258.72 - 257.25	0.00008	613.27	61191.42	61304.82	26.57	17.84	10898.39
	17	258.94 - 256.89	0.00008	579.16	61103.65	68747.11	26.84	18.09	10433.83
NEWPORT	18	256.89 - 253.08	0.00008	547.47	49362.68	55397.15	24.16	16.50	9026.02
	19	253.08 - 248.95	0.00008	581.84	41782.55	40325.94	23.78	18.20	10660.04
	20	247.80 - 240.36	0.00008	576.31	10646.74	15234.87	23.69	18.31	10370.73
	21	240.36 - 238.48	0.00008	633.82	8589.52	19204.26	23.88	16.78	10599.39
	22	238.48 - 234.98	0.00008	531.30	10795.91	27144.78	28.15	19.90	10497.09
	23	234.98 - 234.22	0.00008	589.67	12905.60	22950.12	24.17	17.55	10339.12
	24	232.55 - 231.45	0.00008	543.11	20201.56	34673.31	26.00	19.67	10229.39
	25	231.45 - 228.89	0.00008	489.63	22102.41	35852.90	32.87	24.99	12150.51
	26	228.89 - 227.78	0.00008	495.79	29417.08	39629.71	32.07	22.44	10912.89
	27	227.78 - 226.14	0.00008	513.82	36166.88	37677.83	27.47	20.33	10411.45
	28	226.14	0.00002	521.44	32922.67	37017.26	28.15	21.62	11204.03
	29	223.9 - 221.53	0.00002	470.24	32000.80	36751.80	33.74	21.94	10194.81
	30	221.53	0.00002	507.34	33165.45	35596.92	29.23	20.29	11046.79
	31	219.41	0.00002	504.03	34981.10	35047.44	28.01	20.92	9362.12
	32	219.41 - 216.97	0.00002	452.65	33342.99	34692.03	30.26	22.08	10000.77
	33	216.97 - 215.33	0.00002	456.49	31459.16	38049.64	30.33	21.04	9607.93
	34	215.33 - 213.33	0.00002	498.97	29761.69	44210.28	26.37	19.35	9588.14
	35	213.33 - 207.17	0.00002	486.42	35664.34	56381.93	25.75	18.93	9257.03
	36	207.17 - 203.71	0.00002	430.34	40406.53	64144.24	29.60	22.40	9521.11
	37	201.56 - 201.01	0.00002	515.50	33630.84	65068.43	29.72	20.75	10679.13
	38	201.01 - 197.27	0.00002	535.71	35144.47	66907.53	26.15	19.33	10135.04
AUGUSTA	39	197.27 - 195.01	0.00008	558.33	39330.31	70751.84	25.40	16.40	9167.75
	40	195.01 - 192.68	0.00008	523.75	38359.84	71276.26	25.35	17.06	8825.65
	41	192.68 - 191.64	0.00008	515.10	38368.67	67691.17	22.55	18.38	9382.37
	42	191.64 - 189.95	0.00008	519.24	34197.87	78284.27	28.52	17.63	9111.04
	43	189.95 - 188.59	0.00008	445.20	35490.42	65550.18	31.74	18.60	8277.34
	44	188.59 - 187.55	0.00008	527.93	37560.06	65906.84	25.73	17.77	9275.85
	45	187.55 - 186.26	0.00008	522.43	38734.66	79162.36	26.03	17.77	9173.51
	46	186.26 - 181.29	0.00008	558.24	34617.44	71639.49	25.11	16.59	9036.93
	47	181.29 - 177.81	0.00008	484.84	16688.70	58432.34	30.13	19.76	9587.13
	48	177.81 - 176.00	0.00008	603.18	20536.13	50154.89	28.34	19.91	12101.51
	49	175.50 - 172.65	0.00008	613.60	14936.86	55403.14	29.13	18.60	11346.52
	50	172.65 - 169.52	0.00008	533.36	13809.43	54414.76	28.94	20.43	10498.83
	51	169.52 - 167.08	0.00008	560.36	23585.02	50433.32	23.64	17.20	9576.04
	52	167.08 - 166.08	0.00008	542.56	18801.55	48463.17	25.74	18.43	9951.80
	53	166.08 - 164.39	0.00008	470.75	20712.21	44848.64	32.69	22.54	10529.76
	54	164.39 - 163.40	0.00008	451.14	31311.28	39907.01	32.12	20.90	9321.76
	55	163.40 - 161.91	0.00008	535.46	30366.96	33160.47	23.33	17.79	9527.82
	56	161.91 - 161.23	0.00008	618.14	12261.80	23218.46	23.02	15.80	9598.39
	57	161.23 - 158.63	0.00008	646.73	13785.87	37963.34	23.07	14.86	9552.47
	58	158.63	0.00008	562.32	15054.01	60790.64	22.85	15.74	9224.85
	59	155.71 - 155.04	0.00008	500.27	14423.39	19090.14	30.02	22.90	11142.08
	60	155.04 - 152.68	0.00008	642.77	11966.09	23334.70	25.90	20.22	13208.89
	61	152.68 - 149.03	0.00008	730.53	15393.10	33802.45	31.30	19.55	13797.88
	62	149.03 - 147.19	0.00008	613.52	33800.82	52693.34	30.25	16.35	9993.54
DES ARC	63	147.19 - 145.72	0.00008	610.03	11771.09	42195.23	31.95	20.97	11393.91
	64	145.72 - 143.75	0.00008	560.17	12098.90	22885.90	38.53	20.82	11024.18
	65	143.75 - 141.78	0.00008	530.18	15506.98	28359.78	31.55	17.84	9829.70
	66	141.78 - 140.39	0.00008	554.98	19168.37	30936.36	29.46	17.03	9990.17
	67	140.39 - 139.21	0.00008	598.86	16068.82	26459.51	34.63	19.70	10004.05
	68	139.21 - 138.01	0.00008	508.28	12868.22	21526.16	28.98	18.45	9613.13
	69	138.01 - 136.03	0.00008	521.07	11513.46	35044.71	33.00	17.33	10781.86
	70	136.03 - 135.16	0.00008	633.46	11218.02	25574.45	29.74	15.90	8700.07
	71	133.65 - 132.61	0.00008	555.36	9649.51	27805.52	30.76	20.51	9345.93
	72	132.61 - 130.54	0.00008	455.60	11484.63	21404.70	27.46	17.63	9969.94
	73	130.54 - 128.70	0.00008	571.36	11950.02	15843.43	30.49	19.83	10005.16
	74	128.70 - 124.33	0.00008	509.27	7918.71	12463.75	35.12	22.79	11428.12

Table E.1(Continued...). The Unified Table of Data.

Location	Section	Station	Channel Slope	Width (ft)	Flood Prone Width 50-yr (ft)	Flood Prone Width 100-yr (ft)	Max Depth (ft)	Hydraulic Depth (ft)	Flow Area (sq. ft)
DEVALLS BLUFF	75	124.33 - 122.36	0.00003	514.31	7099.41	15847.85	40.25	25.52	12121.82
	76	122.36 - 118.19	0.00003	476.57	15395.48	10436.37	38.26	26.06	14526.27
	77	118.19 - 116.4	0.00003	555.76	38517.75	26000.29	32.59	21.65	13233.00
	78	116.4 - 114.53	0.00003	616.02	34098.18	39367.44	41.75	24.63	14725.35
	79	114.53 - 112.77	0.00003	547.05	31940.30	37462.03	48.52	30.83	19341.24
	80	111.34	0.00003	624.66	28883.91	43557.18	49.54	31.97	22257.74
	81	109.77 - 108.75	0.00003	696.18	31241.97	50989.80	31.81	25.89	11555.45
	82	108.75 - 107.67	0.00003	446.29	32610.54	32375.32	28.09	22.53	10387.87
	83	107.67	0.00006	463.58	31357.16	31449.71	24.36	19.17	9220.28
	84	107.67 - 103.51	0.00006	503.04	31312.77	32328.97	25.03	19.93	8650.62
	85	104.31 - 103.51	0.00006	482.16	31290.58	32768.61	25.37	20.31	8365.79
	86	103.51 - 102.25	0.00006	411.81	26135.80	32326.10	25.91	19.10	8813.56
	87	102.25 - 101.14	0.00006	464.16	20832.36	31541.12	26.96	20.06	10520.66
CLARENDON	88	101.14 - 100.34	0.00006	524.71	15823.33	24089.47	26.59	21.70	11492.86
	89	100.34 - 98.48	0.00006	529.73	19012.65	22482.35	31.12	24.88	12827.75
	90	98.48 - 96.72	0.00006	547.03	24827.73	26424.47	29.79	23.74	12318.44
	91	96.72 - 94.57	0.00006	677.52	23357.68	26559.39	29.53	18.25	11676.88
	92	94.57 - 92.42	0.00006	653.46	23124.02	26504.15	32.34	19.37	14466.00
	93	89.46 - 87.41	0.00006	629.36	21196.11	25610.01	30.41	23.33	11765.88
	94	87.41 - 84.62	0.00006	670.46	18676.91	26329.63	24.51	19.24	11888.09
	95	84.62 - 81.65	0.00006	627.07	22524.36	29572.36	27.75	17.71	11932.64
	96	80.31 - 78.89	0.00006	533.57	27153.65	28189.88	33.39	20.22	11888.23
	97	78.89	0.00006	544.63	27112.23	28729.76	34.25	18.35	11093.09
	98	76.87 - 75.73	0.00006	593.02	29022.43	30179.45	30.28	19.81	10583.37
	99	75.73 - 73.62	0.00006	533.60	27111.79	29288.22	28.67	17.91	9890.16
	100	75.73 - 68.51	0.00006	521.54	26184.10	29685.54	30.12	19.01	10818.25
	101	71.59 - 68.51	0.00006	621.46	24710.25	30082.86	31.57	19.09	11746.34
	102	68.51 - 67.21	0.00006	591.23	27516.67	30092.93	30.81	20.35	12007.98
	103	67.21 - 64.72	0.00006	630.86	28272.04	30224.16	30.55	18.99	11975.50
	104	64.72	0.00006	555.10	29068.69	30683.76	32.76	18.89	12361.67
	105	64.72 - 60.12	0.00006	480.12	28441.07	31270.29	30.88	21.10	11646.96
	106	62.7 - 60.12	0.00006	518.38	28127.27	31653.02	29.94	22.21	11289.61
ST. CHARLES	107	60.12 - 58.79	0.00006	473.02	22176.63	28967.89	28.53	24.05	11345.59
	108	58.79 - 57.61	0.00006	517.45	20393.39	25922.35	27.37	21.42	11067.76
	109	57.61 - 55.30	0.00006	558.75	21567.87	22829.29	24.45	18.73	10425.26
	110	55.30 - 54.33	0.00006	517.82	21596.80	27095.66	31.69	19.19	9933.45
	111	54.33 - 53.38	0.00006	438.69	27994.14	32560.72	31.83	18.88	8258.27
	112	54.33 - 51.45	0.00006	430.84	29057.15	32169.25	30.37	17.66	8712.55
	113	51.45	0.00006	475.29	31183.16	31386.32	27.44	15.22	9621.12
	114	49.77 - 49.08	0.00006	723.61	24809.89	25094.58	27.29	17.77	14225.30
	115	49.08 - 47.19	0.00006	449.13	23621.05	23826.36	27.30	18.74	14755.53
	116	47.19	0.00006	437.71	23560.79	23748.32	25.31	20.58	9243.07
	117	45.31	0.00006	481.16	17766.32	18435.05	27.61	20.83	10230.00
	118	45.31 - 42.00	0.00006	471.48	17653.05	19588.38	27.70	20.69	9754.85
	119	42.00 - 40.52	0.00006	480.59	16312.83	19228.38	26.38	19.83	9508.57
	120	40.52	0.00011	466.17	15085.88	17715.06	24.98	19.12	9737.44
	121	40.52 - 38.69	0.00011	457.82	15082.72	18562.23	30.54	22.18	11597.24
	122	38.69	0.00011	525.89	16701.65	20014.62	35.31	25.23	13457.04
	123	36.00	0.00011	518.35	18323.73	20619.83	34.52	20.64	10699.38
	124	36.00	0.00011	554.73	18323.73	20619.83	34.52	20.64	10699.38
	125	34.42 - 32.81	0.00011	532.50	18361.18	31695.99	31.90	19.69	10438.75
	126	30.88 - 29.74	0.00011	560.17	28212.27	34581.96	27.62	20.57	11566.68
	127	29.74 - 29.13	0.00011	538.08	28554.82	38439.41	33.22	23.50	12623.17
	128	29.13 - 26.38	0.00011	538.14	31011.92	35539.21	29.31	19.76	10550.14
	129	26.38 - 24.47	0.00011	518.03	33784.20	37462.32	26.26	18.51	9576.90
	130	24.47	0.00011	537.66	35014.42	42287.02	28.29	19.41	9827.11
	131	22.01	0.00011	499.35	33202.91	48456.75	32.73	20.90	10976.93
	132	22.01 - 17.64	0.00011	472.69	33235.78	49273.04	30.02	22.71	10642.02
	133	17.64	0.00011	474.81	33268.64	50089.33	27.30	24.52	10307.11
	134	14.01	0.00011	730.62	40513.17	46076.14	29.97	15.58	14548.14
	135	14.01 - 11.80	0.00011	834.42	30146.57	45673.07	31.06	17.06	14088.00
	136	11.80	0.00011	735.00	19779.96	45270.00	32.15	18.54	13627.85
	137	9.97 - 6.92	0.00011	689.35	22675.42	49697.69	33.26	20.83	15682.17
	138	6.92 - 5.32	0.00011	668.41	8631.56	39081.92	33.01	23.66	15809.97
	139	4.31 - 3.26	0.00011	703.68	1910.15	63567.10	39.44	22.94	16154.34
	140	3.26 - 1.36	0.00011	648.26	1926.17	60535.60	45.32	25.29	16298.64
	141	1.36 - 0.00	0.00011	735.97	2346.44	65351.81	46.75	23.56	17291.30

Table E.1(Continued...). The Unified Table of Data.

Location	Section	Station	Velocity (ft/s)	Discharge (cfs)	Stream Power (lb/ft s)	Shear Force (lb/sq ft)	Manning's n value	Sinuosity 1984	Sinuosity 2003	ΔSinuosity
BATESVILLE	1	295.27 - 293.21	2.70	18747.65	0.16	0.06	0.026	1.13	1.13	0.004
	2	293.21 - 291.27	2.68	18750.00	0.16	0.06	0.026	1.08	1.08	0.000
	3	290.54 - 287.90	3.50	18745.17	0.34	0.10	0.026	1.80	1.82	0.023
	4	286.54 - 285.34	3.22	18743.97	0.28	0.08	0.026	1.20	1.21	0.011
	5	285.34 - 283.60	3.10	17159.51	0.26	0.08	0.026	2.71	2.86	0.151
	6	281.04 - 280.00	3.18	16949.70	0.28	0.09	0.026	1.03	1.02	0.003
	7	280.00 - 276.57	4.01	16150.83	0.75	0.16	0.026	1.51	1.60	0.088
	8	276.57	5.22	17152.26	1.30	0.25	0.026	2.79	2.99	0.196
	9	276.57 - 274.71	4.01	17405.54	0.74	0.16	0.026	1.45	1.52	0.063
	10	270.75	3.88	16729.22	0.46	0.12	0.026	2.16	2.39	0.227
	11	270.75 - 268.78	3.84	17825.71	0.44	0.12	0.026	1.05	1.07	0.015
	12	268.78 - 266.28	3.47	18428.15	0.35	0.10	0.026	1.71	1.82	0.111
	13	266.28 - 262.47	2.94	18392.87	0.22	0.07	0.026	1.31	1.34	0.026
	14	262.47 - 260.98	2.12	17694.72	0.07	0.04	0.026	1.09	1.11	0.016
	15	260.98 - 258.72	2.17	20723.40	0.07	0.04	0.026	1.55	1.61	0.056
	16	258.72 - 257.25	2.13	23087.23	0.07	0.03	0.026	2.06	2.06	0.005
NEWPORT	17	258.94 - 256.89	2.25	23485.22	0.10	0.05	0.029	1.41	1.43	0.020
	18	256.89 - 253.08	2.64	23557.52	0.18	0.07	0.029	1.40	1.43	0.028
	19	253.08 - 248.95	2.31	23733.00	0.12	0.05	0.029	1.43	1.47	0.032
	20	247.80 - 240.36	2.31	23905.60	0.11	0.05	0.029	2.08	2.10	0.025
	21	240.36 - 238.48	2.26	23919.72	0.11	0.05	0.029	1.36	1.44	0.079
	22	238.48 - 234.98	2.30	23952.34	0.11	0.05	0.029	2.11	2.17	0.061
	23	234.98 - 234.22	2.40	23949.31	0.15	0.06	0.029	1.20	1.17	0.028
	24	232.55 - 231.45	2.41	23975.31	0.14	0.05	0.029	2.33	2.40	0.076
	25	231.45 - 228.89	1.98	23966.35	0.07	0.03	0.029	1.83	1.89	0.058
	26	228.89 - 227.78	2.24	23964.57	0.11	0.05	0.029	1.09	1.07	0.013
	27	227.78 - 226.14	2.27	23523.17	0.10	0.05	0.029	1.04	1.07	0.031
	28	226.14	2.05	23010.27	0.07	0.04	0.029	1.71	1.72	0.012
	29	223.9 - 221.53	2.11	21434.84	0.08	0.04	0.029	2.10	2.14	0.036
	30	221.53	2.07	22912.23	0.08	0.04	0.029	1.13	1.16	0.028
	31	219.41	1.28	11951.97	0.02	0.01	0.029	1.25	1.36	0.112
	32	219.41 - 216.97	1.71	17345.29	0.05	0.03	0.029	1.10	1.15	0.052
	33	216.97 - 215.33	2.40	22789.96	0.13	0.05	0.029	1.24	1.29	0.055
	34	215.33 - 213.33	2.33	22161.78	0.12	0.05	0.029	1.59	1.67	0.072
	35	213.33 - 207.17	2.30	20292.23	0.13	0.05	0.029	1.79	1.87	0.077
	36	207.17 - 203.71	2.68	25531.03	0.19	0.07	0.033	1.78	1.84	0.057
	37	201.56 - 201.01	1.23	13135.33	0.02	0.02	0.031	1.64	1.71	0.073
AUGUSTA	38	201.01 - 197.27	2.12	21315.04	0.14	0.06	0.033	1.35	1.36	0.009
	39	197.27 - 195.01	2.83	25876.94	0.28	0.10	0.033	1.65	1.72	0.066
	40	195.01 - 192.68	2.95	25858.19	0.31	0.11	0.033	1.05	1.08	0.027
	41	192.68 - 191.64	2.90	27221.56	0.29	0.10	0.033	1.15	1.19	0.034
	42	191.64 - 189.95	2.35	21615.80	0.18	0.07	0.033	1.08	1.18	0.103
	43	189.95 - 188.59	2.14	17570.26	0.13	0.06	0.033	1.09	1.18	0.085
	44	188.59 - 187.55	2.54	23598.69	0.21	0.08	0.033	1.05	1.12	0.068
	45	187.55 - 186.26	3.04	27248.46	0.36	0.12	0.033	1.27	1.35	0.080
	46	186.26 - 181.29	2.98	26604.98	0.34	0.11	0.034	2.33	2.34	0.007
	47	181.29 - 177.81	2.54	22947.00	0.27	0.09	0.033	2.21	1.80	0.410
	48	177.81 - 176.00	2.38	27975.21	0.17	0.07	0.033	1.22	1.24	0.020
	49	175.50 - 172.65	2.51	28249.06	0.19	0.08	0.033	1.43	1.45	0.018
	50	172.65 - 169.52	2.68	28081.11	0.22	0.08	0.033	2.33	2.33	0.005
	51	169.52 - 167.08	2.94	28003.01	0.28	0.10	0.032	1.19	1.16	0.030
	52	167.08 - 166.08	2.91	28752.64	0.25	0.09	0.030	1.52	1.63	0.116
	53	166.08 - 164.39	2.42	25598.14	0.14	0.06	0.030	1.20	1.39	0.183
	54	164.39 - 163.40	2.79	25577.09	0.25	0.08	0.030	1.05	1.04	0.015
	55	163.40 - 161.91	3.16	29925.70	0.32	0.10	0.030	1.29	1.42	0.125
	56	161.91 - 161.23	3.04	29142.82	0.29	0.10	0.030	1.80	1.92	0.120
	57	161.23 - 158.63	3.06	29195.92	0.30	0.10	0.030	1.17	1.21	0.044
DES ARC	58	158.63	3.22	29700.87	0.34	0.11	0.030	1.19	1.24	0.057
	59	155.71 - 155.04	2.81	29871.69	0.24	0.08	0.030	2.54	2.60	0.065
	60	155.04 - 152.68	2.56	29931.93	0.21	0.08	0.034	1.93	1.05	0.878
	61	152.68 - 149.03	2.35	29487.48	0.16	0.07	0.034	1.85	1.98	0.128
	62	149.03 - 147.19	3.05	29774.07	0.31	0.10	0.030	1.35	1.37	0.017
	63	147.19 - 145.72	2.67	30050.42	0.19	0.07	0.030	1.64	1.74	0.092
	64	145.72 - 143.75	2.79	29988.48	0.23	0.08	0.030	1.02	1.02	0.004
	65	143.75 - 141.78	2.68	26046.79	0.21	0.07	0.030	2.50	2.63	0.129
	66	141.78 - 140.39	2.69	26937.77	0.20	0.07	0.030	1.49	1.58	0.090
	67	140.39 - 139.21	2.99	29719.53	0.26	0.09	0.030	1.04	1.04	0.001
	68	139.21 - 138.01	3.04	29181.34	0.28	0.09	0.030	1.44	1.54	0.099
	69	138.01 - 136.03	2.82	29072.56	0.24	0.08	0.030	1.03	1.24	0.204
	70	136.03 - 135.16	3.37	29257.13	0.39	0.12	0.030	1.29	1.37	0.080
	71	133.65 - 132.61	3.22	30082.63	0.31	0.10	0.030	2.73	2.86	0.135
	72	132.61 - 130.54	3.01	29330.40	0.29	0.09	0.030	1.96	1.99	0.033
	73	130.54 - 128.70	3.08	29534.18	0.33	0.10	0.030	1.09	1.10	0.002
	74	128.70 - 124.33	2.68	30045.32	0.19	0.07	0.030	1.29	1.31	0.029

Table E.1(Continued...). The Unified Table of Data.

Location	Section	Station	Velocity (ft/s)	Discharge (cfs)	Stream Power (lb/ft s)	Shear Force (lb/sq ft)	Manning's n value	Sinuosity 1984	Sinuosity 2003	ΔSinuosity
DEVALLS BLUFF	75	124.33 - 122.36	2.44	29600.12	0.13	0.05	0.030	1.41	1.30	0.111
	76	122.36 - 118.19	1.95	27535.18	0.07	0.03	0.030	1.53	1.66	0.126
	77	118.19 - 116.4	2.07	27297.57	0.08	0.04	0.030	2.05	2.09	0.035
	78	116.4 - 114.53	1.94	28295.73	0.07	0.04	0.030	1.83	2.05	0.220
	79	114.53 - 112.77	1.46	27242.09	0.03	0.02	0.030	2.17	2.31	0.136
	80	111.34	1.15	25512.41	0.01	0.01	0.030	1.86	1.88	0.021
	81	109.77 - 108.75	1.72	19823.25	0.04	0.03	0.030	1.42	1.46	0.041
	82	108.75 - 107.67	2.18	22097.49	0.11	0.05	0.030	1.69	1.80	0.106
	83	107.67	2.64	24371.73	0.18	0.07	0.030	1.30	1.32	0.027
	84	107.67 - 103.51	2.95	25422.13	0.25	0.08	0.030	1.26	1.27	0.012
	85	104.31 - 103.51	3.11	25947.33	0.28	0.09	0.030	1.08	1.14	0.059
CLARENDON	86	103.51 - 102.25	2.57	22047.27	0.19	0.07	0.030	2.53	2.73	0.201
	87	102.25 - 101.14	1.98	20856.75	0.08	0.04	0.030	1.32	1.32	0.005
	88	101.14 - 100.34	1.95	22443.26	0.07	0.04	0.030	1.98	2.17	0.187
	89	100.34 - 98.48	1.98	25299.13	0.08	0.04	0.031	1.03	1.02	0.010
	90	98.48 - 96.72	2.45	29997.77	0.20	0.08	0.035	1.86	2.02	0.156
	91	96.72 - 94.57	2.54	29622.65	0.22	0.09	0.035	1.23	1.27	0.042
	92	94.57 - 92.42	2.17	30981.21	0.13	0.06	0.035	1.31	1.34	0.029
	93	89.46 - 87.41	2.70	31359.17	0.27	0.10	0.035	2.66	2.77	0.114
	94	87.41 - 84.62	2.63	31048.98	0.25	0.09	0.035	1.03	1.04	0.006
	95	84.62 - 81.65	2.19	25875.16	0.15	0.06	0.035	1.58	1.58	0.007
	96	80.31 - 78.89	2.27	27056.13	0.14	0.07	0.035	1.39	1.43	0.044
ST. CHARLES	97	78.89	2.14	23760.04	0.12	0.06	0.035	1.67	1.77	0.100
	98	76.87 - 75.73	2.48	26265.31	0.21	0.08	0.035	1.32	1.36	0.044
	99	75.73 - 73.62	2.44	23999.42	0.19	0.08	0.035	1.74	1.80	0.060
	100	75.73 - 68.51	2.35	25210.59	0.17	0.07	0.035	1.04	1.04	0.004
	101	71.59 - 68.51	2.26	26421.76	0.15	0.06	0.035	2.41	2.54	0.124
	102	68.51 - 67.21	1.81	21860.03	0.08	0.04	0.035	1.24	1.26	0.017
	103	67.21 - 64.72	2.03	24456.49	0.13	0.06	0.035	1.82	1.87	0.045
	104	64.72	2.47	30589.05	0.20	0.08	0.035	1.11	1.09	0.025
	105	64.72 - 60.12	2.44	28475.30	0.19	0.08	0.035	1.62	1.68	0.063
	106	62.7 - 60.12	2.43	27418.42	0.18	0.08	0.035	1.92	2.06	0.140
	107	60.12 - 58.79	2.36	26709.85	0.16	0.07	0.035	1.07	1.10	0.029
	108	58.79 - 57.61	2.40	26511.57	0.18	0.08	0.035	1.30	1.32	0.023
ST. CHARLES	109	57.61 - 55.30	2.02	21054.22	0.12	0.06	0.035	1.11	1.09	0.020
	110	55.30 - 54.33	2.22	21970.35	0.15	0.07	0.035	1.42	1.48	0.055
	111	54.33 - 53.38	2.65	21681.53	0.24	0.09	0.035	1.23	1.29	0.054
	112	54.33 - 51.45	2.40	20572.33	0.19	0.08	0.035	1.34	1.45	0.106
	113	51.45	1.91	18353.93	0.10	0.05	0.035	1.12	1.14	0.019
	114	49.77 - 49.08	2.27	30166.93	0.18	0.07	0.035	1.65	1.61	0.039
	115	49.08 - 47.19	2.20	29037.49	0.17	0.07	0.035	2.19	2.40	0.205
	116	47.19	2.80	25918.44	0.28	0.10	0.035	1.80	1.94	0.144
	117	45.31	2.98	30488.62	0.34	0.11	0.035	1.05	1.06	0.011
	118	45.31 - 42.00	3.18	30918.57	0.42	0.13	0.035	2.80	3.06	0.260
	119	42.00 - 40.52	3.25	30814.59	0.44	0.14	0.035	1.20	1.25	0.047
	120	40.52	3.11	30280.66	0.39	0.13	0.035	1.28	1.35	0.070
	121	40.52 - 38.69	2.75	31171.17	0.28	0.10	0.035	1.74	1.82	0.076
	122	38.69	2.38	32061.67	0.16	0.07	0.035	2.00	1.99	0.007
	123	36.00	2.97	31801.35	0.33	0.11	0.035	1.21	1.23	0.024
	124	36.00	2.97	31801.35	0.33	0.11	0.035	1.33	1.38	0.045
	125	34.42 - 32.81	3.05	31846.45	0.37	0.12	0.035	1.33	1.37	0.041
	126	30.88 - 29.74	2.74	30814.25	0.29	0.10	0.035	1.60	1.68	0.079
	127	29.74 - 29.13	2.43	30529.46	0.18	0.07	0.035	1.62	1.82	0.200
	128	29.13 - 26.38	2.66	28156.29	0.25	0.09	0.035	1.30	1.36	0.054
	129	26.38 - 24.47	2.74	26286.26	0.29	0.10	0.035	1.78	1.71	0.062
	130	24.47	3.10	30508.60	0.39	0.12	0.035	1.49	1.73	0.246
	131	22.01	2.63	28900.73	0.23	0.09	0.035	1.04	1.03	0.010
	132	22.01 - 17.64	2.79	29671.35	0.27	0.10	0.035	1.80	1.86	0.060
	133	17.64	2.95	30441.97	0.31	0.10	0.035	1.77	1.82	0.051
	134	14.01	2.23	32468.80	0.15	0.07	0.035	1.02	1.03	0.008
	135	14.01 - 11.80	2.29	32264.77	0.16	0.07	0.035	1.50	1.63	0.129
	136	11.80	2.35	32060.74	0.17	0.07	0.035	1.03	1.05	0.023
	137	9.97 - 6.92	2.07	32409.48	0.13	0.07	0.035	1.31	1.38	0.071
	138	6.92 - 5.32	2.02	31761.86	0.10	0.05	0.035	1.04	1.05	0.001
	139	4.31 - 3.26	1.89	30397.99	0.08	0.05	0.035	1.21	1.23	0.015
	140	3.26 - 1.36	1.85	30004.98	0.08	0.04	0.035	1.12	1.13	0.006
	141	1.36 - 0.00	1.59	27395.46	0.05	0.03	0.035	1.50	1.56	0.066

Table E.1(Continued...). The Unified Table of Data.

Location	Section	Station	Radius of Curvature (ft)	Wavelength (ft)	Bend Length	Amplitude (ft)	Meander Belt Width (ft)	Meander Width Ratio	W/D Ratio	Entrenchment Ratio	Mobility Index
BATESVILLE	1	295.27 - 293.21	4837.48	11153.87	15762.00	3026.00	14695.45	29.45	35.32	9.91	10
	2	293.21 - 291.27	2993.44	5742.96	8866.00	1082.29	15342.79	30.31	35.01	13.87	10
	3	290.54 - 287.90	1579.26	10749.63	20426.00	4951.58	15901.50	41.66	26.60	22.46	10
	4	286.54 - 285.34	4344.72	9099.06	11386.00	2946.90	15771.80	29.45	47.42	13.19	10
	5	285.34 - 283.60	2007.61	4020.92	15408.00	6513.34	17631.76	33.02	48.95	24.56	10
	6	281.04 - 280.00	17589.58	10877.99	12027.00	908.19	17498.83	34.17	46.66	32.93	10
	7	280.00 - 276.57	3068.09	5195.24	12991.00	4641.87	17407.42	32.76	65.60	52.28	17
	8	276.57	1310.36	9099.06	8130.00	3398.06	18030.50	41.52	57.44	76.26	12
	9	276.57 - 274.71	4260.61	7902.01	16132.00	5061.69	18129.01	37.45	49.95	70.65	12
	10	270.75	1515.90	4928.47	12022.00	2826.24	18492.44	45.48	38.33	114.63	12
	11	270.75 - 268.78	3005.46	5547.10	6451.00	1001.46	18608.63	41.58	42.92	91.47	15
	12	268.78 - 266.28	1523.25	7011.70	13573.00	2867.02	19003.09	40.03	42.26	85.90	16
	13	266.28 - 262.47	2724.44	15612.44	24034.00	3906.83	19436.28	37.33	41.79	96.94	16
	14	262.47 - 260.98	2233.23	5792.67	6695.00	1106.65	20352.17	35.61	38.84	108.90	8
	15	260.98 - 258.72	1863.83	7064.76	11474.00	2408.94	21546.53	35.87	37.90	105.22	9
	16	258.72 - 257.25	2723.72	5913.37	14070.00	5286.00	23839.74	38.87	34.38	99.78	9
NEWPORT	17	258.94 - 256.89	2750.06	7703.79	14462.00	2380.12	21273.47	36.73	32.02	105.50	150
	18	256.89 - 253.08	2784.67	13266.12	23048.00	4504.81	20171.03	36.84	33.17	90.17	151
	19	253.08 - 248.95	3568.23	13266.12	23903.00	3825.14	21696.94	37.29	31.97	71.81	151
	20	247.80 - 240.36	3678.18	19211.27	43933.00	9406.01	23467.68	40.72	31.48	18.47	152
	21	240.36 - 238.48	2937.70	6552.95	10106.00	3219.23	22448.05	35.42	37.77	13.55	152
	22	238.48 - 234.98	1466.08	5800.94	14285.00	4668.42	21961.19	41.34	26.70	20.32	152
	23	234.98 - 234.22	1866.99	6425.52	7749.00	1977.10	21034.33	35.67	33.61	21.89	152
	24	232.55 - 231.45	1844.76	6222.41	14392.00	4244.31	20294.49	37.37	27.61	37.20	152
	25	231.45 - 228.89	2395.00	6688.12	10160.00	2954.42	20294.49	41.45	19.59	45.14	152
	26	228.89 - 227.78	2031.36	4785.06	5787.00	1207.80	17035.63	34.36	22.10	59.33	152
	27	227.78 - 226.14	3886.28	7905.77	10679.00	1371.32	16598.75	32.30	25.27	70.39	150
	28	226.14	1150.57	3639.37	7599.00	2647.14	16596.59	31.83	24.12	63.14	37
	29	223.9 - 221.53	2008.38	3733.31	13839.00	3105.12	16269.30	34.60	21.43	68.05	36
	30	221.53	2264.61	5469.54	8136.00	1694.11	16059.44	31.65	25.00	65.37	37
	31	219.41	1859.32	4639.95	7373.00	2096.90	15969.23	31.68	24.09	69.40	27
	32	219.41 - 216.97	1709.55	7768.82	10171.00	1203.37	15965.51	35.27	20.50	73.66	32
	33	216.97 - 215.33	1564.46	5495.93	7585.00	1977.53	16419.89	35.97	21.70	68.92	37
	34	215.33 - 213.33	1624.06	7649.93	14563.00	4079.52	13383.84	26.82	25.79	59.65	37
	35	213.33 - 207.17	2074.91	14797.98	29319.00	4619.98	13302.09	27.35	25.70	73.32	35
	36	207.17 - 203.71	1875.34	7619.92	24631.00	4187.90	13305.94	30.92	19.21	93.89	39
	37	201.56 - 201.01	1868.15	5255.00	9627.00	3126.65	15113.01	29.32	24.85	65.24	28
AUGUSTA	38	201.01 - 197.27	2133.58	6309.58	18253.00	3450.66	16712.05	31.20	27.71	65.60	51
	39	197.27 - 195.01	2168.97	7684.09	14067.00	3109.45	16625.46	29.78	34.04	70.44	224
	40	195.01 - 192.68	2663.58	9302.07	10815.00	1197.49	16575.61	31.65	30.70	73.24	223
	41	192.68 - 191.64	2024.95	6540.52	8548.00	1612.34	16495.23	32.02	28.03	74.49	229
	42	191.64 - 189.95	1326.19	4986.03	6080.00	967.43	16318.33	31.43	29.46	65.86	204
	43	189.95 - 188.59	1285.07	4765.61	6226.00	1283.68	16224.03	36.44	23.94	79.72	184
	44	188.59 - 187.55	1514.71	5194.33	7618.00	986.29	18295.85	34.66	29.71	71.15	213
	45	187.55 - 186.26	1429.44	3329.87	6177.00	1772.83	19220.57	36.79	29.40	74.14	229
	46	186.26 - 181.29	2213.75	8863.67	24447.00	7883.40	18623.35	33.36	33.65	62.01	227
	47	181.29 - 177.81	1434.95	5840.82	19602.00	4376.75	17423.26	35.94	24.54	34.42	210
	48	177.81 - 176.00	2332.12	6604.15	10751.00	1638.79	17374.71	28.81	30.30	34.05	232
	49	175.50 - 172.65	1988.48	7371.99	15231.00	2615.31	17642.94	28.75	32.98	24.34	234
	50	172.65 - 169.52	1885.42	6352.85	17046.00	3475.74	17476.88	32.77	26.11	25.89	233
	51	169.52 - 167.08	1777.32	8012.48	11377.00	2282.26	17479.66	31.19	32.57	42.09	233
	52	167.08 - 166.08	1025.54	4005.46	7886.00	2341.02	17466.51	32.19	29.44	34.65	236
	53	166.08 - 164.39	845.41	6262.58	9008.00	1708.43	17416.57	37.00	20.89	44.00	222
	54	164.39 - 163.40	1935.63	3767.87	5400.00	487.66	17416.57	38.61	21.59	69.41	222
	55	163.40 - 161.91	1780.85	5065.62	7878.00	1943.25	17416.57	32.53	30.10	56.71	240
	56	161.91 - 161.23	3554.61	4982.33	7812.00	3212.28	17395.76	28.14	39.14	19.84	237
	57	161.23 - 158.63	2410.86	6369.44	8067.00	1645.51	17399.36	26.90	43.54	21.32	237
DES ARC	58	158.63	2067.70	4581.01	6633.00	1795.45	17628.21	31.35	35.73	26.77	239
	59	155.71 - 155.04	2802.42	5592.50	15618.00	5709.18	17628.21	35.24	21.85	28.83	240
	60	155.04 - 152.68	2264.92	5517.83	8030.00	1112.31	17628.21	27.43	31.80	18.62	240
	61	152.68 - 149.03	1288.05	5938.95	9330.00	2432.59	17140.88	23.46	37.37	21.07	239
	62	149.03 - 147.19	1920.93	7860.58	11491.00	3801.81	16970.90	27.66	37.52	55.09	240
	63	147.19 - 145.72	1695.80	5257.54	9138.00	3050.60	16840.06	27.61	29.09	19.30	241
	64	145.72 - 143.75	5013.58	5993.68	7818.00	549.28	16737.69	29.88	26.91	21.60	241
	65	143.75 - 141.78	1760.77	3463.27	9955.00	4308.35	15479.43	29.20	29.71	29.25	224
	66	141.78 - 140.39	1804.74	4965.53	9584.00	2986.00	15512.95	27.95	32.59	34.54	228
	67	140.39 - 139.21	3436.15	6100.94	7203.00	654.43	15562.79	25.99	30.41	26.83	240
	68	139.21 - 138.01	1509.01	4686.14	10126.00	1783.21	15655.94	30.80	27.56	25.32	237
	69	138.01 - 136.03	3473.99	4298.41	5870.00	718.28	15732.85	30.19	30.07	22.10	237
	70	136.03 - 135.16	1691.17	4835.95	7317.00	2105.77	15770.94	24.90	39.84	17.71	238
	71	133.65 - 132.61	1634.29	5685.80	11756.00	3369.79	15834.90	28.51	27.08	17.38	241
	72	132.61 - 130.54	1781.09	5253.69	11950.00	2406.20	14859.90	32.62	25.85	25.21	238
	73	130.54 - 128.70	2627.88	7030.29	9274.00	1307.11	14673.79	25.68	28.82	20.92	239
	74	128.70 - 124.33	1806.46	6574.61	10417.00	2267.87	14500.61	28.47	22.35	15.55	170

Table E.1(Continued...). The Unified Table of Data.

Location	Section	Station	Radius of Curvature (ft)	Wavelength (ft)	Bend Length	Amplitude (ft)	Meander Belt Width (ft)	Meander Width Ratio	W/D Ratio	Entrenchment Ratio	Mobility Index
DEVALLS BLUFF	75	124.33 - 122.36	2527.78	7261.50	20170.00	3795.01	14302.66	27.81	20.15	13.80	63
	76	122.36 - 118.19	1662.76	6625.83	12672.00	2844.88	14791.76	31.04	18.29	32.30	61
	77	118.19 - 116.4	2187.12	5960.60	20652.00	5150.01	15907.48	28.62	25.67	69.31	61
	78	116.4 - 114.53	1934.94	5571.88	12222.00	2848.42	15905.71	25.82	25.01	55.35	62
	79	114.53 - 112.77	1187.56	3853.55	9558.00	2435.16	16493.20	30.15	17.74	58.39	61
	80	111.34	1446.44	5896.52	11359.00	2822.58	16493.20	26.40	19.54	46.24	59
	81	109.77 - 108.75	2157.11	6445.00	8337.00	2855.32	16787.92	24.11	26.89	44.88	52
	82	108.75 - 107.67	1287.50	3570.55	7700.00	2351.97	17103.38	38.32	19.81	73.07	55
	83	107.67	1354.46	3122.96	5400.00	1463.75	17252.04	37.22	24.18	67.64	115
	84	107.67 - 103.51	1274.64	3301.42	5488.00	1580.24	17456.67	34.70	25.24	62.25	117
	85	104.31 - 103.51	3471.25	4199.58	5691.00	947.14	17554.67	36.41	23.75	64.90	119
	86	103.51 - 102.25	1276.32	3257.82	10966.00	4256.90	17716.11	43.02	21.56	63.47	109
	87	102.25 - 101.14	1626.11	5188.35	7950.00	1563.79	17929.03	38.63	23.14	44.88	106
	88	101.14 - 100.34	1739.36	4855.14	10325.00	3137.53	17929.03	34.17	24.18	30.16	156
	89	100.34 - 98.48	12393.46	8123.95	9008.00	800.40	17929.03	33.85	21.29	35.89	166
	90	98.48 - 96.72	1526.64	3777.35	10384.00	3389.10	20484.61	37.45	23.05	45.39	180
	91	96.72 - 94.57	2773.51	9418.76	12956.00	2060.84	20532.71	30.31	37.13	34.48	179
	92	94.57 - 92.42	3499.13	12651.92	20207.00	3509.07	20588.06	31.51	33.74	35.39	183
CLARENDON	93	89.46 - 87.41	1790.31	6574.93	18943.00	3621.51	20657.86	32.82	26.98	33.68	185
	94	87.41 - 84.62	9814.67	8012.48	9967.00	972.10	20744.80	30.94	34.85	27.86	184
	95	84.62 - 81.65	2873.13	9740.80	18600.00	6532.36	20808.90	33.18	35.40	35.92	168
	96	80.31 - 78.89	2598.47	6243.29	10181.00	2933.95	17716.18	33.20	26.39	50.89	171
	97	78.89	1482.31	5383.90	10106.00	2104.53	17551.61	32.23	29.68	49.78	161
	98	76.87 - 75.73	2085.52	5749.56	9596.00	2459.75	17493.59	29.50	29.94	48.94	169
	99	75.73 - 73.62	3131.72	6499.83	13155.00	2904.39	17391.25	32.59	29.79	50.81	161
	100	75.73 - 68.51	3001.58	4601.27	5458.00	538.14	17299.78	33.17	27.44	50.21	165
	101	71.59 - 68.51	1296.46	4881.07	16485.00	4463.66	17259.87	27.77	32.56	39.76	169
	102	68.51 - 67.21	2058.25	8893.75	11340.00	1991.43	17204.73	29.10	29.06	46.54	154
	103	67.21 - 64.72	1752.56	5722.68	10403.00	3766.31	17107.86	27.12	33.22	44.82	163
	104	64.72	1337.10	4220.76	4320.00	875.74	17089.08	30.79	29.39	52.37	182
	105	64.72 - 60.12	1605.37	2975.78	6548.00	2432.35	17020.00	35.45	22.75	59.24	176
	106	62.7 - 60.12	1921.91	5466.70	13002.00	2683.03	17033.26	32.86	23.34	54.26	173
	107	60.12 - 58.79	2646.46	5160.38	6479.00	1305.46	16920.58	35.77	19.67	46.88	170
	108	58.79 - 57.61	1439.52	4768.86	7041.00	1771.92	16916.03	32.69	24.16	39.41	170
	109	57.61 - 55.30	2647.91	7579.80	10727.00	1769.68	16774.63	30.02	29.84	38.60	107
ST. CHARLES	110	55.30 - 54.33	1451.85	5423.35	9268.00	1884.18	16644.99	32.14	26.99	41.71	109
	111	54.33 - 53.38	1191.36	4703.66	6583.00	1167.87	16571.85	37.78	23.24	63.81	108
	112	54.33 - 51.45	1029.37	2940.40	5689.00	863.80	16472.71	38.23	24.40	67.44	106
	113	51.45	2264.08	3237.53	5172.00	916.56	16418.71	34.54	31.23	65.61	100
	114	49.77 - 49.08	1810.01	7646.90	9745.00	3154.00	16378.13	22.63	40.72	34.29	128
	115	49.08 - 47.19	1075.56	5031.63	7966.00	2403.80	16494.87	36.73	23.97	52.59	125
	116	47.19	1063.81	3454.06	7503.00	1923.34	16849.84	38.50	21.27	53.83	119
	117	45.31	2173.31	4637.26	5307.00	689.34	16203.14	33.68	23.10	36.92	129
	118	45.31 - 42.00	1551.21	4402.46	13102.00	2730.08	16133.03	34.22	22.79	37.44	129
	119	42.00 - 40.52	1132.36	4449.66	8086.00	1151.67	16053.87	33.40	24.24	33.94	129
	120	40.52	2055.49	3466.38	5054.00	1631.42	15974.26	34.27	24.38	32.36	235
	121	40.52 - 38.69	841.54	2766.96	4977.00	1521.19	15844.91	34.61	20.65	32.95	238
	122	38.69	1035.75	5398.44	11000.00	2355.96	15752.92	29.95	20.84	31.76	242
	123	36.00	2218.27	6463.95	9004.00	2454.23	15661.35	30.21	25.11	35.35	241
	124	36.00	2039.90	4101.69	5858.00	1830.37	15513.76	27.97	26.88	33.03	241
	125	34.42 - 32.81	2187.59	7759.11	10677.00	2593.27	15388.91	28.90	27.05	34.48	241
	126	30.88 - 29.74	1608.59	5776.76	10307.00	2197.98	15228.35	27.19	27.23	50.36	237
	127	29.74 - 29.13	1035.72	3675.76	7326.00	1415.65	15073.04	28.01	22.90	53.07	236
	128	29.13 - 26.38	1684.28	6280.09	11043.00	1947.28	14965.85	27.81	27.23	57.63	226
	129	26.38 - 24.47	1420.62	4983.76	11739.00	3718.97	14852.33	28.67	27.99	65.22	219
	130	24.47	1124.36	4973.53	8296.00	1985.06	15610.18	29.03	27.70	65.12	236
	131	22.01	2164.51	4176.54	5085.00	654.54	14675.52	29.39	23.89	66.49	229
	132	22.01 - 17.64	1739.68	7018.52	21110.00	3419.36	14721.28	31.14	20.81	70.31	232
	133	17.64	2023.11	5253.93	13913.00	4248.60	14779.05	31.13	19.36	70.07	235
	134	14.01	3709.69	5908.00	6075.00	602.80	14893.54	20.38	46.89	55.45	243
	135	14.01 - 11.80	1709.75	10235.65	16197.00	2156.35	14942.83	17.91	48.91	36.13	242
	136	11.80	45669.61	8507.08	8495.00	1020.79	14815.93	20.16	39.64	26.91	242
	137	9.97 - 6.92	1564.26	7649.91	11855.00	2383.29	15062.25	21.85	33.09	32.89	243
	138	6.92 - 5.32	16273.70	11443.28	12049.00	1513.82	15711.39	23.51	28.25	12.91	241
	139	4.31 - 3.26	2323.23	7356.52	9374.00	2362.29	14196.84	20.18	30.67	2.71	235
	140	3.26 - 1.36	3232.98	8789.82	11726.00	1475.26	14318.53	22.09	25.63	2.97	234
	141	1.36 - 0.00	3506.07	9569.78	13062.00	4524.58	14689.87	19.96	31.24	3.19	223

Table E.1(Continued...). The Unified Table of Data.

Location	Section	Station	Channel Curvature (Rc/W)	Water Surface Angle (Degree)	Janderson Product (Rcτ/W)	Near Bank Stress	Channel Migration (ft)
BATESVILLE	1	295.27 - 293.21	9.69	0.000068	171.07	0.43	181
	2	293.21 - 291.27	5.91	0.000064	104.34	0.38	262
	3	290.54 - 287.90	4.14	0.000112	42.80	0.38	358
	4	286.54 - 285.34	8.11	0.000136	97.35	0.40	136
	5	285.34 - 283.60	3.76	0.000135	46.99	0.42	542
	6	281.04 - 280.00	34.35	0.000129	404.13	0.31	58
	7	280.00 - 276.57	5.77	0.000333	36.09	0.29	707
	8	276.57	3.02	0.000531	12.07	0.24	402
	9	276.57 - 274.71	8.80	0.000308	56.79	0.28	100
	10	270.75	3.73	0.000182	31.07	0.70	327
	11	270.75 - 268.78	6.72	0.000165	57.56	0.72	299
	12	268.78 - 266.28	3.21	0.000120	31.05	0.51	227
	13	266.28 - 262.47	5.23	0.000080	70.71	0.46	201
	14	262.47 - 260.98	3.91	0.000034	111.64	0.47	185
	15	260.98 - 258.72	3.10	0.000032	88.66	0.59	231
	16	258.72 - 257.25	4.44	0.000022	148.04	0.57	310
	17	258.94 - 256.89	4.75	0.000041	94.97	0.42	320
NEWPORT	18	256.89 - 253.08	5.09	0.000066	75.35	0.47	254
	19	253.08 - 248.95	6.13	0.000047	116.81	0.46	255
	20	247.80 - 240.36	6.38	0.000044	127.65	0.40	186
	21	240.36 - 238.48	4.63	0.000046	99.32	0.55	252
	22	238.48 - 234.98	2.76	0.000039	61.32	0.46	180
	23	234.98 - 234.22	3.17	0.000057	57.57	0.49	130
	24	232.55 - 231.45	3.40	0.000049	67.93	0.50	220
	25	231.45 - 228.89	4.89	0.000022	163.05	0.51	87
	26	228.89 - 227.78	4.10	0.000038	91.05	0.47	154
	27	227.78 - 226.14	7.56	0.000038	162.08	0.53	169
	28	226.14	2.21	0.000027	55.16	0.62	187
	29	223.9 - 221.53	4.27	0.000029	106.78	0.52	134
	30	221.53	4.46	0.000030	111.59	0.34	206
	31	219.41	3.69	0.000011	368.89	0.48	226
	32	219.41 - 216.97	3.78	0.000019	151.07	0.60	152
	33	216.97 - 215.33	3.43	0.000041	68.54	0.64	213
	34	215.33 - 213.33	3.25	0.000042	65.10	0.43	229
	35	213.33 - 207.17	4.27	0.000044	85.31	0.40	435
	36	207.17 - 203.71	4.36	0.000051	62.25	0.43	249
	37	201.56 - 201.01	3.62	0.000014	181.20	0.34	156
AUGUSTA	38	201.01 - 197.27	3.98	0.000049	68.67	0.34	264
	39	197.27 - 195.01	3.88	0.000097	38.85	0.49	250
	40	195.01 - 192.68	5.09	0.000103	47.09	0.48	247
	41	192.68 - 191.64	3.93	0.000088	39.31	0.36	174
	42	191.64 - 189.95	2.55	0.000065	36.49	0.34	218
	43	189.95 - 188.59	2.89	0.000048	52.48	0.48	200
	44	188.59 - 187.55	2.87	0.000073	35.86	0.63	229
	45	187.55 - 186.26	2.74	0.000104	23.79	0.54	180
	46	186.26 - 181.29	3.97	0.000104	36.53	0.36	108
	47	181.29 - 177.81	2.96	0.000074	33.63	0.32	503
	48	177.81 - 176.00	3.87	0.000056	55.23	0.36	201
	49	175.50 - 172.65	3.24	0.000070	43.21	0.58	183
	50	172.65 - 169.52	3.53	0.000068	44.19	0.52	395
	51	169.52 - 167.08	3.17	0.000091	33.39	0.48	475
	52	167.08 - 166.08	1.89	0.000078	22.24	0.53	500
	53	166.08 - 164.39	1.80	0.000041	32.65	0.44	208
	54	164.39 - 163.40	4.29	0.000069	53.63	0.40	208
	55	163.40 - 161.91	3.33	0.000091	33.26	0.43	258
	56	161.91 - 161.23	5.75	0.000098	60.53	0.49	273
	57	161.23 - 158.63	3.73	0.000107	37.28	0.43	144
	58	158.63	3.68	0.000110	33.43	0.42	212
	59	155.71 - 155.04	5.60	0.000058	74.69	0.40	175
	60	155.04 - 152.68	3.52	0.000061	46.98	0.35	590
	61	152.68 - 149.03	1.76	0.000057	27.13	0.45	352
	62	149.03 - 147.19	3.13	0.000097	32.39	0.50	296
DES ARC	63	147.19 - 145.72	2.78	0.000051	39.71	0.41	243
	64	145.72 - 143.75	8.95	0.000068	116.74	0.43	0
	65	143.75 - 141.78	3.32	0.000067	47.44	0.64	359
	66	141.78 - 140.39	3.25	0.000084	44.34	0.66	453
	67	140.39 - 139.21	5.74	0.000080	67.50	0.73	208
	68	139.21 - 138.01	2.97	0.000059	32.99	0.67	409
	69	138.01 - 136.03	6.67	0.000096	80.01	0.62	498
	70	136.03 - 135.16	2.67	0.000104	22.25	0.49	489
	71	133.65 - 132.61	2.94	0.000066	29.43	0.57	549
	72	132.61 - 130.54	3.91	0.000057	41.89	0.53	324
	73	130.54 - 128.70	4.60	0.000097	47.17	0.50	332
	74	128.70 - 124.33	3.55	0.000056	51.49	0.50	311

Table E.1(Continued...). The Unified Table of Data.

Location	Section	Station	Channel Curvature (Rc/W)	Water Surface Angle (Degree)	Janderson Product (Rc τ /W)	Near Bank Stess	Channel Migration (ft)
DEVALLS BLUFF	75	124.33 - 122.36	4.91	0.000036	98.30	0.43	644
	76	122.36 - 118.19	3.49	0.000024	102.62	0.50	346
	77	118.19 - 116.4	3.94	0.000031	98.38	0.55	227
	78	116.4 - 114.53	3.14	0.000026	89.74	0.52	653
	79	114.53 - 112.77	2.17	0.000010	108.54	0.52	512
	80	111.34	2.32	0.000005	231.56	0.22	340
	81	109.77 - 108.75	3.10	0.000025	103.28	0.48	134
	82	108.75 - 107.67	2.88	0.000021	57.70	0.60	516
	83	107.67	2.92	0.000016	41.74	0.70	477
	84	107.67 - 103.51	2.53	0.000032	30.41	0.61	265
	85	104.31 - 103.51	7.20	0.000040	79.99	0.57	235
	86	103.51 - 102.25	3.10	0.000062	44.28	0.52	222
	87	102.25 - 101.14	3.50	0.000073	87.58	0.71	208
	88	101.14 - 100.34	3.31	0.000046	90.41	0.52	393
CLARENDON	89	100.34 - 98.48	23.40	0.000022	584.89	0.36	174
	90	98.48 - 96.72	2.79	0.000043	34.88	0.49	224
	91	96.72 - 94.57	4.09	0.000071	48.16	0.49	100
	92	94.57 - 92.42	5.35	0.000056	89.25	0.42	183
	93	89.46 - 87.41	2.84	0.000054	28.45	0.44	168
	94	87.41 - 84.62	14.64	0.000081	156.84	0.58	138
	95	84.62 - 81.65	4.58	0.000068	72.35	0.56	156
	96	80.31 - 78.89	4.87	0.000037	74.92	0.58	242
	97	78.89	2.72	0.000046	45.36	0.71	225
	98	76.87 - 75.73	3.52	0.000061	43.96	0.52	156
	99	75.73 - 73.62	5.87	0.000074	78.25	0.54	171
	100	75.73 - 68.51	5.76	0.000071	85.26	0.47	132
	101	71.59 - 68.51	2.09	0.000034	34.77	0.39	188
	102	68.51 - 67.21	3.48	0.000049	87.03	0.48	103
	103	67.21 - 64.72	2.78	0.000069	50.51	0.42	166
	104	64.72	2.41	0.000069	30.11	0.29	190
	105	64.72 - 60.12	3.34	0.000060	43.61	0.30	164
	106	62.7 - 60.12	3.71	0.000055	49.43	0.31	218
	107	60.12 - 58.79	5.59	0.000046	79.93	0.37	264
	108	58.79 - 57.61	2.78	0.000056	37.09	0.66	313
	109	57.61 - 55.30	4.74	0.000048	86.16	0.48	156
ST. CHARLES	110	55.30 - 54.33	2.80	0.000057	43.13	0.47	182
	111	54.33 - 53.38	2.72	0.000080	30.17	0.63	171
	112	54.33 - 51.45	2.39	0.000072	31.16	0.69	418
	113	51.45	4.76	0.000055	95.27	0.81	217
	114	49.77 - 49.08	2.50	0.000066	34.11	0.39	459
	115	49.08 - 47.19	2.39	0.000056	36.84	0.41	283
	116	47.19	2.43	0.000080	24.30	0.37	214
	117	45.31	4.52	0.000089	41.06	0.47	90
	118	45.31 - 42.00	3.29	0.000102	25.31	0.50	181
	119	42.00 - 40.52	2.36	0.000115	16.83	0.44	300
	120	40.52	4.41	0.000115	33.92	0.34	170
	121	40.52 - 38.69	1.84	0.000111	18.38	0.36	288
	122	38.69	1.97	0.000076	28.14	0.39	230
	123	36.00	4.28	0.000044	38.90	0.65	225
	124	36.00	3.68	0.000044	33.43	0.65	114
	125	34.42 - 32.81	4.11	0.000092	34.23	0.59	125
	126	30.88 - 29.74	2.87	0.000116	28.72	0.75	210
	127	29.74 - 29.13	1.92	0.000083	27.50	0.59	486
	128	29.13 - 26.38	3.13	0.000071	34.78	0.51	337
	129	26.38 - 24.47	2.74	0.000091	28.87	0.52	600
	130	24.47	2.09	0.000069	17.43	0.54	302
	131	22.01	4.33	0.000104	48.16	0.45	126
	132	22.01 - 17.64	3.68	0.000086	38.74	0.47	291
	133	17.64	4.26	0.000068	42.61	0.49	173
	134	14.01	5.08	0.000070	72.54	0.47	122
	135	14.01 - 11.80	2.05	0.000071	29.27	0.47	832
	136	11.80	62.14	0.000064	887.65	0.47	190
	137	9.97 - 6.92	2.27	0.000051	34.04	0.38	449
	138	6.92 - 5.32	24.35	0.000034	486.94	0.37	163
	139	4.31 - 3.26	3.30	0.000032	73.37	0.50	262
	140	3.26 - 1.36	4.99	0.000027	115.09	0.55	205
	141	1.36 - 0.00	4.76	0.000021	158.80	0.51	175

Table E.1(Continued...). The Unified Table of Data.

Location	Section	Station	Types of Meander Migration	Descriptions of Channel Metamorphoses
BATESVILLE	1	295.27 - 293.21	Lateral	180.8 ft shift
	2	293.21 - 291.27	Lateral	261.96 ft shift and channel widening
	3	290.54 - 287.90	Lateral	358 ft shift
	4	286.54 - 285.34	Lateral	136.27 ft shift
	5	285.34 - 283.60	Lateral	542 ft shift and slight channel widening
	6	281.04 - 280.00	Lateral	58 ft shift
	7	280.00 - 276.57	Lateral & Rotational	707 ft shift
	8	276.57	Lateral & Rotational	402 ft shift, channel widening, and enhancements in streampower/velocity
	9	276.57 - 274.71	Lateral & Rotational	100 ft shift
	10	270.75	Lateral & Rotational	326.7 ft shift and channel widening
	11	270.75 - 268.78	Lateral	299 ft shift and perceivable channel widening
	12	268.78 - 266.28	Lateral	227 ft shift and channel widening
	13	266.28 - 262.47	Lateral	200.5 ft shift
	14	262.47 - 260.98	Lateral	184.5 ft shift
	15	260.98 - 258.72	Lateral	231 ft shift and slight channel widening
	16	258.72 - 257.25	Lateral & Rotational	309.66 ft shift and an anterior neck cut-off
	17	258.94 - 256.89	Lateral & Rotational	320 ft shift and slight channel narrowing
	18	256.89 - 253.08	Lateral	253.5 ft shift and perceivable channel widening
	19	253.08 - 248.95	Lateral	254.77 ft shift
	20	247.80 - 240.36	Lateral & Rotational	186 ft shift *
	21	240.36 - 238.48	Lateral & Rotational	252.35 ft shift and close to cut-off
	22	238.48 - 234.98	Lateral & Rotational	180 ft shift and close to cut-off
	23	234.98 - 234.22	Lateral	130 ft shift
	24	232.55 - 231.45	Lateral & Rotational	219.67 ft shift and close to cut-off
	25	231.45 - 228.89	Lateral	87 ft shift and close to cut-off
	26	228.89 - 227.78	Lateral	154 ft shift and perceivable channel widening
	27	227.78 - 226.14	Lateral	168.56 ft shift
	28	226.14	Lateral & Rotational	187.4 ft shift and slight channel widening
	29	223.9 - 221.53	Lateral	134.19 ft shift
	30	221.53	Lateral	206.3 ft shift and channel widening
	31	219.41	Lateral	225.59 ft shift, perceivable channel widening, and close to cut-off
	32	219.41 - 216.97	Lateral	151.8 ft shift
	33	216.97 - 215.33	Lateral & Rotational	213 ft shift and very perceivable channel widening the entire bend
	34	215.33 - 213.33	Lateral	228.91 ft shift and very perceivable channel widening
	35	213.33 - 207.17	Lateral & Rotational	435 ft shift and very perceivable channel widening
	36	207.17 - 203.71	Lateral & Rotational	248.65 ft shift and perceivable channel widening
	37	201.56 - 201.01	Lateral & Rotational	156.29 ft shift, slight channel widening, and very close to cut-off
AUGUSTA	38	201.01 - 197.27	Lateral	264.2 ft shift and very close to cut-off
	39	197.27 - 195.01	Lateral & Rotational	250.28 ft shift, slight channel widening, and very close to cut-off
	40	195.01 - 192.68	Lateral	246.75 ft shift and close to cut-off
	41	192.68 - 191.64	Lateral & Rotational	173.94 ft shift and perceivable channel widening
	42	191.64 - 189.95	Lateral & Rotational	217.60 ft shift and very close to cut-off
	43	189.95 - 188.59	Lateral & Rotational	199.70 ft shift and very perceivable channel widening the entire bend
	44	188.59 - 187.55	Lateral	228.89 ft shift and perceivable channel widening
	45	187.55 - 186.26	Lateral & Rotational	179.6 ft shift and very perceivable channel widening *
	46	186.26 - 181.29	Lateral	108 ft shift and perceivable channel widening
	47	181.29 - 177.81	Lateral & Rotational	503.1 ft shift, very perceivable channel widening, and two anterior neck cut-offs *
	48	177.81 - 176.00	Lateral	200.76 ft shift and an anterior neck cut-off
	49	175.50 - 172.65	Lateral & Rotational	183.20 ft shift *
	50	172.65 - 169.52	Lateral & Rotational	395.4 ft shift and very perceivable channel widening the entire bend *
	51	169.52 - 167.08	Lateral & Rotational	475 ft shift, very perceivable channel widening, and an anterior neck cut-off
	52	167.08 - 166.08	Lateral & Rotational	500 ft shift, very perceivable channel widening, and an anterior neck cut-off
	53	166.08 - 164.39	Lateral & Rotational	207.5 ft shift, very perceivable channel widening, and close to cut-off
	54	164.39 - 163.40	Lateral	207.5 ft shift and close to cut-off
	55	163.40 - 161.91	Lateral & Rotational	258.0 ft shift and very perceivable channel widening
	56	161.91 - 161.23	Lateral & Rotational	272.59 ft shift and very perceivable channel widening the entire bend
	57	161.23 - 158.63	Lateral	143.7 ft shift and slight channel widening
DES ARC	58	158.63	Lateral & Rotational	211.87 ft shift and perceivable channel widening the entire bend
	59	155.71 - 155.04	Lateral & Rotational	174.98 ft shift and slight channel widening *
	60	155.04 - 152.68	Lateral & Rotational	590 ft shift, slight channel widening, and an anterior neck cut-off
	61	152.68 - 149.03	Lateral & Rotational	352.3 ft shift and very perceivable channel widening
	62	149.03 - 147.19	Lateral & Rotational	295.77 ft shift, perceivable channel widening, and an anterior neck cut-off
	63	147.19 - 145.72	Lateral & Rotational	242.89 ft shift, very perceivable channel widening, and an anterior neck cut-off
	64	145.72 - 143.75	N/A	No shift and a perceivable channel widening
	65	143.75 - 141.78	Lateral, Rotational, & Elongated	358.8 ft shift and perceivable channel widening and narrowing
	66	141.78 - 140.39	Lateral & Rotational	453 ft shift, very perceivable channel widening the entire bend, and an anterior neck cut-off
	67	140.39 - 139.21	Lateral	208.33 ft shift and slightly perceivable channel widening
	68	139.21 - 138.01	Lateral & Rotational	409.14 ft shift and perceivable channel widening
	69	138.01 - 136.03	Lateral	498 ft shift and very perceivable channel widening entire bend
	70	136.03 - 135.16	Lateral & Rotational	488.6 ft shift and perceivable channel widening
	71	133.65 - 132.61	Lateral & Rotational	548.77 ft shift and perceivable channel widening
	72	132.61 - 130.54	Lateral & Rotational	323.8 ft shift, perceivable channel widening, an anterior neck cut-off
	73	130.54 - 128.70	Lateral	332.16 ft shift and perceivable channel widening
	74	128.70 - 124.33	Lateral & Rotational	311.35 ft shift

Table E.1(Continued...). The Unified Table of Data.

Location	Section	Station	Types of Meander Migration	Descriptions of Channel Metamorphoses
DEVALLS BLUFF	75	124.33 - 122.36	Lateral & Rotational	643.65 ft shift, perceivable channel widening, multiple anterior neck cut-offs, and slope changes
	76	122.36 - 118.19	Lateral & Rotational	346.39 ft shift and an anterior neck cut-off
	77	118.19 - 116.4	Lateral & Rotational	227.25 ft shift, perceivable channel widening the entire bend, and extremely close to cut-off
	78	116.4 - 114.53	Lateral & Rotational	652.8 ft shift, perceivable channel widening the entire bend, and two anterior neck cut-offs
	79	114.53 - 112.77	Lateral & Rotational	512.28 ft shift and perceivable channel widening the entire bend
	80	111.34	Lateral & Rotational	339.70 ft shift and very perceivable channel widening the entire bend
	81	109.77 - 108.75	Lateral	134 ft shift, perceivable channel widening, and an anterior neck-cut off
	82	108.75 - 107.67	Lateral & Rotational	516.4 ft shift, perceivable channel widening the entire bend, and an anterior neck cut-off
	83	107.67	Rotational	476.5 ft shift and very perceivable channel widening the entire bend
	84	107.67 - 103.51	Lateral & Rotational	265.33 ft shift, perceivable channel widening entire bend, and extremely close to neck-cut-off
	85	104.31 - 103.51	Lateral & Rotational	234.5 ft shift, perceivable channel widening entire bend, and extremely close to neck-cut-off
CLARENDON	86	103.51 - 102.25	Lateral & Rotational	221.67 ft shift and very perceivable channel widening entire bend
	87	102.25 - 101.14	Lateral & Rotational	208.27 ft shift (perceivable, mainly lateral, slightly rotational shifts entire bend)
	88	101.14 - 100.34	Lateral & Rotational	393 ft shift, perceivable channel widening the entire bend, and an anterior neck cut-off
	89	100.34 - 98.48	Lateral	174.03 ft shift and slight channel widening
	90	98.48 - 96.72	Lateral & Rotational	223.69 ft shift and perceivable channel widening entire bend
	91	96.72 - 94.57	Lateral	100 ft shift and slight channel widening
	92	94.57 - 92.42	Lateral	182.79 ft shift
	93	89.46 - 87.41	Lateral & Rotational	167.6 ft shift and slight channel widening
	94	87.41 - 84.62	Lateral	138 ft shift and perceivable channel widening
	95	84.62 - 81.65	Lateral	156.49 ft shift
	96	80.31 - 78.89	Lateral	242.3 ft shift, slight channel widening, and an anterior neck cut-off
	97	78.89	Lateral	224.5 ft shift and an anterior cut-off
	98	76.87 - 75.73	Lateral	155.79 ft shift and slight channel widening
	99	75.73 - 73.62	Lateral & Rotational	171.3 ft shift
	100	75.73 - 68.51	Lateral	132 ft shift and slight channel widening
	101	71.59 - 68.51	Lateral & Rotational	188.29 ft shift, slight channel widening, and an oval loop planform
	102	68.51 - 67.21	Lateral	103 ft shift and slight channel widening
	103	67.21 - 64.72	Lateral & Rotational	165.99 ft shift and slight channel widening
	104	64.72	Lateral	189.75 ft shift and slight channel widening
	105	64.72 - 60.12	Lateral & Rotational	163.75 ft shift (perceivable lateral and rotational shifts entire bend)
	106	62.7 - 60.12	Lateral & Rotational	217.54 ft shift and slight channel widening
	107	60.12 - 58.79	Lateral	264.2 ft shift
	108	58.79 - 57.61	Lateral & Rotational	313.3 ft shift and slight channel widening
	109	57.61 - 55.30	Lateral	155.66 ft shift and slight channel widening
ST. CHARLES	110	55.30 - 54.33	Lateral	181.8 ft shift and slight channel widening
	111	54.33 - 53.38	Lateral & Rotational	170.8 ft shift and slight channel widening
	112	54.33 - 51.45	Rotational	418 ft shift, and fluctuation in mobility index and stream power
	113	51.45	Lateral & Rotational	216.68 ft shift and perceivable channel widening the entire bend
	114	49.77 - 49.08	Lateral & Rotational	458.70 ft shift and slight channel narrowing *
	115	49.08 - 47.19	Lateral & Rotational	283.36 ft shift and close to cut-off *
	116	47.19	Lateral & Rotational	214.19 ft shift and slight channel widening *
	117	45.31	Lateral	90 ft shift and slight channel widening
	118	45.31 - 42.00	Lateral	181.05 ft shift and an s-loop planform *
	119	42.00 - 40.52	Lateral & Rotational	300 ft shift and longitudinal gradient changes *
	120	40.52	Lateral	170 ft shift and perceivable channel widening the entire bend *
	121	40.52 - 38.69	Lateral & Rotational	287.79 ft shift and slight channel narrowing *
	122	38.69	Lateral & Rotational	230 ft shift and slight channel widening the entire bend *
	123	36.00	Lateral	225 ft shift and slight channel widening *
	124	36.00	Lateral	113.5 ft shift *
	125	34.42 - 32.81	Lateral	125 ft shift and slight channel widening *
	126	30.88 - 29.74	Lateral & Rotational	209.8 ft shift *
	127	29.74 - 29.13	Lateral & Rotational	485.85 ft shift and perceivable channel widening/narrowing the entire bend
	128	29.13 - 26.38	Lateral & Rotational	336.66 ft shift and perceivable channel widening
	129	26.38 - 24.47	Lateral & Rotational	600 ft shift and very perceivable channel widening the entire bend
	130	24.47	Lateral & Rotational	301.70 ft shift and slight channel narrowing
	131	22.01	Lateral	126.20 ft shift and slight channel widening the entire bend
	132	22.01 - 17.64	Lateral & Rotational	290.8 ft shift and slight channel widening
	133	17.64	Lateral & Rotational	172.60 ft shift
	134	14.01	Lateral & Rotational	122 ft shift
	135	14.01 - 11.80	Lateral & Rotational	832 ft shift, extreme channel widening the entire bend, and a tortuous s-loop planform
	136	11.80	Lateral	190 ft shift and slight channel widening the entire bend
	137	9.97 - 6.92	Lateral & Rotational	448.8 ft shift and perceivable channel widening/narrowing the entire bend
	138	6.92 - 5.32	Lateral	163 ft shift
	139	4.31 - 3.26	Lateral	261.80 ft shift and perceivable channel widening the entire bend
	140	3.26 - 1.36	Lateral & Rotational	204.7 ft shift and perceivable channel widening
	141	1.36 - 0.00	Lateral	175 ft shift and very perceivable channel widening the entire bend

Note: Red font denotes diminishment in sinuosity over time

Note: * denotes nearby levee

Table E.2. Sediment Analyses.

Location	Section	Station	S _o	V (ft/s)	y _o (ft)	d ₅₀ (ft)	d ₉₀ (ft)	Flow (cfs)	Width (ft)	q (ft ² /s)	d _s	w _f (ft/s)	τ _{ec}	μ _{sc} (ft/s)	μ _s (ft/s)	μ _s /w _f	Dominant Trans. Mech	
BATESVILLE	1	295.27 - 293.21	0.00010	2.70	14.13	0.00062	0.20997	18747.65	499.03	37.57	4.82	0.08180	0.05500	0.04240	0.21330	2.61	Bed Load	
	2	293.21 - 291.27	0.00010	2.68	14.46	0.00062	0.20997	18750.00	506.27	37.04	4.82	0.08180	0.05500	0.04240	0.21578	2.64	Bed Load	
	3	290.54 - 287.90	0.00010	3.50	14.35	0.00062	0.20997	18745.17	381.69	49.11	4.82	0.08180	0.05500	0.04240	0.21496	2.63	Bed Load	
	4	286.54 - 285.34	0.00010	3.22	11.29	0.00062	0.20997	18743.97	535.55	35.00	4.82	0.08180	0.05500	0.04240	0.19069	2.33	Bed Load	
	5	285.34 - 283.60	0.00010	3.10	10.91	0.00062	0.20997	17159.51	534.01	32.13	4.82	0.08180	0.05500	0.04240	0.18743	2.29	Bed Load	
	6	281.04 - 280.00	0.00010	3.18	10.98	0.00062	0.20997	16949.70	512.05	33.10	4.82	0.08180	0.05500	0.04240	0.18799	2.30	Bed Load	
	7	280.00 - 276.57	0.00017	4.01	8.10	0.00062	0.20997	16150.83	531.38	30.39	4.82	0.08180	0.05500	0.04240	0.21057	2.57	Bed Load	
	8	276.57	0.00012	5.22	7.56	0.00062	0.20997	17152.26	434.21	39.50	4.82	0.08180	0.05500	0.04240	0.17091	2.09	Bed Load	
	9	276.57 - 274.71	0.00012	4.01	9.69	0.00062	0.20997	17405.54	484.03	35.96	4.82	0.08180	0.05500	0.04240	0.19350	2.37	Bed Load	
	10	270.75	0.00012	3.88	10.61	0.00062	0.20997	16729.22	406.63	41.14	4.82	0.08180	0.05500	0.04240	0.20248	2.48	Bed Load	
	11	270.75 - 268.78	0.00015	3.84	10.43	0.00062	0.20997	17825.71	447.53	39.83	4.82	0.08180	0.05500	0.04240	0.22441	2.74	Bed Load	
	12	268.78 - 266.28	0.00015	3.47	11.23	0.00062	0.20997	18428.15	474.75	38.82	4.82	0.08180	0.05500	0.04240	0.23293	2.85	Bed Load	
	13	266.28 - 262.47	0.00015	2.94	12.46	0.00062	0.20997	18392.87	520.70	35.32	4.82	0.08180	0.05500	0.04240	0.24532	3.00	Bed Load	
	14	262.47 - 260.98	0.00008	2.12	14.72	0.00062	0.20997	17694.72	571.52	30.96	4.82	0.08180	0.05500	0.04240	0.19469	2.38	Bed Load	
	15	260.98 - 258.72	0.00008	2.17	15.85	0.00062	0.20997	20723.40	600.64	34.50	4.82	0.08180	0.05500	0.04240	0.20206	2.47	Bed Load	
	16	258.72 - 257.25	0.00008	2.13	17.84	0.00062	0.20997	23087.23	613.27	37.65	4.82	0.08180	0.05500	0.04240	0.21435	2.62	Bed Load	
	17	258.94 - 256.89	0.00008	2.25	18.09	0.00062	0.00164	23485.22	579.16	40.55	4.82	0.08180	0.05500	0.04240	0.21584	2.64	Suspended Load	
NEWPORT	18	256.89 - 253.08	0.00008	2.64	16.50	0.00062	0.00164	23557.52	547.47	43.03	4.82	0.08180	0.05500	0.04240	0.20618	2.52	Suspended Load	
	19	253.08 - 248.95	0.00008	2.31	18.20	0.00062	0.00164	23733.00	581.84	40.79	4.82	0.08180	0.05500	0.04240	0.21653	2.65	Suspended Load	
	20	247.80 - 240.36	0.00008	2.31	18.31	0.00062	0.00164	23905.60	576.31	41.48	4.82	0.08180	0.05500	0.04240	0.21715	2.65	Suspended Load	
	21	240.36 - 238.48	0.00008	2.26	16.78	0.00062	0.00164	23919.72	633.82	37.74	4.82	0.08180	0.05500	0.04240	0.20793	2.54	Suspended Load	
	22	238.48 - 234.98	0.00008	2.30	19.90	0.00062	0.00164	23952.34	531.30	45.08	4.82	0.08180	0.05500	0.04240	0.22641	2.77	Suspended Load	
	23	234.98 - 234.22	0.00008	2.40	17.55	0.00062	0.00164	23949.31	589.67	40.62	4.82	0.08180	0.05500	0.04240	0.21259	2.60	Suspended Load	
	24	232.55 - 231.45	0.00008	2.41	19.67	0.00062	0.00164	23975.31	543.11	44.14	4.82	0.08180	0.05500	0.04240	0.22510	2.75	Suspended Load	
	25	231.45 - 228.89	0.00008	1.98	24.99	0.00062	0.00164	23966.35	489.63	48.95	4.82	0.08180	0.05500	0.04240	0.25372	3.10	Suspended Load	
	26	228.89 - 227.78	0.00008	2.24	22.44	0.00062	0.00164	23964.57	495.79	48.34	4.82	0.08180	0.05500	0.04240	0.24040	2.94	Suspended Load	
	27	227.78 - 226.14	0.00008	2.27	20.33	0.00062	0.00164	23523.17	513.82	45.78	4.82	0.08180	0.05500	0.04240	0.22886	2.80	Suspended Load	
	28	226.14	0.00002	2.05	21.62	0.00062	0.00164	23010.27	521.44	44.13	4.82	0.08180	0.05500	0.04240	0.11800	1.44	Mixed Load	
	29	223.9 - 221.53	0.00002	2.11	21.94	0.00062	0.00164	21434.84	470.24	45.58	4.82	0.08180	0.05500	0.04240	0.11887	1.45	Mixed Load	
	30	221.53	0.00002	2.07	20.29	0.00062	0.00164	22912.23	507.34	45.16	4.82	0.08180	0.05500	0.04240	0.11431	1.40	Mixed Load	
	31	219.41	0.00002	1.28	20.92	0.00062	0.00164	11951.97	504.03	23.71	4.82	0.08180	0.05500	0.04240	0.11607	1.42	Mixed Load	
	32	219.41 - 216.97	0.00002	1.71	22.08	0.00062	0.00164	17345.29	452.65	38.32	4.82	0.08180	0.05500	0.04240	0.11925	1.46	Mixed Load	
	33	216.97 - 215.33	0.00002	2.40	21.04	0.00062	0.00164	22789.96	456.49	49.92	4.82	0.08180	0.05500	0.04240	0.11640	1.42	Mixed Load	
	34	215.33 - 213.33	0.00002	2.33	19.35	0.00062	0.00164	22161.78	498.97	44.41	4.82	0.08180	0.05500	0.04240	0.11162	1.36	Mixed Load	
	35	213.33 - 207.17	0.00002	2.30	18.93	0.00062	0.00164	22092.23	486.42	41.72	4.82	0.08180	0.05500	0.04240	0.11040	1.35	Mixed Load	
	36	207.17 - 203.71	0.00002	2.68	22.40	0.00062	0.00164	25531.03	430.34	59.33	4.82	0.08180	0.05500	0.04240	0.12011	1.47	Mixed Load	
	37	201.56 - 201.01	0.00002	1.23	20.75	0.00062	0.00164	13135.33	515.50	25.48	4.82	0.08180	0.05500	0.04240	0.11558	1.41	Mixed Load	
		38	201.01 - 197.27	0.00002	2.12	19.33	0.00031	0.00164	21315.04	535.71	39.79	2.40	0.02526	0.09000	0.03830	0.11158	4.42	Suspended Load
	AUGUSTA	39	197.27 - 195.01	0.00008	2.83	16.40	0.00031	0.00164	25876.94	558.33	46.35	2.40	0.02526	0.09000	0.03830	0.20554	8.14	Suspended Load
		40	195.01 - 192.68	0.00008	2.95	17.06	0.00031	0.00164	25858.19	523.75	49.37	2.40	0.02526	0.09000	0.03830	0.20963	8.30	Suspended Load
		41	192.68 - 191.64	0.00008	2.90	18.38	0.00031	0.00164	27221.56	515.10	52.85	2.40	0.02526	0.09000	0.03830	0.21759	8.61	Suspended Load
		42	191.64 - 189.95	0.00008	2.35	17.63	0.00031	0.00164	21615.80	519.24	41.63	2.40	0.02526	0.09000	0.03830	0.21308	8.44	Suspended Load
		43	189.95 - 188.59	0.00008	2.14	18.60	0.00031	0.00164	17570.26	445.20	39.47	2.40	0.02526	0.09000	0.03830	0.21889	8.67	Suspended Load
		44	188.59 - 187.55	0.00008	2.54	17.77	0.00031	0.00164	23598.69	527.93	44.70	2.40	0.02526	0.09000	0.03830	0.21395	8.47	Suspended Load
		45	187.55 - 186.26	0.00008	3.04	17.77	0.00031	0.00164	27248.46	522.43	52.16	2.40	0.02526	0.09000	0.03830	0.21395	8.47	Suspended Load
		46	186.26 - 181.29	0.00008	2.98	16.59	0.00031	0.00164	26604.98	558.24	47.66	2.40	0.02526	0.09000	0.03830	0.20671	8.18	Suspended Load
		47	181.29 - 177.81	0.00008	2.54	19.76	0.00031	0.00164	22947.00	484.84	47.33	2.40	0.02526	0.09000	0.03830	0.22561	8.93	Suspended Load
		48	177.81 - 176.00	0.00008	2.38	19.91	0.00031	0.00164	27975.21	603.18	46.38	2.40	0.02526	0.09000	0.03830	0.22645	8.96	Suspended Load
		49	175.50 - 172.65	0.00008	2.51	18.60	0.00031	0.00164	28249.06	613.60	46.04	2.40	0.02526	0.09000	0.03830	0.21891	8.67	Suspended Load
50		172.65 - 169.52	0.00008	2.68	20.43	0.00031	0.00164	28081.11	533.36	52.65	2.40	0.02526	0.09000	0.03830	0.22941	9.08	Suspended Load	
51		169.52 - 167.08	0.00008	2.94	17.20	0.00031	0.00164	28003.01	560.36	49.97	2.40	0.02526	0.09000	0.03830	0.21051	8.33	Suspended Load	
52		167.08 - 166.08	0.00008	2.91	18.43	0.00031	0.00164	28752.64	542.56	52.99	2.40	0.02526	0.09000	0.03830	0.21789	8.63	Suspended Load	
53		166.08 - 164.39	0.00008	2.42	22.54	0.00031	0.00164	25598.14	470.75	54.38	2.40	0.02526	0.09000	0.03830	0.24094	9.54	Suspended Load	
54		164.39 - 163.40	0.00008	2.79	20.90	0.00031	0.00164	25577.09	451.14	56.69	2.40	0.02526	0.09000	0.03830	0.23203	9.19	Suspended Load	
55		163.40 - 161.91	0.00008	3.16	17.79	0.00031	0.00164	29925.70	535.46	55.89	2.40	0.02526	0.09000	0.03830	0.21407	8.47	Suspended Load	
56		161.91.																

Table E.2(Continued...). Sediment Analyses.

Location	Section	Station	S _o	V (ft/s)	y _o (ft)	d ₅₀ (ft)	d ₉₀ (ft)	Flow (cfs)	Width (ft)	q (ft ² /s)	d _s	w _r (ft/s)	τ _o	μ _o (ft/s)	μ _s (ft/s)	μ _s /w _r	Dominant Trans. Mech
DEVALLS BLUFF	75	124.33 - 122.36	0.00003	2.44	25.52	0.00062	0.00082	29600.12	514.31	57.55	4.82	0.08180	0.05500	0.04240	0.15701	1.92	Mixed Load
	76	122.36 - 118.19	0.00003	1.95	26.06	0.00062	0.00082	27535.18	476.57	57.78	4.82	0.08180	0.05500	0.04240	0.15866	1.94	Mixed Load
	77	118.19 - 116.4	0.00003	2.07	21.65	0.00062	0.00082	27297.57	555.76	49.12	4.82	0.08180	0.05500	0.04240	0.14462	1.77	Mixed Load
	78	116.4 - 114.53	0.00003	1.94	24.63	0.00062	0.00082	28295.73	616.02	45.93	4.82	0.08180	0.05500	0.04240	0.15425	1.89	Mixed Load
	79	114.53 - 112.77	0.00003	1.46	30.83	0.00062	0.00082	27242.09	547.05	49.80	4.82	0.08180	0.05500	0.04240	0.17257	2.11	Mixed Load
	80	111.34	0.00003	1.15	31.97	0.00062	0.00082	25512.41	624.66	40.84	4.82	0.08180	0.05500	0.04240	0.17574	2.15	Mixed Load
	81	109.77 - 108.75	0.00003	1.72	25.89	0.00062	0.00082	19823.25	696.18	28.47	4.82	0.08180	0.05500	0.04240	0.15814	1.93	Mixed Load
	82	108.75 - 107.67	0.00003	2.18	22.53	0.00062	0.00082	22097.49	446.29	49.51	4.82	0.08180	0.05500	0.04240	0.14753	1.80	Mixed Load
	83	107.67	0.00006	2.64	19.17	0.00062	0.00082	24371.73	463.58	52.57	4.82	0.08180	0.05500	0.04240	0.19245	2.35	Mixed Load
	84	107.67 - 103.51	0.00006	2.95	19.93	0.00062	0.00082	25422.13	503.04	50.54	4.82	0.08180	0.05500	0.04240	0.19621	2.40	Mixed Load
	85	104.31 - 103.51	0.00006	3.11	20.31	0.00062	0.00082	25947.33	482.16	53.82	4.82	0.08180	0.05500	0.04240	0.19806	2.42	Mixed Load
	86	103.51 - 102.25	0.00006	2.57	19.10	0.00062	0.00082	22047.27	411.81	53.54	4.82	0.08180	0.05500	0.04240	0.19210	2.35	Mixed Load
	87	102.25 - 101.14	0.00006	1.98	20.06	0.00062	0.00082	20856.75	464.16	44.93	4.82	0.08180	0.05500	0.04240	0.19687	2.41	Mixed Load
	88	101.14 - 100.34	0.00006	1.95	21.70	0.00020	0.05249	22443.26	524.71	42.77	1.59	0.01146	0.12500	0.03675	0.20475	17.87	Suspended Load
CLARENDON	89	100.34 - 98.48	0.00006	1.98	24.88	0.00020	0.05249	25299.13	529.73	47.76	1.59	0.01146	0.12500	0.03675	0.21923	19.13	Suspended Load
	90	98.48 - 96.72	0.00006	2.45	23.74	0.00020	0.05249	29997.77	547.03	54.84	1.59	0.01146	0.12500	0.03675	0.21414	18.69	Suspended Load
	91	96.72 - 94.57	0.00006	2.54	18.25	0.00020	0.05249	29622.65	677.52	43.72	1.59	0.01146	0.12500	0.03675	0.18775	16.38	Suspended Load
	92	94.57 - 92.42	0.00006	2.17	19.37	0.00020	0.05249	30981.21	653.46	47.41	1.59	0.01146	0.12500	0.03675	0.19342	16.88	Suspended Load
	93	89.46 - 87.41	0.00006	2.70	23.33	0.00020	0.05249	31359.17	629.36	49.83	1.59	0.01146	0.12500	0.03675	0.21228	18.52	Suspended Load
	94	87.41 - 84.62	0.00006	2.63	19.24	0.00020	0.05249	31048.98	670.46	46.31	1.59	0.01146	0.12500	0.03675	0.19278	16.82	Suspended Load
	95	84.62 - 81.65	0.00006	2.19	17.71	0.00020	0.05249	25875.16	627.07	41.26	1.59	0.01146	0.12500	0.03675	0.18499	16.14	Suspended Load
	96	80.31 - 78.89	0.00006	2.27	20.22	0.00020	0.05249	27056.13	533.57	50.71	1.59	0.01146	0.12500	0.03675	0.19765	17.25	Suspended Load
	97	78.89	0.00006	2.14	18.35	0.00020	0.05249	23760.04	544.63	43.63	1.59	0.01146	0.12500	0.03675	0.18829	16.43	Suspended Load
	98	76.87 - 75.73	0.00006	2.48	19.81	0.00020	0.05249	26265.31	593.02	44.29	1.59	0.01146	0.12500	0.03675	0.19561	17.07	Suspended Load
	99	75.73 - 73.62	0.00006	2.44	17.91	0.00020	0.05249	23999.42	533.60	44.98	1.59	0.01146	0.12500	0.03675	0.18602	16.23	Suspended Load
	100	75.73 - 68.51	0.00006	2.35	19.01	0.00020	0.05249	25210.59	521.54	48.34	1.59	0.01146	0.12500	0.03675	0.19162	16.72	Suspended Load
	101	71.59 - 68.51	0.00006	2.26	19.09	0.00020	0.05249	26421.76	621.46	42.52	1.59	0.01146	0.12500	0.03675	0.19202	16.76	Suspended Load
	102	68.51 - 67.21	0.00006	1.81	20.35	0.00020	0.05249	21860.03	591.23	36.97	1.59	0.01146	0.12500	0.03675	0.19826	17.30	Suspended Load
	103	67.21 - 64.72	0.00006	2.03	18.99	0.00020	0.05249	24456.49	630.86	38.77	1.59	0.01146	0.12500	0.03675	0.19154	16.71	Suspended Load
	104	64.72	0.00006	2.47	18.89	0.00020	0.05249	30589.05	555.10	55.11	1.59	0.01146	0.12500	0.03675	0.19104	16.67	Suspended Load
	105	64.72 - 60.12	0.00006	2.44	21.10	0.00020	0.05249	28475.30	480.12	59.31	1.59	0.01146	0.12500	0.03675	0.20190	17.62	Suspended Load
	106	62.7 - 60.12	0.00006	2.43	22.21	0.00020	0.05249	27418.42	518.38	52.89	1.59	0.01146	0.12500	0.03675	0.20712	18.07	Suspended Load
	107	60.12 - 58.79	0.00006	2.36	24.05	0.00020	0.05249	26709.85	473.02	56.47	1.59	0.01146	0.12500	0.03675	0.21556	18.81	Suspended Load
	108	58.79 - 57.61	0.00006	2.40	21.42	0.00020	0.05249	26511.57	517.45	51.24	1.59	0.01146	0.12500	0.03675	0.20341	17.75	Suspended Load
ST. CHARLES	109	57.61 - 55.30	0.00006	2.02	18.73	0.00062	0.20997	21054.22	558.75	37.68	4.82	0.08180	0.05500	0.04240	0.19020	2.33	Mixed Load
	110	55.30 - 54.33	0.00006	2.22	19.19	0.00062	0.20997	21970.35	517.82	42.43	4.82	0.08180	0.05500	0.04240	0.19252	2.35	Mixed Load
	111	54.33 - 53.38	0.00006	2.65	18.88	0.00062	0.20997	21681.53	438.69	49.42	4.82	0.08180	0.05500	0.04240	0.19096	2.33	Mixed Load
	112	54.33 - 51.45	0.00006	2.40	17.66	0.00062	0.20997	20572.33	430.84	47.75	4.82	0.08180	0.05500	0.04240	0.18470	2.26	Mixed Load
	113	51.45	0.00006	1.91	15.22	0.00062	0.20997	18353.93	475.29	38.62	4.82	0.08180	0.05500	0.04240	0.17148	2.10	Mixed Load
	114	49.77 - 49.08	0.00006	2.27	17.77	0.00062	0.20997	30166.93	723.61	41.69	4.82	0.08180	0.05500	0.04240	0.18529	2.27	Mixed Load
	115	49.08 - 47.19	0.00006	2.20	18.74	0.00062	0.20997	29037.49	449.13	64.65	4.82	0.08180	0.05500	0.04240	0.19028	2.33	Mixed Load
	116	47.19	0.00006	2.80	20.58	0.00062	0.20997	25918.44	437.71	59.21	4.82	0.08180	0.05500	0.04240	0.19940	2.44	Mixed Load
	117	45.31	0.00006	2.98	20.83	0.00062	0.20997	30488.62	481.16	63.36	4.82	0.08180	0.05500	0.04240	0.20061	2.45	Mixed Load
	118	45.31 - 42.00	0.00006	3.18	20.69	0.00062	0.20997	30918.57	471.48	65.58	4.82	0.08180	0.05500	0.04240	0.19991	2.44	Mixed Load
	119	42.00 - 40.52	0.00006	3.25	19.83	0.00062	0.20997	30814.59	480.59	64.12	4.82	0.08180	0.05500	0.04240	0.19573	2.39	Mixed Load
	120	40.52	0.00011	3.11	19.12	0.00062	0.20997	30280.66	466.17	64.96	4.82	0.08180	0.05500	0.04240	0.26024	3.18	Suspended Load
	121	40.52 - 38.69	0.00011	2.75	22.18	0.00062	0.20997	31171.17	457.82	68.09	4.82	0.08180	0.05500	0.04240	0.28026	3.43	Suspended Load
	122	38.69	0.00011	2.38	25.23	0.00062	0.20997	32061.67	525.89	60.97	4.82	0.08180	0.05500	0.04240	0.29894	3.65	Suspended Load
	123	36.00	0.00011	2.97	20.64	0.00062	0.20997	31801.35	518.35	61.35	4.82	0.08180	0.05500	0.04240	0.27038	3.31	Suspended Load
	124	36.00	0.00011	2.97	20.64	0.00062	0.20997	31801.35	554.73	57.33	4.82	0.08180	0.05500	0.04240	0.27038	3.31	Suspended Load
	125	34.42 - 32.81	0.00011	3.05	19.69	0.00062	0.20997	31846.45	532.50	59.81	4.82	0.08180	0.05500	0.04240	0.26405	3.23	Suspended Load
	126	30.88 - 29.74	0.00011	2.74	20.57	0.00062	0.20997	30814.25	560.17	55.01	4.82	0.08180	0.05500	0.04240	0.26992	3.30	Suspended Load
	127	29.74 - 29.13	0.00011	2.43	23.50	0.00062	0.20997	30529.46	538.08	56.74	4.82	0.08180	0.05500	0.04240	0.28848	3.53	Suspended Load
	128	29.13 - 26.38	0.00011	2.66	19.76	0.00062	0.20997	28156.29	538.14	52.32	4.82	0.08180	0.05500	0.04240	0.26456	3.23	Suspended Load
	129	26.38 - 24.47	0.00011	2.74	18.51	0.00062	0.20997	26286.26	518.03	50.74	4.82	0.08180	0.05500	0.04240	0.25602	3.13	Suspended Load
	130	24.47	0.00011	3.10	19.41	0.00062	0.20997	30508.60	537.66	56.74	4.82	0.08180	0.05500	0.04240	0.26220	3.21	Suspended Load
	131	22.01	0.00011	2.63	20.90	0.00062	0.20997	28900.73									

Table E.2(Continued...). Sediment Analyses (the Van Rijn Method).

μ^* (ft/s)	τ^*	T	Bedform	q_b (ft ² /s)	β	R_o	Δ	a	Ca	ΔR_o	R'_o	I_f	q_b (ft ² /s)	q_t (ft ² /s)	g_t (tons/day)	C_t (ppm)
0.19347	1.15	19.82	Transition	0.00195	1.29	0.74085	0.00	0.00123	0.41305	0.96871	1.70955	0.00003	0.00041	0.00236	16.86	166.50
0.19125	1.12	19.35	Transition	0.00185	1.29	0.73616	0.00	0.00123	0.39828	0.94593	1.68209	0.00003	0.00041	0.00227	16.18	162.11
0.25004	1.91	33.78	Flat Bed/Antidunes	0.00597	1.29	0.73771	0.00	0.00123	0.91877	1.32554	2.06325	0.00002	0.00070	0.00667	47.66	360.01
0.23981	1.76	30.99	Flat Bed/Antidunes	0.00498	1.37	0.78393	0.00	0.00123	0.80750	1.38541	2.16934	0.00002	0.00053	0.00551	39.38	417.34
0.23224	1.65	29.00	Flat Bed/Antidunes	0.00433	1.38	0.79011	0.00	0.00123	0.73100	1.34985	2.13996	0.00002	0.00048	0.00481	34.38	396.95
0.23798	1.73	30.50	Flat Bed/Antidunes	0.00482	1.38	0.78906	0.00	0.00123	0.78847	1.38804	2.17710	0.00002	0.00051	0.00533	38.06	426.55
0.31828	3.10	55.36	Flat Bed/Antidunes	0.01684	1.30	0.74603	0.00	0.00123	1.92741	1.81245	2.55849	0.00002	0.00121	0.01804	128.88	1572.93
0.42060	5.41	97.41	Flat Bed/Antidunes	0.05517	1.46	0.82059	0.00	0.00123	4.49935	3.00628	3.82688	0.00001	0.00192	0.05709	407.83	3829.88
0.30773	2.90	51.68	Flat Bed/Antidunes	0.01457	1.36	0.77859	0.00	0.00123	1.73877	1.86100	2.63959	0.00001	0.00099	0.01557	111.20	1147.10
0.29267	2.62	46.65	Flat Bed/Antidunes	0.01175	1.33	0.76146	0.00	0.00123	1.49114	1.68772	2.44917	0.00002	0.00093	0.01268	90.61	817.06
0.29035	2.58	45.90	Flat Bed/Antidunes	0.01136	1.27	0.71997	0.00	0.00123	1.45528	1.53934	2.25931	0.00002	0.00106	0.01242	88.74	826.52
0.25921	2.06	36.38	Flat Bed/Antidunes	0.00697	1.25	0.70426	0.00	0.00123	1.02678	1.29958	2.00384	0.00002	0.00088	0.00785	56.09	536.07
0.21540	1.42	24.81	Flat Bed/Antidunes	0.00312	1.22	0.68198	0.00	0.00123	0.57832	0.99100	1.67298	0.00003	0.00069	0.00381	27.23	285.98
0.15028	0.69	11.56	Dunes	0.00063	1.35	0.77631	0.00	0.00123	0.18401	0.75413	1.53045	0.00004	0.00021	0.00084	6.00	71.88
0.15183	0.71	11.82	Dunes	0.00066	1.33	0.76225	0.00	0.00123	0.19027	0.74191	1.50415	0.00004	0.00024	0.00090	6.39	68.76
0.14612	0.65	10.88	Dunes	0.00055	1.29	0.73886	0.00	0.00123	0.16789	0.67313	1.41199	0.00004	0.00026	0.00082	5.84	57.54
0.08425	0.22	2.95	Ripples	0.00004	1.29	0.73605	1.54	0.77218	0.00004	0.02325	0.75930	0.16065	0.00025	0.00028	2.02	18.46
0.09962	0.30	4.52	Dunes	0.00009	1.31	0.75439	1.56	0.78129	0.00007	0.03102	0.78541	0.16382	0.00051	0.00059	4.23	36.48
0.08626	0.23	3.14	Dunes	0.00004	1.29	0.73476	1.58	0.78966	0.00004	0.02387	0.75862	0.16253	0.00028	0.00032	2.27	20.61
0.08650	0.23	3.16	Dunes	0.00004	1.28	0.73358	1.59	0.79435	0.00004	0.02386	0.75744	0.16291	0.00028	0.00032	2.30	20.59
0.08535	0.22	3.05	Dunes	0.00004	1.31	0.75106	1.48	0.74032	0.00004	0.02488	0.77593	0.15908	0.00025	0.00029	2.06	20.29
0.08545	0.22	3.06	Dunes	0.00004	1.26	0.71626	1.67	0.83485	0.00004	0.02219	0.73845	0.16528	0.00028	0.00032	2.27	18.72
0.08994	0.25	3.50	Dunes	0.00005	1.30	0.74219	1.58	0.78976	0.00005	0.02585	0.76804	0.16356	0.00033	0.00038	2.71	24.74
0.08935	0.24	3.44	Dunes	0.00005	1.26	0.71869	1.71	0.85256	0.00004	0.02371	0.74241	0.16746	0.00034	0.00039	2.79	23.46
0.07178	0.16	1.87	Ripples	0.00001	1.21	0.66731	1.60	0.79936	0.00002	0.01532	0.68262	0.15674	0.00014	0.00016	1.11	8.43
0.08222	0.21	2.76	Dunes	0.00003	1.23	0.69074	1.76	0.87908	0.00003	0.01947	0.71021	0.16738	0.00025	0.00028	2.03	15.56
0.08420	0.22	2.94	Dunes	0.00004	1.26	0.71173	1.68	0.83779	0.00003	0.02146	0.73318	0.16507	0.00026	0.00030	2.15	17.39
0.07550	0.17	2.17	Dunes	0.00002	1.96	0.88371	1.56	0.77805	0.00002	0.03128	0.91499	0.10606	0.00011	0.00013	0.93	7.81
0.07742	0.18	2.33	Dunes	0.00002	1.95	0.88356	1.62	0.81169	0.00003	0.03193	0.91549	0.10824	0.00013	0.00015	1.06	8.62
0.07669	0.18	2.27	Dunes	0.00002	2.02	0.88382	1.52	0.75943	0.00003	0.03328	0.91710	0.10888	0.00012	0.00014	1.00	8.17
0.04729	0.07	0.24	Ripples	0.00000	1.99	0.88388	0.29	0.14292	0.00000	0.01681	0.90069	0.02921	0.00000	0.00000	0.03	0.45
0.06286	0.12	1.20	Ripples	0.00001	1.94	0.88348	1.12	0.56017	0.00001	0.02476	0.90824	0.08201	0.00004	0.00005	0.34	3.26
0.08862	0.24	3.37	Dunes	0.00005	1.99	0.88387	1.78	0.88945	0.00004	0.03901	0.92287	0.11830	0.00024	0.00029	2.04	15.19
0.08683	0.23	3.19	Dunes	0.00004	2.07	0.88332	1.66	0.82790	0.00004	0.04021	0.92352	0.11927	0.00021	0.00026	1.83	15.27
0.08576	0.23	3.09	Dunes	0.00004	2.10	0.88292	1.62	0.80819	0.00004	0.04016	0.92308	0.11917	0.00020	0.00024	1.72	15.26
0.09848	0.30	4.39	Dunes	0.00008	1.93	0.88326	1.93	0.96620	0.00005	0.04317	0.92643	0.11939	0.00039	0.00048	3.40	21.27
0.04547	0.06	0.15	Ripples	0.00000	2.00	0.88388	0.18	0.08999	0.00000	0.01519	0.89907	0.02019	0.00000	0.00000	0.01	0.21
0.07904	0.38	3.26	Dunes	0.00002	1.10	0.51334	1.35	0.67508	0.00003	0.01420	0.52754	0.23110	0.00029	0.00031	2.23	20.76
0.10695	0.70	6.80	Dunes	0.00009	1.03	0.29824	1.21	0.60556	0.00010	0.01414	0.31238	0.38500	0.00185	0.00194	13.85	110.89
0.11100	0.76	7.40	Dunes	0.00011	1.03	0.29275	1.21	0.60736	0.00012	0.01463	0.30737	0.38568	0.00227	0.00238	17.01	127.78
0.10843	0.72	7.02	Dunes	0.00010	1.03	0.28261	1.30	0.65034	0.00010	0.01338	0.29599	0.39555	0.00213	0.00223	15.90	111.64
0.08802	0.48	4.28	Dunes	0.00003	1.03	0.28828	1.32	0.66182	0.00005	0.01005	0.29832	0.39954	0.00078	0.00082	5.83	51.94
0.07992	0.39	3.35	Dunes	0.00002	1.03	0.28102	1.32	0.66159	0.00003	0.00850	0.28952	0.40221	0.00053	0.00055	3.90	36.68
0.09508	0.55	5.16	Dunes	0.00005	1.03	0.28716	1.34	0.66756	0.00006	0.01117	0.29833	0.39958	0.00112	0.00117	8.35	69.32
0.11402	0.80	7.86	Dunes	0.00012	1.03	0.28716	1.22	0.61166	0.00013	0.01488	0.30205	0.38706	0.00267	0.00279	19.92	141.65
0.11266	0.78	7.65	Dunes	0.00011	1.03	0.29665	1.18	0.58872	0.00013	0.01528	0.31194	0.38123	0.00240	0.00252	17.97	139.86
0.09418	0.54	5.05	Dunes	0.00005	1.03	0.27306	1.44	0.71972	0.00006	0.01024	0.28331	0.41059	0.00115	0.00119	8.53	66.88
0.08833	0.48	4.32	Dunes	0.00003	1.02	0.27211	1.44	0.72115	0.00004	0.00929	0.28140	0.41189	0.00086	0.00089	6.38	51.06
0.09383	0.54	5.00	Dunes	0.00005	1.03	0.28100	1.38	0.69163	0.00006	0.01062	0.29162	0.40454	0.00108	0.00113	8.08	65.13
0.09904	0.60	5.69	Dunes	0.00006	1.02	0.26876	1.46	0.73011	0.00007	0.01080	0.27956	0.41230	0.00148	0.00154	11.02	77.61
0.11061	0.75	7.34	Dunes	0.00010	1.03	0.29160	1.22	0.61248	0.00011	0.01446	0.30606	0.38688	0.00225	0.00235	16.81	124.76
0.10877	0.73	7.07	Dunes	0.00010	1.03	0.28225	1.30	0.65022	0.00010	0.01343	0.29567	0.39555	0.00217	0.00226	16.18	113.26
0.08861	0.48	4.35	Dunes	0.00004	1.02	0.25647	1.57	0.78698	0.00004	0.00858	0.26505	0.42449	0.00094	0.00098	6.99	47.66
0.10308	0.65	6.24	Dunes	0.00007	1.02	0.26587	1.46	0.73127	0.00008	0.01131	0.27718	0.41251	0.00182	0.00189	13.50	88.35
0.11864	0.86	8.60	Dunes	0.00015	1.03	0.28701	1.18	0.58959	0.00015	0.01593	0.30293	0.38234	0.00325	0.00340	24.28	161.19
0.11529	0.82	8.06	Dunes	0.00013	1.03	0.30356	1.12	0.55775	0.00015	0.01643	0.31999	0.37353	0.00260	0.00273	19.52	153.56
0.11673	0.84	8.29	Dunes	0.00014	1.03	0.31241	1.06	0.52816	0.00016	0.01750	0.32992	0.36563	0.00266	0.00279	19.95	163.92
0.12216	0.92	9.17	Dunes	0.00017	1.03	0.30405	1.05	0.52388	0.00019	0.01823	0.32229	0.36528	0.00347	0.00364	26.01	182.70
0.10277	0.65	6.20	Dunes	0.00007	1.02	0.25453	1.56	0.78047	0.00007	0.01058	0.26511	0.42205	0.00190	0.00197	14.08	87.44
0.09478	0.55	5.12	Dunes	0.00005	1.02	0.27012	1.46	0.73086	0.00006	0.01018	0.28030	0.41275	0.00120	0.00125	8.91	70.99
0.08736	0.47	4.20	Dunes	0.00003	1.03	0.27445	1.42	0.71050	0.00004	0.00927	0.28372	0.40996	0.00081	0.00084	6.01	55.19
0.10833	0.72	7.00	Dunes	0.00010	1.03	0.29867	1.20	0.59952	0.00011	0.01447	0.31314	0.38358	0.00209	0.00219	15.63	119.49
0.09269	0.53	4.86	Dunes	0.00004	1.02	0.26544	1.50	0.75086	0.00005	0.00961	0.27506	0.41693	0.00118	0.00122	8.73	65.71
0.09680	0.57	5.39	Dunes	0.00005	1.02	0.26637	1.49	0.74372	0.00006	0.01030	0.27667	0.41511	0.00143	0.00149	10.63	73.63
0.09436	0.55	5.07	Dunes	0.00005												

Table E.2(Continued...). Sediment Analyses (the Van Rijn Method).

μ^* (ft/s)	τ^*	T	Bedform	q_b (ft ² /s)	β	R_o	Δ	a	Ca	ΔR_o	R'_o	I_r	q_b (ft ² /s)	q_t (ft ² /s)	g_t (tons/day)	C_t (ppm)
0.08329	0.21	2.86	Dunes	0.00003	1.54	0.84420	1.95	0.97321	0.00003	0.02684	0.87104	0.12035	0.00021	0.00025	1.77	11.41
0.06644	0.14	1.46	Dunes	0.00001	1.53	0.84156	1.43	0.71396	0.00001	0.02010	0.86165	0.09603	0.00007	0.00008	0.55	3.54
0.07149	0.16	1.84	Dunes	0.00001	1.64	0.86232	1.44	0.71816	0.00002	0.02487	0.88719	0.10517	0.00009	0.00011	0.77	5.81
0.06642	0.13	1.45	Dunes	0.00001	1.56	0.84853	1.37	0.68587	0.00001	0.02087	0.86941	0.09562	0.00007	0.00008	0.54	4.35
0.04888	0.07	0.33	Ripples	0.00000	1.45	0.81762	0.49	0.24687	0.00000	0.01177	0.82939	0.04128	0.00001	0.00001	0.06	0.45
0.03851	0.05	0.17	Ripples	0.00000	1.43	0.81189	0.28	0.14059	0.00000	0.00994	0.82183	0.02675	0.00000	0.00000	0.02	0.20
0.05864	0.11	0.91	Ripples	0.00000	1.54	0.84239	1.03	0.51529	0.00001	0.01735	0.85973	0.07590	0.00003	0.00004	0.26	3.35
0.07521	0.17	2.15	Ripples	0.00002	1.61	0.85839	1.59	0.79665	0.00002	0.02574	0.88413	0.11099	0.00012	0.00014	1.02	7.61
0.09237	0.26	3.75	Dunes	0.00006	1.36	0.78059	1.70	0.85090	0.00005	0.02830	0.80889	0.15037	0.00037	0.00043	3.09	21.79
0.10298	0.32	4.90	Dunes	0.00010	1.35	0.77342	1.79	0.89262	0.00007	0.03212	0.80554	0.15223	0.00063	0.00073	5.22	38.29
0.10827	0.36	5.52	Dunes	0.00013	1.34	0.76988	1.80	0.89860	0.00008	0.03415	0.80404	0.15140	0.00079	0.00093	6.63	45.68
0.08977	0.25	3.48	Dunes	0.00005	1.36	0.78126	1.67	0.83731	0.00004	0.02731	0.80857	0.14918	0.00033	0.00038	2.70	18.67
0.06900	0.15	1.65	Ripples	0.00001	1.35	0.77217	1.28	0.64022	0.00002	0.01903	0.79121	0.12422	0.00009	0.00010	0.75	6.16
0.10555	1.03	7.25	Dunes	0.00006	1.01	0.13905	1.28	0.63961	0.00008	0.00683	0.14588	0.55593	0.00191	0.00197	14.07	122.03
0.10483	1.02	7.13	Dunes	0.00006	1.01	0.12997	1.41	0.70714	0.00007	0.00615	0.13613	0.56804	0.00200	0.00206	14.69	114.13
0.13054	1.58	11.61	Dunes	0.00017	1.01	0.13303	1.05	0.52599	0.00020	0.00946	0.14248	0.54147	0.00627	0.00644	46.02	311.34
0.14027	1.82	13.56	Dunes	0.00023	1.01	0.15147	0.75	0.37451	0.00035	0.01321	0.16468	0.50193	0.00822	0.00845	60.36	512.13
0.11891	1.31	9.47	Dunes	0.00011	1.01	0.14709	1.05	0.52630	0.00015	0.00907	0.15616	0.53522	0.00330	0.00341	24.34	190.43
0.14422	1.92	14.40	Dunes	0.00026	1.01	0.13418	0.83	0.41251	0.00035	0.01194	0.14612	0.52007	0.01149	0.01175	83.95	625.02
0.14447	1.93	14.45	Dunes	0.00027	1.01	0.14757	0.72	0.35871	0.00041	0.01366	0.16123	0.50000	0.01028	0.01054	75.32	603.34
0.12167	1.37	9.96	Dunes	0.00012	1.01	0.15369	0.96	0.47970	0.00017	0.01006	0.16375	0.52408	0.00353	0.00366	26.12	234.79
0.12357	1.41	10.30	Dunes	0.00013	1.01	0.14398	1.03	0.51478	0.00017	0.00946	0.15345	0.53446	0.00417	0.00430	30.74	224.91
0.11832	1.30	9.36	Dunes	0.00011	1.01	0.15104	1.02	0.50997	0.00015	0.00932	0.16036	0.53081	0.00311	0.00321	22.96	195.22
0.13568	1.70	12.63	Dunes	0.00020	1.01	0.14546	0.86	0.42881	0.00028	0.01160	0.15706	0.51731	0.00706	0.00726	51.83	434.14
0.13508	1.69	12.51	Dunes	0.00020	1.01	0.15286	0.81	0.40354	0.00029	0.01230	0.16516	0.50822	0.00645	0.00664	47.45	391.36
0.12916	1.54	11.35	Dunes	0.00016	1.01	0.14845	0.92	0.45892	0.00022	0.01076	0.15922	0.52210	0.00515	0.00531	37.93	291.08
0.12428	1.43	10.43	Dunes	0.00013	1.01	0.14814	0.98	0.49020	0.00018	0.00995	0.15810	0.52828	0.00416	0.00429	30.65	267.43
0.09867	0.90	6.21	Dunes	0.00005	1.01	0.14355	1.27	0.63512	0.00006	0.00640	0.14995	0.55404	0.00132	0.00136	9.74	97.68
0.11143	1.15	8.19	Dunes	0.00008	1.01	0.14851	1.11	0.55730	0.00011	0.00819	0.15670	0.54001	0.00232	0.00240	17.14	163.97
0.13602	1.71	12.69	Dunes	0.00020	1.01	0.14890	0.83	0.41263	0.00029	0.01204	0.16094	0.51214	0.00695	0.00715	51.10	343.99
0.13253	1.63	12.00	Dunes	0.00018	1.01	0.14099	0.94	0.47062	0.00023	0.01057	0.15156	0.52783	0.00638	0.00656	46.86	293.09
0.13090	1.59	11.68	Dunes	0.00017	1.01	0.13748	1.00	0.49944	0.00021	0.00995	0.14743	0.53477	0.00612	0.00629	44.96	315.31
0.12552	1.46	10.66	Dunes	0.00014	1.01	0.13216	1.14	0.56760	0.00016	0.00867	0.14083	0.54836	0.00505	0.00520	37.11	243.81
0.12992	1.56	11.49	Dunes	0.00016	1.01	0.13996	0.99	0.49373	0.00021	0.01004	0.15000	0.53256	0.00573	0.00590	42.13	305.02
0.13753	0.58	9.52	Dunes	0.00042	1.37	0.78486	1.43	0.71407	0.00024	0.05364	0.83850	0.12800	0.00115	0.00156	11.17	109.98
0.15065	0.69	11.63	Dunes	0.00064	1.36	0.78045	1.26	0.63114	0.00036	0.06291	0.84335	0.11405	0.00176	0.00239	17.08	149.38
0.17998	0.99	17.02	Dunes	0.00141	1.37	0.78342	0.75	0.37328	0.00108	0.09820	0.88162	0.07174	0.00388	0.00529	37.82	283.87
0.16519	0.83	14.18	Dunes	0.00096	1.39	0.79526	0.97	0.48282	0.00064	0.08155	0.87681	0.09286	0.00251	0.00347	24.78	192.55
0.13490	0.56	9.12	Dunes	0.00038	1.46	0.81959	1.26	0.63231	0.00025	0.05963	0.87922	0.12625	0.00092	0.00130	9.31	89.42
0.15607	0.75	12.55	Dunes	0.00075	1.39	0.79415	1.11	0.55744	0.00046	0.07137	0.86552	0.10533	0.00195	0.00270	19.27	171.44
0.14955	0.68	11.44	Dunes	0.00061	1.37	0.78472	1.26	0.62921	0.00035	0.06297	0.84769	0.11474	0.00167	0.00229	16.33	93.69
0.18777	1.08	18.61	Transition	0.00171	1.34	0.76733	0.63	0.31742	0.00146	0.10680	0.87413	0.06029	0.00506	0.00677	48.35	302.87
0.19944	1.22	21.13	Transition	0.00223	1.33	0.76503	0.39	0.19414	0.00288	0.13960	0.90462	0.03721	0.00665	0.00888	63.44	371.39
0.21307	1.39	24.26	Transition	0.00298	1.33	0.76636	0.07	0.03710	0.01854	0.29483	1.06119	0.00514	0.00626	0.00924	66.02	373.44
0.21898	1.47	25.67	Flat Bed/Antidunes	0.00335	1.35	0.77433	0.11	0.05551	0.01349	0.26406	1.03839	0.00850	0.00738	0.01074	76.69	443.70
0.21116	1.36	23.81	Transition	0.00286	1.20	0.65618	0.11	0.05640	0.01186	0.19966	0.85584	0.01722	0.01214	0.01500	107.18	612.12
0.18181	1.01	17.39	Transition	0.00148	1.17	0.62348	0.80	0.39861	0.00105	0.07128	0.69476	0.10673	0.00680	0.00828	59.18	322.42
0.15434	0.73	12.25	Dunes	0.00071	1.15	0.59501	1.46	0.72929	0.00034	0.04309	0.63810	0.16318	0.00332	0.00403	28.77	175.03
0.19908	1.21	21.05	Transition	0.00221	1.18	0.63933	0.39	0.19692	0.00282	0.10907	0.74840	0.06020	0.01042	0.01263	90.21	545.46
0.19908	1.21	21.05	Transition	0.00221	1.18	0.63933	0.39	0.19692	0.00282	0.10907	0.74840	0.06020	0.01042	0.01263	90.21	583.75
0.20607	1.30	22.62	Transition	0.00257	1.19	0.64977	0.23	0.11451	0.00541	0.14419	0.79397	0.03642	0.01183	0.01440	102.89	638.19
0.18343	1.03	17.72	Transition	0.00154	1.18	0.64008	0.72	0.36187	0.00119	0.07722	0.71729	0.09922	0.00662	0.00816	58.31	393.21
0.15909	0.77	13.08	Dunes	0.00081	1.16	0.61071	1.30	0.64918	0.00042	0.04831	0.65902	0.15150	0.00362	0.00444	31.69	207.17
0.17983	0.99	16.99	Transition	0.00141	1.19	0.64894	0.77	0.38693	0.00104	0.07450	0.72344	0.10471	0.00574	0.00715	51.09	362.26
0.18674	1.07	18.40	Transition	0.00167	1.20	0.66336	0.61	0.30462	0.00149	0.08828	0.75164	0.08674	0.00655	0.00821	58.68	428.98
0.20995	1.35	23.52	Transition	0.00279	1.19	0.65287	0.14	0.07058	0.00931	0.18013	0.83300	0.02216	0.01241	0.01520	108.57	709.76
0.17592	0.95	16.22	Transition	0.00128	1.18	0.63656	0.88	0.44130	0.00085	0.06721	0.70377	0.11547	0.00541	0.00669	47.76	306.09
0.18407	1.04	17.85	Transition	0.00156	1.17	0.61821	0.76	0.38089	0.00114	0.07304	0.69125	0.10312	0.00745	0.00901	64.36	380.37
0.19219	1.13	19.55	Transition	0.00189	1.15	0.60129	0.61	0.30633	0.00162	0.08162	0.68291	0.08766	0.01030	0.01219	87.11	503.99
0.15686	0.75	12.69	Dunes	0.00076	1.24	0.70065	1.01	0.50285	0.00052	0.06192	0.76257	0.13288	0.00239	0.00315	22.52	187.97
0.15855	0.77	12.98	Dunes	0.00080	1.22	0.68110	1.05	0.52303	0.00052	0.05960	0.74070	0.13459	0.00271	0.00351	25.07	240.53
0.16040	0.79	13.31	Dunes	0.00084	1.20	0.66294	1.08	0.53939	0.00052	0.05780	0.72075	0.13595	0.00307	0.00392	27.97	237.87
0.13854	0.59	9.68	Dunes	0.00043	1.18	0.63730	1.52	0.76214	0.00023	0.03968	0.67698	0.17184	0.00168	0.00212	15.12	119.33
0.13215	0.53	8.72	Dunes	0.00035	1.16	0.60915	1.76	0.88119	0.00017	0.03341	0.64256	0.18647	0.00150	0.00184	13.16	102.77
0.12448	0.47	7.62	D													

Table E.2(Continued...). Sediment Analyses (the Yang Method).

$\mu\text{-d}_{50}/v$	V_r/w_f	V_c (ft/s)	μ_r/w_f	VS/w_f	V_S/w_f	w_{td50}/v	$\log C_t$	C_t (ppm)	q_t (ft ² /s)	g_t (tons/day)
12.47	3.07	0.25140	2.61	0.00330	0.00031	4.78	1.54	34.86	0.00049	3.53
12.62	3.06	0.25045	2.64	0.00328	0.00031	4.78	1.54	34.62	0.00048	3.46
12.57	3.07	0.25076	2.63	0.00428	0.00031	4.78	1.71	51.75	0.00096	6.85
11.15	3.19	0.26113	2.33	0.00393	0.00032	4.78	1.64	43.65	0.00058	4.12
10.96	3.21	0.26271	2.29	0.00378	0.00032	4.78	1.61	40.89	0.00050	3.54
10.99	3.21	0.26244	2.30	0.00388	0.00032	4.78	1.63	42.57	0.00053	3.80
12.31	3.09	0.25247	2.57	0.00832	0.00052	4.78	2.12	131.37	0.00151	10.76
9.99	3.32	0.27161	2.09	0.00766	0.00040	4.78	2.06	113.69	0.00169	12.11
11.31	3.18	0.25981	2.37	0.00588	0.00038	4.78	1.90	79.12	0.00107	7.67
11.84	3.13	0.25581	2.48	0.00569	0.00038	4.78	1.88	76.30	0.00118	8.46
13.12	3.02	0.24729	2.74	0.00704	0.00045	4.78	2.02	105.26	0.00158	11.30
13.62	2.99	0.24437	2.85	0.00637	0.00045	4.78	1.96	91.75	0.00134	9.60
14.35	2.94	0.24047	3.00	0.00539	0.00044	4.78	1.86	72.76	0.00097	6.93
11.38	3.17	0.25925	2.38	0.00207	0.00025	4.78	1.22	16.72	0.00020	1.40
11.82	3.13	0.25598	2.47	0.00212	0.00025	4.78	1.25	17.66	0.00023	1.64
12.53	3.07	0.25099	2.62	0.00208	0.00025	4.78	1.25	17.65	0.00025	1.79
12.62	3.06	0.25043	2.64	0.00220	0.00024	4.78	1.29	19.34	0.00030	2.11
12.06	3.11	0.25425	2.52	0.00258	0.00025	4.78	1.38	24.26	0.00039	2.81
12.66	3.06	0.25017	2.65	0.00225	0.00024	4.78	1.30	20.11	0.00031	2.21
12.70	3.06	0.24993	2.65	0.00226	0.00024	4.78	1.31	20.24	0.00032	2.26
12.16	3.10	0.25353	2.54	0.00221	0.00025	4.78	1.28	19.19	0.00027	1.95
13.24	3.01	0.24658	2.77	0.00225	0.00024	4.78	1.31	20.48	0.00035	2.49
12.43	3.08	0.25168	2.60	0.00234	0.00025	4.78	1.33	21.17	0.00032	2.32
13.16	3.02	0.24704	2.75	0.00235	0.00024	4.78	1.34	21.85	0.00036	2.60
14.84	2.91	0.23801	3.10	0.00193	0.00023	4.78	1.23	17.00	0.00031	2.24
14.06	2.96	0.24197	2.94	0.00219	0.00024	4.78	1.30	20.16	0.00037	2.63
13.38	3.00	0.24574	2.80	0.00222	0.00024	4.78	1.30	20.18	0.00035	2.49
6.90	3.87	0.31657	1.44	0.00050	0.00008	4.78	0.21	1.61	0.00003	0.19
6.95	3.86	0.31550	1.45	0.00051	0.00008	4.78	0.23	1.69	0.00003	0.21
6.68	3.93	0.32130	1.40	0.00051	0.00008	4.78	0.20	1.60	0.00003	0.19
6.79	3.90	0.31900	1.42	0.00031	0.00008	4.78	-0.18	0.67	0.00001	0.04
6.97	3.85	0.31504	1.46	0.00042	0.00008	4.78	0.07	1.18	0.00002	0.12
6.81	3.89	0.31858	1.42	0.00059	0.00008	4.78	0.32	2.09	0.00004	0.28
6.53	3.97	0.32497	1.36	0.00057	0.00008	4.78	0.29	1.93	0.00003	0.23
6.46	3.99	0.32669	1.35	0.00056	0.00008	4.78	0.27	1.87	0.00003	0.21
7.02	3.84	0.31400	1.47	0.00066	0.00008	4.78	0.41	2.57	0.00006	0.41
6.76	3.91	0.31963	1.41	0.00030	0.00008	4.78	-0.21	0.61	0.00001	0.04
3.25	6.19	0.15627	4.42	0.00168	0.00012	0.74	0.54	3.50	0.00005	0.38
5.99	4.14	0.10467	8.14	0.00896	0.00033	0.74	1.82	66.35	0.00116	8.29
6.11	4.10	0.10363	8.30	0.00934	0.00033	0.74	1.85	71.21	0.00133	9.48
6.34	4.03	0.10173	8.61	0.00918	0.00032	0.74	1.84	69.90	0.00139	9.96
6.21	4.07	0.10279	8.44	0.00743	0.00033	0.74	1.69	49.25	0.00077	5.53
6.38	4.02	0.10144	8.67	0.00678	0.00032	0.74	1.63	42.71	0.00064	4.54
6.24	4.06	0.10258	8.47	0.00803	0.00032	0.74	1.75	55.98	0.00094	6.75
6.24	4.06	0.10258	8.47	0.00963	0.00032	0.74	1.88	75.16	0.00148	10.57
6.03	4.13	0.10437	8.18	0.00945	0.00033	0.74	1.86	72.42	0.00130	9.30
6.58	3.96	0.09997	8.93	0.00803	0.00032	0.74	1.75	56.73	0.00101	7.24
6.60	3.95	0.09979	8.96	0.00754	0.00032	0.74	1.71	51.23	0.00090	6.40
6.38	4.02	0.10143	8.67	0.00796	0.00032	0.74	1.74	55.48	0.00096	6.89
6.69	3.93	0.09918	9.08	0.00847	0.00031	0.74	1.79	62.07	0.00123	8.81
6.14	4.09	0.10341	8.33	0.00931	0.00033	0.74	1.85	70.96	0.00134	9.56
6.35	4.02	0.10167	8.63	0.00922	0.00032	0.74	1.85	70.31	0.00141	10.04
7.03	3.84	0.09695	9.54	0.00765	0.00031	0.74	1.73	53.26	0.00109	7.81
6.77	3.91	0.09865	9.19	0.00884	0.00031	0.74	1.82	66.60	0.00142	10.18
6.24	4.06	0.10255	8.47	0.01002	0.00032	0.74	1.90	80.16	0.00169	12.08
5.88	4.18	0.10568	7.99	0.00963	0.00033	0.74	1.87	74.24	0.00132	9.44
5.70	4.25	0.10738	7.74	0.00969	0.00034	0.74	1.87	74.56	0.00127	9.07
5.87	4.19	0.10577	7.97	0.01020	0.00033	0.74	1.91	81.49	0.00162	11.60
7.08	3.82	0.09660	9.61	0.00888	0.00031	0.74	1.83	67.84	0.00153	10.92
6.65	3.94	0.09943	9.03	0.00810	0.00031	0.74	1.76	57.66	0.00101	7.24
6.54	3.97	0.10023	8.88	0.00744	0.00032	0.74	1.70	50.07	0.00076	5.45
5.98	4.15	0.10475	8.12	0.00967	0.00033	0.74	1.88	75.04	0.00137	9.82
6.78	3.90	0.09858	9.20	0.00846	0.00031	0.74	1.79	62.07	0.00115	8.24
6.75	3.91	0.09874	9.17	0.00883	0.00031	0.74	1.82	66.44	0.00134	9.59
6.25	4.06	0.10248	8.49	0.00849	0.00032	0.74	1.79	61.31	0.00114	8.12
6.11	4.10	0.10367	8.29	0.00852	0.00033	0.74	1.79	61.35	0.00112	8.03
6.57	3.96	0.10005	8.92	0.00945	0.00032	0.74	1.87	73.77	0.00138	9.87
6.36	4.02	0.10165	8.63	0.00963	0.00032	0.74	1.88	75.45	0.00163	11.68
6.16	4.09	0.10322	8.36	0.00892	0.00033	0.74	1.82	66.25	0.00139	9.96
5.90	4.18	0.10550	8.01	0.01066	0.00033	0.74	1.94	87.61	0.00153	10.91
6.70	3.92	0.09909	9.10	0.01020	0.00031	0.74	1.92	83.65	0.00171	12.21
6.21	4.07	0.10279	8.44	0.00954	0.00033	0.74	1.87	74.04	0.00180	12.85
6.59	3.95	0.09989	8.95	0.00975	0.00032	0.74	1.89	77.63	0.00151	10.82
14.17	2.95	0.24139	2.96	0.00262	0.00024	4.78	1.43	26.61	0.00059	4.23

Table E.2(Continued...). Sediment Analyses (the Yang Method).

$\mu_s d_{50}/v$	V_c/w_f	V_c (ft/s)	μ_s/w_f	VS/w_f	V_S/w_f	$w_f d_{50}/v$	$\log C_t$	C_t (ppm)	q_b (ft ² /s)	g_t (tons/day)
9.18	3.43	0.28049	1.92	0.00089	0.00010	4.78	0.67	4.68	0.00010	0.73
9.28	3.42	0.27936	1.94	0.00072	0.00010	4.78	0.51	3.26	0.00007	0.51
8.46	3.54	0.28982	1.77	0.00076	0.00011	4.78	0.53	3.38	0.00006	0.45
9.02	3.45	0.28244	1.89	0.00071	0.00010	4.78	0.50	3.17	0.00005	0.39
10.09	3.31	0.27064	2.11	0.00053	0.00010	4.78	0.32	2.09	0.00004	0.28
10.28	3.29	0.26885	2.15	0.00042	0.00010	4.78	0.14	1.39	0.00002	0.15
9.25	3.42	0.27971	1.93	0.00063	0.00010	4.78	0.42	2.63	0.00003	0.20
8.63	3.51	0.28749	1.80	0.00080	0.00011	4.78	0.57	3.74	0.00007	0.50
11.25	3.18	0.26030	2.35	0.00194	0.00019	4.78	1.20	15.76	0.00031	2.23
11.47	3.16	0.25856	2.40	0.00217	0.00019	4.78	1.28	18.91	0.00036	2.58
11.58	3.15	0.25773	2.42	0.00228	0.00019	4.78	1.31	20.55	0.00042	2.98
11.23	3.18	0.26046	2.35	0.00188	0.00019	4.78	1.18	15.05	0.00030	2.17
11.51	3.16	0.25827	2.41	0.00145	0.00019	4.78	1.00	10.11	0.00017	1.22
3.96	5.31	0.06086	17.87	0.01023	0.00032	0.22	1.70	49.69	0.00080	5.73
4.24	5.07	0.05807	19.13	0.01034	0.00030	0.22	1.71	51.39	0.00093	6.62
4.14	5.15	0.05899	18.69	0.01280	0.00031	0.22	1.87	73.69	0.00152	10.89
3.63	5.66	0.06487	16.38	0.01327	0.00034	0.22	1.88	76.69	0.00127	9.04
3.74	5.53	0.06342	16.88	0.01134	0.00033	0.22	1.77	58.76	0.00105	7.51
4.10	5.18	0.05935	18.52	0.01411	0.00031	0.22	1.94	86.89	0.00163	11.67
3.73	5.55	0.06358	16.82	0.01377	0.00033	0.22	1.91	82.08	0.00143	10.25
3.58	5.73	0.06562	16.14	0.01147	0.00034	0.22	1.77	59.34	0.00092	6.60
3.82	5.45	0.06242	17.25	0.01186	0.00033	0.22	1.80	63.71	0.00122	8.71
3.64	5.65	0.06473	16.43	0.01120	0.00034	0.22	1.76	57.21	0.00094	6.73
3.78	5.49	0.06290	17.07	0.01298	0.00033	0.22	1.87	74.36	0.00124	8.88
3.60	5.70	0.06534	16.23	0.01275	0.00034	0.22	1.85	71.41	0.00121	8.66
3.71	5.57	0.06387	16.72	0.01229	0.00033	0.22	1.83	67.39	0.00123	8.78
3.71	5.56	0.06377	16.76	0.01183	0.00033	0.22	1.80	63.12	0.00101	7.23
3.83	5.43	0.06228	17.30	0.00948	0.00033	0.22	1.64	43.24	0.00060	4.31
3.70	5.58	0.06389	16.71	0.01060	0.00033	0.22	1.72	52.15	0.00076	5.45
3.69	5.59	0.06402	16.67	0.01293	0.00034	0.22	1.87	73.54	0.00153	10.92
3.90	5.36	0.06147	17.62	0.01279	0.00032	0.22	1.86	72.87	0.00163	11.65
4.00	5.27	0.06037	18.07	0.01272	0.00032	0.22	1.86	72.51	0.00145	10.34
4.17	5.12	0.05873	18.81	0.01233	0.00031	0.22	1.84	69.19	0.00147	10.53
3.93	5.34	0.06114	17.75	0.01257	0.00032	0.22	1.85	70.75	0.00137	9.77
11.12	3.20	0.26136	2.33	0.00148	0.00019	4.78	1.01	10.24	0.00015	1.04
11.26	3.18	0.26026	2.35	0.00163	0.00019	4.78	1.08	12.00	0.00019	1.37
11.17	3.19	0.26100	2.33	0.00194	0.00019	4.78	1.20	15.75	0.00029	2.10
10.80	3.23	0.26408	2.26	0.00176	0.00019	4.78	1.12	13.31	0.00024	1.71
10.03	3.32	0.27128	2.10	0.00140	0.00020	4.78	0.95	8.85	0.00013	0.92
10.83	3.22	0.26378	2.27	0.00166	0.00019	4.78	1.09	12.20	0.00019	1.37
11.13	3.19	0.26133	2.33	0.00161	0.00019	4.78	1.07	11.72	0.00029	2.04
11.66	3.14	0.25714	2.44	0.00205	0.00019	4.78	1.24	17.54	0.00039	2.80
11.73	3.14	0.25661	2.45	0.00219	0.00019	4.78	1.29	19.36	0.00046	3.31
11.69	3.14	0.25692	2.44	0.00233	0.00019	4.78	1.33	21.34	0.00053	3.77
11.45	3.16	0.25878	2.39	0.00238	0.00019	4.78	1.34	21.82	0.00053	3.77
15.22	2.89	0.23621	3.18	0.00418	0.00032	4.78	1.72	52.68	0.00129	9.23
16.39	2.83	0.23113	3.43	0.00369	0.00031	4.78	1.65	44.95	0.00115	8.25
17.48	2.77	0.22693	3.65	0.00320	0.00031	4.78	1.57	37.26	0.00086	6.12
15.81	2.86	0.23355	3.31	0.00399	0.00031	4.78	1.70	49.86	0.00115	8.25
15.81	2.86	0.23355	3.31	0.00399	0.00031	4.78	1.70	49.86	0.00108	7.71
15.44	2.88	0.23519	3.23	0.00410	0.00032	4.78	1.71	51.44	0.00116	8.29
15.78	2.86	0.23367	3.30	0.00368	0.00031	4.78	1.64	44.11	0.00092	6.54
16.87	2.80	0.22922	3.53	0.00326	0.00031	4.78	1.58	37.80	0.00081	5.78
15.47	2.87	0.23505	3.23	0.00358	0.00032	4.78	1.62	42.10	0.00083	5.94
14.97	2.90	0.23737	3.13	0.00368	0.00032	4.78	1.64	43.29	0.00083	5.92
15.33	2.88	0.23568	3.21	0.00417	0.00032	4.78	1.72	52.57	0.00113	8.04
15.91	2.85	0.23312	3.33	0.00354	0.00031	4.78	1.62	41.74	0.00091	6.51
16.58	2.82	0.23034	3.47	0.00375	0.00031	4.78	1.66	46.24	0.00110	7.82
17.23	2.79	0.22784	3.60	0.00397	0.00031	4.78	1.71	50.84	0.00123	8.79
13.74	2.98	0.24372	2.87	0.00300	0.00033	4.78	1.49	30.72	0.00052	3.68
14.37	2.94	0.24032	3.00	0.00308	0.00032	4.78	1.51	32.59	0.00048	3.40
14.98	2.90	0.23730	3.13	0.00316	0.00032	4.78	1.54	34.45	0.00057	4.05
15.88	2.85	0.23324	3.32	0.00278	0.00031	4.78	1.46	29.07	0.00052	3.68
16.93	2.80	0.22899	3.54	0.00271	0.00031	4.78	1.46	28.68	0.00051	3.67
16.67	2.81	0.23000	3.48	0.00254	0.00031	4.78	1.41	25.80	0.00042	3.00
17.50	2.77	0.22685	3.66	0.00248	0.00031	4.78	1.41	25.43	0.00044	3.17
16.89	2.80	0.22913	3.53	0.00213	0.00031	4.78	1.30	19.74	0.00028	1.98

Table E.2(Continued...). Sediment Analyses (the Karim-Kennedy and Kennedy Methods).

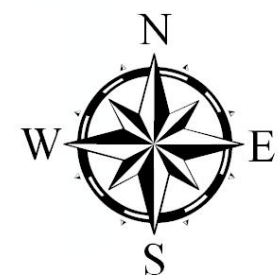
$V/[(SG-1)gd_{50}]^{0.5}$	$(\mu_o - \mu_{oc})/[(SG-1)gd_{50}]^{0.5}$	y_o/d_{50}	$[(SG-1)gd_{50}^3]^{0.5}$	q_t (ft ² /s)	C_t (ppm)	g_t (tons/day)		q_t (ft ² /s)	C_t (ppm)	g_t (tons/day)
14.95	0.94535	22969.73	0.00011	0.00157	110.83	11.22		0.00195	137.53	13.93
14.84	0.95905	23506.18	0.00011	0.00159	114.08	11.39		0.00194	138.80	13.86
19.38	0.95450	23327.36	0.00011	0.00346	186.69	24.72		0.00426	229.80	30.42
17.79	0.82029	18358.44	0.00011	0.00182	137.52	12.97		0.00277	209.84	19.80
17.12	0.80224	17735.30	0.00011	0.00154	126.68	10.97		0.00241	198.72	17.21
17.56	0.80532	17840.96	0.00011	0.00167	133.62	11.92		0.00261	209.01	18.65
22.15	0.93023	13167.36	0.00011	0.00481	419.53	34.37		0.00615	536.03	43.92
28.87	0.71088	12289.54	0.00011	0.00498	334.00	35.57		0.00994	666.66	70.99
22.18	0.83581	15752.06	0.00011	0.00362	266.65	25.85		0.00545	401.60	38.93
21.46	0.88547	17247.62	0.00011	0.00383	246.80	27.37		0.00528	340.24	37.73
21.22	1.00680	16949.59	0.00011	0.00523	347.74	37.34		0.00594	395.38	42.45
19.21	1.05392	18260.91	0.00011	0.00439	299.42	31.33		0.00467	318.92	33.37
16.27	1.12245	20254.98	0.00011	0.00314	235.44	22.42		0.00308	230.98	21.99
11.70	0.84242	23920.70	0.00011	0.00058	49.24	4.11		0.00082	70.40	5.88
11.98	0.88318	25765.76	0.00011	0.00069	53.02	4.93		0.00093	71.51	6.65
11.76	0.95116	28995.29	0.00011	0.00079	55.29	5.61		0.00096	67.79	6.88
12.45	0.95938	29398.98	0.00011	0.00095	61.92	6.77		0.00115	75.16	8.22
14.59	0.90595	26826.46	0.00011	0.00131	80.61	9.35		0.00172	106.16	12.31
12.75	0.96317	29585.92	0.00011	0.00103	66.76	7.34		0.00124	80.66	8.87
12.79	0.96662	29756.61	0.00011	0.00105	66.88	7.48		0.00126	80.42	8.99
12.52	0.91561	27282.99	0.00011	0.00086	60.30	6.13		0.00111	77.80	7.92
12.74	1.01786	32349.44	0.00011	0.00118	69.17	8.41		0.00132	77.68	9.44
13.25	0.94142	28521.15	0.00011	0.00109	70.89	7.76		0.00135	88.35	9.67
13.30	1.01060	31975.55	0.00011	0.00132	78.98	9.40		0.00149	89.51	10.65
10.92	1.16892	40623.74	0.00011	0.00105	56.86	7.50		0.00099	53.62	7.08
12.39	1.09524	36470.34	0.00011	0.00130	71.52	9.32		0.00133	72.91	9.50
12.57	1.03142	33053.87	0.00011	0.00117	67.80	8.37		0.00129	74.82	9.23
11.34	0.41817	35145.47	0.00011	0.00009	5.52	0.66		0.00036	21.56	2.56
11.64	0.42298	35665.66	0.00011	0.00010	5.88	0.72		0.00039	22.83	2.80
11.45	0.39778	32983.42	0.00011	0.00008	4.92	0.60		0.00035	20.70	2.52
7.08	0.40752	34007.55	0.00011	0.00003	2.90	0.19		0.00009	9.67	0.62
9.46	0.42508	35893.25	0.00011	0.00006	4.14	0.43		0.00021	14.72	1.52
13.28	0.40936	34202.62	0.00011	0.00013	6.95	0.94		0.00056	29.84	4.02
12.91	0.38290	31449.94	0.00011	0.00010	6.20	0.74		0.00049	29.00	3.47
12.72	0.37616	30767.19	0.00011	0.00010	6.11	0.69		0.00046	29.11	3.27
14.84	0.42984	36413.44	0.00011	0.00020	8.77	1.40		0.00082	36.59	5.85
6.80	0.40483	33723.07	0.00011	0.00002	2.40	0.17		0.00008	7.95	0.55
16.64	0.57405	63026.77	0.00004	0.00019	12.84	1.38		0.00205	136.26	14.62
22.17	1.31000	53462.25	0.00004	0.00443	253.30	31.65		0.01178	673.35	84.13
23.09	1.34208	55613.78	0.00004	0.00540	289.60	38.54		0.01369	734.65	97.77
22.72	1.40442	59916.83	0.00004	0.00586	293.67	41.84		0.01377	690.48	98.36
18.37	1.36905	57455.61	0.00004	0.00280	178.42	20.02		0.00710	452.25	50.75
16.76	1.41459	60634.01	0.00004	0.00231	155.07	16.50		0.00563	378.23	40.24
19.86	1.37590	57928.30	0.00004	0.00362	214.89	25.89		0.00901	534.04	64.35
23.81	1.37590	57928.30	0.00004	0.00639	324.55	45.63		0.01545	785.04	110.38
23.38	1.31916	54072.31	0.00004	0.00533	296.31	38.07		0.01390	773.07	99.32
19.86	1.46725	64415.49	0.00004	0.00437	244.57	31.20		0.00975	545.95	69.65
18.64	1.47380	64893.60	0.00004	0.00362	206.98	25.88		0.00812	463.90	58.00
19.68	1.41471	60642.16	0.00004	0.00382	219.79	27.28		0.00907	522.26	64.81
20.95	1.49696	66599.61	0.00004	0.00548	275.78	39.14		0.01171	589.33	83.64
23.03	1.34892	56078.31	0.00004	0.00543	287.97	38.79		0.01366	724.39	97.58
22.79	1.40674	60079.83	0.00004	0.00595	297.46	42.49		0.01394	697.02	99.57
18.92	1.58727	73461.69	0.00004	0.00470	229.08	33.58		0.00929	452.64	66.35
21.85	1.51751	68131.76	0.00004	0.00652	304.53	46.54		0.01349	630.61	96.38
24.78	1.37684	57993.50	0.00004	0.00725	343.58	51.76		0.01740	825.18	124.32
23.81	1.28003	51490.01	0.00004	0.00517	290.44	36.91		0.01417	796.44	101.22
23.97	1.23229	48425.71	0.00004	0.00472	277.06	33.72		0.01381	810.72	98.66
25.22	1.27727	51310.72	0.00004	0.00613	307.64	43.80		0.01677	841.19	119.77
21.97	1.60228	74635.25	0.00004	0.00779	345.62	55.63		0.01466	650.54	104.71
20.03	1.48748	65898.74	0.00004	0.00467	265.62	33.34		0.01017	578.57	72.63
18.41	1.45783	63730.91	0.00004	0.00337	221.50	24.10		0.00772	506.55	55.12
23.92	1.30755	53299.25	0.00004	0.00557	304.37	39.82		0.01472	804.01	105.18
20.91	1.52056	68359.96	0.00004	0.00570	306.77	40.74		0.01187	638.51	84.79
21.83	1.51389	67860.11	0.00004	0.00644	319.03	46.04		0.01340	663.52	95.75
20.99	1.37936	58167.36	0.00004	0.00434	234.25	31.02		0.01066	574.93	76.14
21.07	1.34064	55515.98	0.00004	0.00405	220.93	28.91		0.01041	568.56	74.39
23.38	1.46434	64203.59	0.00004	0.00725	387.39	51.82		0.01578	842.89	112.76
23.81	1.40743	60128.73	0.00004	0.00683	315.27	48.79		0.01588	733.00	113.44
22.06	1.35502	56493.95	0.00004	0.00482	228.72	34.40		0.01209	574.37	86.39
26.36	1.28527	51832.30	0.00004	0.00716	410.55	51.12		0.01925	1104.62	137.53
25.22	1.50048	66860.41	0.00004	0.00991	484.83	70.79		0.02037	996.41	145.50
23.60	1.36913	57461.05	0.00004	0.00612	252.12	43.75		0.01496	615.92	106.89
24.13	1.47015	64627.38	0.00004	0.00810	415.35	57.88		0.01741	892.45	124.36
14.84	1.10565	37043.81	0.00011	0.00230	103.40	16.44		0.00230	103.19	16.41





Table E.2(Continued...). Sediment Analyses (the Karim-Kennedy and Kennedy Methods).

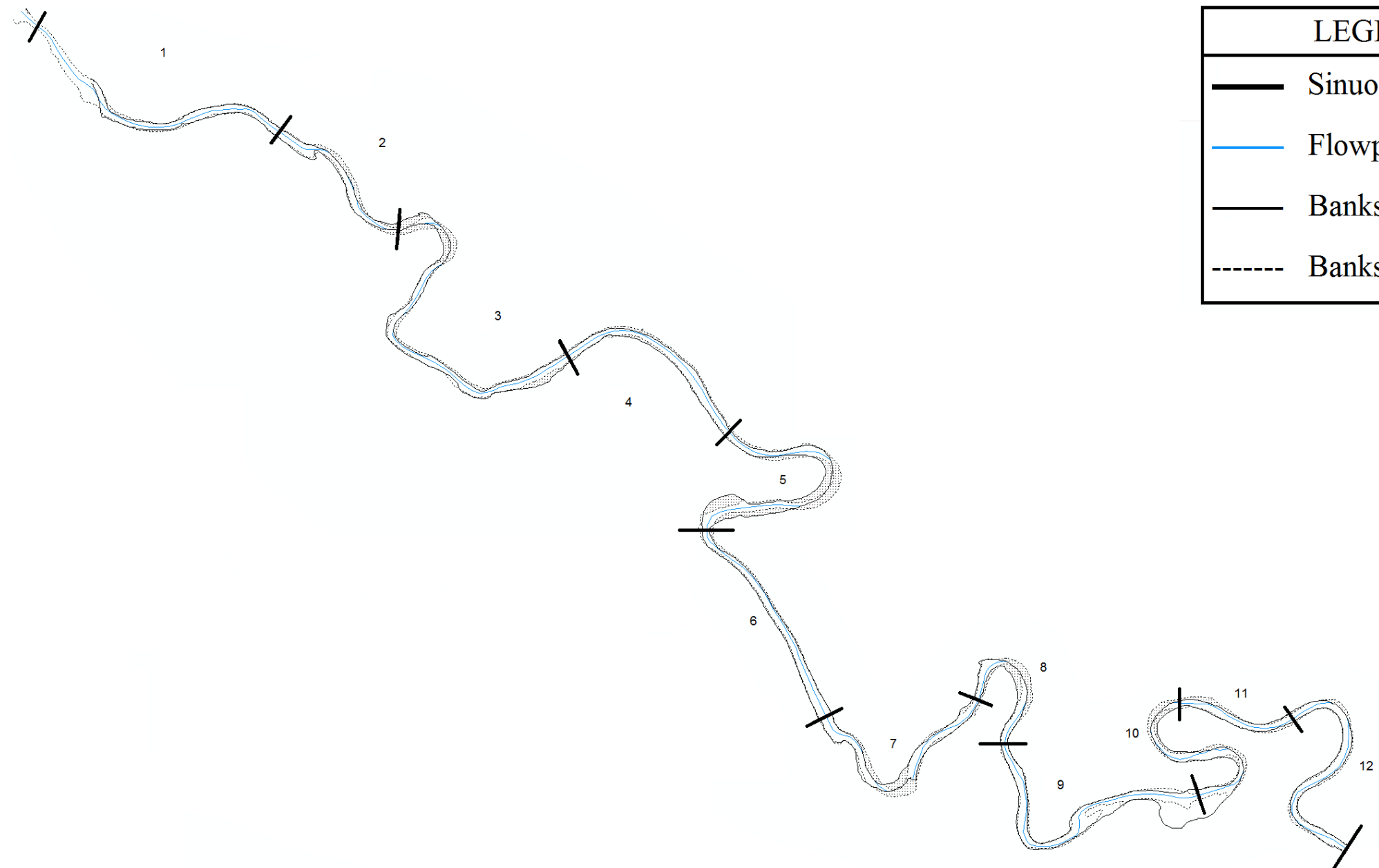
$V/[(SG-1)gd_{50}]^{0.5}$	$(\mu_s - \mu_{sc})/[(SG-1)gd_{50}]^{0.5}$	y_o/d_{50}	$[(SG-1)gd_{50}^3]^{0.5}$	q_b (ft ² /s)	C_t (ppm)	g_b (tons/day)		q_b (ft ² /s)	C_t (ppm)	g_b (tons/day)
13.50	0.63397	41485.31	0.00011	0.00041	19.01	2.95		0.00092	42.20	6.55
10.79	0.64308	42359.88	0.00011	0.00023	10.55	1.64		0.00048	21.94	3.42
11.42	0.56541	35194.24	0.00011	0.00020	10.68	1.41		0.00049	26.70	3.53
10.73	0.61869	40038.53	0.00011	0.00021	11.93	1.48		0.00045	26.07	3.23
8.05	0.72006	50117.25	0.00011	0.00013	7.04	0.94		0.00023	12.07	1.62
6.36	0.73755	51970.43	0.00011	0.00007	4.66	0.51		0.00012	7.52	0.83
9.51	0.64024	42086.78	0.00011	0.00016	14.96	1.15		0.00033	30.52	2.34
12.06	0.58151	36624.77	0.00011	0.00025	13.13	1.75		0.00060	32.03	4.28
14.60	0.82999	31162.75	0.00011	0.00105	52.69	7.47		0.00156	78.74	11.16
16.34	0.85080	32392.79	0.00011	0.00154	80.80	11.01		0.00224	117.59	16.02
17.20	0.86105	33007.81	0.00011	0.00185	90.95	13.19		0.00265	130.54	18.94
14.19	0.82805	31048.96	0.00011	0.00096	47.33	6.83		0.00143	70.79	10.22
10.95	0.85442	32609.54	0.00011	0.00049	28.82	3.49		0.00069	40.53	4.91
18.79	1.61603	106680.00	0.00002	0.00267	165.68	19.10		0.01237	766.27	88.35
19.00	1.75528	122296.90	0.00002	0.00355	196.85	25.34		0.01415	784.88	101.05
23.52	1.70632	116684.32	0.00002	0.00647	312.75	46.23		0.02573	1243.58	183.83
24.38	1.45244	89694.77	0.00002	0.00444	268.96	31.70		0.02361	1431.21	168.68
20.84	1.50705	95200.84	0.00002	0.00302	168.92	21.59		0.01548	865.03	110.55
25.92	1.68845	114668.71	0.00002	0.00857	455.58	61.19		0.03392	1804.22	242.34
25.30	1.50088	94569.94	0.00002	0.00551	315.09	39.34		0.02738	1567.03	195.62
21.07	1.42594	87081.03	0.00002	0.00265	170.38	18.95		0.01496	960.95	106.89
21.79	1.54768	99404.13	0.00002	0.00377	196.81	26.90		0.01823	952.52	130.20
20.59	1.45763	90210.97	0.00002	0.00263	159.94	18.81		0.01434	870.97	102.43
23.86	1.52807	97363.94	0.00002	0.00483	289.02	34.51		0.02350	1406.00	167.87
23.42	1.43579	88047.87	0.00002	0.00378	222.53	26.98		0.02067	1217.84	147.65
22.58	1.48968	93431.03	0.00002	0.00376	206.13	26.86		0.01937	1061.74	138.35
21.74	1.49355	93824.32	0.00002	0.00336	209.51	24.01		0.01735	1081.71	123.97
17.41	1.55355	100018.65	0.00002	0.00187	133.96	13.35		0.00941	674.17	67.20
19.48	1.48895	93357.29	0.00002	0.00236	161.01	16.83		0.01248	853.07	89.15
23.76	1.48409	92865.68	0.00002	0.00436	209.90	31.18		0.02243	1078.44	160.20
23.50	1.58861	103730.32	0.00002	0.00519	231.73	37.05		0.02355	1052.41	168.26
23.37	1.63882	109162.64	0.00002	0.00561	280.82	40.04		0.02406	1205.43	171.87
22.65	1.71994	118232.90	0.00002	0.00588	275.84	41.99		0.02325	1090.90	166.05
23.09	1.60306	105278.90	0.00002	0.00504	260.47	35.97		0.02258	1167.85	161.30
11.16	0.81757	30439.36	0.00011	0.00046	32.66	3.32		0.00069	48.64	4.94
12.28	0.83041	31187.14	0.00011	0.00063	39.64	4.53		0.00093	58.35	6.67
14.63	0.82177	30683.20	0.00011	0.00102	54.95	7.32		0.00155	83.28	11.09
13.28	0.78711	28702.68	0.00011	0.00070	38.62	4.97		0.00111	61.49	7.91
10.57	0.71400	24741.63	0.00011	0.00029	19.75	2.06		0.00050	34.60	3.60
12.56	0.79039	28886.91	0.00011	0.00060	38.10	4.28		0.00094	59.97	6.74
12.14	0.81799	30463.74	0.00011	0.00059	24.27	4.23		0.00089	36.39	6.34
15.49	0.86845	33454.85	0.00011	0.00139	62.30	9.94		0.00196	87.72	14.00
16.48	0.87513	33861.25	0.00011	0.00170	71.19	12.16		0.00238	99.51	17.00
17.59	0.87126	33625.54	0.00011	0.00203	82.14	14.52		0.00287	116.02	20.51
17.95	0.84816	32235.65	0.00011	0.00201	82.98	14.34		0.00296	122.16	21.11
17.20	1.20496	31081.47	0.00011	0.00451	183.99	32.22		0.00396	161.56	28.29
15.18	1.31570	36047.68	0.00011	0.00389	151.34	27.78		0.00305	118.62	21.77
13.16	1.41904	41013.89	0.00011	0.00305	132.49	21.77		0.00219	95.35	15.67
16.43	1.26108	33552.38	0.00011	0.00443	191.18	31.62		0.00365	157.81	26.10
16.43	1.26108	33552.38	0.00011	0.00443	204.60	31.62		0.00365	168.89	26.10
16.87	1.22607	31999.94	0.00011	0.00445	197.28	31.80		0.00382	169.19	27.28
15.13	1.25854	33438.59	0.00011	0.00342	164.55	24.40		0.00285	137.44	20.38
13.41	1.36117	38193.47	0.00011	0.00290	135.24	20.68		0.00220	102.79	15.72
14.73	1.22885	32121.86	0.00011	0.00296	149.70	21.11		0.00256	129.66	18.29
15.13	1.18162	30081.73	0.00011	0.00289	151.03	20.66		0.00264	137.85	18.86
17.15	1.21583	31552.90	0.00011	0.00458	213.66	32.68		0.00397	185.22	28.33
14.55	1.27047	33975.04	0.00011	0.00310	142.14	22.18		0.00257	117.66	18.36
15.43	1.33429	36917.38	0.00011	0.00425	179.27	30.33		0.00326	137.42	23.25
16.32	1.39561	39859.71	0.00011	0.00571	235.87	40.77		0.00406	167.99	29.03
12.34	1.06489	25326.85	0.00011	0.00120	71.29	8.54		0.00127	75.65	9.06
12.67	1.12520	27732.74	0.00011	0.00149	101.89	10.62		0.00147	100.56	10.48
13.00	1.18296	30138.62	0.00011	0.00183	110.95	13.05		0.00168	102.33	12.03
11.45	1.26795	33861.25	0.00011	0.00148	83.23	10.55		0.00126	70.96	8.99
11.16	1.36682	38464.41	0.00011	0.00165	91.91	11.77		0.00128	71.35	9.14
10.45	1.34221	37291.26	0.00011	0.00129	78.90	9.19		0.00103	63.27	7.37
10.21	1.42111	41116.84	0.00011	0.00138	79.11	9.87		0.00103	59.22	7.39
8.77	1.36338	38299.14	0.00011	0.00077	55.05	5.52		0.00062	44.40	4.46

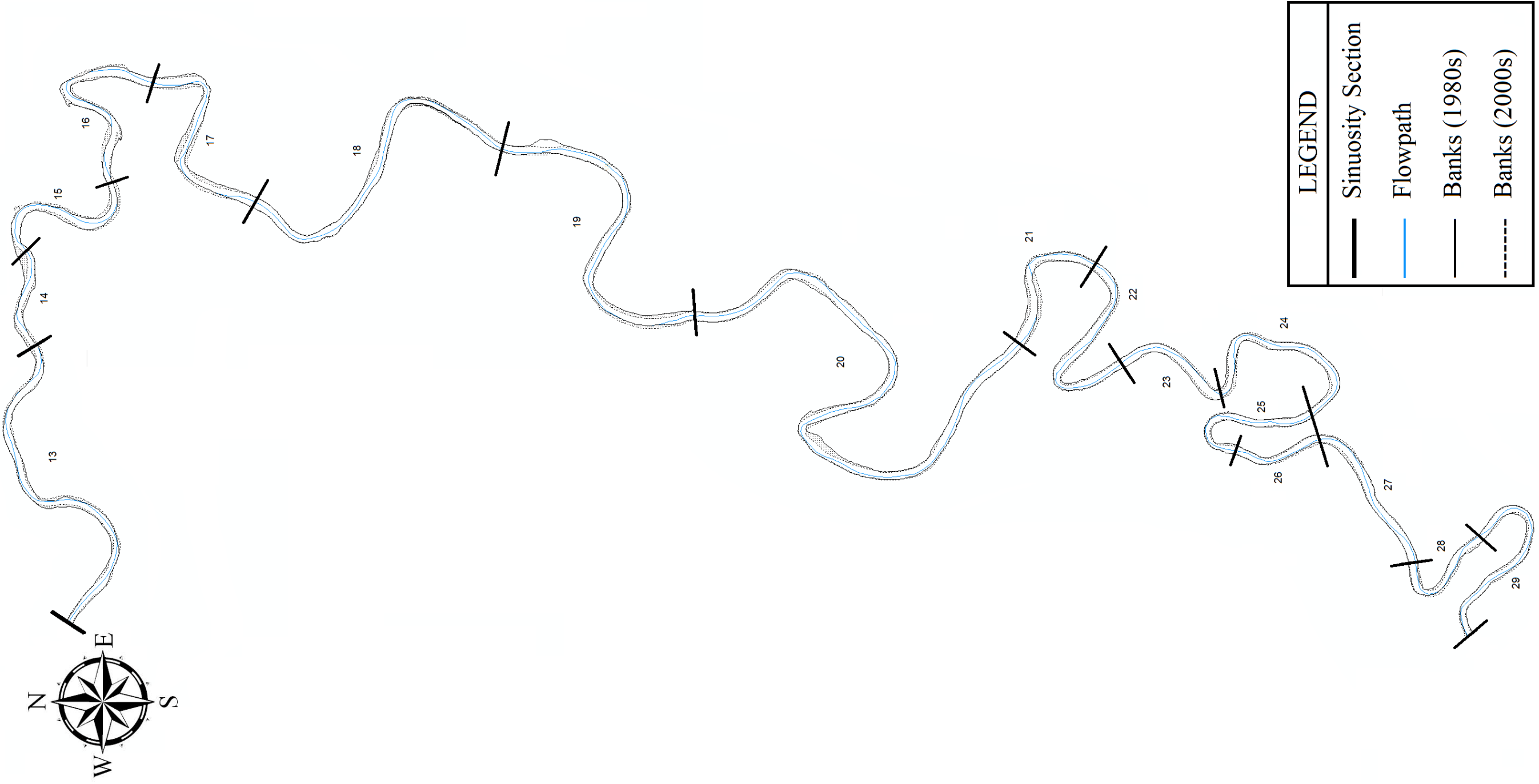
*Red fonts denote flat bed with a reference level *a* of approximately two times the dominant bed material.





APPENDIX F: LARGE PLOTS

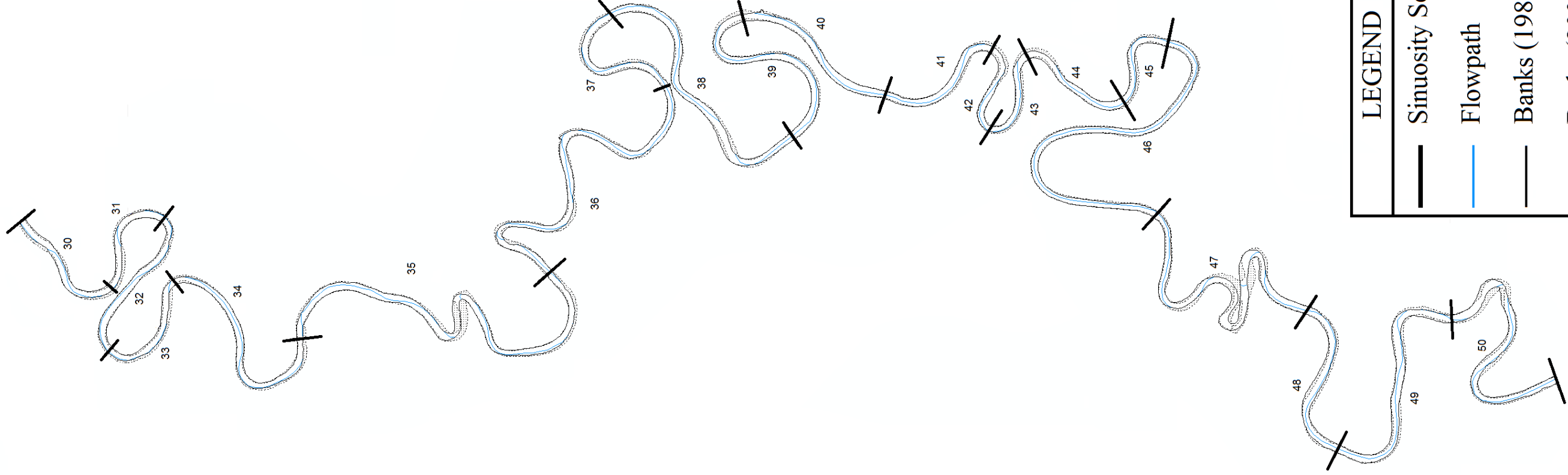






LEGEND	
	Sinuosity Section
	Flowpath
	Banks (1980s)
	Banks (2000s)

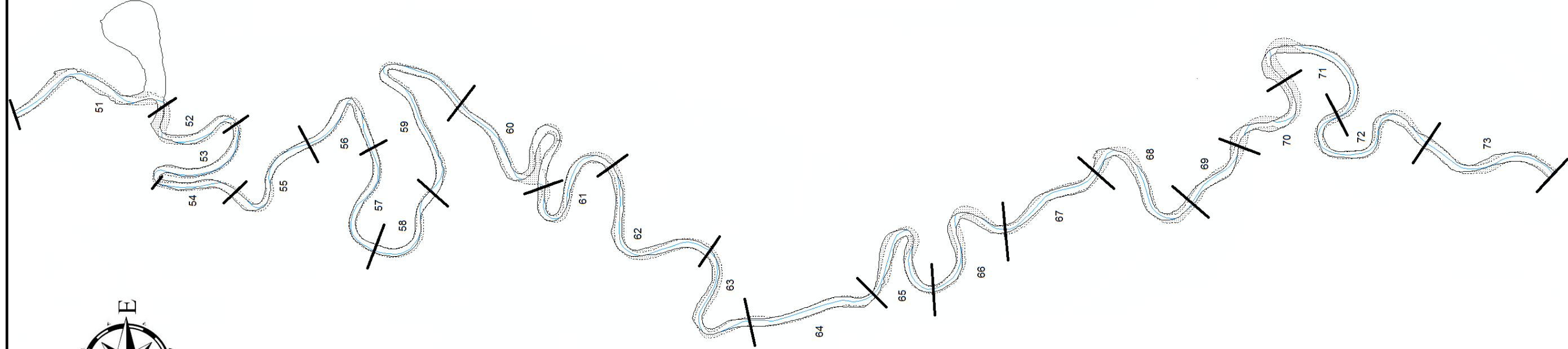







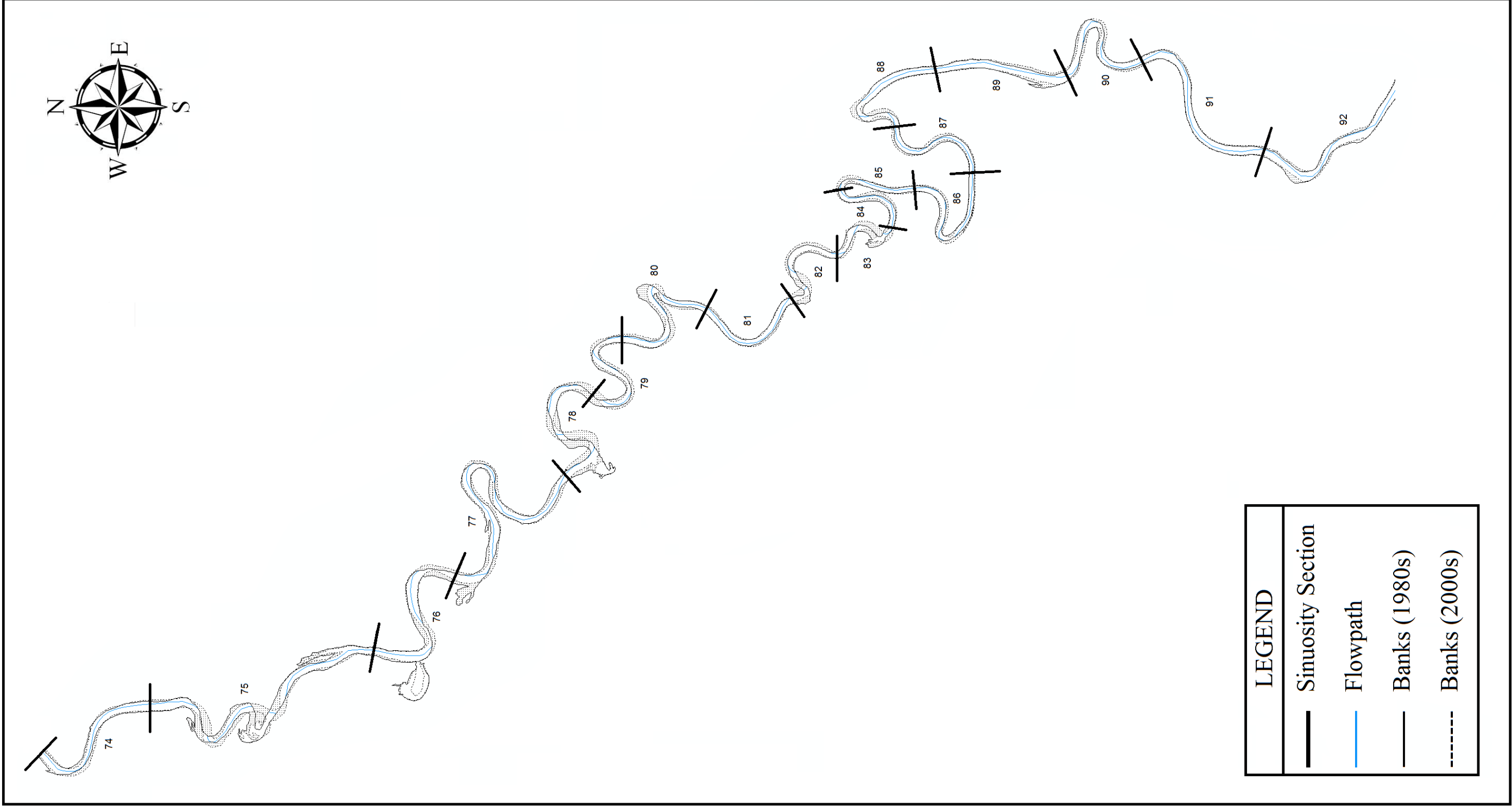
LEGEND	
	Sinuosity Section
	Flowpath
	Banks (1980s)
	Banks (2000s)

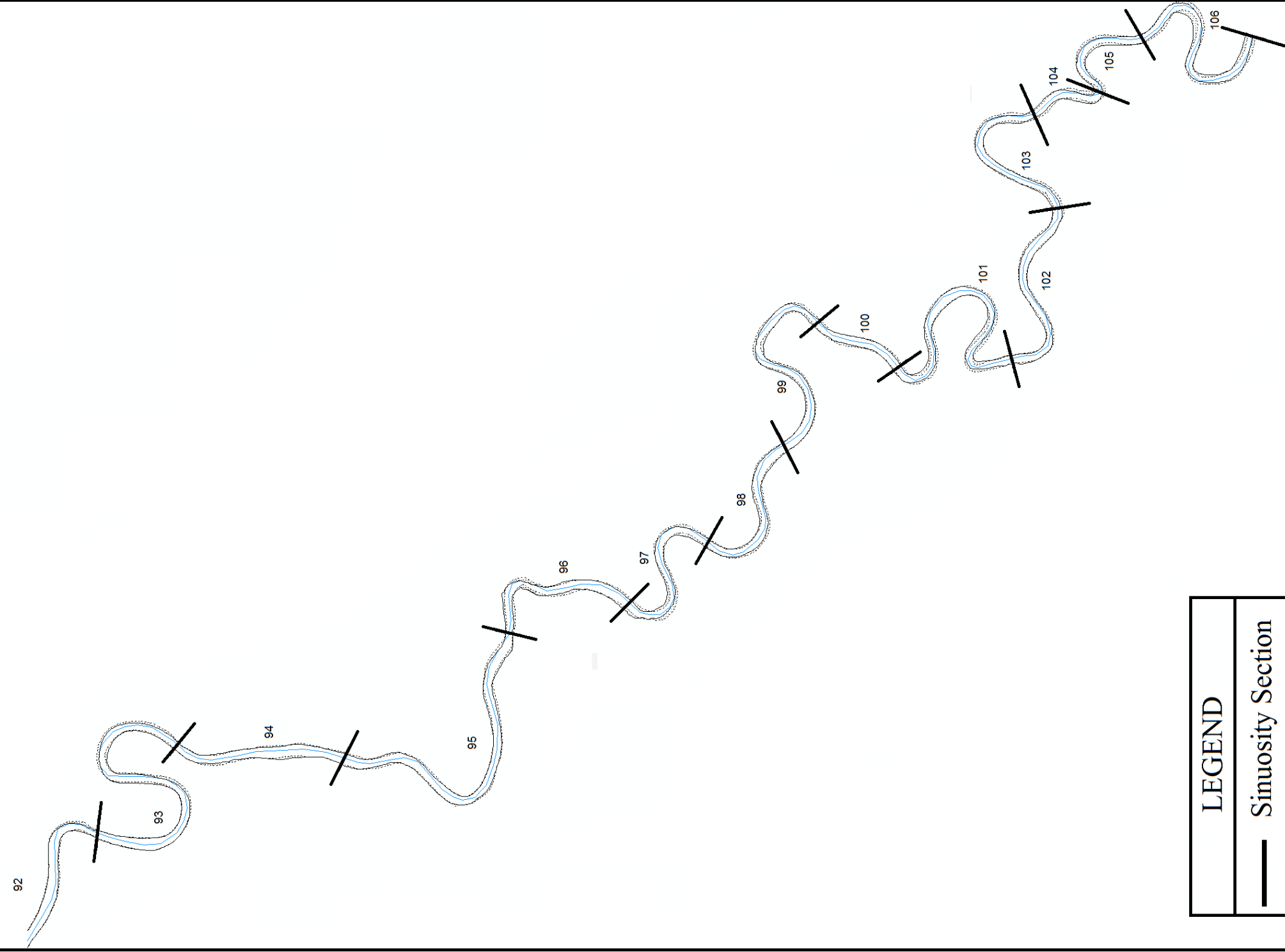


LEGEND	
	Sinuosity Section
	Flowpath
	Banks (1980s)
	Banks (2000s)

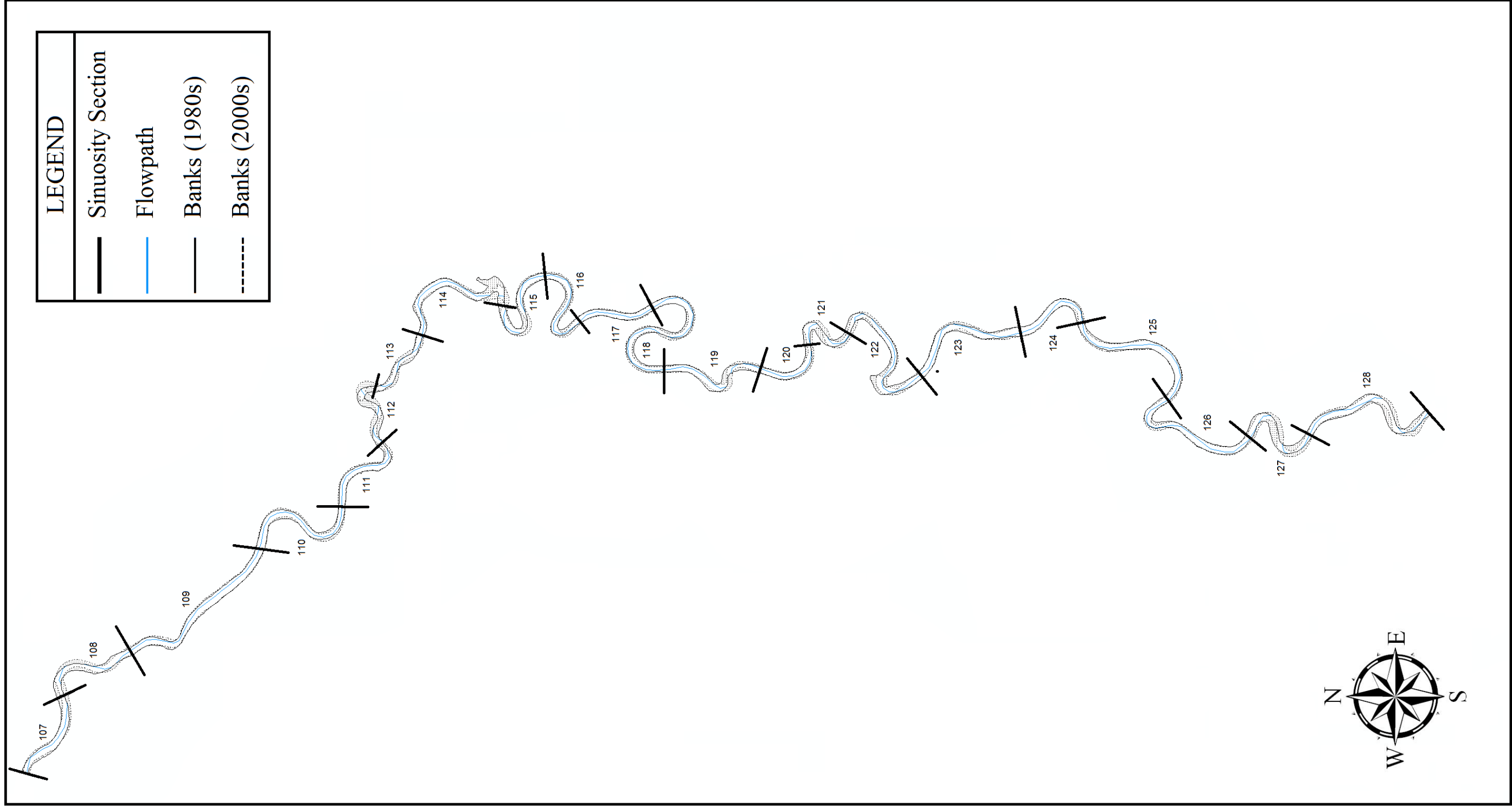






LEGEND	
	Sinuosity Section
	Flowpath
	Banks (1980s)
	Banks (2000s)

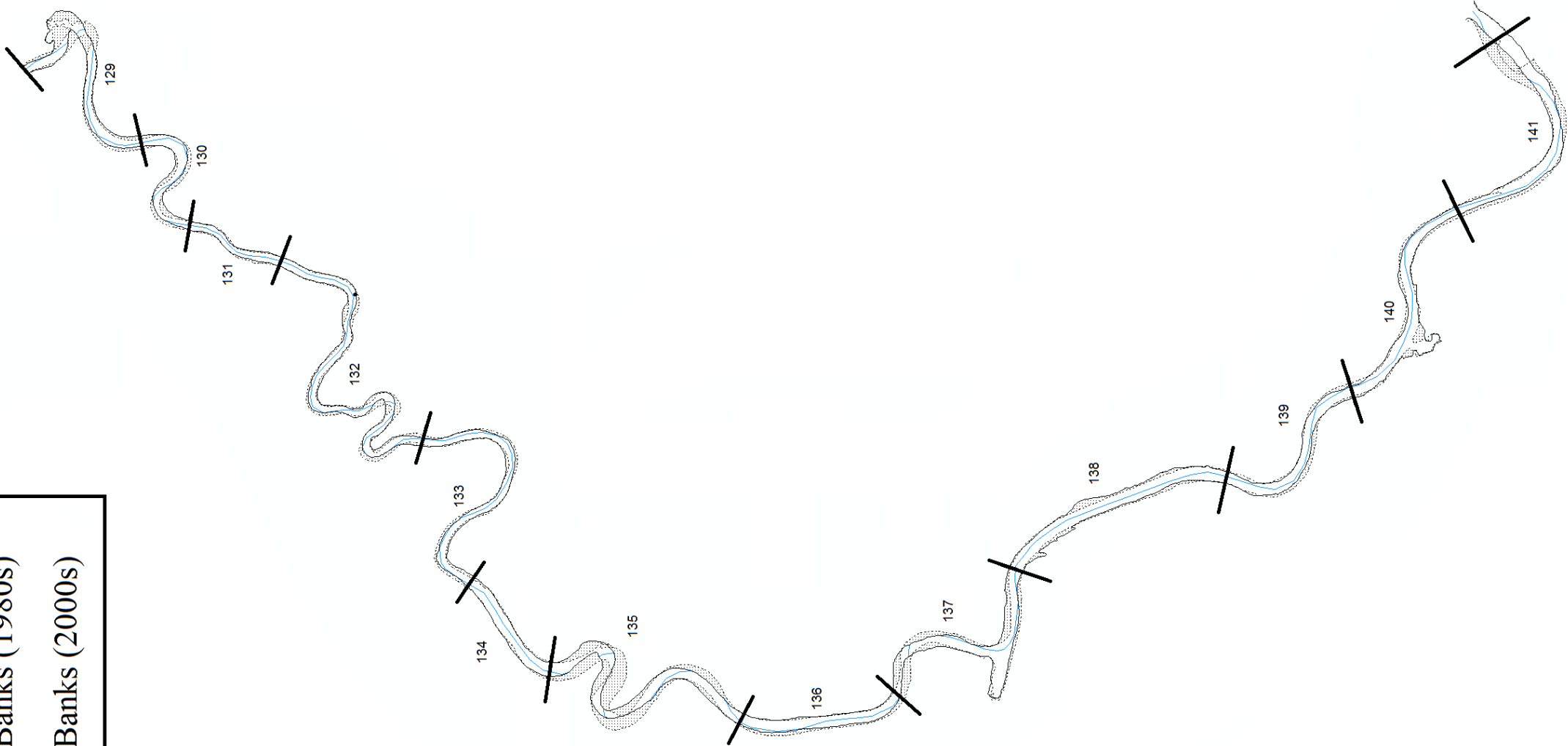


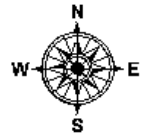


LEGEND	
	Sinuosity Section
	Flowpath
	Banks (1980s)
	Banks (2000s)



LEGEND	
	Sinuosity Section
	Flowpath
	Banks (1980s)
	Banks (2000s)

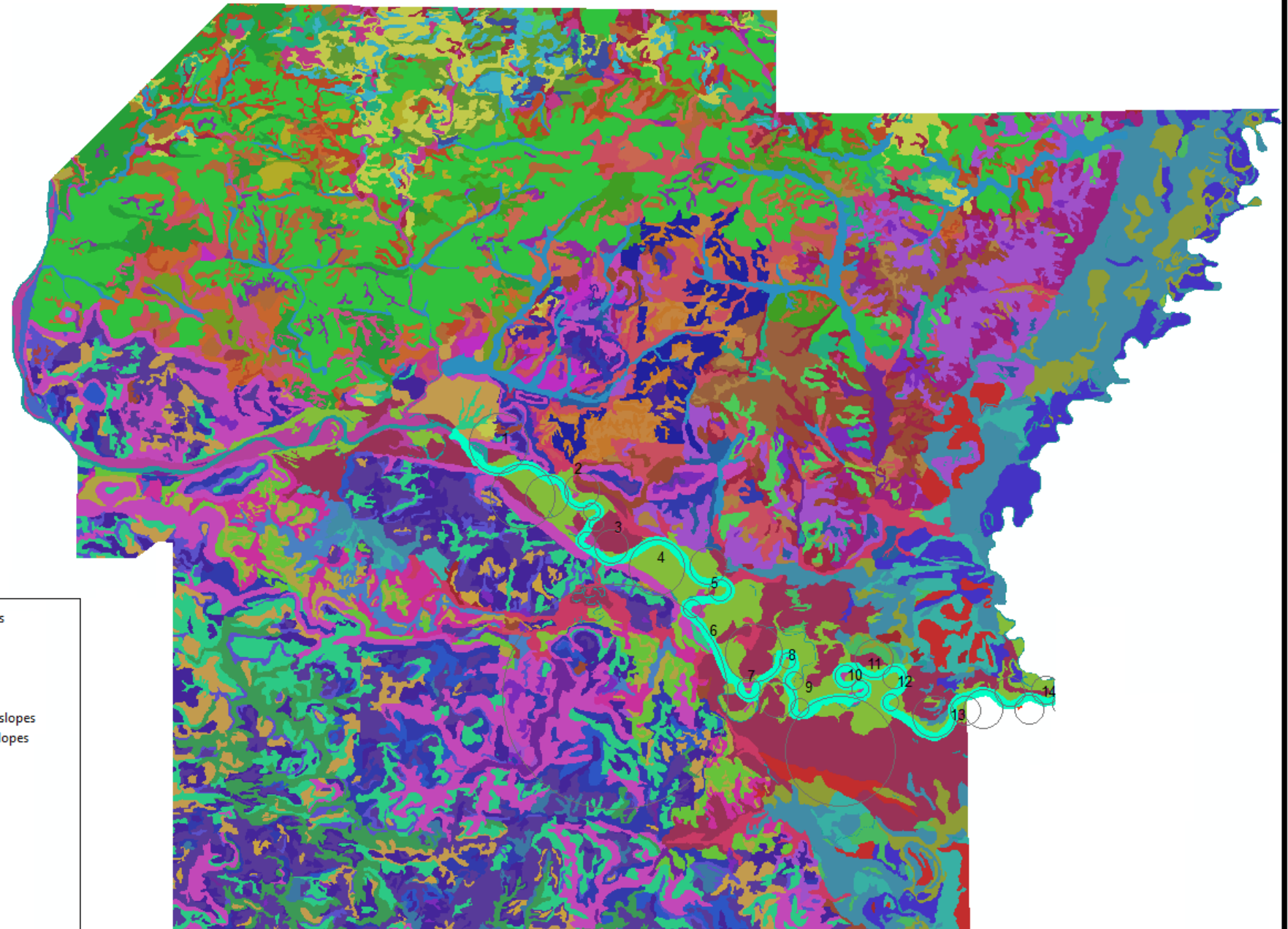


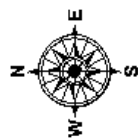


LEGEND

- Amagon silt loam, frequently flooded
- Arkana-Moko complex, 3 to 8 percent slopes
- Arrington silt loam, gently undulating
- Askew silt loam, gently undulating
- Boden fine sandy loam, 3 to 8 percent slopes
- Boden fine sandy loam, 8 to 12 percent slopes
- Boden stony fine sandy loam, 8 to 20 percent slopes
- Brockwell fine sandy loam, 3 to 8 percent slopes
- Captina silt loam, 1 to 3 percent slopes
- Captina silt loam, 3 to 8 percent slopes
- Clarksville very cherty silt loam, 20 to 40 percent slopes
- Clarksville very cherty silt loam, 3 to 8 percent slopes
- Clarksville very cherty silt loam, 8 to 20 percent slopes
- Clarksville-Udorthents complex, 20 to 40 percent slopes
- Crowley silt loam, 0 to 1 percent slopes
- Dubbs silt loam, gently undulating
- Egam silt loam, 0 to 1 percent slopes
- Egam silty clay loam, occasionally flooded
- Enders fine sandy loam, 3 to 8 percent slopes
- Enders fine sandy loam, 8 to 12 percent slopes
- Enders stony fine sandy loam, 20 to 45 percent slopes
- Enders stony fine sandy loam, 8 to 20 percent slopes
- Foley silt loam, 0 to 1 percent slopes
- Forestdale silt loam, frequently flooded
- Gepp very cherty silt loam, 12 to 30 percent slopes
- Gepp very cherty silt loam, 3 to 8 percent slopes
- Gepp very cherty silt loam, 8 to 12 percent slopes
- Hontas silt loam, occasionally flooded
- Jackport silty clay loam, 0 to 1 percent slopes
- Lily fine sandy loam, 3 to 8 percent slopes
- Lily fine sandy loam, 8 to 12 percent slopes
- Lily-Ramsey-Rock outcrop complex, 8 to 30 percent slopes
- Linker fine sandy loam, 3 to 8 percent slopes
- Linker fine sandy loam, 8 to 12 percent slopes
- Linker gravelly fine sandy loam, 12 to 30 percent slopes
- Linker gravelly fine sandy loam, 3 to 8 percent slopes
- Linker gravelly fine sandy loam, 8 to 12 percent slopes
- Loring silt loam, 1 to 3 percent slopes
- Loring silt loam, 3 to 8 percent slopes
- Loring silt loam, 8 to 12 percent slopes
- Moko-Rock outcrop complex, 3 to 20 percent slopes
- Mountainburg stony fine sandy loam, 3 to 12 percent slopes
- Newnata silty clay loam, 3 to 8 percent slopes
- Newnata silty clay loam, 8 to 12 percent slopes
- Noark very cherty silt loam, 12 to 30 percent slopes
- Noark very cherty silt loam, 3 to 8 percent slopes

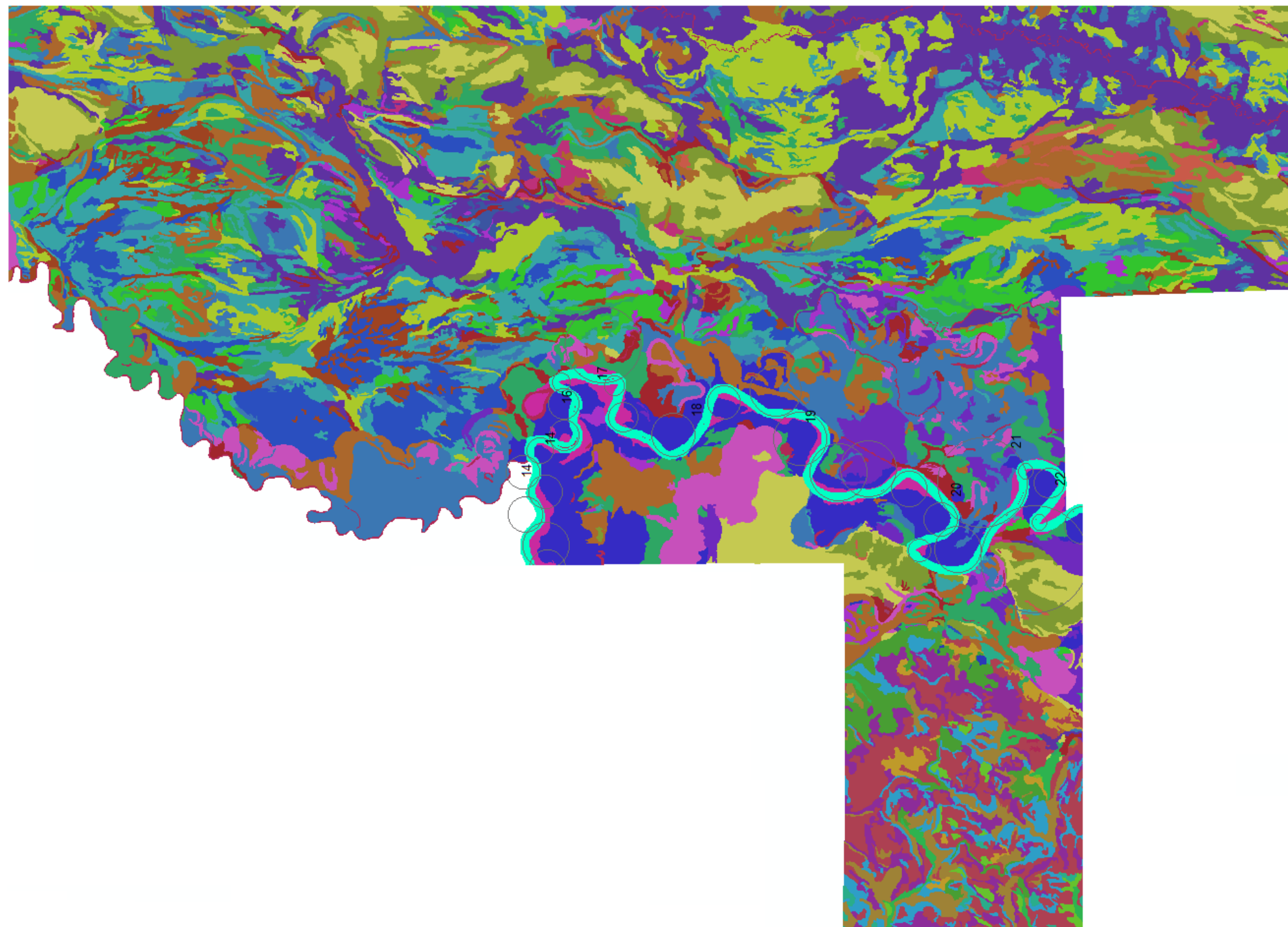
- Noark very cherty silt loam, 8 to 12 percent slopes
- Peridge silt loam, 3 to 8 percent slopes
- Pits-Dumps complex, 20 to 40 percent slopes
- Portia fine sandy loam, 3 to 8 percent slopes
- Portia fine sandy loam, 8 to 12 percent slopes
- Saffell gravelly fine sandy loam, 12 to 20 percent slopes
- Saffell gravelly fine sandy loam, 8 to 12 percent slopes
- Secesh silt loam, frequently flooded
- Sidon silt loam, 1 to 3 percent slopes
- Sidon silt loam, 3 to 8 percent slopes
- Sidon silt loam, 8 to 12 percent slopes
- Spadra fine sandy loam, 0 to 1 percent slopes
- Sturkie silt loam, frequently flooded
- Taft silt loam, 0 to 2 percent slopes
- Wallen gravelly silt loam, 12 to 30 percent slopes
- Wallen gravelly silt loam, 3 to 8 percent slopes
- Wallen gravelly silt loam, 8 to 12 percent slopes
- Water
- Wideman loamy fine sand, frequently flooded

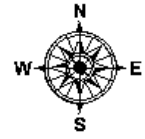




LEGEND

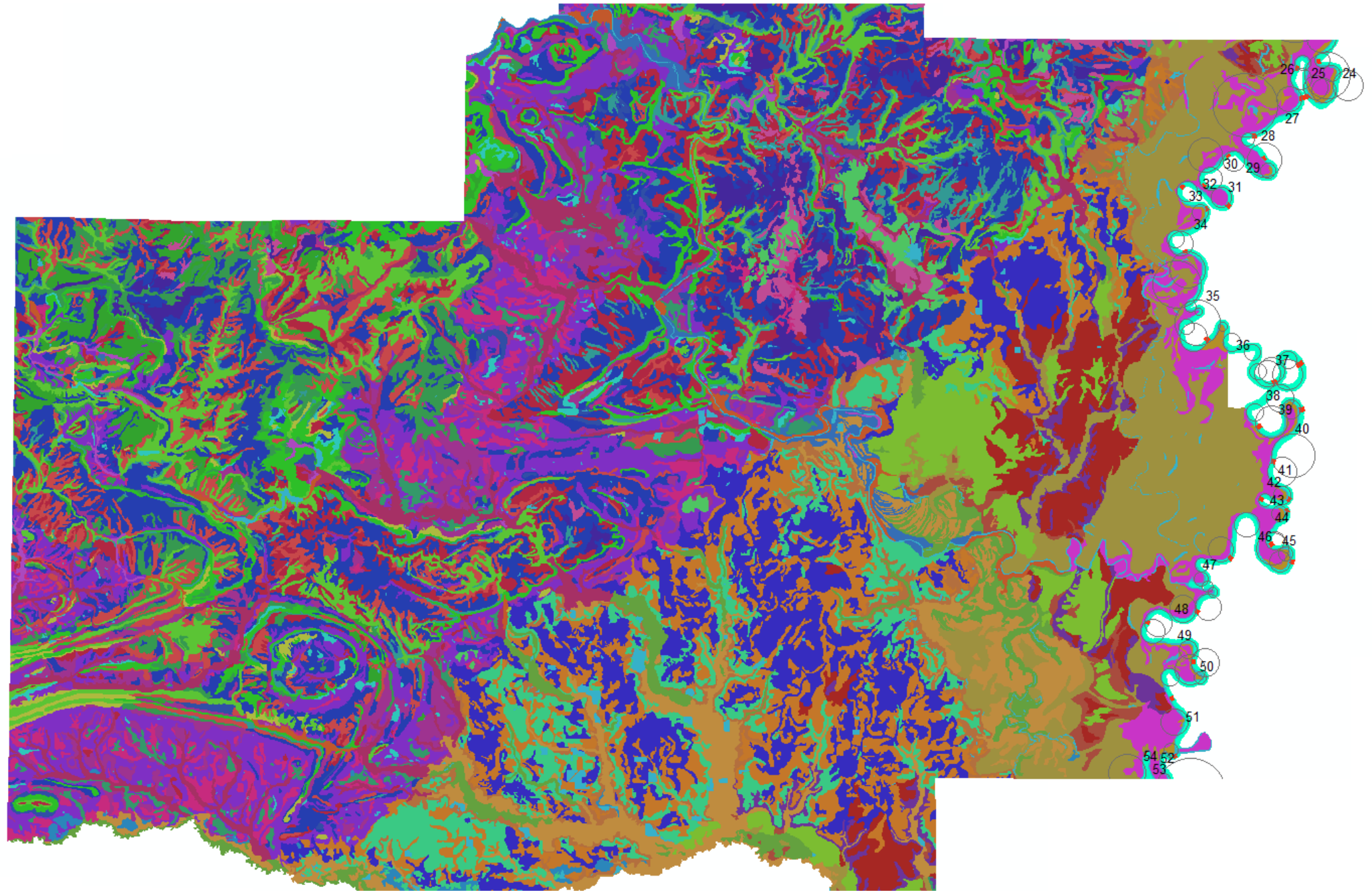
- Amagon and Forestdale silt loams
- Beulah fine sandy loam, undulating
- Bosket fine sandy loam, 0 to 1 percent slopes
- Bosket fine sandy loam, undulating
- Crowley and Hillemann silt loams
- Crowley silt loam
- Dexter silt loam, 0 to 1 percent slopes
- Dexter silt loam, undulating
- Dundee silt loam, 0 to 1 percent slopes
- Dundee silt loam, undulating
- Egam silt loam
- Enders silt loam, 3 to 12 percent slopes
- Enders stony silt loam, 12 to 25 percent slopes
- Foley-Calhoun complex
- Foley-Calhoun-McCrory complex
- Forestdale silty clay loam
- Grubbs silt loam
- Jackport silty clay loam
- Lafe silt loam
- Leadvale silt loam, 1 to 3 percent slopes
- Leadvale silt loam, 3 to 8 percent slopes
- Leadvale stony silt loam, 3 to 12 percent slopes (linker stony fine sandy loam)
- Linker fine sandy loam, 3 to 8 percent slopes
- Linker-Hector complex, 12 to 40 percent slopes
- Mountainburg stony fine sandy loam, 3 to 12 percent slopes
- Patterson fine sandy loam
- Pits, borrow
- Pits, gravel
- Sequatchie loam
- Sharkey silty clay loam
- Staser silt loam
- Water

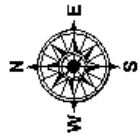




LEGEND

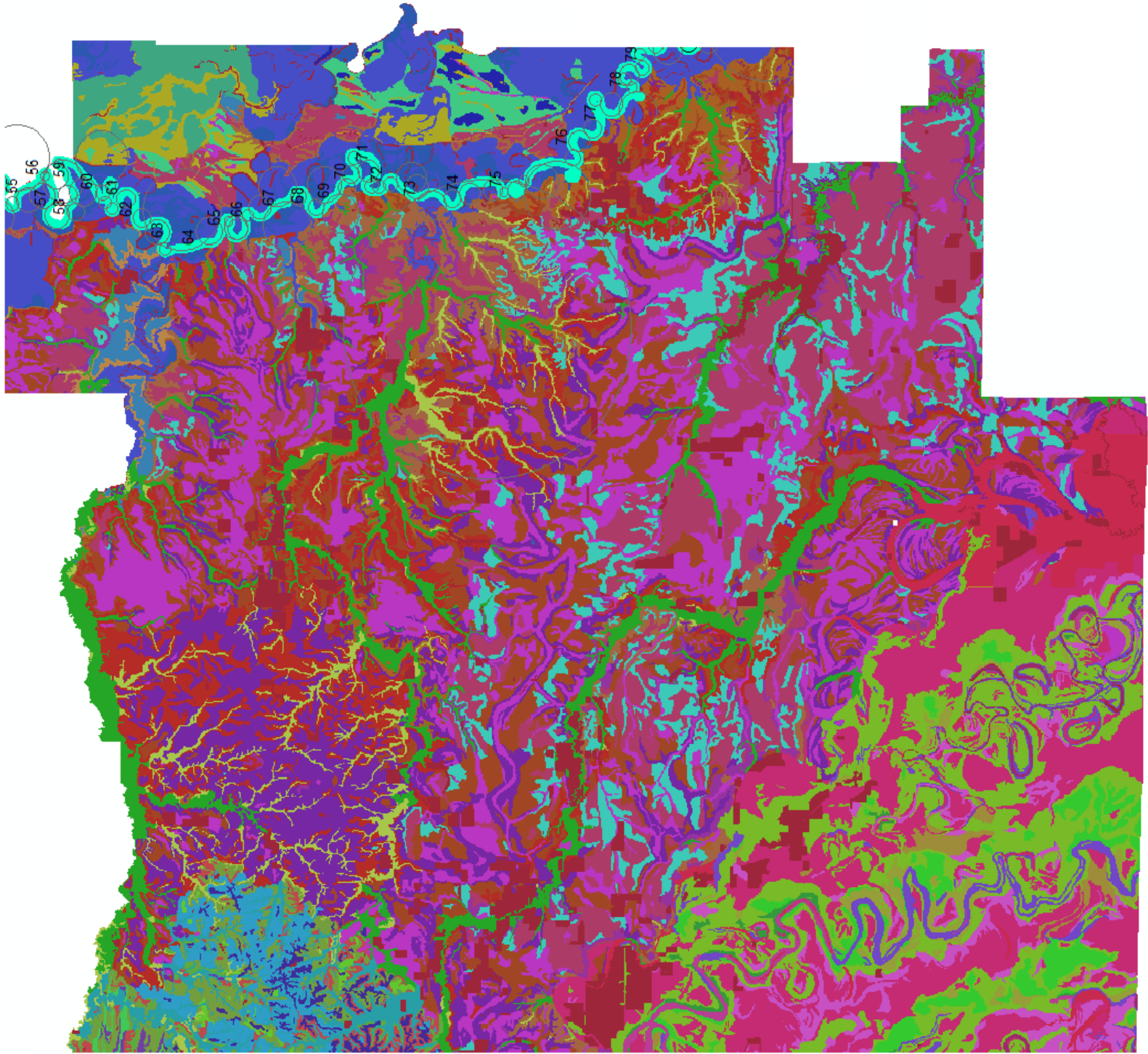
- Allen fine sandy loam, 3 to 8 percent slopes
- Barling silt loam, occasionally flooded
- Bonn silt loam, 0 to 1 percent slopes
- Calhoun silt loam, 0 to 1 percent slopes
- Calloway silt loam, 0 to 1 percent slopes
- Commerce silty clay loam, frequently flooded
- Crowley silt loam, 0 to 1 percent slopes
- Enders fine sandy loam, 3 to 8 percent slopes
- Enders gravelly fine sandy loam, 8 to 12 percent slopes
- Enders stony fine sandy loam, 3 to 12 percent slopes
- Enders-Steprock complex, 12 to 30 percent slopes
- Gore silt loam, 1 to 3 percent slopes
- Guthrie silt loam, 0 to 1 percent slopes
- Jackport silty clay loam, 0 to 1 percent slopes
- Jackport silty clay loam, gently undulating
- Kobel silty clay, frequently flooded
- Large water
- Leadvale silt loam, 1 to 3 percent slopes
- Leadvale silt loam, 3 to 8 percent slopes
- Linker fine sandy loam, 3 to 8 percent slopes
- Linker gravelly fine sandy loam, 3 to 8 percent slopes
- Loring silt loam, 1 to 3 percent slopes
- Loring silt loam, 3 to 8 percent slopes
- Mountainburg stony fine sandy loam, 3 to 12 percent slopes
- Nauvoo fine sandy loam, 3 to 8 percent slopes
- Nugent loamy fine sand, occasionally flooded
- Oaklimeter silt loam, frequently flooded
- Rexor silt loam, occasionally flooded
- Robinsonville fine sandy loam, frequently flooded
- Sidon loam, 1 to 3 percent slopes
- Sidon loam, 3 to 8 percent slopes
- Spadra fine sandy loam, occasionally flooded
- Steprock-Enders complex, 12 to 30 percent slopes
- Steprock-Linker complex, 3 to 8 percent slopes
- Steprock-Mountainburg complex, 8 to 12 percent slopes
- Taft silt loam, 0 to 2 percent slopes
- Tichnor silt loam, frequently flooded

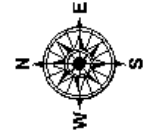




LEGEND

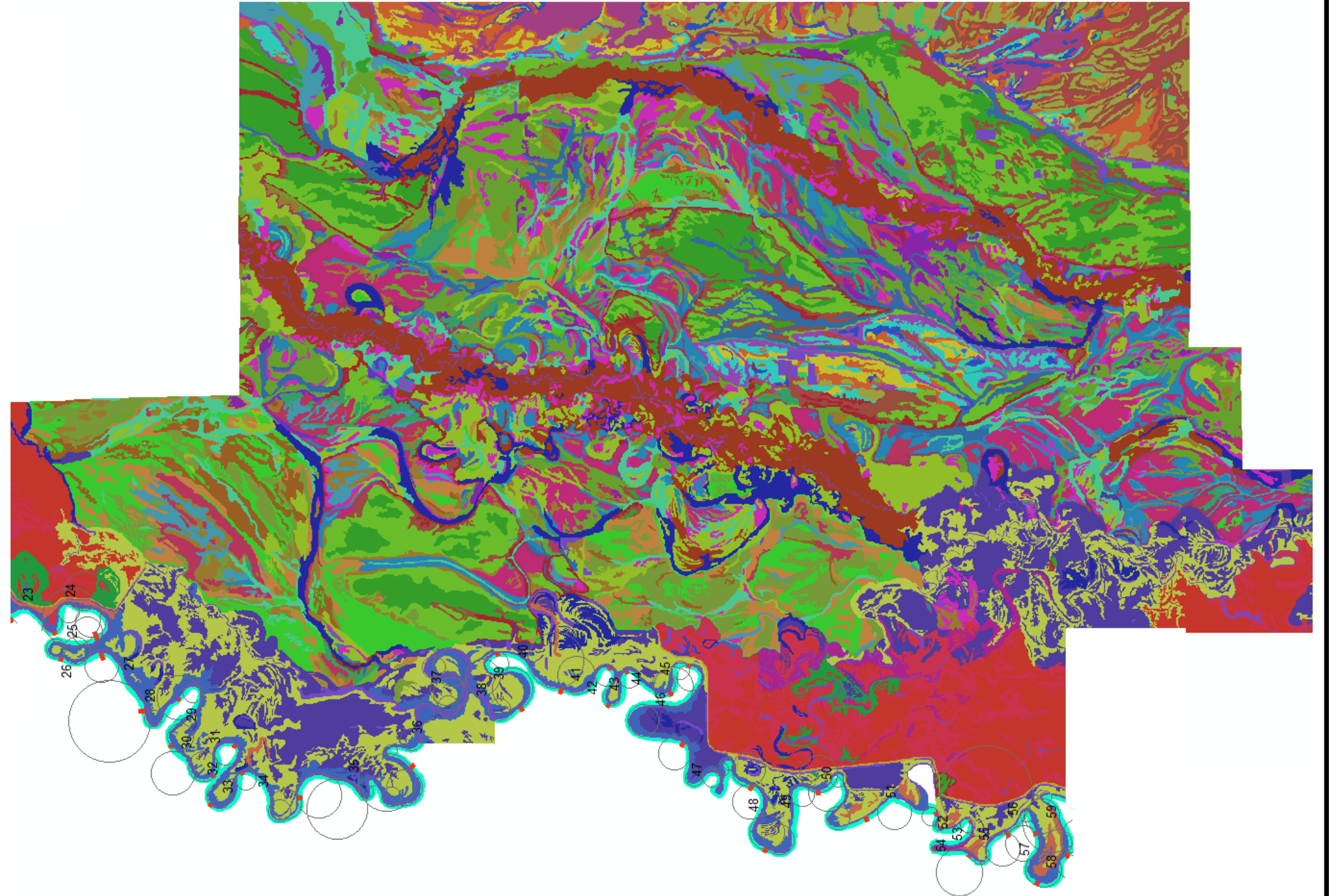
- Amy silt loam, frequently flooded
- Calhoun silt loam, 0 to 1 percent slopes
- Calloway silt loam, 0 to 1 percent slopes
- Caspiana silt loam, 0 to 1 percent slopes
- Commerce silt loam, 0 to 1 percent slopes
- Commerce silt loam, frequently flooded
- Crowley silt loam, 0 to 1 percent slopes
- Dubbs silt loam, 0 to 1 percent slopes
- Dubbs silt loam, 1 to 3 percent slopes
- Enders stony fine sandy loam, 8 to 15 percent slopes
- Hebert silt loam, 0 to 1 percent slopes
- Jackport silty clay loam, 0 to 1 percent slopes
- Jackport silty clay loam, 1 to 3 percent slopes
- Keo silt loam, 0 to 1 percent slopes
- Keo silt loam, 1 to 3 percent slopes
- Kobel silty clay loam, 0 to 1 percent slopes
- Kobel silty clay loam, frequently flooded
- Leadvale silt loam, 1 to 3 percent slopes
- Leadvale silt loam, 3 to 8 percent slopes
- Levee
- Linker-Enders-Mountainburg complex, 12 to 25 percent slopes
- Loring silt loam, 1 to 3 percent slopes
- Loring silt loam, 3 to 8 percent slopes
- Loring-McKamie complex, 8 to 20 percent slopes
- Moreland silty clay, 0 to 1 percent slopes
- Muskogee silt loam, 3 to 8 percent slopes
- Oaklimeter silt loam, occasionally flooded
- Perry silty clay, 0 to 1 percent slopes
- Perry silty clay, frequently flooded
- Pits, borrow
- Portland silty clay, 0 to 1 percent slopes
- Rilla silt loam, 0 to 1 percent slopes
- Rilla silt loam, 1 to 3 percent slopes
- Sacul fine sandy loam, 3 to 8 percent slopes
- Sawyer silt loam, 3 to 8 percent slopes
- Smithdale sandy loam, 5 to 8 percent slopes
- Stuttgart silt loam, 0 to 1 percent slopes
- Stuttgart silt loam, 1 to 3 percent slopes
- Taft silt loam, 0 to 2 percent slopes
- Tichnor silt loam, frequently flooded
- Water
- Yorktown silty clay

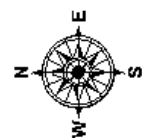




LEGEND

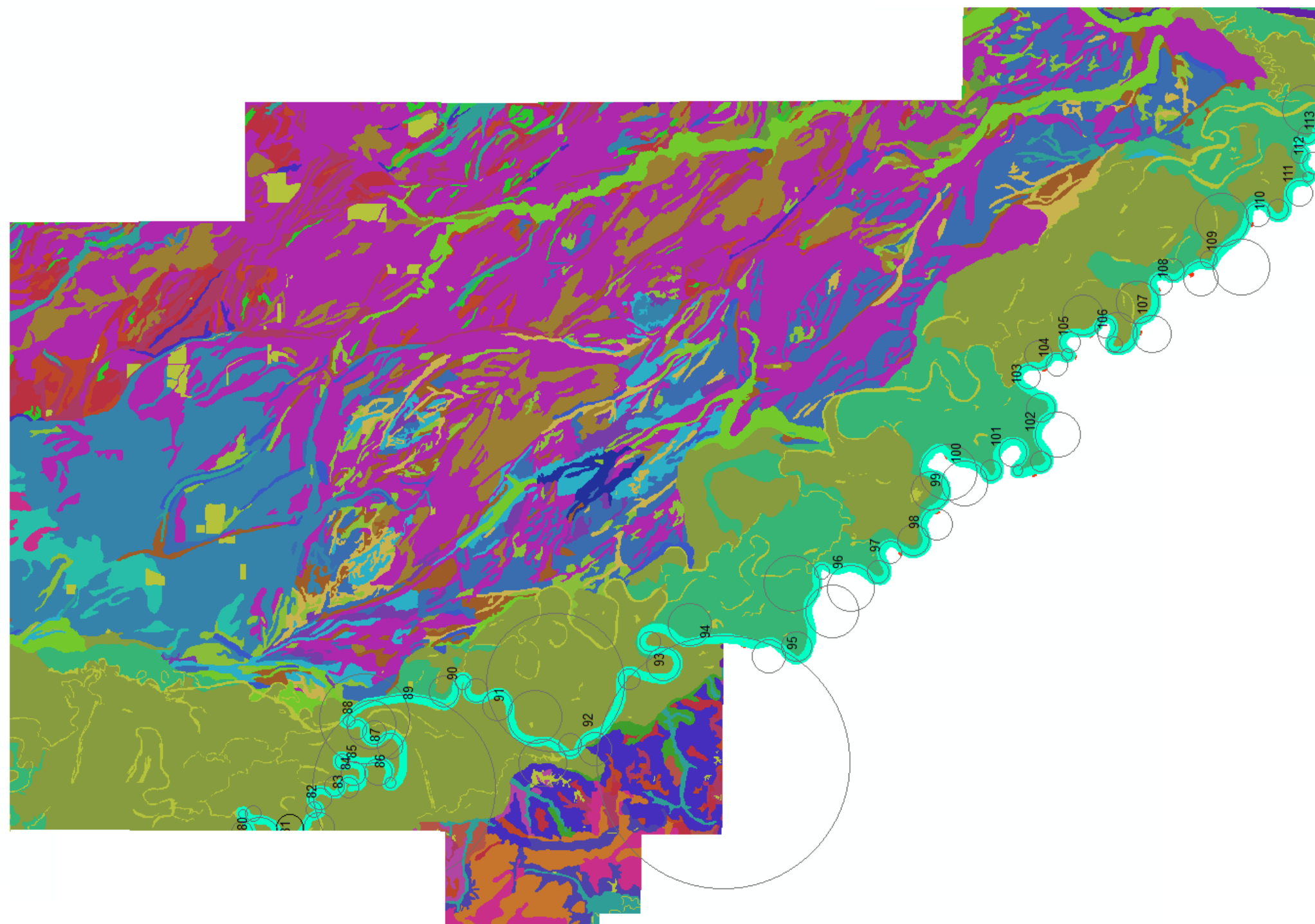
- Amagon silt loam, 0 to 1 percent slopes
- Askew fine sandy loam, 1 to 3 percent slopes
- Bulltown loamy fine sand, 1 to 8 percent slopes
- Calhoun silt loam, 0 to 1 percent slopes
- Calloway silt loam, 0 to 1 percent slopes
- Calloway silt loam, 1 to 3 percent slopes
- Dubbs silt loam, 0 to 1 percent slopes
- Dubbs silt loam, 1 to 3 percent slopes
- Dubbs silt loam, 3 to 8 percent slopes
- Dundee silt loam, 0 to 1 percent slopes
- Foley-Bonn complex, 0 to 1 percent slopes
- Forestdale silty clay loam, 0 to 1 percent slopes, frequently flooded
- Grenada silt loam, 1 to 3 percent slopes
- Grenada silt loam, 3 to 8 percent slopes, eroded
- Grubbs silt loam, 1 to 3 percent slopes
- Grubbs silt loam, 3 to 8 percent slopes, eroded
- Henry silt loam, 0 to 1 percent slopes
- Hillemann silt loam, 0 to 1 percent slopes
- Hillemann silt loam, 1 to 3 percent slopes
- Jackport silty clay loam, 0 to 1 percent slopes
- Kobel silty clay loam, 0 to 1 percent slopes, frequently flooded
- Kobel silty clay loam, 0 to 1 percent slopes, ponded
- Kobel silty clay loam, 0 to 1 percent slopes, rarely flooded
- Lafe silt loam, 0 to 1 percent slopes
- Levee
- McCrary fine sandy loam, 0 to 1 percent slopes
- Oaklimeter silt loam, 0 to 2 percent slopes, occasionally flooded
- Overcup silt loam, 0 to 1 percent slopes
- Patterson fine sandy loam, 0 to 2 percent slopes
- Taylorbay silt loam, 0 to 3 percent slopes, frequently flooded
- Taylorbay silt loam, 0 to 3 percent slopes, rarely flooded
- Teksob loam, 0 to 1 percent slopes
- Teksob loam, 1 to 3 percent slopes
- Teksob loam, 3 to 8 percent slopes
- Tichnor silt loam, 0 to 1 percent slopes, frequently flooded
- Tipp silty clay loam, 0 to 3 percent slopes, frequently flooded
- Tipp silty clay loam, 0 to 3 percent slopes, rarely flooded
- Tuckerman loam, 0 to 1 percent slopes, frequently flooded
- Tuckerman silty clay loam, 0 to 1 percent slopes, frequently flooded
- Water
- Wiville fine sandy loam, 0 to 1 percent slopes
- Wiville fine sandy loam, 1 to 3 percent slopes
- Wiville fine sandy loam, 3 to 8 percent slopes
- Yancopin silty clay loam, 0 to 3 percent slopes, frequently flooded
- Yancopin silty clay loam, 0 to 3 percent slopes, rarely flooded

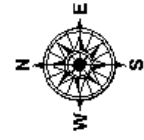




LEGEND

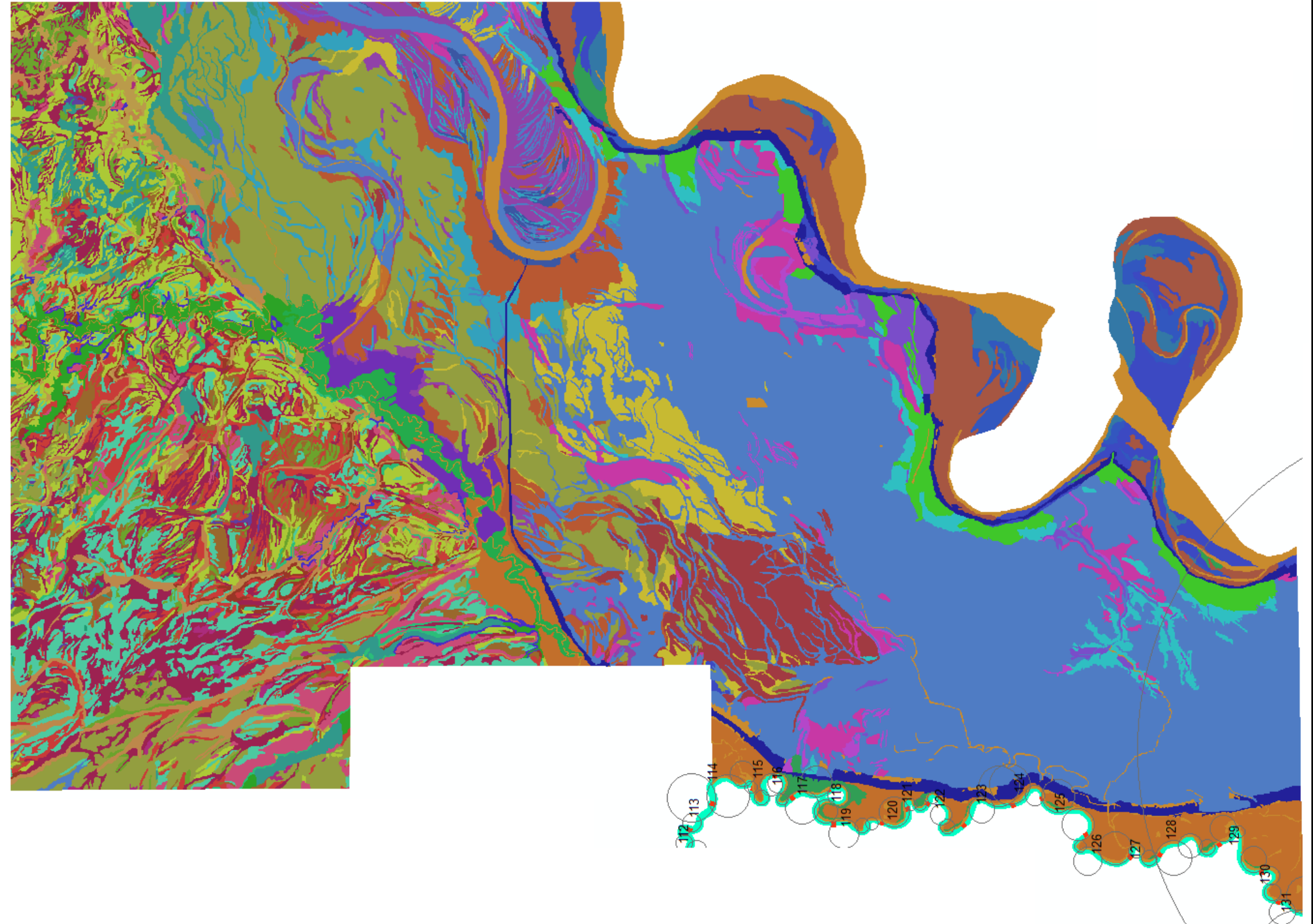
- Amagon silt loam
- Bosket fine sandy loam, 0 to 1 percent slopes
- Bosket fine sandy loam, gently undulating
- Calhoun silt loam
- Calloway silt loam
- Commerce soils, frequently flooded
- Crowley silt loam
- Dubbs silt loam, 0 to 1 percent slopes
- Dubbs silt loam, gently undulating
- Dundee silt loam, 0 to 1 percent slopes
- Dundee silt loam, gently undulating
- Foley-Calhoun-Bonn complex
- Gore silt loam, 3 to 8 percent slopes
- Grenada silt loam, 0 to 1 percent slopes
- Grenada silt loam, 1 to 3 percent slopes
- Grenada silt loam, 3 to 8 percent slopes
- Grubbs silt loam
- Jackport silty clay loam
- Lafe-Bonn complex
- Loring silt loam, 3 to 8 percent slopes
- Loring silt loam, 8 to 12 percent slopes
- McCrary fine sandy loam
- Memphis silt loam, 0 to 1 percent slopes
- Memphis silt loam, 1 to 3 percent slopes
- Memphis silt loam, 3 to 8 percent slopes
- Mhoon soils, frequently flooded
- Sharkey silty clay
- Sharkey soils, frequently flooded
- Stuttgart silt loam, 0 to 1 percent slopes
- Stuttgart silt loam, 1 to 3 percent slopes
- Tichnor soils, frequently flooded
- Water

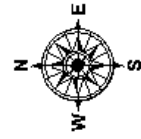




LEGEND

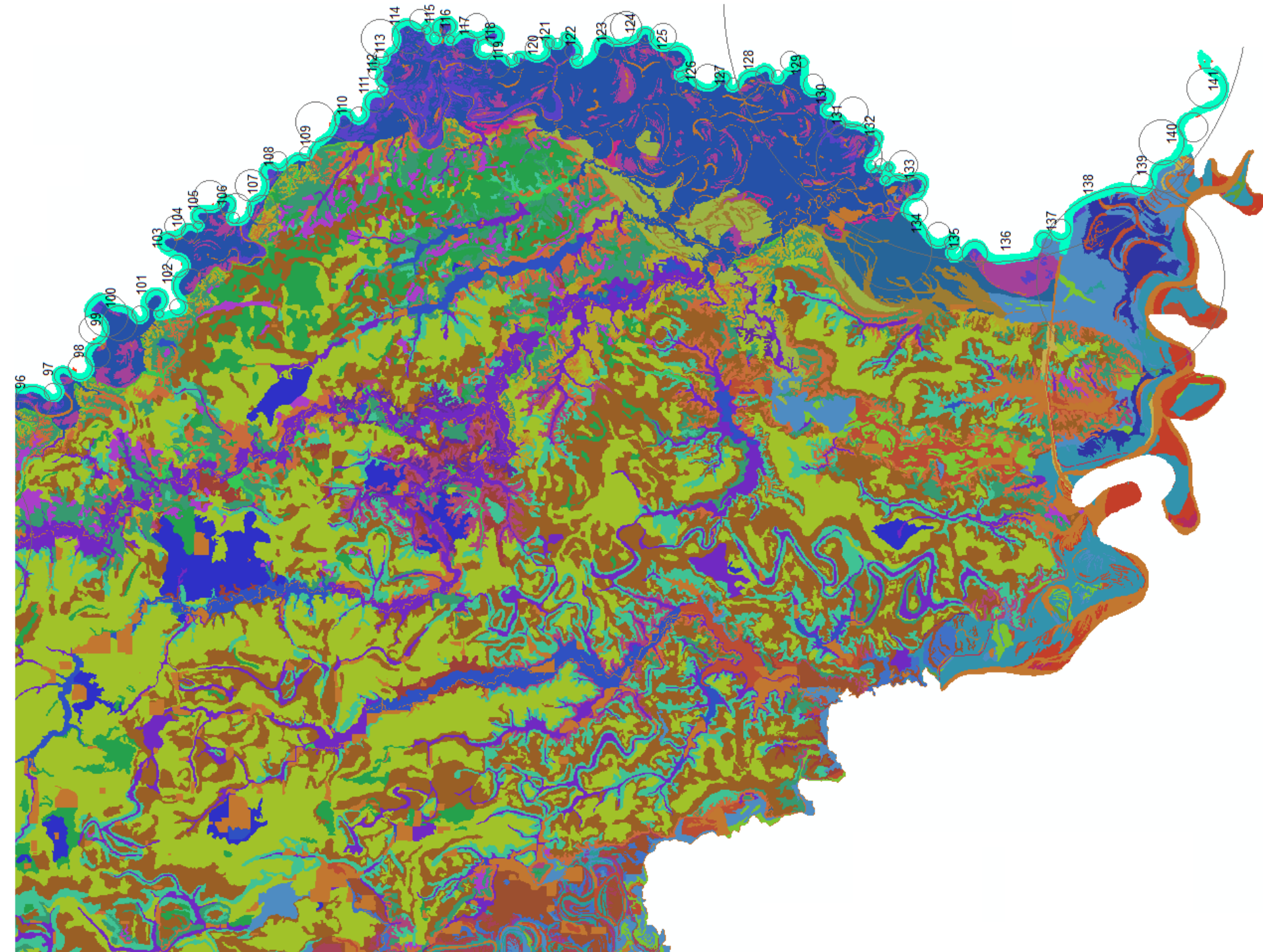
- Alligator clay
- Alligator soils, frequently flooded
- Amagon silt loam
- Arkabutla silty clay loam
- Arkabutla soils, frequently flooded
- Beulah fine sandy loam, gently undulating
- Bonn silt loam
- Calhoun silt loam
- Calloway silt loam, 0 to 1 percent slopes
- Calloway silt loam, 1 to 3 percent slopes
- Commerce silt loam
- Commerce soils, frequently flooded
- Convent silt loam
- Crevasse soils, frequently flooded
- Dubbs silt loam, gently undulating
- Dundee silt loam
- Falaya silt loam
- Fluvaquents, frequently flooded
- Foley silt loam
- Grenada silt loam, 1 to 3 percent slopes
- Henry silt loam
- Jeanerette silt loam
- Lagrange fine sandy loam
- Levee
- Loring silt loam, 1 to 3 percent slopes
- Loring silt loam, 3 to 8 percent slopes, eroded
- Marvell fine sandy loam
- Memphis silt loam, 1 to 3 percent slopes
- Memphis silt loam, 12 to 40 percent slopes
- Memphis silt loam, 3 to 8 percent slopes, eroded
- Memphis silt loam, 8 to 12 percent slopes, eroded ent slopes
- Mhoon soils, frequently flooded
- Natchez silt loam, 20 to 40 percent slopes
- Newellton silty clay
- Newellton silty clay, gently undulating
- Newellton soils, frequently flooded
- Pits, gravel
- Robinsonville fine sandy loam
- Robinsonville soils, frequently flooded
- Sharkey silty clay
- Sharkey soils, frequently flooded
- Tunica silty clay
- Tunica silty clay, gently undulating
- Tunica soils, frequently flooded
- Water
- Zachary soils, frequently flooded

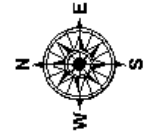




LEGEND

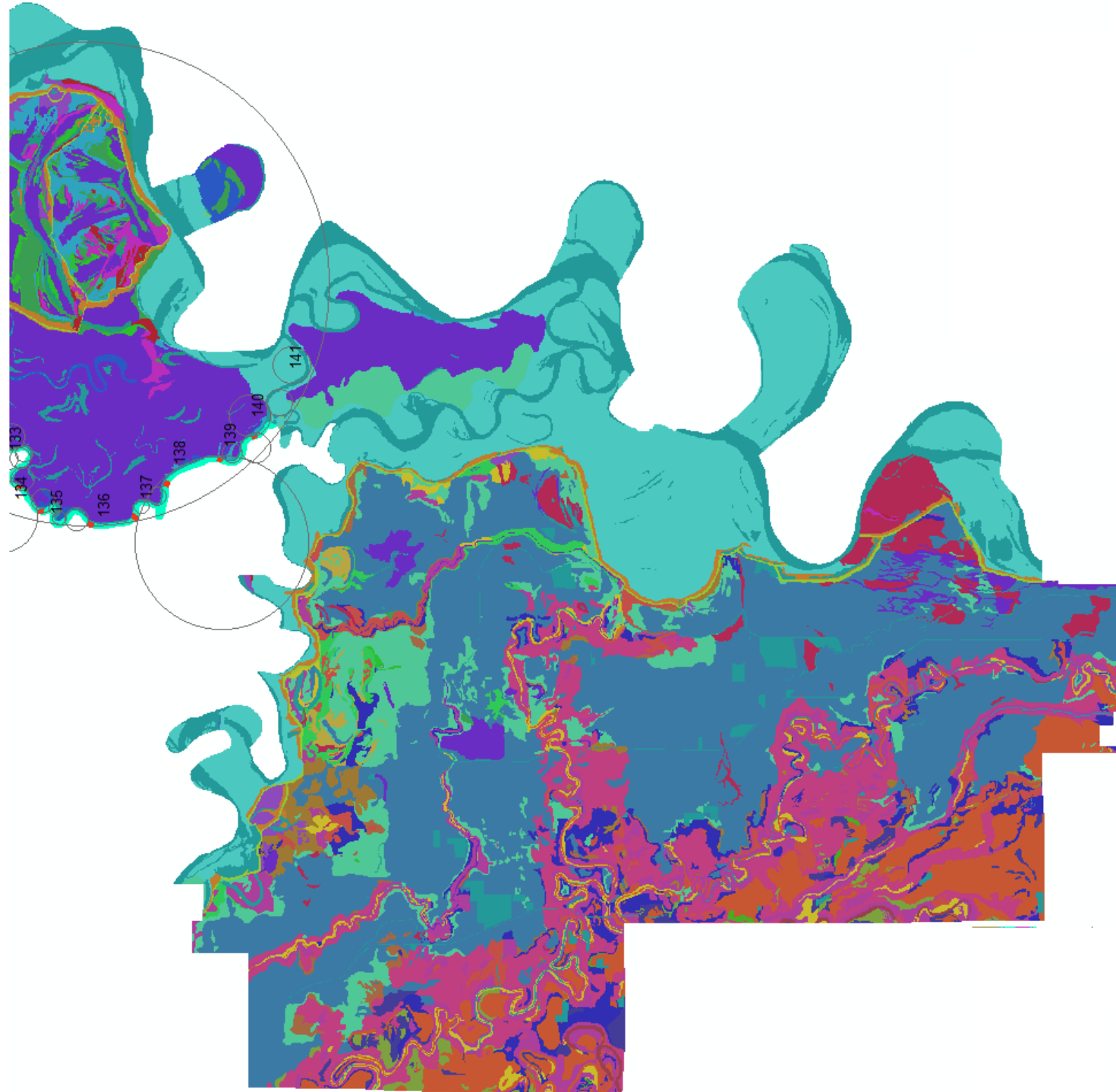
- Crevasse loamy fine sand, 0 to 5 percent slopes, occasionally flooded
- Dam
- Desha silty clay, 0 to 3 percent slopes, occasionally flooded
- Dewitt silt loam, 0 to 1 percent slopes
- Dubbs silt loam, 0 to 3 percent slopes
- Dundee silt loam, 0 to 2 percent slopes, occasionally flooded
- Ethel silt loam, 0 to 1 percent slopes
- Forestdale silty clay loam, 0 to 1 percent slopes, frequently flooded
- Hebert silt loam, 0 to 1 percent slopes
- Immanuel silt loam, 0 to 1 percent slopes
- Immanuel silt loam, 1 to 3 percent slopes
- Immanuel silt loam, 15 to 25 percent slopes
- Immanuel silt loam, 3 to 8 percent slopes
- Immanuel silt loam, 8 to 15 percent slopes
- Keo loam, 0 to 1 percent slopes, occasionally flooded
- Keo loam, 1 to 6 percent slopes, occasionally flooded
- Kobel silty clay, 0 to 1 percent slopes, frequently flooded
- Kobel silty clay, ponded, 0 to 1 percent slopes, frequently flooded
- Lagruie silty clay loam, 0 to 1 percent slopes
- Levee
- Muskogee silt loam, 1 to 3 percent slopes
- Muskogee silt loam, 3 to 8 percent slopes
- Muskogee silt loam, 8 to 15 percent slopes
- Oaklimeter silt loam, 0 to 1 percent slopes, occasionally flooded
- Overcup silt loam, 0 to 1 percent slopes
- Perry clay, 0 to 1 percent slopes
- Perry clay, 0 to 1 percent slopes, frequently flooded
- Portland clay, 0 to 1 percent slopes
- Portland clay, 0 to 1 percent slopes, frequently flooded
- Rilla silt loam, 0 to 1 percent slopes
- Rilla silt loam, 1 to 3 percent slopes
- Riverwash, sandy, frequently flooded
- Stuttgart silt loam, 0 to 1 percent slopes
- Stuttgart silt loam, 1 to 3 percent slopes
- Tichnor silt loam, 0 to 1 percent slopes, frequently flooded
- Tichnor silt loam, ponded, 0 to 1 percent slopes, frequently flooded
- Udipsamments, 0 to 8 percent slopes
- Water
- Yancopin silty clay loam, 1 to 3 percent slopes, frequently flooded
- Yorktown silty clay, ponded, 0 to 1 percent slopes, frequently flooded





LEGEND

- Bowdre, Desha, and Robinsonville soils, gently undulating
- Bruno loamy sand, gently undulating
- Commerce silt loam, 0 to 1 percent slopes
- Commerce silt loam, gently undulating
- Coushatta complex, 0 to 1 percent slopes
- Dam
- Desha clay
- Desha silt loam
- Hebert silt loam
- Levee
- McGehee silt loam
- Newellton clay, 0 to 1 percent slopes
- Newellton clay, gently undulating
- Not complete
- Perry clay
- Perry silt loam
- Pits, borrow
- Portland clay
- Portland silt loam
- Rilla silt loam, 0 to 1 percent slopes
- Rilla silt loam, 1 to 3 percent slopes
- Sharkey and Desha clays, 0 to 1 percent slopes
- Sharkey and Desha clays, gently undulating
- Sharkey and Desha silt loams
- Sharkey clay
- Sharkey-Commerce-Coushatta association, frequently flooded
- Tunica clay, 0 to 1 percent slopes
- Tunica clay, 1 to 3 percent slopes
- Tunica clay, frequently flooded
- Tutwiler silt loam
- Water



THE WHITE RIVER PLANFORM
(RM 295.27 - 0.00)

Legend

WS 100 yr

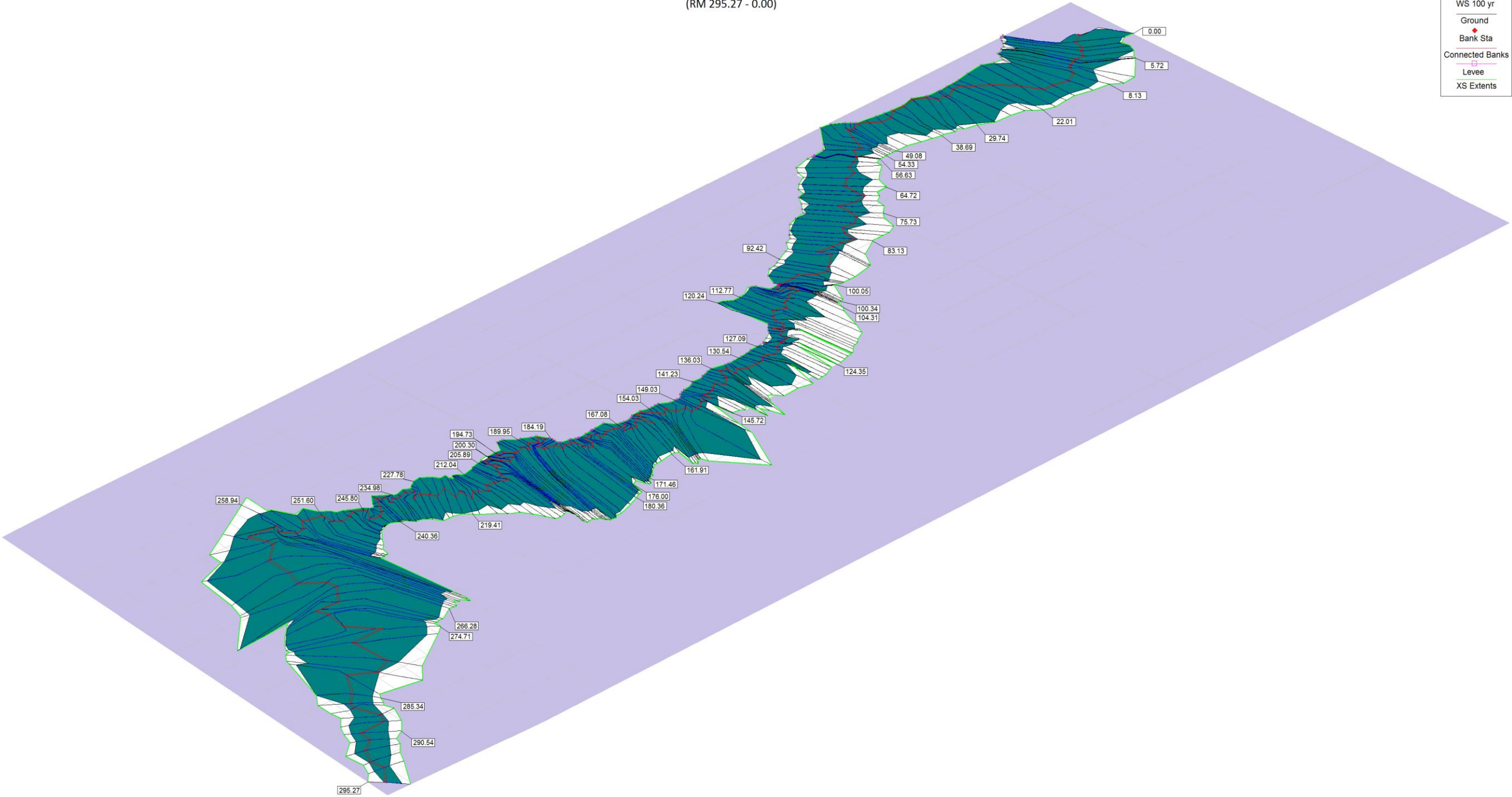
Ground

Bank Sta

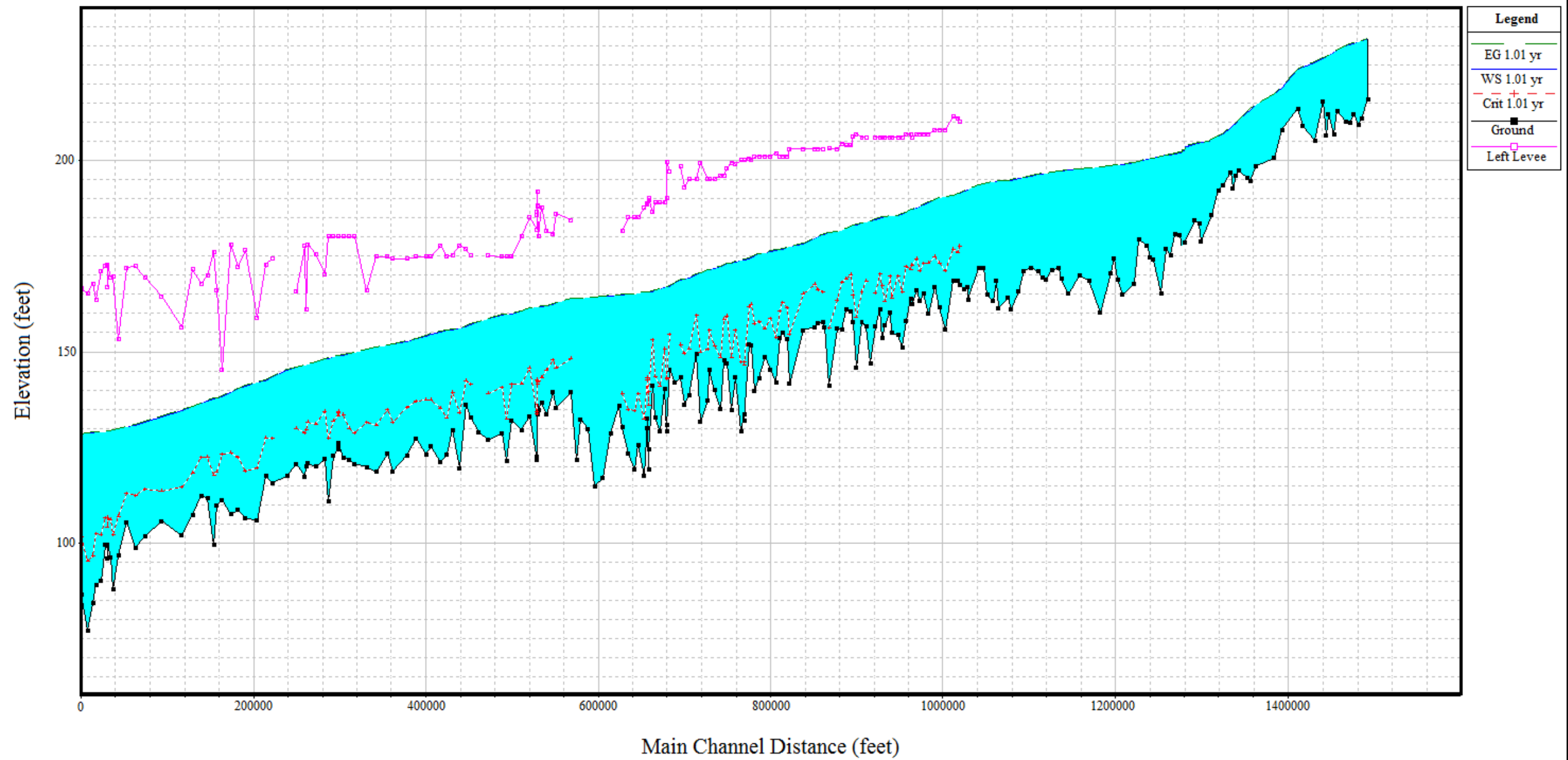
Connected Banks

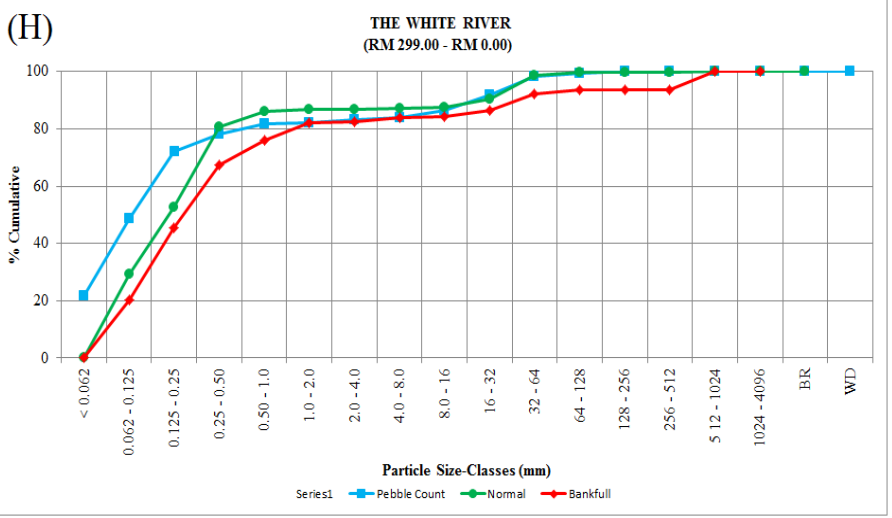
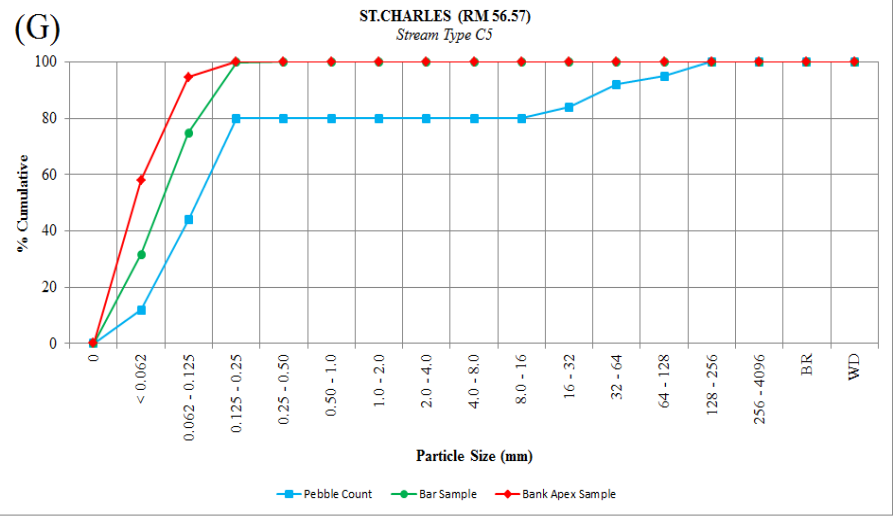
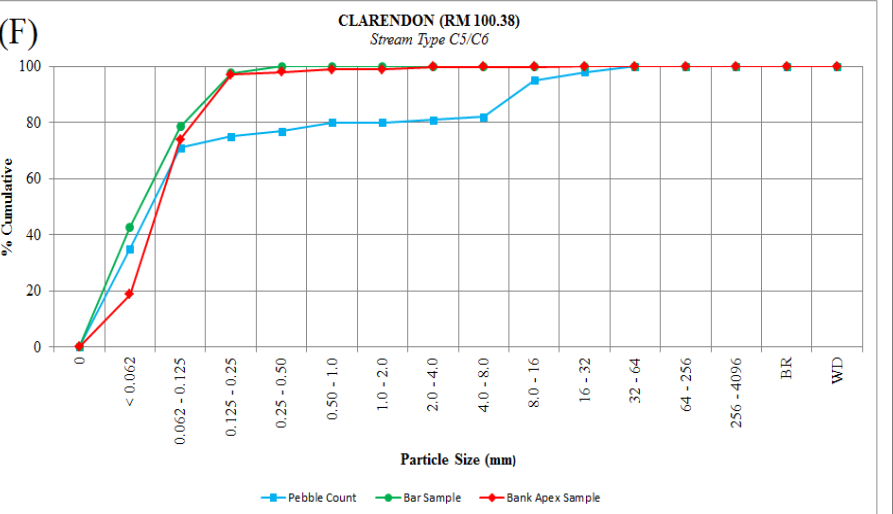
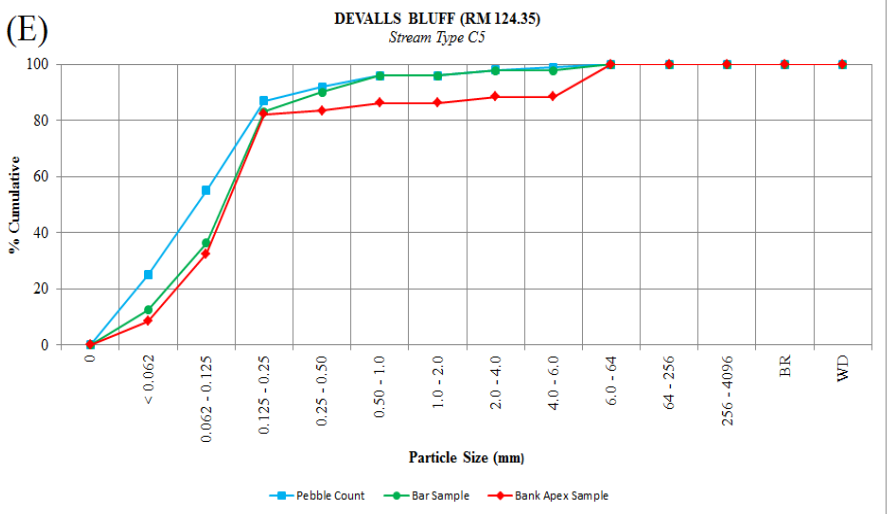
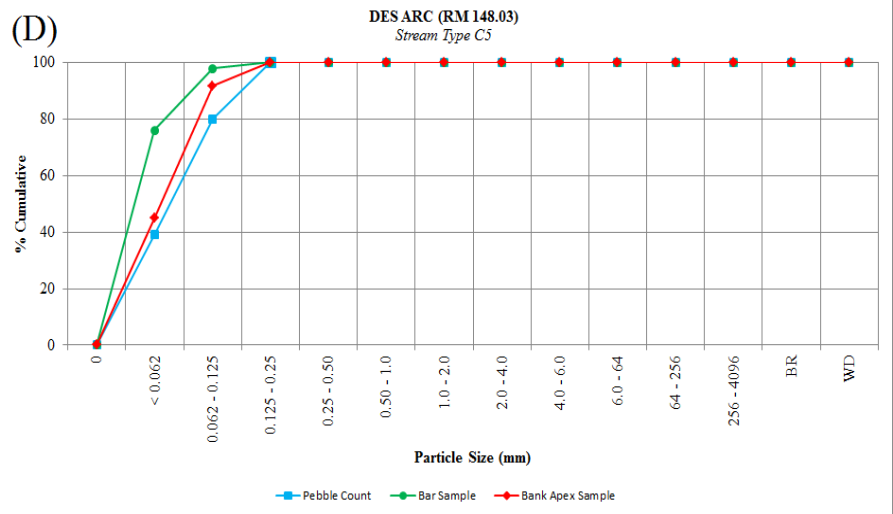
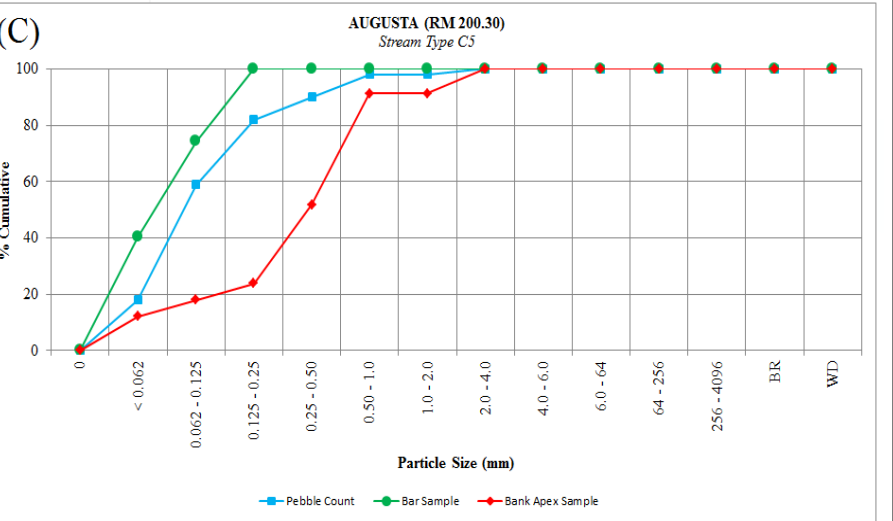
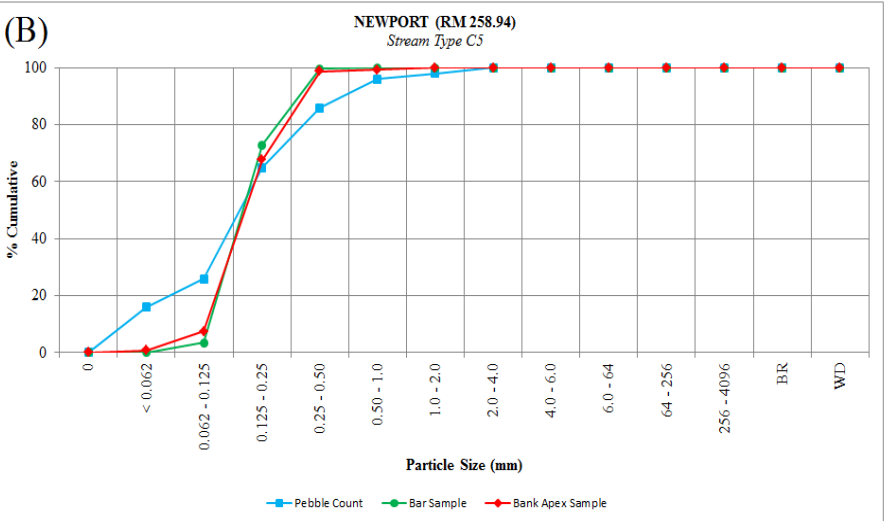
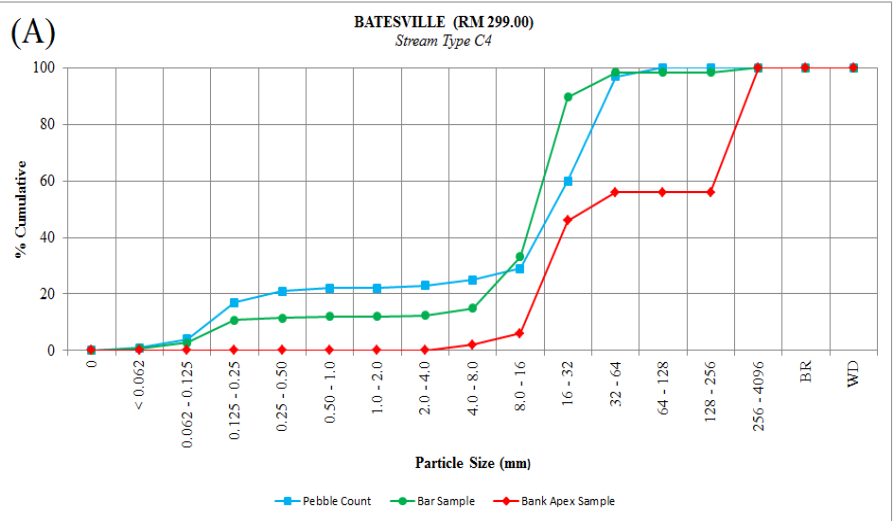
Levee

XS Extents



WHITE RIVER PROFILE





**PARTICLE SIZE DISTRIBUTION CURVES
(WHITE RIVER, RM 299.00 - RM 0.00)**

(A) Batesville, Arkansas at RM 299.00
(B) Newport, Arkansas at RM 258.94
(C) Augusta, Arkansas at RM 200.30
(D) Des Arc, Arkansas at RM 148.03
(E) Devalls Bluff, Arkansas at RM 124.35
(F) Clarendon, Arkansas at RM 100.38
(G) St. Charles, Arkansas at RM 56.57
(H) Composite Plot (RM 299.00 - RM 0.00)